SOVIET PHYSICS

JETP

A translation of the Zhurnal Éksperimental'noĭ i Teoreticheskoĭ Fiziki.

Vol. 14, No. 2, pp 225-483 (Russ. orig. Vol. 41, No. 2, pp 313-669, August, 1961) February, 1962

ANGULAR DISTRIBUTIONS FOR ELASTIC SCATTERING OF 14-Mev NEUTRONS

V. I. STRIZHAK, V. V. BOBYR', L. Ya. GRONA

Physics Institute, Academy of Sciences, Ukrainian S.S.R.

Submitted to JETP editor January 9, 1961

J. Exptl. Theoret. Phys. (U.S.S.R.) 41, 313-316 (August, 1961)

We have measured the differential cross section for elastic scattering of 14-Mev neutrons from carbon, nitrogen and silver at angles from 20 to 140° and from molybdenum, cadmium, and tellurium at angles from 15 to 160°. After some necessary corrections have been made, the experimental data are compared with cross sections calculated on the basis of the optical model of the nucleus.

THERE are many experimental data which are well accounted for by the optical model of the nucleus, particularly by the more recent modifications of this model.[1-4] This is especially true of cross sections for the elastic scattering of neutrons at an energy of 14 Mev.[5-19]

The purpose of the present paper is to present experimental results on the differential cross section for elastic scattering of 14-Mev neutrons by carbon, nitrogen, sulfur, molybdenum, cadmium, and tellurium.

The measurements were made on toroidal scatterers.

The 14-Mev neutrons were produced by bombarding a T-Zr target with 120-kev deuterons in the neutron generator of the Physics Institute of the Academy of Sciences of the Ukrainian S.S.R.[18]

A scintillation counter was used to detect neutrons from molybdenum, cadmium, and tellurium. The counter was sensitive only to neutrons having energy greater than a threshold of 11 Mev. This threshold was not high enough to discriminate completely against inelastically scattered neutrons, and this effect was significant at large angles. However, a higher threshold could not be used partly because a lower counting rate would lead to larger statistical errors and also because of instabilities in the electronic circuitry.

Neutrons scattered from carbon, nitrogen, and sulfur were detected with a scintillation spectrometer using a stilbene crystal and an FÉU-14A photomultiplier. Pulses from the photomultiplier were fed to an AI-100-1 amplitude analyzer. The resolution of the spectrometer was 3% (400 kev). The neutron spectra obtained made it possible to distinguish reliably between elastic and inelastic scattering events.

We measured the relative sensitivity $A(\alpha)$ of the neutron detector as a function of the direction of flight of the incident neutrons.

The scatterers were rings of diameter 13, 20, 25 and 30 cm. The cross-section diameters of the rings were 2 cm for carbon, 3 cm for cadmium, molybdenum, and tellurium, and 4 cm for nitrogen and sulfur.

In the case of nitrogen, the scatterer was made by filling a toroidal Dewar flask with liquid nitrogen. The flask walls were made of 0.5 mm copper.

The measurements were normalized by using scintillation counters to monitor neutrons and α particles from the $T(d, n)\alpha$ reaction.

The differential cross section $\sigma_{el}(\vartheta)$ for elastic

scattering was computed from the experimentally measured values of the quantity

$$S(\vartheta) = (N_{sc} - N_b) / N_d, \quad (1)$$

where N_{SC} is the number of counts with the scatterer and shield in, N_b is the number of counts without the scatterer (background), and N_d is the number of counts without the scatterer and without the shield.

The differential cross section for elastic scattering through an angle ϑ was calculated from the formula

$$\sigma_{el}(\vartheta) = S(\vartheta)(R_1R_2/R_0)^2 \exp(n\sigma_{in}d) / NA(\alpha) B(E_n), \quad (2)$$

where R_1 is the distance from the source to the scatterer, R_2 is the distance from the scatterer to the detector, and R_0 is the distance from the source to the detector. n is the number of nuclei per cc in the scatterer, σ_{in} is the cross section for inelastic scattering, d is the thickness of the scatterer, N is the number of scattering nuclei, and $B(E_n)$ is a correction factor to account for the dependence of the detector sensitivity on energy.

No correction was made for multiple scattering, although it may be considered that these effects are partially accounted for by using σ_{in} in formula (2) instead of the total cross section σ_t.

The measurements did not take long, so that drift in the electronics was not important. For angles less than 70°, statistical errors were less than 4%, while for larger angles these amounted to 7 or 8%.

Measurements were made for angles in the range 20 — 40° for carbon, nitrogen and sulfur, and in the range 15 — 160° for molybdenum, cadmium, and tellurium. The results are shown in Figs. 1 — 6. The solid curves are theoretical, being calculated using the optical model.

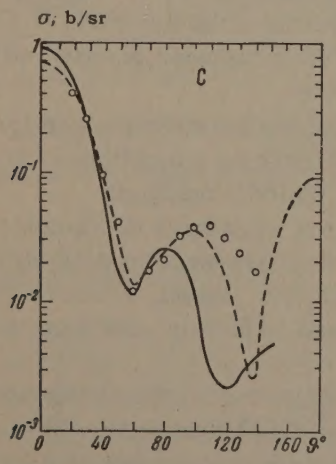

FIG. 1. Differential cross section for the elastic scattering of 14-Mev neutrons on carbon (in the laboratory frame of reference). Theoretical curves: the solid line in this and the following figures is taken from Bjorklund and Fernbach, the dashed line from Beister et al.[16]

Our data agree well with the results of other authors: for carbon, Anderson et al[19]; for nitrogen, Hughes[16]; for sulfur, Elliot[9] and St. Pierre et al[15]; for cadmium (at large angles), Anderson et al.[12]

For carbon, sulfur, molybdenum, cadmium, and tellurium the experimental data are compared with calculations based on the potential given by Bjorklund and Fernbach (Fig. 1, solid curve). There are no theoretical curves for scattering from molybdenum and tellurium, so the data have been compared with existing calculations for the neighboring nuclei zirconium and antimony.

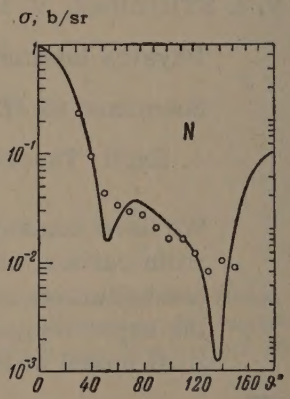

FIG. 2. Differential cross section from elastic scattering on nitrogen.

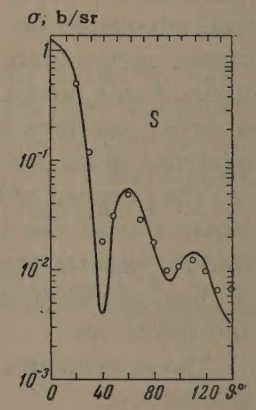

FIG. 3. Differential cross section for elastic scattering on sulfur.

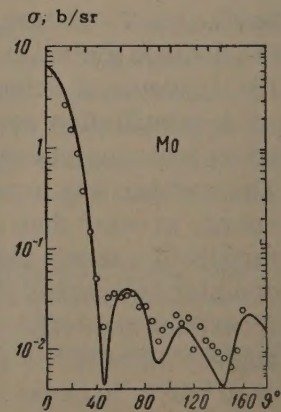

FIG. 4. Differential cross section for elastic scattering on molybdenum.

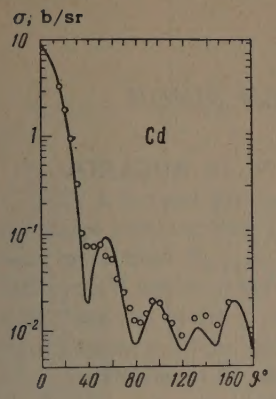

FIG. 5. Differential cross section for elastic scattering on cadmium.

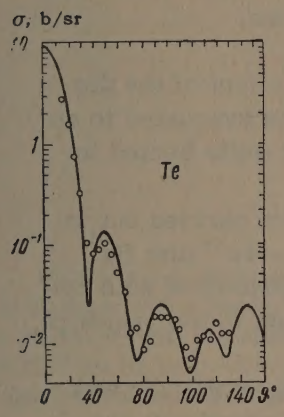

FIG. 6. Differential cross section for elastic scattering on tellurium.

The theoretical curves calculated by Bjorklund and Fernbach are in good agreement with the experimental data for sulfur, molybdenum, cadmium, and tellurium. The calculations disagree with experiment for carbon. Better agreement is obtained by comparing the experimental data with the curve calculated by Beister et al[16] (and shown as the dashed curve in Fig. 1).

[1] Culler, Fernbach, and Sherman, Phys. Rev. **101**, 1047 (1956).

[2] Bjorklund, Fernbach, and Sherman, Phys. Rev. **101**, 1832 (1956).

[3] F. Bjorklund and S. Fernbach, Phys. Rev. **109**, 1295 (1958).

[4] Luk'yanov, Orlov, and Turovtsev, JETP **35**, 750 (1958), Soviet Phys. JETP **8**, 521 (1959).

[5] J. P. Conner, Phys. Rev. **89**, 712 (1953).

[6] J. R. Smith, Phys. Rev. **95**, 730 (1954).

[7] W. J. Rhein, Phys. Rev. **98**, 1300 (1955).

[8] M. M. Khaletskii, DAN SSSR **113**, 305 (1957), Soviet Phys. Dokl. **2**, 129 (1958).

[9] J. O. Elliot, Phys. Rev. **101**, 684 (1956).

[10] H. Nauta, Nucl. Phys. **2**, 124 (1956).

[11] Berko, Whitehead, and Groseclose, Nucl. Phys. **6**, 210 (1958).

[12] Nakada, Anderson, Gardner, and Wong, Phys. Rev. **110**, 1439 (1958).

[13] Coon, Davis, Felthauser, and Nicodemus, Phys. Rev. **111**, 250 (1958).

[14] K. Yuasa, J. Phys. Soc. Japan **13**, 1248 (1958).

[15] St. Pierre, Machwe, and Lorrain, Phys. Rev. **115**, 999 (1959).

[16] D. Hughes, Proc. Second International Conference on the Peaceful Uses of Atomic Energy, Neutron Physics, p. 39 (1959).

[17] L. A. Rayburn, Phys. Rev. **116**, 1571 (1959).

[18] Bobyr', Grona, and Strizhak, JETP **41**, 24 (1961), Soviet Phys. **14**, 18 (1962).

[19] V. I. Strizhak and N. S. Nazarov, Pribory i Tekhnika Éksperimenta (Instrum. and Exptl. Techniques), in press.

[20] Anderson, Gardner, McClure, Nakada, and Wong, Phys. Rev. **111**, 572 (1958).

Translated by R. Krotkov
63

MAGNETOACOUSTIC OSCILLATIONS AND INSTABILITY OF AN INDUCTION PINCH

A. V. BORODIN, P. P. GAVRIN, I. A. KOVAN, B. I. PATRUSHEV, S. L. NEDOSEEV, V. D. RUSANOV, and D. A. FRANK-KAMENETSKII

Submitted to JETP editor January 27, 1961

J. Exptl. Theoret. Phys. (U.S.S.R.) **41**, 317-321 (August, 1961)

The results of an experimental investigation of an induction pinch are presented. It is shown that the radial oscillations that arise in rapid compression of the plasma are of magnetoacoustic nature. Pinch instabilities are also noted at high shock-wave intensities.

FREE magnetoacoustic oscillations in a dense plasma have been investigated by means of an experimental arrangement similar to that usually used for induction compression and heating of a plasma.[1-3]

A schematic diagram of the experiment is shown in Fig. 1. The magnetic field is excited by a uniform turn with an inductance of 30 cm;* preionization is obtained by means of an rf generator with a nominal power of 200 kw, which is connected through a $\frac{3}{4}\lambda$ coaxial cable to a coil arranged coaxially with the turn that produces the main magnetic field. This scheme makes it possible to avoid trapping of the rf magnetic field in the plasma since the frequency of the main field is 59 kc/sec while the frequency of the generator is 50 Mc/sec. The magnetic field strength in the main coil is 25,000 oe while the amplitude of the rf field is 50 — 70 oe.

The discharge is produced in a quartz vacuum chamber. When a glass chamber was used it deteriorated gradually under the effect of the discharge. The vacuum chamber is evacuated to an initial pressure of 10^{-7} mm Hg while heated to 450 — 500° C.

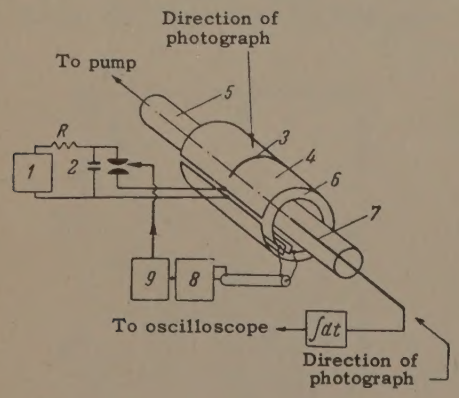

FIG. 1. Schematic diagram of the apparatus; 1) 50-kv charging supply, 2) capacitor bank (C = 50 μf, U_{max} = 50 kv), 3) slit in turn, for photography, 4) main magnetic field coil, 5) quartz vacuum chamber, 6) coil for rf ionization generator, 7) magnetic probe, 8) ionization rf generator (f = 50 Mc/sec, P = 200 kw), 9) trigger unit.

*1 cm = 10^{-9} henry.

Most of the experiments were carried out in air in the pressure range $10^{-1} - 10^{-2}$ mm Hg; some experiments were also performed with hydrogen, argon, xenon, and helium in the pressure range $10^{-1} - 10^{-3}$ mm Hg.

The investigation of discharge behavior was carried out by means of a high-speed camera (SFR-2M) and a magnetic probe, which was located at the axis of the vacuum chamber. The discharge was photographed laterally through vertical slits in the main coil and in the radio-frequency coil and was also photographed axially from the end of the system. Framing operation and the streak mode were both used.

In Fig. 2 we show lateral photographs of discharges in hydrogen, air, and argon. In the pictures in Figs. 2b and 2c it is evident that the emission intensity of the discharge is small in the first half-cycle as compared with the subsequent half-cycles.

Figure 2b was obtained with rather strong preionization; no preionization was used in Figs. 2a and 2c. Similar pictures were obtained through the end face.

In Fig. 3 we show photographs obtained by frame photography of a preionized discharge in air. Radial oscillations of the plasma tube are noticeable in each half-cycle of the magnetic field; the strength of these oscillations increases markedly from the first half-cycle to subsequent half-cycles. This feature is illustrated in Figs. 3a and 3b and in Fig. 4, which are end photographs of discharges in air with strong preionization. In the end photograph obtained with frame operation (Fig. 3) it is evident that the emission from the gas is distributed in the form of a circular layer in the first half-cycle; it can be assumed that the

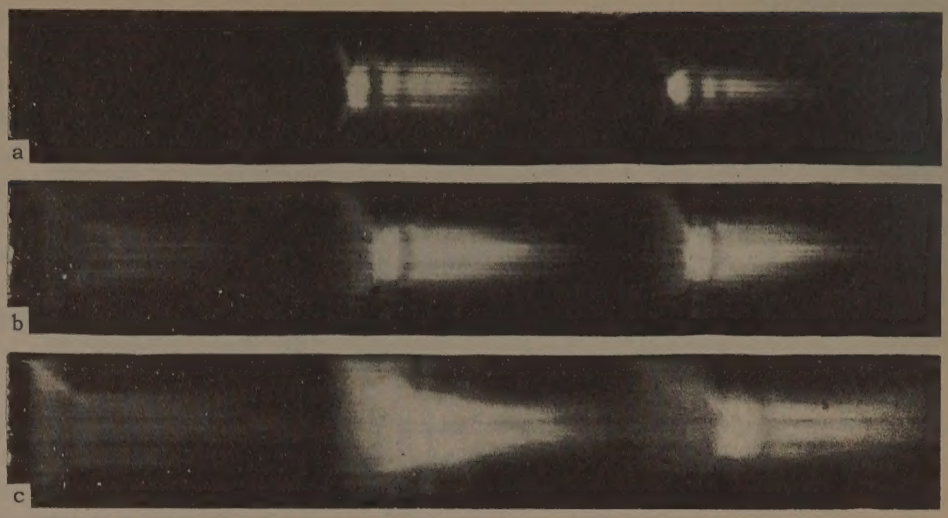

FIG. 2. Lateral photographs of the discharge obtained with a streak camera (peak field H_{max} = 25,000 oe, half-cycle 8 μsec); a) hydrogen, p = 1.3 $\times 10^{-1}$ mm Hg; b) air, p = 8 $\times 10^{-2}$ mm Hg, c) argon, p = 7.8 $\times 10^{-2}$ mm Hg.

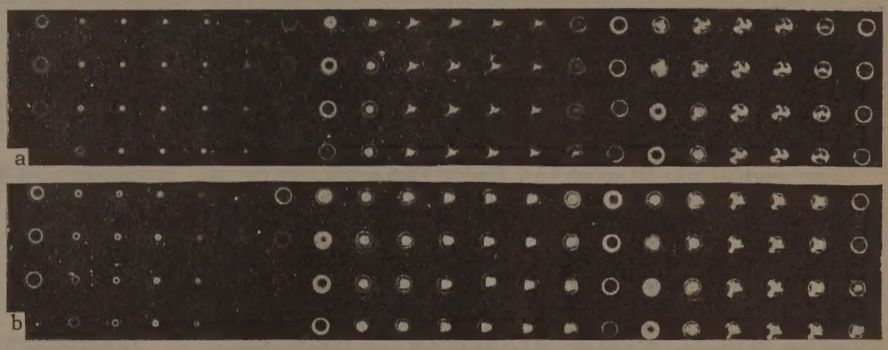

FIG. 3. Axial photographs of discharges in air taken with a framing camera (H_{max} = 25,000 oe, with preionization): a) p = 4 $\times 10^{-2}$ mm Hg, b) p = 8 $\times 10^{-2}$ mm Hg. The time interval between frames is 0.3 μsec.

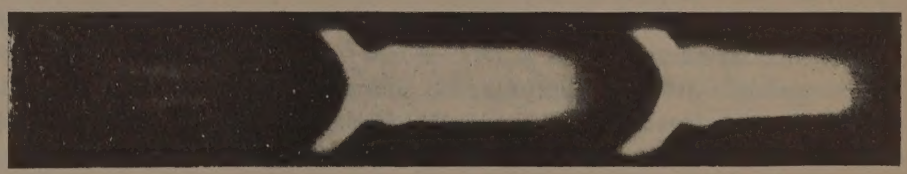

FIG. 4. Axial photographs of discharges in air taken with a streak camera (preionization. p = 8 $\times 10^{-2}$ mm Hg.)

radial oscillations are oscillations of the cold plasma located inside this circular layer. The fields outside the circular tube and outside the plasma are in the same direction.

A similar treatment of the effect is given in a paper by Niblett,[2] in which the oscillation period is described by the following formula:

$$\tau = 2\pi \sqrt{NM_i}/H,$$

where N is the total number of ions over the cross section of the pinch and M_i is the ion mass.

Great interest attaches to the behavior of the plasma during the second, third, and subsequent half-cycles of the magnetic field, because in these cases the density distribution (as is evident from the frame photographs) is approximately uniform.

Magnetic-probe measurements show that in the second half-cycle (preionization) or in the third half-cycle (no preionization, Fig. 5) the magnetic field trapped in the plasma is in the opposite direction to the field outside the plasma. As a result, mixing of these fields at the periphery of the plasma column leads to the formation of a circular plasma layer in which there is no magnetic field. Field growth inside the plasma is inhibited in this stage.

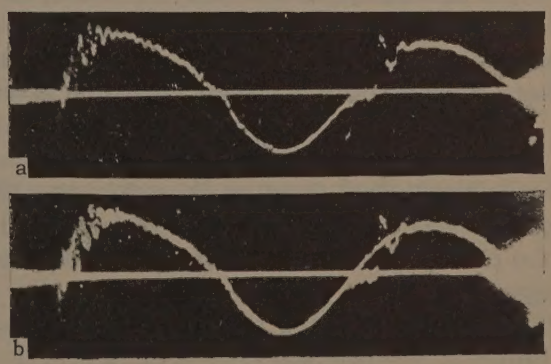

FIG. 5. Oscillogram of the magnetic field at the axis of the discharge chamber (H_{max} = 25 koe, T/2 = 8.5 μsec, p = 8 $\times 10^{-2}$ mm Hg): a) with plasma, b) combined oscillograms of the magnetic field outside the plasma and in the center of the plasma column. No preionization.

After this stage there is a sharp discontinuity in magnetic field at the axis of the plasma column (up to values exceeding the field outside the plasma by 1.5 — 2 times). Oscillations of the magnetic field are observed (with decreasing amplitude) inside the plasma both in the growth suppression stage and immediately after the break; the field oscillates about a variable value close to that of the field outside the plasma. To an accuracy of 20 — 30% the period of these oscillations coincides with that obtained by photography.

The initial compression can be attributed to the formation of a relatively weak shock wave. The velocity of the shock wave $v = 2.3 \times 10^6$ cm/sec and the width of the front is approximately 0.7 cm for a discharge in air ($p = 8 \times 10^{-2}$ mm Hg). The discontinuity in magnetic field at the axis can be explained by the collision of strong shock waves coming together from two sides of the circular plasma layer in which there is no magnetic field.

The radial oscillations of the visible boundary of the plasma column and the oscillations in the intensity of magnetic field would appear to indicate that we are observing magnetoacoustic oscillations of a plasma cylinder. It is somewhat difficult to give an exact description of the boundary conditions for the present experiment since the plasma is surrounded by a copper shield with a longitudinal break.

Foregoing a detailed analysis, we consider two limiting cases. If it is assumed that the shield does not prevent free radiation of the electromagnetic waves at infinity the boundary condition is that of a cylinder executing axially symmetric oscillations in an infinite space.[4] In the absence of surface currents this boundary condition gives

$$J_0(kR)\,H_1^{(2)}(k_0R) = J_1(kR)\,H_0^{(2)}(k_0R)\,/\,n_\perp,$$

where J is the Bessel function, k and k_0 are the wave numbers in the plasma and in vacuum, and $n_\perp$ is the plasma refractive index transverse to the magnetic field. In the present case $n_\perp \gg 1$ so that the boundary condition reduces approximately to $J_0(kR) \approx 0$, whence $\mu \equiv kR = 2.4, 5.5, \ldots$.

The opposite limiting case corresponds to the assumption that the plasma oscillates as though it were completely surrounded by a copper shield.[5] In this case the lowest natural frequency corresponds to the asymmetric oscillation characterized by m = 1; in this case the boundary condition is of the form $J_1(kR) = 0$, whence $\mu = 1.84, 5.3, \ldots$. This condition applies for the magnetoacoustic region, i.e., the frequency should be appreciably lower than the ion cyclotron frequency, as is observed in the present case. For comparison with the experiment we can use the results obtained by Frank-Kamenetskii[5,6] and write the natural frequencies of the magnetoacoustic oscillations in the form

$$f = \frac{\mu_{nm} H_0}{2\pi R \sqrt{4\pi\rho^*}}, \qquad \rho^* = Mn_i \Big/ \left(1 - \frac{n_0}{n_0 + n_i}\,\frac{\tilde{\nu}^2}{\tilde{\nu}^2 + \omega^2}\right),$$

where ρ^* is the effective density, μ_{nm} is the n-th root of the m-th Bessel function, M is the ion mass, n_i is the ion density, and n_0 is the neutral particle density

$$\tilde{\nu}^2 = \nu_{ni}\,(n_0 + n_i)/n_i = \nu_{in}\,(n_0 + n_i)/n_0.$$

Inasmuch as the condition $\tilde{\nu}^2 \gg \omega^2$ applies in the present case, the neutral particles are effectively carried along and $\rho^* = M(n_0 + n_i)$. Thus,

$$f = \mu_{nm} H_0 / 2\pi R \sqrt{4\pi M\,(n_0 + n_i)}.$$

Substitution in this expression of the experimental values for three different gases allows us to form the table below.

The following conclusions can be drawn from this work:

1) The dependence of the natural oscillation frequencies on gas mass is in good agreement with theory;

2) The agreement between the absolute values of the computed and observed frequencies is somewhat worse because we have not taken account of a number of factors such as plasma temperature, nonlinearities, multiply charged heavy-gas ions, etc.

The largest contribution is probably due to the nonlinearity of the oscillations, since the magnetic-probe oscillograms show that the amplitude of the radial oscillations is generally not small (cf. Fig. 5). Poorer agreement is found for argon, where only the first oscillation can be seen clearly, that is to say, the oscillation is almost a weak shock wave.

In control experiments with xenon at high pres-

Gas	p, 10^{-2} mm Hg	$10^{-17} A(n_e + n_i)$	$10^{-4} H_0$, oe	Frequency f, Mc/sec			f_{calc}/f_{exptl}	
				exptl.		calc.		
				μ=1.84	μ=2.4		μ=1,84	μ=2.4
H_2	13.4	1	1	2.1	2.7	1.6	1.3	1.6
N_2	8.0	8	1.7	1.3	1.6	1	1.3	1.6
Ar	7.8	11	2	1.3	1.6	0.8	1.6	2.0

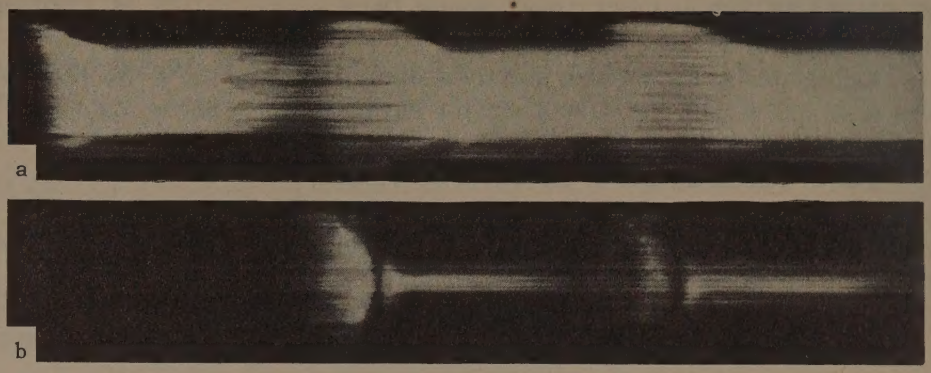

FIG. 6. Lateral photographs of discharges in xenon taken with a streak camera: a) $p = 1.5 \times 10^{-1}$ mm Hg. b) $p = 1.5 \times 10^{-2}$ mm Hg. No preionization.

sures (Fig. 6a) it is impossible to observe a strong plasma compression since the quantity $M(n_i + n_0)$ becomes appreciable and the characteristic times become comparable with the period of the main magnetic field. In addition, the stronger dissipation in these gases leads to weaker trapping of the magnetic field.

The experiments on the heavy gases at low pressures are of interest in themselves. Thus, the oscillogram (Fig. 6b) shows the effect of compression and formation of a shock wave at $p = 1.5 \times 10^{-2}$ mm Hg. Under these conditions the frequency of collisions may be comparable with the natural frequency of the plasma column and this should lead to incomplete entrainment of the neutral particles and strong attenuation due to charge exchange. These effects would explain the inability to excite oscillations under these conditions.

The experimental data given above also give qualitative information concerning the stability of the plasma under conditions of rapid radial compression.

As first noted by Kvartskhava,[7] end-view pictures disclose a clearly defined discharge instability which manifests itself in irregular expulsion of plasma "tongues" in approximately the radial direction. This result is completely verified in the present work. This form of instability is characteristic of a discharge in a long cylinder in which the radial distribution of magnetic field is approximately uniform.*

Analyzing the end-view frame photographs we note that the instabilities arise in the second, third, and subsequent half-cycles of magnetic field. The first half-cycle, which is characterized by slow compression and low temperature is, on the other hand, completely stable.

*A special case of an induction compression of plasma has been considered by Osovets and his co-workers;[8-10] in this case the discharge was produced in a chamber with small ratio of length to diameter, in which a specially chosen stable magnetic field configuration was produced.

Since the instability appears in photographs taken along the axis of the discharge (cf. Fig. 3) but is not seen in the lateral photographs, it may be assumed that the expelled plasma tongues extend along the lines of force of the magnetic field. The formation of plasma tongues starts at the time of maximum plasma compression. It may be assumed that this effect is associated with accelerated plasma motions, so that we are observing some kind of inertia instability.

CONCLUSIONS

Rapid transverse compression of a plasma leads to the excitation of free time-damped magnetoacoustic oscillations of the plasma column. Effects associated with the expulsion of plasma tongues are observed at maximum compression of the circular plasma layer; these tongues extend along the field lines and are evidently due to some form of inertia instability.

The excitation of oscillations can be regarded as the result of rapid compression, by shock waves, of a circular layer of plasma in which there is no field; this layer is formed as a result of mixing of the fields inside and outside the plasma, which are in opposite directions.

The authors wish to thank E. K. Zavoĭskii for his continued interest in this work and L. I. Rudakov for many valuable discussions.

[1] G. B. F. Niblett and T. S. Green, Proc. Phys. Soc. (London) **74**, 732 (1959); **74**, 743 (1959).

[2] G. B. F. Niblett, Proc. Inst. Elec. Eng. (London) **A106**, 152 (1959).

[3] Zolototrubov, Ryzhov, Skoblik, and Tolok, J. Tech. Phys. (U.S.S.R.) **30**, 769 (1960), Soviet Phys.-Tech. Phys. **5**, 722 (1961).

[4] K. Körper, Z. Naturforsch. **15a**, 220 (1960).

[5] D. A. Frank-Kamenetskii, JETP **39**, 669 (1960), Soviet Phys. JETP **12**, 469 (1961).

[6] D. A. Frank-Kamenetskii, J. Tech. Phys.

(U.S.S.R.) **30**, 893 and 899 (1960), Soviet Phys.-Tech. Phys. **5**, 842 and 847 (1961).

[7] Kvartskhava, Kervalidze and Gvaladze, J. Tech. Phys. (U.S.S.R.) **30**, 297 (1960), Soviet Phys.-Tech. Phys. **5**, 274 (1960).

[8] Yu. F. Nasedkin and S. M. Osovets, Fizika plazmy i problema upravlyaemykh termoyadernykh reaktsii (Plasma Physics and the Problem of Controlled Thermonuclear Reactions) AN SSSR Press, 1958, Vol. 3, p. 182.

[9] S. M. Osovets and N. I. Shchedrin, ibid. Vol. 3, p. 196.

[10] S. M. Osovets, Yu. F. Petrov, and N. I. Shchedrin, ibid. Vol. 3, p. 242.

Translated by H. Lashinsky
64

A SEARCH FOR BREMSSTRAHLUNG PRODUCED IN ELASTIC SCATTERING OF NEGATIVE PIONS BY PROTONS

P. F. ERMOLOV and V. I. MOSKALEV

Joint Institute for Nuclear Research

Submitted to JETP editor February 7, 1961

J. Exptl. Theoret. Phys. (U.S.S.R.) 41, 322-326 (August, 1961)

In 1500 cases of elastic scattering of 128- and 162-Mev π^- mesons in a hydrogen-filled cloud chamber, no cases were found in which the angle of emission of the recoil proton exceeded the angle calculated from the conservation laws by more than 3°. On this basis, it was found that the upper limit for the bremsstrahlung cross section for π^- mesons scattered by nuclei is 5×10^{-29} cm^2.

1. INTRODUCTION

THE emission of bremsstrahlung by π mesons in a nuclear force field has been considered from the theoretical viewpoint.[1-5] In particular, Solov'ev[2] used perturbation theory to calculate the angular and energy distributions of the γ quanta and the total cross section for the process $\pi^- + p \to \pi^- + p + \gamma$ for a π^--meson kinetic energy close to the π-meson rest mass. The theory has been further developed by Low,[3] who showed that one can calculate in general form not only the first term of the expansion of the differential cross section in powers of the γ-quantum energy (as was done by Solov'ev[2]), but also the second term, which contains derivatives of the nonradiative scattering amplitude with respect to the energies and angles. This theory was used by Cutkosky[4,5] to calculate, in the fixed-nucleon approximation model, the basic characteristics of bremsstrahlung emission by π^+ mesons of energy close to 200 Mev scattered by protons. In particular, it was shown[5] that the high-energy γ-quantum intensity is smaller than that determined from perturbation theory.[2]

The emission of bremsstrahlung by π^+ mesons has been studied experimentally in the 80 — 300 Mev range in a freon bubble chamber.[6] On the basis of 25 observed cases of bremsstrahlung emission, the cross section for the process was found to be about 7×10^{-27} cm^2 in the case of the fluorine nucleus, which is in satisfactory agreement with the theoretical estimates. We recently learned of the results obtained by Deahl et al,[7] who studied elastic scattering of 225-Mev π^- mesons by protons (1570 cases) in a liquid-hydrogen bubble chamber. They observed five cases of bremsstrahlung of energy $E_{\gamma\,lab} > 50$ Mev, which corresponds to a cross section of 5×10^{-29} cm^2.

In the present experiment we have attempted to estimate the bremsstrahlung cross section in elastic scattering of 128- and 162-Mev π^- mesons by protons in a hydrogen-filled cloud chamber.

2. METHOD AND RESULTS

In a previous experiment,[8] we studied the elastic scattering of π^- mesons by protons in a cloud chamber operating at a hydrogen pressure of 23 atm in a magnetic field of 9000 oe. In 90 000 stereophotographs we found 385 and 1136 cases of elastic scattering for pion kinetic energies E_0 of 128 ± 8 and 162 ± 10 Mev, respectively. Since most of the γ quanta from the process $\pi^- + p \to \pi^- + p + \gamma$ should be of low energy, it was not possible to separate the cases of radiative scattering by means of measurements in which the scattered π^--meson and recoil-proton momenta are determined from the radii of curvature or by measurements of the noncoplanarity angle, since the accuracy of measurement of these quantities is of the same order as the expected variation. (If, however, the proton momentum is determined from the range, then the accuracy of the momentum measurement is 2.5% when the range measurement error is 10%.)

Hence, to search for cases of bremsstrahlung, we employed measurements of the quantity

$$\Delta\theta = \theta_p^{obs} - \theta_p^{calc}(\theta_\pi^{obs}), \qquad (1)$$

i.e., the difference between the measured recoil-proton angle θ_p^{obs} and the proton angle $\theta_p^{calc}(\theta_\pi^{obs})$ corresponding to the kinematical conditions for

elastic scattering of a π meson by the measured angle θ_π^{obs}. From the total number of cases of scattering at the two energies, we selected cases satisfying certain criteria based on the following: a) the angle between the scattering plane and the horizontal should be less than 60°; b) the length of the projection of each of the three tracks on the horizontal plane should be greater than 2 cm; in those cases in which the proton range could be determined, the length of the range should be at least 5 mm; c) the incident π^- meson should not be deflected from the basic beam direction by more than 5°.

A total of 844 cases satisfied the selection criteria. For these cases, we measured simultaneously the angles θ_p and θ_π on a reprojector; the measurements were always made in the azimuthal plane which simultaneously coincided best with the projections of the scattered π-meson and proton tracks on the reprojector screen. The histogram of Fig. 1 represents the distribution of all measured cases of elastic scattering as a function of the quantity $\Delta\theta$. The smooth curve represents the normal distribution $A \exp[-(\Delta\theta)^2/2\delta^2]$ with a standard deviation of $\delta = 0.7°$. As seen from Fig. 1, no cases of elastic scattering were observed with $\Delta\theta > 3°$.

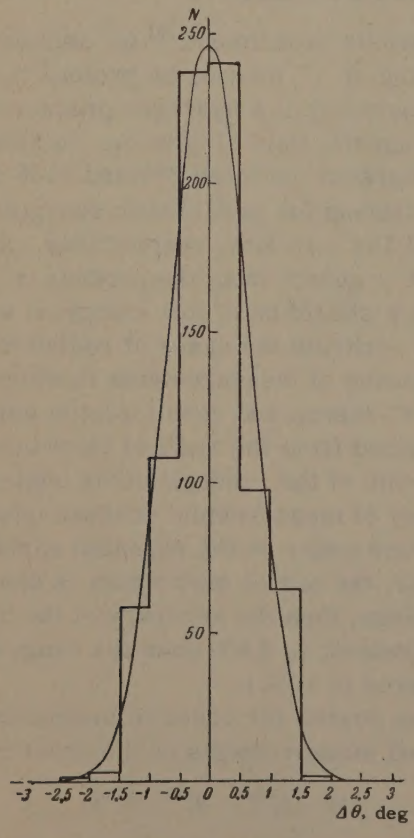

FIG. 1. Experimental distribution of cases of elastic scattering as a function of the quantity $\Delta\theta$ in the laboratory system. The smooth curve represents the normal distribution with a standard deviation of 0.7°.

Figure 2 represents the c.m.s. momentum distribution of the protons for cases in which this momentum could be determined from the measured range of the proton (the total number of cases at the two energies was 112). The numbers beside the arrows indicate the proton momentum for elastic π^-p scattering at the given meson energy. These distributions also indicate the absence of bremsstrahlung, since no cases with smaller momentum were found, within the limits of error of the measurements. (For example, for $E_\gamma = 20$ Mev, the c.m.s. proton momentum for the process $\pi^- + p \to \pi^- + p + \gamma$ should have values from 201 to 170 Mev/c for $E_0 = 162$ and from 176 to 143 Mev/c for $E_0 = 128$ Mev).

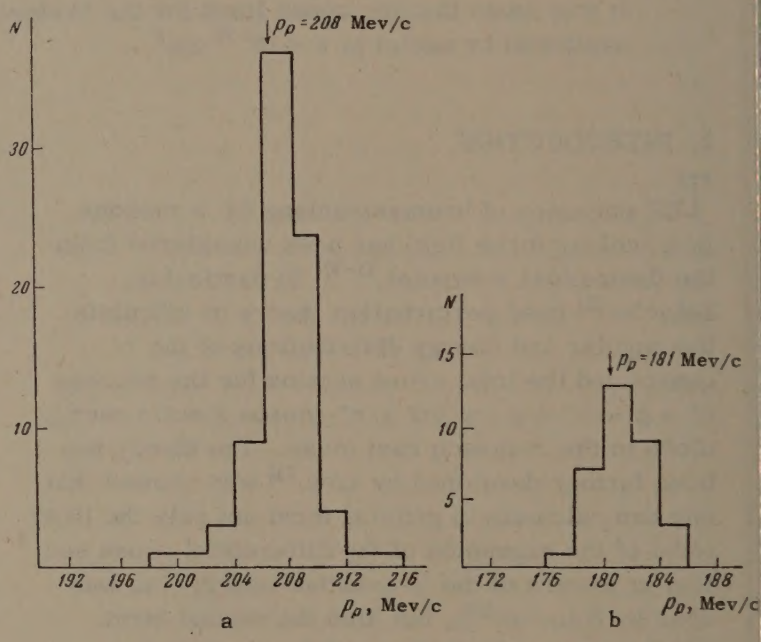

FIG. 2. Recoil proton c.m.s. momentum distribution determined from the ranges: a – $E_0 = 162$ Mev; b – $E_0 = 128$ Mev.

The main process which can resemble bremsstrahlung production in our experiment is quasi-elastic π^-p scattering by complex nuclei of impurities (methyl alcohol). Analysis of the stars produced on complex nuclei indicated that none could have been attributed to the process under investigation.

3. ESTIMATE OF THE UPPER LIMIT OF THE CROSS SECTION FOR THE PROCESS $\pi^- + p \to \pi^- + p + \gamma$

The bremsstrahlung cross section was calculated in the form

$$\sigma_\gamma < \sigma_{el}\, C/NK, \qquad (2)$$

where σ_{el} is the elastic scattering cross section for 154-Mev π^- mesons and was taken as the weighted mean for the number of cases at each energy; N is the total number of cases of elastic

scattering; C is a correction to the number N which takes into account the contribution from Coulomb scattering and interference between Coulomb and nuclear scattering; K is the relative number of cases of scattering with radiation for the entire spectrum of γ quanta with $\Delta\theta > 3°$. The quantity K is determined from the expression

$$K = \frac{\int_{E_\gamma = 10\ \text{Mev}}^{E_{\gamma\,max}} \omega(E_\gamma)\, a(E_\gamma)\, dE_\gamma}{\int_{E_\gamma = 10\ \text{Mev}}^{E_{\gamma\,max}} \omega(E_\gamma)\, dE_\gamma}, \qquad (3)$$

where $\omega(E_\gamma)$ is the theoretical c.m.s. energy spectrum of the γ quanta, which was taken from [5]; the function $a(E_\gamma)$ expresses the probability of bremsstrahlung production with a change in angle $\Delta\theta > 3°$ as a function of the γ-quantum energy. For simplicity, this function was first calculated without taking into account the angular correlation between the direction of scattering of the π meson and the γ quantum; the angular distribution of the scattered π mesons was taken in the same form as that obtained in [8]. The lower limit of integration over E_γ in formula (3) was chosen as 10 Mev, since the probability of recording γ quanta with $E_\gamma < 10$ Mev was small under our conditions.

In Figure 3, curve 1 represents the energy spectrum $\omega(E_\gamma)$ and curve 2 represents the product $\omega(E_\gamma)\,a(E_\gamma)$, i.e., the effective energy spectrum. Graphical integration of these curves gave the value $K = 0.6$. A correction taking into account the angular correlation between the π meson and γ quantum, given by Eq. (1) in Solov'ev's article, [2] was then applied to this value of K. The calculation showed that the average value of this correction over the entire γ-quantum spectrum is about 20%. We finally obtained for K the value 0.5. The upper limit of the total cross section for the production of bremsstrahlung with $E_\gamma > 10$ Mev, calculated from formula (2), is 5×10^{-29} cm^2.

The obtained value can be compared with the total cross section calculated from the perturbation theory formula [2]

$$\sigma_\gamma = \frac{\alpha}{\pi} \ln \frac{E_0}{E_{\gamma\,min}} \left(\frac{1}{\beta_0} \ln \frac{1+\beta_0}{1-\beta_0} + \frac{1}{\beta'} \ln \frac{1+\beta'}{1-\beta'} - 4 \right) \sigma_{el}, \qquad (4)$$

where $E_{\gamma\,min} = 10$ Mev; β_0 and β' are the mean velocities of the π^- mesons before and after scattering. For a meson energy of 154 Mev, the cross section σ_γ found from formula (4) is 2.3×10^{-28} cm^2. However, integration of the energy spectrum obtained by Cutkosky [5] for bremsstrahlung production by π^+ mesons gives for the ratio $\sigma_\gamma/\sigma_{el}$ a value approximately 1/1.5 — 1/1.8 as great as

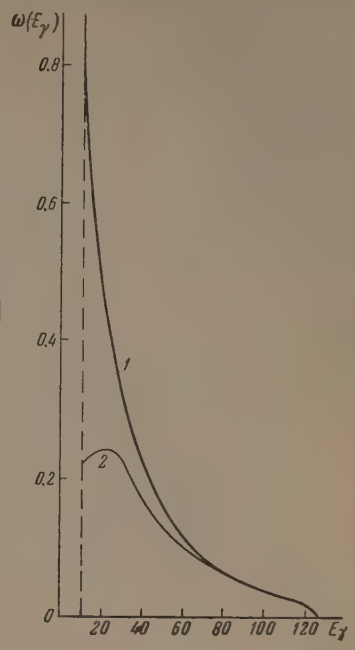

FIG. 3. 1 — C.m.s. energy spectrum of γ quanta $\omega(E_\gamma)$;[5] 2 — effective energy spectrum $\omega(E_\gamma)\,a(E_\gamma)$.

that calculated from (4). (The ratio $\sigma_\gamma/\sigma_{el}$ for π^- mesons should not differ essentially from this ratio for π^+ mesons.) Hence, the upper limit 5×10^{-29} cm^2 obtained by us for the bremsstrahlung cross section is evidently not in sharp contradiction to the theoretical estimates. Comparison of this result with the cross section obtained by Deahl et al. [7] is difficult because of the lack of detailed information on that experiment, but estimates made with allowance for the difference in π-meson energies, different cut-off energies in the γ-quantum spectrum, and the experimental errors indicate that these results are not in contradiction with one another.

The authors express their gratitude to V. P. Dzhelepov and S. M. Bilen'kii for discussion of this work and to Yu. A. Budagov for aid in carrying out the experiment.

[1] L. D. Landau and I. Ya. Pomeranchuk, JETP **24**, 505 (1953).

[2] V. G. Solov'ev, JETP **29**, 242 (1955), Soviet Phys. JETP **2**, 159 (1956).

[3] F. Low, Phys. Rev. **110**, 974 (1958).

[4] R. E. Cutkosky, Phys. Rev. **109**, 209 (1958).

[5] R. E. Cutkosky, Phys. Rev. **113**, 727 (1959).

[6] Lomanov, Meshkovskii, Shalamov, Shebanov, and Grashin, JETP **35**, 887 (1958), Soviet Phys. JETP **8**, 615 (1959).

[7] Deahl, Derrick, Fetkovich, Fields, and Yodh, Proc. 1960 Annual Intern. Conf. on High Energy Physics at Rochester, Univ. of Rochester, 1960.

[8] Budagov, Viktor, Dzhelepov, Ermolov, and Moskalev, JETP **38**, 734 (1960), Soviet Phys. JETP **11**, 531 (1960).

Translated by E. Marquit
65

SOME FEATURES OF MULTIPLE FRAGMENT PRODUCTION BY 9-Bev PROTONS

P. A. GORICHEV, O. V. LOZHKIN, N. A. PERFILOV, and Yu. P. YAKOVLEV

Radium Institute, Academy of Sciences, U.S.S.R.

Submitted to JETP editor February 21, 1961

J. Exptl. Theoret. Phys. (U.S.S.R.) **41**, 327-333 (August, 1961)

The disintegration of Ag and Br nuclei induced by 9-Bev protons and accompanied by the emission of two or more multicharged particles ($Z = 3 - 9$) is investigated. Various characteristics of the multiple emission of fragments, such as the probability of disintegration with the emission of N_f fragments, the charge and energy distributions of the fragments, and their angular correlations, are analyzed. It is concluded that multiply produced fragments are emitted independently.

1. INTRODUCTION

AN interesting phenomenon connected with the production of fragments with $Z \geq 3$ in the disintegration of complex nuclei by fast particles is the emission of two or more fragments in one disintegration. This multiple fragment production becomes rather conspicuous at proton energies greater than 1 Bev. If, for 660-Mev protons, the cross section for disintegration with a production of two or more fragments with $Z \geq 4$ amounts to ~ 0.5 mb[1] (roughly 4% of the total cross section for fragment production), then, for 9-Bev protons, this cross section is equal to ~ 16 mb[2] (this amounts to $\sim 16\%$ of the total fragment-production cross section). In the $1 - 3$ Bev energy range, one should expect that the multiple production constitutes a still greater fraction of the total fragment production cross section, judging from the available preliminary data.[3,4]

In addition to the above, rather scanty, information on the energy dependence of the fragment production multiplicity, very little is known about other features of this phenomenon. Thus, it was mentioned by Perkins[5] that, in disintegrations involving two or more fragments, the fragment with the greater charge has a greater velocity. Lozhkin[6] indicates a strong angular correlation of two fragments in the disintegration, and confirms the tendency mentioned by Perkins.[5]

At the same time, it is absolutely clear that the study of the multiplicity can provide relevant information on the mechanism of the fragmentation process. The question whether some of the fragmentation process characteristics, such as the multiplicity, can be calculated[7] makes it even more necessary to carry out an experimental study of this feature of the fragmentation process. Results of a study of multiple fragment production at 9-Bev proton energy are presented in this article.

The nuclear emulsion method used has great advantages, since it permits us to study many features of the multiplicity at the same time.

In order to determine the fragment charge, the width of the fragment tracks was measured on fine-grain emulsion of the P-9ch type. The measurements were carried out using a special photometer whose optical system enables us, while observing the measured track through a binocular attachment, to scan a certain portion of the track by a narrow slit placed in front of a photomultiplier tube. The pulse from the photomultiplier, representing the transverse profile of a given section of the particle track, was fed to an electronic circuit (Fig. 1). This circuit produced a number of pulses proportional to the half-width of the photomultiplier pulse. The instrument had a dispersion of $\sim 1\%$ for a multiple measurement of one object. The length of the measured track portion could be varied. To exclude the necessity of introducing corrections, only the tracks of particles having an angle of dip less than 12° with the emulsion surface (in the developed emulsion) were selected.

2. EXPERIMENTAL RESULTS

1. Statistics of the disintegrations. From the scanning of nuclear emulsions irradiated by 9-Bev protons, 405 disintegrations with two or more fragments ($N_f \geq 2$) were found. This number of disintegrations corresponds to about 2000 disintegrations involving one fragment. The determination

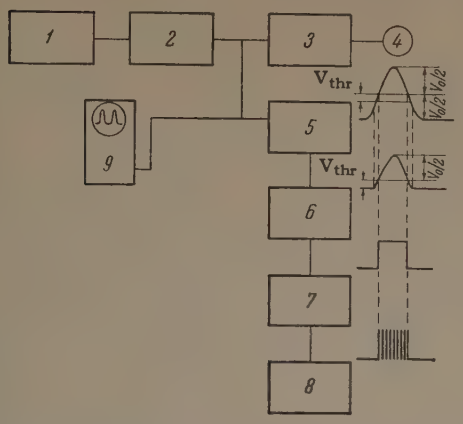

FIG. 1. Block diagram of the apparatus: 1 – photomultiplier with preamplifier, 2 – main amplifier, 3 – memory device, 4 – milliammeter, 5 – limiting circuit, 6 – Schmitt trigger circuit, 7 – blocking generator, 8 – scaler, 9 – oscilloscope. The shape of pulses at various points is indicated at the right-hand side of the figure.

of the fragment charge revealed that the majority of the fragments had charge between 4 and 9. Fragments with charge 3 were almost completely rejected in the selection of the disintegrations because of the small difference between them and the He nuclei. An exception was the isotope $_3Li^8$, which produces a characteristic T-shaped track.

The classification of the found disintegrations involving several fragments is shown in the table.

2. Disintegrations involving two fragments. In order to determine the charge distribution of the fragments in multiple emission and to compare it with the usual charge distribution, 193 tracks were selected from disintegrations with $N_f \geq 2$, and 209 tracks from disintegrations with $N_f = 1$. The distributions of the tracks with respect to the integral width, which was measured on the 38 μ of the residual range, were constructed for both groups. In the distributions, the tracks which did not end in the emulsion were not taken into account. As has been shown by the study of the geometrical conditions of tracks which were suitable for the width measurement, the corrections due to this effect are small, and, what is more important, are the same for both types of selected disintegrations.

Characteristics of the disintegrations	N_f			
	1	2	3	4
Only with fragments with Z = 4–9	~2000	289	35	5
Only with $_3Li^8$ fragments	153	4	1	0
One of fragments $_3Li^8$, the rest with Z = 4–9	–	54	9	2
One of fragments $_5B^8$, the rest with Z = 4–9	14	4	3	2

In view of the small range of the fragments studied, the track distribution with respect to the integral width does not give a sharp differentiation with respect to the fragment charge. Therefore, in order to compare the distributions, we did not pass from the measured track-width distribution to the charge distribution, but analyzed the data obtained directly. To compare the obtained distribution, the χ^2 test was used.

The obtained statistics make it possible to apply the test only in the range of charges Z = 4 – 6 (in this range, the width distribution was divided into 8 intervals). As a result, the probability $P(\chi^2)$ that purely statistical reasons will not make the difference between the distributions smaller than the actually observed value of χ^2, was found to equal 0.8. The value P = 0.8 shows that the compared distributions can be considered as identical.

After having established the above fact, we can, in addition, compare both distributions with respect to the average values of the track width. We can then take into account fragments with Z > 6, which could not be used in comparing the distribution according to the χ^2 test. It has been found that the mean values of the track width in both distributions are fully identical (the difference is less than 2%).

Thus, the results lead to the conclusion that the distribution of the tracks with respect to the width, and consequently the charge distribution of multicharged particles in multiple and single emission events, are identical within the limits of experimental error.

The charge distribution of fragments obtained from the total distribution of the track width of 402 fragments [in disintegrations with $N_f = 1$ and $N_f \geq 2$, after calibrating the latter using particles with Z = 3 ($_3Li^8$) and with Z = 5 ($_5B^8$)] is shown in Fig. 2. The relative frequency of charge pairs Z_n, Z_m in single disintegrations as a function of the sum $Z_n + Z_m$, and the frequency of observation of two fragments with different charges as a function of the fragment charge, are also shown in the figure, based on the study of 36 disintegrations in which the charges of both fragments could be measured.

The distribution of space angles between the two fragments shown in Fig. 3 was obtained from the angle measurements in 303 disintegrations. A marked angular correlation of the fragments in this disintegration is visible: the fragments are emitted predominantly at angles > 120° to each other. No variation of the mean angle between the

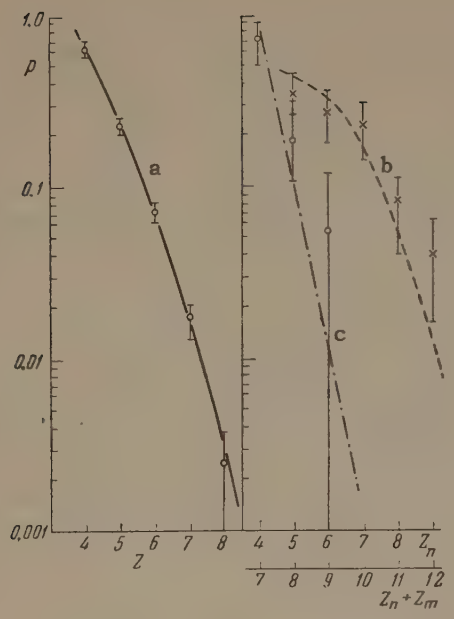

FIG. 2. a – charge distribution of fragments in the disintegration of Ag and Br nuclei; b – probability of the emission per disintegration of fragments with charge Z_n and Z_m as a function of the sum $Z_n + Z_m$: the points represent experimental values, and the curve is calculated; c – probability of emission of two fragments with different charge Z_n as a function of Z_n: points – experimental values, curve – calculated.

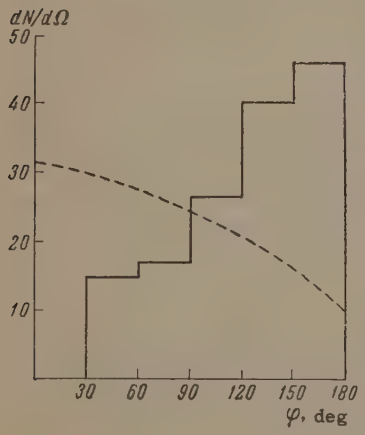

FIG. 3. Distribution of spatial angles between fragments. Histogram – experimental values, curve – calculation for the case of independent fragment emission.

fragments from the sum of their charges has been established; for a variation of the fragment charges from 6 to 10, the mean angle between the fragments remains about 110°.

The energy spectra of fragments in disintegrations with $N_f = 2$ for Z equal to 4, 5, and 6 are shown in Fig. 4. In the same figure, the distribution of the ratio of the energy per nucleon in heavy and light fragments emitted in the same disintegration is also shown. The energy spectra of the fragments are similar to those observed in disintegrations involving one fragment[2] and the most probable ratio of the energy per nucleon in heavy and light fragments is close to unity.

3. Disintegrations involving three fragments. Because of the small statistics of disintegrations

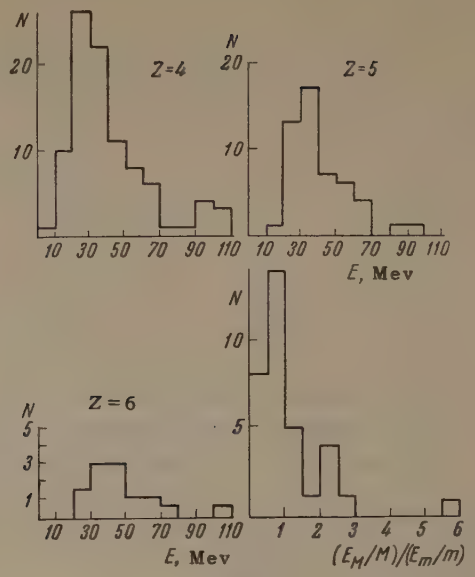

FIG. 4. Energy spectra of fragments in disintegrations with two fragments for Z = 4–6, and the ratios of energy per nucleon in heavy and light fragments $(E_M/M)/(E_m/m)$.

involving three fragments (44 cases), it was impossible to carry out a sufficiently complete study of the characteristics of such disintegrations. The most reliable information is obtained for the angular distribution of the fragments in these disintegrations. The distribution of the projected angles between adjacent fragments in disintegrations with three fragments is shown in Fig. 5, which clearly shows the predominance of large angles between fragments.

The measurement of the fragment charges in the disintegrations gave the following charge distribution of fragments for $Z \geq 4$; the number of fragments corresponding to charge 4, 5, 6, and 7 is equal to 18, 9, 2, and 1 respectively. The comparison of these numbers with the total charge dis-

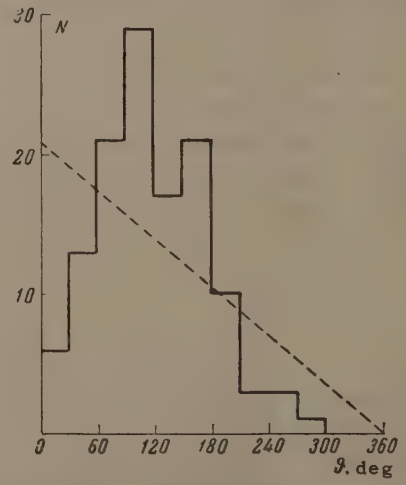

FIG. 5. Distribution of projected angles (ϑ) between fragments in disintegrations involving three fragments. Histogram – experimental results, dotted line – calculation carried out assuming independent fragment emission.

tribution for disintegrations with $N_f = 1$ and $N_f = 2$ (Fig. 2) shows that they agree, within the limits of statistical error.

3. ANALYSIS OF EXPERIMENTAL RESULTS AND CONCLUSIONS

The experimental results presented above were analyzed assuming independent fragment production in disintegrations involving several fragments. This problem can be considered independently of the actual mechanism of the fragment production. The idea of independent fragment production already follows from the study of the charge distribution of the fragments in disintegrations with different numbers of fragments. Identical charge distributions in disintegrations with one and two fragments will be obtained if the probability p_{nm} of observing a pair of charges Z_n and Z_m is equal to the product of the probabilities for the production of each charge: $p_{nm} = p_n p_m$. Thus, if

$$\sum_n p_n = 1, \qquad \sum_m p_m = 1,$$

then the probability of observing fragments with a charge Z_n in disintegrations involving two fragments will be given by

$$P_n = \sum_m p_{mn} = p_n \sum_m p_m = p_n,$$

i.e., is found to equal the probability of observing a charge Z_n in a disintegration with one fragment.

Figure 2 shows the calculated probabilities p_{nn} as a function of the sum of charges $Z_n + Z_m$, and the probability of observing identical charges P_{nm} as a function of charge Z_n. It can be seen that the experimental functions p_{nm} and p_{nn} are close to the theoretical ones.

The relative probabilities of observing a different number of fragments in a single disintegration, assuming their independent production, will follow, to a first approximation, a geometrical series with the common ratio determined by the probability of the production of one fragment in a disintegration. If we denote the probability of emission of $_3Li^8$ in a disintegration by p_1, and the probability of emission of fragments with $Z \geq 4$ by p_2, we can expect the following relation between the numbers of disintegrations with different numbers of fragments:

$$N(2_{fr})/N(1_{fr}) = N(3_{fr})/N(2_{fr}) = N(4_{fr})/N(3_{fr}) = p_2 \quad (1)$$

$$N(2Li_3^8)/N(1Li_3^8) = N(3Li_3^8)/N(2Li_3^8) = p_1, \quad (2)$$

$$N(1_{fr} + Li_3^8)/N(1_{fr}) = N(2_{fr} + Li_3^8)/N(2_{fr}) = N(3_{fr} + Li_3^8)/N(3_{fr}) = p_1, \quad (3)$$

$$N(2_{fr} + Li_3^8)/N(1_{fr} + Li_3^8) = N(3_{fr} + Li_3^8)/N(2_{fr} + Li_3^8) = p_2. \quad (4)$$

The probabilities p_1 and p_2 are calculated as a ratio of corresponding cross sections to the total cross section for the inelastic interaction of 9-Bev protons with Ag and Br nuclei.

We shall analyze the number of disintegrations with a different number of fragments, substituting the data from the table into Eqs. (1) to (4).

For row (1), we have the experimental values 0.14, 0.12, and 0.06. Within the limits of statistical error of the experiment these coincide with the value of $p_2 = 0.09$. Because of the small statistics available, this value cannot be considered as contradicting the values 0.17 and 0.22 of row (4).

For row (2), the values are 0.026 and 0.25, while for row (3) we have 0.030, 0.032, and 0.057, which are somewhat greater than the value $p_1 = 0.01$ but are in good agreement with each other with the exception of the ratio $N(3\,_3Li^8)/N(2\,_3Li^8)$, but this ratio is statistically inaccurate.

Thus, the study of separate probabilities of observation of different numbers of fragments in each disintegration also does not contradict the assumption of the independent emission of fragments in disintegrations involving several fragments.

The energy spectra of fragments in disintegrations involving two fragments, and the ratio of the energy per nucleon in light and heavy fragments (Fig. 4), also do not contradict the hypothesis of an independent emission of fragments.

At the same time, the angular correlation of fragments in disintegrations involving two and three fragments (Figs. 3 and 5) are very unusual for such a picture of an independent emission. In Fig. 3, the dotted line shows the distribution of spatial angles between the two fragments for an independent emission from the nucleus. This distribution was calculated by the Monte Carlo method, and the angular distribution of fragments was taken from [2]. In contrast to the experimentally observed distribution, the expected distribution falls off monotonously from 0 to 180°, while in the interval 0 to 30° there is not a single event in the experimental distribution.

For distributions with three fragments, the expected distribution of the projected angles between two adjoining fragments can be constructed according to the formula given in [8] (dotted line in Fig. 5). The experimental distribution is substantially different from that expected for an independent fragment emission.

Thus, while the relative emission probabilities of different numbers of fragments and the correlations of their energies and charges are in agreement with the hypothesis of their independent production, the angular correlation of fragments contradicts it. The situation is not changed if we take into account the fact that the fragments emitted from the nucleus may interact with each other through their Coulomb field. Because of the fact that the interaction with the residual nucleus is much stronger than that of the fragments with each other, we cannot expect a shift of the angular distribution between fragments to the region around 180°. The effect of the Coulomb interaction can only deplete the range of small angles between the fragments. In addition, the Coulomb interaction between the fragments should depend substantially on the fragment charge. No dependence of the mean angle of the sum of the fragment charges for the given distribution was observed in the experiment.

However, we cannot at present discard the hypothesis of an independent production of fragments only because of the angular correlation, but, on the contrary, should try to understand it assuming an independent fragment emission. Moreover, in contrast to other features of the independent emission of several fragments, it is necessary to have recourse to models in the study of angular correlation.

There are, in principle, two possible explanations. Since, in the picture in which the fragments are produced in a cascade process in a nucleus (both assuming quasi-elastic collisions of cascade nucleons with groups of nucleons in the nucleus[2,3] or assuming ruptured bonds during the passage in the nucleus[7]), the existence of an angular correlation of produced fragments demands the assumption of a spatial non-uniformity in the distribution of nucleons in the nucleus, it is not very probable for two large nucleon groups to occupy nearby locations in the nucleus. Thus, the emission of fragments will occur from regions of the nucleus far from each other, and the requirement that the emitted fragments have small orbital momenta will lead to large angles of emission between them.

The other possibility of explaining the angular correlation of fragments lies in assuming that the fragments may be produced as a result of a so-called direct nuclear decay, whose characteristics are determined by the statistical distribution of the energy and momentum between the products of disintegration before their emission from the interaction volume. In such a case, the angular correlations of fragments follows from conservation laws.

It is difficult at present to draw final conclusions supporting this or the other model. It is necessary to develop the methods of calculating the processes under question, and further increase the accuracy of the experimental data.

In conclusion, the authors would like to thank the workers of the Joint Institute for Nuclear Research I. V. Chuvilo, V. A. Sviridov, and É. N. Tsyganov for help in irradiating the emulsions, and the workers of the Radium Institute V. F. Darovskikh, N. P. Kocherov, and M. M. Makarov for discussion of the results.

[1] O. V. Lozhkin and N. A. Perfilov, JETP **31**, 913 (1956), Soviet Phys. JETP **4**, 790 (1957).

[2] Perfilov, Ivanova, Lozhkin, Makarov, Ostroumov, Solov'eva, and Shamov, JETP **38**, 345 (1960), Soviet Phys. JETP **11**, 250 (1960).

[3] Lozhkin, Perfilov, Rimskii-Korsakov, and Fremlin, JETP **38**, 1388 (1960), Soviet Phys. JETP **11**, 1001 (1960).

[4] E. Baker and S. Katcoff, Bull. Am. Phys. Soc. **2**, ser. II, 222 (1957).

[5] D. H. Perkins, Proc. Roy. Soc. **203**, 399 (1950).

[6] F. P. Lozhkin, Materialy soveshchaniya po primeneniyu radiokhimicheskikh metodov izucheniya yadernykh reaktsii (Proceedings of the Conference on the Application of the Radio-Chemical Method to the Study of Nuclear Reactions), Dubna, Vol. I, OIYaI, 1958, p. 116.

[7] Denisov, Kosareva, and Cerenkov, Tr. Konf. po mirnomu ispol'zovaniyu atomnoĭ energii (Proceedings of the Conference on Peaceful Uses of Atomic Energy), Tashkent, 1959.

[8] G. Lovera, Nuovo cimento **6**, 233 (1949).

Translated by H. Kasha
66

ENERGY SPECTRUM OF μ MESONS IN EXTENSIVE AIR SHOWERS

T. SÁNDOR, A. SOMOGYI, and F. TELBISZ

Central Physics Research Institute, Hungarian Academy of Sciences, Budapest

Submitted to JETP editor February 21, 1961; resubmitted May 19, 1961

J. Exptl. Theoret. Phys. (U.S.S.R.) **41**, 334-336 (August, 1961)

The power exponent of the energy spectrum of μ mesons in EAS has been determined by comparing the intensity of the penetrating component of EAS at a depth of 40 m water equivalent with that at sea level. The result is $F(>E) \sim E^{-\alpha}$, where $\alpha = 0.46 \pm 0.09$.

OBSERVATIONS of EAS at a depth of 40m water equivalent (below 18 m of earth and 15 cm of lead) were initiated in our laboratory in 1960. A diagram of the arrangement (top view) is shown in Fig. 1a. Each of the areas S, S_1, or S_2 is covered by two layers of counters. A vertical section of the setup is shown in Fig. 1b. The trays S_1 and S_2 constitute part of an array used for other measurements and described in detail in [1].

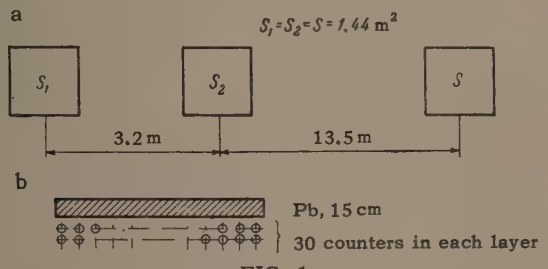

FIG. 1

Sixfold coincidences were recorded. The counting rate was $C_6 = 1.93 \pm 0.05$ hr^{-1}, as determined from the total number of showers recorded (1464). This rate was compared with the rate of EAS measured at the earth's surface under 20 cm of lead[2] in order to find the energy spectrum of μ mesons. The corresponding number of fourfold coincidences $C_4 = 0.29 \pm 0.01$ hr^{-1} refers, however, to the array shown in Fig. 2.

We can compare the rates C_6 and C_4 only after introducing the following corrections:

1. Since the effective areas S of the two arrangements differ, C_4 should be multiplied by $(S/S')^{\gamma_1}$, where γ_1 is the density spectrum exponent for showers detected under 20 cm of lead. According to our measurements carried out with the same apparatus (Fig. 2), $\gamma_1 = 1.89 \pm 0.17$.[2] Thus we have

$$C_4 (S/S')^{\gamma_1} = 5.0 \pm 1.3 \text{ hr}^{-1}.$$

2. Because of the difference in the geometry of the arrangements, we should multiple C_4 by C_3/C_4,

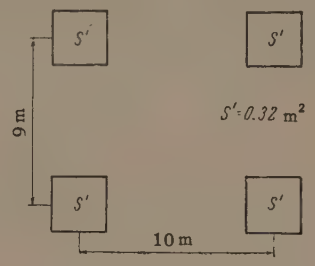

FIG. 2

where C_3 is the rate of triple coincidences at the earth's surface under 20 cm of lead for the array geometry shown in Fig. 1.

Since the difference between the lateral distributions of the electrons and μ mesons over distances of the order of several meters can introduce only a negligible error, we measured, the factor C_3/C_4 without lead (C_3'/C_4'). This applies to a change of the distance between the counters from 10 to 16.8 m. Since a distance of 16.8 m could not be realized in the underground laboratory, the measurements of the coincidence rate C_3' were carried out with the configuration of Fig. 1 at distances of 8.9 m and 13.4 m. From the two results, we determined the power exponent β of the function used for extrapolating the C_3' coincidence rate at 16.8 m. The following results were obtained:

distance between counters, m	8.9	13.4
coincidence rate, hr^{-1}	144.7±1.7	133.6±1.7

Hence $\beta = -0.20 \pm 0.04$, and for 16.8 m we found $C_3' = 128.0 \pm 3.6$ hr^{-1}.

Since the coincidence rate C_4' was found to be 79.6 ± 1.0 hr^{-1}, we have

$$C = C_4 (S/S')^{\gamma_1} (C_3'/C_4') = 8.0 \pm 2.1 \text{ hr}^{-1}.$$

Thus the rate of EAS at 40 m water equivalent is 4.1 ± 1.1 times less than at the earth's surface under 20 cm of lead.

If we denote the mean μ-meson density at the

earth's surface (under 20 cm of lead) by x, and the density at the depth of 40 m water equivalent by px, we find

$$\frac{C}{C_6} = \int_0^\infty (1 - e^{-Sx})^3 x^{-\gamma_1 - 1} dx \Big/ \int_0^\infty (1 - e^{-Spx})^3 x^{-\gamma_2 - 1} dx, \quad (1)$$

where $S = 1.44\ m^2$, and γ_1 and γ_2 are the exponents of the μ-meson density spectrum under 20 cm of lead and at a depth of 40 m water equivalent respectively.

From our previous experiments[2] we have $\gamma_1 = 1.89 \pm 0.17$; according to George et al[3] $\gamma_2 = 2.2 \pm 0.2$. The latter value was found at 60 m water equivalent by means of an arrangement similar to the one used in the present experiment, but with a different effective area. From Eq. (1), it follows that

$$p = 0.47 \pm 0.07.$$

Thus, at 40 m water equivalent the flux density amounts to 50% of the μ mesons under 20 cm of lead at the earth's surface.

Assuming that the energy of the μ mesons is proportional to their residual range, and that the integral energy spectrum can be represented by a power law $E^{-\alpha}$, we can determine the exponent α. The calculations give $\alpha = 0.46 \pm 0.09$ (only statistical errors are indicated).

The results on the energy spectrum, as obtained by different investigators, are shown in the table. The value of α obtained by us agrees well with that obtained by others for the same energy range. As can be seen from the table, the exponents differ greatly for different energy ranges, i.e., the spectrum cannot be represented by a power law. No final conclusion can be drawn as to the variation of the energy spectrum with the shower size.

[1] Sándor, Somogyi, and Telbisz, KFKI Közlémenyek **6**, 117 (1958); Nuovo cimento **16**, Suppl., 209 (1960).

[2] T. Sándor and A. Somogyi, Acta Phys. Acad. Sci. Hung. (in press).

[3] George, MacAnuff, and Sturgess, Proc. Phys. Soc. **A66**, 346 (1953).

[4] Andronikashvili, Bibilashvili, Sakvarelidze, and Khushchishvili, Izv. Akad. Nauk SSSR, ser. fiz. **19**, 681 (1955), Columbia Tech. Transl. p. 619; JETP **32**, 403 (1957), Soviet Phys. JETP **5**, 341 (1957).

[5] E. L. Andronikashvili and R. E. Kazarov, Proc. Cosmic Ray Conf. IUPAP, Moscow, 1959, vol. II, p. 159.

[6] Vernov, Tulupov, Khrenov, and Khristiansen, ibid. p. 169.

[7] Higashi, Mikani, Oshiyo, Shibata, and Watanabe, ibid. p. 181.

Translated by H. Kasha
67

Experimental values of the μ-meson spectrum exponent in EAS

Reference	Depth, m w.e.	Distance from axis	Shower size, N	Energy range E, Bev	Spectrum exponent, α
[3]	12—1600			$0.4<E<400$	0.66
[4]	14—162			$0.4<E<35$	0.60±0.05
[5]	13—160	~28	$1.4\cdot10^4$	$0.4<E<35$	0.54±0.07
		~28	$2.9\cdot10^5$	$0.4<E<15$	0.34*
				$15<E<35$	1.25±0.20
[6]	12—52	~25	$10^4<N<10^5$	$0.4<E<5$	0.08±0.08
				$5<E<10$	0.33±0.3
		~25	$10^5<N<6\cdot10^5$	$0.4<E<5$	0.1±0.08
				$5<E<10$	0.17±0.2
		~100	$10^5<N<6\cdot10^5$	$0.4<E<5$	0.13±0.1
				$5<E<10$	0.45±0.25
[7]	50—250			$10<E<50$	1.1±0.4
Present experiment	12—50			$0.4<E<10$	0.46±0.09

*This value has been computed by us from the first two points of Fig. 3 from reference 5.

HYPERFINE STRUCTURE OF ELECTRON PARAMAGNETIC RESONANCE LINES IN SUPERCOOLED SOLUTIONS OF Ti^{+++}

N. S. GARIF'YANOV and E. I. SEMENOVA

Kazan' Branch, Academy of Sciences, U.S.S.R.

Submitted to JETP editor March 8, 1961

J. Exptl. Theoret. Phys. (U.S.S.R.) **41**, 337-339 (August, 1961)

The hyperfine structure of the electron paramagnetic resonance lines in supercooled glycerine solutions of $Ti_2(SO_4)_3$, enriched in the isotopes Ti^{47} and Ti^{49}, is investigated at a frequency $\nu = 450$ Mc/sec and a temperature $T = 77°$ K. The nuclear spins obtained are $I = 5/2$ for Ti^{47} and $I = 7/2$ for Ti^{49}. The hyperfine splitting constants $|A|$ and $|B|$ are determined. The hyperfine structure of the electron paramagnetic resonance lines in liquid alcohol solutions of Ti^{49} are not resolved at a frequency of 9430 Mc/sec at $T = 295°$ K.

THE hyperfine structure (hfs) of the electron paramagnetic resonance (e.p.r.) lines of the odd, rare isotopes of titanium in solid solutions of its trivalent compounds has not been studied, due to the great width ΔH of the absorption curves.

In a previous work[1] we reported the existence of narrow symmetric e.p.r. lines in liquid alcohol solutions of Ti^{+++} salts in the frequency range 300 — 9460 Mc/sec. The absorption line is also narrow and symmetric in supercooled alcohol and glycerine solutions of Ti^{+++} at a temperature $T = 77°$ K at a frequency $\nu = 300$ Mc/sec, but becomes broad and asymmetric for $\nu = 9460$ Mc/sec, due to the considerable anisotropy of the g-factor. The g-factors were calculated from an analysis of the curves as: for a supercooled glycerine solution $g_{\parallel} = 1.99$, $g_{\perp} = 1.93$, and for alcohol $g_{\parallel} = 2.00$, $g_{\perp} = 1.90$.

We have studied the hfs of the e.p.r. lines in liquid and in supercooled solutions of $Ti_2(SO_4)_3$, enriched in the Ti^{47} and Ti^{49} isotopes to 43.3 and 71.5% respectively. In liquid alcohol and glycerine solutions of Ti^{+++} the measurements were made at $\nu = 9430$ Mc/sec and at $T = 295°$ K, and in supercooled glycerine solutions at frequencies of 450 — 270 Mc/sec and $T = 77°$ K. The concentrations of the solutions were ~ 0.05 mole/liter. The method of measurement has been described earlier[2,3].

As is well known, a double hfs is observed for the e.p.r. lines of supercooled solutions[4] and glasses[5] containing VO^{++} and Cu^{++} under strong field conditions, with hyperfine splitting constants: A for $g_{\parallel}$ and B for $g_{\perp}$, with $|A| > |B|$. This spectrum is described by a Hamiltonian with axial symmetry, dependent on the spin I, of the form

$$\mathcal{H} = g_{\parallel}\beta H_z S_z + g_{\perp}\beta (H_x S_x + H_y S_y) + A I_z S_z + B (I_x S_x + I_y S_y).$$

The greater the anisotropy of the g-factor, the stronger the hfs anisotropy. We would expect an analogous picture for the e.p.r. lines in supercooled Ti^{+++} solutions. If the g-factor is isotropic, as in supercooled Mn^{++} solutions,[4] then A = B and the hyperfine structure spectrum is described by an isotropic spin Hamiltonian.

RESULTS OF THE MEASUREMENTS

The hfs of the e.p.r. lines of supercooled glycerine solutions of $^{47}Ti^{+++}$ and $^{49}Ti^{+++}$ are not resolved at a frequency $\nu = 9430$ Mc/sec at 77° K, owing firstly to the large width of the absorption curves, and secondly to the small hyperfine splitting constant. As has been indicated above already, the e.p.r. line width at these frequencies in supercooled Ti^{+++} solutions is determined by the anisotropy of the g-factor. The further experiments were therefore carried out at frequencies 450 — 270 Mc/sec.

We were able to achieve resolution of the hfs of the e.p.r. lines for supercooled $^{47}Ti^{+++}$ and $^{49}Ti^{+++}$ solutions under high field conditions at $\nu = 450$ Mc/sec. Although further narrowing of the e.p.r. line is observed at lower frequencies, the strong field condition is destroyed, and at $\nu = 270$ Mc/sec the hfs for the intermediate field condition is observed.

At a frequency $\nu = 450$ Mc/sec at 77° K the hfs of the e.p.r. lines of supercooled glycerine solutions of $^{47}Ti^{+++}$ consist of five partially resolved peaks (see Fig. 1). We consider that these hfs

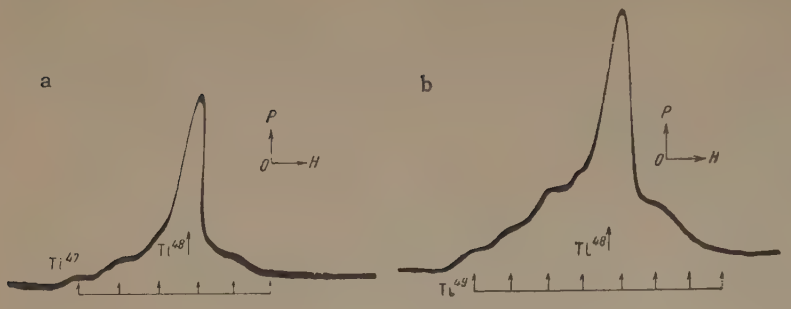

FIG. 1. The hyperfine structure of the e.p.r. lines of supercooled glycerine solution of $Ti_2(SO_4)_3$: a – isotope Ti^{47}, b – isotope Ti^{49} ($\nu \approx 450$ Mc/sec, T = 77°K).

peaks belong to the e.p.r. line produced by the term with $g_{\parallel}$ and the constant A. The more intense e.p.r. line from $^{48}Ti^{+++}$ lies between the third and fourth hfs peaks. These peaks are therefore badly resolved. On the other hand, the e.p.r. line from $^{48}Ti^{+++}$ at the given frequency should lie practically in the center of the spectrum and the total number of hfs peaks from $^{47}Ti^{+++}$ should be six. The last, sixth, peak is not observed because of its great width.

As a result, the hfs spectrum of the e.p.r. line from the $^{47}Ti^{+++}$ ion is explained if the spin of the Ti^{47} isotope is given by the value $I = 5/2$. The hyperfine splitting constant A is of the order of 30 oe: it was determined from the resolved hfs peaks. Besides this hfs there is a second, unresolved, hfs of the line, determined by the terms with $g_{\perp}$ and the constant B. This unresolved hfs is superimposed on the e.p.r. line from Ti^{48}, so that the difference between the resonance values of the field H* for the lines corresponding to the factors $g_{\parallel}$ and $g_{\perp}$ amounts to less than 4 oe.

From a graphical analysis of the width of the combined curve, consisting of the unresolved hfs components and the e.p.r. line from $^{48}Ti^{+++}$, the value of $|B|$ was calculated as ~ 2 oe.

At a frequency $\nu = 450$ Mc/sec the hfs spectrum of the e.p.r. lines of supercooled glycerine solutions of $^{49}Ti^{+++}$ at T = 77° K has seven partially resolved peaks (see Fig. 1). The intense e.p.r. line from $^{48}Ti^{+++}$ lies between the fourth and fifth hfs peaks. In addition, the absorption line from $^{48}Ti^{+++}$ at this frequency should lie practically in the center of the hfs spectrum. The total number of peaks of the hfs spectrum of $^{49}Ti^{+++}$ for the line related to $g_{\parallel}$ should therefore equal eight. Due to the anisotropy of the hfs, the sixth and seventh peaks are broadened and merge into one broad peak, while the eighth peak is not observed at all. The spectrum of the e.p.r. line from $^{49}Ti^{+++}$ is thus produced by a nuclear spin of the isotope $^{49}Ti^{+++}$ equal to $I = 7/2$. $|A|$ is of the order of 30 oe.

The unresolved hfs lines, determined by the terms with $g_{\perp}$ in the Hamiltonian are superimposed on the absorption line of $^{48}Ti^{+++}$. A graphical analysis of this total curve gives $|B| = 2$ oe.

At a frequency $\nu = 9430$ Mc/sec at T = 295° K, the hfs of the e.p.r. line of an alcohol solution of $Ti_2(SO_4)_3$, enriched in the isotope Ti^{49}, is not resolved. The e.p.r. line consists of two parts, a broad base and a narrow peak.

The broad curve is produced as a result of the superposition of unresolved hfs peaks from $^{49}Ti^{+++}$, and the peak is from the e.p.r. line from $^{48}Ti^{+++}$. The hyperfine splitting constant was determined from a graphical analysis of the broad curve as $|a| \approx 12$ oe. As is well known, in liquid solutions an averaged hfs is observed with $|a| = (A+2B)/3$. Substituting the values of A and B determined for the hfs of the e.p.r. line in supercooled $^{49}Ti^{+++}$ solutions, we obtain $|a| \approx 11$ oe.

We did not study the hfs of the e.p.r. line of liquid alcohol solutions of $^{47}Ti^{+++}$, as Ti^{+++} in alcohol solutions rapidly oxidizes to Ti^{++++}.

DISCUSSION OF THE RESULTS

As was shown above, the hfs components of the e.p.r. lines of supercooled Ti^{+++} solutions, enriched in the Ti^{47} and Ti^{49} isotopes, are not fully resolved. The values of the nuclear spins, $I = 5/2$ for the isotope Ti^{47} and $I = 7/2$ for Ti^{49} were therefore obtained not by means of a simple count of the total number of hfs components, but only from the number of those components which lie in the resolved half of the spectrum.

The values obtained for the spins of the isotopes Ti^{47} and Ti^{49} can also be calculated from the ratio of the hyperfine splitting constants, since the nuclear magnetic moments for these isotopes were determined accurately by the method of nuclear paramagnetic resonance.[6]

We have thus been able by the e.p.r. method to confirm the values of the nuclear spins of Ti^{47} and Ti^{49} obtained earlier indirectly from measurements of nuclear paramagnetic resonance in these titanium isotopes.[6,7]

[1] Avvakumov, Garif'yanov, and Semenov, JETP **39**, 1215 (1960), Soviet Phys. JETP **12**, 847 (1961).
[2] N. S. Garif'yanov, JETP **35**, 612 (1958), Soviet Phys. JETP **8**, 426 (1959).
[3] N. S. Garif'yanov, JETP **37**, 1551 (1959), Soviet Phys. JETP **10**, 1101 (1960).
[4] N. S. Garif'yanov, DAN SSSR **103**, 41 (1955).
[5] R. H. Sands, Phys. Rev. **99**, 1222 (1955).
[6] C. D. Jeffries, Phys. Rev. **92**, 1262 (1953).
[7] H. Kopferman, Kernmomente, Edwards Bros., Ann Arbor, 1945.

Translated by R. Berman
68

FLUCTUATIONS OF THE μ-MESON FLUX IN EXTENSIVE AIR SHOWERS

S. N. VERNOV, V. I. SOLOV'EVA, B. A. KHRENOV, and G. B. KHRISTIANSEN

Nuclear Physics Institute, Moscow State University

Submitted to JETP editor March 13, 1961

J. Exptl. Theoret. Phys. (U.S.S.R.) **41**, 340-353 (August, 1961)

Fluctuations of the μ-meson flux in extensive air showers of a given size N ($N > 10^6$) were studied using an arrangement which simultaneously measured the total number of shower particles and the number of μ mesons in the shower. It is shown that the fluctuations can be explained by fluctuations in the height at which the shower-producing primary particle experiences its first interaction. The data obtained are used to determine the interaction mean free path for the ultra-high energy primary particles producing the extensive showers.

INTRODUCTION

THE experimental study of the fluctuations of the μ-meson flux compared to the total flux of all charged particles in extensive air showers (EAS) is of great interest, since the character of these fluctuations is apparently determined by the fluctuations in the development of the cascade of high-energy nuclear-active particles in the atmosphere.

Recently, a number of models of EAS development were considered which predict the existence of strong fluctuations, in particular of the ratio of all charged particles to μ mesons.[1-3]

The present article presents results of a study of the fluctuations in the μ-meson flux in EAS, carried out using the array for the comprehensive study of EAS at Moscow State University.

EXPERIMENTAL METHOD AND DESCRIPTION OF ARRAY

In order to solve the problem at hand, it is necessary simultaneously to determine the total flux of charged particles and to detect a sufficiently large number of μ mesons in individual extensive air showers. In order to determine the total number of particles, we used an array consisting of a large number of Geiger-Müller counters forming a hodoscope. The position of the counter trays and the number of counters of different areas in each tray are shown in Fig. 1a and in Table I.

The total number of particles and the position of the shower axis were determined by the usual method,[4] assuming that all showers have the same lateral-distribution function of charged particles, closely approximated by the Nishimura-Kamata function with age parameter s = 1.3.

The relative error ΔR/R in the determination of the shower-axis position (R is the distance from the shower axis to the center of the array) for showers detected using the triggering method described below amounted to 20%. The relative error in the determination of the number of particles ΔN/N amounted to ±30% for R < 60 m, and to +100%, −50% for R ~ 150 m.

The μ mesons were detected both on the surface of the earth (chambers 2, 3, 5, 6, 7, 9), and

Table I. Distribution of counters with different areas in different points of the array represented in Fig. 1

Point	Unshielded counters		Shielded counters	Point	Unshielded counters		Shielded counters
	330 cm²	100 cm²	330 cm²		330 cm²	100 cm²	330 cm²
I	264	100	—	*5*	72	48	24×2
II	60	48	—	*6*	96	24	24×2
III	120	48	—	*7*	72	48	24×2
U_1(20 m w.e.)	—	—	96	*8*	96	24	—
U_2(40 m w.e.)	—	—	192	*9*	108	24	24×2
1	72	48	—	*10*	96	24	—
2	108	24	24×2	*11*	36	24	—
3	96	24	24×2	*12*	36	24	—
4	72	48	—	*13*	36	24	—
				14	24	48	—
				15	24	48	—

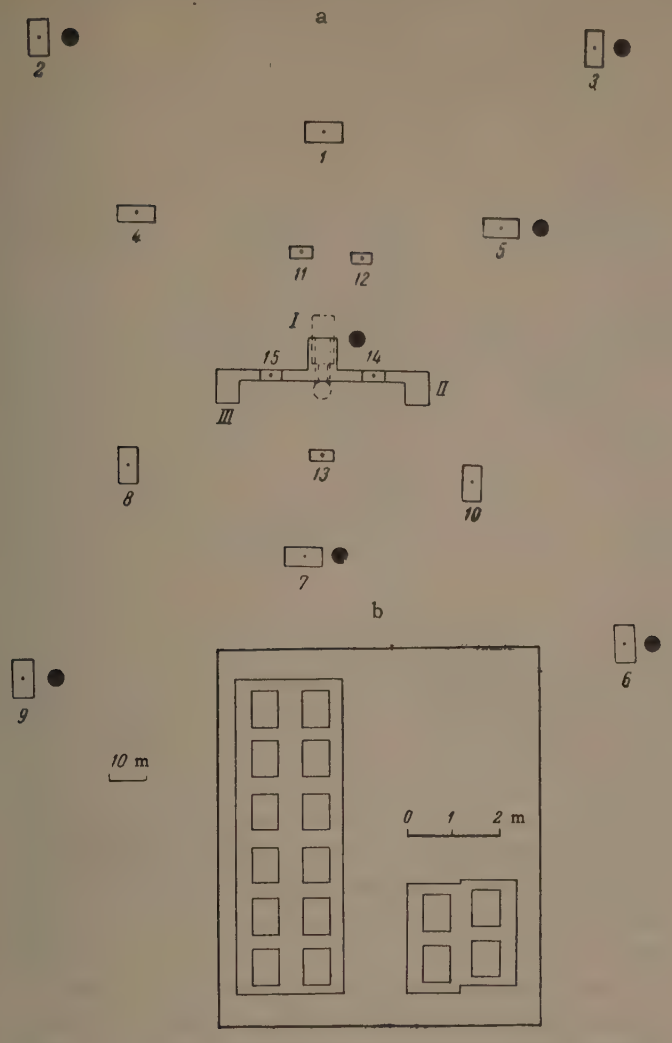

FIG. 1. a – position of the Geiger-Müller counter trays, ● – μ-meson detectors; dashed line – outline of underground chambers; b – positions of detectors in the underground chamber U_2. The squares indicate the effective areas of the counter groups.

underground at 20 and 40 m water equivalent (w.e.) in chambers U_1 and U_2 respectively. On the surface of the earth, we used a hodoscope arrangement of Geiger counters shielded by lead and iron (see Fig. 2) for the detection of μ mesons. Underground, we used for this purpose a hodoscope of Geiger-Müller counters which was similar to the arrangement shown in Fig. 2 but without the top counter layer and the absorber above it.

The total effective area of the μ-meson detectors amounted to 4.75 m^2 on the surface of the earth, 3.2 m^2 at the depth of 20 m w.e., and 6.3 m^2 at 40 m w.e. The position of the μ-meson detectors and the number of counters in them are shown in Fig. 1 and Table I.

EAS were selected by requiring a six-fold coincidence of counters with 0.132 m^2 area in each coincidence channel. The counters of three channels

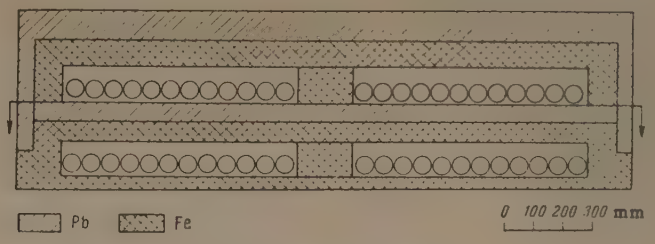

FIG. 2. μ-meson detector.

were placed into one tray, in which the distance between the counter walls amounted to 3 cm (6 × 55 cm counters were used). The distance between the two trays was 2.5 m.

The triggering array was placed in the center of chamber 1, Fig. 1a.

REDUCTION OF DATA

From the total number of detected showers, we selected showers of large size. The selection criterion was the discharge of 100 counters out of 264 with 330 cm^2 area each in chamber 1, and the simultaneous discharge of at least 30 counters out of 72 at trays 1, 4, 5, 7, 8, 10. The shower selected in such a way had a total number of particles $N > 10^5$.

For the determination of the number of μ mesons (with energy $E_\mu > 4 \times 10^8$ ev) detected by the detectors at the surface of the earth, we inspected the hodoscope pictures of counter discharges in the detectors. We regarded either one of the following events as a passage of μ mesons: a) one counter is discharged in each layer of the detector, b) one counter is discharged in one layer, and two counters in the second layer. In one detector (Fig. 2), several events of the types a) or b) could be observed during the passage of several μ mesons, with the order of the discharged counters corresponding to the parallelness of the μ-meson tracks.

In order to exclude the contribution of nuclear-active particles to the detected μ mesons, we analyzed only those cases which occurred at a distance of more than 50 m from the shower axis. For these showers, the probability of a discharge of two counters amounted to 12%. It follows from the experimental data[5,6] that, at distances $r > 50$ m from the shower axis, the fraction of nuclear-active particles as compared to the total number of μ mesons is small (10% at a distance of 50 m), and decreases rapidly (as r^{-1}) with an increasing distance from the shower axis. Using these data, we have calculated the contribution of nuclear-active particles to the detected μ-meson flux for selected

Table II. Distribution of events with respect to the ratio of the number q of detected μ mesons to the mean expected number p of mesons

q/p	A		B		C			
	1	2	3	4	5	6	7	8
0—1/3	13	7	8	2	0	23	4	8
1/3—2/3	18	20	8	10	0	36	20	27
2/3—1	22	26	22	17	65%	22	40	37
1—1 1/3	20	24	12	20	26%	17	38	32
1 1/3—1 2/3	15	14	1	5	6%	18	15	13
1 2/3—2	6	6	4	2	1.6%	2	5	5
2—2 1/3	6	5	1	1		5	2	2
2 1/3—2 2/3	2	2	1	—		—	2	2
2 2/3—3	—	1			1.4%	—	1	1
3—3 1/3	—	1				1	—	—
3 1/3—3 2/3						3		
3 2/3—4								
4—4 1/3	4							
Total number of events	106	106	57	57	100%	127	127	127
$P(\chi^2)$	20 %		0.03%		< 0.01%			

Remark: A — data from all surface detectors for $N \geq 5 \times 10^6$, B — from detector U_1 for $N \geq 4 \times 10^6$, C — from detector U_2 for $N \geq 4 \times 10^6$. Column 5 shows the distribution expected because of the spread of the real distances from the shower axis to U_2. Columns 1, 3, and 6 show the experimental distributions; columns 2, 4, and 7, the distributions expected according to Eq. (2); and column 8, the distribution expected because of the factor shown in column 5 and of statistical fluctuations.

showers. It was found that the contribution amounts to 5%.

The determination of the μ-meson flux density with energy $E_\mu > 5 \times 10^9$ ev and $E_\mu > 10^{10}$ ev was carried out using detectors U_1 and U_2 (at 20 and 40 m w.e. respectively). It was assumed that, when one μ meson traverses the counters, we should observe the discharge of one, two, or more counters of the detector of Fig. 2 (in the lower layer). The probability of a simultaneous discharge of two or more counters due to the passage of one μ meson amounted to 8%, and was due to the production by the μ mesons of δ electrons and of secondary electron-photon showers.

In measuring the μ-meson flux using the U_1 and U_2 detectors placed below the level at which the position of the shower axis was being determined, a certain uncertainty arises in the actual distance from the shower axis, owing to the unknown angle of shower arrival. This uncertainty decreases with increasing distance R from the trace of the shower axis on the surface of the earth to the vertical line passing through U_1 and U_2.

Table II (column 5) shows the probabilities of the deviation of the μ-meson flux density from the average density obtained for R = H (where H is the depth of the underground chamber in meters), assuming an angular distribution as $\cos^7 \theta$ and a lateral μ-meson distribution as 1/r.

For the analysis, we used showers with $R \geq H$.

Using the method for determining the number of μ mesons described above, the average lateral distributions of μ mesons with different threshold energy were obtained for showers of different size (Fig. 3).

The obtained average characteristics of the μ-meson flux permitted us to determine, for each detector, the expected number of μ mesons corresponding to the detected number of shower particles, and the distance of the μ-meson detector from the shower axis.

RESULTS

As a result of the above-described data reduction, we have found for each selected shower the number q of μ mesons detected by the detectors and the number p of μ mesons expected in those detectors for a given total number of particles in the shower and for known distances of the detectors from the shower axis on the surface of the earth.

The investigated showers were divided into the following size intervals:

For the detector on the surface of the earth:
$$\begin{cases} N = (2-5)\cdot 10^6 \\ N = (5-10)\cdot 10^6, \\ N \geqslant 10^7 \end{cases}$$

For U_1:
$$\begin{cases} N = (2-4)\cdot 10^6 \\ N \geqslant 4\cdot 10^6 \end{cases},$$

For U_2:
$$\begin{cases} N = (1-2)\cdot 10^6 \\ N = (2-4)\cdot 10^6 . \\ N \geqslant 4\cdot 10^6 \end{cases}$$

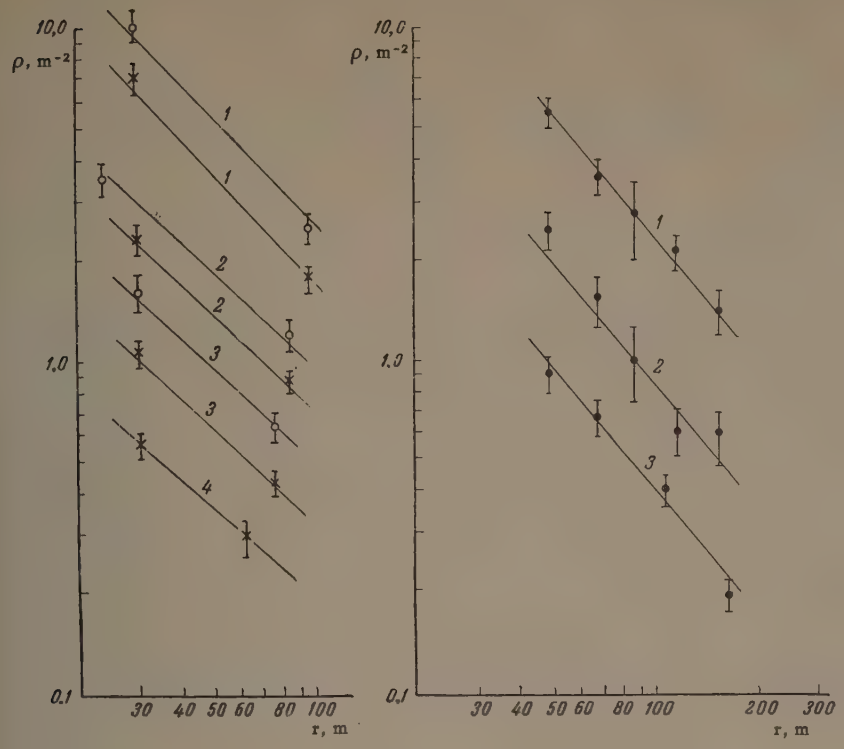

FIG. 3. Mean lateral distributions $\rho(r)$ of μ-meson fluxes in showers with different numbers of particles: $1-\bar{N} = 2\times10^7$ ($N > 10^7$), $2-\bar{N} = 5\times10^6$ ($\Delta N = 4-10\times10^6$), $3-\bar{N} = 2.5\times10^6$ ($\Delta N = 2-4\times10^6$), $4-\bar{N} = 1\times10^6$ ($\Delta N = 1-2\times10^6$). The μ-meson flux density was determined according to the detector U_1(○), U_2 (×), or the surface detector (●).

Table III. Distribution of events with respect to the detected number of μ mesons q

q	A		B		C		D		E	
	exp.	calc.	exp.	calc.	exp.	calc.	exp.	calc.	exp.	calc.
0	47	42	6	5	11	5	24	17	20	4
1	42	51	9	8	19	9	27	28	28	12
2	44	34	8	9	10	15	23	28	19	20
3	12	18	8	8	12	15	17	19	22	25
4	8	8	5	6	10	12	12	13	12	27
5	2	2	8	5	4	10	5	7	10	24
6	2	1	6	4	3	5	7	4	12	18
7	1	1	—	2	—	4	1	2	3	12
8		1	1	1	4	2	2	2	5	7
9			1	1	5	2	—	1	4	4
10				1	1	1	3	1	2	2
11				1	1	1	1	1	4	1
12							—		3	1
13							—		2	
14							1		2	
15									1	
16					1				1	
17										
18										
19										
20										
21									1	
22									1	
23										
24					1					
25										
26									1	
27										
28										
29										
30										
Total number of events	158	158	52	52	82	82	123	123	156	156
$P(\chi^2)$	15%		50%		0.3%		20%		0.01%	

Remark: A – data from all surface detectors for $N = 2-5\times10^6$, B – for $N = 5-10\times10^6$, C – data from detector U_1 for $N = 2-4\times10^6$, D – from detector U_2 for $N = 1-2\times10^6$, and E – from detector U_2 for $N = 2-4\times10^6$.

The calculation gives the distribution expected according to Eq. (1).

For groups of showers with a relatively small number of particles ($N < 4 \times 10^6$), the distributions with respect to the number of detected μ mesons q are shown in Table III. For shower groups with $N \geq 4 \times 10^6$, the distributions with respect to q/p are shown in Table II.

q/p	0—1	1—2	2—3	3—4	4—5	5—6	6—7	7—8	8—9
$I(q/p)$	240	107	40	11	5	2	1	0	1

In order to estimate the role of purely statistical fluctuations for each group of showers in Table III, we have constructed the distributions with respect to q expected because of statistical fluctuations and calculated according to the formula

$$W(q) = \sum_i w_i, \qquad w_i = p_i^q e^{-p_i} / q! \qquad (1)$$

(The summation is carried out over all showers of the given group.)

For the distributions in Table II, the statistical fluctuations of the values q/p were calculated from the formulae:

$$\sum_{q=0}^{p_i/3} W(q), \qquad (\text{for } q/p = 0 - {}^1/_3),$$

$$\sum_{q=p_i/3}^{2p_i/3} W(q) \quad (\text{for } q/p = {}^1/_3 - {}^2/_3), \text{ etc.} \qquad (2)$$

For underground detectors, the non-statistical fluctuations in the μ-meson flux density may be due to the unknown true distances from the shower axis to the μ-meson detectors, as mentioned above. For the distributions C (Table II), we have calculated the theoretical distribution I(q/p) taking both the spread of the true distances from the shower axis and statistical fluctuations (column 8) into account. From a comparison of columns 7 and 8 of Table II, it follows that the non-statistical fluctuations due to the deviation of the true distance of the shower axis to the underground μ-meson detectors for varying angles of shower incidence are negligible.

A comparison of the experimental distributions with respect to q and q/p with the ones expected from Eqs. (1) and (2) were carried out using the χ^2 test. The values of $P(\chi^2)$ are shown in Tables II and III.

It can be seen from these tables that the fluctuations observed by means of surface detectors can be fully explained by statistical fluctuations. However, the fluctuations in the μ-meson flux observed by means of the underground detectors U_1 and U_2 are greater than purely statistical fluctuations if we consider sufficiently large showers.*

*The data of Tables II and III show only that, for a limited area of μ-meson detectors, the study of fluctuations is possible if N is sufficiently large and R sufficiently small, i.e., the mean number of μ mesons incident on the detector area is large. In a contrary case, purely statistical fluctuations may mask the effect.

For the detector U_2, the distribution with respect to q/p for all detected showers ($N \geq 1 \times 10^6$) is shown below. This enables us to study the fluctuations of the μ-meson flux in the range $q/p > 1$:

The non-statistical character of fluctuations in the latter case is confirmed by the correlation of the deviations from the mean values of the μ-meson flux measured by detectors U_1 and U_2. In fact, let us consider the pair of values $x = q/p$ (for detector U_1) and $y = q/p$ (for detector U_2). If the deviations of x from unity are correlated with the deviations of y, then this means that non-statistical fluctuations in the number of μ mesons exist. However, for a small mean number of detected mesons, a large role is played by the Poisson fluctuations of q/p, which may fully mask the correlation of these values between U_1 and U_2. Therefore, in order to calculate the correlation coefficient between x and y, we have selected showers with a sufficiently large number of particles N and small distances R (ratio $N/R \geq 4 \times 10^5\ m^{-1}$). Table IV shows the distribution of the pair of values of x and y obtained. The events were grouped according to the intervals of q/p used in Table II. The

Table IV

U_1 \ U_2	0-1/3	1/3-2/3	2/3-1	1-4/3	4/3-5/3	5/3-2	2-7/3	7/3-8/3	8/3-3	>3
>3						1			1	1
8/3-3										1
7/3-8/3		1			1					
2-7/3	1			1		1				2
5/3-2	1		1	1	5	1		1		
4/3-5/3	1	6	1	1	3	3		1		1
1-4/3	2	5	6	2		1	1			
2/3-1	5	5	5	5	3					
1/3-2/3	2	3	5	2	1					
0-1/3	8	4	1	2	2		1			

A comparison of the value of $P(\chi^2)$ in columns d and e of Table III shows that a change in the mean number of mesons incident upon the area of detector U_2 from 2.5 to 4.2 leads to a clear-cut manifestation of non-Poisson fluctuations.

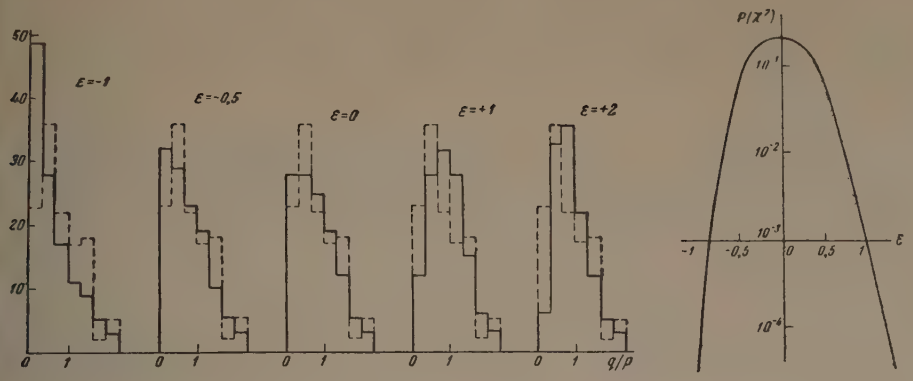

a b

FIG. 4. a – theoretical distributions with respect to q/p calculated using Eq. (10) (solid histograms) and experimental distribution with respect to q/p from Table II (dotted histograms). The quantity q/p ranges from 0 to 2⅓, Δ q/p = ⅓. b – probability $P(\chi^2)$ of different values of ε calculated from the comparison of experimental and theoretical distributions.

correlation coefficient R calculated from the data of Table IV according to the formula

$$r = \left(\sum xy - n\bar{x}\bar{y}\right)\left(\sum x^2 - n\bar{x}^2\right)^{-1/2}\left(\sum y^2 - n\bar{y}^2\right)^{-1/2}$$

where n is the number of (x, y) pairs taken into consideration amounts to 0.60 ± 0.15.

The probability that the resultant value of r (or rather of its lower limit, r = 0.45) occurs when there is no correlation between the quantities x and y amounts to 0.1% (the total number of pairs of the measured values being n = 109). [7] Consequently, the value r = 0.60 ± 0.15 means that a correlation exists between the quantities x and y due to non-statistical fluctuations in the μ-meson flux.

The set of the distributions with respect to q/p gives the total picture of fluctuations in the μ-meson flux with energy $E_\mu > 10^{10}$ ev (detector U_2). In the range q/p > 1, we can represent the dependence I(q/p) as a power law $I(q/p) \sim (q/p)^{-m}$ where m > 3.0.

Table II shows the variation of I(q/p) in the range q/p < 1. In Fig. 4, the data of column 6 of Table II are presented together with the theoretically expected fluctuations discussed below.

DISCUSSION OF RESULTS

Let us consider some methodological problems arising in connection with the experiment.

1. The μ-meson flux is observed over a relatively small area, since a small fraction of the total number of μ mesons in the showers is detected (~ 0.1%). Moreover, for the case of the detectors U_1 and U_2, the detection of μ mesons occurs at one point, and therefore the fluctuations of the detected number of μ mesons may refer both to fluctuations of the total flux of μ mesons and to the fluctuations in the lateral distribution function of the μ mesons.

In the case of surface detectors, the detection takes place at several points at different distances from the axis, which enables us in principle to distinguish the fluctuations in the total μ-meson flux from the fluctuations in their lateral distribution function. However, the area of the detectors is relatively small, and chance variations in the number of detected μ mesons play a large role.

Therefore, in order to compare the experiment with theory, it is necessary to take into account the theoretical prediction both with respect to the fluctuations of the total μ-meson flux and with respect to the fluctuations of the μ-meson lateral distribution function.

2. A number of errors of random nature (random errors in the determination of the shower size, the spread of distances of the μ-meson detectors from the shower axis due to angular distribution of the shower axis, especially for detectors U_1 and U_2, etc.) lead to an increase in the observed fluctuations of the μ-meson flux. Therefore, the observed fluctuations represent an upper limit for possible fluctuations of the μ-meson flux.

3. A decrease in the observed fluctuations of the μ-meson flux may be caused by a systematic selection of showers with a given type of the electron lateral distribution function, if the latter depends on the μ-meson flux. Experimentally, the showers are selected by the triggering arrangement and by means of an additional requirement of a given electron density at two points 60 m apart. As calculations carried out by one of the authors (V. I. Solov'eva) have shown, such a selection leads to a considerable decrease in the selection efficiency only for showers with a lateral distribution function corresponding to electron-photon showers with age s < 1.0. At present, there is a lack of sufficient experimental data on the age distribution of showers. According to preliminary results obtained by the Tokyo group,* there are no sharp deviations from the average lateral distribution function for s = 1.3, at least at distances

*Fukui, Hasegawa, Matano, Miura, Oda, Ogita, Suga, Tanahashi, and Tanaka (private communication).

greater than 30 m from the shower axis. In such a case, a selection of showers according to the electron density should not influence the fluctuations in the μ-meson flux.

Taking the methodological problems mentioned above into consideration, we shall compare the results obtained with the theoretical predictions.

1. Comparison of the results with the model of EAS developing the atmosphere without fluctuations is simplest when the fluctuations of the μ-meson flux in the showers with a given number of particles are only due to the fluctuations in the altitude of the first interaction of the primary particles.[3] In such a case, the shower development in the atmosphere is described by a cascade curve with a maximum, whose depth depends logarithmically ($x_m = B \ln E_0 + \text{const}$) on the energy of the primary particle. The absorption of the shower particles beyond the maximum is exponential with a mean free path $\Lambda = 200$ g/cm^2. The μ-meson flux n_μ with $E_\mu \geq 10^{10}$ ev is not absorbed beyond the shower maximum, while the total number of μ mesons is proportional to the primary energy. In such a model, it is assumed[3] that the lateral distribution functions of all shower particles and of μ mesons do not fluctuate, and our experimental results therefore permit an unambiguous interpretation.

The number of particles in showers whose axes are inclined to the vertical by an angle θ at the observation level x_0 depends on the depth of the first interaction, as shown by

$$N = c_1 N_m E_0^{B/\Lambda} \exp\left[-(x_0 - x)\sec\theta/\Lambda\right], \qquad (3)$$

where $N_m = c_2 E_0$.

The number of primary particles with energy E_0 interacting at the depth x equals

$$I(E_0, x)\, dE_0\, dx = c_3 E_0^{-\gamma-1} \exp\left[-x \sec\theta/\lambda\right] \sec\theta\, dE_0\, dx/\lambda, \qquad (4)$$

where λ is the interaction mean free path of primary particles, and γ is the exponent of their energy spectrum.

Substituting x for N according to Eq. (3), we obtain

$$I(E_0, N)\, dE_0\, dN = c_4 E_0^{(\Lambda+B)/\lambda-\gamma-1} N^{-(1+\Lambda/\lambda)} \exp\left(-x_0 \sec\theta/\lambda\right) dE_0\, dN. \qquad (5)$$

Integrating over E_0 from $E_{0m} = N/c_2$ to $E_{0\max}^{1+B/\Lambda} = N \exp(x_0 \sec\theta/\Lambda)/c_1 c_2$, we obtain the angular distribution and the altitude dependence of showers with a given number of particles, which should satisfy the experimental data (see, e.g., [5,8]).

Obviously, the result depends essentially on the quantity $\epsilon = (\Lambda+B)/\lambda - \gamma - 1$. If $(\Lambda+B)/\lambda < \gamma$, then the angular distribution has the form

$$\exp\left[-\gamma x_0 \sec\theta/(\Lambda + B)\right],$$

If $(\Lambda+B)/\lambda > \gamma$, then $\exp(-x_0 \sec\theta/\lambda)$. The experimentally observed variation is of the form

$$\exp\left(-x_0 \sec\theta/(100 - 120)\right).$$

It is found that the distribution of showers with respect to the number of μ mesons n_μ is very sensitive to ϵ, and, from a comparison of experimental data with the model under consideration, we can determine this quantity and, knowing Λ and γ, also find the value of λ.

The experimental data were obtained with an array which detected EAS with all angles of incidence θ, and we therefore integrate Eq. (5) over θ assuming an isotropic distribution of the primary particles. Two regions of integration are important, $E_0 < E_{01}$ and $E_0 > E_{01}$, where

$$E_{01}^{1+B/\Lambda} = c_1^{-1} c_2^{-1} N \exp\left(x_0/\Lambda\right)$$

is the maximum possible energy for a vertical shower with a given number of particles.

For $E_0 < E_{01}$ we have

$$I(E_0, N)\, dE_0\, dN = c_4 E_0^{\epsilon} N^{-(1+\Lambda/\lambda)} \times \left[\lambda \exp\left(-\frac{x_0}{\lambda}\right) \Big/ x_0 - \int_{x_0/\lambda}^{\infty} \frac{e^{-t}}{t}\, dt\right] dE_0 dN. \qquad (6)$$

At sea level, x_0/λ is large (> 10), and therefore

$$\lambda/x_0 \exp\left(x_0/\lambda\right) - \int_{x_0/\lambda}^{\infty} \frac{e^{-t}}{t}\, dt \sim c_5 \exp\left(-x_0/\lambda\right), \qquad (7)$$

where c_5 is independent of x_0/λ.

For $E_0 > E_{01}$ we have

$$I(E_0, N)\, dE_0\, dN = c_4 E_0^{\epsilon} N^{-(1+\Lambda/\lambda)} \times \int_0^{(\cos\theta)_1} \exp\left(-x_0 \sec\theta/\lambda\right) d\cos\theta\, dE_0\, dN,$$

where

$$(\cos\theta)_1 = \left[1 + (\Lambda + B)\, x_0^{-1} \ln\left(E_0/E_{01}\right)\right]^{-1}.$$

We therefore obtain the expression

$$I(E_0, N)\, dE_0\, dN = c_4 c_5 E_0^{\epsilon} N^{-(1+\Lambda/\lambda)} \times \exp\left\{-x_0 \lambda^{-1}\left[1 + (\Lambda + B)\, x_0^{-1} \ln\left(E_0/E_{01}\right)\right]\right\} dE_0\, dN = c_6 E_0^{-\gamma-1} N^{-(1+\Lambda/\lambda)}\, dE_0\, dN. \qquad (8)$$

Substituting in Eqs. (8) and (6) n_μ instead of E_0, we obtain the distribution of events according to the number of μ mesons of the form

$$I(n_\mu)\,dn_\mu = \begin{cases} n_\mu^{\varepsilon}\,dn_\mu & n_\mu < n_{\mu\,min}^{\Lambda/(\Lambda+B)} \exp\left[x_0/(\Lambda+B)\right] \\ n_\mu^{-\gamma-1}\,dn_\mu & n_\mu > n_{\mu\,min}^{\Lambda/(\Lambda+B)} \exp\left[x_0/(\Lambda+B)\right]. \end{cases} \tag{9}$$

From the distribution (9), we can obtain the theoretically expected distributions shown in Table II. For this, it is necessary for each shower with a number of particles N and falling at a distance R from the μ-meson detectors, to consider its spectrum $I(p', p)\,dp'$ of the μ-meson numbers p' detected by the detectors, which has the form (9) and which, in addition, satisfies the condition

$$\int_{p'_{min}}^{\infty} I(p',\ p)\,dp' = 1, \qquad \int_{p'_{min}}^{\infty} p' I(p', p)\,dp' = p,$$

where p is the average number of μ mesons obtained for showers with a given N and R. We then obtain the theoretically expected distribution $I_T(q/p)$ analogously to formula (2):

$$\sum_i \sum_{q=0}^{p_i/3} \int_{p'_{min}}^{\infty} p'^q e^{-p'} I(p',\ p)\,dp'/q! \qquad \text{for } q/p = 0 - {}^1/_3,$$

$$\sum_i \sum_{q=p_i/3}^{2p_i/3} \int_{p'_{min}}^{\infty} p'^q e^{-p'} I(p',\ p)\,dp'/q! \qquad \text{for } q/p = {}^1/_3 - {}^2/_3. \tag{10}$$

The distributions $I_T(q/p)$ for the detector U_2 calculated according to Eq. (10) are shown in Fig. 4. The separate distributions (solid histograms a — e) are calculated for different values of ϵ.

The comparison with the experimentally observed distributions $I(q/p)$ (the dotted histograms in Fig. 4) for the detector U_2 taken from Table II were carried out using the χ^2 test. Figure 4b shows the probabilities of agreement $P(\chi^2)$ between the experimentally and the theoretically expected distributions for different ϵ. The values of ϵ from -0.5 to $+0.5$ occur with a probability greater than 10%, which, for $\Lambda = 200$ g/cm^2, $B = 30$ g/cm^2, and $\gamma = 2$ corresponds to values of λ from 92 to 66 g/cm^2. As has been mentioned above, methodological errors of the experiment lead to an increase in the observed fluctuations, so that, from the comparison of the experimental and theoretical distributions, it follows only that $\epsilon > -0.5$ or $\lambda < 92$ g/cm^2.

2. In recent years, several models of EAS development were proposed in which an essential role is played by the fluctuations of the nuclear-interaction characteristics [1] and the fluctuations of the height of the nuclear interaction which determines the number of particles in the shower. [2] We shall consider the model of EAS development proposed by Cranshaw and Hillas. [2] This model assumes that electron-photon showers in EAS have a small range, so that the number of particles in the shower at observation level is determined only by the last interactions of nuclear-active particles in the shower core. The altitude of the last interaction may vary, which leads to variations in the age of observed showers and in the lateral distribution function of shower particles. The number of high-energy μ mesons is proportional to the energy lost by the primary particle up to the observation level.

Selecting the showers in our experiment in the manner described above, we choose showers with a lateral distribution function corresponding to $s > 1.0$. (We assume that, according to the model under consideration, there are fluctuations in the lateral distribution function of the shower.) The detection of a given number of particles in a shower then shows that $E_{n.a.} > E_c$, and that the depth of the last interaction $x_0 < x_c$. (The values of E_c and x_c correspond to the case where the shower age parameter $s = 1$.) Because of the falling spectrum of nuclear-active particles, the main contribution to the number of detected showers will be due to particles with energy $E_{n.a.} \sim E_c$ and $x_0 \sim x_c$, and we can therefore assume that the given number of particles in the shower determines $E_{n.a.}$ and x_0. The μ-meson flux, however, may fluctuate, since the given value of $E_{n.a.}$ at the level x_0 can occur for different energies of the primary particle, which undergoes a different number of interactions along its path.

If β is the energy fraction conserved in each interaction by the primary particle, then $E_0 = E_{n.a.}\beta^{-i}$, where i is the number of interactions. The probability that i interactions occur is

$$W_i = \left(\frac{x_0}{\lambda}\sec\theta\right)^i \exp\left(-\frac{x_0}{\lambda}\sec\theta\right) \Big/ i!$$

and the number of primary particles which are responsible for the appearance of a particle with energy $E_{n.a.}$ at the level x_0 is given by the equation

$$I(E_{n.a.})\,dE_{n.a.} = c' \frac{dE_{n.a.}}{E_{n.a.}^{\gamma+1}} \beta^{i\gamma} \exp\left(-\frac{x_0}{\lambda}\sec\theta\right) \frac{1}{i!}\left(\frac{x_0}{\lambda}\sec\theta\right)^i, \tag{11}$$

where c' is the absolute coefficient in the energy spectrum of primary particles.

Carrying out a summation over all values of i, we obtain the angular distribution and altitude dependence of showers with fixed N and age

$$I(E_{n.a.})\,dE_{n.a.} = c' \frac{dE_{n.a.}}{E_{n.a.}^{\gamma+1}} \exp\left[-\frac{x_0}{\lambda}\sec\theta\,(1-\beta^\gamma)\right]. \tag{12}$$

In order to explain the observed angular distribution of showers with a number of particles in the range $10^5 - 10^7$, Cranshaw and Hillas[2] assumed $\lambda = 75$ g/cm^2 and $\beta = 0.5$.

Assuming these values of λ and β, we can obtain the distribution with respect to i from Eq. (11). Since the experimental array detects showers with all angles of incidence θ, we integrate (11) over θ assuming an isotropic angular distribution of the primary particles. The results of the integrations are given below. W is the probability that i collisions of the primary particles occur at any angle θ. The corresponding values of the μ-meson flux n_μ are also given:

i	1	2	3	4	5	6	7	8	9	10	11	12
W	0.12	0.16	0.21	0.17	0.13	0.075	0.046	0.018	0.0074	0.003	$9.3\cdot10^{-4}$	$3.2\cdot10^{-4}$
$n_\mu/n_{\mu min}$	1	3	7	15	31	63	127	255	511	1023	2047	4095

In fact, it follows from our assumptions that the μ-meson flux n_μ is proportional to the energy lost by the primary particle, i.e.,

$$n_\mu \sim (1-\beta) E_0 (1 + \beta + \ldots + \beta^i)$$
$$= (1-\beta) E_{n.a.} (\beta^{-i} + \ldots + 1)$$
$$= (1-\beta) E_{n.a.} (\beta^{-i} - 1) \qquad (13)$$

and $n_\mu/n_{\mu min} = \beta^{-i} - 1$.

From this relation between n_μ and i, we obtain the distribution with respect to n_μ. The mean value of the μ-meson flux is found to be $\bar{n}_\mu/n_{\mu min} = 36$, and the corresponding number of interactions ≈ 5.

Let us consider the number of showers in which $n_\mu < \bar{n}_\mu$ and $n_\mu > \bar{n}_\mu$ (using the nomenclature of the previous section, $q < p$ and $q > p$). From the distribution with respect to $n_\mu/n_{\mu min}$ given above, it follows that $I(q < p)/I(q > p) = 5.6$. The experimental distribution from Table II, column 6 gives $I(q < p)/I(q > p) = 1.75 \pm 0.2$. Consequently, the model under consideration predicts a large number of showers with a relatively small μ-meson flux, which contradicts the experimental data.

We will show that the fluctuations in the lateral distribution of μ mesons cannot, in the model under consideration, lead to the observed difference between the theoretical and experimental distributions $I(q/p)$. In order to explain this difference, it is necessary to assume that the lateral distribution of the μ-meson flux for $i < 5$ is steeper than for $i > 5$. A small number of μ mesons for $i < 5$ will then be compensated by the large concentration of μ mesons and, vice-versa, a large number of μ mesons for $i > 5$ will be compensated by the small concentration of the μ mesons since the μ-meson density will undergo small fluctuations with respect to the mean value.

However, the variation in the lateral distribution of μ mesons would mean a change in the mean altitude of μ-meson production. Since the main contribution to the number of μ mesons is due to the interactions of the primary particle occuring before the last interaction, which determines the number of particles in the shower [see Eq. (13)], and the altitude distribution of these events is independent of the number i, the mean altitude of μ-meson production should not depend on the number of interactions i. This means that the mean lateral distribution of the μ-meson flux should be independent of i, and therefore the fluctuations in the lateral distribution of μ-meson flux cannot lead to the difference between the theoretical and experimental distributions $I(q/p)$.

CONCLUSIONS

1. Experimentally observed small fluctuations in the μ-meson flux in showers with a given number of particles contradict the model of shower development proposed by Cranshaw and Hillas.[2]

2. The fact that the observed fluctuations in the μ-meson flux are not greater than the theoretically predicted fluctuations due only to the altitude fluctuations in EAS indicates a small role of fluctuations in the development of EAS with a large number of particles ($N > 10^6$).

Calculations carried out by Fukui et al[3] and in the present article show that, if EAS develop without fluctuations, the distribution with respect to the μ-meson number n_μ in a shower with a given number of particles is very sensitive to the quantity $\epsilon = (\Lambda + B)/\lambda - \gamma - 1$. The values of Λ and γ are well-known, and therefore the magnitude λ of the interaction mean free path of primary particles follows from the exact shape of the distribution with respect to n_μ. Thus, the study of the exact form of the distribution of μ mesons in EAS with a known number of particles enables us to determine the interaction mean free path of primary ultra-high energy particles producing the EAS. Furthermore, in order to obtain the exact distribution of the μ-meson flux, it is necessary to increase the accuracy of the experimental method. This involves the use of large-

area μ-meson detectors located at several points, the distance between which should be sufficiently large in order to determine the role of fluctuations in the μ-meson lateral distribution function; and also the exact determination of the distance between the μ-meson detectors and the shower axis, etc.

In conclusion, the authors would like to thank I. P. Ivanenko for discussing the results, and also the workers of Moscow State University who took part in the measurement and analysis of the results: K. I. Solov'ev, V. Sokolov, E. Shein, V. Putintsev, I. Vasil'chikov, V. Nazarov, G. Degtyareva, N. Proshina, and I. Massal'skaya.

[1] N. L. Grigorov and V. Ya. Shestoperov, JETP **34**, 1539 (1958), Soviet Phys. JETP **7**, 1061 (1958).

[2] T. E. Cranshaw and A. M. Hillas, Proc. Cosmic Ray Conf. IUPAP, Moscow, 1959, vol. II, p. 231.

[3] Fukui, Hasegawa, Matano, Miura, Oda, Ogita, Suga, Tanahashi, and Tanaka, ibid., p. 31.

[4] Vernov, Khristiansen, Abrosimov, Goryunov, Dmitriev, Kulikov, Nechin, Sokolov, Solov'eva, Solov'ev, Strugal'skii, and Khrenov, ibid., p. 5.

[5] Abrosimov, Goryunov, Dmitriev, Solov'eva, Khrenov, and Khristiansen, JETP **34**, 1077 (1958), Soviet Phys. JETP **7**, 746 (1958).

[6] Cranshaw, de Beer, Galbraith, Porter, and Hillas, Nuovo cimento **8**, Suppl., 567 (1958).

[7] A. G. Worthing and J. Geffner, Treatment of Experimental Data, Wiley, N.Y., 1943.

[8] B. Rossi, Proc. Cosmic Ray Conf. IUPAP, Moscow, 1959, vol. II, p. 17.

Translated by H. Kasha
69

THE FERMI SURFACE OF LEAD

N. E. ALEKSEEVSKII and Yu. P. GAĬDUKOV

Institute for Physics Problems, Academy of Sciences, U.S.S.R.

Submitted to JETP editor March 22, 1961

J. Exptl. Theoret. Phys. (U.S.S.R.) 41, 354-362 (August, 1961)

A detailed study of the galvanomagnetic properties of single crystal lead is carried out. From the experimental data the Fermi surface could be established and is found to be double sheeted: one part of the Fermi surface is an open surface of the "fluted cylinder net" type, the axes of the cylinders being parallel to the [111] crystallographic axis; the other part is a closed surface. The volumes of the open and closed surfaces are equal and opposite in sign (the closed surface corresponds to "hole" conductivity). The model proposed for the Fermi surface of lead is compared with the experimental results on the de Haas–van Alphen effect, known from the literature.

A preliminary study of the anisotropy of the resistivity of single crystals of lead in the range of large magnetic fields showed that lead has an open Fermi surface.[1,2] An open Fermi surface for metals with cubic lattice symmetry can only be a surface of the "fluted cylinder space net" type, with axes parallel to rational axes of the reciprocal lattice. Such surfaces were found in copper,[3] gold and silver.[2,4]* It would be expected that the Fermi surface of lead would also be a "space net." The anisotropy of the galvanomagnetic properties would then be similar to that in gold, silver and copper. However, on the polar diagram of the resistance of lead in a magnetic field there are wide angular ranges with quadratic growth of resistance, and saturation of the resistivity in a magnetic field is only found in some selected directions. (This behavior of the resistivity of lead single crystals is the opposite of the resistance behavior of gold, silver and copper.)

It was established previously that the quadratic resistance growth in a wide range of directions for tin single crystals is connected with the compensation of the "electron" and "hole" volumes of the Fermi surface.[6] An analogous "compensation" can therefore be expected for the Fermi surface of lead.

The purpose of the present work was to determine the topology of the Fermi surface of lead. Lead is also of interest in that the de Haas–van Alphen effect has been studied in most detail for this metal.[7,8] It was therefore possible to compare the results of two different methods of studying the Fermi surface of metals.

SPECIMENS AND MEASUREMENTS

The lead single crystals, grown by the Czochralski method, were 20 — 30 mm long and 2 — 3 mm in diameter. In some cases specimens of the required orientation were in plate form. Such specimens were cut by electro-erosion from a large single crystal obtained by the Obreimov-Shubnikov method. The orientation of the round single crystals was determined optically with an accuracy of 1°. The orientation of the plates was determined by x rays. The resistivity change of the specimens from room temperature to 4.2° K was $\rho_{300}/\rho_{4.2} = 6{,}000 - 10{,}000$, so that measurements could be made in large effective fields, starting at about 1 koe ($\rho_{4.2}$ was determined by extrapolating the $\rho_{4.2}(H)$ dependence to zero magnetic field).

The measurements were carried out at 4.2° K with a potentiometer system having a sensitivity of 10^{-9} v. The angular dependence of the resistivity and the Hall e.m.f. were determined in a field of 23 koe. The magnetic field was rotated in a plane perpendicular to the specimen axis. The Hall e.m.f. was measured both on the plates and on the round specimens. In the latter case the Hall e.m.f. was taken off at two pairs of mutually

*We must point out that we are discussing the topological features, and not the form of the Fermi surface, which are not the same at all![5] For example, the Fermi surface of copper is a system of cubes, the vertices of which intersect in such a way that the "openness" arises in the [001] and [110] directions as well as [111]. For galvanomagnetic properties, the topology of such a surface is equivalent to a "fluted cylinder space net" with axes parallel to the directions [111], [110] and [001]. These are precisely the topological features that show up in the galvanomagnetic properties of gold, silver and copper.

Specimen Pb	Orientation* φ; ϑ′, deg	$\rho_{300}/\rho_{4.2}$	Position of the minima and maxima (in degrees) on the $\rho_H(\vartheta)$ diagrams**
1	[001]	8000	[010] (13) ***; [110] (1)
2	0; 10		0 (6); ± 41 (1.1); ±43 (1.5); ± 45 (1); ± 47 (1.5); ±49 (1.1); ± 90 (5.5)
3	0; 14		0 (4); ± 44 (1,2); ± 47 (1,5); ±49 (1); ±90 (5)
4	0; 20		0 (3.7); ± 30 (2); ±40 (2,3); ±52 (1); 90 (4,5)
5	0; 27	7150	0 (6); ± 25 (3,2); ± 38 (4); ± 51 (1); ± 90 (7.5)
6	0; 31		0 (4,3); ± 3 (4.5); ± 19(3.2); ± 53 (1); ± 90 (6.6)
7	0; 35		0 (1.6); ± 16 (3,2); ± 52 (1); ± 90 (5)
8	[011]	9400	[01$\bar{1}$] (1); ± 20 (10.5); [2$\bar{1}$1] (1); [100] (15,5)
9	45; 6		0 (1.2); ± 45 (6); ± 90 (1)
10	45; 10	9900	0 (1); ± 3 (4); ± 6 (2); ± 45 (17); ± 90 (1,3)
11	45; 16		0 (6,5); ± 2 (8,5); ± 9 (4); ± 43 (20); ± 90 (1)
12	45; 37	10800	0 (8); ± 5 (8.5); ± 23 (3); ± 48 (9); ± 60 (8); ± 72 (9); ± 90 (1)
13	45; 41	8500	0 (8); ± 15 (9); ± 25 (2,5); ± 32 (5.5); ± 36 (4); ± 40 (9.5); ± 90 (1)
14	40; 45	6050	0 (5); + 14 (5.8); + 27 (2); + 34 (3,5); + 36 (2,7); + 48 (6); — 86 (1); — 44 (6); — 23 (1,4); — 10 (5.5);
15	[111]		[112] (4.5); ± 16 (5,5); [011] (1)
16	43; 64		0 (4.8); + 12 (5.5); + 22 (3); + 26 (3.5); + 34 (1,3); + 88 (1)
17	45; 80	10800	0 (12.5); ± 34 (1); ± 72 (8); ± 90 (1)

*φ and ϑ′ are the polar coordinates of the specimen axes: φ is measured from the (010) or (100) plane; ϑ′ is the angle between the [001] axis and the specimen axis.

**The direction of the line of intersection of the plane of rotation of the magnetic field with the plane passing through the specimen axis and the [001] axis is chosen as $\vartheta = 0$.

***The ratio of the resistance for the given direction to the resistance in the deepest minimum is given in parentheses.

perpendicular contacts, placed on a transverse section of the specimen. The table shows data on the specimens.

EXPERIMENTAL RESULTS*

Some characteristic angular dependences of the resistance $\rho_H(\vartheta)$, where ϑ is the angle of rotation of the magnetic field, are shown in Fig. 1. The $\rho_H(\vartheta)$ dependence for the specimen Pb-1 was given previously.[2] One can gain a qualitative idea of the nature of the resistance anisotropy from the table.

Figure 2 shows characteristic examples of the behavior of the resistance in a magnetic field for different directions. A marked anisotropy is also observed in the behavior of the Hall e.m.f. (Fig. 3), and on the $E_x(\vartheta)$ diagrams narrow maxima, which are observed for $\mathbf{H} \parallel [110]$ are characteristic. The principal variations of Hall e.m.f. with magnetic field are shown in Fig. 4.

As mentioned above, a quadratic growth of resistance in a magnetic field is observed over a wide range of angles [broad maxima on the $\rho_H(\vartheta)$ diagrams]. Saturation of the resistance is only observed in special directions, for example for $\mathbf{H} \parallel [110]$, $\mathbf{H} \parallel [112]$ with $\mathbf{I} \parallel [011]$. For these magnetic field directions narrow deep minima appear on the $\rho_H(\vartheta)$ diagrams. All the directions for which narrow minima are observed are plotted on the stereographic projection (Fig. 5). The depth of the narrow minima of resistance (except those corresponding to $\mathbf{H} \parallel [110]$) depends on the current orientation. For example, with $\mathbf{I} \parallel [111]$ a broad maximum of resistance is found in the region of the [112] direction, and $\rho \sim H^2$. This made it essential to make an analysis of current diagrams, which enabled the cause of the quadratic growth and saturation of the resistance to be explained, and made it possible to determine the direction of the open sections of the Fermi surface.

As has already been noted,[6] three types of current diagram $\rho_H(\alpha)$ are possible in the general case; α is the angle between the current and the mean direction of the open sections of the Fermi surface or of some crystallographic direction ($\mathbf{I} \perp \mathbf{H}$).

1. If in some direction of the magnetic field there are no open sections of the Fermi surface, but there is compensation of the "electron" and "hole" volumes of the Fermi surface, $V_{el} = V_{hole}$, then for any angle α the resistance increases quadratically with field: $\rho \sim H^2$.

2. If for some direction of H there are no open sections of the Fermi surface, but $V_{el} \neq V_{hole}$, then the resistance in a magnetic field reaches

*The authors thank A. P. Kir'yanov who made the measurements on a number of specimens.

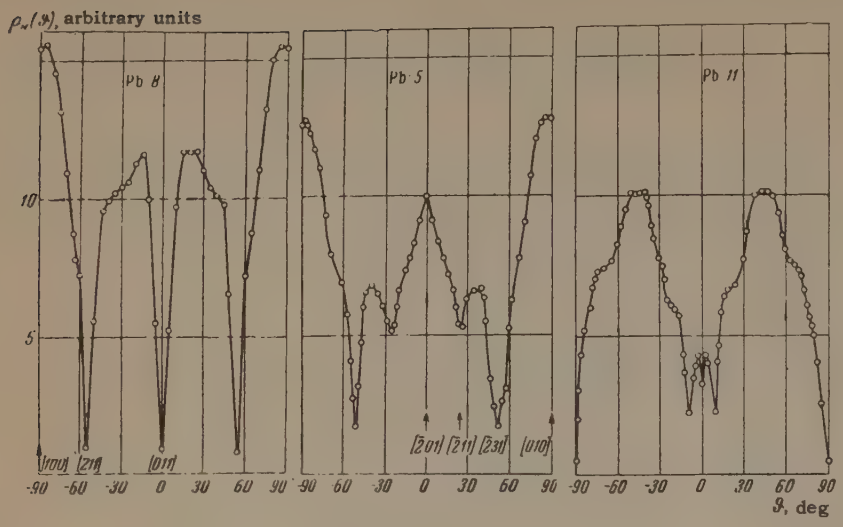

FIG. 1. The anisotropy of the resistance of single crystals of lead; H = 23 koe, T = 4.2°K.

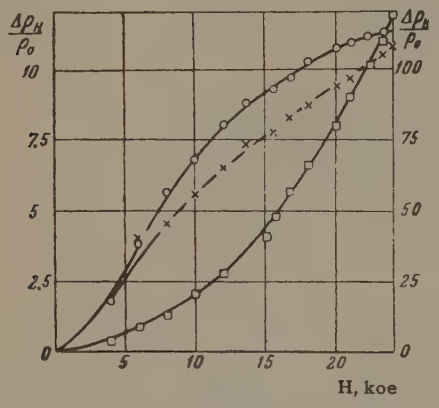

FIG. 2. The change of resistance in a magnetic field for specimen Pb-8 for various values of the angle ϑ: ○ – ϑ = 0°, × – ϑ = 55° (left ordinate scale); □ – ϑ = 90° (right ordinate scale).

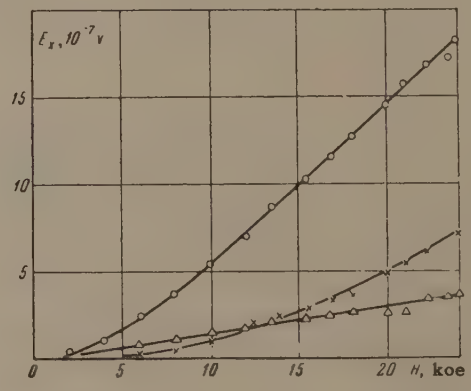

FIG. 4. Dependence of the Hall e.m.f. on the magnitude of the magnetic field for a fixed angle ϑ for specimen Pb-8 (I = 3 amp): ○ – ϑ = 0°, × – ϑ = 55°, Δ – ϑ = 90°.

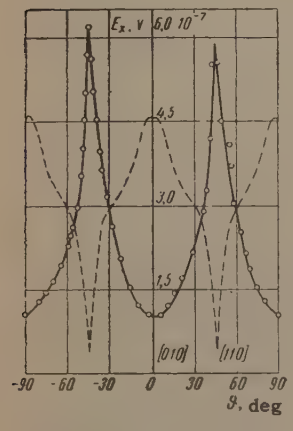

FIG. 3. Anisotropy of the Hall e.m.f. for specimen Pb-1 (specimen diameter 1.8 mm); H = 22 koe, T = 4.2°K, I = 1 amp. For comparison, the angular dependence of the resistance is shown in the figure (dashed curve).

saturation for any α (the resistance behaves in a similar way if there are open sections with a different mean direction).

3. If for a given direction of the magnetic field, there is a layer of open sections of the Fermi surface with a single mean direction, then

$$\rho_H(\alpha) = AH^2\cos^2\alpha + B.$$

An analysis of the experimental angular dependences $\rho_H(\vartheta)$ shows that a current diagram of the first type is met in wide ranges of directions of the magnetic field, grouped round the [001] and [111] axes. The second type of current diagram only occurs for the [110] direction. For direction of H lying in the (111) planes, for which an analysis could be carried out, the current diagrams had a form close to a $\cos^2\alpha$ dependence.

It is natural to suggest that any direction of the magnetic field lying in the (111) planes (except directions near [110]) will have this property. This is borne out by the fact that the narrow minima of resistance lie mainly in the (111) planes. We can thus consider that the directions of the narrow minima are those field directions for which open sections of the Fermi surface exist. The stereographic projection of the narrow minima is, therefore, in fact the projection of the singular directions of the magnetic field for an open Fermi surface of lead. This projection is shown in the upper part of Fig. 5. The dimensions of the two dimensional regions around the [110] direction could be determined very approximately from the disappearance of the minima of resistance in the

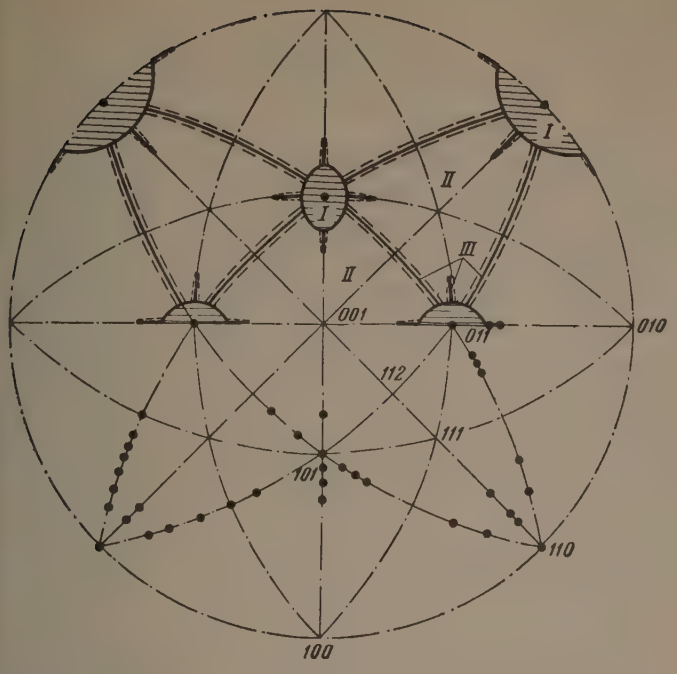

FIG. 5. Stereographic projection of the directions of the narrow minima of resistance (lower half) and of the singular magnetic field directions for the Fermi surface of lead (upper half). Region I – double regions of magnetic field directions for which open sections exist (the thickness of the layer of open sections is zero at the edges of the regions I and in the direction [110]); there are no open sections for regions II, but there is compensation of the "electron" and "hole" volumes: $V_{el} = V_{hole}$; there are considerably drawn out closed sections for the regions III. Open trajectories are only found for those directions of the magnetic field which lie on the "whiskered" lines.

(111) planes as the plane of the magnetic field approached the [110] direction: the diameter of the region is $(20 \pm 2)^\circ$ in the (001) plane; $(14 \pm 2)^\circ$ in the (110) plane; in the (001) and (110) planes the minima of resistance exist at distances somewhat greater than the dimensions of the double region. This feature, which has been studied in detail earlier,[6] is connected with the fact that for rational planes, open sections of the Fermi surface can exist beyond the limits of the double region. There are, therefore, "whiskers" on the projections of the singular directions of H for open sections of the Fermi surface of lead. The ends of the "whiskers" are 15° from the center of the double region.

THE FERMI SURFACE OF LEAD

The stereographic projection of the singular magnetic field directions (Fig. 5) corresponds to a Fermi surface of the "fluted cylinder space net" type, with axes parallel to the [111] directions. Such a surface is one of the simplest possible for metals with cubic lattice symmetry. The diameter of the "cylinders" (assuming that there is some mean constant diameter[9]) can be calculated from the dimensions of the double region on the projection. This "diameter" is (0.18 ± 0.03)b, where b is the period of the reciprocal lattice of lead in the [001] direction, $b = 2(2\pi/a)$, $a = 4.9$ A.

In order to explain the compensation of volumes, which is observed when the magnetic field direction lies in the regions II of the stereographic projection, it must be assumed that the Fermi surface of lead is double sheeted, and it must consist of at least two parts equal in volume and opposite in sign. There are, in general, two possibilities: either both parts are open surfaces, or one is open and the other closed. The second possibility is more likely, since the combination of two open surfaces could hardly give such a simple stereographic projection of the singular magnetic field directions as was found for lead.

Taking one of the surfaces to be closed, we can decide whether it refers to holes or to electrons. For this purpose the sign of the Hall constant for $H \parallel [110]$ must be determined. The sign of the Hall constant is in this case determined by the sign of the closed surface. The sign of the Hall constant found experimentally corresponds to a "hole" surface. The open surface is, correspondingly, electronic.

Some mean diameter d_m of the "fluted cylinders," which form the open Fermi surface of lead, can be determined from the value of the Hall constant R in the [110] direction. For this we use equations (33) and (34) of the paper by Lifshitz and Peschanskii.[9] For the present case the equations can be written in the following form:

$$R_{[011]} = 1/\Delta nec,$$
$$\Delta n = 2h^{-3}(V_{tot} - 0.7b^2 d_m),$$
$$V_{tot} = V_{el} - V_{hole}.$$

As $V_{el} = V_{hole}$ for the Fermi surface of lead, $\Delta n = \pm 1{,}4\, h^{-3} b^2 d_m$. The Hall constant $R_{[110]} = 4.3 \times 10^{-3}$ cgs emu, determined from experiment, leads to the value $d_m \approx 0.16$b, which agrees well with the value found before from the dimensions of the double region of the stereographic projection.

Knowing d_m, the volumes of the open and closed parts of the Fermi surface of lead can be found. With $d = 0.17$b, the volume of the open surface $V_{el} = 0.11\, b^3$. Assuming that the closed surface is a sphere, the radius of this sphere $r \approx 0.3$b. A model of the surface of lead, which does not contradict the experimental results is shown in Fig. 6.

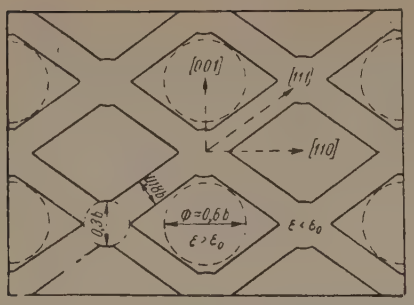

FIG. 6. Section of the Fermi surface of lead by the (110) plane (schematic).

COMPARISON OF THE RESULTS OBTAINED WITH DATA FROM THE DE HAAS–VAN ALPHEN EFFECT

Shoenberg first observed the de Haas–van Alphen effect in lead, using a pulse method to measure the susceptibility in high magnetic fields.[7] Gold later studied the effect in detail.[8]* He was able to propose a model of the Fermi surface from the results obtained, which consists of several parts. One part of the surface is open and other parts of the surface are closed. However, the open surface does not have open sections, and cannot therefore accord with the galvanomagnetic properties of lead. It is thus interesting to analyze Gold's experimental data directly and compare them with the model of the Fermi surface derived from the data of the present work.

Figure 7 shows the periods of oscillation of the susceptibility, observed in Gold's experiments. It can be seen that the periods fall into three groups: α, β, and γ. Gold notes that the short-period α oscillations show insignificant anisotropy of the period for all directions of the magnetic field: the β oscillations have weak anisotropy; roughly the same for all planes containing the [001] axis. The disappearance of the β oscillations for an inclination of the magnetic field 25° from the [001] axis is a characteristic here. The long period group of γ oscillations consists of several branches, showing considerable anisotropy of periods.

Comparing these results with the Fermi surface shown in Fig. 6, it is natural to relate the β oscillations with the closed "hole" surface, as does Gold. The closed surface has, in fact, the largest area of diametral section. The oscillations connected with the closed surface must, therefore, have the shortest period (since the period of the oscillations $P = \Delta(1/H) = 4\pi e/chS_m$, where S_m is the extremal cross-section of the Fermi surface). Knowing the mean dimensions of the closed surface, we can deduce that the corresponding period of the susceptibility oscillations will be $P_\alpha \approx 0.54 \times 10^{-8}$ oe^{-1}, which is in good agreement with Gold's data: $P_\alpha = 0.56 \times 10^{-8}$ oe^{-1}.

The β and γ oscillations can be related to the maximal and minimal sections respectively of the open Fermi surface of lead. The region where four "cylinders" cross one another has the maximal section. When the magnetic field is inclined to the [001] axis these sections increase, leading to a reduction in the corresponding period of oscillations. For some angular distance from the [001] axis, the oscillations of this type disappear. This occurs near those directions of the magnetic field for which open sections of the Fermi surface occur (the thick lines in Fig. 5).

For example, if the magnetic field lies in the (001) plane, the maximal closed section (and, correspondingly, the β oscillations) disappear for an angle of 30° between the field and the [001] axis. There is thus qualitative agreement with Gold's results. It is, however, difficult to make a quantitative calculation for this case. We only note that if the volume of a sphere is deduced from the period of the β oscillations (diameter ~ 0.3 b), then this volume agrees approximately with the volume of the region where the "cylinders" of the open Fermi surface cross.*

The γ oscillations can be ascribed to the minimal sections of the open Fermi surface, i.e., to the sections of the four "cylinders" parallel to the [111] direction. In the general case four sections of different area are possible. All four sections coincide for $\mathbf{H} \parallel [001]$. Taking the diameter of the cylinders equal to 0.17 b, we find that $P_{\gamma[001]} \approx 3.6 \times 10^{-8}$ oe^{-1}. According to Gold's data $P_{\gamma[001]} = 4.1 \times 10^{-8}$ oe^{-1}. Assuming that these periods coincide for [001], we can compare the form of the anisotropy of the γ oscillations with the periods of the oscillations possible for the minimal sections of the "cylinders." The behavior of the anisotropy of the periods of the

*We should also point out that Harrison[10] has recently studied the Fermi surface of lead theoretically.

*We must point out two facts. 1) One concludes from the model of the Fermi surface of lead that β oscillations should exist in the region of the [111] direction as well as the [001] direction (the former direction is also far from directions which lead to open sections). In Gold's work there is no indication of oscillations in this region with a period close to the period of the β oscillations. 2) As soon as open sections of the Fermi surface arise, new closed "hole" sections also arise. It can easily be seen from Fig. 6 that the area of these sections exceeds not only the areas of the sections connected with the β oscillations, but also the areas referring to the α oscillations. Gold's data to not indicate the existence of such large sections.

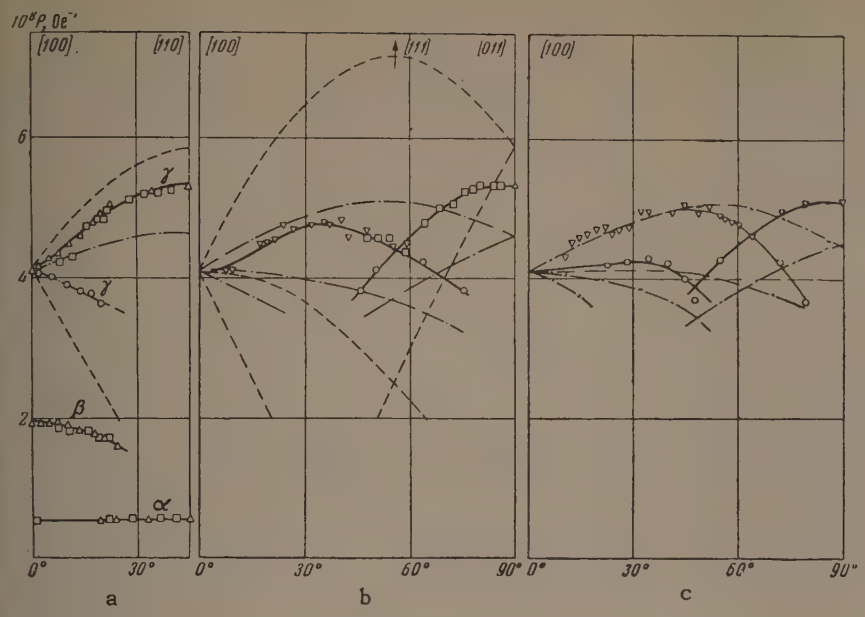

FIG. 7. Periods of oscillations of the susceptibility of lead, found by Gold.[8] The continuous lines are drawn through Gold's experimental points. Case a – $\mathbf{H}\|(001)$, b – $\mathbf{H}\|(0\bar{1}1)$, c – the field parallel to the plane, the normal to which has the orientation [$\varphi = 30°$, $\vartheta = 90°$]. The periods for the α and β oscillations are not shown for cases b and c.

oscillations corresponding to the open Fermi surface of lead is shown by the dotted line (these curves are not shown in Fig. 7c). It can be seen from the figure that there is some qualitative agreement in behavior of the calculated and observed periods of the γ oscillations.

The collapse in the γ oscillations (and also of the β oscillations) for some directions of the magnetic field, associated with the appearance of open sections, is most characteristic. It must be remarked, nevertheless, that there are great quantitative discrepancies in the behavior of the anisotropy of the calculated and observed periods of the γ oscillations. This is not surprising, however, since it was assumed in the calculation that the open Fermi surface is formed by right cylinders. If we make the natural assumption that the cylinders are corrugated, we can obtain better agreement with Gold's data. For example, for corrugation of the cylinders produced by part of an ellipsoidal surface of revolution with axes in the ratio 3:2 (the long axis parallel to the [111] axis), the picture of the behavior of the anisotropy of the γ oscillations is shown in Fig. 7 by the dashed line.

In conclusion, we consider it a pleasure to thank Academician P. L. Kapitza for his constant interest in this work.

[1] N. E. Alekseevskii and Yu. P. Gaĭdukov, JETP **36**, 447 (1959), Soviet Phys. JETP **9**, 311 (1959).

[2] N. E. Alekseevskii and Yu. P. Gaĭdukov, JETP **37**, 672 (1959), Soviet Phys. JETP **10**, 481 (1960).

[3] A. B. Pippard, Phil. Trans. Roy. Soc. **A250**, 325 (1957).

[4] Yu. P. Gaĭdukov, JETP **37**, 1281 (1959), Soviet Phys. JETP **10**, 913 (1960).

[5] J. R. Klauder and J. E. Kunzler, Phys. Chem. Solids **18**, 256 (1961).

[6] Alekseevskii, Gaĭdukov, Lifshitz, and Peschanskii, JETP **39**, 1201 (1960), Soviet Phys. JETP **12**, 837 (1961).

[7] D. Shoenberg, Physica **19**, 791 (1953).

[8] A. V. Gold, Phil. Trans. Roy. Soc. **A251**, 85 (1958).

[9] I. M. Lifshitz and V. G. Peschanskii, JETP **35**, 1251 (1958), Soviet Phys. JETP **8**, 875 (1959).

[10] W. A. Harrison, Phys. Rev. **118**, 1190 (1960).

Translated by R. Berman
70

RECOMBINATION RADIATION OF CESIUM PLASMA IN A HOMOGENEOUS MAGNETIC FIELD

Yu. M. ALESKOVSKII and V. L. GRANOVSKII

Moscow State University

Submitted to JETP editor March 20, 1961

J. Exptl. Theoret. Phys. (U.S.S.R.) **41**, 363-367 (August, 1961)

The recombination radiation from cesium vapor plasma in a longitudinal magnetic field was investigated by spectrophotometric means. It was found that recombination emission is enhanced considerably with increasing field strength and diminishing gas pressure. This increase is due mainly to higher concentration of charge carriers near the column axis and, to a smaller degree, to decreasing electron temperature.

INTRODUCTION. STATEMENT OF THE PROBLEM

A homogeneous magnetic field H_z parallel to the positive column of a low-pressure gas discharge reduces the diffusion of charge carriers from the plasma to the walls.[1] The mean lifetime τ of free carriers in the plasma should thus be lengthened. Consequently, when the current strength i in the column is maintained unchanged, the average concentration of free electrons and ions n_e should increase, while the electron temperature T_e and the longitudinal electric field strength E_z should be reduced.[2] These conclusions are confirmed by probe measurements in helium.[3]

The longer lifetime τ in a field H_z should also increase the probability of volume recombination in the plasma,[4,5] which can then possibly exceed surface recombination on the walls. This effect should be manifested externally by enhanced intensity I of recombination radiation from the plasma. However, in investigations of recombination radiation from cesium plasma in a longitudinal magnetic field, Davies[6] found that, contrary to expectations, application of the field produces almost no changes in I and n_e, while T_e is increased slightly instead of being decreased.

We have performed a new investigation of recombination radiation from cesium plasma,* in order to check the foregoing hypotheses regarding the influence of a magnetic field on the probability of volume recombination. We aimed to determine the influence of the magnetic field on the intensity of electron recombination in an electropositive gas and also on the concentration and temperature of electrons in the plasma.

*E. Mikhalets assisted with some of the experimental work.

EXPERIMENTAL CONDITIONS AND TECHNIQUE

Spectrophotometric measurements were obtained for one of the recombination bands, the 6P "series limit continuum," in cesium vapor plasma. For a Maxwellian velocity distribution of the plasma electrons the spectral intensity distribution in the investigated band is given by Mohler and Boeckner[7,8] as

$$I(\nu) = \text{const} \cdot n_e^2 T_e^{-3/2} \nu^{-1} \exp[-h(\nu - \nu_1)/kT_e],$$

where ν_1 is the frequency limit of the levels at which free electrons are captured. The electron temperature and concentration in the plasma were determined from this relation.

A stationary plasma was produced in a discharge tube 40 cm long and 2.5 cm in diameter. A cylindrical probe along the tube axis was used to measure plasma parameters, simultaneously with the optical measurements. The cesium vapor pressure varied from 2×10^{-3} to 0.13 mm Hg. The tube was placed in a homogeneous magnetic field generated by two solenoids that were separated by a gap through which the central portion of the tube was focused on a UM-2 monochromator. A photomultiplier was used to detect the radiation.

Photometric measurements were performed at several points of the recombination continuum, from its threshold at 4940 A to 4400 A. A standard temperature-calibrated tungsten lamp was used to record the spectral characteristic of the photomultiplier for this region.

The measured spectral distribution was appreciably distorted, especially at low pressures, by the bright Cs doublet $8P_{1/2,3/2} - 6S_{1/2}$, which was scattered in the optical system and was superposed on the recombination band at the monochro-

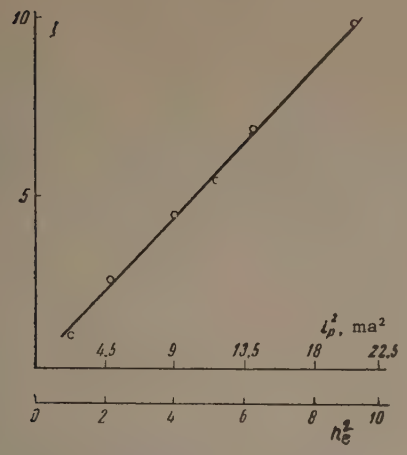

FIG. 1. Recombination radiation as a function of electron concentration. $p = 2.8 \times 10^{-2}$ mm Hg. H = 0.

mator exit. The doublet was excluded as follows. At the lowest values of the pressure and current density, when volume recombination in the plasma can practically be neglected, the intensity distribution was measured in the studied spectral interval; under these conditions the spectrum is determined completely by the scattered light. This distribution does not depend on the discharge conditions, which affect only the intensity of the doublet. Therefore the measured intensity of one of the cesium lines can be used under different discharge conditions to compute the scattered light intensity for any spectral region, thus permitting suitable correction of the recombination radiation measurements.

The spectral function $I(n_e)$ was recorded as a check to determine whether our measurements actually represented recombination radiation. The relative electron concentration was determined by measuring i_p, the ion current to the probe. n_e was varied by changing the discharge current i. Figure 1 shows the result $I \sim n_e^2$, as was to be expected for radiative recombination in two-body collisions.

BASIC EXPERIMENTAL RESULTS

1. The imposition of a magnetic field on a plasma enhances considerably the intensity I of recombination radiation (see the table), especially at low pressures. The simultaneous constriction of the positive column is observed; this effect is magnified, as expected,[9,10] with reduced cesium pressure and with growth of the factor $\omega_e\tau_e\omega_p\tau_p$ determining the effect of the magnetic field on the plasma.

2. The electron temperature T_e was determined from the slopes of the straight-line plots of $\ln [\nu I(\nu)]$ vs ν (Fig. 2). The straight line provide evidence of a Maxwellian electron distribution. The table gives values of T_e at different cesium pressures and in different magnetic fields. The table also includes values of T_e derived from probe measurements at H = 0, and the relative electron concentrations $n_e(H)/n_e(0)$ obtained from optical measurements. The last column gives the measured relative density of the ion current to the probe, $j_p(H)/j_p(0)$. A comparison of the fourth and fifth columns, and of the sixth

Pressure, 10^{-3} mm Hg	H, oe	$I(H)/I(0)$	T_e, °K: From spectrum	T_e, °K: From probe current	$n_e(H)/n_e(0)$	$j_p(H)/j_p(0)$
82	0	1		4200	1	1
	330	17			4.1	3.7
	660	38			6.0	5.7
	980	54			7.3	6.9
18	0	1	3700	3600	1	1
	330	2.6	3300		1.6	1.5
	660	4.8	3070		2.2	2.0
	980	7.3	3040		2.7	2.55
	1300	8.4	2550		2.9	3.08
36	0	1	3080	2900	1	1
	330	1.32	2850		1.14	1.18
	660	1.83	2800		1.33	1.35
	980	2.36	2670		1.49	1.53
	1300	2.64	2500		1.56	1.74
74	0	1	2640	2700	1	1
	330	1.19	2580		1.09	1.12
	660	1.28	2470		1.12	1.2
	980	1.37	2450		1.15	1.3
	1300	1.3	2370		1.12	1.35
130	0	1	2420	2100	1	1
	330	1.07	2440		1.03	1.07
	660	1.09	2410		1.04	1.08
	980	1.08	2400		1.04	1.08
	1300	0.98	2360		1.0	1.09

The data are given for the discharge current density $j = 0.5$ amp/cm^2.

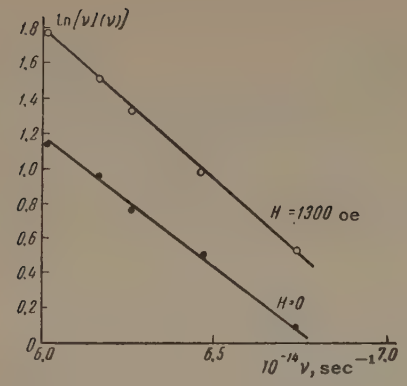

FIG. 2. Graphs used to determine the electron temperature T_e at $p = 36 \times 10^{-3}$ mm Hg.

and seventh columns, shows completely satisfactory agreement between the optical and probe measurements; the discrepancies lie within the limits of experimental error.

The table shows that the concentration n_e grows with increase of H_z for a given current strength; the effect becomes more pronounced as the gas pressure is reduced. On the other hand, the electron temperature T_e drops; this effect is also more pronounced as the pressure is reduced. When the pressure was raised to 0.13 mm we observed practically no influence of magnetic fields up to 1300 oe.

DISCUSSION OF RESULTS. CONTROL EXPERIMENTS

1. Our results agree with the previously derived[4,5] increase, in a magnetic field, of the fraction of charged particles disappearing from the plasma through volume recombination. The lowering of the temperature T_e and the enhanced axial concentration of charged particles in the magnetic field agrees with diffusion theory.

2. The enhancement of recombination radiation in a plasma subjected to a magnetic field is associated a) with the constriction of the positive column and the consequently increased concentration of charged particles along the discharge axis, and b) with the lowered electron temperature resulting in a larger recombination coefficient. A calculation shows that the second cause does not account for more than 10% of the observed enhancement of recombination radiation.

3. In analyzing the causes of the discrepancy between our results and those of Davies[6] obtained in the same range of cesium pressures, considerable differences in the diameter of the positive column and in the discharge current density must be noted. In Davies' investigation the diameter was one-fifth of ours, while the current density was one order of magnitude greater than in our experiments.

The effect of the latter circumstance was checked by performing measurements at different densities of the discharge current j. The measurements of T_e given in Fig. 3 show a diminishing

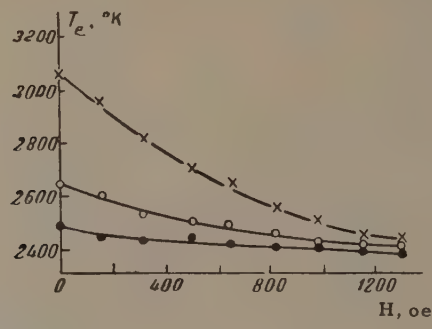

FIG. 3. Electron temperature vs magnetic field at different current densities. × – j = 0.2 amp/cm²; ○ – j = 0.3 amp/cm²; ● – j = 0.5 amp/cm². p = 0.13 mm Hg.

influence of the magnetic field on T_e as the current density increases. A similar conclusion follows from the data for the recombination radiation intensity and the charged particle concentration at $p = 0.2 \times 10^{-2}$ mm and H = 1300 oe:

j, amp/cm²	0,2	0.3	0.4	0,5	0,6	0,7	0,8	1,0
$I(H)/I(0)$:	20	18,5	14,2	11,5	8.8	5.7	3,8	2.9
$n_e(H)/n_e(0)$	4.4	4.0	3,6	3,2	2.8	2.25	1.74	1.64

The high current density (5 amp/cm²) probably prevented Davies from observing the enhancement of recombination radiation and other effects induced by a magnetic field in a discharge with low current density. At the high degree of gas ionization (some tens percent) that characterized Davies' experiments, the electron and ion diffusion rates evidently depended on their Coulomb interaction rather than on collisions with neutral atoms. When electron-ion collisions are taken into account the flux of charged particles to the walls in directions normal to the magnetic field is given by[11]

$$\Gamma_\perp = -\frac{D_a^0 \nabla n}{1 + \omega_e \omega_p / \nu_{pa} (\nu_{ea} + \nu_{ep})},$$

where D_a^0 is the coefficient of ambipolar diffusion at H = 0, ω_e and ω_p are the Larmor frequencies of electrons and ions, and ν_{pa} etc. are the frequencies of collisions between ions and atoms, electrons and atoms etc. The frequency of electron-ion collisions is

$$\nu_{ep} = \frac{4}{3}\sqrt{2\pi}\,\Lambda n\,(e^2/kT_e)^2\,(kT_e/m)^{1/2},$$

where $\Lambda = \frac{3}{2}\ln(3kT_e/2\sqrt{2}\,\pi^{1/3}e^2 n^{1/3})$ is the Cou-

lomb logarithm. Calculations performed subject to the conditions obtaining in Davies' experiments, i.e., $p = 10^{-2}$ mm, $H = 1000$ oe, and $n = 10^{13}$ cm^{-3} (corresponding to ~ 10% cesium ionization) lead to a value of ν_{ep} that is one order of magnitude greater than ν_{ea}. This gives the ratio $\omega_e\omega_p/\nu_{pa}(\nu_{ea} + \nu_{ep}) \approx 0.1$, so that there is only a small reduction of charged particle flux to the walls in a magnetic field. Under the conditions of Davies' experiments we can therefore not expect any appreciable influence of the magnetic field on the electron parameters and recombination processes in a plasma.

[1] J. S. Townsend, Phil. Mag. **25**, 459 (1938).

[2] L. Tonks, Phys. Rev. **56**, 360 (1939).

[3] R. J. Bickerton and A. von Engel, Proc. Phys. Soc. (London) **B69**, 468 (1956).

[4] I. A. Vasil'eva, Radiotekhnika i Elecktronika (Radio Engineering and Electron Physics) No. 12, 2015 (1960).

[5] A. S. Syrgii and V. L. Granovskii, ibid. **5**, 1522 (1960).

[6] L. W. Davies, Proc. Phys. Soc. (London) **B66**, 33 (1953).

[7] F. Mohler and C. Boeckner, Bur. Standards J. Research **2**, 489 (1929).

[8] F. Mohler, ibid. **10**, 771 (1933).

[9] O. Repkova and G. Spiwak, J. Phys. (U.S.S.R.) **9**, 222 (1945).

[10] E. Reikhrudel' and G. Spivak, JETP **10**, 1408 (1940).

[11] V. E. Golant, J. Tech. Phys. (U.S.S.R.) **30**, 881 (1960), Soviet Phys.-Tech. Phys. **5**, 831 (1961).

Translated by I. Emin
71

AN EFFICIENT HIGH-CURRENT MICROTRON

S. P. KAPITZA, V. P. BYKOV, and V. N. MELEKHIN

Physics Laboratory, Institute for Physics Problems, Academy of Sciences, U.S.S.R.

Submitted to JETP editor March 28, 1961

J. Exptl. Theoret. Phys. (U.S.S.R.) 41, 368-384 (August, 1961)

The construction of a high-current microtron is described, in which electrons are accelerated to 6 — 13 Mev, the pulse currents being 20 — 5 ma. The operation of an efficient lanthanum boride thermionic cathode in the rf field of the accelerating resonator is studied. The efficiency of the accelerator is estimated, and its principal calculated and experimentally confirmed parameters are presented.

1. INTRODUCTION

THE electron cyclotron, which is a cyclic accelerator of relativistic particles in a constant magnetic field and at constant frequency of the accelerating voltage, was first suggested by Veksler.[1] The earliest electron accelerators constructed on the new principle[2-4] were inefficient, and interest in microtrons, as these electron accelerators were subsequently called, disappeared during the rapid development of linear electron accelerators.

The low efficiency of earlier microtrons[2-6,15] resulted from the unsatisfactory conditions of electron injection. The uncontrollability of field emission in the strong field of toroidal resonant cavities and the impossibility of predicting electron trajectories precisely resulted in a low efficiency of capture and of the accelerator as a whole.

Theoretical investigations of phase stability in microtrons[7-9] have shown that the range of phase oscillations is small (0 — 32°). This fact directed our attention to the microtron as an accelerator that can produce beams of bunched electrons with constant energy. On the other hand, the small region of stable motion is the basis for all difficulties regarding particle capture into accelerating orbits. Increased efficiency could therefore not be expected without an essential change in the conditions of injection.

We have proposed[10] a resonator based on electron injection from a thermionic cathode through the direct action of the rf resonator field. The use of a simple cavity shape in the E_{010} mode permitted precise calculations of electron motion in a field of known configuration. The accelerator constructed by us yielded a (pulse) current of 20 ma at 7 Mev, and 5 ma at 13 Mev. The new technique of electron injection into the accelerating mode permitted doubling of the magnet field strength, thus doubling the beam energy without changing the diameters of the orbits. The variation of magnetic field strength also permitted the continuous variation of beam energy, which was thus no longer limited to integral multiples of the rest energy as in previous modes of operation.

It should be noted that several authors have suggested independently that a complicated arrangement of electron trajectories in the resonator could be employed. Thus, Aitken[11] suggested placing the electron emitter within the rf field. Poulin[12] suggested a method of injection in a toroidal resonator which in principle also permitted strengthening of the magnetic field, but motion in the given field could not be calculated simply. No experimental results with resonators of these types have been published.

The present paper describes the construction of a high-current microton and discusses the basic physical principles of this type of accelerator.

2. ACCELERATOR MAGNET AND CHAMBER

The electromagnet and vacuum chamber are shown in Fig. 1. The diameter of the vacuum chamber 1 is 700 mm; its top and bottom are formed by the magnet poles 2, which are separated by 110 mm. The magnet coils 3 wound with 25 × 1 mm copper strip insulated by paper tape are mounted directly on the poles. The coils are cooled by water circulating in rubber tubes 4 that are in contact with the coils.

The upper plate of the magnet is clamped to the pillars 5 in the magnetic circuit by four screws, which at the same time fasten down the rubber gasket 6 between the poles and the chamber wall. This magnet is distinguished by 8-mm compensat-

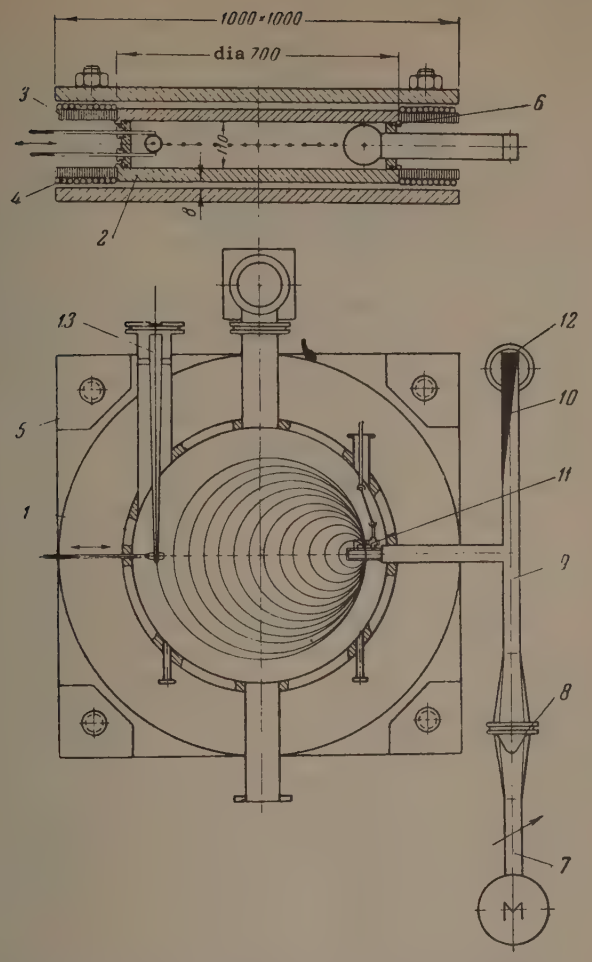

FIG. 1. Microtron vacuum chamber and electromagnet.

ing gaps between the plates and poles. These gaps in the magnetic circuit increase the anisotropy of the demagnetization coefficient of the poles and thus enhance the magnetic field homogeneity in the working space. The effect of the gaps is based essentially on the fact that, with continuity of the tangential field component, the lines of force turn through a greater angle in the air gap than in the iron of the poles. The introduction of these gaps is justified only when the iron of the magnetic circuit and poles is unsaturated. Conventional 12 × 4 mm shims are located at the edges of the poles in order to enlarge the homogeneous field region. The relative field homogeneity depends on the field strength and comprises a few tenths of one percent when the diameter of the working region is about 55 cm in fields up to 1500 oe.

The total weight of the magnet is 1.5 tons; No. 3 steel was used in its construction. The field strength in the chamber reached 2000 oe at 4 kw and 3 amp/mm^2 current density. Power was fed to the magnet from a three-phase selenium rectifier and a motor-generator converter stabilized within 0.1% at 427 cps. The same converter also fed the modulator.

The accelerator chamber and waveguide were evacuated by diffusion pumps with liquid nitrogen traps, to which nitrogen was supplied automatically.[13]

Access to the chamber was obtained by lifting the upper plate together with the pole and coil. After the chamber was closed, hot pumps produced the 10^{-5} mm Hg working vacuum within 15 — 20 min. The numerous insertions and shifts within the chamber were made through rubber and teflon seals in the wall.

The control chamber was separated from the accelerator by a 2-meter shield. The remote electric control was performed with selsyns.

A probe was moved across the chamber to measure the current distribution in the different orbits. The current in the target was registered either oscillographically or by an automatic potentiometer in which the tape motion was synchronized with the probe motion. Figure 4 shows a record obtained in this manner. The target was a water-cooled copper rod or plate coated with a phosphor.

The image of the beam on the target was viewed with a commercial PTU-4 television receiver. Sevenfold magnification of the television screen image permitted the detailed study of the position and size of the beam in any orbit.

3. RADIO-FREQUENCY SYSTEM AND RESONATOR

The rf field in the resonator was excited by means of a standard untunable magnetron and a modulator with a long pulse-shaping line. The rf pulse duration was 3 μsec and its repetition frequency was 427 cps. The waveguide transmission line (Fig. 1) consisted of a phase shifter 7, vacuum port 8, tee 9, water load 10, and resonator 11. Supplementary evacuation of the waveguide can be performed by an oil diffusion pump 12, although evacuation through the resonator produces a sufficiently low pressure. The cooling water circulates first through the load, then through the resonator. Thus the thermocouples measuring the water temperature differential between the input and output of the load and resonator permitted a direct comparison of the power fed to both the load and the resonator. This ratio was usually a little larger than unity.

The most crucial part of the accelerator is the resonator. The first runs were performed with conventional toroidal resonators and 8 — 10 mm accelerating gaps. Very careful selection of the shape and surface of the accelerating gap with direct emission from the copper walls enabled us to attain currents up to 7 ma (with 6 Mev energy in the 12th orbit), but only when the accelerator was tuned very critically.

In our search for an improved injection method and emission control we switched to a cylindrical resonator in which E_{010} oscillations were excited (a "flat" resonator). Electrons in this resonator start from a hot cathode k installed on the flat wall of the resonator (Fig. 2). Inside of the resonator two types of trajectories are possible, the first of which (Fig. 2a) starts at a cathode positioned relatively far from the resonator axis. In this case an electron leaves the resonator when its total energy U is 2 — 2.5 times its rest energy $U_0 = mc^2$; with each successive transit the electron energy is increased by 1 — 1.25 U_0, i.e., 500 — 600 kev. This occurs when the magnetic field is 1 — 1.25 H_0, where $H_0 = 2\pi U_0/\lambda e = 1070$ oe is the magnetic field calculated for the wavelength $\lambda = 10$ cm.

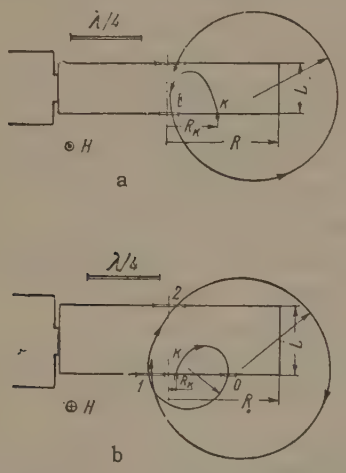

FIG. 2. Electron motion in the resonator.

For trajectories of the second type (Fig. 2b) the cathode is close to the resonator axis. An electron first passes through an additional port O before entering into its resonant orbit, where with each transit its energy is increased by 1.8 — 2.2 U_0 in a magnetic field of 1.8 — 2.2 H_0.

All parameters of electron motion in microtron accelerating modes were calculated. A simulating machine, Prudkovskii's trajectory plotter,[14] was used for preliminary calculations. This machine plots electron paths in a variable electromagnetic field, using a computer for mechanical integration and simulation of the equations of motion.

For a detailed study of electron motion the equations of motion were integrated numerically on the fast Strela computer. The numerical results supplied complete information regarding particle dynamics in the accelerator. Details of the calculation are given in the Appendix.

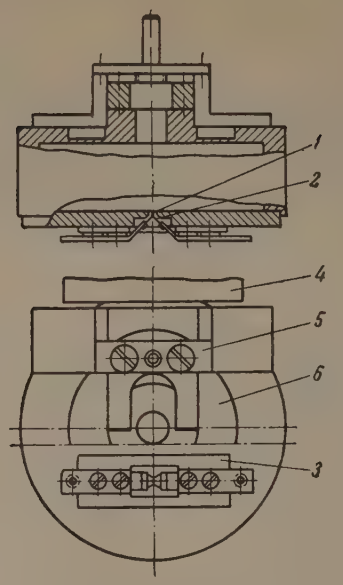

FIG. 3. Cross section of first type of resonator.

Figure 3 is a sketch of the dismountable resonator, made of oxygen-free copper, used for the first mode of electron acceleration. The resonator is excited through a port in its cylindrical wall, which forms a junction with the end of a rectangular waveguide 4. The size of the junction aperture was determined empirically. The Q of the cold resonator when loaded with the waveguide was usually about one-half or one-third of its intrinsic Q.

A simple screw mechanism 5 was used to tune the resonator by bending one of its walls into which a diaphragm 6 (0.2 — 0.3 mm thick) had been inserted. The resonator and its parts around the membrane were water-cooled; the cooling tubes had been soldered to the resonator housing with silver in vacuo.

Table I gives the resonator dimensions R and L, the cathode position (the distance R_k), the constant magnetic field strength H, the amplitude E of the rf electric field, and other data pertaining to the wavelength $\lambda = 10.0$ cm, which are analyzed in Sec. 4.

Table I

Mode	R, cm	L, cm	R_k, cm	H/H_0	H, oe	E, kv/cm	Resonant phase φ_0	Initial phase region $\Delta\varphi$
1	3.83	1.67	1.75	1.1	1180	380	0	0.07
2	3.83	2.31	0.32	1.81	1940	460	0	0.25

4. THE CATHODE AND ELECTRON CAPTURE INTO ACCELERATING MODES

The initial experiments with a flat resonator and tungsten cathode did not produce the required emission and current density. The best cathode, satisfying all requirements, was a lanthanum boride (LaB_6) thermionic cathode (Fig. 3). This cathode 1, a 1.5 mm cube, was cut electrically from a baked rod of the boride. The cube was soldered to a tantalum heater 2, which was 0.2 mm thick and 2 — 2.5 mm wide; the soldering was performed in vacuo at 2000° C with molybdenum disilicide ($MoSi_2$). At 1500 — 1600° C with rf fields in the resonator this cathode supplies a stable emission current of 100 — 200 amp/cm^2. The boride cathode can function in a poor vacuum and at atmospheric pressure when cold. It requires no activation when switched on and the emission is easily monitored by its temperature. The cathode holder 3 was mounted flush with the inner surface of the resonator, precisely in the symmetry plane of the accelerator.

The tantalum strip of the cathode heater was heated by a 427-cycle alternating current with strength up to 50 amp. The magnetic field around the current could perturb electron orbits and deflect electrons from their plane of motion. In order to obviate this defect, the trigger pulse of the modulator was synchronized with the zero phase of the cathode current, at which time the magnetic field vanishes and cannot perturb electron motion, while the cathode temperature and emission remain practically unchanged because of the thermal inertia of the heater. On the other hand, the symmetry of the resonator and cathode adjustments were checked by varying the starting phase and thus perturbing the orbits.

The total cathode emission current and the beam current were recorded oscillographically. The ratio of the current I captured into accelerating orbits to the current I_k emitted from the cathode

$$K = I / I_k$$

is called the capture coefficient, which usually has a value of $1/30$ to $1/40$ in the first mode. Beam losses are usually small during acceleration after the second transit through the resonator. Figure 4 represents the current distribution in different orbits; this was recorded automatically on a target of 5-mm diameter.

The capture coefficient K is determined by two factors, the initial phase region $\Delta\varphi$ within which electrons can be accelerated synchronously and the distribution of cathode emission current during each period of the rf field.

The initial phase region $\Delta\varphi$ was calculated for given parameters of the accelerating field and resonator. In the described modes of operation resonant electrons were emitted at the maximum electric field E in the resonator ($\varphi_0 = 0$ if $E \sim \cos\varphi = \cos\omega t$). The calculated value of $\Delta\varphi$ for the 12th orbit has been given above.

The emitted current distribution during a rf period is determined by processes at the cathode. Since the cathode is not biased, emission evidently occurs only during the positive half-period.

With a field of 380 kv/cm at the cathode in the first mode and 460 kv/cm in the second mode and a current density of ~ 100 amp/cm^2 from the cathode, the current is determined mainly by the cathode temperature and only to a lesser extent by the field strength. The field affects emission through the Schottky effect, which diminishes as the cathode temperature rises.

Emission during the positive rf half-period can be assumed approximately constant. In this case the capture coefficient is practically

$$K \approx \Delta\varphi / \pi.$$

At $\varphi_0 = 0$ nonuniform emission during the half-period only increases the calculated value of K.

We selected $\varphi_0 = 0$ originally in order to simplify the calculations and because we intended to use a cold cathode. In the case of field emission, with exponential current density in strong fields, the entire current from the cathode would be emitted close to the field maximum; thus the phase $\varphi_0 = 0$ would be most advantageous. In the case of a hot cathode, for which emission is only slightly dependent on the field, the calculation shows that an initial phase $\varphi_0 < 0$ should be selected. In this case the region $\Delta\varphi$ can be expanded considerably because of electron bunching in their motion along their initial paths inside of the resonator. The bunching mechanism has been discussed in [16].

Electrons were accelerated at $\varphi \neq 0$ in a flat cylindrical resonator with $R_k = 1.9$ cm and L

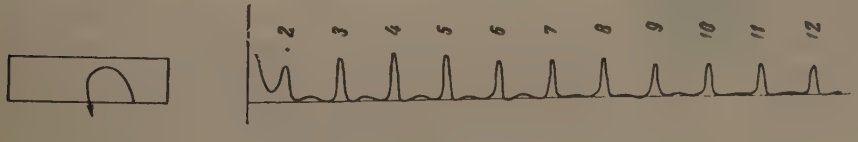

FIG. 4. Current distribution in successive orbits.

= 2.2 cm, with the cathode located farther from the axis than in the case $\varphi_0 = 0$. In this resonator, by varying the magnetic field H from H_0 to 1.5 H_0, the electron energy in the 12th orbit was varied continuously from 6 to 9 Mev with an average current of about 10 ma and capture coefficient $1/30 - 1/20$. Adjustment of the magnetic field was accompanied by a slight shift of the orbits; therefore the orbit ports of the resonator were elongated.

The foregoing modes are of great interest when the beam energy must be varied continuously. With the earlier conventional methods of injection[3] the beam energy was limited to multiples of the rest energy. The more rigorous conditions governing electron capture thus deprived the accelerator of the requisite flexibility.

5. PROPERTIES OF THE ELECTRON BEAM

Electrons in a microtron move within the homogeneous field of the magnet, and the electrons are focused solely by the resonator field, since motion occurs during the zero phases of the electric field.[17]

It should be noted that along the first segment of the trajectory within the resonator (KA in Fig. 2) the vertical motion of electrons is affected by the action of the rf magnetic field; the average effect is a certain amount of beam defocusing along the initial segment. This effect is small, but makes it necessary to position the cathode precisely in the symmetry plane of the resonator and magnet.

The electron orbit ports in the resonator walls are either circular with 10 — 8 mm diameters, or elongated with 18 — 20 mm lengths and 8-mm height. Practically no beam loss resulted from the vertical dimension of the ports. Horizontal focusing was ensured by lengthening of the electron pulses during transits. The beam cross section was 4 × 5 mm in the last orbit. The beam dimensions and orbit positions indicated that the energy spread did not exceed 50 kev in the first mode and 100 kev in the second mode. Some 80% of the beam in the last orbit is easily extracted magnetically through a circular cone (13 in Fig. 1) with soft steel walls. This channel is 500 mm long, with an 8 × 10 mm entrance and 20 × 30 mm exit. The position of the channel in the accelerator is not very critical.

An rf analyzer was used to investigate electron bunching and the charge distribution in bunches accelerated in the first mode.[18] The kinematic design of the accelerator is well confirmed by the measured charge distribution. Most of the charge in a bunch lies within a region 5 — 7 mm long, and the particle density in the bunch is 10^8 cm^{-3}.

The maximum current and energy attainable in a microtron are of interest. Estimates show that because of the strong bunching of the microtron beam, even with currents as low as 1 amp, coherent radiation from bunches moving in a constant magnetic field can be expected to have considerable effect on electron motion.

All bunches progress simultaneously through the resonator, which is thus loaded with a current equal to the beam current multiplied by N, the number of orbits. Interactions between the current and both the resonator and cathode can also limit the range of usefulness of the accelerator, but the extent of this influence requires further study.

6. ACCELERATOR OPERATION AND EFFICIENCY

An accelerator operating mode begins with resonator tuning and excitation of the rated magnetic field. This is followed by adjustment of the cathode current. At a given level of rf power loading the resonator by means of the cathode current, the electric field strength required for resonant acceleration of electrons can be attained. This is accomplished most easily by observing the oscillogram of target and cathode currents or the mean intensity of the beam and of gamma radiation near the target. For low cathode currents the electric field is large and electrons are accelerated only at the beginning and end of each pulse (Fig. 5a). For too high cathode currents, electrons either are not accelerated or are accelerated only at the middle of a pulse (Fig. 5b). With the correct cathode current and electric field in the resonator, acceleration occurs throughout the entire period of stable resonator operation.

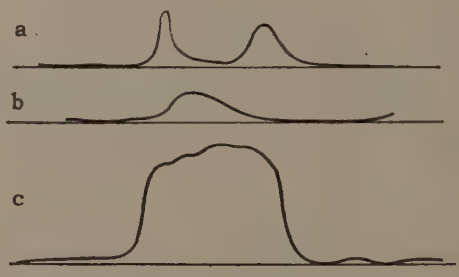

FIG. 5. Shape of current pulses.

Following the adjustment of the cathode current, a further fine adjustment of the resonator in accordance with thermocouple readings usually produces the optimum distribution of power between the load and the resonator. Experience has shown that the established mode is very stable and that the accelerator can function with practically no attention on the part of the operator. Current

pulse duration at the target is usually 1.8 — 2.2 μsec (Fig. 5c).

The field strength in the flat resonator is 300 — 600 kv/cm. In our toroidal resonators the field between the flat or rounded surfaces of the working section of an 8 — 10 mm gap reached 1000 — 1500 kv/cm. No appreciable emission or discharge was detected from the mechanically polished copper surfaces in either case. Cold emission from copper at $E = 10^6$ v/cm is calculated to be $i = 10^{-10}$ amp/cm^2. It is of interest that the field strengths achieved by us in flat resonators are very much higher than the assumed limit[19] of 100 — 150 kv/cm in linear accelerators for field configurations very close to our configuration in each resonator.

Experiments have shown that a lowering of the vacuum to 10^{-4} mm Hg or the absence of a transverse magnetic field was not accompanied by either a discharge or extraneous emission in the flat resonator.

The accelerator efficiency η is determined by the distribution of rf power fed to the resonator. A fraction P_1 of the power is expended in ohmic losses in the resonator walls and, for a given wavelength, depends only on the resonator size and field E. Calculated values of P_1 for the first and second modes are given in Table II for a copper resonator with $\lambda = 10$ cm and depth of penetration $\delta = 1.2 \times 10^{-4}$ cm.

Another fraction P_k of the power is expended in accelerating all emitted electrons in the first segment of their trajectory. We can assume that this fraction equals approximately the product of the emitted current $I_k = I/K$ by the energy $U_1 - U_0$ acquired by the electron in its first passage out of the resonator. The inaccuracy of this estimate lies in the fact that we here neglect the distribution of current and energy with respect to the accelerating-field phase.

The effective power P_a is expended in accelerating resonant electrons, and is the product of three factors, the beam current I, the energy ΔU, and the number N of orbits. The accelerator efficiency is therefore represented approximately by

$$\eta = \frac{P_a}{P_1 + P_k + P_a} = \frac{IN\Delta U}{P_1 + I\Delta U/K + NI\Delta U}.$$

A rise of η will obviously accompany an increase of N, I, or the capture coefficient K. Approximate power distributions and other experimental data are given in Table II.

The current in the 12th orbit of the second mode is considerably lower than the levels attained in the first six orbits. The current loss in the final orbits was evidently associated with defocusing resulting from growing magnetic field inhomogeneity as the field strength became twice as large as the rated value.

The power distribution pertains only to a stable mode. In our case resonator oscillations are built up in a time equal to approximately $\frac{1}{3}$ of the total duration of an rf pulse; this must be taken into account in computing the efficiency of the accelerator. In the cases of pulses that are shorter than this build-up time the accelerator efficiency will decrease; on the other hand, increased pulse duration leads to higher efficiency.

Higher efficiency can result from reduced resonator losses if a toroidal resonator is used with a large shunt resistance across the effective gap. However, the complexity of the field in a resonator of this shape makes it difficult to determine the optimum injection conditions. In a toroidal resonator with a small gap and the conventional geometrical parameters[2,3] it is more advantageous to capture and accelerate electrons from a hot cathode. This is required if we wish to use the condition $\varphi_0 < 0$.

A toroidal resonator with a hot cathode is of interest in the case of an intermittent microtron. In a microtron operating at high levels of pulsed power the reduction of losses in the resonator is not very important.

Microtron modes are also possible in which the magnetic field is stronger than the levels we have indicated. This will be accompanied by higher electron energy without an increase in the number of orbits but, of course, with greater power losses in the resonator.

CONCLUSIONS

The described accelerator is a high-current microtron in which efficient electron acceleration has been achieved for the first time in an operating mode with variable energy increment per cycle. These advantages resulted from the use of an efficient thermionic cathode and exact calculations for motion in a new form of resonator. Experi-

Table II

Mode	N	I, ma	U_{12}, Mev	ΔU, kev	K	U, kev	P_1, kw	P_k, kw	P_a, kw	η, %
1	12	20	7.3	560	1/40	1120	300	465	135	15
2	12	5	13	1000	1/20	500	500	100	65	7

ments performed with this accelerator confirmed the calculations based on an analysis of electron motion in the given electromagnetic field.

The microtron can compete well with linear accelerators at low energies. The principal advantages of the microtron are the constant beam energy, bunching, and the greater operating simplicity and reliability resulting from the simple resonator shape and from energizing by pulsed magnetrons.

In conclusion we wish to thank P. L. Kapitza for supporting this work and S. I. Filimonov for his continued interest. We also wish to thank G. P. Prudkovskii and L. A. Vaĭnshteĭn for useful discussions, A. A. Kolosov and S. V. Melekhin for constant experimental assistance, and engineer L. Zykin for his participation in the construction of the accelerator.

APPENDIX

CALCULATION OF ELECTRON MOTION IN THE MICROTRON

S. P. Kapitza, V. N. Melekhin, I. G. Krutikova, and G. P. Prudkovskii

We shall now present the principal results of the calculations of electron motion in a microtron with a hot cathode. We start with the relativistic equation of electron motion in an electric field **E** and magnetic field **H**:

$$\frac{d}{dt}\frac{m\mathbf{V}}{\sqrt{1-V^2/c^2}} = e\left(\mathbf{E}+\left[\frac{\mathbf{V}}{c}\mathbf{H}\right]\right) \qquad (1)^*$$

in which we then introduce the dimensionless variables

$$\varphi = \omega t, \quad x = kX, \quad y = kY, \quad k = \omega/c,$$
$$u = V_x/c, \quad v = V_y/c, \quad \beta^2 = u^2 + v^2,$$
$$\Gamma = U/mc^2 = 1/\sqrt{1-\beta^2}. \qquad (2)$$

We are thus using natural quantities that are characteristic of relativistic electronics.

We also introduce the relative magnetic field strength

$$\Omega = H/H_0, \qquad (3)$$

where $H_0 = \omega mc/e$ is the nominal magnetic field of a microtron at the frequency ω (the cyclotron field). The electric field amplitude divided by the constant magnetic field gives the quantity

$$\varepsilon = E/H. \qquad (4)$$

We investigated electron motion in a circular cylindrical resonator with E_{010} excitation and in a rectangular resonator with E_{101} excitation (see [20], Secs. 93 and 94). In both cases the rf field has only the components E_y and H_z in the XY plane, independently of the Y coordinate. The dimension L of our resonators in the Y direction was very much smaller than the other dimensions; we therefore speak of flat resonators (Fig. 6).

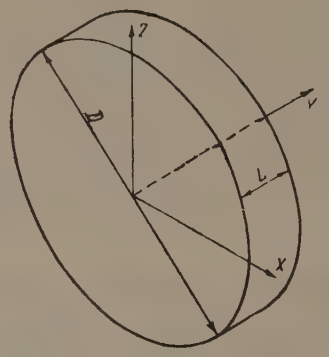

FIG. 6. Cylindrical resonator.

In the cylindrical resonator (1) becomes

$$\frac{d}{d\varphi}\frac{u}{\sqrt{1-\beta^2}} = -\Omega v + \varepsilon\Omega v J_1(x)\sin\varphi,$$
$$\frac{d}{d\varphi}\frac{v}{\sqrt{1-\beta^2}} = \varepsilon\Omega J_0(x)\cos\varphi + \Omega u - \varepsilon\Omega u J_1(x)\sin\varphi. \qquad (5)$$

In the rectangular resonator we have, correspondingly,

$$\frac{d}{d\varphi}\frac{u}{\sqrt{1-\beta^2}} = -\Omega v + \varepsilon\Omega v\varkappa\sin\varkappa x\sin\varphi,$$
$$\frac{d}{d\varphi}\frac{v}{\sqrt{1-\beta^2}} = \varepsilon\Omega\cos\varkappa x\cos\varphi + \Omega u - \varepsilon\Omega u\varkappa\sin\varkappa x\sin\varphi, \qquad (6)$$

with the relative wave number $\varkappa = k_x/k_z$.

Equations (5) or (6) describe electron motion completely in the variable field of the resonator and constant magnetic field. The initial conditions depend on the position of the cathode. Neglecting the thermal velocities of the electrons, the initial conditions are $\varphi = \varphi_0$, $x = x_k$, $y = 0$, $u = 0$, and $v = 0$, where x_k is the coordinate of the cathode.

Electron trajectories outside of the resonator are circular up to the point of entrance into the resonator at $y = l = kL$, where L is the resonator thickness.

The cyclic motion is easily programmed for automatic calculation, which was performed with six-place accuracy as far as the 12th orbit. This program permitted the detailed study of the entire acceleration process, since all fundamental factors were taken into account in the equations. The sole simplification that must be mentioned is the neglect of the way in which the rf field is affected by ports in the resonator walls. The field distor-

*$\left[\frac{\mathbf{V}}{c}\mathbf{H}\right] = \left[\frac{\mathbf{V}}{c}\times\mathbf{H}\right]$.

tions produced by these ports are small and do not affect the results essentially. We also did not take into account the interaction between electrons and radiation emitted by electrons while we were considering the motion of a charge in a given field.

Electron motion is entirely dependent on five parameters—the fields Ω and ϵ, the resonator dimension l, the cathode position x_k, and the initial phase φ_0. In the microtron accelerating mode (sometimes called a mode with variable energy increment[7]) these parameters are independent. Moreover, motion along the first segment of the trajectory within the resonator can be considered separately, being calculated in such a way that upon leaving the resonator the electron enters into the accelerating mode.

We shall write the relations between the accelerator parameters (field strengths, transit phase, and resonator dimensions) characterizing this mode. In each transit the energy of an electron possessing the stable phase φ_s is enhanced in such a way that the period of revolution in a field H is increased by q periods ($T = 2\pi/\omega$) of the variable field. We confine ourselves to the fundamental mode $q = 1$,[9] where the phase-stable region is largest and the energy increment for each transit is

$$\Delta U = eHcT/2\pi \quad \text{or} \quad \Delta\Gamma = \Omega. \tag{7}$$

We shall also determine the energy increment when a fast electron moves along the axis $x = 0$ through a resonator of length l. Integrating the second equation in (5) from the entrance phase φ_n to the exit phase φ_m for $v \approx -1$, while neglecting terms that would take into account the effect of the magnetic field, we obtain

$$\Delta\Gamma \approx \varepsilon\Omega\,(\sin\varphi_n - \sin\varphi_m).$$

In view of (7), after transforming the expression in parentheses, we obtain

$$\sin(l/2) = 1/2\varepsilon\cos\bar{\varphi}, \tag{8}$$

where $\bar{\varphi} = (\varphi_m + \varphi_n)/2$ and $\varphi_m - \varphi_n \approx l$.

The mean phase $\bar{\varphi}$ is determined by the requirement of phase stability during subsequent acceleration, and in the absence of phase oscillations φ should be equal to the stable phase φ_s. On the basis of our calculations and from the theory of phase oscillations in a microtron[7,8] we can take

$$\varphi_s = 0.35\,(20°), \qquad \cos\varphi_s = 0.94, \tag{9}$$

Equation (8) enables us to relate l and ϵ immediately. It is also evident that the resonator thickness l has no bearing on the initial segment of the trajectory if the electron does not strike the wall.

Electron energy at the end of the first transit can be called the injection energy (pertaining to the given system): its dimensionless value should be

$$\Gamma_1 = 2\Omega \text{ (first type of trajectory)}, \quad \Gamma_1 = \Omega \text{ (second type of trajectory)}. \tag{10}$$

These conditions are associated with the fact that an electron must encircle the resonator in its first revolution.

For phase stability of the motion the exit phase φ_{ex} for the first type and the entrance phase φ_1 for the second type of trajectory must satisfy approximately the conditions

$$\varphi_{ex} \approx \varphi_s + l/2 \text{ (first type)}, \quad \varphi_1 \approx \varphi_s - l/2 \text{ (second type)}. \tag{11}$$

Conditions (7) — (11) together with the solution of (5) or (6) provide a basis for deriving the parameters Ω, ϵ, l, x_k and φ_0, corresponding to what we shall call the resonant trajectories of the microtron accelerating mode. It is not necessary to calculate all orbits and the parameter l can be omitted from consideration.

We have calculated only the trajectories with $\varphi_0 = 0$, corresponding to electron exit at the maximum electric field amplitude in the resonator. Table III gives the results for two modes of the first type and one mode of the second type in the circular resonator, and for one mode of the second type in the rectangular resonator.

The resonant trajectory regions for the first mode with $\varphi_0 = 0$ are shown in Fig. 7 in the coordinates Ω and x_k. The resonant region $\Gamma = 2\Omega$ is determined by the following three conditions: Electrons must depart with initial phases within the stable acceleration region ($0.25 < \bar{\varphi} < 0.45$), the exit point must be close to the axis ($-0.2 < x_{ex} < 0.3$), and the extreme point of the orbit within the resonator must lie within the wall ($y_{max} < l$). The corresponding region of values of Ω and x_k is shaded in the figure; the heavy dots represent the experimental operating modes for which data are given in the table.

Figure 8 shows the small resonant trajectory region for the second mode in the cylindrical resonator with $\varphi_0 = 0$, corresponding to the large value $\Omega = 1.9$. The dot represents an experimental result consistent with the calculation.

Figure 9 shows a similar region for the rectangular resonator with $a = 0.9\lambda$ and $b = 0.6\lambda$, in which Ω has still larger values (2.02). This was not confirmed experimentally.

Table III

Type of motion	Type of resonator	Ω	ε	x_k	l	Δφ	z_{ex}	w_{ex}
1	cylindrical	1,10	1,11	1.20	1.00	0,07	0,183	0,031
1	cylindrical	1,10	1,06	1,10	1.05	0.07	0,178	0,029
2	cylindrical	1,81	0,80	0,20	1.45	0,24	—	—
2	rectangular	2,02	0,79	0,20	1.47	0,21	—	—

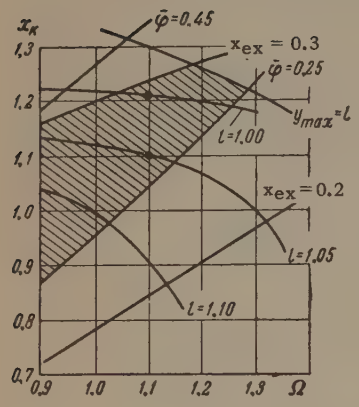

FIG. 7. Region of resonant trajectories for the first type of motion (with $\varphi_0 = 0$) in a cylindrical resonator.

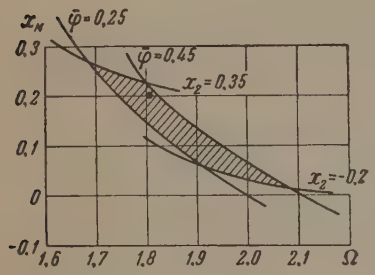

FIG. 8. Region of resonant trajectories for the second mode (with $\varphi_0 = 0$) in a cylindrical resonator.

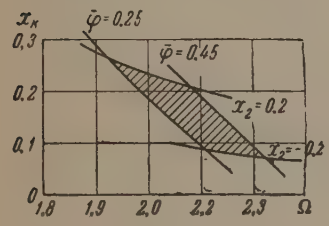

FIG. 9. Region of resonant trajectories for the second mode (with $\varphi_0 = 0$) in a rectangular resonator.

The foregoing modes can be investigated in detail by means of complete exact calculations for several orbits, in order to check the correctness of the preliminary parameters determined from relations some of which, specifically (8) and (11), are only approximate.

Phase oscillations for the first mode are shown in Fig. 10 for $\varphi_0 \sim 0$. By varying φ_0 and finding the boundary of the stable trajectory region we determine the region of electron capture given in the table for N = 12.

In Fig. 10 the phase stable region is outlined with a dashed curve. If the phase trajectory of an electron crosses this limiting line or lies outside of it the electron will sooner or later depart from synchronism and will be lost. The initial points of the phase trajectories lie along straight lines intersecting the limiting curve at two points where the values of φ_0 determine the region of capture. The exact locations of the straight lines depend on x_k, the cathode position, as shown in Fig. 10.

Stable trajectories cannot be determined by numerical computations for an unlimited number of orbits. In practice, however, we are always interested in electron behavior and acceleration during a finite number of revolutions. For example, Fig. 10 shows that the trajectory for $\varphi_0 = -0.04$ and $x_k = 1.10$ begins to depart from synchronism only after twelve revolutions. The tra-

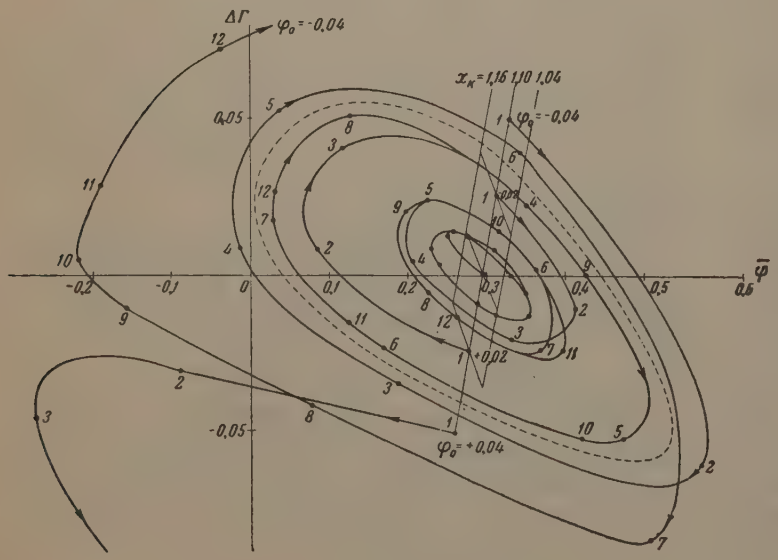

FIG. 10. Phase oscillations of electrons in the first accelerating mode.

jectory will therefore be useful up to this number of orbits, although it is unstable from a formal point of view. The existence of such "limited" trajectory stability accounts for the small current drop always observed between successive orbits. One can therefore speak more properly not of a stability region, but of the dynamic aperture of the accelerator, i.e., the region of initial parameters corresponding to electrons accelerated during a given number of orbits.

Figure 11 shows the position of orbits around the resonator for different numbers N. The orbits are seen to lie very close to the resonator axis.

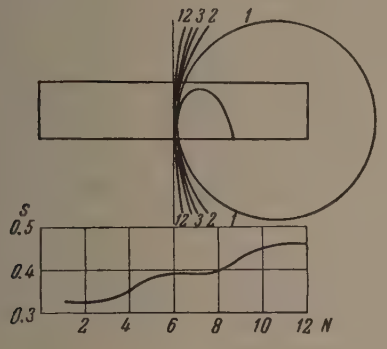

FIG. 11. Positions of orbits and drift of orbit centers.

It is interesting to consider the drift of the center of circular orbits along the y axis in a rf field. Figure 11 shows the position of the center s (the value of which is highly exaggerated along the y axis) as a function of N for a stable trajectory. The slow regular shift of the center is accompanied by oscillations with the period $\Delta N \sim 5$, which are evidently associated with the phase oscillations of the electron.

A constant uniform field does not affect the vertical motion of electrons in a microtron. An rf electric field, unlike that in linear accelerators, performs a focusing function because $\varphi_s > 0$. During acceleration an electron traverses the focusing field of the entrance port at a higher value of the field strength than the defocusing field at the resonator exit. According to Bell's calculations [17] electrons oscillate slowly near the median xy plane with amplitudes that grow slowly as $\Gamma^{1/4}$.

During motion in the first segment of the trajectory, the variable magnetic field H_θ in a circular resonator and H_x in a rectangular resonator perturb motion in the vertical direction whenever the particle departs from the xy plane.

The linearized equations of vertical motion in a circular resonator are, with $z = kZ$,

$$\frac{d}{d\varphi}\frac{w}{\sqrt{1-\beta^2}} + Az = 0, \quad w = \frac{dz}{d\varphi}, \quad A = -\varepsilon\Omega\frac{J_1(x)}{x}v\sin\varphi. \tag{12}$$

The variation of the coefficient $A(\varphi)$ along the trajectory is shown in Fig. 12. Focusing by the acting forces occurs along a part of the trajectory ($A > 0$), while defocusing occurs elsewhere ($A < 0$). The corresponding solution of (12) can be obtained by numerical integration along the first segment of the trajectory. Table III gives values of z_{ex} and w_{ex} derived for the initial conditions $z_0 = 0.1$ and $w_0 = 0$.

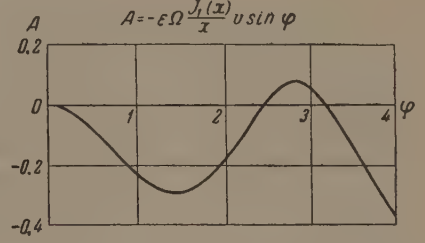

FIG. 12. Variation of the coefficient determining the vertical motion of an electron in the initial segment of its trajectory for the first type of motion in a cylindrical resonator.

The overall effect of the variable magnetic field on the first segment of the trajectory is a slight defocusing; this has been calculated only approximately, since defocusing produced by space charge, which we have neglected, is also possible close to the cathode. The vertical defocusing limits the cathode size and determines the height of the orbit ports of the resonator. Experiment indicates adequate focusing by rf fields during acceleration under actual conditions.

It is also of interest to calculate the power required to excite a suitable rf field. The power loss can be determined by integrating the magnetic field H_θ on the resonator surface (see Sec. 98 of [20], for example):

$$P = \frac{c^2}{32\pi^2}\frac{1}{\sigma d}\oint |H_z|^2 ds, \tag{13}$$

where σ is the conductivity of the metal and $d = (1/2\pi)\sqrt{\lambda c/\sigma}$ is the depth of penetration.

Using the expression for fields in a cylindrical resonator and integrating, we obtain

$$P = \frac{\pi}{4}\nu_{01}J_1^2(\nu_{01})\frac{d}{\lambda}(\nu_{01}+l)\,\Omega^2\varepsilon^2 P_0, \tag{14}$$

where ν_{01} is the first root of the zeroth order Bessel function, and $P_0 = m^2c^5/e^2 = I_0V_0 = 8700$ Mw is the characteristic power of rf electronic devices. This power is independent of the wavelength λ and equals the energy flux transported through a cross section $8\pi\lambda^2$ of a flat wave, whose field is $mc^2/e\lambda$. The power can be represented as the product of the characteristic electron current $I_0 = mc^3/e = 17\,000$ amp by the voltage ($V_0 = 511$ kev) corresponding to the electron rest energy.

Since l depends only on ϵ according to Eq. (8), the power depends only on ϵ and Ω. For an accelerator with a cylindrical resonator operating in a mode of any type we obtain the power

$$P = 1.02\, P_0 \frac{d}{\lambda}\left(1.2 + \arcsin \frac{1}{1.88\,\varepsilon}\right)\varepsilon^2\Omega^2. \qquad (15)$$

The dependence of the ratio $P\lambda/P_0 d$ on Ω and ϵ is shown in Fig. 13.

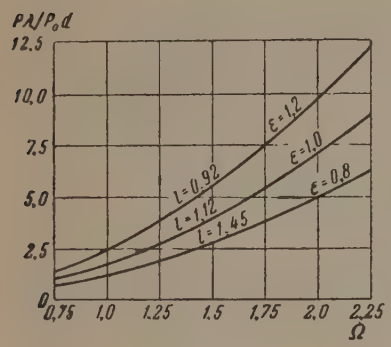

FIG. 13. Ohmic power loss in a cylindrical resonator vs the parameters Ω and ε of an electron accelerating mode.

For copper at room temperature we have $\sigma = 5.7 \times 10^5\,\Omega^{-1}$ cm. Also, for $\lambda = 10$ cm we have $d = 1.2 \times 10^{-4}$ cm and $P_0 d/\lambda \approx 100$ kw. An expression analogous to (15) can also be derived for a rectangular resonator:

$$P = \frac{\pi^2}{8} P_0 \frac{d}{\lambda}\left[\frac{a^3 + b^3}{2ab} + \frac{l\,(a^3 + b^3)}{a^2 b^2}\right]\varepsilon^2\Omega^2, \qquad (16)$$

where a, l, and b are the lengths of the resonator along the x, y, and z axes, respectively. The shape of the resonator has only a small effect on the power, which is influenced most strongly by the parameter Ω. For large Ω, with the previous number of orbits, the energy is increased by the factor Ω compared with the nominal value at $\Omega = 1$. It should be noted that $\epsilon \sim 1$ is always valid; therefore the power loss depends mainly on Ω, the relative magnetic field strength.

Our calculations provided a basis for proposing a microtron resonator differing considerably from all previously suggested and constructed resonators. For this resonator the rf field amplitude ϵ and the associated accelerating gap l in their dimensionless form are close to unity. The length of the transit distance $L = l/k$ therefore considerably exceeds the values proposed and realized by other authors.[7,21] For a given wavelength the accelerating field is correspondingly weaker; the relative reduction is a very favorable factor in enlarging the useful range of an accelerator that can be achieved with higher fields and frequencies.

The value of ϵ is close to unity because a microtron is a cyclic accelerator in which the electric field is not small. This is the fundamental difference between microtrons and other cyclic accelerators of relativistic particles, and makes it difficult to analyze microtrons by the approximation methods that commonly consider an adiabatic accelerating process in accelerators with weak fields. We therefore developed computer procedures for numerical calculations.

On the other hand, the numerical approach required resonators with simple geometrical shapes, in which the expressions for the field ϵ are known. In these resonators a given accelerating voltage requires somewhat higher rf power than in specially selected toroidal resonators. However, the possibility of a complete calculation in this case produces a considerable gain in the final accelerating parameters. We can thus exceed the empirical limits of all previously proposed microtrons, whose currents and efficiencies were found to be more than one order of magnitude smaller than those based on the foregoing calculations.

We can expect that the further development of numerical methods for resonators of all shapes will lead to an accelerating unit that is optimal with respect to rf power dissipation. All calculating difficulties can be overcome.

In conclusion we wish to express our gratitude to P. L. Kapitza and E. S. Kuznetsov for their interest, to M. M. Antimonik for the programming of calculations, and to V. P. Bykov and L. A. Vaĭnshteĭn for useful discussions.

[1] V. I. Veksler, DAN SSSR **43**, 346 (1944); J. Phys. (U.S.S.R.) **9**, 153 (1945).

[2] Redhead, Le Caine, and Henderson, Can. J. Research **A28**, 73 (1950).

[3] Henderson, Heymann, and Jennings, Proc. Phys. Soc. (London) **B66**, 654 (1953).

[4] H. F. Kaiser, Rev. Sci. Instr. **25**, 565 (1955).

[5] D. Aitken and R. E. Jennings, Nature **181**, 1726 (1958).

[6] A. Carrelli and F. Porreca, Nuovo cimento **6**, 729 (1957).

[7] Henderson, Heymann, and Jennings, Proc. Phys. Soc. (London) **B66**, 41 (1953).

[8] A. A. Kolomenskii, J. Tech. Phys. (U.S.S.R.) **30**, 1347 (1960), Soviet Phys.-Tech. Phys. **5**, 1278 (1961).

[9] Kotov, Kuznetsov, and Rubin, Usp. Fiz. Nauk **64**, 197 (1958).

[10] Kapitza, Bykov, and Melekhin, JETP **39**, 997 (1960), Soviet Phys. JETP **12**, 693 (1961).

[11] D. K. Aitken, Proc. Phys. Soc. (London) **A70**, 550 (1957).

[12] A. Poulin, Nuclear Instr. and Methods **5**, 107 (1959).

[13] V. P. Bykov and V. N. Kostryukov, Pribory i Tekhnika Éksperimenta (Instr. and Exptl. Techniques) **3**, 154 (1959).

[14] G. P. Prudkovskii, Collection, Nekotorye Voprosy Inzhenernoĭ Fiziki (Some Problems of Engineering Physics), Moscow Physics and Engineering Institute, No. 2, 1957, p. 36.

[15] H. Reich, Z. angew. Phys. **11**, 481 (1960).

[16] S. P. Kapitza, J. Tech. Phys. (U.S.S.R.) **29**, 729 (1959), Soviet Phys.-Tech. Phys. **4**, 654 (1959).

[17] J. S. Bell, Proc. Phys. Soc. (London) **B66**, 802 (1953).

[18] V. P. Bykov, JETP **40**, 1658 (1961), Soviet Phys. JETP **13**, 1169 (1961).

[19] Chodorow, Ginzton, Hanse, Kyhl, Neal, and Panofsky, Rev. Sci. Instr. **26**, 134 (1955).

[20] L. A. Vaĭnshteĭn, Elektromagnitnye Volny (Electromagnetic Waves), Soviet Radio, Moscow, 1957.

[21] A. Poulin, Nuclear Instr. and Methods **9**, 113 (1960).

Translated by I. Emin
72

TRANSITION RADIATION IN A PLASMA WITH ACCOUNT OF TEMPERATURE

V. M. YAKOVENKO

Institute of Radiophysics and Electronics, Academy of Sciences, Ukrainian S.S.R.

Submitted to JETP editor December 13, 1960

J. Exptl. Theoret. Phys. (U.S.S.R.) 41, 385-388 (August, 1961)

The transition radiation that arises when a charged particle passes through the boundary of a plasma (with dielectric) described by linearized hydrodynamic equations is investigated with account of the effect of the temperature.

GINZBURG and Frank[1] (see also [2,3]) have discovered that radiation is produced when a charged particle passes through the interface between two media with different refractive indices. The formulas were derived in these papers without account of spatial dispersion of the media.

In the case of a plasma, account of the temperature gives rise to spatial dispersion. We consider below the transition radiation in a plasma with account of the temperature. The ions are assumed to be stationary, so that their effect reduces to neutralization of the equilibrium electron density.

Let a particle with velocity $\mathbf{v}$ and charge q move along the z axis and cross at the instant $t = 0$ the interface between a certain medium 1, having a dielectric constant $\epsilon(\omega)$, and a plasma (medium 2). The plasma fills the half-space $z < 0$.

The electromagnetic field excited in the plasma by the moving particle is described by the Maxwell equations

$$\operatorname{rot}\mathbf{E} = -\frac{1}{c}\frac{\partial \mathbf{H}}{\partial t}, \qquad \operatorname{div}\mathbf{E} = 4\pi\left[e\frac{\rho}{m} + q\delta(\mathbf{r} - \mathbf{v}t)\right],$$

$$\operatorname{rot}\mathbf{H} = \frac{1}{c}\frac{\partial \mathbf{E}}{\partial t} + 4\pi\left[e\frac{\rho_0}{m}\mathbf{u} + q\mathbf{v}\delta(\mathbf{r} - \mathbf{v}t)\right], \quad (1)^*$$

where $\mathbf{u}$ is the velocity of motion of the plasma, m is the electron mass, and ρ is the deviation of the electron density from the equilibrium value ρ_0. The values of $\mathbf{u}$ and ρ are determined by the following system of linearized hydrodynamic equations

$$\frac{\partial \rho}{\partial t} + \rho_0 \operatorname{div}\mathbf{u} = 0, \qquad \rho_0\frac{\partial \mathbf{u}}{\partial t} + \nabla p - \frac{e}{m}\rho_0\mathbf{E} = 0,$$

$$\nabla p = v_0^2\nabla\rho, \qquad v_0^2 = T/m, \quad (2)$$

where T is the plasma temperature. The components of the fields in medium 1 are determined from the equations

$$\operatorname{rot}\mathbf{E} = -\frac{1}{c}\frac{\partial \mathbf{H}}{\partial t}, \qquad \operatorname{div}\mathbf{D} = 4\pi q\delta(\mathbf{r} - \mathbf{v}t),$$

$$\operatorname{rot}\mathbf{H} = \frac{1}{c}\frac{\partial \mathbf{D}}{\partial t} + 4\pi q\mathbf{v}\delta(\mathbf{r} - \mathbf{v}t),$$

$$\mathbf{D}(\mathbf{r}, t) = \int_{-\infty}^{+\infty} \varepsilon(\omega)\,\mathbf{E}(\omega, \mathbf{r})\,e^{i\omega t}\,d\omega, \quad (3)$$

and the hydrodynamic equations differ from (2) in that the term with $\mathbf{E}$ is missing. In addition to the continuity of the tangential components of $\mathbf{E}$ and $\mathbf{H}$, the conditions satisfied on the interface are equality of the pressures ($p_1 = p_2$) and equality of the normal velocity components ($u_{1z} = u_{2z}$).

Choosing as solutions waves outgoing from the origin, and using the formulated boundary conditions, we obtain for the fields in the plasma

$$H_1(r, z, t) = \int H_1 e^{i(\omega t - \varkappa_1 z)} J_1(\lambda r)\,\lambda\,d\lambda d\omega,$$

$$H_1 = \frac{q\lambda}{\pi c}\,\frac{\left\{\varepsilon_2 f_1^{-2}(\varkappa_1 \pm \omega/v) - f_2^{-2}\left[\varepsilon_1\gamma(k_2^2 - \omega^2/v^2) \pm \varepsilon_1\omega/v + \varepsilon_2\varkappa_1\right] \pm \dfrac{\gamma\varepsilon_1\omega/v}{\sqrt{k_{02}^2 - \lambda^2} \pm \omega/v}\right\}}{\varepsilon_2\varkappa_1 - \varepsilon_1\varkappa_2 + \varepsilon_1\gamma\lambda^2}, \quad (4)$$

where $J_1(\lambda r)$ are Bessel functions of first order; the plus sign is taken for an incoming particle and the minus sign for a particle outgoing from the plasma.

We introduce here the following notation

$$\varepsilon_2 = 1 - (\omega_0/\omega)^2, \quad \omega_0^2 = 4\pi e^2\rho_{02}/m^2, \quad k_{1,2}^2 = \omega^2\varepsilon_{1,2}/c^2,$$

$$k_{02}^2 = \omega^2\varepsilon_2/v_{02}^2,$$

$$\varkappa_{1,2}^2 = k_{1,2}^2 - \lambda^2, \quad \alpha_1^2 = (\omega/v_{01})^2 - \lambda^2, \quad \alpha_2^2 = \omega^2\varepsilon_2/v_{02}^2 - \lambda^2,$$

$$f_{1,2}^2 = \omega^2/v^2 + \lambda^2 - k_{1,2}^2, \quad \gamma = (1 - \varepsilon_2)/(\varepsilon_2\alpha_1\rho_{02}/\rho_{01} - \alpha_2).$$

*rot = curl.

Let us change to spherical coordinates by means of the relations $r = R \sin\theta$ and $z = -R\cos\theta$ (where R is the distance from the origin to the point of observation). For large values of R the integral (4) is evaluated by the method of steepest descent.[2] Carrying out this integration and calculating the energy flux in a solid angle $d\Omega = \sin\theta\, d\theta\, d\varphi$ over the entire transit time of the particle, we obtain the radiated energy for a charged particle traveling into the plasma:

$$\frac{dW}{d\Omega} = \frac{q^2v^2}{\pi^2c^3}\sin^2\theta\cos^2\theta\int_0^\infty \frac{\sqrt{\varepsilon_2}\,|A|^2\,d\omega}{|\varepsilon_1\cos\theta + \sqrt{\varepsilon_2}\sqrt{\varepsilon_1-\varepsilon_2\sin^2\theta}|^2},$$

$$A = \frac{(\varepsilon_1-\varepsilon_2)(1-\varepsilon_2\beta^2-\beta\sqrt{\varepsilon_1-\varepsilon_2\sin^2\theta})}{(1-\beta^2\varepsilon_2\cos^2\theta)(1-\beta\sqrt{\varepsilon_1-\varepsilon_2\sin^2\theta})} + \frac{v_{02}\varepsilon_1(1-\varepsilon_2)}{v\sqrt{\varepsilon_2}(1+\sqrt{\varepsilon_2\rho_{02}/\rho_{01}})} \times\left[\frac{1}{1+(v/v_{02})\sqrt{\varepsilon_2(1-v_{02}^2\sin^2\theta/c^2)}} - \frac{1-\varepsilon_2\beta^2}{1-\varepsilon_2\beta^2\cos^2\theta}\right]. \quad (5)$$

This formula describes the total energy radiated from the plasma, including the Cerenkov radiation generated in medium 1.[3] When T = 0 this equation is equivalent to the corresponding expression (38) of the paper of Ginzburg and Frank[1] [with v replaced by −v in Eq. (38)].

It follows from (5) that the temperature plays a significant role if the velocity of the charged particle exceeds the average thermal velocity of the plasma electrons. When $v/v_{02} \ll 1$, the transition radiation in the plasma is independent of the temperature. In analogy with the interaction between a particle and an unbounded plasma, we can assume that the intensity is independent of the temperature because the hydrodynamic approximation is used to solve the problem (see [4]). Apparently, a temperature dependence would obtain in the kinetic approximation.

If the particle moves in the opposite direction (from the plasma into medium 1), the formula for the radiation is obtained from (5) by substituting −v for v. The divergence arising when

$$1 - \frac{v}{v_{02}}\sqrt{\varepsilon_2\left(1-\frac{v_{02}^2}{c^2}\sin^2\theta\right)} = 0 \quad (6)$$

is due here to the occurrence in the plasma of a cylindrical Cerenkov wave obtained from (4) (see [2]):

$$H_2 = \frac{q}{c\sqrt{2\pi vR\sin\theta}}\int_{-\infty}^{\infty} C\exp\left\{i\left[\omega t - \frac{\omega}{v}R\left(\sqrt{1-\varepsilon_2\left(\frac{v^2}{v_{02}^2}-\beta^2\right)}\cos\theta + \sin\theta\sqrt{\frac{v^2}{v_{02}^2}\varepsilon_2 - 1}\right)\right]\right\}d\omega,$$

$$C = \frac{\sqrt{i\omega}(1-\varepsilon_2)(v^2\varepsilon_2/v_{02}^2-1)^{1/4}}{\left[\frac{\varepsilon_2}{\varepsilon_1}\sqrt{1-\frac{v^2}{v_{02}^2}\varepsilon_2+\beta^2\varepsilon_1}+\sqrt{1-\varepsilon_2\left(\frac{v^2}{v_{02}^2}-1\right)}\right]} \cdot \frac{\sqrt{i\omega}(1-\varepsilon_2)(v^2\varepsilon_2/v_{02}^2-1)^{1/4}}{\left[1+\frac{v}{v_{02}}\varepsilon_2\sqrt{\frac{\rho_{02}}{\rho_{01}}\left(1+\varepsilon_2-\frac{v_{02}^2}{v^2}\right)}\right]+\frac{v^2}{v_{02}^2}\varepsilon_2(1-\varepsilon_2)}.$$

The angle determined by relation (6) characterizes the cone of the Cerenkov waves reflected from the interface.

Thus, for a particle with velocity greater than the mean thermal velocity of the plasma electrons, we obtain for the transition-radiation energy

$$\frac{dW_{\text{Cer}}}{dr} = \frac{q^2}{v^2}\int_0^\infty \frac{(1-\varepsilon_2)^2\{(v^2\varepsilon_2/v_{02}^2-1)[1-\varepsilon_2(v^2/v_{02}^2-v^2/c^2)]\}^{1/2}\cdot\omega\,d\omega}{\varepsilon_2|S|^2},$$

$$S = \left[\frac{\varepsilon_2}{\varepsilon_1}\sqrt{1-\frac{v^2}{v_{02}^2}\varepsilon_2+\beta^2\varepsilon_1}+\sqrt{1-\varepsilon_2\left(\frac{v^2}{v_{02}^2}-1\right)}\right] \times\left[1+\frac{v}{v_{02}}\varepsilon_2\sqrt{\frac{\rho_{02}}{\rho_{01}}\left(1+\varepsilon_2-\frac{v_{02}^2}{v^2}\right)}\right]+\frac{v^2}{v_{02}^2}\varepsilon_2(1-\varepsilon_2). \quad (9)$$

c

$$\frac{dW_{\text{tr}}}{d\Omega} = \frac{q^2v^2}{\pi^2c^3}\sin^2\theta\cos^2\theta\int_0^\infty \frac{\sqrt{\varepsilon_2}\,|A|^2\,d\omega}{|\varepsilon_1\cos\theta+\sqrt{\varepsilon_2}\sqrt{\varepsilon_1-\varepsilon_2\sin^2\theta}|^2},$$

$$A = \frac{(\varepsilon_1-\varepsilon_2)(1-\varepsilon_2\beta^2+\beta\sqrt{\varepsilon_1-\varepsilon_2\sin^2\theta})}{(1-\beta^2\varepsilon_2\cos^2\theta)(1+\beta\sqrt{\varepsilon_1-\varepsilon_2\sin^2\theta})} + \frac{v_{02}\varepsilon_1(1-\varepsilon_2)(1-\beta^2\varepsilon_2)}{v\sqrt{\varepsilon_2}(1+\sqrt{\varepsilon_2\rho_{02}/\rho_{01}})(1-\beta^2\varepsilon_2\cos^2\theta)}. \quad (8)$$

For the Cerenkov radiation we obtain the energy flux through an annular area r, r+dr over the entire transit time of the particle:

Here, as in formula (7), the integration extends over the frequencies

$$\omega_0\left(1-\frac{v_{02}^2}{v}\right)^{-1/2} \leqslant \omega \leqslant \omega_0\frac{\left[\left(1-\frac{v_{02}^2}{c^2}\sin^2\theta\right)\right]^{1/2}}{\left(1-\frac{v_{02}^2}{v^2}-\frac{v_{02}^2}{c^2}\sin^2\theta\right)}.$$

Let us mention also the transition radiation produced when a particle crosses the interface

between a plasma and a dielectric, on which interface the normal component of the plasma velocity vanishes, $u_{2Z} = 0$. The boundary conditions for the fields **E** and **H** remain the same as before. All the results are obtained for this case from formulas (5) — (9) by putting $\rho_{01} = \infty$. In order to obtain the corresponding expressions for the vacuum-plasma case it is sufficient to put $\epsilon_1 = 1$ and $\rho_{01} = \infty$ in (5) — (9). It is assumed here, naturally, that the interface is a solid wall.

In conclusion, the authors express their gratitude to F. G. Bass for guidance and also to É. A. Kaner for useful advice in carrying out this work.

[1] V. L. Ginzburg and I. M. Frank, JETP **16**, 15 (1945).

[2] G. M. Garibyan, JETP **33**, 1403 (1957), Soviet Phys. JETP **6**, 1079 (1958).

[3] V. E. Pafomov, JETP **36**, 1853 (1959), Soviet Phys. JETP **9**, 1321 (1960).

[4] A. I. Akhiezer and A. G. Sitenko, JETP **23**, 161 (1952).

Translated by J. G. Adashko
73

THE MEAN FREE PATH OF MOLECULES IN A MOLECULAR BEAM

V. S. TROITSKII

Radiophysics Institute of the Gor'kii State University

Submitted to JETP editor January 9, 1961

J. Exptl. Theoret. Phys. (U.S.S.R.) **41**, 389-390 (August, 1961)

It is shown that the mean free path of molecules at any point in a molecular beam with a Maxwellian velocity distribution is almost exactly three times greater than the path length in a gas of the same density.

THE question of the mean free path of molecules in the beam, which limits the possible increase in beam power, arises at the present time in connection with the construction of molecular generators using relatively dense beams of molecules. A determination of the path length enables an estimate of the possible beam density to be made for a given length, and its destruction by diffusion to be calculated.

For the calculation we shall assume that the molecular motion at the point considered is unidirectional. This is clearly justifiable at distances from the beam source greater than its diameter, i.e., in the region usually used in practice. We will neglect impacts with molecules scattered diffusely at collisions, which limits the applicability of the expression derived below to cases where the fraction of diffused molecules is small.

In view of what has been said, the calculation of the path length of a molecule in the beam reduces to the calculation of the path length in a gas with a Maxwellian law for the distribution of velocities c:

$$F(c) = 4\pi(\beta^3/\pi^3)^{1/2} e^{-\beta c^2} c^2, \qquad \beta = m/2kT.$$

Considering two groups of molecules in the beam with velocities c and c_1, lying in the ranges dc and dc_1, we can write for the total number of collisions between them in unit volume per second $d\nu(c, c_1) = n^2 F(c) F(c_1) \pi\sigma^2 g\, dc\, dc_1$,[1] where n is the molecular density at the point of the beam considered, $g = c - c_1$ is the relative velocity of the molecules in the beam, and σ is the effective molecular radius.

The number of collisions in unit volume per second of any molecule of the first group, with velocity c, with all the other molecules equals

$$d\nu_1(c) = n\pi\sigma^2 \int_0^\infty |c - c_1| F(c_1)\, dc_1.$$

The number of collisions, averaged for all possible molecular velocities, will be

$$\nu = n\pi\sigma^2 \int_0^\infty F(c)\, dc \int_0^\infty |c - c_1| F(c_1)\, dc_1.$$

Breaking down the inner integral into two with limits 0, c and c, ∞, integrating, and expressing β in terms of the mean thermal velocity $\bar{c} = 2/\sqrt{\pi\beta}$, we obtain

$$\nu = n\pi\sigma^2\bar{c}\,(7 - 4\sqrt{2})/2\sqrt{2} \approx n\pi\sigma^2\bar{c} \cdot 0{,}475.$$

The mean free path $\bar{c}/\nu$ at the point in the beam with the given density n is

$$\lambda_{\text{beam}} = \frac{4}{7 - 4\sqrt{2}} \frac{1}{n\pi\sigma^2\sqrt{2}} = \frac{4}{7 - 4\sqrt{2}} \lambda_{\text{gas}} \approx 3\lambda_{\text{gas}},$$

where λ_{gas} is the mean free path of molecules in the gas. The path length of molecules in the beam is thus three times greater than the path length in a gas of the same density.

It is of interest to determine the path length in a quasi monokinetic beam, when the molecular velocity is distributed uniformly in some interval Δc around the mean velocity c. The distribution law in this case is $F(c) = 1/\Delta c$. Substituting this into the expression for ν and integrating, we obtain $\nu = n\pi\sigma^2\Delta c/3$, whence the path length $\lambda_{\text{beam}} = \lambda_{\text{gas}} \times c3\sqrt{2}/\Delta c$.

[1] L. Boltzmann, Vorlesungen über Gastheorie, Barth, Leipzig, 1910.

Translated by R. Berman
74

POLARIZATION CROSS SECTION FOR THE SCATTERING OF FAST NUCLEONS

S. CIULLI and J. FISCHER

Joint Institute for Nuclear Research

Submitted to JETP editor January 24, 1961

J. Exptl. Theoret. Phys. (U.S.S.R.) **41**, 391-393 (August, 1961)

The contribution of pion poles to the cross section for the NN → NN process is investigated for the case where the polarization of one of the final nucleons is measured. It is shown that not only the contribution from the quadratic term but also that from the linear term vanishes at all angles. Some practical consequences of this fact are discussed.

In recent times measurements of polarization in the elastic scattering of fast nucleons at small angles have attracted great interest. In the present article we hope to direct attention to the fact that such experiments are also of considerable theoretical interest.

Let us write the NN → NN scattering amplitude in the form of the sum

$$M = P_1 + P_{-1} + X, \tag{1}$$

where P_1 and P_{-1} arise from single-meson poles lying respectively in the regions $\cos\theta > 1$ and $\cos\theta < -1$ of the plane of the cosine of the scattering angle (center-of-mass system). Their explicit form is well known; the principal experimental interest, therefore, lies in the term X, which is determined by more distant singularities (many-pion contributions[1,2]).

As is known, the individual terms of relation (1) have the form (μ is the mass of the π meson)

$$P_1 = \frac{g^2}{\mu^2 - \bar{t}} S_5,$$

$$P_{-1} = \frac{g^2}{\mu^2 - \bar{t}}\left(\frac{1}{4} S_1 - S_2 - \frac{3}{2} S_3 - S_4 + \frac{1}{4} S_5\right); \tag{2}$$

$$X = \sum_{i=1}^{5} x_i S_i, \tag{3}$$

where

$$S_1 = 1, \quad S_2 = \sum_{\mu} \gamma_\mu^1 \gamma_\mu^2, \quad S_3 = \sum_{\mu<\nu} i\gamma_\mu^1 \gamma_\nu^1 i\gamma_\mu^2 \gamma_\nu^2,$$

$$S_4 = \sum_{\mu} i\gamma_\mu^1 \gamma_5^1 i\gamma_\mu^2 \gamma_5^2, \quad S_5 = \gamma_5^1 \gamma_5^2;$$

$$t = -2q^2(1 - \cos\theta), \quad \bar{t} = -2q^2(1 + \cos\theta)$$

(q is the length of the momentum vector in the center-of-mass system). The gamma-matrix superscripts distinguish between the spaces of the first and second fermions.

Let us begin by examining the first single-meson term P_1, and let us write the sum $P_{-1} + X$ as

$$Y = \sum_{i=1}^{5} y_i S_i.$$

The expression for the cross section contains, besides the quadratic terms $|P_1|^2$ and $|Y|^2$, the interference terms $P_1^+ Y$ and $Y^+ P_1$. If it were now possible to assume that all coefficients y_i except y_5 were negligibly small, y_5 could be expressed in terms of the unpolarized cross section by solving a simple quadratic equation. However, since Y contains generally speaking all the structure terms, it is not possible to distinguish further between contributions to the cross section from terms of the type $|Y|^2$ and interference terms.

At high energies this "undesirable" contribution from the interference terms becomes, generally speaking, stronger and stronger, since the poles asymptotically approach the boundary of the physical region (for example, at 9 Bev the cosines of the poles $P_{\pm 1}$ equal ± 1.002 in the center-of-mass system). At small angles (which are important from the experimental point of view) the quadratic term $|P_1|^2$ is of practically no significance for the cross section, since it vanishes together with its derivative at $\cos\theta = 1$.[1] On the other hand, the interference term $P_1^+ X + X^+ P_1$ has a larger derivative at $\cos\theta = 1$. Therefore at small angles the effect of the pole is almost exclusively determined by the sharp dependence of the interference term on the cosine.

In order to find all five coefficients x_i it is necessary to carry out a "complete experiment" consisting of five independent experiments. We wish to draw attention below to the fact that in experiments where the polarization of one of the nucleons is measured the effect of the interference term $P_{\pm 1}^+ X + X^+ P_{\pm 1}$ is completely eliminated

throughout the region $-1 \leq \cos\theta \leq 1$ (the vanishing of the quadratic term $|P_{\pm 1}|^2$ in such experiments is generally known).

The polarization cross section is proportional to the expression

$$\mathrm{Sp}_1\mathrm{Sp}_2\left(M^+\frac{-i\hat{p}+m}{2m}\frac{-i\hat{k}+m}{2m}M\frac{-i\hat{k}'+m}{2m}\frac{-i\hat{p}'+m}{2m}\Sigma\mathbf{e}\right), \tag{4}$$

where $\hat{p} = \gamma_\mu p_\mu$; $\Sigma\mathbf{e}$ is the Racah spin tensor of nucleon polarization; Σ_i here is determined by the relation (σ_i is the Pauli matrix)

$$\Sigma_i \equiv \begin{pmatrix} \sigma_i & 0 \\ 0 & \sigma_i \end{pmatrix} = i\gamma_5\gamma_i\beta \qquad (\beta = \gamma_4).$$

Multiplying this relation by the polarization vector $e \equiv (0, \mathbf{e})$, we obtain $\Sigma\mathbf{e} = i\gamma_5\hat{e}\beta$.

To calculate the interference between amplitude (1) and pole (2) it is necessary to replace one of the M's in (4) by a pseudoscalar term and the other by an expression for X. The computation can be carried out in the rest system of the polarized nucleon. The problem consists of calculating five sums of double traces which are combinations of sixteen expressions of the type

$$i\mathrm{Sp}\left(\frac{-i\hat{p}+m}{2m}\gamma_4\gamma_5\gamma_4\frac{1+\gamma_4}{2}\hat{e}\gamma_4\gamma_5\gamma_A\right)$$
$$\times\,\mathrm{Sp}\left(\frac{-i\hat{k}+m}{2m}\gamma_4\gamma_5\gamma_4\frac{-i\hat{k}'+m}{2m}\gamma_A\right), \tag{5}$$

where γ_A designates any of the sixteen terms of the appropriate γ-algebra. It is necessary to form five sums from these terms so as to obtain the structure terms $S_1, \ldots, S_5$. All these sums equal zero, because the expression $\epsilon^{\alpha\beta\gamma\delta}p_\alpha p'_\beta k'_\gamma k_\delta$ vanishes owing to conservation of energy and momentum ($\epsilon^{\alpha\beta\gamma\delta}$ is a unit antisymmetric tensor).

The second single-meson term P_{-1}, which in the chosen representation has a complicated structure, can be reduced to the form $\gamma_5^1\gamma_5^2$ by the Fierz transformation.

As has been shown above, the effect of the single-meson term on the cross section is completely eliminated in polarization experiments, and it becomes possible to measure directly the contributions of higher meson approximations. Of course, there are some nonsingle-meson terms whose spin structure resembles that of the single-meson terms, and which thus also make no contribution to the polarization cross section. But although it is impossible to determine the magnitude of all x_i ($i = 1, 2, \ldots, 5$) by such an experiment, we can still obtain a lower estimate of the total contribution of nonsingle-meson terms. At the present time very little is known about them theoretically, but it is generally considered that they are small.

---

[1] G. F. Chew, Phys. Rev. 112, 1380 (1958); Ann. Rev. Nucl. Sci. 9, 29 (1959).

[2] Amati, Leader, and Vitale, Nuovo cimento 17, 68 (1960).

Translated by Mrs. J. D. Ullman
75

EVOLUTIONALITY CONDITIONS OF STATIONARY FLOWS

R. V. POLOVIN

Physico-Technical Institute, Academy of Sciences, Ukrainian S.S.R.

Submitted to JETP editor January 25, 1961

J. Exptl. Theoret. Phys. (U.S.S.R.) **41**, 394-399 (August, 1961)

Application of the evolutionality conditions to flows in nozzles and to transonic flows shows that a continuous transition from subsonic to supersonic velocity is possible, whereas transition from supersonic to subsonic velocity is accompanied by the formation of shock waves. Application of the evolutionality conditions to an oblique shock wave attached to a wedge indicates that the flow behind the shock wave is subsonic. The evolutionality conditions are also applied to exothermal and endothermal discontinuities.

1. INTRODUCTION

ANALYSIS of magnetohydrodynamic shock waves has shown that not all shock waves on which the conservation laws are satisfied and the entropy increases can be realized in practice. For magnetohydrodynamic shock waves to exist it is necessary, in addition, that the evolutionality conditions be satisfied,[1] i.e., that the number of outgoing waves be equal to the number of independent boundary conditions on the discontinuity surface.[2,3]

An account of the evolutionality conditions is essential also in the investigation of the possibility of existence of several gasdynamic flows in the absence of a magnetic field. The present article is devoted to this subject.

We investigate the evolutionality conditions of continuous flows and of moving and attached discontinuities. An account of these conditions enables us to conclude that a continuous transition from supersonic to subsonic flow is impossible. In particular, shock waves must occur in the reversed Laval nozzle (which converts supersonic flow into subsonic). Similar shock waves must also occur in transonic flow about a bounded body. We shall advance later on certain arguments in favor of concluding that an attached oblique shock wave is a weak one.

2. CONTINUOUS ONE-DIMENSIONAL FLOWS

The meaning of the evolutionality condition is best seen by analyzing the flow of gas in a nozzle.

Let the stationary values of the velocity, pressure, and entropy experience infintesimal perturbations δv_x, δv_y, δp, and δs (the x axis is directed along the nozzle). These perturbations can be resolved into four terms, each propagating along one of the characteristics. The slopes of these characteristics in the (x, t) plane are determined by the following relations (we confine ourselves to the one-dimensional theory):

$$dx/dt = v, \tag{1}$$
$$dx/dt = v+c, \tag{2}$$
$$dx/dt = v-c. \tag{3}$$

The characteristic (1) is dual and serves the perturbations of both the entropy and the velocity curl. The perturbations of the Riemann invariants propagate along characteristic (2) and (3). The characteristics (1) and (2) are always directed downstream. The characteristic (3) is directed downstream in the case of supersonic velocity of the medium and upstream in the case of subsonic velocity. If the flow is everywhere subsonic or everywhere supersonic, each of the perturbations propagates downstream or upstream along one of the characteristics. Such a flow is evolutional.

In passing through the speed of sound, the two cases shown in Fig. 1 are possible. Figure 1a corresponds to the ordinary Laval nozzle in which

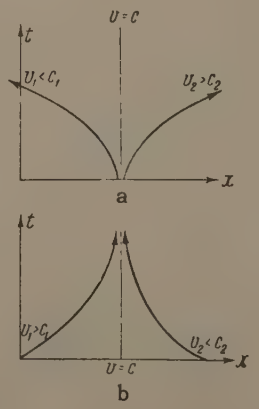

FIG. 1

subsonic flow becomes supersonic. Figure 1b corresponds to the reversed Laval nozzle, in which supersonic flow is transformed into subsonic.

In the former case (Fig. 1a) two characteristics of type (3) go from the sound line v = c. These characteristics carry the same perturbation to the entrance and to the exit from the nozzle. Such a flow is also evolutional.

In the second case (Fig. 1b), the different perturbations occurring at the input and at the output of the nozzle are carried to the sound line. Since these perturbations are independent, a discontinuity is produced on the sound line,* in other words, this flow is non-evolutional.

3. TRANSONIC FLOW

Let a stationary bounded body be placed in a subsonic gas stream. Since the velocity of the gas on the surface of the body is greater than the velocity at infinity, the gas will reach the velocity of sound for a certain critical Mach number at infinity. Starting with this value of the Mach number, the appearance of shock waves is possible. We want to know whether shock waves appear when the velocity of the incoming gas is increased, or whether a continuous flow about a finite body is possible such that the velocity of the gas is subsonic at infinity and bounded regions of supersonic flow exist on the surface of the body. Such continuous solutions do exist formally, but it will be shown presently that they are not evolutional and therefore cannot be realized.†

To prove the non-evolutionality of the transonic flow we note that the flow is one-dimensional near the body, where the deduction made above, concerning flows in nozzles, remains valid; viz., a continuous transition from subsonic to supersonic flow is evolutional and can be realized, but a continous transition from supersonic to subsonic flow is not evolutional, i.e., not realizable.

The reason for the impossibility of having a continuous transonic flow about a body is that infinitesimal perturbations produce a radical change in the entire flow pattern. The impossibility of transonic flow about a body under an infinitesimal perturbation of the stationary state was demonstrated in a different manner by several writers.[6-13]

4. MOVING DISCONTINUITIES

Let us write out the most general form of the conservation laws that hold on the discontinuity surface: the conservation of mass

$$\{\rho v_n\} = 0, \tag{4}$$

the conservation of momentum

$$\{p + \rho v_n^2\} = 0, \tag{5}$$

$$\{v_\tau\} = 0 \tag{6}$$

and the conservation of energy

$$\{w + v_n^2/2\} = \Delta E, \tag{7}$$

where w is the heat function, v_n the normal component of the gas velocity, v_τ the tangential component, and ΔE the change in energy due to dissociation, ionization, chemical reactions, or phase transitions, radiation* or absorption of photons; the subscripts 1 and 2 pertain to the regions in front and behind the discontinuity, respectively; the symbol $\{\ \}$ denotes the difference between the values of the corresponding quantities behind and in front of the discontinuity.

Let us examine now the form assumed by the shock adiabat (connection between the pressure p_2 behind the shock wave and the specific volume $1/\rho_2$). To find the equation of the shock adiabat we must eliminate v_{1n} and v_{2n} from the conservation laws (4), (5), and (7). A plot of the shock adiabat is shown in Fig. 2a, where the point 1 denotes the initial state $(p_1; 1/\rho_1)$. The line 4-1-3 denotes the shock adiabat without change of energy ($\Delta E = 0$), the line 9-8-7-15-5-6 is the shock adiabat with release of energy ($\Delta E > 0$), and finally the line 11-10-16-12-13-14 shows the shock adiabat with absorption of energy ($\Delta E < 0$). On the segments 7-15 and 16-12, bounded by the vertical line 7-1-12 and the horizontal line 16-1-15, the mass flux den-

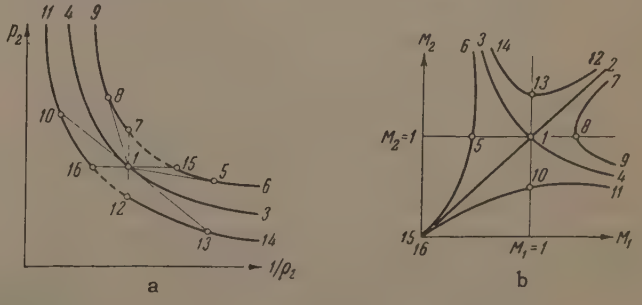

FIG. 2

*That discontinuity is formed on the sound line in the reversed Laval nozzle was demonstrated by Kantrowitz,[4] who investigated the deformation of the profile of the perturbation wave; see also the article by Meyer.[5]

†Experiments show that shock waves are produced in the transition from supersonic to subsonic velocity.

*We have in mind discontinuities in which the energy radiated is not compensated by absorption in the adjacent layers of the matter. Otherwise we must put $\Delta E = 0$, and the presence of radiation affects only the form of the equation of state.

sity $\rho_1 v_{1n}$ becomes imaginary, and these segments cannot be realized.

To determine the evolutionality conditions, it is more convenient to use the shock adiabat in the (M_1, M_2) plane (M_1 and M_2 are the Mach numbers ahead of and behind the discontinuity, respectively). Such an adiabat is shown in Fig. 2b, where the numbers denote the same points as in Fig. 2a. In Fig. 2b the points 15 and 16 coincide with the origin. At 8 and 5 we have $M_2 = 1$ and the lines 1-8 and 1-5 are tangent to the shock adiabat 9-7-15-6 (see Fig. 2a). $M_1 = 1$ at 10 and 13, where the tangent 10-1-13 to the shock adiabat 4-1-3 crosses the shock adiabat 11-16-12-14.

Let us proceed to determine the evolutionality conditions of the discontinuities. We consider the shock waves first.

The speed of propagation of a shock wave depends on its amplitude. Therefore the evolutionality conditions of the shock wave have the form[14] $M_1 > 1$ and $M_2 < 1$. Such waves can propagate either without change of energy (segments 4-1 of Figs. 2a and 2b), with release of energy (segments 9-8), or with absorption of energy (segments 10-11). Corresponding to segment 9-8 is an overcompressed detonation wave; such a wave is a combustion wave in which the medium is heated in the shock wave and point 8 corresponds to the Chapman-Jouguet detonation. Segment 10-11 corresponds to a shock wave in which the heating of the medium is accompanied by absorption of energy resulting from dissociation or ionization. This section corresponds also to a shock wave in a fog, accompanied by evaporation.

Let us proceed now to examine discontinuities with propagation speed independent of the amplitude. In this case the evolutionality conditions have the form[14] $M_1 < 1$, $M_2 < 1$, or $M_1 > 1$, $M_2 > 1$. Such waves can propagate without change of energy only in the trivial case when there is no discontinuity, $M_1 = M_2$ (the line 0-1-2 of Fig. 2b). If energy is released, these waves correspond to segments 15-5 and 7-8 of Figs. 2a and 2b. Segment 15-5 corresponds to the ordinary combustion waves; the segments 7-8 corresponds either to a supersonic combustion wave (such combustion takes place in thermonuclear reactions, when the medium is heated by radiant heat conduction, and also in a supersonic stream) or to a discontinuity with recombination. Segments 15-5 and 7-8 correspond also to condensation jumps.* Discontinuities corresponding to segments 16-10 and 12-13 apparently cannot be realized.

Let us consider, finally, the discontinuities that convert subsonic gas flow into supersonic ($M_1 < 1$, $M_2 > 1$). Such continuities correspond to the segments 5-6, 1-3, and 13-14 of Fig. 2. These discontinuities are non-evolutional[14] and therefore cannot exist. Such flows, however, can be realized in the case of gas flowing in a nozzle. Analogously, segments 13-12, 8-7 and 15-5, 16-10 can be realized in a nozzle without going through the velocity of sound.

5. ATTACHED SHOCK WAVE

Let us proceed to an analysis of a shock wave attached to the vertex of a wedge in the stream.

We consider two-dimensional perturbations δv_x, δv_y, δp, and δs of the velocity, pressure, and entropy. The perturbations of the entropy and of the velocity curl propagate along the characteristic

$$x/t = v_x, \qquad y/t = v_y, \tag{8}$$

while the perturbations of the pressure and the velocity potential propagate along the characteristic cone

$$(x/t - v_x)^2 + (y/t - v_y)^2 = c^2. \tag{9}$$

We consider first the evolutionality conditions of an infinitesimal shock-wave segment located away from the wedge. In the region 1 in front of the shock wave the flow is supersonic; therefore perturbations arising on the shock wave cannot go into this region. These perturbations can be outgoing only in the region 2 behind the shock wave. On the surface of the shock wave, three independent boundary conditions are satisfied, and therefore the number of outgoing shock waves should also be three.

The entropy wave and the wave of the velocity curl are always outgoing. Were the characteristic cone (9) with vertex located on the discontinuity surface, to be located entirely in the region 2 when $t > 0$, then two additional perturbations would propagate along it. Thus, the number of outgoing waves would be four, and the shock wave would be non-evolutional. Were this cone to be wholly situated in region 1, then the number of outgoing waves would be two, i.e., the shock wave would also be non-evolutional. Therefore the characteristic cone

*In view of the confusion in the terminology, we must stop to discuss the term "weak detonation." Courant and Friedrichs[15] call a weak detonation one in which $M_1 > 1$ and $M_2 > 1$, and prove that it cannot exist (an analogous proof was first published by Zel'dovich[16]). Other authors[17-20] speak of "weak detonation," now taken to mean a condensation discontinuity in a supersonic stream. Finally, Ubbelohde[21] and Lewis[22] also speak of the possibility of a weak detonation, but define it as an overcompressed detonation ($M_1 > 1$, $M_2 < 1$) in which the release of energy is small.

(9) should be situated partially in region 1 and partially in region 2. This means that the normal component of the velocity of the medium behind the shock wave should be subsonic

$$v_{2n} < c_2. \qquad (10)$$

Let us consider now the evolutionality conditions of an infinitesimal shock-wave segment adjacent to the vertex of the wedge. Since the angle of inclination of the shock wave is determined uniquely by the size of the wedge and by the velocity of the medium in region 1, the intensity of the shock wave is not an independent perturbation. Therefore four boundary conditions are satisfied on the discontinuity surface, and the number of outgoing waves should be four.

Let us locate the x axis on the wall in region 2. Then the points located on the wall will satisfy in the three-dimensional space (x, y, t) the relations

$$y = 0, \qquad x > 0, \qquad t > 0 \qquad (11)$$

(here $v_{2x} = v_2$ and $v_{2y} = 0$).

The intersection of the characteristic cone (9) with the surface of the wall (11) defines two characteristics $x/t = v_2 + c_2$ and $x/t = v_2 - c_2$ ($y = 0$), which, by virtue of the foregoing, should be outgoing, i.e., should be located in the region $t > 0$, $x > 0$. From this it follows, in turn, that an attached shock wave is evolutional only when the total velocity of the medium behind the shock wave is greater than the velocity of sound:

$$v_2 > c_2. \qquad (12)$$

Thus, flow about a wedge gives rise to weak shock waves, as is indeed observed in practice.

As shown by Thomas,[23] when $v_2 < c_2$ an infinitesimal perturbation of an oblique shock wave causes a sharp change in the entire flow pattern. As is well known, the angle of inclination of the flow in an oblique shock wave cannot exceed a certain maximum value χ_{max}. It follows from the foregoing that detachment of an oblique shock wave occurs at a smaller angle of inclination χ_s. This angle is determined from the condition that the velocity of the gas v_2 behind the shock wave must equal the velocity of sound c_2.

6. INTERSECTION OF DISCONTINUITIES

Let us consider the correct reflection of a shock wave from a solid wall (see Fig. 3; OA — incident wave, OB — reflected wave, α_1 — angle of incidence, α_2 — angle of reflection). The angle of incidence α_1 is specified, and the frame of reference is chosen such as to make the point

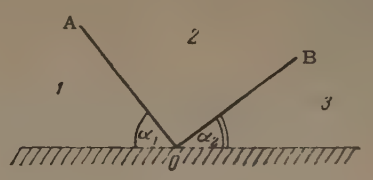

FIG. 3

O stand still. In the regions 1, 2, and 3, the perturbations δp, δs, δv_x, and δv_y are possible; in addition, the velocity of the point O and the angle of reflection α_2 can experience perturbations δU and $\delta\alpha_2$. These perturbations are interrelated by ten boundary conditions: four boundary conditions on the incident wave OA, four boundary conditions on the reflected wave OB, and the two conditions making the velocity of the medium in the regions 1 and 3 parallel to the wall ($\delta v_{1y} = 0$, $\delta v_{3y} = 0$; the x axis is directed along the wall).

By eliminating from these ten boundary conditions the six quantities δp_2, δs_2, δv_{2x}, δv_{2y}, δU, and $\delta\alpha_2$, we obtain four independent boundary conditions, which relate the perturbations in the regions 1 and 3. The evolutionality conditions consist in the fact that the number of characteristics outgoing from the point O should also be four. Repeating the arguments of Sec. 5, we find that the flow in region 3 should be supersonic, $v_3 > c_3$. This means that the shock wave always belongs to the weak family.

Application of the evolutionality conditions to the Mach reflection of shock waves is expected to eliminate the ambiguity of the solution.

The author is grateful to A. I. Akhiezer, L. D. Landau, M. A. Leontovich, and L. I. Sedov for valuable discussions.

[1] I. M. Gel'fand, Usp. Mat. Nauk (Advances in Mathematical Sciences), **14**, 87 (1959).

[2] Akhiezer, Lyubarskii, and Polovin, JETP **35**, 731 (1958), Soviet Phys. JETP **8**, 507 (1959).

[3] R. V. Polovin, Usp. Fiz. Nauk **72**, 33 (1960), Soviet Phys.-Uspekhi **3**, 677 (1961).

[4] A. Kantrowitz, Phys. Rev. **71**, 465 (1947).

[5] R. E. Meyer, Proc. Symp. Appl. Math., McGraw-Hill Co., (1953), vol. 4, p. 41.

[6] G. I. Taylor, J. of London Math. Soc. **5**, 224 (1930).

[7] A. I. Nikol'skii and G. I. Taganov, Prikladnaya matematika i mekhanika (Applied Mathematics and Mechanics) **10**, 481 (1946).

[8] F. I. Frankel', ibid. **11**, 199 (1947).

[9] A. Buseman, J. Aeron. Sci. **16**, 337 (1949).

[10] G. Guderley, Advances in Applied Mechanics **3**, 145 (1953).

[11] A. R. Manwell, Quart. J. Mech. Appl. Math. **7**, 40 (1954).

[12] L. Bers. Comm. Pure Appl. Math. **7**, 79 (1954).

[13] C. S. Morawetz, Comm. Pure Appl. Math. **9**, 45 (1956).

[14] L. D. Landau and E. M. Lifshitz, Mekhanika sploshnykh sred (Mechanics of Continuous Media), Gostekhizdat, 1953, p. 406.

[15] R. Courant and K. Friedrichs, Supersonic Flow and Shock Waves, Interscience, 1948.

[16] Ya. B. Zel'dovich, JETP **10**, 542 (1940).

[17] R. A. Gross and A. K. Oppenheim, ARS Journal **29**, 173 (1959).

[18] S. G. Reed, J. Chem. Phys. **20**, 1823 (1952).

[19] W. D. Hayes, Fundamentals of Gas Dynamics, Vol. 3. High Speed Aerodynamics and Jet Propulsion, Princeton Univ. Press, (1958) p. 417.

[20] G. I. Taylor and R. S. Tankin, ibid. p. 622.

[21] A. R. Ubbelohde, Proc. Roy. Soc. **A204**, 25 (1951).

[22] B. Lewis, Fourth Symposium on Combustion, The Williams and Wilkins Co. (1953), p. 467.

[23] T. Y. Thomas, Proc. Nat. Acad. Sci. **34**, 526 (1948).

Translated by J. G. Adashko
76

"SCALAR" FORM OF THE DIRAC EQUATION AND CALCULATION OF THE MATRIX ELEMENTS FOR REACTIONS WITH POLARIZED DIRAC PARTICLES

Yu. D. USACHEV

P. N. Lebedev Physics Institute, Academy of Sciences, U.S.S.R.

Submitted to JETP editor January 27, 1961

J. Exptl. Theoret. Phys. (U.S.S.R.) 41, 400-409 (August, 1961)

A formalism first proposed by Sommerfeld is developed, in which the wave function in the Dirac equation is a scalar and the corresponding γ matrices behave like a four-vector under Lorentz transformations. The transition to this representation and its various features are investigated. Solutions of the resulting equation are found, and a study is made of the spin operator of the "scalar" Dirac equation, which is a differential operator. A new method is indicated for calculating matrix elements for reactions involving polarized particles. For this purpose a method is also proposed for writing the γ matrices by means of Kronecker δ symbols and certain discontinuous functions.

THE book by Sommerfeld[1] contains a clear statement of the problem as to whether it is possible that there be two points of view regarding the transformation properties of the wave function and the matrices in the Dirac equation. The first, generally accepted, point of view regards the γ matrices as quantities which do not change under any possible linear transformations of the coordinates, while the ψ function turns out to possess the definite transformation properties of a bispinor. In a certain sense the other point of view is the precise opposite of this. Adopting it, we regard the wave function as an invariant under Lorentz transformations, and the γ matrices turn out to have the properties of a four-vector.

Reference [1], however, gives only a statement of the question in principle, and the second point of view has not been developed. The purpose of the present paper is to present an example and some consequences of a formalism entirely based on the second, alternative, statement of the problem.

1. STATEMENT OF THE DIRAC EQUATIONS IN "SCALAR" FORM

Let us define as follows four mutually orthogonal vectors $n^{\mu}{}_{\alpha}$ (the index α written in the second place will always refer to the number of the vector, and the first index μ indicates the component):*

$$g_{\mu\nu}n^{\mu}{}_{\alpha}n^{\nu}{}_{\beta} = g_{\alpha\beta}. \tag{1}$$

*Greek letters run through the values 0, 1, 2, 3. The metric used in this paper is $g_{00} = 1$, $g_{11} = g_{22} = g_{33} = -1$; $\hbar = c = 1$.

It is not hard to verify that the components of the vectors $n^{\mu}{}_{\alpha}$ also satisfy the relations

$$g^{\alpha\beta}n^{\mu}{}_{\alpha}n^{\nu}{}_{\beta} = g^{\mu\nu}. \tag{2}$$

We can change to covariant components in the usual way: $n_{\mu\alpha} = g_{\mu\nu}n^{\nu}{}_{\alpha}$. The relations (1) and (2) allow us to interpret the matrix composed of the components of the vectors $n^{\mu}{}_{\alpha}$ as the matrix of a certain Lorentz transformation.

Let us also define by means of the vectors $n^{\mu}{}_{\alpha}$ certain matrices N^{μ}:

$$N^{\mu} = n^{\mu}{}_{\alpha}\gamma^{\alpha}, \qquad N_{\mu} = g_{\mu\nu}N^{\nu}. \tag{3}$$

Here the four-rowed matrices γ^{α} have the well known properties

$$\gamma^{\mu}\gamma^{\nu} + \gamma^{\nu}\gamma^{\mu} = 2g^{\mu\nu}, \qquad \gamma_{\mu} = g_{\mu\nu}\gamma^{\nu} \tag{4}$$

and with them one can write the Dirac equation in the usual form

$$(-i\gamma^{\mu}\partial/\partial x^{\mu} + m)\psi = 0. \tag{5}$$

It is not hard to verify from Eqs. (1) and (4) that

$$N^{\mu}N^{\nu} + N^{\nu}N^{\mu} = 2g^{\mu\nu}. \tag{6}$$

Owing to this it is possible to construct a first-order equation by means of the matrices N^{μ}

$$(-iN^{\mu}\partial/\partial x^{\mu} + m)\omega = 0. \tag{7}$$

In view of Eq. (6) multiplication of Eq. (7) on the left by the operator $(iN^{\mu}\partial/\partial x^{\mu} + m)$ leads to the second-order equation $(\Box + m^2)\omega = 0$.

Let us now examine the transformation properties of the equation (7). The Lorentz transformation

$$x'^{\mu} = a^{\mu}{}_{\nu}x^{\nu}, \quad n'^{\mu}{}_{\alpha} = a^{\mu}{}_{\nu}n^{\nu}{}_{\alpha}, \quad a^{\nu}{}_{\mu}a_{\lambda}{}^{\mu} = \delta^{\nu}_{\lambda}$$

does not change the form of (7)

$$\left(-iN'^{\mu}\frac{\partial}{\partial x'^{\mu}} + m\right)\omega' = 0, \qquad \omega' = S\omega, \tag{8}$$

if the following relations hold:

$$S\gamma^{\alpha} = \gamma^{\alpha}S \qquad (\alpha = 0, 1, 2, 3). \tag{9}$$

In other words, according to Schur's lemma the matrix S must be the unit matrix, and owing to this the wave function ω is a scalar under Lorentz transformations:

$$S = I, \qquad \omega' = \omega. \tag{10}$$

2. SOLUTIONS OF THE "SCALAR" DIRAC EQUATION

It is easy to find the solutions of our equation (7) by using the usual methods. We note certain features that turn up in this connection.

The condition of solubility of the two systems of equations

$$(N^{\mu}p_{\mu} - m)\,\omega_0{}^{(1)} = 0, \qquad (N^{\mu}p_{\mu} + m)\,\omega_0{}^{(2)} = 0, \tag{11}$$

which correspond to positive-frequency and negative-frequency solutions, is the vanishing of the determinants of their coefficients. This condition takes the form

$$(n^{\mu}{}_0 p_{\mu})^2 - (n^{\mu}{}_1 p_{\mu})^2 - (n^{\mu}{}_2 p_{\mu})^2 - (n^{\mu}{}_3 p_{\mu})^2 - m^2 = 0. \tag{12}$$

We can easily convince ourselves of the truth of Eq. (12) if we go from the system of vectors $n^{\mu}{}_{\alpha}$ to another system of mutually orthogonal vectors $n'^{\mu}{}_{\alpha}$ with the components $n'^{\mu}{}_{\alpha} = \delta^{\mu}_{\alpha}$. In this system of coordinates the condition that the determinant be zero takes the usual form: $p'_{\mu}p'^{\mu} - m^2 = 0$. It is obvious that because of the Lorentz invariance of Eq. (12) the equation holds also in any coordinate system.

We now give a table of the solutions of the "scalar" Dirac equation (the solutions are computed to within a normalization factor)

$$\omega_0 \sim \begin{vmatrix} n^{\mu}{}_0 p_{\mu} + m & 0 & -n^{\mu}{}_3 p_{\mu} & -(n^{\mu}{}_1 - in^{\mu}{}_2)\,p_{\mu} \\ 0 & n^{\mu}{}_0 p_{\mu} + m & -(n^{\mu}{}_1 + in^{\mu}{}_2)\,p_{\mu} & n^{\mu}{}_3 p_{\mu} \\ -n^{\mu}{}_3 p_{\mu} & -(n^{\mu}{}_1 - in^{\mu}{}_2)\,p_{\mu} & n^{\mu}{}_0 p_{\mu} + m & 0 \\ -(n^{\mu}{}_1 + in^{\mu}{}_2)\,p_{\mu} & n^{\mu}{}_3 p_{\mu} & 0 & n^{\mu}{}_0 p_{\mu} + m \end{vmatrix} \tag{13}$$

When one chooses the special coordinate system in which $n'^{\mu}{}_{\alpha} = \delta^{\mu}_{\alpha}$, the solutions (13) take the form of the well known solutions u (first two columns) and v (last two columns) (see, for example, reference 2).

3. THE TRANSFER OF THE TRANSFORMATION PROPERTIES FROM THE ψ FUNCTION TO THE γ MATRICES

Comparing Eqs. (4) and (6), we see that the matrices γ^{μ} and N^{μ} are connected with each other by a similarity transformation (cf., e.g., reference 3)

$$N^{\mu} = R\gamma^{\mu}R^{-1}, \tag{14}$$

where R is a certain nonsingular matrix. On the other hand, remembering the definition of the matrices N^{μ}, we can write the equation

$$R\gamma^{\mu}R^{-1} = n^{\mu}{}_{\alpha}\gamma^{\alpha}. \tag{15}$$

Since the coefficients $n^{\mu}{}_{\alpha}$ are the matrix of a Lorentz transformation, it is easy to identify R^{-1} with the well known transformation matrix that acts on the bispinor in a Lorentz transformation. Thus the change from the usual representation (5) of the Dirac equation to the new "scalar" Dirac equation (7) is made by means of the relations

$$\omega = R\psi, \qquad N^{\mu} = n^{\mu}{}_{\alpha}\gamma^{\alpha} = R\gamma^{\mu}R^{-1}. \tag{16}$$

Thus we have obtained the Dirac equation in a "scalar" form, i.e., in a form in which the wave function does not change in Lorentz transformations and the transformation properties that in the usual theory inhere in the wave function are transferred to the N matrices. We note that the R transformation that accomplishes this transfer preserves eigenvalues, as do the unitary transformations of the bispinor in the usual Dirac equation.

Having in mind Eq. (16), the definition

$$\bar{\omega} = \omega^{+}\gamma^{0}, \tag{17}$$

and also the relation characteristic of Lorentz transformations, $\gamma^0 R^{+}\gamma^0 = R^{-1}$, we can easily show that all quantities bilinear in ω have the same physical natures and transformation properties as in the usual formalism. We shall demonstrate this with the example of the current $\bar{\omega}N^{\mu}\omega$:

$$\bar{\omega}N^{\mu}\omega = \bar{\psi}\gamma^0 R^{+}\gamma^0 N^{\mu}R\psi = \bar{\psi}R^{-1}N^{\mu}R\psi = \bar{\psi}\gamma^{\mu}\varphi.$$

It can also be shown simply in the case of the other bilinear physical quantities, including the spin tensor

$$\tfrac{1}{4}\bar{\omega}(N^{\mu}N^{\nu} - N^{\nu}N^{\mu})\,\omega = \tfrac{1}{4}\bar{\psi}(\gamma^{\mu}\gamma^{\nu} - \gamma^{\nu}\gamma^{\mu})\,\psi. \tag{18}$$

The formal proof of Eq. (18), however, is not enough to establish the fact that the quantity $\frac{1}{4}(N^\mu N^\nu - N^\nu N^\mu)$ actually is the spin operator for the particle described by (7). This question requires some additional investigation.

4. THE SPIN OPERATOR OF THE "SCALAR" EQUATION

In the framework of the usual theory, in the case of the Dirac equation the infinitesimal Lorentz transformation

$$x'^\mu = a^\mu{}_\nu x^\nu \quad (x' = ax), \tag{19}$$

$$a^\mu{}_\nu = \delta^\mu_\nu + \varepsilon^\mu{}_\nu = \delta^\mu_\nu + \varepsilon^{\mu\lambda} g_{\lambda\nu} \quad (\varepsilon^{\mu\nu} = -\varepsilon^{\nu\mu}) \tag{20}$$

generates the well known transformation of the wave function

$$\psi_\alpha(x) \to \psi'_\alpha(x') = S'_{\alpha\beta}\psi_\beta(a^{-1}x') = U_{x'x}S'_{\alpha\beta}\psi_\beta(x). \tag{21}$$

If a^μ_ν is of the form (20), then

$$S'_{\alpha\beta} = \delta_{\alpha\beta} + \tfrac{1}{2}\varepsilon_{\mu\nu}\Sigma^{\mu\nu}_{\alpha\beta}, \quad \Sigma^{\mu\nu} = \tfrac{1}{4}(\gamma^\mu\gamma^\nu - \gamma^\nu\gamma^\mu), \tag{22}$$

and the operator $U_{x'x}$ (an integration over d^4x is understood with respect to the repeated "index" x) can be written in the form

$$U_{x'x} = \delta(x' - x) + \tfrac{1}{2}\varepsilon^{\mu\nu}M_{\mu\nu}\delta(x' - x),$$
$$M_{\mu\nu} = x_\nu\partial/\partial x^\mu - x_\mu\partial/\partial x^\nu. \tag{23}$$

The infinitesimal operators $\Sigma^{\mu\nu}$ and $M_{\mu\nu}$ are closely associated with the spin and orbital angular momentum of the Dirac particle.

It may seem at first glance that the spin of the particle described by Eq. (7) is zero [since in Eq. (8) $S_{\alpha\beta} = \delta_{\alpha\beta}$]. In our case, however, we cannot use the usual formalism expressed in Eqs. (19) — (22). Therefore our problem is to find a mathematical apparatus suitable for the description of the changes of the wave function in (8) which are generated by Lorentz transformations.

On being transformed to a different coordinate system the equation

$$\left(-iN^\mu\frac{\partial}{\partial x^\mu} + m\right)\omega(n^\sigma{}_\alpha, x^\nu) = 0 \quad (\alpha = 0, 1, 2, 3), \tag{24}$$

takes the form

$$\left(-iN'^\mu\frac{\partial}{\partial x'^\mu} + m\right)\omega'(n'^\sigma{}_\alpha, x'^\nu) = 0. \tag{25}$$

It is not hard to find the operator that accomplishes the change from $\omega(n^\sigma{}_\alpha, x^\nu)$ to $\omega'(n'^\sigma{}_\alpha, x'^\nu)$. It can be written in the form

$$\omega'(n'^\sigma{}_\alpha, x'^\nu) = SU_{x'x}T_{n'_\alpha, n_\alpha}\omega(n^\sigma{}_\alpha, x^\nu), \tag{26}$$

where $S_{\alpha\beta} = \delta_{\alpha\beta}$ [by Eq. (10)], the operator $U_{x'x}$ is defined by Eq. (23), and the operator

$$T_{n'_\alpha, n_\alpha} \equiv T_{n'_0 n'_1 n'_2 n'_3,\ n_0 n_1 n_2 n_3} = \prod_{\alpha=0}^{3}\delta'(n'_\alpha - n_\alpha)$$
$$+ \tfrac{1}{2}\varepsilon^{\mu\nu}\left(n_{\nu\beta}\frac{\partial}{\partial n^\mu{}_\beta} - n_{\mu\beta}\frac{\partial}{\partial n^\nu{}_\beta}\right)\prod_{\alpha=0}^{3}\delta(n'_\alpha - n_\alpha) \tag{27}$$

is written here correct to infinitesimals of the second order in ϵ, just as $U_{x'x}$ is in Eq. (23).

It is easy to verify that by means of the operator $ST_{n'_\alpha, n_\alpha}U_{x'x}$ and its reciprocal Eq. (25) can be written in the form (24):

$$S^{-1}T^{-1}_{n'_\alpha, n_\alpha}U^{-1}_{xx'}\left(-iN'^\mu\frac{\partial}{\partial x'^\mu} + m\right)ST_{n'_\alpha, n_\alpha}U_{x'x}\omega(n^\sigma{}_\alpha, x^\nu)$$
$$= \left(-iN^\lambda\frac{\partial}{\partial x^\lambda} + m\right)\omega(n^\sigma{}_\alpha, x^\nu) = 0,$$

As usual, the infinitesimal operator

$$\eta_{\mu\nu} = n_{\nu\beta}\frac{\partial}{\partial n^\mu{}_\beta} - n_{\mu\beta}\frac{\partial}{\partial n^\nu{}_\beta} \tag{28}$$

must be associated with the spin of the particle described by (7). We note that a peculiarity of this representation is that $\eta_{\mu\nu}$ is written in the form of a differential operator, with a structure somewhat reminiscent of that of the four-dimensional generalization of the orbital angular momentum operator. We shall show that (7) nevertheless describes a Dirac particle with the spin $\frac{1}{2}$. To do so we go over to the usual representation of the Dirac equation

$$\bar\omega\eta_{\mu\nu}\omega = \bar\psi R^{-1}\left(n_{\nu\beta}\frac{\partial R}{\partial n^\mu{}_\beta} - n_{\mu\beta}\frac{\partial R}{\partial n^\nu{}_\beta}\right)\psi \equiv \bar\psi R^{-1}R_{\mu\nu}\psi. \tag{29}$$

To find the result of the action of $\eta_{\mu\nu}$ on R and avoid the long and complicated direct calculations, we resort to the following device. On differentiating the equation $R\gamma^\sigma = n^\sigma{}_\alpha\gamma^\alpha R$ with respect to $n^\mu{}_\beta$ and multiplying the result by $n_{\nu\beta}g_{\sigma\lambda}\gamma^\lambda$ from the right, we get

$$4n_{\nu\beta}\frac{\partial R}{\partial n^\mu{}_\beta} = N_\nu R\gamma_\mu + N^\lambda n_{\nu\beta}\frac{\partial R}{\partial n^\mu{}_\beta}\gamma_\lambda.$$

When we now interchange the indices μ and ν and subtract the resulting expression from the one just written, we get the equation for the required quantity

$$R_{\mu\nu} = \tfrac{1}{4}(N_\nu R\gamma_\mu - N_\mu R\gamma_\nu) + \tfrac{1}{4}N^\lambda R_{\mu\nu}\gamma_\lambda. \tag{30}$$

The solution of (30) can be written in the form

$$R_{\mu\nu} \equiv n_{\nu\beta}\partial R/\partial n^\mu{}_\beta - n_{\mu\beta}\partial R/\partial n^\nu{}_\beta = \tfrac{1}{4}R(\gamma_\nu\gamma_\mu - \gamma_\mu\gamma_\nu)$$
$$= \tfrac{1}{4}(N_\nu N_\mu - N_\mu N_\nu)R, \tag{31}$$

which can be verified by direct substitution in (30).

Thus, substituting (31) in (29), we find

$$\bar\omega\eta_{\mu\nu}\omega = \tfrac{1}{4}\bar\psi(\gamma_\nu\gamma_\mu - \gamma_\mu\gamma_\nu)\psi, \tag{32}$$

i.e., (7) indeed still describes a Dirac particle with spin $1/2$, as also follows from (18).

5. QUANTIZATION AND PHYSICAL INTERPRETATION OF THE WAVE FUNCTION OF THE "SCALAR" EQUATION

By simple arguments it is easy to find the method of quantization of the "scalar" equation, corresponding to the usual quantization:

$$[\bar{\omega}_\rho(x'), \omega_\sigma(x)]_+ = -iS_{\sigma\rho}[N^\mu; x - x']. \qquad (33)$$

Here $S_{\sigma\rho}[N^\mu; x-x']$ corresponds to the usual commutator function $S_{\sigma\rho}(x-x')$, with the matrices γ^μ replaced by N^μ. It is obvious that $S_{\sigma\rho}[N^\mu; x-x']$ satisfies the free-particle "scalar" Dirac equation. This method of quantization, and also the replacement of the matrices γ^μ by N^μ in all of the singular functions, establishes the correspondence with the usual formalism and allows us to construct the S-matrix formalism in the standard way.

Let us say a few words about the physical interpretation of the wave function of the "scalar" Dirac equation. Its meaning becomes particularly clear if we transform the "scalar" equation to the coordinate system in which $n'^\mu{}_\alpha = \delta^\mu_\alpha$, and consequently the axes of the new coordinate system coincide with the four unit vectors of the frame formed by the vectors n_α ($\alpha = 0, 1, 2, 3$). As can be seen from Eqs. (7), (3), and (13), in the new coordinate system the "scalar" equation formally coincides with the usual Dirac equation, and its solutions coincide with the solutions of that equation. But the numerical values of the wave function of the scalar equation remain the same in any coordinate system [cf. Eq. (13)], and therefore they are always numerically equal to the wave function of the usual Dirac equation in the coordinate system in which $n'^\mu{}_\alpha = \delta^\mu_\alpha$.

These features of the "scalar" Dirac equation reduce to the fact that the requirement of invariance of its form in any transformed coordinate system is satisfies by changes of the matrices N^μ, without affecting the numerical values of the components of the ω function.

6. THE SIMPLEST SYSTEM OF SOLUTIONS

The considerations given above allow us to find the system of coordinates in which the matrix of the solutions, Eq. (13), takes the simplest possible form—namely, is just a four-rowed unit matrix. For brevity we shall call this coordinate system the system K_0. The required transformation R that accomplishes the change to the system K_0 naturally does not affect the exponential factor in the free-particle solution, and changes only the form of the matrix part.

The transition to K_0 corresponds, in the sense of our previous remarks, to the transition to the coordinate system associated with the Dirac particle at rest. Having then obtained the solutions of the simplest form

$$\varphi_0^{(1)} = \begin{vmatrix} 1 \\ 0 \\ 0 \\ 0 \end{vmatrix}, \qquad \varphi_0^{(2)} = \begin{vmatrix} 0 \\ 1 \\ 0 \\ 0 \end{vmatrix},$$

$$\varphi_0^{(3)} = \begin{vmatrix} 0 \\ 0 \\ 1 \\ 0 \end{vmatrix}, \qquad \varphi_0^{(4)} = \begin{vmatrix} 0 \\ 0 \\ 0 \\ 1 \end{vmatrix}, \qquad (34)$$

we can use them to find the matrix elements of reactions involving polarized Dirac particles by a new method, without using the usual technique of projection operators and the calculation of traces.

In fact, the operator M that stands between the wave functions of the initial and final states, and can be computed, for example, by perturbation theory, is in general a certain four-rowed matrix, independently of how many vertices there are in the process in question. If, however, the initial and final states—solutions of the "scalar" equation—are written in the system K_0 and have the form (34), then the problem of finding the transition probabilities between states of definite polarization reduces in the first stage simply to picking out the corresponding matrix element of M, since $\varphi_0^{(k)} + M\varphi_0^{(l)} = M_{kl}$ ($k, l = 1, 2, 3, 4$). Therefore the solution of the problem breaks up into two steps: a) finding the matrix R that accomplishes the change from the usual Dirac equation to the "scalar" equation with the simplest system of solutions, and b) finding a method for obtaining the matrix element M_{kl}.

7. THE TRANSITION TO THE SYSTEM K_0

The system of four solutions of (5) can be written in the form of a single four-rowed matrix

$$\psi_0 = [2m(\varepsilon + m)]^{-1/2}\{(\varepsilon + m)I - \gamma^0\gamma^k p_k\} \quad (k = 1, 2, 3). \qquad (35)$$

Here I is the four-rowed unit matrix, $\epsilon = |p_0|$, and

$$\gamma^0 = \begin{vmatrix} I' & 0 \\ 0 & -I' \end{vmatrix}, \qquad \gamma^r = \begin{vmatrix} 0 & \sigma_r \\ -\sigma_r & 0 \end{vmatrix} \quad (r = 1, 2, 3) \qquad (36)$$

where I′ is the two-rowed unit matrix and σ_r are the Pauli matrices.

The transition to the "scalar" equation, written in K_0, is accomplished by means of the relations

$$\varphi_0 = R\psi_0 = I, \tag{37}$$

$$R\gamma^\mu R^{-1} = n^\mu{}_\alpha \gamma^\alpha = N^\mu. \tag{38}$$

Hereafter we shall denote by L(p) the matrix R defined by (37), and shall denote by $l^\mu{}_\alpha$ the vectors $n^\mu{}_\alpha$ defined by (37) and (38). From the form of ψ_0, Eq. (35), it is easy to find the operator L(p):

$$R \equiv L(p) = [2m(\varepsilon + m)]^{-1/2}\{(\varepsilon + m) I + \gamma^0\gamma^k p_k\}. \tag{39}$$

In fact, it is easy to verify that (37) is satisfied, and, in addition,

$$L^{-1}(p) = \psi_0 = [2m(\varepsilon + m)]^{-1/2}\{(\varepsilon + m) I - \gamma^0\gamma^k p_k\}, \tag{40}$$

$$\gamma^0 L^+(p)\gamma^0 = L^{-1}(p). \tag{41}$$

The components of the vectors $l^\mu{}_\alpha$ defined by the relations (38) and (39) are given by the table

	l_0	l_1	l_2	l_3
$l^0{}_\alpha$	$\frac{\varepsilon}{m}$	$\frac{p^1}{m}$	$\frac{p^2}{m}$	$\frac{p^3}{m}$
$l^1{}_\alpha$	$\frac{p^1}{m}$	$1+\frac{(p^1)^2}{m(\varepsilon+m)}$	$\frac{p^1p^2}{m(\varepsilon+m)}$	$\frac{p^1p^3}{m(\varepsilon+m)}$
$l^2{}_\alpha$	$\frac{p^2}{m}$	$\frac{p^2p^1}{m(\varepsilon+m)}$	$1+\frac{(p^2)^2}{m(\varepsilon+m)}$	$\frac{p^2p^3}{m(\varepsilon+m)}$
$l^3{}_\alpha$	$\frac{p^3}{m}$	$\frac{p^3p^1}{m(\varepsilon+m)}$	$\frac{p^3p^2}{m(\varepsilon+m)}$	$1+\frac{(p^3)^2}{m(\varepsilon+m)}$

(42)

The table (42) (in which we have changed to the contravariant components of the vector p) can be represented by the formula

$$l^\mu{}_\alpha = \delta_{\mu\alpha} + \frac{p^\mu p^\alpha}{m(\varepsilon+m)} + \frac{1}{\varepsilon+m}[p^\mu\delta_{\alpha 0} + p^\alpha\delta_{\mu 0}] - \frac{2\varepsilon+m}{\varepsilon+m}\delta_{\mu 0}\delta_{\alpha 0}, \tag{43}$$

if we set $p^0 = \epsilon$. The quantities $l^\mu{}_\alpha$ satisfy Eqs. (1) and (2).

The matrices N^0 and N^s (s = 1, 2, 3) can now be represented in the form

$$N^0 = \frac{\varepsilon}{m}\gamma^0 + \frac{p^n}{m}\gamma^n \qquad (n = 1, 2, 3), \tag{44}$$

$$N^s = \frac{p^s}{m}\gamma^0 + \left[\delta_{sn} + \frac{p^s p^n}{m(\varepsilon+m)}\right]\gamma^n \qquad (s, n = 1,2,3). \tag{45}$$

The transformation L(p) diagonalizes the equations (11), converting them into

$$(m\gamma^0 \mp m)\varphi_0 = 0, \tag{46}$$

owing to the relation

$$N^\mu p_\mu = m\gamma^0. \tag{47}$$

8. THE TRANSFORMATION OF THE MATRIX ELEMENT

Let us consider the general form of the matrix element, as calculated, for example, by perturbation theory. For definiteness suppose only one Dirac particle is involved in the process. Then in the framework of the usual theory the general form of the matrix element in the momentum representation, for states with prescribed polarizations k and l, is

$$M_{kl} = \bar{\psi}_0^{(k)}(p_2)\hat{A}\ldots\hat{E}\hat{F}\hat{G}\psi_0^{(l)}(p_1). \tag{48}$$

Here p_1 and p_2 are the initial and final momenta of the particle, $\psi_0^-(k) = \psi_0^{+(k)}\gamma^0$ and $\psi_0^{(l)}$ are particular solutions in Eq. (35), and the notations $\hat{A}$ and so on have their usual meanings: $\hat{A} = A_\mu\gamma^\mu$.

On the basis of Eqs. (37) and (41) the formula (48) can be rewritten in the form

$$M_{kl} = \bar{\varphi}_0^{(k)}L(p_2)\hat{A}\ldots\hat{E}\hat{F}\hat{G}L^{-1}(p_1)\varphi_0^{(l)}, \tag{49}$$

where $\varphi_0^{(l)}$ (l = 1, 2, 3, 4) are as shown in Eq. (34). If one of the matrix vectors, for example $\hat{F}$, is equal to $\hat{p}_1$, then Eq. (49) can be simplified, in view of Eq. (47):

$$M_{kl} = \bar{\varphi}_0^{(k)}L(p_2)\hat{A}\ldots\hat{E}L^{-1}(p_1)m\gamma^0\hat{G}_N\varphi_0^{(l)},$$

where the notation $\hat{G}_N$ has the meaning that one must replace the matrices γ^μ in $\hat{G}$ by the matrices N^μ, i.e.,

$$\hat{G}_N = G_\mu N^\mu = G_\alpha^{(N)}\gamma^\alpha, \quad G_\alpha^{(N)} = G_\mu l^\mu{}_\alpha. \tag{50}$$

Remembering the obvious relations

$$\bar{\varphi}_0^{(k)}L(p_2) = \varphi_0^{+(k)}\hat{V}, \qquad L^{-1}(p_1)\gamma^0\hat{G}_N\varphi_0^{(l)} = \hat{T}\hat{G}_N\varphi_0^{(l)}. \tag{51}$$

$$V_2 = \frac{\varepsilon_2+m}{\sqrt{2m(\varepsilon_2+m)}}, \quad V_r = -\frac{p_2^r}{\sqrt{2m(\varepsilon_2+m)}},$$

$$\varepsilon_2 = |p_2^0| \qquad (r = 1, 2, 3),$$

$$T_0 = \frac{\varepsilon_1+m}{\sqrt{2m(\varepsilon_1+m)}}, \quad T_r = -\frac{p_1^r}{\sqrt{2m(\varepsilon_1+m)}}, \quad \varepsilon_1 = |p_1^0| \tag{52}$$

(in Eq. (52) we have for convenience gone over to the contravariant components of the vectors p_1 and p_2), we can finally rewrite M_{kl} in the form

$$M_{kl} = m\varphi_0{}^{+(k)}\hat{V}\hat{A}\ldots\hat{E}\hat{T}\hat{G}_N\varphi_0{}^{(l)}. \tag{53}$$

In case of need the factor $L(p_2)$ can be taken to the right across one or more of the matrix vectors, in an analogous way. If the original particle was at rest, then $L^{-1}(p_1) = I$ and Eq. (49) for M_{kl} takes the form

$$M_{kl} = \varphi_0{}^{+(k)}\hat{V}\hat{A}\ldots\hat{E}\hat{F}\hat{G}\varphi_0{}^{(l)}. \tag{54}$$

Thus in all cases the operators L and L^{-1} can by simple manipulations be brought into the expression for M_{kl} on an equal footing with the matrix vectors $\hat{A}, \ldots, \hat{E}$, etc.

9. THE STRUCTURE OF THE γ MATRICES AND THE CALCULATION OF MATRIX ELEMENTS

In order to proceed further, it is necessary to find a method for calculating the matrix elements of the matrix $\hat{V}\hat{A}\hat{B}\hat{C}\ldots$. This method can be the ordinary law of matrix multiplication, provided it is possible to represent the γ matrices by means of Kronecker δ symbols.

First let us introduce some step functions of discrete variables*

$$\varepsilon_k = \begin{cases} +1, & k = 1, 2 \\ -1, & k = 3, 4, \end{cases}$$
$$\varkappa_k(1, 2) = \begin{cases} +1, & k = 1, 2 \\ 0, & k = 3, 4, \end{cases} \qquad (55)$$
$$\varkappa_k(3, 4) = \begin{cases} 0, & k = 1, 2 \\ +1, & k = 3, 4. \end{cases}$$

By means of the step functions (55) and the Kronecker δ symbols one can write expressions for the matrix elements of the γ matrices in Eq. (36). In fact, it can easily be verified directly that

$$\gamma^{\mu}_{kl} = \varepsilon_k \{\delta_{\mu 0}\delta(k-l) + [\delta_{\mu 1} + (-1)^k \delta_{\mu 2}]\,\delta(k+l-5) - \delta_{\mu 3}(-1)^k [\varkappa_k(1, 2)\,\delta(k-l+2) + \varkappa_k(3, 4)\,\delta(k-l-2)]\}, \qquad (56)$$

where we have used the notation $\delta(m-n) = \delta_{m,n}$. With this way of writing them, the matrix elements of the matrix vector $(\hat{A})_{kl} = (A_\mu \gamma^\mu)_{kl}$ will have the following appearance:

$$A_\mu \gamma^\mu_{kl} = \varepsilon_k \{A_0\delta(k-l) + [A_1 + (-1)^k iA_2]\,\delta(k+l-5) - A_3(-1)^k [\varkappa_k(1, 2)\,\delta(k-l+2) + \varkappa_k(3, 4)\,\delta(k-l-2)]\}. \qquad (57)$$

*We stipulate that hereafter Greek letters shall as before take the values 0, 1, 2, 3, and Latin letters shall take the values 1, 2, 3, 4.

Then, using the law of matrix multiplication, we get, for example:

$$(\hat{A}\hat{B})_{kl} = \sum_{m=1}^{4} A_\mu \gamma^\mu_{km} \cdot B_\nu \gamma^\nu_{ml}$$
$$= \{A_\mu B^\mu + (-1)^k i (A_1B_2 - A_2B_1)\}\,\delta(k-l) + \{A_0B_1 - A_1B_0 + (-1)^k i (A_0B_2 - A_2B_0)\} \times \delta(k+l-5) - (-1)^k (A_0B_3 - A_3B_0)\,[\delta(k-l+2) + \delta(k-l-2)] - \{(-1)^k (A_1B_3 - A_3B_1) + i(A_2B_3 - A_3B_2)\}\,[\delta(k+l-3) + \delta(k+l-7)]. \qquad (58)$$

We note that it is enough to indicate the range of variation of the indices k and l, and the step functions $\kappa_k(1, 2)$ and $\kappa_k(3, 4)$ can then be omitted in the final formulas. In intermediate steps they are to be kept, however, to avoid possible mistakes.

The set of six δ symbols appearing in Eq. (58) is enough to exhaust all 16 matrix elements of a four-rowed matrix. Therefore no new δ symbols appear subsequently.

The calculation of matrix elements from the product of a large number of matrix vectors can be continued further. The method of calculation is obvious.

The existence of tables of formulas like Eqs. (57) and (58) decidedly facilitates and quickens the calculation of matrix elements for reactions involving polarized Dirac particles.

In conclusion I regard it as my pleasant duty to express my gratitude to Professor M. A. Markov for his interest in this work and for discussions.

[1] A. Sommerfeld, Atombau und Spektrallinien, Vol. 2—Russian translation, GITTL, 1956, page 219.

[2] Bethe, de Hoffmann, and Schweber, Mesons and Fields, Vol. 1 (Row, Peterson, and Co., 1955).

[3] R. H. Good, Jr., Revs. Modern Phys. **27**, 187 (1955).

Translated by W. H. Furry
77

ERRORS DUE TO THE DEAD TIME OF COUNTERS OPERATING IN CONJUNCTION WITH PULSED SOURCES

I. A. GRISHAEV and A. M. SHENDEROVICH

Physico-Technical Institute, Academy of Sciences, Ukrainian S.S.R.

Submitted to JETP editor January 27, 1961

J. Exptl. Theoret. Phys. (U.S.S.R.) **41**, 410-416 (August, 1961)

Expressions are derived for the mean counting rate, mean counting rate loss, and dispersions of the recorded and suppressed counts for different relations between the dead time and the pulse duration and repetition rate. Errors due to the dead time are found to depend greatly on the relations between these quantities. The derived formulas can be used to compute the experimental errors due to the dead time.

INTRODUCTION

THE statistics of counting losses associated with counter dead time in the case of pulsed sources is of considerable practical interest, because many investigations in nuclear and particle physics are performed with various types of pulsed accelerators. Earlier literature[1,2] on this subject had been confined to calculating the mathematical expectation of the counting loss for counters with "unprolonged" dead time[3] not exceeding the interval between pulses.

This last condition is not always satisfied in practice. For example, in some cyclic accelerators[4] the beam is bunched with a repetition period equal to the period of orbital revolution (about 10^{-8} sec). The dead time of real detectors usually exceeds this period, and in some instances is considerably longer than the repetition period of bunches. For example, in traveling-wave linear accelerators[5] oscillators in the 10-cm range are used, so that the bunch repetition period is about 3×10^{-10} sec.

It is of interest to study the statistics for arbitrary relations between the dead time and pulse spacing, and to calculate, in addition to the mean values, the dispersions of counts and counting losses (suppressed counts).

The analysis will be based on a sequence of identical pulses with constant repetition frequency f for both "prolonged" and "unprolonged" dead times.[3] The dead time τ is assumed to be constant and unfluctuating. A Poisson distribution $\eta(t)$ will be assumed for the particles impinging on a counter (hits) during any time interval. Since the pulses are identical, the intensity (the mean number of hits per second), averaged over the time of the experimental run, is

$$n = f \int_0^{t_c} \eta(t)\, dt. \qquad (1)$$

Time is measured here from the start of the pulse.

Since the mean number of particles entering the counter in a time T is nT, which is related simply to the mean count $\overline{M}$ and the mean counting loss $\overline{L}$ in the same time by

$$nT = \overline{M} + \overline{L}, \qquad (2)$$

only the expressions for $\overline{M}$ will be given below. Expressions for the dispersion will be given both in the case of the recorded counts (D_M) and of the suppressed counts (D_L), since these quantities, because of the statistical relation between M and L, do not satisfy any equation analogous to (2). In our derivations it will be assumed that the reciprocal pulse duty factor satisfies the realistic condition $Q > 2$.

1. RELATIONS FOR DEAD TIME SHORTER THAN PULSE SEPARATION

In these cases both the count and the counting loss during any pulse are independent of their values during other pulses. $\overline{M}$, D_M, and D_L can therefore be obtained by summations over all pulses.

We shall confine ourselves to the two extreme cases, $t_c \gg \tau$ and $t_c < \tau$. In the first case, using the formulas for constant intensity,[3] we easily obtain for rectangular pulses the following expressions for the mean counts of counters with prolonged and unprolonged dead times ($\overline{M}_p$ and $\overline{M}_u$, respectively):

$$\overline{M}_p = nTe^{-nQ\tau}, \qquad \overline{M}_u = nT/(1 + nQ\tau). \qquad (3)$$

For small loads $nQ\tau \ll 1$, and

$$\overline{M}_p = \overline{M}_u = nT(1 - nQ\tau). \quad (4)$$

The dispersions (standard deviations) for small loads are thus given directly by

$$D_M = nT(1 - 3nQ\tau), \qquad D_L = \overline{L} = n^2QT\tau. \quad (5)$$

It follows from (3)—(5) that all statistical characteristics depend on the single parameter of reciprocal pulse duty factor Q. All relations have the same form as in the case of constant intensity, but with dead time $Q\tau$.

In the second case ($t_c < \tau$) no more than one count can occur during each pulse. For arbitrary pulse shapes we therefore easily obtain the following expressions for the mean count and the dispersions (which coincide for both types of dead time):

$$\overline{M} = fT\{1 - e^{-n/f}\}, \qquad D_M = fTe^{-n/f}\{1 - e^{-n/f}\},$$

$$D_L = fT\{n/f + e^{-n/f} - e^{-2n/f} - ne^{-n/f}/f\}. \quad (6)$$

Unlike the preceding case, all parameters here depend only on the pulse repetition frequency.

For sufficiently high frequencies or low intensities ($f \gg n$), Eq. (6) is simplified as follows:

$$\overline{M} = nT(1 - n/2f), \qquad D_M = nT(1 - n/f),$$

$$D_L = \overline{L} = n^2T/2f. \quad (7)$$

It is thus seen that the counting loss will be greater or less than in the case of constant intensity equal to n, depending on whether 1/2f is larger or smaller than τ.

2. RELATIONS FOR DEAD TIME LONGER THAN PULSE SEPARATION. EXPRESSIONS FOR THE MEAN COUNT

We first obtain the mean count in the case of a prolonged dead time. It is most convenient to use Schiff's formula[6] for an arbitrary time dependence of the intensity, which in the given case is

$$\overline{M} = fT\int_0^{t_c} \eta(t)\exp\left\{-\int_{t-\tau}^{t}\eta(t')\,dt'\right\}dt.$$

The expression for $\overline{M}$ differs depending on the relation between 1/f and τ (Fig. 1). In one case (Fig. 1a), $\overline{M}$ can be calculated by dividing the integral from 0 to t_c into two integrals, from 0 to $t_c - t_1$ and from $t_c - t_1$ to t_c. In the first of these integrals, the integral in the exponent can obviously be put into the form

$$\int_{t-\tau}^{t}\eta(t')\,dt' = \int_{t_1+t}^{t_c}\eta(t')\,dt' + \lambda\int_0^{t_c}\eta(t')\,dt' + \int_0^{t}\eta(t')\,dt'.$$

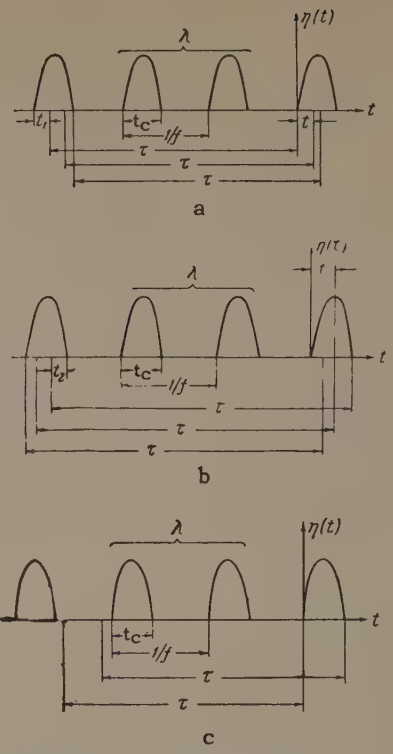

FIG. 1. Three possible relations between τ, f, and t_c. a — the dead time, plotted backward from the start of a given pulse (on the extreme right), includes λ complete pulses and a fraction of an additional pulse; b — the dead time, plotted backward from the end of a given pulse, includes λ complete pulses and a fraction of an additional pulse; c — the dead time, plotted backward from either the start or end of a given pulse, includes only λ complete pulses.

After some elementary transformations involving (1), we have

$$\int_0^{t_c-t_1}\eta(t)\exp\left\{-\int_{t-\tau}^{t}\eta(t')\,dt'\right\}dt = e^{-(\lambda+1)n/f}\int_0^{t_c-t_1}\eta(t)\exp\left\{-\int_{t}^{t+t_1}\eta(t')\,dt'\right\}dt. \quad (10)$$

In the second integral the expression in the exponent is divided into only two terms, the second and third terms in (9). Therefore

$$\int_{t_c-t_1}^{t_c}\eta(t)\exp\left\{-\int_{t-\tau}^{t}\eta(t')\,dt'\right\}dt = e^{-\lambda n/f}\int_{t_c-t_1}^{t_c}\eta(t)\exp\left\{-\int_0^{t}\eta(t')\,dt'\right\}dt. \quad (11)$$

Transforming by means of the identity

$$\int_0^x\eta(t)\exp\left\{-\int_0^t\eta(t')\,dt'\right\}dt = 1 - \exp\left\{-\int_0^x\eta(t)\,dt\right\} \quad (12)$$

and using (8) and (10), we obtain

$$\overline{M} = fTe^{-\lambda n/f}\left\{e^{-n/f}\int_0^{t_u-t_1}\eta(t)\exp\left[\int_t^{t+t_1}\eta(t')\,dt'\right]dt - e^{-n/f} + \exp\left[-\int_0^{t_u-t_1}\eta(t)\,dt\right]\right\}. \quad (13a)$$

In the second and third cases (Fig. 1b and c) similar calculations lead to

$$\overline{M} = fTe^{-(\lambda+1)n/f}\left\{1 - \exp\left[-\int_0^{t_2}\eta(t)\,dt\right] + \int_{t_2}^{t_u}\eta(t)\exp\left[-\int_{t-t_2}^{t}\eta(t')\,dt'\right]dt\right\}, \quad (13b)$$

$$\overline{M} = fTe^{-\lambda n/f}\{1 - e^{-n/f}\}. \quad (13c)$$

In the special case $\lambda = 0$, Eq. (13c) reduces to the expression for $\overline{M}$ in (6).

Equation (13c) depends only on the mean intensity and pulse repetition frequency, while (13a) and (13b) depend also on the pulse shape and on the exact relation between f and τ. The simplest forms of these equations are obtained when the dead time contains an integral number μ of periods:

$$\overline{M} = nTe^{-n\psi/f} = nTe^{-n\tau}, \quad (14)$$

i.e., the count will be the same as in the case of a continuous source with constant intensity n.

These results enable us to estimate the mean count when the exact relation between f and τ or the pulse shape is unknown. It follows from (8) that $\overline{M}$ is a monotonic function of τ. Therefore, when $f\tau$ lies between the integers μ and κ, we have, according to (14),

$$nTe^{-\varkappa n/f} \leqslant \overline{M} \leqslant nTe^{-n\psi/f}. \quad (15)$$

At high repetition frequencies or low intensities ($f \gg n$) Eqs. (13a)—(13c) are simplified. Series expansions of the expressions in the braces give, to second order terms,

$$\overline{M} = nTe^{-\lambda n/f}\left\{1 + n\left(a_1 - \tfrac{1}{2} - b_1 + b_1^2/2\right)/f\right\}, \quad (16a)$$

$$\overline{M} = nTe^{-(\lambda+1)n/f}\{1 - n(a_2 + b_2^2/2)/f\}, \quad (16b)$$

$$\overline{M} = nTe^{-\lambda n/f}\{1 - n/2f\}, \quad (16c)$$

$$a_1 = \left(\frac{f}{n}\right)^2\int_0^{t_u-t_1}\eta(t)\left[\int_t^{t+t_1}\eta(t')\,dt'\right]dt, \quad b_1 = \frac{f}{n}\int_0^{t_u-t_1}\eta(t)\,dt,$$

$$a_2 = \left(\frac{f}{n}\right)^2\int_{t_2}^{t_u}\eta(t)\left[\int_{t-t_2}^{t}\eta(t')\,dt'\right]dt, \quad b_2 = \frac{f}{n}\int_0^{t_2}\eta(t)\,dt. \quad (17)$$

The coefficients a_1, b_1, a_2, and b_2 do not exceed unity.

At very high frequencies, when $\lambda \gg 1$, we have $\tau \approx \lambda/f$ and Eqs. (16a)—(16c) practically coincide, to within a factor of the order $1 - n/f$, with $\overline{M}$ for the case of constant intensity.

We shall now consider the case of unprolonged dead time. The simplest expression for the mean count is obtained either when the dead time includes an integral number of periods or when the dead time considerably exceeds the repetition period. In these instances the mean count can be calculated by the procedure used in references 3 and 7 for constant intensity. Let us assume that M counts have been obtained during a sufficiently prolonged experiment. Then, if τ contains an integral number of periods λ, the total number of periods during which hits could not be registered is $M\lambda$, without considering in which portions of the pulses the counts occurred. It follows that the mean number of inoperative periods is

$$\bar{\nu} = \lambda\overline{M}. \quad (18)$$

The counting loss will be the number of hits during these periods; the mean loss will thus be

$$\overline{L} = n\bar{\nu}/f = n\lambda\overline{M}/f = n\tau\overline{M}. \quad (19)$$

From (2) we finally obtain

$$\overline{M} = nT/(1 + n\tau). \quad (20)$$

It is easily seen that the same result follows in the case $\tau f \gg 1$, independently of the exact relation between these quantities. The dead time following each count then includes an integral number λ of complete pulses and fractions of two pulses at the beginning and end of the dead time. Since $\lambda \gg 1$ the mean number of hits during these fractions can be neglected compared with the mean number during the large number of complete pulses. All considerations leading to (20) therefore remain valid. Equation (20) differs in no way from the corresponding expression for the constant intensity case, i.e., here also the pulsed character of the source does not affect the results.

For an arbitrary relation between f and τ we shall calculate only the upper and lower limits of $\overline{M}$; this can be done easily in the following manner. If λ is the number of complete periods included in the dead time (neglecting fractional periods), in the case of M counts we obviously have

$$\lambda M \leqslant \nu \leqslant (\lambda + 1)M. \quad (21)$$

Hence, by analogy with the foregoing calculations, we have

$$\frac{nT}{1 + \lambda n/f} \geqslant \overline{M} \geqslant \frac{nT}{1 + (\lambda + 1)n/f}. \quad (22)$$

These narrow limits permit a highly accurate determination of $\overline{M}$ in the cases of large λ and small loads ($\lambda n \ll f$).

3. RELATIONS FOR DEAD TIME LONGER THAN PULSE SEPARATION. DERIVATION OF THE DISPERSIONS

The expressions for the dispersions will be derived only in the most interesting practical case of small loads ($n\tau \ll 1$). Since the statistical relations for the different types of dead time coincide in this case,[3] we shall consider only the unprolonged dead time, for which the calculations are easier. The dispersion of the counts can now be derived, as in [3], by passing from the statistics of counts to the statistics of pulse intervals. The number r_i of complete periods between two successive counts obviously does not depend on the exact times when preceding counts occurred. On the other hand, in the present case ($\tau > 1/f - t_c$, $n\tau \ll 1$) the mean value of r_i is considerably greater than unity. Therefore in the case of "good" statistics (large M during the experiment) the total number of periods is approximately

$$R = \sum_{i=1}^{M} r_i. \qquad (23)$$

The mean values $\overline{r}$ and the dispersions D_r of all r_i are obviously identical. Therefore, because of the large number of independent r_i, R has a Gaussian distribution with mean value and dispersion given by

$$\overline{R} = M\overline{r}, \qquad D_R = MD_r. \qquad (24)$$

Passing from the statistics of intervals to the statistics of counts by means of Bayes' formula and confining ourselves to "good" statistics, we obtain (as in Chapter 2, Sec. 6 of [3])

$$\overline{M} = R/\overline{r}, \qquad D_M = RD_r/\overline{r}^3. \qquad (25)$$

D_M will be derived after $\overline{r}$ and D_r are determined. In the given case ($r_i \gg 1$) r_i can be represented, with an error not exceeding unity (Fig. 2), by

$$r_i = \lambda + \rho_i. \qquad (26)$$

It follows from (26) that the probability of r_i complete periods in the time interval between counts equals the probability that no particles arrive during r_i periods but that a particle does hit during the following period:

$$p(r_i) = ne^{-\rho_i n/f}/f. \qquad (27)$$

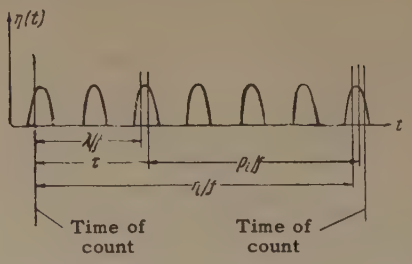

FIG. 2. Relations between r_i, λ, and ρ_i. r_i – number of complete periods between two successive counts; λ – number of complete periods in time τ; ρ_i – number of complete periods between termination of dead time and time of next count.

This formula is used to calculate $\overline{r}$ and D_r (as in Chapter 1, Sec. 6 of [3]):

$$\overline{r} = \lambda + f/n, \qquad D_r = (f/n)^2. \qquad (28)$$

Substituting in (25) and using the formula R = fT, we finally have

$$D_M = nT/(1+\lambda n/f)^3 = nT(1-3\lambda n/f). \qquad (29)$$

This equation is based on the fact that we are considering small loads. When τ contains an integral number of periods or $f\tau \gg 1$, we have $\lambda/f = \tau$, and (29) differs in no way from the corresponding expression for continuous operation with constant intensity n.

The expression for the dispersion of the counting loss can also be derived by a familiar procedure (Chapter 4, Sec. 6 of [3]). Without presenting the calculations, we note only that at small loads and for $f\tau \gg 1$ the result is the same as in the case of constant intensity.

CONCLUSIONS

The foregoing analysis has shown that the counting loss associated with dead time depends essentially on the relation between the dead time and pulse duration and spacing. With increasing pulse repetition frequency and reduced pulse duration for the same mean intensity, the counting loss tends generally to diminish. While for $t_p \gg \tau$ the counting loss increases by a factor Q compared with the case of constant intensity (and Q is often of the order of tens of thousands), when t_p and τ are comparable the counting loss is very close to that obtained with constant intensity (multiplied by no more than a few units). Finally, when $f\tau \gg 1$, there is no difference between these quantities, and all statistical relations are identical for the two cases. The difference also disappears when the condition $f\tau \gg 1$ is unfulfilled in the special case of a dead time containing an integral number of periods.

Our results show particularly that high-frequency bunching of beams in linear accelerators has no effect on the experimental errors associated with the dead time.

[1] C. H. Westcott, Proc. Roy. Soc. (London) **A194**, 508 (1948).

[2] N. Feather, Proc. Cambridge Phil. Soc. **45**, 648 (1949).

[3] Gol'danskii, Kutsenko, and Podgoretskii, Statistika otschetov pri registratsii yadernykh chastits (Counting Statistics in the Registration of Nuclear Particles), Fizmatgiz, 1959.

[4] M. S. Livingston, High-Energy Accelerators, Interscience Publishers, New York, 1954.

[5] E. L. Chu and W. Hansen, J. Appl. Phys. **18**, 996 (1947).

[6] L. I. Schiff, Phys. Rev. **50**, 88 (1936).

[7] B. V. Gnedenko, JETP **11**, 101 (1941).

Translated by I. Emin
78

CAUSE OF VANISHING OF THE RENORMALIZED CHARGE IN THE LEE MODEL

D. A. KIRZHNITS

P. N. Lebedev Physics Institute, Academy of Sciences, U.S.S.R.

Submitted to JETP editor January 30, 1961

J. Exptl. Theoret. Phys. (U.S.S.R.) 41, 417-422 (August, 1961)

With the example of a model which is a relativistic generalization of the models of Ruijgrok-Van Hove and of Lee, it is shown that the difficulties in the latter model arise from the violation of the Bloch consistency condition, and not from violation of crossing symmetry. In the Lee model a covariant S matrix exists only for vanishing renormalized charge. It is found that the Bloch condition in its usual form is too severe. A physical consistency condition is formulated which contains only renormalized quantities.

1. In recent years much attention has been given to the difficulties inherent in the well known Lee model (we refer to the vanishing of the renormalized charge, the existence of nonphysical states, and so on). The interest in these problems is primarily due to the fact that there are definite arguments in favor of the existence of analogous difficulties also in an actual field theory with a point interaction.

There are, however, serious grounds for thinking that the difficulties of the Lee model are specific to it and not directly related to possible difficulties of an actual field theory. This is indicated, for example, by the fact that these difficulties disappear if we go over from the Lee model to the more realistic model proposed by Ruijgrok and Van Hove (cf. [1]). To settle the question finally it is desirable to discover the reasons for the vanishing of the charge in the Lee model and to find out whether these reasons are effective in an actual field theory. The present paper is devoted to the analysis of this question.*

In connection with what has been said we must note an assumption due to Mandelstam,[2] that the difficulties in question are closely connected with the violation of the crossing symmetry (c.s.) of the theory.† If this assumption should turn out to be entirely correct, it would follow that the causes of the vanishing of the charge are specific features of the Lee model and that there are no such difficulties in an actual field theory. The c.s. is indeed strongly violated in the Lee model (the V particle can only emit a meson, and the N particle can only absorb one), whereas in an actual field theory there is complete symmetry between emission and absorption.

There is, however, no direct proof of Mandelstam's assumption. Essentially the only argument in its favor is the situation in simple models of field theory—the Lee model and the statistical scalar model.* If however, we go over to more complex models, we can verify (cf. Sec. 2) that this assumption is by no means always true and does not reflect the true causes of the appearance of the difficulties. It is convenient to use for this purpose a relativistic model considered by Smolyanskii and the writer[1] (hereafter referred to as I), which is a generalization of the models of Lee and Ruijgrok and Van Hove. It then turns out that the theory is free from difficulties even when there are some violations of c.s.†

It is shown in Sec. 3 that the immediate cause of the appearance of the difficulties is not the violation of c.s., but the violation of the Bloch consistency condition. In the light of this last condition the entire set of available facts receives a simple explanation. In particular, the vanishing of the charge in the Lee model is simply due to the fact that for other values of the charge the

*In this paper we are concerned exclusively with relativistic theories (in particular, with the relativistic Lee model). The discussion of nonrelativistic models is of little interest in itself, especially since the difficulties are due precisely to the relativistic range of momenta.

†By c. s. we mean the symmetry of the theory with respect to emission and absorption of particles, i. e., with respect to the interchanges $\varphi_+ \rightleftarrows \varphi_-$, and so on, where the indices + and – correspond to the creation and annihilation parts of the operator φ.

*Ter-Martirosyan[3] has shown that for these models this assumption is valid even outside the framework of the Hamiltonian method.

†On the other hand, a model is known (cf.[4]) in which the renormalized charge vanishes although there is c. s. This property is absent, however, in the relativistic generalization of the model.

correctly stated problem has no solutions at all.

In this connection it is important to note that for a renormalized theory, in which there is no mutually unambiguous correspondence between the bare and renormalized charges, the Bloch condition in its usual form can be excessively severe. This condition must be expressed not in terms of the bare quantities, but in terms of the renormalized quantities. It may be that the problem has no solution in any finite order of perturbation theory, but at the same time an exact solution exists. Precisely this situation exists in the model considered in I (cf. Sec. 4).

2. At first glance the situation existing in the model considered in I corresponds to the Mandelstam hypothesis. In fact, setting $g_N = 0$, we arrive at the Lee model, in which the difficulties under discussion are inherent; at the same time there is violation of c.s. as regards the θ particles. If, however, we set $g_V = g_N$, then the c.s. of the theory is restored, and, as is shown in I, the theory is free from difficulties.

On a more detailed examination, however, facts appear that are in contradiction with the hypothesis under discussion. Namely, it turns out that the theory is free from difficulties even when there are some violations of c.s.

First, in our model c.s. is radically violated with regard to the heavy particles. The usual c.s. condition, which requires interchange between emission of a particle and absorption of the antiparticle cannot be satisfied because of the absence of antiparticles. Even if one formulates a weakened c.s. condition, assuming simply interchange of emission of a particle and its absorption (this is possible if we proceed by the law of conservation of heavy particles, cf. [5]), this condition also is violated in view of the fact that the process $\theta \rightleftarrows V + N$ is forbidden.

Furthermore, in the case of bare charges g_V and g_N which are not equal to each other and to zero the theory also does not possess the property of c.s., and at the same time is free from difficulties. It is true that in this case we always have $g_{0V} = g_{0N}$, so that the renormalized theory is crossing-symmetrical. Therefore it could be thought that in the Mandelstam hypothesis one must be speaking of just the c.s. of the renormalized theory. In this form, however, the hypothesis loses its force. In fact, after charge renormalization the Lee model also acquires the property of c.s., because $g_0 = 0$.

Finally, we must recall the model with complex charge, considered at the end of I, which is also unsymmetrical with respect to interchange of creation and annihilation operators of the θ particles and has a nonvanishing renormalized charge.

It follows from what has been said that violation of c.s. is not the direct cause of the appearance of the difficulties. It is natural to think that these arise when there is at the same time a violation of some more fundamental requirement, which must be obeyed by every internally consistent field theory. It turns out that this requirement is the Bloch consistency condition.

3. A theory in which c.s. is violated is essentially a nonlocal theory. In fact, the Hamiltonian of the model under consideration (for notations see I)

$$H(x) = \bar{\psi}(x)(\sigma_+\varphi_+(x) + \sigma_-\varphi_-(x))\psi(x) \qquad (1)$$

can be written in the typically nonlocal form

$$H(x) = \bar{\psi}(x)\int d\xi F(x-\xi)\varphi(\xi)\psi(x).$$

The Fourier transform of the form-factor F is of the form

$$F(k) = \sigma_+\theta_+(k) + \sigma_-\theta_-(k),$$

where $\varphi = \varphi_+ + \varphi_-$, and $\theta_\pm$ are step functions which accomplish the projection onto the positive and negative frequency ranges.

If the interaction Hamiltonian is nonlocal, the question arises sharply as to whether the consistency conditions are satisfied, i.e., as to whether the S matrix exists as a definite function of the spacelike surface σ. In the case in which the Hamiltonian does not depend explicitly on this surface the condition has the well known form

$$[H(x),\ H(x')] = 0, \qquad (2)$$

where the points x and x' lie on σ, i.e., are separated by a spacelike interval.

We shall show that in the model under consideration the vanishing of the renormalized charge occurs when and only when the condition (2) is violated (for a somewhat sharper form of this condition see Sec. 4). It is easy to understand this statement if we take account of the fact that a theory with the charge equal to zero satisfies Eq. (2) identically. Therefore under the indicated conditions no other solutions are possible.

First we note that in the model in question the fermions have no antiparticles. Therefore the creation and annihilation operators taken separately (and not their sum, as for Dirac particles) anticommute outside the light cone. The corresponding anticommutator

$$\{\psi(x)\bar{\psi}(x')\} \sim \delta(u\xi_0 - \xi u_0),$$

where $\xi = x - x'$, vanishes for $\xi^2 > \xi_0^2$, in virtue of $u_0^2 > u^2$. It is clear that the corresponding violation of c.s. does not prevent the condition (2) from holding, in complete agreement with what was said in Sec. 2 and with the assertion just made.

Using these anticommutation rules for ψ and substituting Eq. (1) in Eq. (2), we get

$$[H(x)H(x')] = is_+(x)s_-(x')\Delta_+(x-x') + is_-(x)s_+(x')\Delta_-(x-x').$$

Here $s_\pm(x) = \bar{\psi}(x)\sigma_\pm\psi(x)$, and $\Delta_\pm$ are the well known commutator functions. Replacing them by the functions $\Delta = \Delta_+ + \Delta_-$, $\Delta_1 = i(\Delta_+ - \Delta_-)$, only the first of which vanishes outside the light cone, we arrive at a condition equivalent to Eq. (2)

$$s_+(x)s_-(x') - s_-(x)s_+(x') = 0. \tag{3}$$

It is well known that this condition holds for a theory with crossing symmetry because $s_+ = s_-$, but this condition is less severe than the condition of c.s.

In particular, for a model with complex charge, where

$$s_+ = g(\bar{\psi}\tau_1\psi), \qquad s_- = g^*(\bar{\psi}\tau_1\psi),$$

the condition (3) is satisfied identically, and this is also in agreement with the present assertion.

The third case of violation of c.s. mentioned in Section 2—that in which the charges g_V and g_N are unequal—will be discussed in the next section.

If there is strong enough violation of c.s., the condition (3) may not be satisfied. In this case, according to our assertion, the theory must contain difficulties. This situation occurs in the Lee model,* where

$$s_+ = g(\bar{\psi}_N\psi_V), \qquad s_- = g(\bar{\psi}_V\psi_N).$$

The left member of Eq. (3) now has the form $g^2[A(x, x') - A(x', x)]$, where

$$A(x, x') = \bar{\psi}_N(x)\bar{\psi}_V(x')\psi_V(x)\psi_N(x')$$

and for it to vanish it is necessary that $g = 0$. From this it is clear that the renormalized charge must also be zero,

$$g_0 = 0. \tag{4}$$

Thus the compatibility condition enables us to determine the value of the renormalized charge without making dynamical calculations. In the general case of charges g_V and g_N which are not zero this condition gives

$$g_V = g_N, \tag{5'}$$

from which it follows by considerations of symmetry that

$$g_{0V} = g_{0N}. \tag{5''}$$

Precisely this relation is obtained by direct calculation (cf. I). If we violate the relation (5″), the corresponding bare charges turn out to be complex, and we have all of the difficulties that come from this.[7] This situation is also in agreement with the statement made earlier.

The only problem that remains unsettled is connected with the relation (5′), which at first glance contradicts the statement in question. In actual fact, as was noted in Sec. 2, the theory is free from difficulties even for charges g_V and g_N which are not equal to each other (and to zero). It turns out, however, that the condition (2) is in certain ways too severe.

4. Let us first look into the properties of the S matrix of the model under consideration in the case $g_V \neq g_N$. Because of the violation of the condition (2) the S matrix does not exist at all in the infinite-time representation of Tomonaga and Schwinger. We emphasize that for the time being the discussion is being conducted in the language of bare charges, which corresponds to the treatment of the unrenormalized theory.

When one uses the usual one-time formalism the violation of the compatibility condition manifests itself in the fact that violations of causality and of relativistic invariance arise at once. The point is that the expression for the S matrix involves retarded commutators of the type $\theta(x-x')\times[H(x)H(x')]$. Since this commutator does not vanish outside of the light cone because of the presence of the function Δ_1 (see above), and the function θ has an invariant meaning only inside the cone, a violation of the two conditions that have been indicated is inevitable. Thus the terms in the expansion of the S matrix can be divided into two classes. The first includes those that contain only the function Δ; terms of the second class contain also the function Δ_1 and thus contradict the conditions of causality and of relativistic invariance.

If, however, we analyze the structure of the terms of the second class, it turns out that their dependence on g_V and g_N is of a very specific type. In the lowest order of perturbation theory the matrix element in question depends on the combination $g_V^2 - g_N^2$ (for $g_V = g_N$ this element must vanish). If now we sum all of the reducible diagrams of higher orders that correspond to this

*The fact that the Bloch condition is not satisfied in the Lee model has been noted previously. [6]

matrix element, then after the renormalization is carried out the combination just mentioned goes over into the difference of the squares of the renormalized charges, $g_{0V}^2 - g_{0N}^2$. This fact is closely connected with the renormalizability of the model under consideration, which was already noted in the first papers on the Ruijgrok-Van Hove model (cf. [7]).

But the equation $g_{0V}^2 - g_{0N}^2 = 0$ holds for any value of g_V and g_N (cf. I). Therefore after renormalization the exact solution for the S matrix has an acceptable structure because of the actual vanishing of the terms of the second class. Returning to the infinite-time formalism, we can say that in this case the renormalized S matrix exists in spite of the violation of the condition (2).

It is important to emphasize that the vanishing of the terms of the second class occurs only in the exact solution; if we confine ourselves to terms of a finite order in g_V and g_N, the combination in question by no means vanishes. What has been said can be illustrated by the impossibility of the inverse expansion of the renormalized expression in terms of the bare constants, because of the nonanalytic behavior of the relation $g_{0V} = g_{0N} = (g_V g_N)^{1/2}$ (cf. I).

Thus the consistency condition in its usual form is in fact too severe. It requires the existence (in the one-time formalism, the causality and relativistic invariance) of each term of the expansion of the S matrix in terms of the bare coupling constants. This requirement is excessive, and, moreover, unphysical. The physical compatibility condition must be formulated in the language of the renormalized quantities only (see below).

Thus even if the original Hamiltonian does not satisfy the condition (2), there is a certain possibility for the theory to be "self-perfecting." For example, in the model considered just now the radiative corrections, which are different for each of the vertex parts, lead finally to the restoration of consistence.

This situation is possible owing to two circumstances. First, it is important that there is no reciprocally unique correspondence between the bare and renormalized charges. Whereas the region of variation of the bare charges is the plane (g_V, g_N), the region of variation of the renormalized charges (the so called normal zone) degenerates into the line $g_{0V} = g_{0N}$. In the Lee model there is an analogous degeneration of the line g into the point $g_0 = 0$. Therefore to a given value of the renormalized charge there corresponds a whole set of values of the bare charge. The degeneration of the normal zone, without which, by the way, the difficulties discussed in this paper are themselves impossible, is due to the great effect of virtual quanta of high energies.*

Second, it is important that the theory is renormalizable. This means that there exists a separation of the Lagrangian into free and interaction Lagrangians, different from the ordinary separation, and such that the bare quantities disappear from the theory; their place is taken by the renormalized charge and mass.[8] The corresponding S matrix is finite and contains only the renormalized quantities.

It is natural to take the physical consistency condition to be the condition of the existence of such a renormalized S matrix. This condition is hard to write in a closed mathematical form because of the presence of derivatives in the new interaction Lagrangian (cf. [8]). Nevertheless we can assert that all of the cases considered above, including the case $g_V = g_N$, are in accordance with this new condition. It is enough to note that this condition is equivalent to the requirement of causality and relativistic invariance, in the sense that has been indicated, for the S matrix written in the one-time formalism.

In conclusion we emphasize once more that in view of the complete equivalence of two theories that differ only in the values of the bare coupling constants but not in the values of the renormalized constants, the question raised at the end of Sec. 3 is completely disposed of.

5. The analysis made here thus shows that in the framework of the model considered the renormalized charge goes to zero only when the existence of a covariant S matrix is impossible with any other value of the charge. Of course we can still not conclude from this that there are no other causes for the vanishing of the renormalized charge.

In any case we can state that the cause that leads to the difficulties in the Lee model is without force in a real field theory (the corresponding Hamiltonian satisfies the consistency condition). Therefore the situation in the Lee model provides no additional arguments for solving the problem of the difficulties of a real field theory.

I express my deep gratitude to I. E. Tamm for his interest in this work and to E. S. Fradkin for numerous discussions.

*If the contribution of these quanta is small, the assertion of the preceding section (and also the Mandelstam hypothesis) loses its force. This applies in particular to the Lee model with a form-factor, and also to the model with a nonrelativistic dispersion law of the nucleons.[9]

[1] D. A. Kirzhnits and S. A. Smolyanskii, JETP **41**, 205 (1961), Soviet Phys. JETP **14**, 149 (1962).

[2] S. Mandelstam, Phys. Rev. **112**, 1344 (1958).

[3] K. A. Ter-Martirosyan, JETP **37**, 1005 (1959), Soviet Phys. JETP **10**, 714 (1960).

[4] V. D. Kukin and A. R. Frenkin, Doklady Akad. Nauk SSSR **133**, 49 (1960), Soviet Phys. Doklady **5**, 698 (1961).

[5] H. Fried, Phys. Rev. **118**, 1427 (1960).

[6] B. L. Ioffe, Proc. All-Union Conference on Quantum Electrodynamics (in Russian), Moscow, 1955. Y. Munakata, Progr. Theoret. Phys. **13**, 455 (1955).

[7] T. Ruijgrok, in: Les problèmes mathematiques de la théorie quantique des champs, Paris, 1959.

[8] P. T. Matthews and A. Salam, Phys. Rev. **94**, 185 (1954). Y. Katayama, Progr. Theoret. Phys. **10**, 31 (1953).

Translated by W. H. Furry
79

RELAXATION ABSORPTION OF SOUND IN A PARAMAGNETIC SUBSTANCE

B. I. KOCHELAEV

Kazan' State University

Submitted to JETP editor, February 3, 1961

J. Exptl. Theoret. Phys. (U.S.S.R.) 41, 423-428 (August, 1961)

The acoustical absorption in paramagnetic crystals due to spin-lattice interactions is considered theoretically. The estimates obtained for the acoustical absorption coefficient show that the effect may be quite easily observed experimentally.

1. The possibility of affecting the spin system of a paramagnet by excitation with acoustical vibrations was first pointed out by Al'tshuler.[1] He developed the theory of the resonance absorption of sound by the spin system, which is the analogue of paramagnetic resonance.

Along with resonance methods of studying the dynamic properties of a spin system, considerable use is made of the susceptibility dispersion and the energy dissipation in the paramagnet on applying an alternating magnetic field parallel to the constant one; these effects are caused by relaxation processes in the spin system. It can be expected that the acoustical analogue of these phenomena exists. In the present paper we discuss the acoustical absorption in paramagnetic crystals due to relaxations between the spin system and the thermal lattice vibrations. The calculation is made semiphenomenologically, using a method developed by Mandel'shtam and Leontovich[2] and by Shaposhnikov,[3] which allows the behavior of a system subject to time-dependent excitation to be considered in a thermodynamic way.

2. We assume that the paramagnet can be subdivided into two subsystems which interact weakly with one another; the spin system belongs to one of the subsystems and the remaining degrees of freedom (of the lattice) belong to the other. The thermodynamic state of the lattice will be taken to be independent of the state of the spin system. In other words, we will consider paramagnets for which the spin-lattice relaxation time τ is much longer than the spin-spin relaxation time τ_S; in addition, the temperature of the paramagnet must not be too low (otherwise the second assumption will not be satisfied).

The state of the spin system in complete thermodynamic equilibrium is completely characterized by a temperature T, equal to the lattice temperature T_1, and by the value of the external magnetic field H. We choose the components of the deformation tensor for the external parameters characterizing the state of the spin system when sound is propagated in the paramagnet.

We consider a small volume of the crystal, of which the linear dimensions, L, are such that $L \ll \lambda$, where λ is the wavelength of the sound; this volume should, however, contain a sufficiently large number of atoms for a macroscopic description to be possible. We assume henceforth that when sound is propagated in the paramagnet both subsystems of the volume under consideration pass through a series of equilibrium states. It is then necessary that the frequency of the sound, ω, be much smaller than $1/\tau_S$.

If the sound propagates along one of the coordinate axes, for example z, and the oscillations are longitudinal (which corresponds to the usual experimental conditions), the number of components of the deformation tensor reduces to one

$$u_{zz} = u = u_0 \cos(qz)\, e^{i\omega t} = u' e^{i\omega t}, \qquad (1)$$

where q is the wave number. The work performed on the spin system of the volume considered when the parameter u is changed is

$$\delta A = \sigma du, \quad \sigma = \sigma(u, H, T) = -\partial\Psi/\partial u. \qquad (2)$$

Here Ψ is the free energy of the spin system in the presence of the external magnetic field H, and σ is the generalized force corresponding to the coordinate u.

If the amplitude of the sound wave is small, the departure of the system from the state of complete thermodynamic equilibrium can be taken as infinitesimal. Therefore, the departure of the parameters σ, T, and T_1 from their equilibrium values σ_0 and T_0 will be small, which we utilize below by writing all equations in a linear approximation in terms of the quantities u, $\xi = \sigma - \sigma_0$, $\theta = T - T_0$, and $\theta_1 = T_1 - T_0$.

The dissipative properties of the spin system can be conveniently described by introducing (in analogy with the magnetic susceptibility) the "acoustical susceptibility of the spin system" by the following equation:

$$\xi / u = \zeta = \zeta' - i\zeta'', \tag{3}$$

where ζ' and ζ'' are real. It is easily seen that the attenuation of a sound wave in the paramagnet, caused by the dissipative properties of the spin system, is determined by the imaginary part of the acoustical susceptibility. The energy absorbed in unit time is

$$\bar{\dot{E}} = \overline{\Lambda U} = \tfrac{1}{2}\omega\zeta''(u')^2, \tag{4}$$

where Λ and U are the real parts of the variables σ and u; the point signifies differentiation, and the bar averaging over time.

Thus, our problem reduces to finding ζ''. A series expansion of σ in terms of θ and u close to equilibrium gives

$$\xi = (\Psi_{uT})_0\,\theta + (\Psi_{uu})_0 u, \qquad \Psi_{xy} \equiv \partial^2\Psi / \partial x \partial y. \tag{5}$$

To determine θ we apply the equation of thermal balance to the spin system. The quantity of heat δQ which the spin system exchanges with its surroundings consists of two parts:

1) The heat given up by the lattice in time dt:

$$\delta Q' = -\varkappa_1 (T - T_1)\, dt = -\varkappa_1 (\theta - \theta_1)\, dt.$$

Here κ_1 is the thermal conductivity between the spin system and the lattice.

2) The heat flowing out to the remaining parts of the spin system:

$$\delta Q'' = -dt \int \operatorname{div} (-\varkappa_2 \operatorname{grad} T)\, dV,$$

where κ_2 is the thermal conductivity for the spin system. The linear dimensions of the volume V are much less than the acoustical wavelength, and, consequently, grad T does not change within its limits, so that we may write $\delta Q'' = \kappa_2 V \nabla^2 \theta$.

Considering what has been said in Sec. 1, the lattice vibrations can be considered adiabatic at each point; thus the difference of the lattice temperature from its equilibrium value will be [4]

$$\theta_1 = -T\alpha_V \rho \left(v_l^2 - \tfrac{4}{3} v_t^2\right) u c_1^{-1} = -Bu. \tag{6}$$

Here α_V is the thermal expansion coefficient, ρ is the density of the crystal, v_l and v_t are the velocities of sound polarized longitudinally and transversely, and c_1 is the lattice thermal capacity under constant pressure. From the equation of thermal balance we find

$$\theta = [T(\Psi_{Tu})_0\, i\omega - B\varkappa_1] / [i\omega c_H + \varkappa_1 + \varkappa_2 V], \tag{7}$$

where c_H is the thermal capacity of the spin system under constant magnetic field.

Using (3), (5), and (7), we obtain the imaginary part of the acoustical susceptibility for unit volume of the paramagnet:

$$\zeta'' = -\left[\frac{T(\psi_{Tu})_0 (1 + \varkappa_2\tau\omega^2 / v_l^2 C_H) + BC_H}{(1 + \varkappa_2\tau\omega^2 / v_l^2 C_H)^2 + \omega^2\tau^2}\right] \frac{(\psi_{Tu})_0\, \omega\tau}{C_H}, \tag{8}$$

where $\tau = C_H/\kappa_1$ is the spin lattice relaxation time, C_H is the thermal capacity of the spin system for unit volume, and $\psi = \Psi/V$.

3. In order to express ζ'' in terms of known quantities, it remains to find $(\Psi_{Tu})_0$ explicitly. By definition

$$\Psi = -kT \ln\left[\operatorname{Sp} \exp\left(-\frac{\hat{\mathcal{H}}}{kT}\right)\right]. \tag{9}$$

Because the parameter u is small, the Hamiltonian of the spin system, $\hat{\mathcal{H}}$, can be expanded in power series of u:

$$\hat{\mathcal{H}} = \hat{\mathcal{H}}_0 + \hat{F}u + \ldots, \tag{10}$$

where $\hat{\mathcal{H}}_0$ is the spin-system Hamiltonian in the absence of sound.

We assume that the spectrum of the spin system consists of two groups of levels, separated in energy by an interval $\Delta E \gg \kappa T$ while the lower group of levels lies within the limits $\Delta E' \ll \kappa T$. This assumption is true for the majority of paramagnets in a wide temperature range (down to liquid-helium temperature). In this case the effect of the upper levels on the behavior of the system in the acoustical field is insignificant, and, expanding (9) in powers of 1/kT, we obtain the following formula for $(\Psi_{Tu})_0$ on taking into account the first nonzero term of the expansion:

$$(\Psi_{Tu})_0 = \frac{1}{kT^2\eta}\left[\operatorname{Sp}\hat{\mathcal{H}}_0\hat{F} - \frac{1}{\eta}\operatorname{Sp}\hat{\mathcal{H}}_0 \operatorname{Sp}\hat{F}\right], \tag{11}$$

where η is the number of states of the spin system.

Substituting (11) and (8) in (4), and averaging throughout the volume of the crystal, the general formula can be written down for the acoustical absorption coefficient, defined as the ratio of the energy absorbed in unit volume to twice the flux of acoustical energy. We will write down the formula for the absorption coefficient, taking into account the following facts. Bloembergen [5] has evaluated the thermal conductivity: $\kappa_2 = C_H a^2/50\tau_s$, where a is the shortest distance between spins. This estimate shows that, at temperatures above liquid helium, for reasonable acoustical frequencies and for the majority of paramagnets, we have

$$\varkappa_2\tau\omega^2 / v_l^2 C_H = 4\pi^2 a^2 \tau / 50\,\lambda^2\tau_s \ll 1. \tag{12}$$

It is seen from formulae (6) and (8) that the part of ζ'' caused by the change of lattice temperature under the effect of acoustical vibrations leads to a multiplier C_H/C_l, the value of which is insignificant at not too low a temperature. Thus we obtain the following formula for the acoustical absorption coefficient in unit volume of the paramagnet:

$$\alpha = \frac{1}{\rho v_l^3 k^2 T^3 C_H \eta^2}\left[\mathrm{Sp}\ \hat{\mathcal{H}}_0\hat{F} - \frac{1}{\eta}\mathrm{Sp}\ \hat{\mathcal{H}}_0\ \mathrm{Sp}\ \hat{F}\right]^2 \frac{\omega^2\tau}{1+\omega^2\tau^2}. \quad (13)$$

4. We now make numerical estimates of the acoustical absorption coefficient for typical paramagnets.

1) We consider first paramagnetic salts with ions whose spin, S, is greater than $1/2$; e.g. Cr^{3+} and Ni^{2+} ions ($S = 3/2$ and $S = 1$, respectively) surrounded octahedrally by diamagnetic particles X. In the absence of sound the Hamiltonian of the spin system has the form

$$\hat{\mathcal{H}}_0 = \sum_j \Big[g\beta\,(H_x\hat{S}_{jx} + H_y\hat{S}_{jy} + H_z\hat{S}_{jz}) + \tfrac{1}{6}D\,(\hat{S}_{jx} + \hat{S}_{jy} + \hat{S}_{jz})^2\Big] + \hat{\mathcal{H}}_{ss}. \quad (14)$$

Here H is the strength of the external magnetic field, $\hat{S}_x$, $\hat{S}_y$, $\hat{S}_z$ are the operators projecting the spin onto the coordinate axes directed at the X particles, D is the constant describing the splitting of the spin levels in the crystalline electric field of trigonal symmetry, $\hat{\mathcal{H}}_{ss}$ is the spin-spin interaction Hamiltonian, β is the Bohr magneton. We neglect g-factor anisotropies.

Using the results obtained by van Vleck,[6] we write down the operator $\hat{F}$ for the case when the electric charge of the X particles is zero (water molecules):

$$\hat{F} = \sum_j \{\varepsilon_1 R^{-3}[(\gamma_1^2+\gamma_2^2-2\gamma_3^2)(2\hat{S}_{jz}^2 - \hat{S}_{jx}^2 - \hat{S}_{jy}^2) + 3(\gamma_1^2-\gamma_2^2)(\hat{S}_{jy}^2 - \hat{S}_{jx}^2)] + \varepsilon_2 R[\gamma_1\gamma_2(\hat{S}_{jx}\hat{S}_{jy} + \hat{S}_{jy}\hat{S}_{jx}) + \gamma_1\gamma_3(\hat{S}_{jx}\hat{S}_{jz} + \hat{S}_{jz}\hat{S}_{jx}) + \gamma_2\gamma_3(\hat{S}_{jy}\hat{S}_{jz} + \hat{S}_{jz}\hat{S}_{jy})]\};$$

$$\varepsilon_1 = \frac{54}{\sqrt{3}}\frac{l^2}{\Delta^2}\left(\frac{e\mu}{R^3}\right)\frac{\overline{r^4}}{R^4},$$

$$\varepsilon_2 = \frac{12324}{175}\frac{l^2}{\Delta^2}\left(\frac{e\mu}{R^3}\right)\left(\frac{\overline{r^2}}{R^2} - \frac{55}{36}\frac{\overline{r^4}}{R^4}\right), \quad (15)$$

where γ_1, γ_2, γ_3 are the direction cosines of the acoustical propagation direction, l is the spin-orbit coupling constant, r is the radius of the d electron, Δ is the total splitting of the orbital levels of the paramagnetic ion in the crystalline cubic field, μ is the electric dipole moment of particle X, and R is the distance to it.

Substituting (15) and (14) in (13) gives

$$\alpha = (AN^2/T^3C_H)\,\omega^2\tau/(1+\omega^2\tau^2);$$

$$A = 2\cdot 10^{-3}(\varepsilon_2^2 D^2 R^2/\rho v_l^3 k^2)\,[4S^2(S+1)^2 - 3S(S+1)]^2\,(\gamma_1\gamma_2 + \gamma_1\gamma_3 + \gamma_2\gamma_3)^2, \quad (16)$$

where N is the number of paramagnetic ions in unit volume. It is clear from this formula that a strong variation of the acoustical absorption coefficient on the propagation direction of the sound in the crystal should be observed. In particular, α has a maximum if the sound propagates along the trigonal symmetry axis of the crystalline field, and becomes zero if it is directed along the cubic axis. For example, if in potassium chromium alum the sound is directed along the principal cubic axis of the crystal, then $\alpha = 0$. (Strictly speaking $\alpha \neq 0$, since van Vleck,[6] neglected in the calculation of F a small contribution proportional to H, which will give acoustical absorption four orders of magnitude smaller than that being considered.) If the sound is directed along the trigonal symmetry axis of the crystalline field of one of the ions in the elementary cell (the elementary cell of alums contains four non-equivalent ions, whose trigonal axes are directed in space along the diagonals of a cube), then the absorption coefficient is $\alpha \approx 10^{-6}$ cm^{-1} when the following values for the constants are assumed: $l = 88$ cm^{-1}, $\Delta = 50{,}000$ cm^{-1}, $v_l = 2.3\times10^5$ cm sec^{-1}, $\overline{r^2} = 1.23\times10^{-16}$ cm^2, $\overline{r^4} = 2.46\times10^{-32}$ cm^4, $R = 2\times10^{-8}$ cm, $\mu = 2\times10^{-18}$ cgs esu units, $\omega = 3\times10^7$ cps, $T = 300°$ K, $H = 0$, $\tau = 0.5\times10^{-8}$ sec.

2) For the case of paramagnetic ions with spin $S = 1/2$, the spin-lattice interaction energy in crystals is proportional to the magnetic field, as a consequence of Kramer's theorem. We take magnetic dipole-dipole interactions into account by considering the magnetic field close to the paramagnetic ion to consist of the external magnetic field plus a local field created by all the remaining magnetic particles.

As a concrete example we consider a salt of divalent copper, in which the Cu^{2+} ion is in octahedral surroundings. As a rule, one of the four-fold axes (we choose it as the z axis) is different-the octahedron is compressed or extended along this axis. Using the spin-lattice interaction operator of Bashkirov[7] we obtain, after calculations analogous to those made in Item 1, the following expression for the acoustical absorption coefficient:

$$\alpha = (A'N^2/T^3C_H)\,\omega^2\tau/(1+\omega^2\tau^2);$$

$$A' = (\varepsilon^2\beta^4/\rho v_t^3\hbar^2)\left[(\varphi_1^2-\varphi_2^2)^2H^4 + \tfrac{4}{3}(\varphi_1^2+\varphi_2^2)H^2K^2 + \tfrac{4}{9}K^4\right](\gamma_1^2-\gamma_2^2)^2,$$

$$\varepsilon = \tfrac{64}{7}(e\mu l\sqrt{r^2}/\Delta\delta R^4). \qquad (17)$$

Here the local magnetic field values have been averaged assuming that they are distributed for the various ions according to a Gaussian law with an effective field constant of K. The quantities δ and Δ are the splittings of the orbital levels in the tetragonal and cubic internal crystalline fields, respectively, and φ_1, φ_2, φ_3 are the direction cosines of the external magnetic field.

It should be noted that the angular variation of the absorption coefficient in formula (17) may be inaccurate, since, when calculating the spin lattice interaction, Bashkirov[7] only took into account the quadratic terms of the expansion in the electronic coordinates of the d electron energy in the electric field of the crystal; there is reason to suppose that the following term in the expansion (of fourth degree in the coordinates) may be important (cf.[6]).

If the sound and field are directed so that for one of the ions in the elementary cell of a $CuSO_4 \cdot 5H_2O$ crystal we have $(\gamma_1^2 - \gamma_2^2) = 1$ and $(\varphi_1^2 - \varphi_2^2) = 1$, and we use the following values for the constants, $\delta = 1400\ cm^{-1}$, $\Delta = 12300\ cm^{-1}$, $l = 695\ cm^{-1}$,[7] $H = 10^4$ oe, $K \ll H$ (the remaining values of the constants are the same as for the alums), the acoustical absorption coefficient is $\alpha \approx 10^{-5}\ cm^{-1}$.

The estimates made for the acoustical absorption coefficient show that the effect considered can be experimentally observed. The strong variation of the acoustical absorption coefficient on the value of the external magnetic field simplifies the separation of the paramagnetic absorption of sound from other mechanisms. The mechanism we have considered will, apparently, always play an unimportant role in the general absorption of acoustical energy in the crystal. We note that the variation $\alpha = \alpha(H)$ is markedly different for ions with spin $S = 1/2$ and $S > 1/2$. When $S > 1/2$ the paramagnetic absorption of sound in most cases apparently disappears as H increases; if $S = 1/2$ the acoustical absorption coefficient increases according to the law $\alpha \propto H^2$ as $H \to \infty$.

Apart from its intrinsic interest, the experimental study of the effect we have considered will give important information on the spin-lattice interaction in paramagnetic crystals, which, as is well known, has been studied so far quite inadequately.

In conclusion, the author thanks S. A. Al'tshuler for constant interest in this work and for discussion of the results.

[1] S. A. Al'tshuler, JETP **28**, 38, 49 (1955), Soviet Physics - JETP **1**, 29, 37 (1955).

[2] L. I. Mandel'shtam and M. A. Leontovich, JETP **7**, 438 (1937).

[3] I. G. Shaposhnikov, JETP **17**, 824 (1947) and **18**, 533 (1948).

[4] L. D. Landau and E. M. Lifshitz, Statisticheskaya fizika (Statistical Physics), Gostekhizdat, 1951.

[5] N. Bloembergen, Physica **15**, 386 (1949)

[6] J. H. van Vleck, Phys. Rev. **57**, 426 (1940).

[7] Sh. Sh. Bashkirov, JETP **34**, 1465 (1958), Soviet Physics - JETP **7**, 1013 (1958).

Translated by K. F. Hulme
80

FERMI SYSTEMS WITH ATTRACTIVE AND REPULSIVE INTERACTIONS

M. Ya. AMUS'YA

Physico-Technical Institute, Academy of Sciences, U.S.S.R.

Submitted to JETP editor February 4, 1961

J. Exptl. Theoret. Phys. (U.S.S.R.) **41**, 429-440 (August, 1961)

We have used quantum field theoretical methods to consider a uniform, infinite system of fermions with pair interactions. The interaction consists of two parts: an attraction U of range b and a strong repulsion V of range a, with $b \gg a$. The ground-state energy expression is expanded in terms of two parameters— $a\rho^{1/3}$ and $1/b\rho^{1/3}$ —for the intermediate range of densities ρ ($b^3\rho \gg 1$ and $a^3\rho \ll 1$). All diagrams, the contribution of which to the energy is not less than the contribution which in the gas approximation is cubic in a, are taken into account. We show under what conditions there are states of the system for which $E_{av} < 0$, $\partial E_{av}/\partial\rho = 0$, and $\partial^2 E_{av}/\partial\rho^2 > 0$ (E_{av} is the energy per particle). We obtain in the two-parameter approximation a set of equations that enable us to find the ground-state energy. We compare this set of equations, obtained in the present paper, with Brueckner's equation which corresponds to the gas approximation.

1. INTRODUCTION

We obtained in a previous paper,[1] in the approximation of weak correlations, a set of equations for the ground state of nuclei (or of nuclear matter). We then essentially left out of the discussion the nature of the forces that must act between isolated particles in order that the weak correlation approximation be valid. A similar situation occurs also in other papers[2] on nuclear matter or on atomic nuclei as many-body systems.

It is well known that at distances of 1.5 to 2.5 fermi units the nucleon-nucleon interaction potential is negative. A study of experimental data on nucleon-nucleon scattering and on high-energy pick-up processes and similar ones enables one to assume that there are strong repulsive forces acting at distances of 0.4 to 0.5 fermi units.[3,4] We base our assumptions upon these data and assume that the nucleon-nucleon interaction potential consists of two parts: an attraction U and a repulsion V with ranges b and a, respectively, where $U \ll V$, $a < b$.

A consistent consideration of nuclear matter as a many-body system is made difficult by the fact that there is no small parameter which could be used reliably to estimate the perturbation-theory diagrams and to sum them. Indeed, the quantity that characterizes the contribution from different diagrams of the same order is $p_0 b$, where p_0 is the Fermi-momentum. If $p_0 b \ll 1$, the so-called gas approximation is valid,[5] and if $p_0 b \gg 1$ and U is not large, the high-density approximation is valid.[6] For the inner regions of heavy nuclei (and also for nuclear matter) p_0 is such that $p_0 b \approx 3$ and the large value of V makes it impossible to use the high-density approximation.

However, the fact that the assumed interaction consists of two parts enables us to introduce not one but two parameters, $p_0 a < 1$ and $p_0 b > 1$, and to expand the ground-state energy, the energy of single-particle excitations, and so on in powers of $p_0 a$ and $1/p_0 b$. The approximate equations obtained by this method for the single-particle and pair wave functions enable us to verify the validity of the weak correlations approximation.

Since the system considered here, with two kinds of interaction, is of interest not only as a model for nuclear matter, we shall consider the problem from a more general point of view, restricting ourselves only to the following assumption about the forces: $|V| \gg |U|$, $a \ll b$ and $ap_0 \ll 1$, $bp_0 \gg 1$. For the sake of simplicity we restrict ourselves to homogeneous systems of infinite extent in space, we determine their binding energy, and we show under what condition a state can be realized for which $\partial E_{av}/\partial\rho = 0$.

2. A SYSTEM WITH TWO KINDS OF INTERACTIONS. ESTIMATES OF DIAGRAMS

We shall use the apparatus of quantum field theory as a general method of considering systems with a large number of particles. We write the S-

matrix of the system under consideration in the form

$$S = T\exp\left\{-\frac{i}{2}\int [V(x_1 - x_2) + U(x_1 - x_2)]\,\psi^+(r_1, t_1)\,\psi^+(r_2, t_2) \times \psi(r_2, t_2)\,\psi(r_1, t_1)\,dr_1\,dr_2\,dt_1 dt_2\right\},$$

$$V(x_1 - x_2) + U(x_1 - x_2) = [V(r_1 - r_2) + U(r_1 - r_2)]\,\delta(t_1 - t_2),$$

$$\hbar = m = 1. \qquad (1)$$

Regarding the ground state of a system of non-interacting particles as the vacuum state and changing from the T- to the N-product, we can use a diagram technique.* Then:

1. In each vertex there enter three lines, one of which corresponds to a factor $-iU(q)$ or $-iV(q)$ while the other two are either internal or external lines that correspond to the motion of virtual and real particles and holes.

2. An internal line corresponds to a propagator which in the momentum representation is equal to

$$G^{-1}(p) = p_e - p^2/2 + i\delta\theta(p),$$
$$\theta(p) = 1 - 2n_p = \begin{cases} 1, & |p| > p_0 \\ -1, & |p| < p_0 \end{cases}, \qquad (2)$$

where p_e is the energy and n_p the occupation number of non-interacting particles in the ground state.

3. The law of conservation of four-momentum is valid at each vertex.

4. The diagram of n-th order in U and V is multiplied by

$$i^n \frac{k\ldots(k-m+1)}{2^n m!\,n!}(-1)^P,$$

where P is the number of closed particle-hole loops, and k and m the number of U- or V-lines ($k > m$) which are arranged over the diagram in such a way that interchange of U and V does not change the matrix element. We depict in each diagram V by a dotted line and U by a wavy line.

We consider first diagrams containing V only.

Since $ap_0 \ll 1$, we can restrict ourselves to the ladder (gas) approximation, which corresponds to multiple scattering of one particle of an isolated pair by the other particle of the pair (Fig. 1). Since $Va^2 \gg 1$ one must everywhere perform the summation over V instead of the separate diagrams of Fig. 1. We denote the sum depicted in Fig. 2 by V_{eff}.

Of all the diagrams containing only U, the main contribution is made by the diagrams of Fig. 3, where in each order of the perturbation theory the maximum number of particles (which is equal to the

FIG. 1

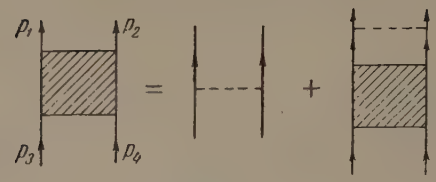

FIG. 2

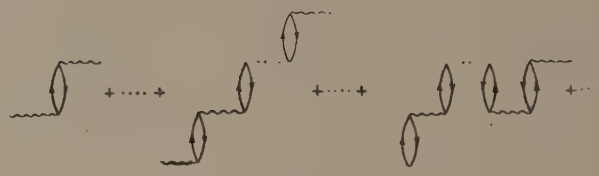

FIG. 3

order) is excited. The ratio of any diagram of Fig. 1 to another of the same order is less than $(ap_0)^{-1}$, and the same ratio for the diagrams of Fig. 3 is of higher order in bp_0.* We denote the sum of diagrams in Fig. 3 by U_{eff} and depict it by a double wavy line.

From the calculation given in Galitskii's paper[5] it follows that we can assume—at any rate to get estimates—that the effective short-range interaction V_{eff} is the same as the scattering amplitude of hard spheres of radius a.† One can assume that the scattering amplitude is constant for not too large values of the momentum. Moreover, if $V_{eff} \approx 4\pi a$, then $p_0 V_{eff} \ll 1$. The scattering amplitude is independent of the magnitude of V for sufficiently large V. It will become clear in the following that all expressions for the total energy, the single-particle Green's function, the effective interaction, and so on, contain in the integrand steeply decreasing functions of the type $(x-a)^{-1}$ and the integration over the intermediate momenta is thus limited to momenta not larger than a few times p_0, and this means that for estimates one must everywhere substitute a instead of V_{eff}.

We shall take into account all diagrams whose contribution to the ground-state energy E_0 is larger than that from the term proportional to a^3 in the gas approximation. We must thus drop all

*For details see references [5], [7], and [8].

*We shall give a more detailed and accurate comparison of different diagrams in another paper, where we shall use as an example the value of p_0 corresponding to nuclear matter, and where V, U, a, and b are taken from nucleon-nucleon interaction data.

†In the system of units in which $m = \hbar = 1$, V_{eff} is nearly equal to f, i.e., to the scattering amplitude.

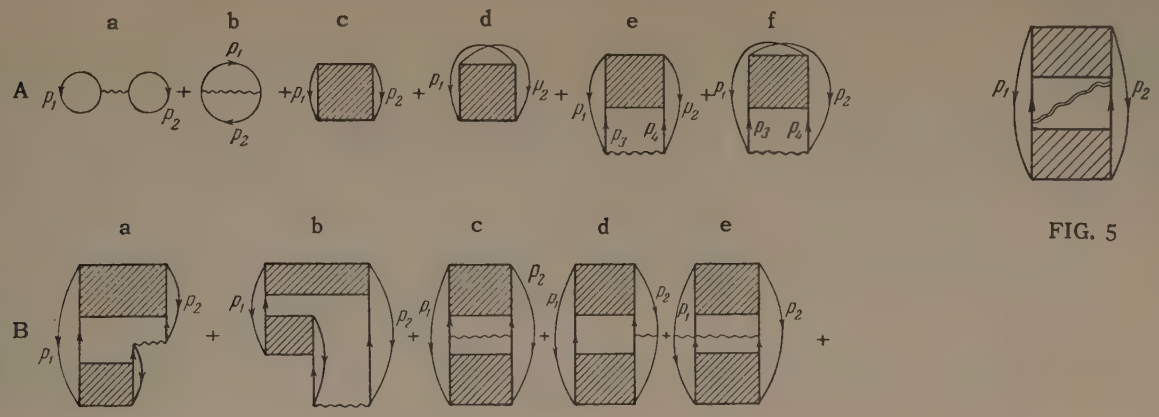

FIG. 5

FIG. 4

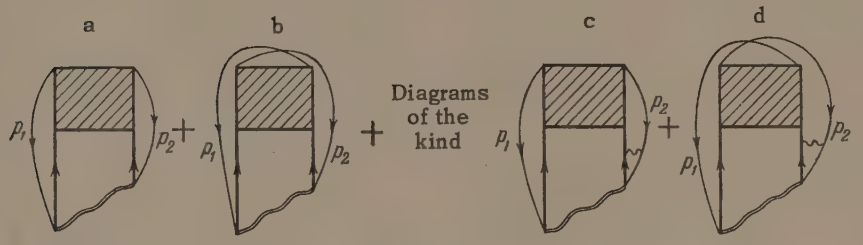

FIG. 6

diagrams which contain powers of V_{eff} larger than the second. All irreducible diagrams* which determine E_0 and which do not contain higher powers of U than the first are depicted in Fig. 4.

We now consider irreducible diagrams containing higher powers of U. The main contribution is in each order in U given by the diagrams containing the smallest number of integrations of U(q) over the momentum transfer q, since U(q) is different from zero only for small values of q. Thus, of all the possible complications when we go from the n-th to the (n+1)st order in U, we must take into account the diagrams depicted in Fig. 3. We must then take into account, apart from the diagrams of Fig. 4B, the five diagrams that are obtained from Fig. 4B by replacing U by U_{eff} (for instance, the diagram of Fig. 5).

In first order in V_{eff} one must take into account the diagrams of Fig. 6, as becomes clear from the estimates given in the following. In zeroth order in V_{eff} one must take into account, apart from the correlation energy diagrams (Fig. 7a), also the exchange diagrams. One must, of course, take into account irreducible diagrams in which instead of the Green's function (2) one must substitute the Green's function that takes the self energy into account†

*Diagrams are called irreducible if they do not contain parts of the self-energy type.

†A consideration of $\Sigma(p)$ will be the subject of a subsequent paper.

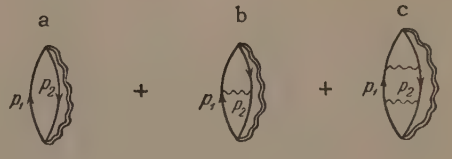

FIG. 7

$$G^{-1}(p) = p_e - p^2/2 - \Sigma(p) + i\delta\theta(p). \qquad (3)$$

Before we go over to estimate the reduced diagrams, we must note that should it ever become necessary to take into account terms proportional to V_{eff}^3, the main difficulty would lie in the appreciable increase in the number of mixed diagrams.

To elucidate the conditions for the existence of a state of the system for which $\partial E_{av}/\partial\rho = 0$, it is necessary to know how the matrix elements depend on p_0. Since the dependence on p_0 is different for different potentials, we perform the estimates for three potentials: $U = (U_{01}/r\nu_1)e^{-\nu_1 r}$, $U = U_{02}e^{-\nu_2 r}$, and a potential which is a square well of depth U_0 and width b. For the diagrams of Fig. 4A we have*

a: $U_{01}p_0^6/\nu_1^3$, $U_{02}p_0^6/\nu_2^3$, $U_0 b^3 p_0^6$; b: $U_{01}p_0^3$, $U_{02}p_0^3$, $U_0 p_0^3$;

c, d: ap_0^6; e, f: $U_{01}ap_0^5/\nu_1$, $U_{02}ap_0^3\nu_2 \ln(p_0/\nu_2)$, $U_0 ap_0^4$,

and for the diagrams of Fig. 4B

a, b, c, d, e: $\sim a^2 p_0^6 U_{01}/\nu_1$, $a^2 p_0^4 U_{02}\nu_2$, $a^2 p_0^5 U_0$.

*We shall give elsewhere more detailed estimates of the diagrams for nuclear matter.

It is somewhat more difficult to estimate the terms containing U_{eff}.

For the correction to the correlation energy, which is described by the diagram of Fig. 7a, we find by summing the diagrams of Fig. 3 in the approximation $p_0 b \gg 1$ (see [6] and [9])

$$E_{corr} = \frac{3}{8\pi p_0^2} \int_0^{p_0} q^3 dq \int_{-\infty}^{+\infty} ds \, [\ln(1-B) + B], \qquad (4)$$

$$B = \frac{p_0 |U(q)|}{2\pi^2} \left\{ \left(1 - s \operatorname{arctg} \frac{1}{s}\right) + \frac{q}{4p_0} \left[(1+s^2) \ln\left(1 + \frac{1}{s^2}\right) - \frac{2+s^2}{1+s^2} \right] \right\}. \qquad (5)^*$$

If for our estimate we replace V_{eff} by $4\pi a$, we get for the diagram of Fig. 6a

$$E^a_{corr} = \frac{3a}{2p_0^2} \int_0^{p_0} q^3 \frac{dq}{|U(q)|} \int_{-\infty}^{+\infty} ds \left[\ln(1-B) + B + \frac{B^2}{2} \right]. \qquad (6)$$

It is expedient to distinguish two cases in (4) and (6), namely $B \gg 1$ and $B \ll 1$. If $B \ll 1$ we find from (4) after some straightforward but tedious calculations

$$E_{corr} = -\frac{1}{16\pi^4} \int_0^{p_0} q^3 dq \, U^2(q) \left[(1 - \ln 2) + \frac{3q}{16 p_0} (4 \ln 2 - 1) \right]. \qquad (7)$$

For all long-range potentials with finite range, $U(q)$ tends with increasing q to zero at least as fast as $1/q^2$. The main contribution is thus given by that part of B which does not contain a factor q, and this makes it possible to drop in E^a_{corr} the term proportional to q. We get then

$$E^a_{corr} = -\frac{0.23}{16\pi^6} a p_0 \int_0^{p_0} q^3 dq U^2(q). \qquad (8)$$

The exchange diagram of Fig. 6 contributes the same. An estimate yields

$$E_{corr} \approx (U_{01}^2/\nu_1^2) \ln(p_0/\nu_1), \quad U_{02}^2/\nu_2^2, \quad U_0^2 b^2 \ln p_0 b;$$
$$E^a_{corr} \approx a p_0 (U_{01}^2/\nu_1^2) \ln(p_0/\nu_1), \quad a p_0 U_{02}^2/\nu_2^2, \quad a p_0 U_0^2 b^2 \ln(p_0 b). \qquad (9)$$

We consider now the case when $B > 1$. One can easily verify that the main contribution to E_{corr} and E^a_{corr} will be made by the integration over q from a q_m such that $B(q_m) \approx 1$ to p_0 (i.e., $q_m \sim \nu_1, \nu_2, 1/b$). To obtain estimates when $B > 1$ we must thus replace the quantities $\ln(p_0 b)$, $\ln(p_0/\nu_1)$ in (9) by $\ln(p_0/q_m)$.

When choosing the diagrams occurring in the correlation energy (Fig. 3 and the diagram of Fig. 7a) we have noted that in each order the ratio of the retained diagram to any dropped one is larger than $p_0 b$. This means that the contribution from the diagram of Fig. 7b and from the diagrams of Fig. 6c and d is smaller by approximately $1/p_0 b$ than the contribution from the diagrams of Figs. 7a and 6a, while that from the diagram of Fig. 7c is less than that from the diagram of Fig. 7a by a factor $1/p_0^2 b^2$.

The estimates performed here enable us to reach some qualitative conclusions.

1. If $a \gg U_0 b^3$ the attraction U is taken into account only in first order and the energy is evaluated from the hard-sphere formula:[10]

$$E_{av} = \frac{3}{10} p_0^2 \left[1 + \frac{20}{27\pi} U_0 b^3 p_0 + \frac{10}{9\pi} p_0 a + \frac{4}{21\pi^2} (11 - 2\ln 2) p_0^2 a^2 \right] - \frac{1}{2} U_0. \qquad (10)$$

2. If $a \approx U_0 b^3$ the expression for the energy is given by Eq. (10). Of most interest is the case where $a \ll U_0 b^3$ since it corresponds to the possibility of forming a state with negative total energy.

3. GROUND STATE ENERGY AND EQUATION OF STATE OF A SYSTEM WITH TWO KINDS OF INTERACTION

We evaluate the energy pertaining to one nucleon in the ground state when $U_0 b^3 \gg a$.* For the diagrams of Fig. 4A a and b we find

$$E^a = \rho \int U(\mathbf{r}) \, d\mathbf{r},$$

$$E^b = -\frac{1}{2\rho (2\pi)^6} \int n_{p_1} n_{p_2} U(|p_1 - p_2|) \, dp_1 \, dp_2 \approx -\frac{U_0}{2}, \qquad (11)$$

where $\rho = p_0^3/6\pi^2$ is the density of the particles with spins in the same direction.

We now find the contributions from the diagrams of Fig. 4A c and d. The difficulty in solving this problems lies in the difference between (3) and the free-particle Green's function (2). In the present paper we shall not attempt to solve this problem exactly, and assume only that $\Sigma(p)$ can be approximated in the momentum range $0 < p < 1/a$ by a quadratic parabola; this corresponds to replacing the kinetic energy $p^2/2$ in the Green's function by $p^2/2\mu_1$.† The effective interaction V_{eff} is expressed in terms of the amplitude for hard sphere-hard sphere scattering:[5]

* arctg = $\tan^{-1}$.

*We assume that the interaction potentials are spin-independent. $G_0(p)$ contains $\delta_{ss'}$ where s' and s are the spin components at the ends of the line G in the diagrams. In all results given here we have summed over s.

†One can hope that the results given here will not change appreciably when the dispersion law differs from a quadratic one.

$$V_{\text{eff}} \sim [f + O(f^2)].$$

If one replaces $p^2/2$ in the single-particle Green's functions by $p^2/2\mu_1$, i.e., if one takes into account that the scattering takes place in a dispersive medium, then $V_{\text{eff}} \sim \mu_1^{-1}[f + O(f^2)]$, as one can verify using the derivation of V_{eff} given by Galitskii.[5]

Since the function f is equal to a for the momenta $pa \ll 1$ which are of interest to us, and is independent of μ_1, the effective interaction V_{eff} is proportional to a/μ_1 and this expresses the change in the effective repulsive potential by a factor μ_1 if the presence in the system of a long-range attraction is taken into account. Such an approximation is unsatisfactory for $p \approx p_0$. However, if integration over a wide range is important in the matrix element (short-range potential) the contribution from the $p \approx p_0$ region is negligibly small. We can thus evaluate it assuming that the above-mentioned method of taking the change in the single-particle Green's function into account is sufficiently accurate. The contribution from the diagrams of Fig. 4A c and d is then equal to

$$E^{cd} = p_0^2(ap_0/3\pi\mu_1) + p_0^2(2a^2p_0^2/35\pi^2\mu_1)(11 - 2\ln 2). \quad (12)$$

If, however, the $p \approx p_0$ region is important, we must use a different approximation:

$$\Sigma(p) = \Sigma(p_0) + q\Sigma'(p_0)$$

or

$$\tfrac{1}{2}p^2 \approx \tfrac{1}{2}p_0^2 + qp_0 \to \tfrac{1}{2}p_0^2 + qp_0/\mu_2 \qquad (q = p - p_0). \quad (13)$$

One can verify that μ_2 differs less from unity than μ_1.

We now consider the diagrams of Fig. 4A e and f. If we restrict ourselves to the term proportional to a in V_{eff}, we find after integrating over the fourth component of the momentum

$$E^{ef} = -\frac{6ap_0}{(2\pi)^6\mu_1}\int d\mathbf{p}_1 d\mathbf{p}_2 d\mathbf{p}_3 n_{\mathbf{p}_1} n_{\mathbf{p}_2}(1 - n_{\mathbf{p}_3})$$
$$\times (1 - n_{\mathbf{p}_1+\mathbf{p}_2-\mathbf{p}_3})\, U'(p_0|\mathbf{p}_1 - \mathbf{p}_3|)$$
$$\times [\tfrac{1}{2}p_3^2 + \tfrac{1}{2}(\mathbf{p}_1 + \mathbf{p}_2 - \mathbf{p}_3)^2$$
$$- \tfrac{1}{2}p_1^2 - \tfrac{1}{2}p_2^2 + \Sigma(p_3) + \Sigma(|\mathbf{p}_1 + \mathbf{p}_2 - \mathbf{p}_3|)$$
$$- \Sigma(p_1) - \Sigma(p_2) + 2i\delta(n_{\mathbf{p}_1+\mathbf{p}_2-\mathbf{p}_3} + n_{\mathbf{p}_3} - n_{\mathbf{p}_1} - n_{\mathbf{p}_2})]^{-1}. \quad (14)$$

Terms of the type

$$\int \frac{n_{\mathbf{p}_1} n_{\mathbf{p}_2} n_{\mathbf{p}_3} n_{\mathbf{p}_4} \delta(\mathbf{p}_1 + \mathbf{p}_2 - \mathbf{p}_3 - \mathbf{p}_4)}{p_1^2 + p_2^2 - p_3^2 - p_4^2}\, d\mathbf{p}_1\, d\mathbf{p}_2\, d\mathbf{p}_3\, d\mathbf{p}_4$$

which we obtain on integrating, vanish because the domain of integration is the same for all variables while the denominator is antisymmetric. To display explicitly the way the energy depends on the density, the momenta are expressed in units p_0. Writing $\mathbf{q} = \mathbf{p}_1 - \mathbf{p}_3$ and using the fact that $U(q)$ decreases steeply with increasing q we expand the integrand [apart from $U(q)$] in a power series in q, retaining the first two terms. After straightforward but very tedious calculations we get

$$E^{ef} = -\frac{ap_0\mu_2}{2\mu_1\pi^3}\int_0^1 dq\, U'(qp_0)\, q^3$$
$$\times\left[(1 - \ln 2) + \frac{3}{16}q(4\ln 2 - 1)\right],$$
$$U'(p_0q) \equiv p_0^3 U(p_0q). \quad (15)$$

The contribution from the diagrams of Fig. 7a and those of Fig. 6 a, b is obtained by analogy with (4) and (6):

$$E_{\text{corr}} = \frac{3p_0^2}{8\pi^2\mu_2}\int_0^1 q^3 dq \int_{-\infty}^{+\infty} ds\, [\ln(1 - \mu_2 B) + \mu_2 B], \quad (16)$$

$$E^a_{\text{corr}} = \frac{3ap_0^2}{2\mu_1\mu_2}\int_0^1 \frac{q^3 dq}{|U(qp_0)|}\int_{-\infty}^{+\infty} ds\left[\ln(1 - \mu_2 B) + \mu_2 B + \frac{\mu_2^2 B^2}{2}\right]; \quad (17)$$

the quantity B is defined in (5).

If $ap_0^2 b > 1$ and E^a_{corr} is of the order of the part E^{cd} which is proportional to a^2, then (11), (12), and (15) to (17) determine the ground state energy of the system $E_0 = E_{av}N$, where N is the number of particles in the system up to terms of the order a^2.

As an example we give the expression for E_0 for an exponential attractive potential $U_0 e^{-\nu r}$ for the case where $B < 1$:

$$E_0/N = \frac{3}{10}p_0^2 + \frac{4}{3\pi}U_0\frac{p_0^3}{\nu^3} - \frac{1}{2}U_0$$
$$+ \frac{3}{2}U_0\frac{\nu}{p_0}\left\{\frac{1}{\pi}\ln\frac{2p_0}{\nu} + \frac{1}{\pi} + \frac{\nu}{p_0}\right\}$$
$$+ \frac{1}{3\pi\mu_1}ap_0^3 + \frac{2}{35\pi^2\mu_1}(11 - 2\ln 2)p_0^4a^2$$
$$- U_0a\nu\frac{\mu_2}{\mu_1\pi^2}\left\{4(1 - \ln 2)\left(2\ln\frac{p_0}{\nu} - 1\right)\right.$$
$$\left. + \frac{3}{2}\left(1 - \frac{3}{4}\pi\frac{\nu}{p_0}\right)(4\ln 2 - 1)\right\} - \frac{U_0^2\mu_2}{\pi^2\nu^2}\left\{\frac{1}{3}(1 - \ln 2)\right.$$
$$\left. + \frac{3}{64}(4\ln 2 - 1)\left(\frac{\pi}{2}\frac{\nu}{p_0} - 1\right) + 0.08\frac{ap_0}{\mu_1\pi^2}\right\}. \quad (18)$$

The equation of state of the gas considered is obtained from (18) by differentiating with respect to ρ:

$$P = \rho^2\partial E_{av}/\partial\rho. \quad (19)$$

For a density for which $(U_0/\nu^2)(p_0/\nu) > 1$ the

pressure is basically determined by the attractive potential. Therefore $P < 0$, corresponding to a tendency of the system to compress without limit. However, the presence of a repulsion, the energy of which increases very steeply with increasing density (together with the term $\sim p_0^2 a^2$ in (18), an important contribution to E_0 is starting to be made by the terms proportional to $p_0^3 a^3$ and by all higher powers of $p_0 a$) and this leads to the fact that at high densities the rate of growth $(\partial E/\partial \rho)$ of the energy of the attraction and of the repulsion compensate one another and the pressure is determined by the kinetic energy.

We shall, however, be interested in the case where $P = 0$, and we shall now consider that case.

4. SPONTANEOUSLY CONDENSED SYSTEMS

If the system is not closed, the condition $P = 0$ may not be satisfied for its internal energy, and there is no connection between ρ, a, b, V, and U. Closed systems will spontaneously condense to such a density that $P = 0$, and there is thus a well-defined connection between ρ and the parameters of the potentials. In the present section we shall study systems for which

$$\partial E_{av}/\partial \rho = 0, \qquad \partial^2 E_{av}/\partial \rho^2 > 0. \tag{20}$$

These are precisely of greatest interest to us, since they apply to practically all atomic nuclei.[1] Condition (20) was proposed in [1] on the basis of a set of equations obtained to describe the ground state of atomic nuclei. In the present paper (20) appears as an additional condition.

Let us consider what requirements are imposed on the potentials U and V by the existence of a minimum of the ground state energy with respect to ρ when $ap_0 \ll 1$ and $bp_0 \gg 1$. It is of certain interest to show that a many-particle system with two-body interactions taken from experimental data* can be in the state (20). It is well known that (20) is not satisfied when there are only attractive forces (Wigner's theorem). Exchange forces by themselves lead to the possibility of satisfying (20).

If the interaction potential is negative and contains together with an exchange part also a non-exchange part, (20) is not satisfied. We consider under what conditions strong repulsions at small distances can lead to (20) being satisfied. It is clear that one can always find a ρ for which (20) is valid if V is sufficiently large. However, we shall in the present paper be interested in the possibility of satisfying (20) just for an intermediate density when E_{av} is determined with sufficient accuracy by the sum of the contributions from the diagrams of Figs. 4 to 7 or simply by (18). One sees easily that in order that condition (20) be satisfied it is necessary that the expression for the energy E_{av} contain terms that increase more rapidly than ρ with increasing density.

*For example, for nuclear matter from nucleon-nucleon scattering experiments.

Estimates of the diagrams which were given in the foregoing, and also Eq. (18), show that the only term which increases more rapidly than ρ is the term proportional to $\rho^{4/3}$:

$$E_s = \tfrac{12}{35}\mu_1^{-1}(6\pi^2)^{1/3}a^2(11 - 2\ln 2)\rho^{4/3} \approx 13a^2\rho^{4/3}/\mu_1. \tag{21}$$

The remaining terms, either those corresponding to the presence in the system of only a long-range attraction or the mixed ones, cannot contain ρ in powers higher than the first, as can be seen from the estimates.

We shall see under what conditions condition (20) can be satisfied. We find from (18) and (20)

$$\begin{aligned}
&\frac{3}{5} + \frac{4}{\pi}\xi\eta - \frac{3}{2}\xi\frac{1}{\eta^3}\left\{\frac{1}{\pi}\ln 2\eta + \frac{2}{\eta}\right\} \\
&\quad + \frac{\zeta}{\pi\mu_1} + \frac{8}{35\pi^2\mu_1}(11 - 2\ln 2)\zeta^2 \\
&\quad - \frac{\mu_2}{\mu_1\pi^2}\xi\zeta\frac{1}{\eta^3}\left\{8(1 - \ln 2) + \frac{9\pi}{8\eta}(4\ln 2 - 1)\right\} \\
&\quad - \frac{\mu_2}{\pi^2}\frac{\xi^2}{\eta^2}\left\{0.08\frac{\zeta}{\mu_1\pi^2} - \frac{3}{64}(4\ln 2 - 1)\frac{\pi}{2}\frac{1}{\eta}\right\} = 0,
\end{aligned} \tag{22}$$

$$\begin{aligned}
&-\frac{3}{5} + \frac{6}{\pi}\xi\frac{1}{\eta^3}\ln 2\eta - \frac{3}{2\pi}\xi\frac{1}{\eta^3} + 15\xi\frac{1}{\eta^4} \\
&\quad + \frac{8}{35\pi^2\mu_1}(11 - 2\ln 2)\zeta^2 + \frac{0.16\mu_2}{\mu_1\pi^2}\zeta\xi^2\frac{1}{\eta^2} \\
&\quad + \frac{\mu_2}{\mu_1\pi^2}\xi\zeta\frac{1}{\eta^3}\left\{24(1 - \ln 2) + \frac{9\pi}{2\eta}(4\ln 2 - 1)\right\} \\
&\quad - \frac{3}{32}\frac{\mu_2}{\pi}\xi^2\frac{1}{\eta^3}(4\ln 2 - 1) > 0,
\end{aligned} \tag{23}$$

where

$$\xi = U_0/v^2, \qquad \eta = p_0/v, \qquad \zeta = p_0 a.$$

Let U be the Wigner potential. Then $\xi < 0$ and one can show that μ_1 and $\mu_2 > 1$. The calculation given here had a meaning only because $\zeta \ll 1$ and $\eta \gg 1$. But under those conditions (23) is not satisfied since all terms in (23), apart from those proportional to ζ^2 and $\zeta\xi^2/\eta^2$, are negative. It is perfectly clear that the average energy E_{av} of the ground state of the system considered must be negative. We find from (18) and (22)

$$\begin{aligned}
E_{av} \approx &\frac{1}{5}p_0^2 - \frac{U_0}{2} + \frac{2}{\pi}\frac{U_0}{\eta}\ln\eta + \frac{3}{2\pi}U_0\frac{1}{\eta} \\
&- \frac{8\mu_2}{\mu_1}(1 - \ln 2)U_0\frac{\zeta}{\eta}\ln\eta,
\end{aligned} \tag{24}$$

from which we see that $E_{av} > 0$.

We consider a system such as a neutron fluid, since we neglect the Coulomb interaction and do not take the isotopic spin of the particles into account. The result obtained here means thus that it is impossible for a neutron fluid of intermediate density to exist if its interaction potential is the Wigner potential. This conclusion does, of course, not exclude the possibility that there exists a bound state at densities so high that $\zeta \approx 1$ and $\eta \gg 1$.

We now see what changes occur if we take the Majorana potential into account along with the Wigner potential. We shall assume for the sake of simplicity that their radial dependences are the same and we denote the respective parts in the mixture by the letters W and M. (18) is then changed and using (20) we find instead of (24)

$$E_{av} \approx \frac{1}{5} p_0^2 - \left(\frac{W}{2} - M\right) U_0 + \frac{2}{\pi}\left(\frac{W}{2} - M\right) U_0 \frac{\ln \eta}{\eta} + \frac{3}{2\pi}\left(W - \frac{M}{2}\right) U_0 \frac{1}{\eta} - \frac{2}{105\mu_1}\zeta^2 p_0^2 - \frac{8\mu_2}{\mu_1}(1 - \ln 2)\left(W - \frac{M}{2}\right) U_0 \frac{\zeta}{\eta} \ln \eta < 0 \qquad (25)$$

or

$$M > W/2, \qquad 5\,|\,W/2 - M\,|\,|\,\xi\,|\,| > \eta^2 (1 - 2\zeta^2/21\,\mu_1). \qquad (26)$$

If $M \geq W/2$ we have $\mu_1 \leq 1$. For sufficiently large M ($M \gtrsim W$) the quantity μ_1 is appreciably less than unity.* If, moreover, $\eta\zeta \gg 1$, we have from (23)

$$\zeta^2 > 2.7\,\mu_1, \qquad (27)$$

and we get from (22) an equation for η, which in first approximation can be written as

$$0.6 + 1.27\,(W - M/2)\,\xi\eta + 0.32\,\zeta/\mu_1 + 0.22\,\zeta^2/\mu_1 = 0. \qquad (28)$$

The appearance of the factor μ_1 leads to terms $\sim a^2$ being able to contribute to the energy to approximately the same extent as the kinetic energy even if ζ is appreciably less than unity. (One must therefore take into account terms proportional to a^3, for instance when studying nuclear matter.) It is clear that the introduction of an exchange interaction does not only enable us to achieve $E_{av} < 0$, but also increases the repulsive energy so that (27) can be satisfied. One can show that E_{av} and the density corresponding to (20) depend strongly on the radius of the core (of the short-range potential) a, while the above-mentioned strong dependence arises from the requirement that (20) be satisfied.

The presence of two kinds of particles in the system increases the repulsive energy. Indeed, if $\zeta \ll 1$, the repulsion is important only in states for which the spatial part of the pair wave function is symmetric. The statistical weight of such a state is equal to unity for identical particles, while it is equal to four for different particles. The repulsive energy per particle is thus increased threefold. For smaller values of η when $\eta\zeta \approx 1$ we get from (23) instead of (17)

$$-1.9\,(M - W/2)\,\xi\zeta^3 \ln 2\zeta + 0.22\zeta^2/\mu_1 > 0.6 \qquad (29)$$

and from (22) we get an estimate for ξ

$$\xi \approx -0.25/\mu_1 (W - M/2). \qquad (30)$$

Equations (30) and (25) go together. We note that (27) is satisfied if ζ is not too small. One must then take into account the contribution from the diagrams of Fig. 4B, which leads to a decrease of the kinetic energy, as is clear from estimates.

Up to now we have considered the possibility that there exists a bound state when $\zeta \ll 1$ and $\eta \gg 1$. However, one can verify by a direct calculation that the contribution of the correlation energy is altogether very small even if $\eta \gtrsim 1$. Equation (18) is in that case incorrect since it does not take into account the contribution of the diagrams of Figs. 6c, d and 7 b, c. However, for estimates one can neglect them in $\partial^2 E_{av}/\partial\rho^2$ compared to the exchange terms in (23), i.e.,

$$(W/2 - M)\,\xi\,(\ln 2\eta - 0.25 + 0.8/\eta) > 0.3\,|\,\eta^3.$$

There is thus a possibility for the existence of a bound state when $\zeta \ll 1$ and $\eta \gg 1$, if exchange forces are taken into account.

Although the density-dependence of the matrix elements containing U is different for different potentials, one can conclude on the basis of estimates given earlier that the results of the present section are qualitatively independent of the form of U. If we take into account that the nucleon-nucleon interaction consists of two parts, it is possible to show that (20) is satisfied for nuclear matter at intermediate densities only if there is a strong repulsion at small distances (a core) and also an appreciable admixture of exchange forces in U. The equilibrium density ρ will depend strongly on the core radius.

5. A COMPARISON WITH BRUECKNER'S METHOD

Recently Brueckner's method,[2] which is based upon replacing the true interaction by a t-matrix which is obtained from an integral equation, has been used very widely for studying systems with interactions of the kind considered, in

*μ_1 depends, generally speaking, on the density in such a way that $\partial^2(\rho^{4/3}/\mu_1)/\partial\rho^2 < \mu_1 \partial^2\rho^{4/3}/\partial\rho^2$. In that case, however, $\partial^2(\rho^{4/3}/\mu_1)/\partial\rho^2 > \partial^2\rho^{4/3}/\partial\rho^2$.

particular for nuclear matter. The ground state energy, the single-particle energy, and the basis functions,[2,1] and also the t-matrix are determined from the following relations

$$E_0 = -\sum_{i=1}^{N}\left(i\left|\frac{\Delta}{2}\right|i\right)+\frac{1}{2}\sum_{i,k=1}^{N}(ik|t|Aik),$$

$$(ik|t|lq) = (ik|V+U|lq) + \sum_{s,p>F}\frac{(ik|V+U|sp)(sp|t|lq)}{E_l+E_q-E_s-E_p},$$

$$E_l = -\left(l\left|\frac{\Delta}{2}\right|l\right)+\sum_{q\leqslant F}(lq|t|Alq), \qquad (31)$$

where the notation is the same as in [1].

The equation for the t-matrix is obtained in the ladder approximation[11] and is valid only at low density. Since, however, p_0b is about 3 to 3.5 for nuclear forces, such an equation has no exact theoretical foundation. Doubt was therefore often expressed as to the validity of the method, and astonishment in connection with the good agreement with experiment both for the average energy per particle in nuclear matter and for the density for which the energy is a minimum. Apart from the agreement with experiment, arguments in favor of this method are based either on qualitative considerations (see a discussion in [12] on the influence of the Pauli principle and the "healing length") or on calculations of some of the dropped perturbation-theory diagrams.

Hugenholtz[13] has, however, already shown that in the high density approximation (corresponding to $p_0b \approx 3$ to 3.5) the main contribution is not made by the ladder diagrams (compare estimates of the diagrams of Figs. 4a, b, c and 7a). Moreover, in Brueckner's method some formal difficulties are raised by the possibility that the t-matrix may have poles below the Fermi surface, which would make it wrong to drop terms containing higher powers in t than in (31). Many attempts have been made to get rid of these poles but they have not been successful. The appearance of poles need not cause surprise since in the low-density approximation the presence of an attraction (however small) leads to a logarithmic divergence in the scattering amplitude near the Fermi surface. It is, however, not clear whether this singularity is real in the case of nuclear matter, for instance, or whether it appears because of an application of the Brueckner method.*

In the present paper a different method is proposed, which as far as we can see is free from the above-mentioned deficiencies. For comparison we obtain the set of equations of the type (31) in the two-parameter approximation. The contribution from the diagrams of Fig. 4A c, d can in the notation of (31) be written in the form

$$E^{cd} = \frac{1}{2}\sum_{i,k=1}^{N}(ik|Q|Aik),$$

where Q is determined from the integral equation

$$(ik|Q|lq) = (ik|V|lq) + \sum_{s,p>F}\frac{(ik|V|sp)(sp|Q|lq)}{E_l+E_q-E_s-E_p}. \qquad (32)$$

Summing the contribution from the diagrams of Fig. 4A a to f, we find

$$E_0 = -\sum_{i=1}^{N}\left(i\left|\frac{\Delta}{2}\right|i\right)+\frac{1}{2}\sum_{i,k=1}^{N}(ik|\tau|Aik),$$

$$(ik|\tau|lq) = (ik|V+U|lq) + \sum_{s,p>F}\frac{(ik|V+U|sp)(sp|Q|lq)}{E_l+E_q-E_s-E_p},$$

$$E_l = -\left(l\left|\frac{\Delta}{2}\right|l\right)+\sum_{q\leqslant F}(lq|\tau|Alq). \qquad (33)$$

Equations (33) can be generalized in such a way that one can take into account the diagrams of Figs. 7a and 6a, b. We leave for the moment the problem of the application of these equations to a nucleus or to nuclear matter; this requires considerably more accurate estimates of diagrams than the ones given here. At the present more accurate estimates are being made.

In conclusion I consider it a pleasant duty to express my deep gratitude to Professor L. A. Sliv and also to G. M. Shklyarevskii for many discussions and valuable hints and to D. A. Kirzhnits for interesting discussions about the problems of this paper.

*The problem under what conditions poles appear in the pair scattering amplitude will be considered elsewhere.

[1] M. Ya. Amus'ya, JETP **39**, 639 (1960), Soviet Phys. JETP **12**, 449 (1961).

[2] K. A. Brueckner and J. L. Gammel, Phys. Rev. **109**, 1023 (1958).

[3] Gammel, Christian, and Thaler, Phys. Rev. **105**, 311 (1957).

[4] J. L. Gammel and R. M. Thaler, Phys. Rev. **107**, 291, 1337 (1957).

[5] V. M. Galitskii, JETP **34**, 151 (1958), Soviet Phys. JETP **7**, 104 (1958).

[6] M. Gell-Mann and K. A. Brueckner, Phys. Rev. **106**, 364 (1957).

[7] J. Hubbard, Proc. Roy. Soc. (London) **A240**, 539 (1957).

[8] V. M. Galitskii and A. B. Migdal, JETP **34**, 139 (1958), Soviet Phys. JETP **7**, 96 (1958).

[9] D. A. Kirzhnits, JETP **37**, 585 (1959), Soviet Phys. JETP **10**, 414 (1960).

[10] T. D. Lee and C. N. Yang, Phys. Rev. **105**, 1119 (1957).

[11] N. M. Hugenholtz, Physica **23**, 481 (1957).

[12] Gomes, Waleska, and Weisskopf, Ann. Phys. **3**, 241 (1958).

[13] N. M. Hugenholtz, Physica **23**, 533 (1957).

Translated by D. ter Haar
81

RESULTS OF MEASUREMENT OF THE ELECTRICAL CONDUCTIVITY OF INSULATING LIQUIDS

G. A. OSTROUMOV

Leningrad State University

Submitted to JETP editor February 4, 1961

J. Exptl. Theoret. Phys. (U.S.S.R.) **41**, 441-444 (August, 1961)

A hydrodynamical explanation is proposed for the deviation from "Ohm's law" encountered in measurements of the specific electric conductivity of some liquids. The explanation is confirmed by the experimental data reported in the literature.

In studying the electric conductivity of liquids, experimenters frequently encounter "deviations from Ohm's law": the voltage is found to be proportional to neither the current nor the distance between electrodes. Explanations for this circumstance are sought on the basis of gas electronics with the possible motion of the liquid medium neglected.

For example, Goodwin and Macfadyen [1] (see also [2], p. 340) report measurements of the resistance of highly purified n-hexane between flat electrodes (no dimensions indicated) spaced 550 to 420 μ apart. The plotted results (Fig. 6 of [1] or Fig. 230 of [2]) show that the current increases strongly with increasing voltage. An explanation, which is not too rigorously confirmed by experiment (the bending of the lines in Fig. 7) is sought in the "simplest theory of impact ionization": the liquid is considered to be as a whole a stationary medium, through which the ions move and are sometimes recombined.

Yet the possible role of hydrodynamic phenomena in the process involved in the passage of current through liquids (and gases) has been mentioned earlier on several occasions, for example in [3,4]. In particular, even primitive dimensionality considerations, say the very listing of the possible cases, make it possible to establish (neglecting the inhomogeneity of the dielectric constant and electrostriction) that a real liquid capable of electrolysis cannot be immobile in a strong electric field between stationary electrodes. The spontaneous motion of the liquid under these conditions was noted many times (see, for example, [5], Fig. 5). In the case of laminar spontaneous motion of the liquid, the electric current flowing is proportional to the cube of the field intensity [[4], formula (19)], so that "Ohm's first law" is not satisfied.

If we replot Fig. 6 of [1] in new coordinates (the cube root of the flowing current i vs. the potential difference between the electrodes $El = U$) we obtain the plot shown in Fig. 1. It is seen from this

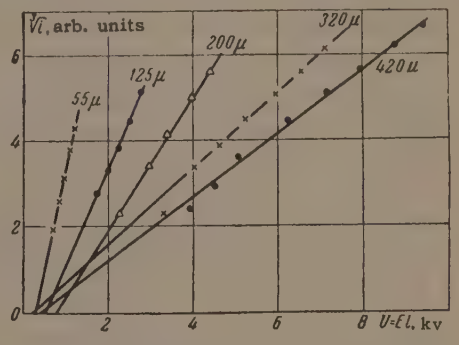

FIG. 1. Results of replotting Fig. 6 of [1] for n-hexane. The numbers on the curves denote the interelectrode distance in microns. The liquid was in spontaneous laminar motion.

plot that the experimental points (with several isolated exceptions) fit well straight lines with abscissa intercepts whose average is approximately 500 volts. This shows that the applied voltage produces essentially in the liquid an electric field, the cube of which is proportional to the mean density of the electric current in the spontaneously moving liquid. The remaining small part of the voltage is needed to overcome the surface resistance on the boundary of the electrodes (and perhaps also to remove the electrons from the metal of the electrodes), and to produce a current of sufficient strength (see Fig. 49 in the book by Levich, [6] Sec. 46, p. 252).

If we now relate the slope of the resultant lines with the interelectrode distance, we obtain from Fig. 1 the plot shown in Fig. 2, from which it is seen that for a specified current the voltage applied to the liquid (i.e., after subtracting the voltage drops at the electrodes) is proportional to the distance between electrodes: "Ohm's second

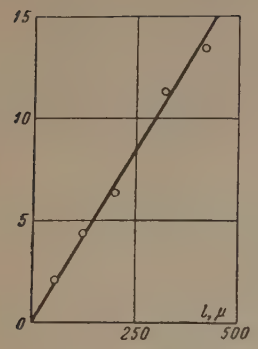

FIG. 2. Reciprocal of the slopes of the lines of Fig. 1, in arbitrary scale, as a function of the distance between electrodes. The "effective resistance" is proportional to the distance between electrodes.

law" holds. This means that we indeed deal here with a relation between the current density and the field intensity within the layer of moving medium (averaged values), and not with an edge or wall effect.

If these considerations are true, then we must recall (see [4]) that the coefficient of proportionality between the current and the cube of the field intensity is not at all connected with the specific electric conductivity of the liquid, but is obtained essentially by dividing the square of the dielectric constant of the liquid by its dynamic coefficient of viscosity. To measure the intrinsic conductivity of an electric insulating liquid it is necessary to use a low electric field intensity (see [4], table on p. 1918, with benzene as an example).

G. A. Skanavi ([2], p. 270, Fig. 156) gives the measured values of the electric conductivity of transformer oil. These show once more that the current is not proportional to the voltage, and that certain differences in the five cited curves can be attributed to the shapes and finishes of the electrodes. Figure 3 shows curves 1, 2, 3, and 5 replotted as in Fig. 1, but for different electrode shapes. It is seen that the lines drawn through the points pass either through the origin or very close to it. We can therefore conclude that here, too, the liquid was in spontaneous laminar motion during the measurements.

Curve 4 corresponds to a particular set of carefully cleaned flat copper electrodes, has a different form and is therefore not included in the foregoing group of replotted curves. In the text this curve is pointed out as being one example of particularly precise results. Yet, as shown in [4] (formula 22), if the liquid is in turbulent spontaneous motion the current density is proportional to the square of the field intensity, the coefficient of proportionality being essentially determined by the dielectric constant and by the density of the liquid and also by the linear dimensions of the instrument, and is not at all connected with the electric conductivity.

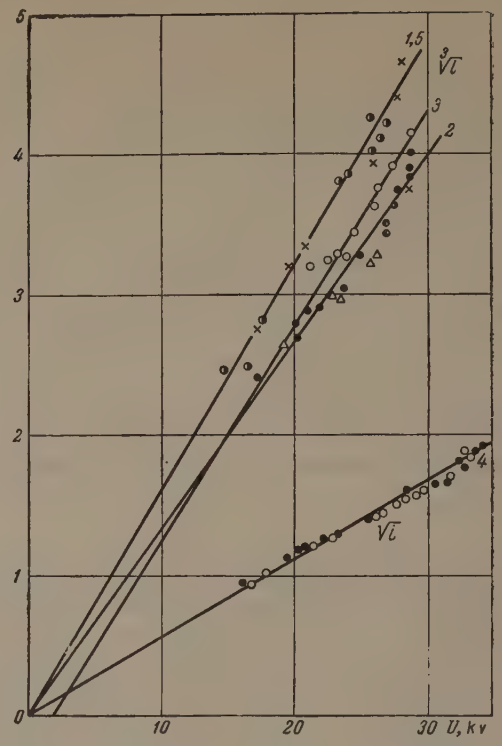

FIG. 3. Result of replotting Fig. 156 of [2] for transformer oil. Curve 4 is for liquid in spontaneous turbulent motion, while the remaining curves are plotted for laminar flow.

Curve 4 of Fig. 3 is the mate of curve 4 in Fig. 156 of [2], having the same values of the voltage (abscissa), but the ordinates are now the square roots of the current (arbitrary scale). It is seen that the points all fit quite well a straight line passing through the origin. This means that the liquid was in spontaneous turbulent motion during the measurements. The conciseness of the original text does not enable us to advance any hypothesis to explain the change of the laminar motion of curves 1, 2, 3, and 5 into the turbulent motion of curve 4.

Some light is cast on this question by Fig. 10 of the paper of Toriyama [7] on the electric conductivity of transformer oil. In Fig. 4 we show in

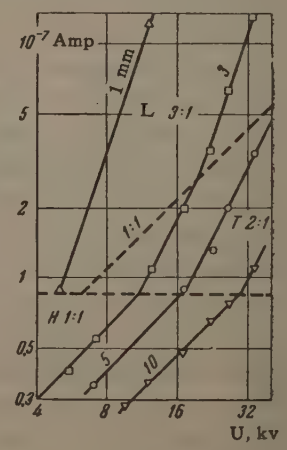

FIG. 4. Result of replotting Fig. 10 of [7] for transformer oil. The figures on the curves are the distances between flat electrodes, in millimeters. In the regions S, L, and T the liquid was stationary, laminar, and turbulent, respectively.

logarithmic coordinates the dependence of the current on the applied voltage, obtained from the aforementioned diagram. The entire diagram consists evidently of regions demarcated by the dashed lines and marked S, L, and T. In the region corresponding to low current densities (less than 8.5×10^{-8} amp/cm^2), the current is approximately proportional to the voltage and inversely proportional to the distance between the plane electrodes (diameter 25 mm), so that both "Ohm's laws" are obeyed satisfactorily. It must be assumed that the liquid was stationary during the measurements (region S). The specific resistivity, calculated from the data for this region, is found to be 2.1×10^{12} ohm-cm ± 13 percent.

The region corresponding to large currents but small distances between the electrodes, i.e., to small applied voltages, shows a cubic dependence of the current on voltage (the slope of the lines is 3:1) and therefore indicates that the spontaneous motion of the liquid is laminar (region L).

At large distances between the electrodes, and accordingly at large applied voltages, the two foregoing regions become separated by a third one, characterized by a quadratic dependence of current on the voltage (slope of curves 2:1). It must be assumed that this is a region where the liquid is in turbulent spontaneous motion (region T).

It is possible to see on this diagram that as the distance between electrodes is increased and if the applied voltage is high (for example, 16 kv), the liquid between electrodes is first stationary (region S), and the current is low and obeys "Ohm's law." After a certain sufficient field intensity is reached (about 40 kv/cm) the liquid goes into spontaneous turbulent motion and the current increases as the square of the field intensity; the effective resistance is then inversely proportional to the field intensity. As the electrodes come closer together, the motion of the liquid begins to be slowed down by the viscous boundary layer adhering to the electrodes and becomes laminar in spite of the continuing increase in field intensity; the effective resistance decreases as the inverse square of the field intensity. No region of turbulent motion was observed at low voltages.

The small number of points on the last diagram and their relative spread did not enable us to establish with sufficient reliability the limits of the indicated regions. More detailed experimental investigations are therefore necessary, as well as attempts at a theoretical solution of the nonlinear problem of electric convection, following, Benard and Rayleigh,* for example.

A. Shteĭnberg and R. Shatrova participated in the reduction of the curves.

*We note that an error has crept into[4], namely that in Sec. IV of the article the letter μ denotes (unlike the remaining sections of the article) not the dynamic but the kinematic viscosity of the liquid. This error occurred also in the numerical values for air, listed in the table on p. 1918. The error was corrected in[5].

[1] D. W. Goodwin and K. A. Macfadyen. Proc. Phys. Soc. **B66**, 85 (1953).

[2] G. A. Skanavi, Fizika dielektrikov (Physics of Dielectrics) Fizmatgiz, (1958).

[3] A. Nikuradze, Zhidkie dielektriki (Liquid Dielectrics), Gostekhizdat, (1936), p. 65.

[4] G. A. Ostroumov, J. Tech. Phys. (U.S.S.R.) **24**, 1915 (1954).

[5] G. A. Ostroumov, JETP **30**, 282 (1956), Soviet Phys. JETP **3**, 259 (1956).

[6] V. G. Levich, Fiziko-khimicheskaya gidrodinamika (Physico-Chemical Hydrodynamics), Fizmatgiz, (1959).

[7] Y. Toriyama. Arch. Elektrotechnik **19**, 31 (1927).

[8] G. A. Ostroumov, J. Tech. Phys. (U.S.S.R.) **25**, 366 (1955).

Translated by J. G. Adashko
82

EFFECT OF ROTATION ON PAIR CORRELATION IN NUCLEI

Yu. T. GRIN'

Submitted to JETP editor February 4, 1961

J. Exptl. Theoret. Phys. (U.S.S.R.) **41**, 445-450 (August, 1961)

Corrections are determined to the quantity Δ characterizing the pair correlation, in the second order of perturbation theory in the rotation. Corrections are estimated to the rotation spectrum, arising from the dependence of Δ and consequently of the moment of inertia on the nuclear spin.

IT is well known that a magnetic field reduces the magnitude of the energy gap 2Δ in a superconductor. Since a magnetic field is equivalent to a rotation, the rotation of a system of "paired" particles will also lead to this same effect. The reduction of Δ results in an increase in the moment of inertia. Since the change of Δ depends on the rate of rotation or the spin I of the system, this will lead to corrections to the moment of inertia which are proportional to $I(I+1)$ and consequently to corrections to the energy proportional to $I^2(I+1)^2$.

The calculation of the change in Δ is conveniently done by the method of Gor'kov and Migdal,[1] using the equation for the Green's function. In the present paper we shall find the diagonal corrections to the solutions of the Gor'kov equation in the second order of perturbation theory and find the dependence of Δ on I. Using the dependence $\Delta(I)$ thus found, we can estimate the corrections to the energy of the rotating system proportional to $I^2(I+1)^2$.

We shall write these equations for the Green's functions

$$G(x_1, x_2) = -i\langle T[\psi(x_1)\psi^*(x_2)]\rangle,$$

$$F = -i\langle T[\psi^*(x_1)\psi^*(x_2)]\rangle \exp(-i2\mu t)$$

in the usual form

$$(i\partial/\partial t - H)\,G - i\Delta F = \delta(\mathbf{r}_1 - \mathbf{r}_2),$$

$$(i\partial/\partial t + H^* - 2\mu)\,F + i\Delta^* G = 0, \qquad (1)$$

where $\psi(x)$ and $\psi^+(x)$ are the operators for annihilation and creation of particles, μ is the chemical potential, and Δ is a quantity characterizing the pair correlation. The quantity Δ is found from the equation

$$\Delta = \gamma \int_C F^*(\mathbf{r}, \mathbf{r}, \omega)\frac{d\omega}{2\pi}. \qquad (2)$$

Here $F(\mathbf{r}, \mathbf{r}, \omega)$ is the time Fourier component of the function F, γ is the interaction constant of the particles, while the contour C consists of the real axis and the infinite semicircle in the upper half plane.

The total Hamiltonian of the system of particles has the form

$$H = H^0 + H' = H^0 - M^x\Omega,$$

where H is the Hamiltonian of the nucleus in the rotating system, M^x is the angular momentum along the x axis, coinciding with the axis of rotation, and Ω is the angular velocity.

Treating the term $M^x\Omega$ as a perturbation, it is easy to calculate the diagonal corrections (which are the only ones we are interested in for what follows) in the second order of perturbation theory in the functions G and F. For the case where the functions G and F are expanded in eigenfunctions of the Hamiltonian H^0, these corrections have the form

$$\begin{aligned} G''_{\lambda\lambda} = \sum_{\lambda_1}\{&H'_{\lambda\lambda_1}H'_{\lambda_1\lambda}[G_\lambda G_{\lambda_1}G_\lambda - G_\lambda F_{\lambda_1}F_\lambda - F_\lambda D_{\lambda_1}F_\lambda - F_\lambda F_{\lambda_1}G_\lambda \\ &+ iH'_{\lambda\lambda_1}\Delta'_{\lambda_1\lambda}[G_\lambda G_{\lambda_1}F_\lambda - G_\lambda F_{\lambda_1}G_\lambda - F_\lambda F_{\lambda_1}F_\lambda - F_\lambda D_{\lambda_1}G_\lambda] \\ &+ i\Delta'_{\lambda\lambda_1}H'_{\lambda_1\lambda}[-F_\lambda G_{\lambda_1}G_\lambda + F_\lambda F_{\lambda_1}F_\lambda + G_\lambda D_{\lambda_1}F_\lambda + G_\lambda F_{\lambda_1}G_\lambda \\ &+ \Delta'_{\lambda\lambda_1}\Delta'_{\lambda_1\lambda}[F_\lambda G_{\lambda_1}F_\lambda - F_\lambda F_{\lambda_1}G_\lambda - G_\lambda F_{\lambda_1}F_\lambda - G_\lambda D_{\lambda_1}G_\lambda]\} \\ &+ i\Delta''_{\lambda\lambda}2F_\lambda G_\lambda - 2\mu'' F_\lambda F_\lambda, \end{aligned} \qquad (3)$$

$$\begin{aligned} F''_{\lambda\lambda} = \sum_{\lambda_1}\{&H'_{\lambda\lambda_1}H'_{\lambda_1\lambda}(D_\lambda D_{\lambda_1}F_\lambda + D_\lambda F_{\lambda_1}G_\lambda + F_\lambda G_{\lambda_1}G_\lambda - F_\lambda F_{\lambda_1}F_\lambda \\ &+ iH'_{\lambda\lambda_1}\Delta'_{\lambda_1\lambda}(D_\lambda F_{\lambda_1}F_\lambda + D_\lambda D_{\lambda_1}G_\lambda + F_\lambda G_{\lambda_1}F_\lambda - F_\lambda F_{\lambda_1}G_\lambda) \\ &+ i\Delta'_{\lambda\lambda_1}H'_{\lambda_1\lambda}(F_\lambda D_{\lambda_1}F_\lambda + F_\lambda F_{\lambda_1}G_\lambda + D_\lambda G_{\lambda_1}G_\lambda - D_\lambda F_{\lambda_1}F_\lambda) \\ &- \Delta'_{\lambda\lambda_1}\Delta'_{\lambda_1\lambda}(F_\lambda F_{\lambda_1}F_\lambda + F_\lambda D_{\lambda_1}G_\lambda + D_\lambda G_{\lambda_1}F_\lambda - D_\lambda F_{\lambda_1}G_\lambda)\} \\ &+ 2\mu'' D_\lambda F_\lambda + i\Delta''(F_\lambda F_\lambda - D_\lambda G_\lambda). \end{aligned} \qquad (4)$$

Here G_λ, F_λ, and D_λ are given by the formulas

$$G_\lambda = \frac{(E_\lambda + \varepsilon_\lambda)}{2E_\lambda(\omega - E_\lambda + i\delta)} + \frac{(E_\lambda - \varepsilon_\lambda)}{2E_\lambda(\omega + E_\lambda - i\delta)},$$

$$F_\lambda = -\frac{i\Delta}{2E_\lambda}\left[\frac{1}{\omega - E_\lambda + i\delta} - \frac{1}{\omega + E_\lambda - i\delta}\right],$$

$$D_\lambda = \frac{(E_\lambda - \varepsilon_\lambda)}{2E_\lambda(\omega - E_\lambda + i\delta)} + \frac{(E_\lambda + \varepsilon_\lambda)}{2E_\lambda(\omega + E_\lambda - i\delta)}. \qquad (5)$$

The equation for determining Δ'' has the form

$$\Delta''(\mathbf{r}) = \gamma \sum_{\lambda} F''_{\lambda\lambda}(0)\, \varphi_\lambda(\mathbf{r})\, \varphi^*_\lambda(\mathbf{r}). \tag{6}$$

In the present paper we shall be interested in the quantity Δ'' averaged over the nuclear volume V:

$$\overline{\Delta''} = \frac{1}{V}\int \Delta''(\mathbf{r})\, dV.$$

From formula (6) we then obtain an equation for $\overline{\Delta''}$:

$$\overline{\Delta''} = \gamma \sum_{\lambda} F''_{\lambda}(0). \tag{6'}$$

Using Eqs. (6) and (2) for the unperturbed Δ, we easily find (assuming that $\Delta''(\mathbf{r})$ depends smoothly on $\mathbf{r}$) that

$$\sum_{\lambda} F''_{\lambda}(0) + \overline{\Delta''} \sum_{\lambda} \frac{1}{2E_\lambda} = 0. \tag{7}$$

Using formulas (4) and (5) this equation takes the form

$$\sum_{\lambda\lambda_1} \Big\{ H'_{\lambda\lambda_1} H'_{\lambda_1\lambda} \left[\frac{\Delta(\varepsilon_{\lambda_1} - \varepsilon_\lambda)^2 (\varepsilon_{\lambda_1}\varepsilon_\lambda - \Delta^2)}{4(E_\lambda E_{\lambda_1})^3 (E_\lambda + E_{\lambda_1})} + \frac{\Delta(\Delta^2 + \varepsilon_\lambda \varepsilon_{\lambda_1} - E_\lambda E_{\lambda_1})}{4(E_\lambda E_{\lambda_1})^2 (E_\lambda + E_{\lambda_1})} \right]_1$$

$$+ (H'_{\lambda\lambda_1}\Delta'_{\lambda_1\lambda} - \Delta'_{\lambda\lambda_1} H'_{\lambda_1\lambda}) \left[\frac{(\varepsilon_\lambda - \varepsilon_{\lambda_1})}{4E_\lambda E_{\lambda_1}(E_\lambda + E_{\lambda_1})} \right.$$

$$\left. + \frac{\Delta^2(\varepsilon_{\lambda_1} - \varepsilon_\lambda)(2\Delta^2 + (\varepsilon_\lambda - \varepsilon_{\lambda_1})^2 + 2\varepsilon_\lambda\varepsilon_{\lambda_1} + E_\lambda E_{\lambda_1})}{4(E_\lambda E_{\lambda_1})^3 (E_\lambda + E_{\lambda_1})} \right]_2$$

$$+ \Delta'_{\lambda\lambda_1}\Delta'_{\lambda_1\lambda} \left[\frac{\Delta(\varepsilon_\lambda - \varepsilon_{\lambda_1})^2 (\varepsilon_\lambda \varepsilon_{\lambda_1} - \Delta^2)}{4(E_\lambda E_{\lambda_1})^3 (E_\lambda + E_{\lambda_1})} \right.$$

$$\left. + \frac{\Delta(E_\lambda E_{\lambda_1} + \varepsilon_\lambda \varepsilon_{\lambda_1} + \Delta^2)}{4(E_\lambda E_{\lambda_1})^2 (E_\lambda + E_{\lambda_1})} \right]_3 \Big\}$$

$$+ \mu'' \Delta \sum_{\lambda} \frac{\varepsilon_\lambda}{2E_\lambda^3} - \overline{\Delta''}\Delta^2 \sum_{\lambda} \frac{1}{2E_\lambda^3} = 0. \tag{8}$$

The corrections associated with the change in the chemical potential μ'' can be calculated from the equation

$$\sum_{\lambda} G''_{\lambda\lambda} = 0. \tag{9}$$

Evaluating μ'' from this equation, we can show that the corrections to $\overline{\Delta''}$ resulting from a change in the chemical potential will be $\sim (\Delta/\epsilon_0)^2 \sim A^{-4/3}$ and can be neglected.

The quantities in square brackets which appear in (8) have sharp maxima, as a function of ϵ_λ for fixed $\epsilon_\lambda - \epsilon_{\lambda_1} = d$, of width $\sim \Delta$ at the point $\epsilon_\lambda + \epsilon_{\lambda_1}$. Thus these quantities can be calculated by the quasiclassical method developed by Migdal.[1] One easily sees, by calculating the elementary integrals, that the sums in square brackets can be replaced by the expressions

$$[\ldots]_1 \to -\frac{(1+2x^2)g - 1}{2\Delta(1+x^2)}\delta(\varepsilon_\lambda), \tag{10}$$

$$[\ldots]_2 \to -\frac{x(x^2 g - 1)\delta(\varepsilon_\lambda)}{2\Delta(1+x^2)}, \tag{11}$$

$$[\ldots]_3 \to -\frac{(x^2 g - 1)}{(1+x^2)}\delta(\varepsilon_\lambda), \tag{12}$$

where

$$g(x) = \frac{\ln|x + \sqrt{1+x^2}|}{x\sqrt{1+x^2}}, \quad x = \frac{\varepsilon_\lambda - \varepsilon_{\lambda_1}}{2\Delta}.$$

It is easy to calculate the sum in the last term in (8) by changing to an integral over ϵ_λ:

$$\sum_{\lambda} \frac{1}{2E_\lambda^3} = \frac{\rho_0}{\Delta^2}, \tag{13}$$

where ρ_0 is the level density at the Fermi surface. As a result, Eq. (8) for $\overline{\Delta''}$ takes the form

$$\rho_0 \overline{\Delta''} = -\sum_{\lambda\lambda_1} \Big\{ \frac{(1+2x^2)g - 1}{2\Delta(1+x^2)} H'_{\lambda\lambda_1} H'_{\lambda_1\lambda}$$

$$+ \frac{x^2 g - 1}{2\Delta(1+x^2)} [(H'_{\lambda\lambda_1}\Delta'_{\lambda_1\lambda} - \Delta'_{\lambda\lambda_1} H'_{\lambda_1\lambda})x + \Delta'_{\lambda\lambda_1}\Delta'_{\lambda_1\lambda}] \Big\} \delta(\varepsilon_\lambda). \tag{14}$$

We shall carry out the further calculations for the model of an axially symmetric deformed oscillator.

In this model the operator $\dot{M}^X$ is different from zero only for transitions with $n'_X = n_X \pm 1$, $n'_Z = n_Z \pm 1$. To quasiclassical accuracy all possible matrix elements $\dot{M}^X_{\lambda\lambda_1}$ are equal, and the energies of the transitions are $\epsilon_\lambda - \epsilon_{\lambda_1} = \pm(\omega_Z \pm \omega_Y)$.

In this model, as shown by Migdal,[1]

$$\Delta' = -i\frac{\alpha}{2\Delta}\dot{M}^x \Omega, \tag{15}$$

where

$$\alpha = \frac{g_1 + g_2}{g_1 x_1^2 + g_2 x_2^2}, \quad g_1 = g(x_1), \; g_2 = g(x_2), \; x_1 = \frac{\omega_z - \omega_x}{2\Delta},$$

$$x_2 = \frac{\omega_x + \omega_y}{2\Delta} \approx \frac{\omega_0}{\Delta},$$

while the rigid moment of inertia J_0 is equal to

$$J_0 = \frac{x_1^2 + x_2^2}{x_1^2 x_2^2} \frac{1}{8\Delta^2} \sum_{\lambda\lambda_1} |\dot{M}^x_{\lambda\lambda_1}|^2 \delta(\varepsilon_\lambda). \tag{16}$$

Then calculating the sum (14) by using (15) and (16), we get

$$\frac{\overline{\Delta''}}{\Delta} = -\frac{J_0 I(I+1)}{2\rho_0 \Delta^2 J^2} \left\{ \frac{x_1^2 x_2^2}{(x_1^2 + x_2^2)} \left[\frac{(x_1^2 g_1 - 1)(1 + 2\alpha x_1^2 - \alpha^2 x_1^2)}{x_1^2 (1 + x_1^2)} + \frac{g_1}{x_1^2} \right. \right.$$

$$\left. \left. + \frac{(x_2^2 g_2 - 1)(1 + 2\alpha x_2^2 - \alpha^2 x_2^2)}{x_2^2 (1 + x_2^2)} + \frac{g_2}{x_2^2} \right] \right\} \tag{17}$$

or, abbreviated,

$$\frac{\overline{\Delta''}}{\Delta} = -\frac{J_0 I(I+1)}{2\rho_0 \Delta^2 J^2} L(x_1, x_2). \tag{17a}$$

Formula (17) supplies the answer to our problem. From (17) we see that in order of magnitude $\overline{\Delta''}/\Delta$ is equal to the ratio of the rotational energy $I(I+1)/2J$ to the total pairing energy $-\rho_0\Delta^2/4$. The numerical coefficient in the curly brackets is approximately equal to 0.4 for actual deformed nuclei. Formula (17) enables us to estimate the change in Δ at the point of transition from the superfluid state to the normal state. This change is of the order of 40%. In fact, at the transition point we have the relation

$$-\rho_0\Delta^2/4 + I_c(I_c+1)/2J = I_c(I_c+1)/2J_0. \qquad (18)$$

In our qualitative estimates we neglect the slight difference in Δ for neutrons and protons, and we always write the total density ρ_0. For a more precise computation it would be necessary to write the energy of the pair correlation $-\rho_0\Delta^2/4$ separately for protons and neutrons. However, this produces an insignificant change in the results.

The critical spin for the transition is equal to

$$I_c(I_c+1) = \rho_0\Delta^2 JJ_0/2\,(J_0 - J). \qquad (19)$$

For angular momenta $I < I_C$ the superconducting state will be stable and $J < J_0$, while for $I > I_C$ the normal state of the system is stable, in which $\Delta = 0$ and $J = J_0$.

In first approximation we shall assume that Δ is not changed at the transition point. Then, substituting (19) in formula (17), we get an estimate for the change of Δ at the transition point:

$$\frac{\overline{\Delta_c''}}{\Delta} \approx -\frac{L}{(4J/J_0)(1-J/J_0)}. \qquad (20)$$

Since $J/J_0 \approx 1/2$, $\overline{\Delta_C''}/\Delta \approx 0.4$, i.e., it is only in first approximation that we can regard the value of Δ as being unchanged at the transition point.

Let us compute I_C on this assumption. To quasiclassical accuracy $\rho_0 = 3A/2\epsilon_0$. The Fermi energy of the nucleus is $\epsilon_0 \approx 36$ Mev, while $J/J_0 = 0.5$. The moments of inertia in the region of the rare earths are $J \approx 33$ Mev^{-1}, while in the region of heavy elements $J \approx 72$ Mev^{-1}. Estimating I_C according to formula (19), we find $I_C \approx 11$ for the rare earths, while $I_C \approx 17$ for the heavy elements.

Similar estimates of this effect were first made by Mottelson.[3] These moments agree with the maximum moments observed in experiments on Coulomb excitation.[4]

The observation of rotational states with $I > I_C$ by using electromagnetic transitions from states with $I < I_C$ will be difficult, since we must then excite a state in which $\Delta = 0$ and consequently there must occur a marked readjustment of the internal state of the nucleus. As we have pointed out earlier,[5] in a transition with a marked change in Δ, a retardation factor

$$K = \left[\prod_\lambda (u_\lambda^i u_\lambda^f + v_\lambda^i v_\lambda^f)\right]^2 = \exp\left\{2\sum_\lambda \ln (u_\lambda^i u_\lambda^f + v_\lambda^i v_\lambda^f)\right\} \qquad (21)$$

appears, where $u_\lambda = \frac{1}{2}(1 + \epsilon_\lambda/E_\lambda)$, $v_\lambda = \frac{1}{2}(1 - \epsilon_\lambda/E_\lambda)$, while the superscripts i and f denote the initial and final states, in which the nucleus has different values of Δ. Assuming, for example, that in the final state $\Delta^f = 0$, we obtain, by changing from summation to integration,

$$2\sum_{\substack{\lambda>0\\ \epsilon_\lambda-\epsilon_0>0}} \ln\frac{1}{2}\left(1+\frac{|\,\varepsilon_\lambda\,|}{\sqrt{\Delta^2+\varepsilon_\lambda^2}}\right) = \int_0^\infty \rho_0 \ln\frac{1}{2}\left(1+\frac{\varepsilon}{\sqrt{\varepsilon^2+\Delta^2}}\right)d\varepsilon = -\frac{\rho_0\Delta(\pi-2)}{2}, \qquad (22)$$

$$K = \exp\{-\rho_0\Delta(\pi-2)\}. \qquad (23)$$

Since, when we include the change in Δ for large values of I, $\rho_0\Delta(\pi-2) \sim 5$ for the heavy elements and ~ 4 for the rare earths, $K \sim 10^{-2}$.

We can also estimate the corrections to the rotational spectrum of the system, $\delta E = -BI^2(I+1)^2$, resulting from the change in Δ and the consequent change in the moment of inertia.

As was shown by Migdal,[1] moments of inertia can be described well by the expression $J = Cx_1$, where C = const. Then the change in the rotational energy when Δ is changed will be

$$\delta E \approx -\frac{\hbar^2 I(I+1)}{2J^2}\delta J = \frac{\hbar^2 I(I+1)}{2J}\frac{\delta\Delta}{\Delta}. \qquad (24)$$

Substituting for $\delta\Delta$ in (24) from formula (17), we get

$$\delta E \approx -\frac{J_0 L(x_1, x_2)}{4\rho_0\Delta^2 J^3} I^2(I+1)^2. \qquad (25)$$

Thus we obtain as an estimate for the coefficient B

$$B \approx -J_0 L/4\rho_0\Delta^2 J^3. \qquad (26)$$

The usual nonadiabatic correction to the rotation spectrum, omitting the pair correlation, was calculated previously by us[5] and has the form (for a deformation $\beta \gg A^{-2/3}$):

$$B \sim 1/\rho_0 J_0^2 (\omega_0\beta)^2. \qquad (27)$$

Since $\omega_0\beta \sim \Delta \sim \epsilon_0 A^{-2/3}$, the two corrections have just the same order of magnitude with respect to A. Numerically estimated coefficients B from formula (26) also turn out to be close to the experimentally observed values.

For the rare earths

$$B_{th} \approx 25\times10^{-3} \text{ kev}, \quad B_{exp} \approx 20\times10^{-3} \text{ kev},$$

while for heavy elements

$$B_{th} \approx 6\times10^{-3} \text{ kev}, \quad B_{exp} \approx (3-5)\times10^{-3} \text{ kev}.$$

Thus rotation has a sizable effect on the pairing correlation, and this effect must be taken into account in computing the nonadiabatic corrections proportional to $I^2(I+1)^2$. In the case of the estimate of I_c we can neglect the change in Δ only in first approximation. However, for more precise computations this change must be taken into account.

The author expresses his gratitude to V. M. Galitskii and A. B. Migdal for interesting discussions.

[1] A. Migdal, JETP **37**, 249 (1959), Soviet Phys. JETP **10**, 176 (1960).

[2] Yu. Grin', JETP **39**, 138 (1960), Soviet Phys. JETP **12**, 100 (1961).

[3] B. Mottelson and J. Valatin, Phys. Rev. Letters **5**, 511 (1960).

[4] Stephens, Diamond, and Perlman, Phys. Rev. Letters **3**, 435 (1959).

[5] Yu. Grin', JETP **41**, 222 (1961), Soviet Phys. **14**, 162 (1961).

Translated by M. Hamermesh
83

NUCLEON CORRELATIONS AND PHOTONUCLEAR REACTIONS. II. (γ, p) *AND* (γ, n) *REACTIONS IN THE NONRESONANCE REGION* ($E_\gamma \gtrsim 30$ Mev)

G. M. SHKLYAREVSKII

Physico-Technical Institute, Academy of Sciences, U.S.S.R.

Submitted to JETP editor February 6, 1961

J. Exptl. Theoret. Phys. (U.S.S.R.) **41**, 451-455 (August, 1961)

It is shown that the inclusion of pair correlation of nucleons is absolutely necessary for explaining the cross sections for single nucleon photonuclear reactions [i.e., (γ, p) and (γ, n) reactions] in the energy region beyond the giant resonance.

1. In the present paper we shall consider the question of the effect of pair correlation of nucleons on the cross section for photoreactions with the emission of a single nucleon [i.e., (γ, p) and (γ, n) reactions] in light nuclei, under the condition that the product nucleus is left in the ground state or weakly excited states ($E^* \lesssim 10$ Mev). All the assumptions concerning the properties of correlators which were made by us previously[1] are retained here, including the assumption that the correlators are small.

The wave function of the nucleus Ψ^A can be written as*

$$\Psi^A \approx \Psi^A_{IPM} + \sum_{ij} \{Z^1_{ij}\}^{-1} \hat{q}\chi_{ij} \hat{Q}^1 \Psi^A_{IPM} \qquad (\chi_{ij} \equiv \chi^1_{ij}), \qquad (1)$$

where we include only triplet correlators. A simple estimate shows that if $r_c^0 \leq r_c^1/3$, the contribution of the singlet correlators to the reaction cross section does not exceed 10% even for $E_\gamma \sim 100$ Mev.

2. The basis of the method proposed here is the expansion of the nuclear wave function, written taking account of pair correlation of nucleons, in terms of a complete set of suitably chosen functions of the independent motion. For this purpose it is first necessary to separate in Ψ^A_{IPM} the wave function of the pair of correlating nucleons. Suppose that in the LS-coupling approximation the initial nucleus has the configuration $S^{n_1}[\lambda_1]p^{n_2}[\lambda_2]$ where $n_1 + n_2 = n \equiv A$. Then

$$\Psi^A_{IPM}(L\Lambda, S\Sigma, TM_T)$$

$$= \sqrt{\frac{n_2(n_2-1)}{n(n-1)}} \sum_{\xi'\xi_0} \mathcal{R}^{pp}_{\xi'\xi_0} \{\Psi^{A-2}_{p^{n_2}}(\xi'), \Psi^{p^2}(\xi_0)\}_{LST} + (-)^{n_2-1}$$

$$\times \sqrt{\frac{2n_1n_2}{n(n-1)}} \sum_{\xi'\xi_0} \mathcal{R}^{sp}_{\xi'\xi_0} \{\Psi^{A-2}_{s^{n_1-1}p^{n_2-1}}(\xi'), \Psi^{sp}(\xi_0)\}_{LST} + \ldots. \qquad (2)$$

*The notation is the same as in[1].

Here $\mathcal{R}^{pp}_{\xi'\xi_0}$ and $\mathcal{R}^{sp}_{\xi'\xi_0}$ are fractional parentage coefficients of the type $\langle s^{n_1}p^{n_2-2}, p^2 | \} s^{n_1}p^{n_2}\rangle$ and $\langle s^{n_1-1}p^{n_2-1}sp | \} s^{n_1}p^{n_2}\rangle$ respectively; $\xi' \equiv L'S'T'$ are the quantum numbers of the system of $A-2$ nucleons; $\xi_0 \equiv LST$ are the quantum numbers of the pair which are selected, and $\{\ ,\ \}_{LST}$ denotes the vector coupling of the angular momenta ξ' and ξ_0 in the state LST. In formula (2) we have omitted the term corresponding to the separating out of two s-nucleons, since correlations of such pairs lead to final states of the nucleus $A-1$ with high excitation energy. (These will be states $s^{n_1-1}p^{n_2}$.) We shall not consider such excitations. Furthermore

$$\Psi(\xi_0) \equiv |n_{i0}l_{i0}, n_{j0}l_{j0}; \xi_0\rangle$$

$$= \sum C^{L_0\Lambda_0}_{l_{i0}m_{i0}l_{j0}m_{j0}} |n_{i0}l_{i0}m_{i0}\rangle |n_{j0}l_{j0}m_{j0}\rangle X_{S_0\Sigma_0}\Omega_{T_0\tau}, \qquad (3)$$

where $|n_{i0}l_{i0}m_{i0}\rangle$ are the single particle wave functions from which Ψ^A_{IPM} is constructed, and X and Ω are respectively the spin and isotopic spin functions for the pair of nucleons.

The wave function (3) of the pair is expressed in the coordinates $\mathbf{r}_i$, $\mathbf{r}_j$. We go over to the coordinates $\mathbf{r} = \mathbf{r}_i - \mathbf{r}_j$, $\mathbf{R} = (\mathbf{r}_i + \mathbf{r}_j)/2$. For oscillator functions this transformation is known as the Talmi transformation; the properties of the coefficients of this transformation have been treated in papers by Moshinsky[2] and Arima and Terasawa.[3] We find

$$|n_{i0}l_{i0}, n_{j0}l_{j0}; \xi_0\rangle$$

$$= \sum_{\tilde{n}\tilde{l}\tilde{N}\tilde{L}} \langle n_{i0}l_{i0}, n_{j0}l_{j0}; \xi_0 | \tilde{n}\tilde{l}, \tilde{N}\tilde{L}; \xi_0\rangle |\tilde{n}\tilde{l}, \tilde{N}\tilde{L}; \xi_0\rangle;$$

$$|\tilde{n}\tilde{l}, \tilde{N}\tilde{L}; \xi_0\rangle = \sum C^{L_0\Lambda_0}_{\tilde{l}\tilde{m}\tilde{L}\tilde{\Lambda}} |\tilde{n}\tilde{l}\tilde{m}\rangle |\tilde{N}\tilde{L}\tilde{\Lambda}\rangle X_{S_0\Sigma_0}\Omega_{T_0\tau}. \qquad (4)$$

Here $\tilde{n}\tilde{l}\tilde{m}$ and $\tilde{N}\tilde{L}\tilde{\Lambda}$ are the quantum numbers of the relative motion and the motion of the center of gravity of the pair respectively.

We now apply the operator $\hat{q}\chi_{ij}\hat{Q}^1$ to the function (4) and expand the result in the complete set of functions $|n_i l_i, n_j l_j; \xi_0\rangle$.* We then obtain

$$\hat{q}\chi_{ij}\hat{Q}^1 |n_{i0}l_{i0}, n_{j0}l_{j0}; \xi_0\rangle$$

$$= \sum_{n=1}^{\infty} \sum_{n_i l_i n_j l_j}^{q} c_n \langle n_{i0}l_{i0}, n_{j0}l_{j0}; \xi_0 | 00, \tilde{N}_0\tilde{L}_0; \xi_0\rangle$$

$$\times \langle n0, \tilde{N}_0\tilde{L}_0; \xi_0 | n_i l_i, n_j l_j; \xi_0\rangle | n_i l_j, n_j l_j; \xi_0\rangle \delta_{\xi_0\xi_0'}, \quad (5)$$

where ξ_0' corresponds to $S_0 = 1$, $T_0 = 0$ and the coefficients c_n are given by the expansion

$$\chi_{ij} |000; r\rangle = \sum_{n=0}^{\infty} c_n |n00; r\rangle.$$

Substituting (2) — (5) in formula (1), we get

$$\Psi^A(L\Lambda, S\Sigma, TM_T) = \Psi^A_{IPM}(L\Lambda, S\Sigma, TM_T)$$

$$+ \{Z^1\}^{-1} \sum_{ij} \Big[\sqrt{\frac{n_2(n_2-1)}{n(n-1)}} \sum_{\xi'\xi_0'} \mathcal{R}^{pp}_{\xi'\xi_0'}$$

$$\times \sum C^{L\Lambda}_{L'\Lambda' L_0\Lambda_0} C^{S\Sigma}_{S'\Sigma' 1\Sigma_0} \Psi^{A-2}_{p^{-2}}(\xi')$$

$$\times \sum_{n=1}^{\infty} \sum_{n_i l_i n_j l_j}^{q} c_n d^n_{n_i l_i n_j l_j} |n_i l_i, n_j l_j; \xi_0'\rangle$$

$$+ (-)^{n_2-1} \sqrt{\frac{2n_1n_2}{n(n-1)}} \sum_{\xi'\xi_0'} \mathcal{R}^{sp}_{\xi'\xi_0'} \sum C^{L\Lambda}_{L'\Lambda' L_0\Lambda_0} C^{S\Sigma}_{S'\Sigma' 1\Sigma_0}$$

$$\times \Psi^{A-2}_{s^{-1}p^{-1}}(\xi') \sum_{n=1}^{\infty} \sum_{n_i l_i n_j l_j}^{q} c_n f^n_{n_i l_i n_j l_j} |n_i l_i, n_j l_j; \xi_0'\rangle \Big], \quad (6)$$

where the superscript q on the summation sign indicates that it is necessary to exclude states which are occupied in Ψ^A_{IPM}, and we have introduced the notation

$$d^n_{n_i l_i, n_j l_j} \equiv \langle 01, 01; \xi_0' | 00, \tilde{N}_0\tilde{L}_0; \xi_0'\rangle \langle n0, \tilde{N}_0\tilde{L}_0; \xi_0'' | n_i l_i^3, n_j l_j; \xi_0'\rangle,$$

$$f^n_{n_i l_i, n_j l_j} \equiv \langle 00, 01; \xi_0' | 00, 0\tilde{L}_0; \xi_0'\rangle \langle n0, 0\tilde{L}_0; \xi_0' | n_i l_i, n_j l_j; \xi_0'\rangle.$$

3. We are interested in reactions where the product nucleus is produced in a state with configuration $s^{n_1}[\lambda_1]p^{n_2-1}[\lambda]$. In the approximation of weak correlators which we are using, it is not necessary to take account of the correlation in the final state wave function; it can therefore be written in the form

$$\Psi^{A-1}_{IPM}(L_1\Lambda_1, S_1\Sigma_1, T_1M_{T_1})$$

$$= \sum_{\xi_1'} Q^{s_1p}_{\xi_1} \sum C^{L_1\Lambda_1}_{L_1'\Lambda_1' \bar{l}\bar{m}} C^{S_1\Sigma_1}_{S_1'\Sigma_1' 1/2\bar{\sigma}} C^{T_1M_{T_1}}_{T_1'M_{T_1'} 1/2\bar{\tau}}$$

$$\times \Psi^{A-2}(\xi_1') |\bar{n}\bar{l}\bar{m}\rangle \chi_{1/2\bar{\sigma}} \omega_{1/2\bar{\tau}}. \quad (7)$$

Here $Q^p_{\xi_1'}$ and $(-1)^{n_2-1}Q^s_{\xi_1'}$ are fractional parentage coefficients of type $\langle s^{n_1}p^{n_2-2}, p | \} s^{n_1}p^{n_2-1}\rangle$ and $\langle s^{n_1-1}p^{n_2-1}, s | \} s^{n_1}p^{n_2-1}\rangle$; $\bar{n}\bar{l}\bar{m}\bar{\sigma}\bar{\tau}$ are the quantum numbers of the final state of that nucleon of the correlating pair which remains in the nucleus; $\xi_1' \equiv L_1'S_1'T_1'$ are the quantum numbers of the system of $A-2$ nucleons. In formula (7) one should keep the index p or s depending on whether one is calculating the matrix element with the second or third term of the wave function (6). In the first case $\bar{n} = 0$, $\bar{l} = 1$, and in the second $\bar{n} = \bar{l} = 0$.

The second nucleon of the correlating pair makes a transition to the continuous spectrum. Its wave function is

$$\Psi^{(-)}_{\mathbf{k}} = (4\pi k)^{-1}$$

$$\times \sum i^l \sqrt{4\pi(2l+1)}\, e^{-i\delta_l} |El\rangle Y_{l0}(\cos\theta)\, \chi_{1/2\sigma}\omega_{1/2\tau}, \quad (8)$$

where $\hbar\mathbf{k}$ is the relative momentum in the final state, $|El\rangle$ are the radial wave functions normalized to $\delta(k-k')$. The total wave function of the system in the final state can be taken as a product $\Psi^{A-1}_{IPM}\Psi^{(-)}_{\mathbf{k}}$.

In calculating the total reaction cross section, we can restrict ourselves to the E1 term in the interaction operator H_ζ, i.e., we can set

$$H_\zeta \sim e_1 \sum h_i O_+ + e_2 \sum h_i O_-,$$

$$h_i \sim P \sum_\mu D^1_{\mu P}(\alpha\beta)\, Y_{1\mu}(\theta, \varphi)\, \varkappa r_i,$$

$$P = \pm 1, \quad (9)$$

where e_1 and e_2 are the effective charges, and $O_\pm$ are the projection operators for the proton and neutron respectively. Standard computations give the matrix elements as linear combinations of the quantities

$$M^+_{El0, n_l l_i m_l} \langle \bar{n}\bar{l}\bar{m} | n_j l_j m_j\rangle, \qquad M^-_{\bar{n}\bar{l}\bar{m}, n_j l_j m_j} \langle El0 | n_l l_l m_l\rangle,$$

where we use the notation $M^+ = \langle | e_1 h_i O_+ | \rangle$ and $M^- = \langle | e_2 h_i O_- | \rangle$. Omitting the complicated formulas, we remark that the various terms in the wave function (6) give different types of transitions, which are shown schematically in Fig. 1, and different sets of final states of the product nucleus. Thus, for example, if the state of the initial nucleus is described by the Young pattern [44], the transitions of type α and β give only states [43], while the transitions γ_1 also give states [421] and [331].

*We should point out the following: we are assuming that the wave functions corresponding to bound states of particles in Ψ^A_{IPM} are well approximated by oscillator functions with some value of the parameter $\hbar\omega$; then it is convenient to choose the complete set of functions $|n_i l_i, n_j l_j; \xi_0\rangle$ with this same value of the parameter $\hbar\omega$. Under this condition the further computations are significantly simplified.

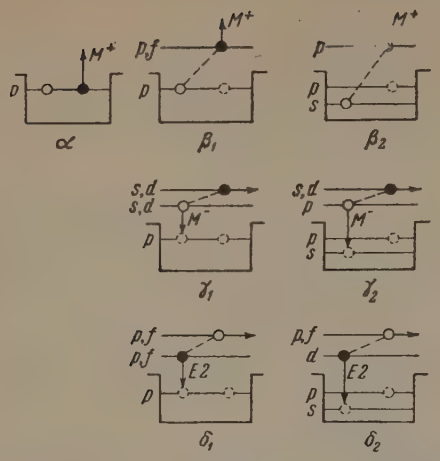

FIG. 1. Classification of terms of the wave function (6) and electromagnetic transitions: o – neutrons, • – protons; the dashed line joins the correlating nucleons. The vertical arrows correspond to the operators M^+ or M^-, and the horizontal lines to the matrix element $< E\,l|n_j l_j >$.

4. Calculations have been made for the $C^{12}(\gamma, p)B^{11}$ reaction in the interval $30 \lesssim E_\gamma \lesssim 70$ Mev. We took for the classification for the levels of B^{11} that given by Inglis[4] for the limiting case of LS coupling. The interaction in the final state was taken into account by using the complex potential:

$$V = V_0 + iW_0 \quad \text{for} \quad R \leqslant R_0,$$
$$V = 0 \quad \text{for} \quad R > R_0;$$

here $R_0 = 1.25\,A^{1/3} \times 10^{-13}$ cm, V_0 and W_0 are chosen to depend on the proton energy in accordance with Fig. 1 of Glassgold's summary.[5] The phase shifts were computed using the approximate formulas of Pargamanik and Ul'yanov.[6] The Coulomb interaction was neglected.

The parameter $\hbar\omega$ of the single-particle oscillator functions was set equal to 16 Mev. The correlator χ_{ij} was taken in the form $\exp\{-\beta r_{ij}^2\}$. We used terms in the expansion up to n = 4 inclusive.

The results of the computation of the total cross section for the $C^{12}(\gamma, p)$ reaction for final states ^2P [43] are given in Fig. 2. Here we also give the experimental data of Penner and Leiss.[7] As we see, for $\beta \approx 0.55 \times 10^{26}$ cm^{-2}, there is satisfactory agreement of computation with experiment. Thus the radius of correlation of triplet pairs of nucleons in nuclei like He^4 and C^{12} is apparently approximately the same. In Fig. 2 we also give the result of computation omitting the correlation. It is easy to see that correlation of the nucleons has an extremely important effect on the reaction cross section, especially at high energies.

With this same value of $\beta = 0.55 \times 10^{26}$ cm^{-2} we calculated the cross section for transitions with excitation of the B^{11} nucleus to the states ^2D [43], ^2F [43], and ^4P [421]. The overall total cross section and the experimental data of Penner and Leiss[7] are given in Fig. 3.

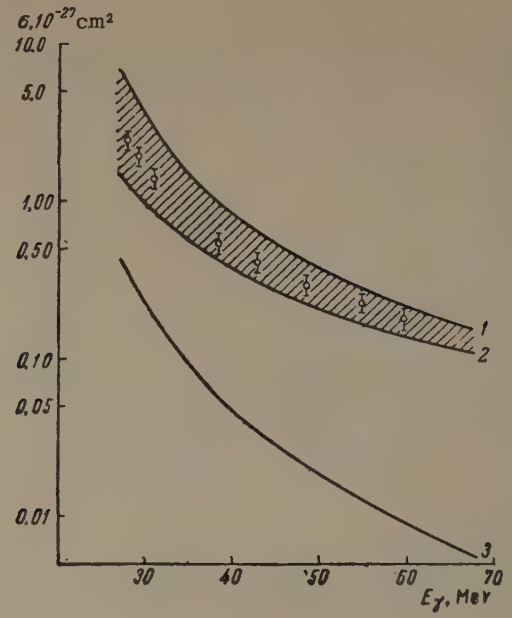

FIG. 2. Total cross section for the $C^{12}(\gamma, p)B^{11}$ reaction with transition to the state ^2P [43]. Curves 1 and 2 correspond to $\beta = 0.5 \times 10^{26}$ and 0.6×10^{26}; curve 3 is calculated omitting correlation. The experimental points are taken from the work of Penner and Leiss[7].

Calculations of the angular distributions of the protons were not made because of the complexity of the formulas. However, there is no doubt that if one includes E2 and higher multipoles, one can obtain the characteristic forward angular distribution of (γ, p) reactions. More interesting is the fact that in a model with correlations it is possible to explain the shift toward the forward direction in the angular distribution of neutrons from

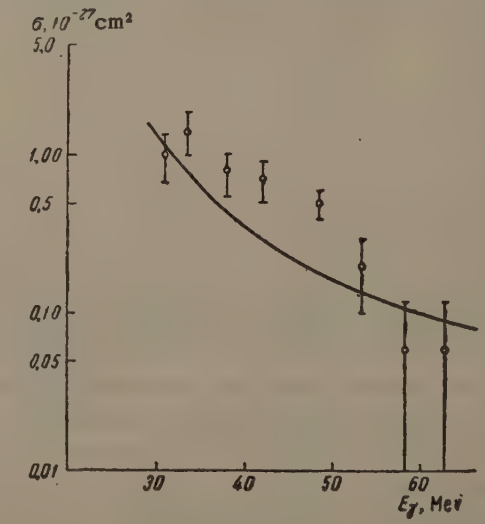

FIG. 3. Overall total cross section for the $C^{12}(\gamma, p)B^{11*}$ reaction with transition to the states ^2D [43], ^2F [43], and ^4P [421]. The curve is calculated for $\beta = 0.55 \times 10^{26}$. The experimental data are those of reference 7. In addition to the statistical errors shown, there is an uncertainty of ± 50%.

the $C^{12}(\gamma, n)$ reaction which has been observed by Kul'chitskii and Presperin[8] and others.

In fact, all the E1 transitions shown in Fig. 1 are also possible for neutrons, and, in the region of p-shell nuclei, for example, they give even partial waves in the continuous spectrum. Furthermore even though the neutron does not possess an "effective charge" with respect to EL transitions for $L \geq 2$, nevertheless the transitions δ_1 and δ_2 shown in Fig. 1 are possible. It is easy to see that for such transitions the neutron is in the continuous spectrum with an odd orbital angular momentum. The interference of these transitions with those previously mentioned leads to an asymmetry in the angular distribution of the neutrons.

5. The results obtained lead one to think that, despite the somewhat arbitrary method of introduction of the correlation, the model used correctly reflects the properties of atomic nuclei which are important for reactions at high energy. This applies especially to the assumption that the correlators are small, which is a self-consistent assumption in the sense that a comparison of the computations with experiment leads to this same conclusion. A check of the whole model is the satisfactory result of the calculation of transitions with excitation of the product nucleus.

Another important question is the choice of the specific form of the correlators. In connection with wellknown properties of photonuclear reactions (the smallness of the momentum of a photon even when its energy is large) it is especially significant that the introduction of correlators leads to large gradients of the two-particle function $\psi^S_{\alpha\beta}(ij)$ at small distances. Thus any function which falls off sufficiently rapidly with increasing r_{ij} gives the same results as the function used in the present paper. This also leads to the result that the choice (within reasonable limits) of the specific form and the parameters of the function Ψ_{IPM} has little effect on the final results.

[1] G. M. Shklyarevskii, JETP **41**, 234 (1961), Soviet Phys. JETP **14**, 170 (1962).

[2] M. Moshinsky, Nucl. Phys. **13**, 104 (1959).

[3] A. Arima and T. Terasawa, Progr. Theor. Phys. **23**, 115 (1960).

[4] D. R. Inglis, Revs. Modern Phys. **25**, 390 (1953).

[5] A. Glassgold, Revs. Modern Phys. **30**, 419 (1958).

[6] L. Pargamanik and V. Ul'yanov, JETP **35**, 258 (1958), Soviet Phys. JETP **8**, 177 (1958).

[7] S. Penner and J. Leiss, Phys. Rev. **114**, 1101 (1959).

[8] L. Kul'chitskii and V. Presperin, JETP **37**, 1524 (1959), Soviet Phys. JETP **10**, 1082 (1960).

Translated by M. Hamermesh
84

LINE SHAPE AND DISPERSION IN THE VICINITY OF AN ABSORPTION BAND, AS AFFECTED BY INDUCED TRANSITIONS

S. G. RAUTIAN and I. I. SOBEL'MAN

P. N. Lebedev Physics Institute, Academy of Sciences, U.S.S.R.

Submitted to JETP editor February 11, 1961

J. Exptl. Theoret. Phys. (U.S.S.R.) **41**, 456-464 (August, 1961)

The problem treated is that of the effect of a strong monochromatic electromagnetic field of frequency close to one of the characteristic frequencies of a system on the spectral composition of the radiation. The dielectric permittivity of the medium in the presence of the field is calculated.

1. The effect of an external electromagnetic field on the macroscopic characteristics of a medium has been treated in many papers. Karplus and Schwinger,[1] and also Basov and Prokhorov,[2] have calculated the absorption coefficient and the dielectric permittivity at the frequency of the applied field as affected by the change of the populations of the levels that is produced by the field (the "saturation effect"). A number of authors[3-6] have treated the change of shape of the spectral lines associated with one of the levels i or k when the system is in a field of frequency ω close to ω_{ik}. In particular it has been shown that at large amplitudes of the field the probability that the system is in the levels i and k oscillates with time. This leads to a splitting of the spectral lines associated with the levels i and k. In these papers, however, there was no study of the shape of the line of the transition $i \rightarrow k$ itself in the presence of a field with $\omega \sim \omega_{ik}$. Precisely this problem is the main one treated in the present paper.

As is well known, the necessity of taking induced transitions into account arises in systems with an inverted population of the levels. There has recently been special interest in systems with transitions that lie in the infrared and optical regions of the spectrum.[7-9] Here conditions arise which differ in a number of important respects from those in the microwave region. Namely, in all methods that have been proposed the inversion of the populations is produced owing to excitation with a broad spectrum (radiationless transitions,[7,9-17] or optical excitation by means of radiation with a broad spectral composition[7,8]). This means that the model of a monochromatic field used in [3-6] to describe the excitation of the system does not correspond to the actual conditions.

The second important difference is that the lifetimes of the levels considered are usually quite different. In the case of gaseous systems, for example, at small densities the lifetimes of the excited states are determined by spontaneous transitions, which have different probabilities for the different levels. In crystals the lifetime of the upper state can be determined by a spontaneous transition and that of the lower state by radiationless transitions or, for the ground state, by the probability of excitation. Moreover, as the result of various elastic processes the line widths may not correspond to the decay probabilities (Doppler effect, Weisskopf broadening mechanism, inhomogeneity of the crystal, etc.).

All of these circumstances must be included in the treatment. At first, however, we shall consider radiative processes, and shall take into account all the other causes of line broadening later on.

2. Let us consider an atom[1)] with nondegenerate levels $E_3 > E_2 > E_1$, E_j, E_m. It is obvious that the production of an inverted population of the levels E_3, E_2 is possible only if the probability $2\gamma_2$ of decay of level 2 is larger (in practice, much larger) than the probability $2\gamma_{32}$ of the spontaneous transition $3 \rightarrow 2$. Therefore our further calculation is made under the condition

$$\gamma_{32} \ll \gamma_2. \qquad (1)$$

There is no restriction on the decay probability $2\gamma_3$ of level 3.

We shall assume that the atom is in a strong electromagnetic field of frequency $\omega_\lambda \sim \omega_{32}$

[1)] For definiteness we shall speak of an atom, although all of the further treatment applies to any quantized system.

$= (E_3 - E_2)/\hbar$ and a weak field with a continuous spectrum, which must be considered for the calculation of the induced emission and absorption at frequencies ω_λ, ω_μ. At the initial time t = 0 let the atom be in level 3 and let there be in the radiation field n_λ, n_μ photons with frequencies ω_λ, ω_μ. As the result of the interaction with the field there can be various transitions accompanied by emission and absorption of photons ω_λ, ω_μ. We shall denote the probability amplitudes of the states of the system "atom + field" by $a(3, n_\lambda, n_\mu)$, $a(2, n_\lambda+1, n_\mu)$, etc. When Eq. (1) holds and n_μ is small we can take into account only the transitions shown in Fig. 1. In fact, under these conditions the probability amplitudes of the states formed through the emission and absorption of photons ω_μ [i.e., $a(3, n_\lambda-1, n_\mu+1)$, $a(2, n_\lambda, n_\mu+1)$, $a(3, n_\lambda+1, n_\mu-1)$, $a(2, n_\lambda+2, n_\mu-1)$] are small in comparison with $a(3, n_\lambda, n_\mu)$ and $a(2, n_\lambda+1, n_\mu)$. Therefore transitions of types

$$2, n_\lambda, n_\mu+1 \to 3, n_\lambda, n_\mu+1, n_{\mu'}-1;$$
$$3, n_\lambda-1, n_\mu+1 \to 2, n_\lambda-1, n_\mu+1, n_{\mu'}+1 \text{ etc.}$$

from these four states can be neglected. We note that the transition

$$2, n_\lambda+1, n_\mu \to 3, n_\lambda+1, n_\mu-1$$

must be taken into account, since for large n_λ[2] the probability of this process is comparable with the probability of induced emission with the transition $3, n_\lambda, n_\mu \to 2, n_\lambda, n_\mu+1$.

Within the framework of this approximation the system of perturbation-theory equations for the probability amplitudes $a(3, n_\lambda, n_\mu)$, $a(2, n_\lambda+1, n_\mu)$, ... can be integrated for arbitrary values of n_λ. The exact solutions of the system, valid for arbitrary t, are of the form

$$a(3, n_\lambda, n_\mu) = A_1 e^{\alpha_1 t} + A_2 e^{\alpha_2 t},$$
$$a(2, n_\lambda+1, n_\mu) = ic^*_{32\lambda}\sqrt{n_\lambda}\, e^{i\Omega_\lambda t}\left\{\frac{A_1}{\alpha_2+\gamma_3}e^{\alpha_1 t} + \frac{A_2}{\alpha_1+\gamma_3}e^{\alpha_2 t}\right\},$$
$$a(3, n_\lambda-1, n_\mu+1) = -\frac{c^*_{32\mu}\sqrt{1+n_\mu}\, c_{32\lambda}\sqrt{n_\lambda}}{\alpha_1-\alpha_2}\{A_1[\varphi_{11}-\varphi_{12}] + A_2[\varphi_{21}-\varphi_{22}]\},$$
$$a(2, n_\lambda, n_\mu+1) = -i\frac{c^*_{32\mu}\sqrt{1+n_\mu}}{\alpha_1-\alpha_2}\{A_1[(\alpha_1+\gamma_3)\varphi_{11} - (\alpha_2+\gamma_3)\varphi_{12}]$$
$$+ A_2[(\alpha_1+\gamma_3)\varphi_{21} - (\alpha_2+\gamma_3)\varphi_{22}]\}e^{i\Omega_\lambda t},$$
$$a(3, n_\lambda+1, n_\mu-1) = -\frac{c_{32\mu}\sqrt{n_\mu}\, c^*_{32\lambda}\sqrt{n_\lambda}}{\alpha_1-\alpha_2}$$
$$\times\left\{A_1\left[\varphi_{11} - \frac{\alpha_1+\gamma_3}{\alpha_2+\gamma_3}\varphi_{21}\right] + A_2\left[\frac{\alpha_2+\gamma_2}{\alpha_1+\gamma_3}\varphi_{12} - \varphi_{22}\right]\right\}e^{i(\Omega_\lambda-\Omega_\mu)t},$$
$$a(2, n_\lambda+2, n_\mu-1) = i\frac{c_{32\mu}\sqrt{n_\mu}\, c^{*2}_{32\lambda}\, n_\lambda}{\alpha_1-\alpha_2}\left\{\frac{A_1}{\alpha_2+\gamma_3}[\varphi_{11}-\varphi_{21}]\right.$$
$$\left. + \frac{A_2}{\alpha_1+\gamma_3}[\varphi_{12}-\varphi_{22}]\right\}e^{i(2\Omega_\lambda-\Omega_\mu)t}. \quad (2)$$

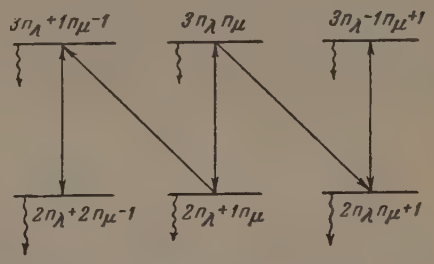

FIG. 1. Scheme of transitions. The wavy arrows denote spontaneous transitions to all lower levels.

Here we have introduced the following notations:

$$\Omega_\lambda = \omega_\lambda - \omega_{32}, \qquad \Omega_\mu = \omega_\mu - \omega_{32};$$

the coefficients $c_{32\lambda}$ and $c_{32\mu}$ are connected with the matrix elements of the interaction Hamiltonian:

$$\hbar c_{32\lambda}\sqrt{n_\lambda} = H_{2n_\lambda;\,3n_\lambda-1}, \qquad \hbar c_{32\mu}\sqrt{n_\mu} = H_{2n_\mu;\,3n_\mu-1} \text{ etc.};$$

A_1 and A_2 are constants of integration, which can be determined from the initial conditions; the functions φ_{11}, φ_{12}, φ_{21}, φ_{22} are given by

$$\varphi_{ij} = \frac{\exp\{[i(\Omega_\mu-\Omega_\lambda)+\alpha_i]t\} - \exp\{\alpha_j t\}}{i(\Omega_\mu-\Omega_\lambda)+\alpha_i-\alpha_j} \quad (i, j = 1, 2); \quad (3)$$

and finally, α_1 and α_2 are the roots of the characteristic equation:

$$\alpha_{1,2} = i\delta_{1,2} - \Gamma_{1,2} = -\frac{i}{2}\Omega_\lambda - \frac{1}{2}(\gamma_2+\gamma_3)$$
$$\mp\sqrt{(i\Omega_\lambda+\gamma_2-\gamma_3)^2/4 - G^2},$$
$$G^2 = \pi c^3\omega_{32}^{-2}\gamma_{32}N_\lambda, \quad (4)$$

where N_λ is the total number of photons of frequency ω_λ in unit volume, and δ_1, δ_2, $-\Gamma_1$, $-\Gamma_2$ are the real and imaginary parts of α_1 and α_2.

The formulas (1) — (4) enable us to obtain all needed characteristics of the radiation in the transition of the atom from an excited state.

3. With $a(3, n_\lambda, n_\mu)$ as an example, let us investigate the special features of the solutions that can arise for various relations between γ_2, γ_3, and N_λ. For simplicity let us consider the case of greatest practical interest, that of exact resonance, that is, the case in which the frequency of the external field coincides with that of the transition ($\Omega_\lambda = 0$). For $N_\lambda \to 0$ we have $\alpha_1 = -\gamma_2$, $\alpha_2 = -\gamma_3$, and Eq. (2) goes over into the well known solution of the problem of the purely spontaneous transition of the atom to the ground state. As N_λ increases the roots α_1, α_2 at first remain real and negative:

[2] If n_λ is sufficiently large, the probability of induced transitions exceeds the probability of spontaneous transitions and the populations of levels 3 and 2 are of the same order of magnitude.

$$-\alpha_{1,2}=\Gamma_{1,2}=\tfrac{1}{2}(\gamma_2+\gamma_3)\pm\sqrt{(\gamma_2-\gamma_3)^2/4-G^2}. \quad (5)$$

Under this condition

$$a(3, n_\lambda, n_\mu)|^2 = |A_1 e^{-\Gamma_1 t}+A_2 e^{-\Gamma_2 t}|^2$$

decreases monotonically with the time. The complexity of the damping curve is physically due to the "mixing" of the states 2 and 3 of the atom owing to the interaction with the field. For small $G^2/(\gamma_2-\gamma_3)^2$ we have

$$\Gamma_1=\gamma_2-G^2/(\gamma_2-\gamma_3), \qquad \Gamma_2=\gamma_3+G^2/(\gamma_2-\gamma_3), \quad (6)$$

that is, we can suppose that the induced transitions act along with the spontaneous transitions in changing the lifetime. With further increase of G^2, however, it turns out that the induced and spontaneous transitions are quite different from this point of view.

For $G^2=(\gamma_2-\gamma_3)^2/4$ we have $\alpha_{1,2}=-(\gamma_2+\gamma_3)/2$; that is, γ_2 and γ_3 have equal effects in determining the transition from the excited state. If $\gamma_2>\gamma_3$, as is so in the majority of cases, the decay occurs more rapidly than for $G=0$. If, on the other hand, $\gamma_2<\gamma_3$, there is a lengthening of the lifetime.

When the external field is still stronger the radical becomes imaginary, and the real part no longer depends on the field:

$$\alpha_{1,2}=-\tfrac{1}{2}(\gamma_2+\gamma_3)\pm i\sqrt{G^2-(\gamma_2-\gamma_3)^2/4}, \quad (7)$$

and the time dependence of $|a(3, n_\lambda, n_\mu)|^2$ takes on the character of damped oscillations:

$$|a(3, n_\lambda, n_\mu)|^2 = A\cos^2[\delta t+\psi]\,e^{-(\gamma_2+\gamma_3)t},$$
$$\delta^2=G^2-(\gamma_2-\gamma_3)^2/4. \quad (8)$$

We note that for $\gamma_2=\gamma_3$, i.e., in the only case considered in the papers cited earlier,[3-6] the oscillatory behavior begins at once at the smallest values of N_λ. At the same time, as will be shown below, a considerable saturation can be attained even in the "aperiodic case" of Eq. (5), if $\gamma_2\gg\gamma_3$.

Since the character of the solutions is determined by the sign of the radicand, the features we have noted will also appear in the other functions of Eq. (2).

4. In many cases the excitation is selective (for example, optical excitation), and we can assume that at the initial time $t=0$ the atom is in the level 3. Then

$$A_1=-(\alpha_2+\gamma_3)/(\alpha_1-\alpha_2),$$
$$A_2=(\alpha_1+\gamma_3)/(\alpha_1-\alpha_2). \quad (9)$$

In the opposite case it is necessary to use also the solution under the initial condition $a(2, n_\lambda+1, n_\mu)=1$ for $t=0$, for which solution

$$A_1=-A_2=-ic_{32\lambda}\sqrt{n_\lambda}/(\alpha_1-\alpha_2). \quad (10)$$

The analysis here will be for the practically most interesting case, that of Eq. (9).

Let us consider the probability W_λ of induced emission of a photon of frequency ω_λ, and the integrated probability[3)] W_μ of spontaneous emission in the transition $3\to 2$. Calculations by the usual rules, by means of Eq. (2), lead to the following expressions:

$$W_\lambda=\frac{\gamma_2+\gamma_3}{\gamma_3}\frac{G^2}{\Omega_\lambda^2+(\gamma_2+\gamma_3)^2+G^2(\gamma_2+\gamma_3)^2/\gamma_2\gamma_3},$$
$$W_\mu=\frac{\gamma_{32}}{\gamma_3}\frac{\Omega_\lambda^2+(\gamma_2+\gamma_3)^2+G^2(\gamma_2+\gamma_3)/\gamma_2}{\Omega_\lambda^2+(\gamma_2+\gamma_3)^2+G^2(\gamma_2+\gamma_3)^2/\gamma_2\gamma_3}. \quad (11)$$

The dependence of W_λ and W_μ on $G^2/\gamma_2\gamma_3$ is shown in Fig. 2. For small N_λ the probability of induced emission increases in proportion to N_λ, and thereafter it reaches a limiting value (saturation effect)

$$W_\lambda=\gamma_2/(\gamma_2+\gamma_3), \quad N_\lambda\gg N_\lambda^0\equiv(\omega_{32}^2/\pi c^3)\,\gamma_2\gamma_3/\gamma_{32}. \quad (12)$$

If $\gamma_2\gg\gamma_3$, then $\gamma_2/(\gamma_2+\gamma_3)\sim 1$, i.e., practically every act of excitation leads to the induced emission of a photon of the frequency of the external field.

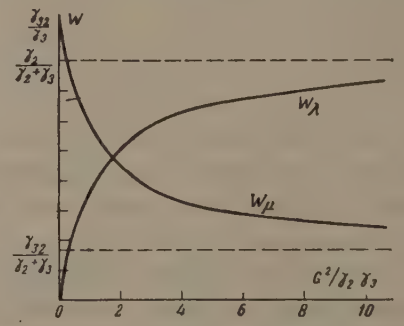

FIG. 2. Integrated probabilities of emission.

In Eq. (12) the quantity N_λ^0 obviously gives the number of photons per cm^3 for which W_λ reaches about half of its limiting value. Besides the well known dependence on the frequency ($\sim\omega_{32}^2$) we must also note that the larger the value of $\gamma_2\gamma_3/\gamma_{32}$ the greater the field intensity required to give saturation. The value of the parameter G^2 that corresponds to N_λ^0 is $\gamma_2\gamma_3$.

The integrated probability of spontaneous emission falls with increasing N_λ, and the larger the value of γ_2/γ_3 the larger is the amount by which this probability decreases (Fig. 2):

$$W_\mu=\gamma_{32}/\gamma_3 \quad (N_\lambda\ll N_\lambda^0),$$
$$W_\mu=\gamma_{32}/(\gamma_2+\gamma_3) \quad (N_\lambda\gg N_\lambda^0). \quad (13)$$

[3)] The term probability is used here in denoting two different quantities: the transition probability per unit time (the Einstein coefficient $2\gamma_{ik}$), and the probability of emission of a photon (W_λ, W_μ), which is identical with the ordinary concept of probability.

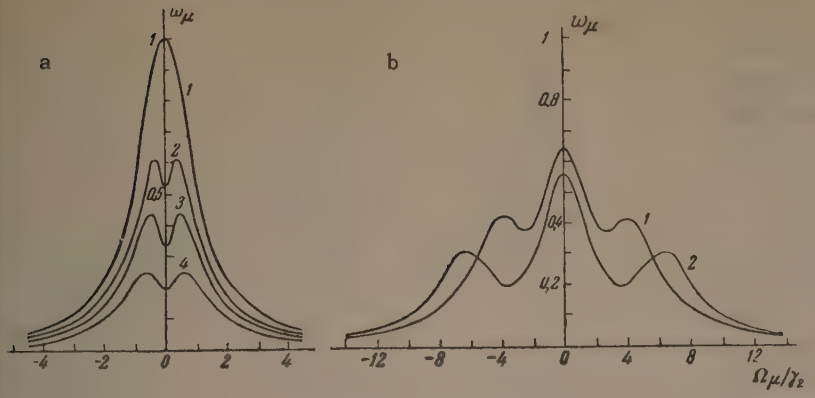

FIG. 3. Spectral density of the probability of spontaneous emission (in units $\gamma_{32}/\pi\gamma_3(\gamma_2+\gamma_3)$. Case a is for $\gamma_3 = \gamma_{32} = 0.1\,\gamma_2$; curve 1 is for G = 0, curve 2 $G^2 = 0.04\,\gamma_2^2$, curve 3 for $G^2 = 0.08\,\gamma_2^2$, and curve 4 for $G^2 = (\gamma_2-\gamma_3)^2/4$. Case b is for $\gamma_3 = \gamma_2$; curve 1 is for $G^2 = 4\,\gamma_2^2$ and curve 2 for $G^2 = 9\,\gamma_2^2$.

Thus as N_λ is increased there is a redistribution of the probabilities of the decay of the excited state between the two channels, one of which is the induced transition 3, n_λ, $n_\mu \to 2$, $n_\lambda+1$, n_μ, and the other the spontaneous transition 3, n_λ, $n_\mu \to 2$, n_λ, $n_\mu+1$. In the generators in the short-wave region that are described at the present time, $\gamma_2 \gg \gamma_3$, and with sufficiently powerful excitation these changes in the integrated probabilities should be observed.

5. As has already been pointed out, the transitions induced by the field cause changes of the spectral composition of the spontaneous radiation and of the shape of the absorption line. For the case in which Eq. (7) holds the cause of the change in the line shape is obvious: the probability of finding the atom in the excited states oscillates with the time, and it is easy to see that this leads to a splitting of the line. In the "aperiodic case" of Eq. (5) there are no oscillations, but the amplitudes of the different states of the system "atom + field" fall off with different damping constants Γ_1 and Γ_2, which also leads to a change of the shapes of the emission and absorption lines.

The spectral density (in the frequency scale) w_μ of the probability of spontaneous emission of a photon can be put in the form

$$w_\mu = \frac{\gamma_{32}\gamma_2}{\pi^2|\alpha_1-\alpha_2|^2}\int_{-\infty}^{\infty}\left|\frac{A_1}{x+\Omega_\mu-i\alpha_1}-\frac{A_2}{x+\Omega_\mu-i\alpha_2}\right|^2 \times\left\{\left|\frac{\alpha_1+\gamma_3}{x+\Omega_\lambda-i\alpha_1}-\frac{\alpha_2+\gamma_3}{x+\Omega_\lambda-i\alpha_2}\right|^2 + \frac{\gamma_3}{\gamma_2}G^2\left|\frac{1}{x+\Omega_\lambda-i\alpha_1}-\frac{1}{x+\Omega_\lambda-i\alpha_2}\right|^2\right\}dx. \quad (14)$$

It can be seen from this that w_μ will contain resonance terms with denominators of the forms

$$(\Omega_\mu-\Omega_\lambda)^2+4\Gamma_1^2,\quad (\Omega_\mu-\Omega_\lambda)^2+4\Gamma_2^2,$$
$$(\Omega_\mu+2\delta_1)^2+(\Gamma_1+\Gamma_2)^2,\quad (\Omega_\mu+2\delta_2)^2+(\Gamma_1+\Gamma_2)^2. \quad (15)$$

The coefficients of these terms, which depend on $\delta_{1,2}$, $\Gamma_{1,2}$, and Ω_λ, can be calculated by integrating Eq. (14). The general formulas for the coefficients are very cumbersome, however, and we shall not give them, but shall confine ourselves to a qualitative analysis of the line shape and numerical illustrations.

Let us first consider the case $\Omega_\lambda = \omega_\lambda - \omega_{32} = 0$, in which the line is symmetrical with respect to $\Omega_\mu = \omega_\mu - \omega_{32} = 0$. If the inducing field is not too large, so that $G^2 < (\gamma_2-\gamma_3)^2/4$, then $\delta_1 = \delta_2 = 0$, and $\Gamma_1 \neq \Gamma_2$ are determined by Eq. (5), from which it can be seen that $\Gamma_1 > \Gamma_2$. Consequently, $2\Gamma_1 > \Gamma_1+\Gamma_2 > 2\Gamma_2$, and of the four terms listed in Eq. (15) the one that decreases most sharply with increase of Ω_μ is the term with Γ_2. It can be shown that the coefficient of this term is negative and increases in absolute value with increasing G. Therefore the general picture of the change of the line shape reduces to the following (Fig. 3, a): for $G^2 \ll (\gamma_2-\gamma_3)^2/4$ there is an ordinary line of the dispersion shape with width $\gamma_2+\gamma_3$ and integrated emission probability γ_{32}/γ_2 (curve 1); as G increases a minimum appears in the center of the line (curves 2 — 4), and remains right up to the value $G^2 = (\gamma_2-\gamma_3)^2/4$.

Further increase of the external field leads to the appearance of imaginary parts $\delta_{1,2}$, and for $\Omega_\lambda = 0$ we have

$$\Gamma_1 = \Gamma_2 = (\gamma_2+\gamma_3)/2,$$
$$\delta_1 = -\delta_2 = \sqrt{G^2-(\gamma_2-\gamma_3)^2/4}. \quad (16)$$

Consequently, the emission line in this case consists of three components with equal widths $\gamma_2+\gamma_3$, separated from each other by distances $2\delta_1$. The splitting of the line becomes detectable, however, only for $\delta_1 \gtrsim \gamma_2+\gamma_3$, i.e., for

$$G^2 \gtrsim \gamma_2\gamma_3\left[\frac{3\gamma_2}{4\gamma_3}+\frac{1}{2}+\frac{3\gamma_3}{4\gamma_2}\right]. \quad (17)$$

Different values of G are required, depending on the value of γ_2/γ_3, but in any case the splitting of the line will be appreciable only when there is comparatively strong saturation, i.e., for $G^2 \gg \gamma_2\gamma_3$. Thus from the very start of the splitting the integrated intensity of the line is practically unchanged, and as G increases its two equal components move farther and farther apart. This can be seen well in curves 1 and 2 of Fig. 3, b. The former case

corresponds to $N_\lambda = 4N_\lambda^0$, the latter to $N_\lambda = 9N_\lambda^0$. We note, finally, that at the indicated values of the field the oscillations of a $(3, n_\lambda, n_\mu)$ are still very strongly damped; in the former case the mean lifetime $1/(\gamma_2+\gamma_3)$ of an atom in level 3 is about $1/3$ of the period of oscillation, and in the latter case it is $2/3$ of the period.

With departure from resonance ($\Omega_\lambda \neq 0$) the line becomes extremely asymmetrical: the maximum of one of the side components approaches ω_{32}, and its magnitude increases sharply. At the same time the other two terms become smaller and the positions of their maxima go farther from ω_{32}.

Let us turn to the transitions induced by a weak field. For the initial conditions (9) the induced emission coefficient k_μ (dimensions cm^{-1}) is given by[4)]

$$k_\mu = \frac{\lambda^2}{4\pi^2}\frac{Q\gamma_{32}\gamma_2}{|\alpha_1-\alpha_2|^4}\int_{-\infty}^{\infty}\left\{\left|\frac{\alpha_2+\gamma_3}{x+\Omega_\mu-i\alpha_1}-\frac{\alpha_1+\gamma_2}{x+\Omega_\mu-i\alpha_2}\right|^2\right.$$
$$\times\left|\frac{\alpha_1+\gamma_3}{x+\Omega_\lambda-i\alpha_1}-\frac{\alpha_2+\gamma_3}{x+\Omega_\lambda-i\alpha_2}\right|^2$$
$$\left.-G^4\left|\frac{1}{x+\Omega_\mu-i\alpha_1}-\frac{1}{x+\Omega_\mu-i\alpha_2}\right|^2\left|\frac{1}{x+\Omega_\lambda-i\alpha_1}\right.\right.$$
$$\left.\left.-\frac{1}{x+\Omega_\lambda-i\alpha_2}\right|^2\right\}dx, \qquad (18)$$

where Q is the number of acts of excitation per unit volume and unit time. For the initial conditions (10) the formula for k_μ differs from Eq. (18) by a change of sign and replacement of γ_2 by γ_3 in the coefficient of the integral.

For $G^2 < (\gamma_2-\gamma_3)^2/4$ the nature of the change of the frequency dependence of k_μ is approximately the same as for the spontaneous emission line (Fig. 4, a). In the case $G^2 > (\gamma_2-\gamma_3)^2/4$, on the other hand, there is a decided difference between k_μ and w_μ: for sufficiently large G, k_μ is negative in a certain range of frequencies, i.e., there is absorption of a weak field of these frequencies (curves 3 and 4 in Fig. 4, b).

An interesting property of k_μ is that for $\omega_\mu \to \omega_\lambda$ it is not equal to the absorption coefficient for a strong field, $k_\lambda = \lambda^2 Q W_\lambda / 4N_\lambda$; k_λ is always larger than k_μ, as can be seen from Fig. 4, where k_μ/k_λ is plotted as the ordinate. We note that the discontinuity of the emission coefficient is of great importance for understanding the operation of quantum generators.

[4)] The formula (18) is for the case of a gas and $k_\mu\lambda \ll 1$. By using the results of Ginzburg[18] one can easily extend the formula to the case of a medium with $\varepsilon \neq 1$ and small $k_\mu\lambda$. This comment also applies to the subsequent formulas for the dielectric permittivity.

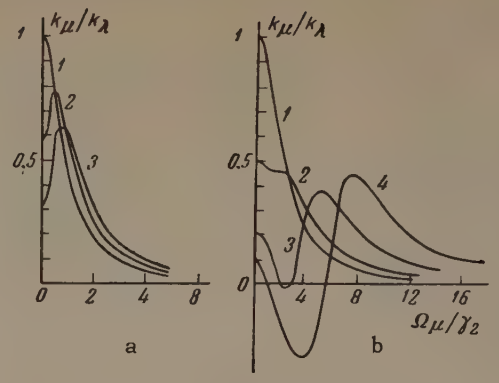

FIG. 4. Emission coefficient k_μ. Case a is for $\gamma_3 = \gamma_{32} = 0.1\,\gamma_2$; curve 1 is for $G^2 = 0$, curve 2 $G^2 = 0.08\,\gamma_2^2$, curve 3 for $G^2 = (\gamma_2-\gamma_3)^2/4$. Case b is for $\gamma_3 = \gamma_2$; curve 1 is for $G^2 = 0.2$, curve 2 for $G^2 = 4\,\gamma_2^2$, and curve 3 for $G^2 = 9\,\gamma_2^2$.

In a number of problems arising in the analysis of devices with negative resistance it is necessary to know the complex dielectric constant $\epsilon = \epsilon' + i\epsilon''$ of the medium. The imaginary part of ϵ is determined from the emission coefficient (for $k_\mu\lambda \ll 1$, cf. footnote [4)])

$$\varepsilon''(\omega_\mu) = -(\lambda/2\pi)\,k_\mu. \qquad (19)$$

For $\omega_\mu \neq \omega_\lambda$ the real part of ϵ can be found by means of the Kramers-Kronig formula:[19]

$$\varepsilon'(\omega_\mu) = 1 - \frac{\lambda}{2\pi^2}\,P\int_{-\infty}^{\infty}\frac{k_\mu(x)}{x-\omega_\mu}\,dx. \qquad (20)$$

Curves of $\epsilon' - 1$ for the cases considered above are shown in Fig. 5, a for $\omega_\mu > \omega_{32}$ [$\epsilon'(\Omega_\mu) - 1 = -\epsilon'(-\Omega_\mu) + 1$]. Like the emission coefficient, $\epsilon' - 1$ decreases in absolute value with increase of G. For $G^2 < (\gamma_2-\gamma_3)^2/4$ (Fig. 5, a) we note the fact that near ω_{32} the dispersion is positive and $\epsilon' - 1$ is zero at three points. For $\gamma_2 = \gamma_3$ and comparatively small G^2 there is negative dispersion (curves 1, 2 of Fig. 5, b). For sufficiently large G^2, when the splitting of the spontaneous emission line is appreciable, $\epsilon' - 1$ goes to zero at five points, and near ω_{32} the dispersion is still negative.

The dielectric permittivity at the frequency ω_λ must be determined separately because of the discontinuity at the point ω_λ. Calculating the energy of the interaction of the atom with the field by means of perturbed wave functions, we arrive at the following formulas:

$$\varepsilon'' = -\frac{\lambda^3}{8\pi^2}\,Q\,\frac{\gamma_2+\gamma_3}{\gamma_3}\,\frac{\gamma_{32}}{\Omega_\lambda^2 + (\gamma_2+\gamma_3)^2 + G^2(\gamma_2+\gamma_3)^2/\gamma_2\gamma_3}, \qquad (21)$$

$$\varepsilon' - 1 = -\varepsilon''\frac{\Omega_\lambda}{\gamma_2+\gamma_3}.$$

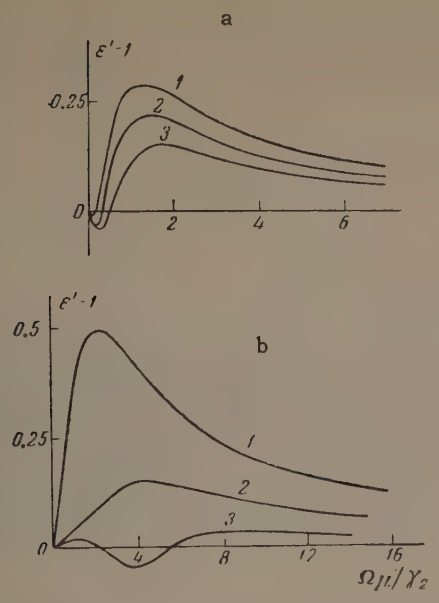

FIG. 5. Real part of the dielectric permittivity [in units $\gamma_{32}\lambda^3 Q/8\pi^2(\gamma_3+\gamma_2)^2$]. Case a is for $\gamma_3=\gamma_{32}=0.1\,\gamma_2$; curve 1 is for $G^2=0.04\,\gamma_2^2$, curve 2 for $G^2=0.08\,\gamma_2^2$, and curve 3 for $G^2=0.14\,\gamma_2^2$. Case b is for $\gamma_3=\gamma_2$; curve 1 for $G^2=0$, curve 2 for $G^2=4\,\gamma_2^2$, and curve 3 for $G^2=9\,\gamma_2^2$.

If $\gamma_2=\gamma_3$, Eq. (21) agrees with the formulas of Basov and Prokhorov[2] if we set $2\gamma_2=1/\tau$, where τ is the lifetime of the excited state.

In conclusion let us consider the extension of the formulas we have given to cases in which the widths of the levels are not due to spontaneous transitions only. Here we must distinguish between elastic and inelastic processes. If all inelastic processes, including also spontaneous transitions, lead to lifetimes τ_2 and τ_3 for levels 2 and 3, then in all of the formulas we must set $2\gamma_2=1/\tau_2$, $2\gamma_3=1/\tau_3$. Elastic processes (Doppler effect, inhomogeneity of the medium) lead to broadening of the lines on account of changes of the frequency ω_{32} of the transition. Since ω_{32} is involved in α_1, α_2, A_1, A_2, we must average the quantity in question over the possible values of ω_{32} with appropriate weights. For example, if the probability distribution for the various values of ω_{32} is of the form

$$\psi(\omega_{32})=\frac{\Delta\nu/\pi}{(\omega_{32}-\bar{\omega}_{32})^2+(\Delta\nu)^2}, \qquad (22)$$

the probability of induced emission is

$$\overline{W}_\lambda=\int_{-\infty}^{\infty}W_\lambda\psi(\omega_{32})\,d\omega_{32}$$

$$=\frac{\Delta\nu+(\gamma_2+\gamma_3)\sqrt{1+G^2/\gamma_2\gamma_3}}{\gamma_3\sqrt{1+G^2/\gamma_2\gamma_3}}\frac{G^2}{\bar{\Omega}_\lambda^2+[\Delta\nu+(\gamma_2+\gamma_3)\sqrt{1+G^2/\gamma_2\gamma_3}\,]^2},$$

$$\bar{\Omega}_\lambda=\omega_\lambda-\bar{\omega}_{32}. \qquad (23)$$

In particular, it can be seen from Eq. (23) that for $\Delta\nu\gg\gamma_2+\gamma_3$ the degree of saturation is determined by the parameter $G(\gamma_2+\gamma_3)/[\Delta\nu(\gamma_2\gamma_3)^{1/2}]$, which involves the characteristics of both the elastic and the inelastic processes.

[1] R. Karplus and J. Schwinger, Phys. Rev. **73**, 1020 (1949).

[2] N. G. Basov and A. M. Prokhorov, Usp. Fiz. Nauk **57**, 485 (1955).

[3] V. M. Kontorovich and A. M. Prokhorov, JETP **33**, 1428 (1957), Soviet Phys. JETP **6**, 1100 (1958).

[4] A. Javan, Phys. Rev. **107**, 1579 (1957).

[5] A. Di Giacomo, Nuovo cimento **14**, 1082 (1959).

[6] P. N. Butcher, in Quantum Electronics, edited by C. H. Townes, New York, 1960, page 189.

[7] F. A. Butaeva and V. A. Fabrikant, Issledovanie po eksperimental'noi i teoreticheskoi fizike (Studies in Experimental and Theoretical Physics), AN SSSR, 1959, page 62.

[8] A. L. Schawlow and C. H. Townes, Phys. Rev. **112**, 1940 (1958).

[9] Basov, Krokhin, and Popov, Usp. Fiz. Nauk **72**, 161 (1960), Soviet Phys. Uspekhi **3**, 702 (1961).

[10] J. H. Sanders, Phys. Rev. Letters **3**, 86 (1959).

[11] A. Javan, Phys. Rev. Letters **3**, 87 (1959).

[12] S. G. Rautian and I. I. Sobel'man, JETP **39**, 217 (1960), Soviet Phys. JETP **12**, 156 (1961).

[13] S. G. Rautian and I. I. Sobel'man, Optika i spektroskopiya (Optics and Spectroscopy) **10**, 134 (1961).

[14] Ablekov, Pesin, and Fabelinskii, JETP **39**, 892 (1960), Soviet Phys. JETP **12**, 618 (1961).

[15] T. H. Maiman, Nature **187**, 493 (1960).

[16] Collins, Nelson, Schawlow, Bond, Garrett, and Kaiser, Phys. Rev. Letters **5**, 303 (1960).

[17] P. P. Sorokin and M. J. Stevenson, Phys. Rev. Letters **5**, 557 (1960).

[18] V. L. Ginzburg, JETP **10**, 589, 601 (1940).

[19] L. D. Landau and E. M. Lifshitz, Élektrodinamika sploshnykh sred (Electrodynamics of Continuous Media), Gostekhizdat, 1957.

Translated by W. H. Furry
85

JUSTIFICATION OF THE RULE FOR SUCCESSIVE FILLING OF (n + l) GROUPS

V. M. KLECHKOVSKII

K. I. Timiryazev Agricultural Academy

Submitted to JETP editor February 16, 1961

J. Exptl. Theoret. Phys. (U.S.S.R.) **41**, 465-466 (August, 1961)

It is demonstrated that the rule previously formulated on the basis of a generalization from the empirical data, according to which the filling of the electronic levels of atoms occurs (with increasing atomic number of the element) in a sequence corresponding to increasing values of the sum of the principal and orbital quantum numbers, can be derived theoretically on the basis of the Thomas-Fermi statistical model. A comparison is made of two independently derived values of the interval within which the set of levels with a given value of the sum $n+l$ is filled.

As has been shown previously,[1] the solution of the question of the first appearance of atomic electrons with given l on the basis of statistical theory[2] leads to expressions which not only numerically, but also in their mathematical form, are similar to the analogous expressions arising from the rule of successive filling of $(n+l)$ groups.[3] In this connection the question arises whether this same rule, which was formulated as a result of the generalization of the empirical data concerning the distribution of electrons in electron shells of neutral, unexcited atoms, can also be derived theoretically on the basis of the statistical model of the atom.

Using the equation of the statistical theory[4] for the Thomas-Fermi model

$$N_k = 2\,(6Z/\pi^2)^{1/3}\,k\int [x\varphi_0(x) - (4/3\pi Z)^{2/3}k^2]^{1/2}\frac{dx}{x}, \qquad (1)$$

and the approximation[5]

$$\varphi_0(x) = (1+ax)^{-2}, \qquad a = (\pi/8)^{2/3} \qquad (2)$$

for the function $\varphi_0(x)$, Tietz[6] obtained the following description of the relation between Z and the number N_k of electrons which occupy a level with a given value of the quantum number k in an atom ($k = \frac{1}{2}, \frac{3}{2}, \frac{5}{2}\ldots$ etc.):

$$N_k = 4\,(6Z)^{1/3}\,k\,[1 - (4/3Z)^{1/3}k]. \qquad (3)$$

It is not difficult to see that, taking $k = l + \frac{1}{2}$, Eq. (3) can be transformed to

$$N_l = 2\,(2l+1)\,(6Z)^{1/3} - 2\,(2l+1)^2. \qquad (4)$$

To the limits of the intervals of Z, within which the statistical model predicts the filling of each individual subgroup with given l, there correspond on the surface $N_l = f(Z)$ the points of intersection of the curve N_l with lines parallel to the Z axis at values of the ordinates N_l which are multiples of $2(2l+1)$. Equation (4) enables one to find the general expression for these points of intersection,

$$N_l = 2\,(2l+1)\,(x-1), \text{ if } Z = \tfrac{1}{6}(2l+x)^3, \qquad (5)$$

where x is the order number of the subgroup with given l, whose filling according to this model should occur within the interval

$$\tfrac{1}{6}(2l+x)^3 \leqslant Z \leqslant \tfrac{1}{6}(2l+x+1)^3. \qquad (6)$$

Since the order number of the subgroup with a given l is equal to $n-l$, and consequently $2l + x = n + l$, Eq. (6) is equivalent to

$$\tfrac{1}{6}(n+l)^3 \leqslant Z \leqslant \tfrac{1}{6}(n+l+1)^3. \qquad (7)$$

From this it follows that in the statistical model of the atom, for which relations (1), (2), and (3) are valid, filling of a set of subgroups with a given value of $n+l$ should occur within the limits between $Z = (n+l)^3/6$ and $Z = (n+l+1)^3/6$. In other words, this proves that in the statistical model the $(n+l)$ group of quantum levels should be filled successively, starting from groups of levels with smaller values of the sum of principal and orbital quantum numbers to those level groups with larger values of this sum, i.e., precisely in the order which is dictated by the rule of successive filling of $(n+l)$ groups.

The limiting values of Z in (7) are very close to the empirical values, but do not coincide with them precisely; this is related to the statistical character of the theory which is the basis of this model. A more precise description of the limits of the interval within which there is a filling of all the levels with given value of $n+l$ in the elec-

tron shells of neutral, unexcited atoms, which follows from the rule of successive filling of $n+l$ groups, has the form

$$\tfrac{1}{6}(n+l)^3+(n+l)\left[\tfrac{1}{2}\cos^2\tfrac{1}{2}\pi(n+l)-\tfrac{1}{6}\right]$$
$$\leqslant Z\leqslant \tfrac{1}{6}(n+l+1)^3$$
$$+(n+l+1)\left[\tfrac{1}{2}\sin^2\tfrac{1}{2}\pi(n+l)-\tfrac{1}{6}\right]. \quad (8)$$

The additional terms appearing in (8) and absent in (7) can here be regarded as corrections to the description (7) obtained on the basis of the statistical model, where one takes account of the integral nature of Z and the condition that Z be kept equal to the total number of electrons in a neutral atom.

[1] V. M. Klechkovskii, Doklady Akad. Nauk S.S.S.R. **92**, 923 (1953); JETP **26**, 760 (1954); JETP **30**, 199 (1956), Soviet Phys. JETP **3**, 125 (1956).

[2] A. Sommerfeld, Wave Mechanics, vol. II, 1933; D. Ivanenko and S. Larin, Doklady Akad. Nauk S.S.S.R. **88**, 45 (1953).

[3] V. M. Klechkovskii, Doklady Akad. Nauk S.S.S.R. **80**, 603 (1951); JETP **23**, 115 (1952).

[4] P. Gombás, Die statistische Theorie des Atoms und ihre Anwendungen, Vienna, Springer, 1949.

[5] T. Tietz, Ann. Physik. **15**, 186 (1955).

[6] T. Tietz, Ann. Physik **5**, 237 (1960).

Translated by M. Hamermesh
86

THEORY OF SCATTERING OF HIGH-ENERGY PHOTONS BY PHOTONS

S. S. SANNIKOV

Physico-Technical Institute, Academy of Sciences, Ukrainian S.S.R.

Submitted to JETP editor February 17, 1961, resubmitted April 24, 1961

J. Exptl. Theoret. Phys. (U.S.S.R.) **41**, 467-477 (August, 1961)

Scattering of high-energy photons by photons is investigated by the dispersion-relation technique. The cross sections for zero and small angle scattering and the total scattering cross section are determined.

THE dispersion relation technique [1-3] is being used more widely for the study of various processes involving the scattering of particles. In the present article, this technique is applied to the investigation of photon-photon scattering in the high energy region.* The dispersion relation technique considerably simplifies the calculation of the scattering amplitude and cross section and enables one to obtain the integral cross section, which has not been calculated until now.

First, from the unitary condition we shall find an expression for the imaginary part of the scattering amplitude. Then, after investigating the symmetry properties and analytic properties of the total amplitude, we shall find the real part with the aid of the dispersion relations. The differential cross section for photon-photon scattering is calculated for scattering angles $\theta \gg m/\omega$ (m is the electron mass, ω is the c.m.s. photon frequency) and for zero angle. In addition to the main terms containing the fourth degree of the logarithm, we shall calculate terms containing the third degree of the logarithm.

1. The dispersion relations can be used to investigate the analytic properties of the photon-photon invariant scattering amplitude A which is related to the matrix element M in the following way:

$$M = \tfrac{1}{4}(2\pi)^4 (\omega_1\omega_2\omega_3\omega_4)^{-1/2} A\delta(k_1 + k_2 - k_3 - k_4),$$

where ω_i and k_i are the frequencies and the wave vectors of the photons.

The amplitude A can be represented in the form

$$A = A_s + A_c + A_a + A_{s,e} + A_{c,e} + A_{a,e},$$

where the partial amplitudes A_s, A_c, and A_a correspond to the scattering processes

$$(s)\quad (k_1, e_1) + (k_2, e_2) \to (k_3, e_3) + (k_4, e_4),$$
$$(c)\quad (k_1, e_1) + (-k_4, e_4) \to (k_3, e_3) + (-k_2, e_2),$$
$$(a)\quad (k_1, e_1) + (-k_3, e_3) \to (-k_2, e_2) + (k_4, e_4).$$

The partial amplitudes $A_{s,e}$, $A_{c,e}$, and $A_{a,e}$ correspond to exchange scattering processes with the photons in the final states (k_3, e_3), (k_4, e_4) and are obtained from A_s, A_c, and A_a by means of the interchange

$$(k_3, e_3) \leftrightarrow (k_4, e_4). \tag{1}$$

The amplitudes A_c and A_a can be obtained from A_s by means of the interchange

$$\begin{aligned} A_s &\to A_c \text{ for } (k_2, e_2) \leftrightarrow (-k_4, e_4), \\ A_s &\to A_a \text{ for } (k_2, e_2) \leftrightarrow (-k_3, e_3), \end{aligned} \tag{2}$$

and it is therefore sufficient to consider only the amplitude A_s.

In order to determine the imaginary part of this amplitude, we shall start from the unitary condition for the scattering matrix S:

$$S^+S = SS^+ = 1.$$

Setting $S = 1 + iT$, we obtain

$$T - T^+ = iT^+T. \tag{3}$$

The amplitude A_s is related to the matrix element of the operator T in the following way:

$$i\langle k_3e_3, k_4e_4 \mid T \mid k_1e_1, k_2e_2\rangle = \tfrac{1}{4}(2\pi)^4 (\omega_1\omega_2\omega_3\omega_4)^{-1/2} A_s\delta(k_1 + k_2 - k_3 - k_4).$$

It follows from (3) that

$$\operatorname{Im}\langle k_3e_3, k_4e_4 \mid T \mid k_1e_1, k_2e_2\rangle = \tfrac{1}{2}\sum_n \langle k_3e_3, k_4e_4 \mid T^+ \mid n\rangle\langle n \mid T \mid k_1e_1, k_2e_2\rangle. \tag{4}$$

If from all the intermediate states in (4) we retain only the states of a free electron-positron

*Photon-photon scattering was first investigated by Euler [4] in the low-energy region and by Akhiezer [5] in the high-energy region. Karplus and Neuman investigated photon-photon scattering with the aid of invariant quantum electrodynamics. [6]

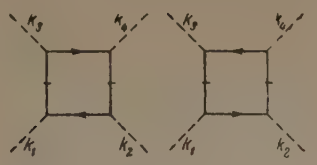

FIG. 1

pair, we obtain the following expression for the imaginary part of the amplitude A_S in the first nonvanishing approximation of perturbation theory (in the order e^4):

$$\operatorname{Im} A_s = \frac{(2\pi)^4}{2} \sum_{\substack{p_1 s_1 \\ -p_2 s_2 \\ (p_1+p_2=k_1+k_2)}} \frac{m^2}{p_1^0 p_2^0} A^+(k_3 e_3, k_4 e_4, p_1 s_1, -p_2 s_2)$$

$$\times A(p_1 s_1, -p_2 s_2, k_1 e_1, k_2 e_2). \qquad (5)$$

In the first-order approximation of perturbation theory (in the order e^2), the expressions occurring in (5) for the amplitudes of the creation and annihilation of a pair in which two free photons take part are well known:

$$A(p_1 s_1, -p_2 s_2, k_1 e_1, k_2 e_2) = ie^2 \bar{u}(p_1) \left[\frac{\hat{e}_1 (i(\hat{p}_1 - \hat{k}_1) - m) \hat{e}_2}{-2p_1 k_1} + \frac{\hat{e}_2 (i(\hat{p}_1 - \hat{k}_2) - m) \hat{e}_1}{-2p_1 k_2} \right] v(-p_2),$$

$$A^+(k_3 e_3, k_4 e_4, p_1 s_1, -p_2 s_2) = -ie^2 \bar{v}(-p_2) \left[\frac{\hat{e}_4 (i(\hat{p}_1 - \hat{k}_3) - m) \hat{e}_3}{-2p_1 k_3} + \frac{\hat{e}_3 (i(\hat{p}_1 - \hat{k}_4) - m) \hat{e}_4}{-2p_1 k_4} \right] u(p_1)$$

(Invariant normalization factors were chosen here, for the spinors u and v.)

It is seen directly from (5) and from similar expressions for Im A_C and Im A_a that the following equalities hold:

$$A_{s,e} = A_s, \qquad A_{c,e} = A_c, \qquad A_{a,e} = A_a.$$

Introducing the notation

$$A_s = \tfrac{1}{2}(A_1 + A_{1,e}), \qquad A_c = \tfrac{1}{2}(A_2 + A_3),$$
$$A_a = \tfrac{1}{2}(A_{2,e} + A_{3,e}),$$

we write the total amplitude A in the form

$$A = A_1 + A_2 + A_3 + A_{1,e} + A_{2,e} + A_{3,e}.$$

In the first nonvanishing approximation of perturbation theory, it follows from (5) that the imaginary part of the amplitude A_1 is depicted by the two Feynman diagrams shown in Fig. 1 (the electron lines with the horizontal stroke denote free particles).

The amplitudes A_i are functions of the scalar products $k_i e_j$ and of two independent scalar invariants associated with the total energy and momentum transfer. We introduce the following notation for these invariants:

$$s = -(k_1 + k_2)^2 = -(k_3 + k_4)^2,$$
$$t = (k_1 - k_3)^2 = (k_2 - k_4)^2,$$
$$u = (k_1 - k_4)^2 = (k_2 - k_3)^2.$$

By the law of conservation, s, t and u satisfy the equality $-s + t + u = 0$. Using the properties of crossing symmetry (1) and (2), we have

$A_1 \to A_2$ for $(k_2, e_2) \leftrightarrow (-k_4, e_4)$, $s \to -u$, $t \to t$;
$A_1 \to A_3$ for $(k_2, e_2) \leftrightarrow (-k_3, e_3)$, $s \to -t$, $u \to u$;
$A_1 \to A_{1,e}$ for $(k_3, e_3) \leftrightarrow (k_4, e_4)$, $s \to s$, $t \to u$;
$A_1 \to A_{2,e}$ for $(k_1, e_4) \to (-k_2, e_2)$,
$(k_3, e_3) \to (k_4, e_4)$, $(k_2, e_2) \to (-k_3, e_3)$;
$s \to -t$, $t \to u$, $u \to -s$;
$A_1 \to A_{3,e}$ for $(k_2, e_2) \to (-k_4, e_4)$,
$(k_4, e_4) \to (k_3, e_3)$, $(k_3, e_3) \to (-k_2, e_2)$,
$s \to -u$, $u \to t$, $t \to -s$. (6)

The kinematics of all scattering process with four external free-photon lines is shown in Fig. 2. The energetically allowed region for the processes described by the amplitudes A_1 and $A_{1,e}$ is the half-plane $s \geq 0$, and the processes described by the amplitudes A_2, $A_{3,e}$ and A_3, $A_{2,e}$ are energetically possible in the half-planes $s - t \leq 0$ and $t \leq 0$, respectively. The imaginary parts of the amplitudes A_i and $A_{i,e}$, as will be seen below, are nonzero in the regions

$$\operatorname{Im} A_1, \operatorname{Im} A_{1,e} \neq 0 \text{ for } s \geqslant 4m^2,$$
$$\operatorname{Im} A_2, \operatorname{Im} A_{3,e} \neq 0 \text{ for } u \leqslant -4m^2,$$
$$\operatorname{Im} A_3, \operatorname{Im} A_{2,e} \neq 0 \text{ for } t \leqslant -4m^2.$$

The physical regions (regions in which the scattering angles are real) are shown crosshatched in Fig. 2.

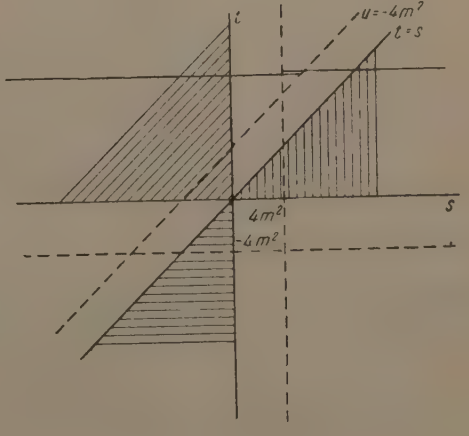

FIG. 2

2. We introduce the notation

$$p_1 - p_2 = v, \quad k_1 + k_2 = k_3 + k_4 = q, \quad k_1 - k_2 = p,$$
$$k_3 - k_4 = p' \quad (-q^2 = p^2 = p'^2 = s, \quad qp = qp' = 0),$$

and represent $\mathrm{Im}\, A_1$ in the form

$$\mathrm{Im}\, A_1 = \frac{e^4}{8\pi^2}\int d^4v\,\delta(qv)\,\delta(v^2 - s + 4m^2)\,\frac{S_1 + S_2}{(vp - s)(vp' - s)}; \tag{7}$$

$$S_1 = \mathrm{Sp}\Big(\frac{i}{2}(\hat q + \hat v) - m\Big)\gamma_\mu\Big(\frac{i}{2}(\hat v - \hat p) - m\Big)\gamma_\nu$$
$$\times\Big(\frac{i}{2}(\hat q - \hat v) + m\Big)\gamma_\rho\Big(\frac{i}{2}(\hat v - \hat p') - m\Big)\gamma_\sigma e_\mu^1 e_\nu^2 e_\sigma^3 e_\rho^4,$$

$$S_2 = \mathrm{Sp}\Big(\frac{i}{2}(\hat q - \hat v) - m\Big)\gamma_\nu\Big(\frac{i}{2}(\hat v - \hat p) + m\Big)\gamma_\mu$$
$$\times\Big(\frac{i}{2}(\hat q + \hat v) + m\Big)\gamma_\sigma\Big(\frac{i}{2}(\hat v - \hat p') + m\Big)\gamma_\rho e_\mu^1 e_\nu^2 e_\sigma^3 e_\rho^4$$
$$(\hat q = \gamma_\mu q_\mu). \tag{8}$$

The calculation of the spurs (8) leads to the following general expression for $\mathrm{Im}\, A_1$:

$$\mathrm{Im}\, A_1 = \frac{e^4}{8\pi^2}\,\mathrm{Im}\, T^{(1)}_{\mu\nu\rho\sigma} e_\mu^1 e_\nu^2 e_\sigma^3 e_\rho^4,$$

where the components of the tensor $T^{(1)}_{\mu\nu\rho\sigma}$ have the form

$$T^{(1)}_{\mu\nu\rho\sigma} = (\delta_{\mu\nu}\delta_{\rho\sigma}A + \delta_{\mu\rho}\delta_{\nu\sigma}B + \delta_{\mu\sigma}\delta_{\nu\rho}C)$$
$$+ (\delta_{\mu\nu}q_\rho q_\sigma A^{(qq)} + \delta_{\mu\rho}q_\nu q_\sigma B^{(qq)} + \delta_{\mu\sigma}q_\nu q_\rho C^{(qq)} + \delta_{\nu\rho}q_\mu q_\sigma D^{(qq)}$$
$$+ \delta_{\nu\sigma}q_\mu q_\rho E^{(qq)} + \delta_{\rho\sigma}q_\mu q_\nu F^{(qq)} + \dots) + (q_\mu q_\nu p_\rho p_\sigma A^{(qqpp)}$$
$$+ q_\mu q_\rho p_\nu p_\sigma B^{(qqpp)} + q_\mu q_\sigma p_\nu p_\rho C^{(qqpp)} + q_\nu q_\rho p_\mu p_\sigma^{(qqpp)}$$
$$+ q_\nu q_\sigma p_\mu p_\rho E^{(qqpp)} + q_\rho q_\sigma p_\mu p_\nu F^{(qqpp)} + \dots)$$
$$+ (p_\mu p_\nu p_\rho p'_\sigma A^{(pppp')} + p_\mu p_\nu p_\sigma p'_\rho B^{(pppp')} + p_\mu p_\rho p_\sigma p'_\nu C^{(pppp')}$$
$$+ p_\nu p_\rho p_\sigma p'_\mu D^{(pppp')} + \dots) + (q_\mu q_\nu q_\rho q_\sigma A^{(qqqq)} + \dots) \tag{9}$$

(To obtain the omitted terms from the written ones, we replace the pairs qq by pp, p′p′, pp′, p′p, qp, pq, qp′, p′q; the tetrads qqpp by qqp′p′, qqpp′, qqp′p, qp′pp, p′qpp, qpp′p′, pqp′p′, ppp′p′, the tetrads pppp′ by p′p′p′p, qppp, qp′p′p′, pqqq, p′qqq, and the tetrads qqqq by pppp, p′p′p′p′.) The scalar coefficients $A, \dots, A^{(qq)}, \dots, A^{(qqpp)}, \dots, A^{(pppp')}, \dots, A^{(qqqq)}, \dots$ are functions of the variables s and t.

The conditions of gauge invariance and invariance with respect to the CPT and CP transformations lead to a number of relations between the scalar coefficients in the expression for the tensor $T^{(1)}_{\mu\nu\rho\sigma}$. These transformations have the form

gauge invariance: $(q+p)_\mu T^{(1)}_{\mu\nu\rho\sigma} = 0,$

CPT transformation: $q \to q,\ p \leftrightarrow p',\ \mu \leftrightarrow \sigma,\ \nu \leftrightarrow \rho,$

CP transformation: $q \to q,\ p \to -p,$

$$p' \to -p'\ \ \mu \leftrightarrow \nu,\ \ \rho \leftrightarrow \sigma.$$

We have obtained the following relations ($\eta = t/s$):

$$A = -s[A^{(qp')} + A^{(p'p')} + (1-2\eta)A^{(pp')}],$$
$$A^{(qq)} = F^{(qq)} = s^{-1}A + A^{(qp')} + (1-2\eta)A^{(qp)},$$
$$B = -s[B^{(qp)} + B^{(pp)} + (1-2\eta)B^{(p'p)}],$$
$$B^{(qq)} = E^{(qq)} = s^{-1}B + B^{(qp')} + (1-2\eta)B^{(qp)},$$
$$C = -s[C^{(qp)} + C^{(pp)} + (1-2\eta)C^{(p'p)}],$$
$$C^{(qq)} = D^{(qq)} = s^{-1}C - C^{(qp')} - (1-2\eta)C^{(qp)},$$
$$A^{(pp)} = F^{(p'p')} = -(1-2\eta)^{-1}(A^{(qp)} + A^{(pp')}),$$
$$B^{(pp)} = E^{(pp)} = B^{(p'p')} = E^{(p'p')} = -(1-2\eta)^{-1}(B^{(qp')} + B^{(pp')}),$$
$$C^{(pp)} = D^{(pp)} = C^{(p'p')} = D^{(p'p')} = -(1-2\eta)^{-1}(C^{(qp')} + C^{(pp')}),$$
$$A^{(p'p)} = F^{(p)p'} = A^{(pp')} = F^{(p'p)} = A^{(qp)} + B^{(qp)} - C^{(qp)} - B^{(qp')}$$
$$- sA^{(p'qqq)} + sB^{(qp'pp)} + s(1-2\eta)C^{(qpp'p')},$$
$$B^{(pp')} = E^{(pp')} = B^{(qp')} - C^{(qp')} + sA^{(qpp'p')} - sA^{(pqqq)}$$
$$+ s(1-2\eta)C^{(qp'pp)},$$
$$C^{(pp')} = D^{(pp')} = -[B^{(qp')} - C^{(qp')} + sA^{(qpp'p')} - sA^{(pqqq)}$$
$$+ s(1-2\eta)B^{(qp'pp)}],$$
$$B^{(p'p)} = E^{(p'p)},\ C^{(p'p)} = D^{(p'p)},\ A^{(qp)} = F^{(p'q)} = -A^{(pq)}$$
$$= -F^{(qp')},$$
$$B^{(qp)} = E^{(p'q)} = -E^{(qp)} = -B^{(p'q)},\ C^{(qp)} = C^{(p'q)}$$
$$= -D^{(qp)} = -D^{(p'q)},$$
$$A^{(qp')} = F^{(pq)} = -A^{(p'q)} = -F^{(qp)},\ B^{(qp')} = E^{(pq)}$$
$$= -E^{(qp')} = -B^{(pq)},$$
$$C^{(qp')} = C^{(pq)} = -D^{(qp')} = -D^{(pq)},$$
$$A^{(qqpp)} = s^{-1}(B^{(qp)} + C^{(qp)} + A^{(qp')} + A^{(pp)}) - A^{(qppp)}$$
$$- (1-2\eta)A^{(qp'pp)},$$
$$B^{(qqpp)} = s^{-1}(A^{(qp)} + B^{(qp')} + C^{(qp')} + B^{(pp)}) - A^{(qp'p'p')}$$
$$- (1-2\eta)B^{(qpp'p')},$$
$$C^{(qqpp)} = -s^{-1}(A^{(qp)} + B^{(qp')} + C^{(qp')} - C^{(pp)}) + A^{(qp'p'p')}$$
$$+ (1-2\eta)C^{(qpp'p')},$$
$$A^{(qqpp')} = s^{-1}(A^{(qp)} + B^{(qp)} - C^{(qp)}) - A^{(p'qqq)},$$
$$B^{(qqpp')} = s^{-1}(A^{(qp')} + B^{(qp')} - C^{(qp')}) - A^{(pqqq)},$$
$$C^{(qqpp')} = -s^{-1}(A^{(qp')} + B^{(qp')} - C^{(qp')}) + A^{(pqqq)},$$
$$A^{(qqp'p')} = s^{-1}A^{(p'p')} - A^{(qpp'p')} - (1-2\eta)A^{(qp'p'p')},$$
$$B^{(qqp'p)} = s^{-1}(B^{(p'p)} + C^{(qp)}) - C^{(qpp'p')} - (1-2\eta)A^{(qp'pp)},$$
$$C^{(qqp'p)} = s^{-1}(C^{(p'p)} - B^{(qp)}) + B^{(qpp'p')} + (1-2\eta)A^{(qp'pp)},$$
$$A^{(ppp'p')} = -s^{-1}A^{(p'p')} + A^{(qpp'p')} - (1-2\eta)A^{(p'p'p'p)},$$
$$B^{(ppp'p')} = E^{(ppp'p')} = -s^{-1}B^{(pp)} + B^{(qpp'p')}$$
$$- (1-2\eta)A^{(p'p'p'p)},$$
$$C^{(ppp'p')} = D^{(ppp'p')} = -s^{-1}C^{(pp)} + C^{(qpp'p')}$$
$$- (1-2\eta)A^{(p'p'p'p)},$$
$$F^{(ppp'p')} = -(1-2\eta)^{-1}[s^{-1}(B^{(p'p)} + C^{(p'p)})$$
$$- A^{(qp'pp)} + A^{(p'p'p'p)}],$$
$$A^{(qqqq)} = s^{-1}(A^{(qq)} + B^{(qq)} + C^{(qq)}) + A^{(pqqq)}$$
$$+ (1-2\eta)A^{(p'qqq)},$$

$$A^{(pppp)} = -s^{-1}(A^{(pp)} + B^{(pp)} + C^{(pp)}) + A^{(qppp)} - (1-2\eta)A^{(p'p'p'p)},$$

$$A^{(p'p'p'p')} = -(1-2\eta)^{-1}[s^{-1}(A^{(p'p')} + B^{(pp)} + C^{(pp)}) + A^{(pppp')} - A^{(qp'p'p')}],$$

$$A^{(pppp')} = D^{(p'p'p'p)} = B^{(pppp')} = C^{(p'p'p'p)},$$

$$A^{(p'p'p'p)} = B^{(p'p'p'p)} = C^{(pppp')} = D^{(pppp')}$$

$$A^{(pqqq)} = D^{(p'qqq)} = -B^{(pqqq)} = -C^{(p'qqq)},$$

$$A^{(p'qqq)} = D^{(pqqq)} = -B^{(p'qqq)} = -C^{(pqqq)}. \quad (10)$$

(The relations between coefficients with the tetrads qqpp, qqp'p', qqpp', qqp'p and qp'pp, p'qpp, qpp'p', pqp'p' are the same as between the coefficients with the pairs pp, p'p', pp', p'p and qp, pq, qp', p'q, and the relations between the coefficients with qppp and qp'p'p' are the same as those between the coefficients with pqqq and and p'qqq.) Hereafter, we shall take as the independent coefficients the functions

$A^{(qp)}$, $B^{(qp)}$, $C^{(qp)}$, $A^{(qp')}$, $B^{(qp')}$, $C^{(qp')}$, $A^{(p'p')}$, $B^{(p'p)}$, $C^{(p'p)}$, $sA^{(pqqq)}$, $sA^{(p'qqq)}$, $sA^{(qppp)}$, $sA^{(qp'p'p')}$, $sA^{(qp'pp)}$, $sB^{(qp'pp)}$, $sC^{(qp'pp)}$, $sA^{(qpp'p')}$, $sB^{(qpp'p')}$, $sC^{(qpp'p')}$, $sA^{(pppp')}$, $sA^{(p'p'p'p)}$.

We give explicit expressions for the imaginary parts of the independent functions $A^{(qp)}$, $B^{(qp)}$, ... obtained in the calculation of the spurs (8) (in the approximation $s, t \gg 4m^2$):

$$\operatorname{Im} A^{(qp)} = \operatorname{Im} B^{(qp)} = \operatorname{Im} C^{(qp)} = s(a_2/2 - a_3) = st(tF_2 + F_1)/2(s-t)^2 + F_0/4(s-t),$$

$$\operatorname{Im} A^{(qp')} = \operatorname{Im} B^{(qp')} = \operatorname{Im} C^{(qp')} = s(a_2/2 - a_3) + (a_0' - a_1')/2 = st(tF_2 + F_1)/2(s-t)^2 + (1/4(s-t) - 1/2s)F_0,$$

$$\operatorname{Im} A^{(p'p')} = 2s(b_4 - a_3) + s(b_2 - a_1) + (b_2' - a_1') = s^2(5s - 9t)(tF_2 + F_1)/6(s-t)^3 + (-1/4t + 1/4(s-t) - t/3(s-t)^2 + 1/2s)F_0,$$

$$\operatorname{Im} B^{(p'p)} = 2sc_4 - (s-t)c_2 + sa_1 + s(a_2 - a_0)/2 = -s(s^2 - 8st + 3t^2)(tF_2 + F_1)/6(s-t)^3 - (1/4t + 1/3(s-t) + t/3(s-t)^2)F_0,$$

$$\operatorname{Im} C^{(p'p)} = 2sc_4 - tc_2 - sa_1 + s(a_0 - a_2)/2 = -s(2s^2 + 5st - 3t^2)(tF_2 + F_1)/6(s-t)^3 - (7/12(s-t) + t/3(s-t)^2)F_0,$$

$$\operatorname{Im} sA^{(pqqq)} = \operatorname{Im} sA^{(p'qqq)} = s(a_3 - a_2) = s(s-2t)(tF_2 + F_1)/2(s-t)^2 - F_0/4(s-t),$$

$$\operatorname{Im} sA^{(qppp)} = \operatorname{Im} sA^{(qp'p'p')} = s(b_3 - b_2) = s^3(tF_2 + F_1)/2(s-t)^3 + (-1/8t + 3/8(s-t) + t/4(s-t)^2)F_0,$$

$$\operatorname{Im} sA^{(qp'pp)} = \operatorname{Im} sA^{(qpp'p')} = s(c_3 - c_2) = s^2t(tF_2 + F_1)/2(s-t)^3 + (-1/8t + 1/8(s-t) + t/4(s-t)^2))F_0,$$

$$\operatorname{Im} sB^{(qp'pp)} = \operatorname{Im} sC^{(qp'pp)} = \operatorname{Im} sB^{(qpp'p')} = \operatorname{Im} sC^{(qpp'p')} = sc_3 + s(a_1 - b_2 - c_2)/2 = s^2t(tF_2 + F_1)/2(s-t)^3 + (1/8t + 1/8(s-t) + t/4(s-t)^2)F_0,$$

$$\operatorname{Im} sA^{(pppp')} = 2s(e_4 - c_3) - s(b_3 - b_2) = -\frac{s^3(s-3t)}{2(s-t)^4}(tF_2 + F_1) + (1/24t - 5/24(s-t) + t/2(s-t)^2 + t^2/2(s-t)^3)F_0,$$

$$\operatorname{Im} sA^{(p'p'p'p)} = s(2e_4 - c_3) = \frac{s^3(s+t)}{2(s-t)^4}(tF_2 + F_1) + (1/24t + 13/24(s-t) + t/(s-t)^2 + t^2/2(s-t)^3)F_0, \quad (11)$$

where a_i, b_i, ..., F_i are given by formulas (A.1) and (A.2).

3. Singularities of the total scattering amplitude are represented in Fig. 2 as functions of two independent complex variables. In the real plane (s, t), the total amplitude breaks off at $2\operatorname{Im}(A_1 + A_{1,e})$ in the half-plane $s \geq 4m^2$, at $2\operatorname{Im}(A_2 + A_{3,e})$ in the half-plane $u \leq -4m^2$, and at $2\operatorname{Im}(A_3 + A_{2,e})$ in the half-plane $t \leq -4m^2$. The cuts in the complex plane s (for a given t) run from $4m^2$ to ∞ and from $-4m^2 + t$ to $-\infty$.

The analytic properties of the total scattering amplitude with respect to s are expressed by the dispersion relation (without subtraction)

$$A^{(i)}(s,t) = \frac{1}{\pi}\int_{4m^2}^{\infty}\frac{\operatorname{Im}A_1^{(i)}(s',t)}{s'-s}ds' - \frac{1}{\pi}\int_{-\infty}^{-4m^2+t}\frac{\operatorname{Im}A_2^{(i)}(s',t)}{s'-s}ds' + \frac{1}{\pi}\int_{4m^2}^{\infty}\frac{\operatorname{Im}A_{1,e}^{(i)}(s',t_1)}{s'-s}ds' - \frac{1}{\pi}\int_{-\infty}^{-4m^2+t}\frac{\operatorname{Im}A_{3,e}^{(i)}(s',t_1)}{s'-s}ds', \quad (12)$$

where $t_1 = s' - u$, or by the relation

$$A^{(i)} = \frac{1}{\pi}\int_{4m^2}^{\infty}\frac{\operatorname{Im}A_1^{(i)}(s',t)}{s'-s}ds' + \frac{1}{\pi}\int_{4m^2}^{\infty}\frac{\operatorname{Im}A_1^{(i_e)}(s',u)}{s'-s}ds' + \frac{1}{\pi}\int_{4m^2}^{\infty}\frac{\operatorname{Im}A_1^{(i_c)}(u',t)}{u'+u}du' + \frac{1}{\pi}\int_{4m^2}^{\infty}\frac{\operatorname{Im}A_1^{(i_a)}(u',-s)}{u'+u}du'. \quad (12')$$

In Fig. 2 the contour of integration lies in the upper half-plane ($t \geq 0$) and, for $t > 4m^2$, partially enters the nonphysical region. Hence, no contribution comes from the contour of integration of the quantities $\operatorname{Im} A_3$ and $\operatorname{Im} A_{2,e}$. In (12) we understand by $\operatorname{Im} A_1^{(i)}$ the imaginary part of any of the independent scalar functions $A^{(qp)}$ and $B^{(qp)}$, and we understand by $\operatorname{Im} A_2^{(i)}$, $\operatorname{Im} A_{1,e}^{(i)}$, $\operatorname{Im} A_{3,e}^{(i)}$ the imaginary parts of the same independent functions in the expansion (9) for A_2, $A_{1,e}$, $A_{3,e}$. In (12') all the functions under the integral sign are expressed in terms of independent coeffi-

cients of the expansion (9) for A_1 [which is possible owing to (6)].

4. Inserting in (12′) the expressions for the imaginary parts of the functions $A^{(qp)}$, $B^{(qp)}$, . . . (11), we find the expressions for the real parts of these functions. We note that for those terms in (11) which do not decrease (they remain constant) as $s \to \infty$, the subtraction should be carried out at the point $s = t$.

Using (A.3), we obtain, for $s, t \gg 4m^2$, the following expression for the real parts:

$$\mathrm{Re}\,A^{(qp)} = \frac{t}{4(s-t)^2}\ln^2\frac{t}{s} + \frac{1}{2(s-t)}\ln\frac{t}{s},$$

$$\mathrm{Re}\,A^{(qp')} = \frac{t}{4(s-t)^2}\ln^2\frac{t}{s} - \frac{s-2t}{2s(s-t)}\ln\frac{t}{s},$$

$$\mathrm{Re}\,A^{(p'p')} = \frac{s}{12}\frac{5s-9t}{(s-t)^3}\ln^2\frac{t}{s} - \frac{3s^3-15s^2t+22st^2-6t^3}{6st(s-t)^2}\ln\frac{t}{s} - \frac{2}{3(s-t)},$$

$$\mathrm{Re}\,B^{(p'p)} = -\frac{1}{12}\frac{s^2-8st+3t^2}{(s-t)^3}\ln^2\frac{t}{s} - \frac{3s^2-10st+3t^2}{6t(s-t)^2}\ln\frac{t}{s} + \frac{2}{3(s-t)},$$

$$\mathrm{Re}\,C^{(p'p)} = -\frac{1}{12}\frac{2s^2+5st-3t^2}{(s-t)^3}\ln^2\frac{t}{s} - \frac{7s-3t}{6(s-t)^2}\ln\frac{t}{s} - \frac{2}{3(s-t)},$$

$$\mathrm{Re}\,sA^{(pqqq)} = \frac{s-2t}{4(s-t)^2}\ln^2\frac{t}{s} - \frac{1}{2(s-t)}\ln\frac{t}{s},$$

$$\mathrm{Re}\,sA^{(qppp)} = \frac{s^2}{4(s-t)^3}\ln^2\frac{t}{s} - \frac{s^2-5st+2t^2}{4t(s-t)^2}\ln\frac{t}{s} + \frac{1}{2(s-t)},$$

$$\mathrm{Re}\,sA^{(qp'pp)} = \frac{st}{4(s-t)^3}\ln^2\frac{t}{s} - \frac{s(s-3t)}{4t(s-t)^2}\ln\frac{t}{s} + \frac{1}{2(s-t)},$$

$$\mathrm{Re}\,sB^{(qp'pp)} = \frac{st}{4(s-t)^3}\ln^2\frac{t}{s} + \frac{s^2-st+2t^2}{4t(s-t)^2}\ln\frac{t}{s} + \frac{1}{2(s-t)},$$

$$\mathrm{Re}\,sA^{(pppp')} = -\frac{s^2}{4}\frac{s-3t}{(s-t)^4}\ln^2\frac{t}{s} + \frac{s^3-8s^2t+25st^2-6t^3}{12t(s-t)^3}\ln\frac{t}{s} + \frac{s+t}{2(s-t)^2},$$

$$\mathrm{Re}\,sA^{(p'p'p'p)} = \frac{s^2}{4}\frac{s+t}{(s-t)^4}\ln^2\frac{t}{s} + \frac{s(s^2+10st+t^2)}{12t(s-t)^3}\ln\frac{t}{s} + \frac{3s-t}{2(s-t)^2}. \qquad (13)$$

We now write the general expression for the scattering amplitude in the center-of-mass system:

$$A = 4\alpha^2\{(e_1e_2)(e_3e_4)\,a + (e_1e_4)(e_2e_3)\,b + (e_1e_3)(e_2e_4)\,c + s^{-1}[(e_1e_2)(pe_3)(pe_4) + (e_3e_4)(p'e_1)(p'e_2)]\,d + s^{-1}[(e_1e_4)(p'e_2)(pe_3) + (e_2e_3)(p'e_1)(pe_4)]\,e + s^{-1}[(e_1e_3)(p'e_2)(pe_4) + (e_2e_4)(p'e_1)(pe_3)]\,f + s^{-2}(p'e_1)(p'e_2)(pe_3)(pe_4)\,g\}, \qquad (14)$$

where α is the fine-structure constant and

$$a = A + A_e + B_c + B_a, \quad b = B + C_e + A_c + C_a,$$

$$c = C + B_e + C_c + A_a,$$

$$d = s[A^{(pp)} + A_e^{(pp)} + \tfrac{1}{4}(B_c^{(qq)} + 2B_c^{(pp)} + B_c^{(pp')} + B_c^{(p'p)} + C_a^{(qq)} + 2C_a^{(pp)} + C_a^{(pp')} + C_a^{(p'p)} + 2C_a^{(qp)} + 2C_a^{(qp')})],$$

$$e = s[B^{(p'p)} - C_e^{(p'p)} + \tfrac{1}{4}(A_c^{(qq)} + A_c^{(pp)} + A_c^{(p'p')} + 2A_c^{(pp')} + A_a^{(qq)} + A_a^{(pp)} + A_a^{(p'p')} + 2A_a^{(pp')})],$$

$$f = s[C^{(p'p)} - B_e^{(p'p)} + \tfrac{1}{4}(C_c^{(qq)} + 2C_c^{(pp)} + C_c^{(pp')} + C_c^{(p'p)} + 2C_c^{(qp)} + 2C_c^{(qp')} + B_a^{(qq)} + 2B_a^{(pp)} + B_a^{(pp')} + B_a^{(p'p)})],$$

$$g = s^2[F^{(ppp'p')} + F_e^{(ppp'p')} + \tfrac{1}{16}(2B_c^{(qqpp)} + 2C_c^{(qqpp)} - A_c^{(ppp'p')} + 2B_c^{(ppp'p')} - 2C_c^{(ppp'p')} - F_c^{(ppp'p')} + 2A_c^{(qppp)} - 2A_c^{(qp'p'p')} + 2A_c^{(pqqq)} - 2A_c^{(p'qqq)} + A_c^{(qqqq)} + A_c^{(pppp)} + A^{(p'p'p'p)} + 4C_a^{(qqpp)} - A_a^{(ppp'p')} - 2B_a^{(ppp'p')} + 2C_a^{(ppp'p')} - F_a^{(ppp'p')} - 2A_a^{(qppp)} - 2A_a^{(qp'p'p')} - 2A_a^{(pqqq)} - 2A_a^{(p'qqq)} + A_a^{(qqqq)} + A_a^{(pppp)} + A_a^{(p'p'p'p')})]. \qquad (15)$$

It follows from (6) that the functions with the indices e, c, and a can be obtained from the corresponding functions without the indices by means of the substitutions $s \to s$, $t \to u$; $s \to -u$, $t \to t$; and $s \to -u$, $t \to -s$.

5. The differential cross section for photon-photon scattering is related to the scattering amplitude A by the expression

$$d\sigma = (16\pi)^{-2}\omega^{-2}\,|A|^2 do.$$

Inserting expression (14) in place of A and averaging over the polarizations of the initial photons and summing over the polarizations of the final photons, we obtain

$$d\sigma = (\alpha^4/2^6\pi^2)\,\omega^{-2} do\,[4|a|^2 + |b|^2 + |c|^2 + 2\mathrm{Re}\,(ab^* + ac^* + bc^*) + 2\cos^2\theta\,(|b|^2 + |c|^2 + \mathrm{Re}\,(ab^* + ac^* + bc^*)) + 4\sin^2\theta\,\mathrm{Re}\,(2ad^* - be^* - 2cf^*) - 4\sin^2\theta\cos\theta\,\mathrm{Re}\,(e+f)\,a^* + \cos^4\theta\,(|b|^2 + |c|^2) + 2\sin^4\theta\,(3|d|^2 + 2|e|^2 + 2|f|^2 + \mathrm{Re}\,(a+b+c)\,g^*) + 4\sin^2\theta\cos^2\theta\,\mathrm{Re}\,(bd^* - be^* + cd^*) - 4\sin^2\theta\cos^3\theta\,(bf^* + ce^*) - 8\sin^4\theta\cos\theta\,\mathrm{Re}\,(e+f)\,d^* + 4\sin^6\theta\,\mathrm{Re}\,(d-e-f)\,g^* + 2\sin^4\theta\cos^2\theta\,(|e|^2 + |f|^2 + 4\,\mathrm{Re}\,ef^*) + \sin^8\theta\,|g|^2]. \qquad (16)$$

If in the initial state the polarizations of the photons are orthogonal to each other and if the polarizations reverse as a result of the scattering, then the cross section has the form

$$d\sigma(1_\perp, 2_\parallel, 3_\parallel, 4_\perp) = (\alpha^4/2^6\pi^2)\,\omega^{-2} do\,[|b|^2\cos^2\theta + 2\,\mathrm{Re}\,(be^*)\sin^2\theta\cos\theta + |e|^2\sin^4\theta]. \qquad (17)$$

For small scattering angles ($m/\omega \ll \theta \ll 1$), the greatest contribution to the scattering amplitude (14) comes from terms containing the functions a, b, and c, which, in this case, are equal to (we neglect the contribution from the imaginary parts)

$$a = b \approx -\frac{4}{3}\ln\frac{t}{s}, \quad c \approx \ln^2\frac{t}{s} + \frac{8}{3}\ln\frac{t}{s},$$

the cross section is then expressed by the formula

$$d\sigma \approx (\alpha^4/\pi^2)\,\omega^{-2}do\,[(e_1e_3)^2\,(e_2e_4)^2\ln^4\theta + \tfrac{4}{3}(e_1e_3)\,(e_2e_4)((2-3\ln 2)\,(e_1e_3)\,(e_2e_4) - (e_1e_2)\,(e_3e_4) - (e_1e_4)\,(e_2e_3))\ln^3\theta]. \quad (18)$$

If we restrict ourselves to the first term in (18), we obtain the formula first found by Akhiezer.[5] In this case, the cross section averaged over the polarizations has the form

$$d\sigma \approx (4\alpha^4/\pi^2)\,\omega^{-2}do\,[\ln^4\theta - 4\,(\ln 2 - 1/3)\ln^3\theta]. \quad (19)$$

6. We shall also find an expression for zero-angle scattering cross section. In the center-of-mass system, the zero-angle scattering amplitude has the form

$$A = 4\alpha^2\,[(e_1e_2)\,(e_3e_4)\,a + (e_1e_4)\,(e_2e_3)\,b + (e_1e_3)\,(e_2e_4)\,c].$$

Using (A.1) and (A.2) for $t = 0$ [we now retain in (8) terms containing the electron mass] and determining the real parts of the scalar functions from the dispersion relations (12′), we obtain for a, b, and c the expressions

$$a = b \approx \frac{4}{3}\ln\frac{s}{m^2}, \quad c \approx \ln^2\frac{s}{m^2} - \frac{20}{3}\ln\frac{s}{m^2}$$

(we neglect the contribution from the imaginary parts).

In this case, the differential cross section is expressed by the formula

$$(d\sigma/do)_{\theta=0} \approx (\alpha^4/\pi^2)\,\omega^{-2}\,[(e_1e_3)^2\,(e_2e_4)^2\ln^4(\omega/m) - \tfrac{4}{3}(e_1e_3)\,(e_2e_4)\,((5-3\ln 2)\,(e_1e_3)\,(e_2e_4) - (e_1e_2)\,(e_3e_4) - (e_1e_4)\,(e_2e_3))\ln^3(\omega/m)]. \quad (20)$$

The cross section averaged over the polarizations has the form

$$(d\sigma/do)_{\theta=0} \approx (4\alpha^4/\pi^2)\,\omega^{-2}\,[\ln^4(\omega/m) - 4\,(4/3 - \ln 2)\ln^3(\omega/m)] \quad (21)$$

(the first term was obtained by Karplus and Neuman[6]).

7. Finally, we give expressions for the total cross section in the case of definite polarizations of the colliding and scattered photons (17). In (17) the real and imaginary parts of the functions b and e have the form

$$\mathrm{Re}\,b = \frac{x}{6}\frac{6-9x+3x^2+x^3}{(1-x)^2}\ln^2 x + \frac{2-2x-3x^2+5x^3+x^4}{6x^2}\ln^2(1-x) + \frac{1}{3}(3-5x-x^2)\ln x\ln(1-x) - \frac{4-4x-x^2}{3(1-x)}\ln x + \frac{2+x+x^2}{3x}\ln(1-x),$$

$$\mathrm{Re}\,e = \frac{1+4x+20x^2-36x^3+27x^4-8x^5}{24(1-x)^3}\ln^2 x + \frac{8+2x-6x^2-5x^3+5x^5}{24x^3}\ln^2(1-x) - \frac{3-3x+8x^2}{12}\ln x\ln(1-x) - \frac{6-23x+11x^3-10x^3+8x^4}{12x(1-x)^2}\ln x - \frac{6-x^2+4x^4}{6x(1-x)}\ln(1-x) + \frac{1+6x-3x^2}{6x(1-x)},$$

$$\mathrm{Im}\,b = \frac{x}{3}\frac{6-9x+3x^2+x^3}{(1-x)^2}\ln x + \frac{12-3x-5x^2-x^3}{3x}\ln(1-x) + \frac{3-3x+x^2}{3(1-x)},$$

$$\mathrm{Im}\,e = \frac{1+4x+20x^2-36x^3+27x^4-8x^5}{12(1-x)^3}\ln x + \frac{8+2x-6x^2+5x^3-5x^5}{12x^3}\ln(1-x) + \frac{8-13x+12x^2-4x^3+5x^4-4x^5}{6x^2(1-x)^2},$$

where $x = \sin^2 1/2\,\theta$.

Integrating (17) over x from 0 to 1 (we note that all divergences occurring here drop out), we obtain

$$\sigma(1_\perp, 2_\parallel, 3_\parallel, 4_\perp) = C\alpha^4/\omega^2,$$

$$C \approx \{2^2/\pi)\,\{2\,[8\zeta(2) - 11\zeta(3) + 17\zeta(4) - 7\zeta(5) + \xi(3) - 3] + \pi^2\,[7 - \zeta(2) - 4\zeta(3)]\} \approx 27, \quad (22)$$

where $\zeta(s)$ is the Riemann zeta function and $\xi(s)$ is the series of Riemann functions (A.4).

In conclusion I express my deep gratitude to Professor A. I. Akhiezer for valuable advice and discussion.

APPENDIX

1. In (7) the following integrals are encountered:

$$F_0(s) = \int d^4v\,\delta(qv)\,\delta(v^2 - s + 4m^2) = 2\pi\theta(s-4m^2)\,r_1,$$

$$F_1(s) = \int \frac{\delta(qv)\,\delta(v^2-s+4m^2)}{vp-s}\,d^4v = -\frac{\pi}{s}\,\theta(s-4m^2)\ln\frac{1+r_1}{1-r_1},$$

$$F_2(s,t) = \int \frac{\delta(qv)\,\delta(v^2-s+4m^2)}{(vp-s)\,(vp'-s)}\,d^4v = \frac{\pi}{str_2}\,\theta(s-4m^2)\ln\frac{r_1+r_2}{|r_1-r_2|}$$

$$(r_1 = \sqrt{1-\gamma\eta}, \qquad r_2 = \sqrt{1+\gamma(1-\eta)},$$

$$\eta = t/s, \qquad \gamma = 4m^2/t);$$

$$\int \frac{v_\mu\delta(qv)\,\delta(v^2-s+4m^2)}{vp-s}\,d^4v = p_\mu a_1', \quad \int \frac{v_\mu v_\nu\delta(qv)\,\delta(v^2-s+4m^2)}{vp-s}\,d^4v = (q_\mu q_\nu + s\delta_{\mu\nu})\,a_2' + p_\mu p_\nu b_2',$$

$$\int \frac{v_\mu\delta(qv)\,\delta(v^2-s+4m^2)}{(vp-s)\,(vp'-s)}\,d^4v = (p+p')_\mu a_1,$$

$$\int \frac{v_\mu v_\nu\delta(qv)\,\delta(v^2-s+4m^2)}{(vp-s)\,(vp'-s)}\,d^4v = (q_\mu q_\nu + s\delta_{\mu\nu})\,a_2 + (p_\mu p_\nu + p_\mu' p_\nu')\,b_2 + (p_\mu p_\nu' + p_\nu p_\mu')\,c_2,$$

$$\int \frac{v_\mu v_\nu v_\rho \delta(qv)\,\delta(v^2-s+4m^2)}{(vp-s)(vp'-s)}\,d^4v = [(q_\mu q_\nu + s\delta_{\mu\nu})(p+p')_\rho + \ldots]\,a_3 + (p_\mu p_\nu p_\rho + p'_\mu p'_\nu p'_\rho)\,b_3 + (p_\mu p'_\nu p'_\rho + \ldots + p'_\mu p_\nu p_\rho + \ldots)\,c_3,$$

$$\int \frac{v_\mu v_\nu v_\rho v_\sigma \delta(qv)\,\delta(v^2-s+4m^2)}{(vp-s)(vp'-s)}\,d^4v = \left[\frac{s^2}{3}(\delta_{\mu\nu}\delta_{\rho\sigma}+\ldots) + \frac{s}{3}(\delta_{\mu\nu}q_\rho q_\sigma + \ldots) + q_\mu q_\nu q_\rho q_\sigma\right] a_4 + [(p_\mu p_\nu + p'_\mu p'_\nu)(q_\rho q_\sigma + s\delta_{\rho\sigma}) + \ldots]\,b_4 + [(p_\mu p'_\nu + p_\nu p'_\mu)(q_\rho q_\sigma + s\delta_{\rho\sigma}) + \ldots]\,c_4 + (p_\mu p_\nu p_\rho p_\sigma + p'_\mu p'_\nu p'_\rho p'_\sigma)\,d_4 + (p_\mu p'_\nu p'_\rho p'_\sigma + \ldots + p'_\mu p_\nu p_\rho p_\sigma + \ldots)\,e_4 + (p'_\mu p'_\nu p_\rho p_\sigma + \ldots)\,f_4 \qquad \text{(A.1)}$$

(the omitted terms are obtained from the written ones by all possible permutations of the indices μ, ν, ρ, σ), where the quantities a'_1, a'_2, ... are expressed in terms of the integrals F_0, F_1, and F_2:

$$a'_0 = F_1, \quad a'_1 = F_1 + F_0/s, \quad a'_2 = -F_0/2s - 2m^2F_1/s,$$

$$b'_2 = F_1 + 3F_0/2s + 2m^2F_1/s, \quad a_0 = F_2,$$

$$a_1 = (sF_2 + F_1)/2(s-t),$$

$$a_2 = -(tF_2 + F_1)/(s-t) - 4m^2F_2/s,$$

$$b_2 = s^2F_2/2(s-t)^2 + (2s-t)F_1/2(s-t)^2 - (s-2t)F_0/4st(s-t) + m^2sF_2/t(s-t),$$

$$c_2 = s(tF_2+F_1)/2(s-t)^2 + F_0/4t(s-t) - m^2(s-2t)F_2/t(s-t),$$

$$a_3 = -s(tF_2+F_1)/2(s-t)^2 - F_0/4s(s-t) - 2m^2F_2/(s-t) - m^2F_1/s(s-t),$$

$$b_3 = s^3F_2/2(s-t)^3 + (3s(s-t)+t^2)F_1/2(s-t)^3 - (3s-2t)(s-3t)F_0/8st(s-t)^2 + 3m^2s^2F_2/2t(s-t)^2 + m^2(3s-2t)F_1/2s(s-t)^2,$$

$$c_3 = s^2(tF_2+F_1)/2(s-t)^3 + (s+t)F_0/8t(s-t)^2 - m^2s(s-4t)F_2/2t(s-t)^2 + m^2F_1/2(s-t)^2,$$

$$b_4 = -s^2(tF_2+F_1)/3(s-t)^3 - (3s-t)F_0/12s(s-t)^2 - 5m^2sF_2/3(s-t)^2 - 4m^4F_2/3t(s-t) - m^2(2s-t)F_1/s(s-t)^2 + m^2(s-2t)F_0/3ts^2(s-t),$$

$$c_4 = -s(s+t)(tF_2+F_1)/6(s-t)^3 - F_0/6(s-t)^2 - m^2(s+4t)F_2/3(s-t)^2 + 4m^4(s-2t)F_2/3st(s-t) - m^2F_1/(s-t)^2 - m^2F_0/3st(s-t),$$

$$e_4 = s^3(tF_2+F_1)/2(s-t)^4 + (s^2+2st-t^2)F_0/8t(s-t)^3 - m^2s^2(s-5t)F_2/2t(s-t)^3 - m^4s(s-2t)F_2/t^2(s-t)^2 + m^2(3s-t)F_1/2(s-t)^3 + m^2(s^2-2st+2t^2)F_0/4st^2(s-t)^2. \qquad \text{(A.2)}$$

(We have given here the expressions for the coefficients used in the calculations.)

2. We now give the asymptotic integrals, for $s, t \gg 4m^2$, occurring in the first term of (12'):

$$\frac{1}{\pi}\int_{4m^2}^{\infty} \frac{s'^k[tF_2(s',t)+F_1(s')]}{(s'-t)^n(s'-s)}\,ds' \approx \frac{s^{k-1}}{2(s-t)^n}\ln^2\frac{t}{s},$$

$$\frac{1}{\pi}\int_{4m^2}^{\infty} \frac{F_0(s')}{(s'-t)^n(s'-s)}\,ds' \approx \frac{2}{(s-t)^n}\left[\ln\frac{t}{s} - \sum_{k=1}^{n-1}\frac{(-1)^k}{k}\left(\frac{s-t}{t}\right)^k\right]. \qquad \text{(A.3)}$$

3. We finally give the expressions for the integrals occurring in integration of (17):

$$\int_0^1 \ln^n\frac{1}{x}\frac{dx}{1-x} = n!\,\zeta(n+1),$$

$$\int_0^1 \ln^n\frac{1}{x}\ln\frac{1}{1-x}\frac{dx}{1-x} = n!\,\xi(n+1),$$

$$\xi(s) = \sum_{n=1}^{\infty}\frac{\zeta(s,n+1)}{n} \qquad \text{(A.4)}$$

and $\zeta(s, n)$ is the Riemann function of two arguments:

$$\zeta(s,n) = \sum_{k=0}^{\infty}\frac{1}{(k+n)^s}, \qquad \zeta(s) = \zeta(s,1).$$

[1] Gell-Mann, Goldberger, and Thirring, Phys. Rev. 95, 1612 (1954).

[2] Bogolyubov, Medvedev, and Polivanov, Voprosy teorii dispersionnykh sootnoshenii (Problems in the Theory of Dispersion Relations), Fizmatgiz, 1958.

[3] S. Mandelstam, Phys. Rev. **112**, 1344 (1958); **115**, 1741 (1959).

[4] H. Euler, Ann. Physik **26**, 398 (1936).

[5] A. I. Akhiezer, Physik Zeits. Sowjetunion **11**, 263 (1937).

[6] R. Karplus and M. Neuman, Phys. Rev **80**, 380 (1950).

Translated by E. Marquit
87

ON THE THEORY OF THE SCATTERING OF SLOW NEUTRONS IN A FERMI LIQUID

A. I. AKHIEZER, I. A. AKHIEZER, and I. Ya. POMERANCHUK

Physico-Technical Institute, Academy of Sciences, Ukrainian S.S.R. and
Institute of Theoretical and Experimental Physics, Academy of Sciences, U.S.S.R.

Submitted to JETP editor February 24, 1960

J. Exptl. Theoret. Phys. (U.S.S.R.) **41**, 478-487 (August, 1961)

The scattering of slow neutrons in a Fermi liquid is investigated theoretically. The cross sections for direct scattering and scattering involving the excitation of zero and ordinary sound are determined.

1. The purpose of the present paper is the theoretical investigation of the scattering of slow neutrons in a Fermi liquid. It is known that, for sufficiently low temperatures, specific sound waves —the so-called zero sound (Landau,[1] Klimontovich and Silin[2])—may propagate in such a system. We shall show that these waves can be excited by irradiating the Fermi liquid with slow neutrons whose velocity exceeds the velocity of the zero sound.

The investigation of the scattering of slow neutrons in liquid He^3, which is a Fermi liquid, can therefore serve, in principle, to verify the existence of the zero sound.

Besides the scattering with excitation of the zero sound (and ordinary sound), direct scattering of the neutrons by the nuclei of the Fermi liquid is also possible. In these scattering processes the energy transfer and the scattering angle are not correlated, whereas in scattering processes connected with the excitation of collective degrees of freedom and having the character of Cerenkov radiation, the scattering angle is a unique function of the energy transfer.

2. The Hamiltonian for the interaction of a slow neutron with the nuclei of the Fermi liquid is given by a sum of Fermi pseudopotentials:

$$\mathcal{H} = -\frac{2\pi\hbar^2}{m'}\sum_i (a + b\mathbf{s}\mathbf{K}_i)\,\delta(\mathbf{r} - \mathbf{r}_i), \tag{1}$$

where $\mathbf{r}$, $\mathbf{r}_i$, and $\mathbf{s}$, $\mathbf{K}_i$ are the radius vectors and the spins of the neutron and the i-th nucleus, m' is the reduced mass of the neutron-nucleus system, and a and b are the coherent and incoherent scattering lengths for the scattering of a neutron from a free nucleus of the Fermi liquid (the quantities a and b are complex owing to the absorption of the neutrons by the nuclei). The effect of the Fermi liquid comes most clearly into play for small neutron momentum transfers Δp_n. We shall therefore assume in the following that $|\Delta p_n| \ll p_0$, where p_0 is the limiting momentum of the Fermi liquid. Under these conditions we can replace the summation over i in (1) by an integration over $\rho(\mathbf{r}_i, \alpha_i, t)\,d\mathbf{r}_i$, where ρ is the density of nuclei with spin projection α_i at the point $\mathbf{r}_i$ of the Fermi liquid:

$$\mathcal{H} = -(2\pi\hbar^2/m')\,(a + b\mathbf{s}\mathbf{K}(\mathbf{r}))\,\rho(\mathbf{r}, \alpha, t). \tag{2}$$

The deviation of the density of the Fermi liquid from its equilibrium value ρ_0 is clearly equal to $\delta\rho = \int \delta n_p d\tau_p$, where $d\tau_p = (2\pi\hbar)^{-3}dp$ ($\mathbf{p}$ is the momentum of a quasiparticle of the Fermi liquid) and δn_p is the deviation of the quasiparticle distribution function from its equilibrium value

$$n_p^0 = \left[\exp\left(\frac{\varepsilon_p - \zeta}{T}\right) + 1\right]^{-1}$$

(ε_p is the energy of the quasiparticle, ζ is the chemical potential). δn_p satisfies, according to Landau,[3] the equation

$$\left(\frac{\partial}{\partial t} + \frac{\partial\varepsilon_p}{\partial\mathbf{p}}\frac{\partial}{\partial\mathbf{r}}\right)\delta n_p(\mathbf{r}, t) - \frac{\partial n_p^0}{\partial\mathbf{p}}\,\mathrm{Sp}_{k'}\int f\frac{\partial}{\partial\mathbf{r}}\,\delta n_{p'}(\mathbf{r}, t)\,d\tau_{p'} = I\{\delta n_p\}. \tag{3}$$

Here I is the collision integral, and $f = f(\mathbf{p}, \mathbf{p}') + \mathbf{K}\cdot\mathbf{K}'q(\mathbf{p}, \mathbf{p}')$ is a quantity which characterizes the interaction of the quasiparticles. At absolute zero $\delta n_p = (\nu + \mathbf{K}\cdot\mu)\,\delta(\varepsilon_p - \zeta)$, where ν and μ are certain functions of $\mathbf{n} = \mathbf{p}/p$ and $\mathbf{r}$, t. The monochromatic oscillations $\delta n_p (\sim e^{i(\mathbf{q}\cdot\mathbf{r} - \omega t)})$ satisfy the equations

$$(\eta_i - \cos\theta)\,\nu_{qi}(\mathbf{n}) = \cos\theta\int F(\tilde{\chi})\,\nu_{qi}(\mathbf{n}')\,do'/4\pi,$$
$$(\eta_i' - \cos\theta)\,\mu_{qi}(\mathbf{n}) = \cos\theta\int G(\tilde{\chi})\,\mu_{qi}(\mathbf{n}')\,do'/4\pi, \tag{4}$$

where θ is the angle between $\mathbf{n}$ and $\mathbf{q}$, $\tilde{\chi}$ is the angle between $\mathbf{p}$ and $\mathbf{p}'$, do' is the angular part

of the volume element of p', $\eta_i = s_i/v_0$, $\eta_i' = s_i'/v_0$, $s_i = \omega_i/q$, $s_i' = \omega_i'/q$ are the propagation velocities of the oscillations of the quantities ν and μ (the index i denotes the kind of oscillation), v_0 is the Fermi velocity, and the quantities F and G, which are proportional to $f(p, p')$ and $g(p, p')$, determine the change of the energy of the quasiparticle, which is related to the change of the distribution function by

$$\delta\varepsilon_p = \int \left(F\nu' + \tfrac{1}{4} G\mu' K\right) do'/4\pi, \qquad \nu' = \nu(n', r, t), \quad \mu' = \mu(n', r, t). \tag{5}$$

For sufficiently low temperatures, when there is very little absorption of zero sound, the scattering of the neutron and the excitation of the zero sound can be interpreted as the emission of a quantum of zero sound by the neutron. This process is described by a Hamiltonian which differs from (2) in that ρ is replaced by the change of the density of the Fermi liquid caused by the zero sound oscillations.

In order to calculate the emission probability for a quantum of zero sound, we must quantize the zero sound. For this purpose we must first determine the energy of the oscillations of the zero sound,

$$E = \int dr\, \mathrm{Sp} \int_{p=p_0}^{p_0+\delta p_0} \varepsilon_p\, d\tau_p + \frac{1}{2}\int dr\, \mathrm{Sp} \int \delta\varepsilon_p\, \delta n_p\, d\tau_p, \tag{6}$$

where $\varepsilon_p = v_0(p - p_0)$ and $\delta p_0 = (\nu + K\cdot\mu)/v_0$ is the change of the Fermi momentum connected with the oscillations of the Fermi surface [the second term in (6) takes account of the interaction between the quasiparticles]. Using (5), we obtain

$$E = \frac{p_0^2}{(2\pi\hbar)^3 v_0}\int dr \left\{\int\int \left(\nu^2 + \frac{1}{4}\mu^2\right) do + \int\int\int \left(F\nu\nu' + \frac{1}{16} G\mu\mu'\right)\frac{do\, do'}{4\pi}\right\}. \tag{7}$$

This expression should, of course, have the form

$$E = \sum_{qi}\left(N_{qi} + \frac{1}{2}\right)\hbar\omega_i + \sum_{q,\, i,\, \lambda}\left(N_{qi\lambda} + \frac{1}{2}\right)\hbar\omega_i', \tag{8}$$

where N_{qi} is the number of quanta of zero sound of the type ν_i and frequency ω_i, and $N_{qi\lambda}$ is the number of quanta of zero sound of the type μ_i, frequency ω_i', and polarization $\lambda = 1, 2, 3$. Expression (8) follows from (7), if we expand ν and μ in terms of plane waves:

$$\nu = \frac{(2\pi\hbar)^{3/2}}{p_0}\sum_{q,\, i}\left(\frac{1}{2} v_0\hbar\omega_i\right)^{1/2}\{\nu_{qi}(n)\, c_{qi} e^{i(qr-\omega_i t)} + \nu_{qi}^*(n)\, c_{qi}^+ e^{-i(qr-\omega_i t)}\},$$

$$\mu = \frac{(2\pi\hbar)^{3/2}}{p_0}\sum_{q,\, i,\, \lambda}(2v_0\hbar\omega_i')^{1/2}\{\mu_{qi\lambda}(n)\, c_{qi\lambda} e^{i(qr-\omega_i' t)} + \mu_{qi\lambda}^*(n)\, c_{qi\lambda}^+ e^{-i(qr-\omega_i' t)}\} \tag{9}$$

interpret the quantities c_{qi}, c_{qi}^+, $c_{qi\lambda}$, $c_{qi\lambda}^+$ as boson absorption and creation operators for the corresponding zero sound quanta, and subject the functions $\nu_{qi}(n)$ and $\mu_{qi\lambda}(n)$ to the normalization conditions*

$$\eta_i \int |\nu_{qi}(n)|^2\, do/\cos\theta = 1, \qquad \eta_i' \int |\mu_{qi\lambda}(n)|^2\, do/\cos\theta = 1. \tag{10}$$

Substituting (9) in (2), we find for the energy of the interaction of a neutron with the zero sound oscillations

$$\mathcal{H}^{(0)} = -\frac{m^*}{m'}\sqrt{\frac{\hbar v_0}{\pi}}\left\{a\sum_{qi}\sqrt{\hbar\omega_i}\,(A_i c_{qi}^+ e^{-i(qr-\omega_i t)} + \text{h.c.}) + 2[(a + bsK)K]_c \sum_{qi\lambda}\sqrt{\hbar\omega_i'}\,(B_{i\lambda} c_{qi\lambda}^+ e^{-i(qr-\omega_i' t)} + \text{h.c.})\right\}, \tag{11}$$

where

$$A_i = \int \nu_{qi}(n)\, do, \qquad B_{i\lambda} = \int \mu_{qi\lambda}(n)\, do, \tag{12}$$

and the bracket $[Y]_c$ denotes the part of Y which is coherent in the spins of the nuclei and does not contain the nuclear spin operators K linearly; $m^* = p_0/v_0$.

Using the expression for $\mathcal{H}^{(0)}$, we can easily determine the cross sections for the scattering of a neutron (from a single nucleus) with emission of the different types of zero sound quanta:

$$d\sigma_{\uparrow\uparrow}^{(\nu_i)} = \tfrac{3}{2}(m^*/m')^2 |A_i|^2 |a|^2 (s_i v_0/v_n^2)(\hbar^3 q^2\, dq/p_0^3), \quad d\sigma_{\uparrow\downarrow}^{(\nu_i)} = 0,$$

$$d\sigma_{\uparrow\uparrow}^{(\mu_i)} = \frac{3}{2}\left(\frac{m^*}{m'}\right)^2 |B_{iz}|^2 \frac{|b|^2}{16}\frac{s_i' v_0}{v_n^2}\frac{\hbar^3 q^2\, dq}{p_0^3},$$

$$d\sigma_{\uparrow\downarrow}^{(\mu_i)} = \frac{3}{2}\left(\frac{m^*}{m'}\right)^2 |B_i^+|^2 \frac{|b|^2}{16}\frac{s_i' v_0}{v_n^2}\frac{\hbar^3 q^2\, dq}{p_0^3}, \tag{13}$$

where v_n is the velocity of the neutron, $B_i^+ = B_{ix} + iB_{iy}$ (the z axis is directed along s), the arrows indicate whether the directions of the neutron spin before and after the scattering are parallel or antiparallel with respect to each other, and the indices ν_i and μ_i denote the type of zero sound quantum emitted.

It is very probable [1] that the simultaneous propagation of ν_i and μ_i waves in the Fermi liquid is not possible (at least, if $F(\tilde{\chi}) = \text{const}$). In the following we shall therefore only consider the excitation of ν_i waves. In this case the conservation laws

$$p_n = p_n' + \hbar q, \qquad E_n = E_n' + \hbar q s_i, \tag{14}$$

*To derive these conditions, we must use the relations

$$\int\int F\nu_{qi}\nu_{qi}'\, do\, do'/4\pi = \int(\eta_i/\cos\theta - 1)\,|\nu_{qi}|^2\, do,$$

$$\int\int G\mu_{qi\lambda}\mu_{qi\lambda}'\, do\, do'/4\pi = \int(\eta_i'/\cos\theta - 1)\,|\mu_{qi\lambda}|^2\, do.$$

which follow from (4).

must hold, where $\mathbf{p_n}$, E_n and $\mathbf{p'_n}$, E'_n are the momentum and energy of the neutron before and after the scattering. It follows from (14) that the angle ϑ between $\mathbf{p_n}$ and $\mathbf{q}$, as well as the scattering angle χ, are uniquely determined by the energy transfer:

$$\cos\vartheta = \frac{s}{v_n} + \frac{\hbar q}{2p_n}, \qquad \cos\chi = \frac{2p_n^2 - 2ms\hbar q - (\hbar q)^2}{2p_n\sqrt{p_n^2 - 2ms\hbar q}}, \quad (15)$$

where $s = s_i$ and m is the mass of the neutron. The first relation shows that v_n must be larger than s.

For small scattering angles we have

$$\cos\vartheta = s/v_n, \qquad \chi^2 = (\hbar q/p_n)^2\,(1 - s^2/v_n^2), \quad (15')$$
$$\hbar q \ll p_n.$$

In this case the zero-sound quanta are emitted under a rigorously defined angle with respect to the direction of motion of the neutron (as in the Cerenkov radiation). The largest possible momentum of the quantum is equal to $\hbar q_{max} = 2(p_n - ms)$ and the smallest momentum of the neutron after the scattering is equal to $p'_{n\,min} = |p_n - 2ms|$ (the neutrons with the minimal energy will move along the initial direction of the beam; all these relations hold for $\hbar q_{max} \ll p_0$).

It is easy to see that the scattering angle χ reaches a maximum for $\hbar q = (2/3ms)(p_n^2 - m^2s^2)$. This limiting angle is equal to (with $p_n \approx ms$)

$$\chi_0 = \arccos\left[\frac{(1+2\xi_0^2)\sqrt{4-\xi_0^2}}{3\sqrt{3}\xi_0}\right] \approx 2\left(\frac{\xi_0^2-1}{3}\right)^{3/2}, \quad \xi_0 = \frac{p_n}{ms} \quad (16)$$

Near the maximal scattering angle χ_0 the scattering cross section behaves like

$$d\sigma^{(\nu_i)} \sim q^2\,dq \sim \sin\chi\,d\chi/\sqrt{\cos\chi - \cos\chi_0}, \qquad \chi \approx \chi_0, \quad (17)$$

i.e., it contains an integrable singularity. However, this result, as well as the proof of the existence of χ_0 itself, was obtained under the assumption that the absorption of the zero sound can be neglected (see Sec. 4).

For small scattering angles the cross section $d\sigma^{(\nu_i)}$ has the form

$$d\sigma^{(\nu_i)} = \frac{3}{2}\left(\frac{m}{m'}\right)^2 |A_i|^2\,|a|^2\,\frac{s_i p_n}{v_0 p_0}\left(1 - \frac{s_i^2}{v_n^2}\right)^{-3/2}\chi^2\,d\chi. \quad (18)$$

If $\hbar q_{max} \ll p_0$, we can determine the total cross section for the emission of a quantum of zero sound:

$$\sigma^{(\nu_i)} = 4\left(\frac{m^*}{m'}\right)_i^2 |A_i^2|\,a\,^2\,\frac{s_i v_0}{v_n^2}\left(\frac{p_n - ms_i}{p_0}\right)^3. \quad (19)$$

The quantity A_i depends on the form of the function $F(\tilde{\chi})$. If we assume that $F(\tilde{\chi}) = \text{const}$, we have, according to (10) and (12),

$$A = \sqrt{2\pi(\eta_0^2 - 1)}\left(\eta_0 \ln\frac{\eta_0+1}{\eta_0-1} - 2\right)$$
$$\times\left[2 - (\eta_0^2 - 1)\left(\eta_0 \ln\frac{\eta_0+1}{\eta_0-1} - 2\right)\right]^{-1/2}, \qquad \eta_0 = \frac{s}{v_0}. \quad (20)$$

We note that A vanishes for $F \to 0$.

3. We now turn to the calculation of the cross section for the direct scattering of the neutron by the nuclei of the Fermi liquid and to the consideration of the absorption of the zero sound in the scattering accompanied by the excitation of zero sound. For simplicity we shall assume that the energy of the quasiparticle does not depend on the orientation of its spin. The cross section for the coherent scattering of the neutron without change of orientation of its spin, $d\sigma_c$, is, according to (2), determined by the Fourier component of the deviation of the density of the Fermi liquid $\delta\rho(\mathbf{r}, t)$ from its equilibrium value ρ_0, i.e., by the quantity $\int \delta\rho(\mathbf{r}, t)\,e^{-i(\mathbf{q}\cdot\mathbf{r}-\omega t)}\,d\mathbf{r}dt$, where $\hbar\mathbf{q} = \mathbf{p_n} - \mathbf{p'_n}$ and $\hbar\omega = E_n - E'_n$ are the changes of the momentum and energy of the neutron:

$$d\sigma_c = 2\pi\,(|a|^2/v_n\rho_0)\,(2\pi\hbar/m')^2\,\Phi(q, \omega)\,dp'_n/(2\pi\hbar)^3, \quad (21)$$

where Φ is the correlation function of the density of the nuclei,

$$\Phi(q, \omega) = \frac{1}{2\pi}\int d\mathbf{r}_1\,e^{-iq(\mathbf{r}_1-\mathbf{r}_2)}\int dt_1\,e^{i\omega(t_1-t_2)}$$
$$\times\langle\delta\rho(\mathbf{r}_1, t_1)\,\delta\rho(\mathbf{r}_2, t_2)\rangle, \quad (22)$$

and the brackets $\langle\ldots\rangle$ indicate the (quantum mechanical and thermodynamical) average.* According to the general theory of fluctuations, one can calculate the quantity Φ (for $T, \hbar\omega \ll \zeta$) first in the temperature region $T \gg \hbar\omega$, and then multiply the result by the factor $\hbar\omega(N_\omega + 1)/T$, where N_ω is Planck's distribution function:†

$$\Phi(q, \omega) = \frac{\hbar\omega}{T}\,(N_\omega + 1)\,\frac{1}{2\pi}\int d\mathbf{r}_1\,e^{-iq(\mathbf{r}_1-\mathbf{r}_2)}\int dt_1\,e^{i\omega(t_1-t_2)}$$
$$\times\,\overline{\delta\rho(\mathbf{r}_1, t_1)\,\delta\rho(\mathbf{r}_2, t_2)} \quad (23)$$

(the bar denotes the thermodynamical average).

In order to calculate the correlation function $\Phi(\mathbf{q}, \omega)$ with account of the collisions we use the method of Abrikosov and Khalatnikov.[5] Introducing the stray force $\mathbf{y}(\mathbf{p}, \mathbf{r}, t)$ in the kinetic equation (3) and choosing the collision integral $I\{\nu\}$ in the simplest form satisfying the requirements of conservation of the number of particles, momentum, and energy,

*The general relation between the neutron scattering cross section and the correlation function of the density of nuclei was established by Van Hove.[4]

†This method was used by Abrikosov and Khalatnikov[5] in their calculation of the correlation function with neglect of the collisions.

$$I\{\nu\} = -\tau^{-1}\Big\{\nu(\mathbf{n}) - \nu_0 - \sum_{m=-1}^{1} \nu_1^m P_1^m(\cos\theta)\, e^{im\varphi}\Big\}, \tag{24}$$

where ν_l^m are the coefficients in the expansion of the function $\nu(\mathbf{n})$ in terms of spherical harmonics, we obtain the following expression for the average value of the product of stray forces:

$$\overline{y(\mathbf{p}, \mathbf{r}, t)\, y(\mathbf{p}', \mathbf{r}', t')} = \frac{2T}{\tau}\left(\frac{d\varepsilon_p}{d\tau_p}\right)_\zeta \delta(\mathbf{r}-\mathbf{r}')\,\delta(t-t') \times \delta(\varepsilon-\zeta)\delta(\varepsilon'-\zeta)\sum_{l=2}^{\infty}\frac{2l+1}{1+F_l/(2l+1)}P_l(\cos\tilde{\chi}),$$

$$(d\tau_p/d\varepsilon_p)_\zeta = m^* p_0/\pi^2\hbar^3, \tag{25}$$

where F_l are the spherical harmonics of the function $F(\tilde{\chi})$. Solving the kinetic equation (3) with the stray force y, we obtain a relation between the Fourier components of the functions $\delta\rho$ and y ($\sim e^{i(\mathbf{q}\cdot\mathbf{r}-\omega t)}$). Considering only the first two harmonics in the expansion of F in terms of spherical harmonics, we find

$$\delta\rho = -i\left(\frac{d\tau_p}{d\varepsilon_p}\right)_\zeta \frac{1}{qv_0 D}\int y(\mathbf{n})\, h(\mathbf{n})\,\frac{do}{4\pi}, \tag{26}$$

where

$$D = 1 + (A_1F_0 + i\eta\xi A_0) - g(A_2F_0 + i\eta\xi A_1),$$

$$h(\mathbf{n}) = \frac{1-g\cos\theta}{\cos\theta - \eta(1+i\xi)},$$

$$g = \frac{3i\xi\eta + A_2F_1}{1+3i\xi\eta A_2 + F_1A_3}, \qquad A_n = \frac{1}{2}\int_{-1}^{1}\frac{x^n\,dx}{x-\eta(1+i\xi)}$$

($\eta = \omega/qv_0$, $\xi = 1/\omega\tau$). Using (24) and (25), we obtain finally the following expression for Φ:

$$\Phi(q,\omega) = \frac{2\hbar\omega}{\tau(qv_0)^2}\left(\frac{d\tau_p}{d\varepsilon_p}\right)_\zeta (N_\omega+1)\frac{1}{|D|^2}\left\{\int|h(\mathbf{n})|^2\frac{do}{4\pi} - \left|\int h(\mathbf{n})\frac{do}{4\pi}\right|^2 - 3\left|\int h(\mathbf{n})\cos\theta\frac{do}{4\pi}\right|^2\right\}. \tag{27}$$

If the condition $|\omega|\tau \gg 1$ ($\tau \sim T^{-2}$) is satisfied, the function $\Phi(q, \omega)$ has poles for values of ω which are close to the real axis, $\omega = \eta_0 v_0 q - i\gamma_0$ ($\eta_0 v_0$ is the velocity of the zero sound and γ_0 is its damping coefficient; an expression for γ_0 was found in reference 6). Separating out the poles of the function $\Phi(q, \omega)$, we write the latter in the form

$$\Phi(q,\omega) = \Phi_0(q,\omega) + \Phi_d(q,\omega), \tag{28}$$

where the function Φ_0 contains the poles of Φ, while Φ_d is free of singularities. Assuming for simplicity that F = const, we have

$$\Phi_0(q,\omega) = \frac{\hbar\omega}{\pi}\left(\frac{d\tau_p}{d\varepsilon_p}\right)_\zeta (N_\omega+1)\frac{\eta_0^2-1}{F_0(1-\eta_0^2+F_0)} \times\left\{\frac{\gamma_0}{(\omega-\eta_0v_0q)^2+\gamma_0^2} + \frac{\gamma_0}{(\omega+\eta_0v_0q)^2+\gamma_0^2}\right\}. \tag{29}$$

The quantity Φ_d is a smooth function of ω. We can therefore neglect the collisions of the quasiparticles in the computation of Φ_d.

If F = const, we have*

$$\Phi_d(q,\omega) = \frac{\hbar\omega}{2qv_0}\left(\frac{d\tau_p}{d\varepsilon_p}\right)_\zeta (N_\omega+1)\,R_0\left(\frac{\omega}{qv_0}\right)\theta\left(1-\frac{|\omega|}{qv_0}\right),$$

$$R_0\left(\frac{\omega}{qv_0}\right) = \left\{(1+F_0w)^2 + \left(\frac{\pi}{2}\frac{\omega}{qv_0}F_0\right)^2\right\}^{-1},$$

$$w = 1 - \frac{\omega}{2qv_0}\ln\left|\frac{qv_0+\omega}{qv_0-\omega}\right|, \qquad \theta(x) = \begin{cases}0, & x<0\\ 1, & x>0\end{cases}. \tag{30}$$

The separation of the poles out of the correlation function corresponds to the separation of the coherent neutron scattering cross section into two parts:

$$d\sigma_c = d\sigma^{(0)} + d\sigma_c^{(d)},$$

$$d\sigma^{(0)} = \frac{2\pi|a|^2}{v_n p_0}\left(\frac{2\pi\hbar}{m'}\right)^2\Phi_0(q,\omega)\frac{d\mathbf{p}_n'}{(2\pi\hbar)^3},$$

$$d\sigma_c^{(d)} = \frac{2\pi|a|^2}{v_n p_0}\left(\frac{2\pi\hbar}{m'}\right)^3\Phi_d(q\omega)\frac{dp_n'}{(2\pi\hbar)^3}. \tag{31}$$

For F = const we find, according to (29) and (30),

$$d\sigma^{(0)} = \frac{3}{\pi}\left(\frac{m^*}{m'}\right)^2|a|^2\omega(N_\omega+1)\frac{v_0}{v_n}\frac{\eta_0^2-1}{F_0(1-\eta_0^2+F_0)} \times\left\{\frac{\gamma_0}{(\omega-\eta_0v_0q)^2+\gamma_0^2} + \frac{\gamma_0}{(\omega+\eta_0v_0q)^2+\gamma_0^2}\right\}\frac{d\mathbf{p}_n'}{p_0^3}, \tag{32}$$

$$d\sigma_c^{(d)} = \frac{3}{2}\left(\frac{m^*}{m'}\right)^3|a|^2\frac{\omega}{qv_n}(N_\omega+1)\,R_0\left(\frac{\omega}{qv_0}\right)\theta\left(1-\frac{|\omega|}{qv_0}\right)\frac{d\mathbf{p}_n'}{p_0^3}. \tag{33}$$

The quantity $d\sigma^{(0)}$ is the cross section for the scattering of the neutron with excitation (or absorption) of zero sound, and $d\sigma_c^{(d)}$ is the cross section for the direct scattering of the neutron without change of orientation of its spin.

If $\gamma_0 \to 0$, we find†

$$\Phi_0(q,\omega) = \frac{\hbar\omega}{qv_0}\left(\frac{d\tau_p}{d\varepsilon_p}\right)_\zeta (N_\omega+1)\frac{\eta_0^2-1}{F_0(1-\eta_0^2+F_0)}\left\{\delta\left(\frac{\omega}{qv_0}-\eta_0\right) + \delta\left(\frac{\omega}{qv_0}+\eta_0\right)\right\}. \tag{29'}$$

Substitution of this expression in $d\sigma^{(0)}$ leads immediately to formulas (13) and (20) for the cross section for the scattering of the neutron with excitation of zero sound for F = const.

We note that the validity of expression (29) is limited by the inequalities $\tau^{-1} \ll |\omega| \ll T/\hbar$. If $T \lesssim \hbar\omega$, we can use only expression (29′) for Φ_0, since expression (29) does not take account of the quantum mechanical effect in the absorption of the

*The expression for Φ_d with $\gamma = 0$ and F = const can be taken directly from formula (23) of the paper of Abrikosov and Khalatnikov.[5]

†Expression (29′) can be taken directly from formula (23) of[3]. Replacing in this formula

$$\delta(\Delta\omega \pm \eta_0v_0q) \text{ by } \pi^{-1}\gamma\,[(\Delta\omega \pm \eta_0v_0q)^2+\gamma^2]^{-1},$$

we take account of the effect of the absorption of zero sound on the scattering of light in a Fermi liquid.

zero sound, as pointed out by Landau.[1] According to the results of[1], however, we may expect that formula (29) remains valid also for $T \lesssim \hbar\omega$, if we replace γ_0 by $\gamma = \gamma_0\{1 + (\hbar\omega/2\pi T)^2\}$.

4. We have seen above that for $\gamma \to 0$ and $\eta_0 v_0 < v_n < 2\eta_0 v_0$ the scattering angle of the neutron in the scattering with excitation of zero sound cannot exceed a certain limiting value χ_0, and the cross section for this process becomes infinite for $\chi \sim \chi_0$. If the absorption of the zero sound is taken into account, the scattering cross section for $\chi \sim \chi_0$ will, according to (32), have the form

$$d\sigma^{(0)} = G(J + O(\xi)) \sin\chi\, d\chi, \qquad J = \int \frac{\xi\, dt}{(\eta - \eta_0)^2 + \xi^2},$$

where

$$t = p_n/m\eta_0 v_0, \quad \xi = \xi(\chi) = \gamma/qv_0, \quad \eta = \eta(\chi, t) = \omega/qv_0$$

and G is some function of χ. The limiting angle χ_0 is evidently determined by the conditions

$$\eta(\chi_0, t_0) = \eta_0, \qquad \partial\eta(\chi_0, t)/\partial t\,|_{t_0} = 0.$$

For $\chi > \chi_0$ the difference $\eta(\chi, t) - \eta_0$, regarded as a function of t, does not become zero and the integral J is of the order of ξ: $J = 0(\xi)$. For $\chi < \chi_0$ and $\xi \ll 1$ the integral J is equal to

$$J = \pi \int \delta(\eta - \eta_0)\, dt + O(\xi) = \pi\, |\partial\eta/\partial t\,|_{t_0}^{-1} + O(\xi) \sim 1,$$

and $d\sigma^{(0)}$ is given by (13) with an accuracy up to terms of order ξ.

Finally, if $\chi \approx \chi_0$, we use the expansion

$$\eta_0 - \eta = \alpha(\chi - \chi_0) + \beta(t - t_0)^2,$$

where

$$\alpha = -(\partial\eta/\partial\chi)\,|_{\chi_0, t_0}, \qquad \beta = -\tfrac{1}{2}(\partial^2\eta/\partial t^2)\,|_{\chi_0, t_0},$$

and write J in the form

$$J = \int_{-\infty}^{\infty} \frac{\xi\, dz}{[\alpha(\chi - \chi_0) + \beta z^2]^2 + \xi^2}, \qquad z = t - t_0.$$

For $\chi = \chi_0$ we then obtain $J \sim (\beta\xi)^{-1/2} \gg 1$.

We see that the absorption of the zero sound leads to a "smearing out" of the limiting scattering angle.

5. The cross section for the direct coherent scattering of the neutron by the nuclei of the Fermi liquid (without change of orientation of the neutron spin), given by formula (33), differs from the cross section for the coherent scattering of the neutron without change of orientation of its spin in a Fermi gas of the same density by the factor R_0. For $|\omega|/qv_0 \ll 1$ this factor is independent of the transferred energy and momentum and is equal to $R_0 \cong (1 + F_0)^{-2}$. $R_0 \to 0$ for $|\omega|/qv_0 \to 1$. Therefore the cross section for direct coherent scattering into angles close to

$$\chi_d = \arccos\left\{\frac{1}{2p_n p_n'}[p_n^2 + p_n'^2 - (2mv_0)^{-2}(p_n^2 - p_n'^2)^2]\right\}$$

is appreciably smaller in a Fermi liquid than in an ideal gas.

If we keep only the first two harmonics in the expansion of F, we find for the direct scattering cross section

$$d\sigma_c^{(d)} = \frac{3}{2}\left(\frac{m^*}{m'}\right)^2 |a|^2 \frac{\omega}{qv_n}(N_\omega + 1)\, R_1\left(\frac{\omega}{qv_0}\right)\theta\left(1 - \frac{|\omega|}{qv_0}\right)\frac{dp_n'}{p_n^3}, \tag{33'}$$

where the factor R_1, which distinguishes this cross section from the corresponding cross section in the ideal Fermi gas, is equal to

$$R_1\left(\frac{\omega}{qv_0}\right) = \left(1 + \frac{F_1}{3}\right)^2 L^{-2}\left\{(1 + F_0 Q_1)^2 + \left(\frac{\pi}{2}\eta F_0 Q_2\right)^2\right\}^{-1},$$

$$Q_1 = w - \frac{\eta^2 F_1}{Q}\left\{L\left(w^2 - \frac{\pi^2}{4}\eta^2\right) + \frac{\pi^2}{2} w\eta^4 F_1\right\},$$

$$Q_2 = 1 + \frac{\eta^2 F_1}{Q}\left\{\eta F_1\left(w^2 - \frac{\pi^2}{4}\eta^2\right) - 2wL\right\},$$

$$L = 1 + F_1\left(\tfrac{1}{3} + \eta^2 w\right), \qquad Q = L^2 + \frac{\pi^2}{4}\eta^6 F_1^2.$$

6. Let us now consider the incoherent scattering of the neutron in a Fermi liquid. This scattering, which is due to the quantity b in the pseudopotential (1), is of the same type as the scattering of a neutron in an ideal Fermi gas of nuclei whose mass is equal to the effective mass m* of the quasiparticles of the Fermi liquid. The total cross section for the incoherent scattering (with and without change of orientation of the neutron spin) per nucleus is equal to

$$d\sigma' = \frac{9}{32}\left(\frac{m^*}{m'}\right)^2 |b|^2 \frac{\omega}{qv_n}(N_\omega + 1)\,\theta\left(1 - \frac{|\omega|}{qv_0}\right) p_0^{-3} dp_n'. \tag{34}$$

We note that this expression does not contain (as $d\sigma_c^{(d)}$ does) the factor R which depends on the correlation between the nuclei.

It follows from (33) and (34) that there is no unique relation between the transferred energy and momentum for the direct scattering, whereas such a relation does exist (for $\gamma \to 0$) in the scattering with excitation of the zero sound [owing to the presence of the δ functions in formula (29')]. This circumstance allows us, in principle, to distinguish between the two types of scattering.

Let us finally discuss the angular distribution of the neutrons for the direct scattering in the region of small angles, $\chi \ll 1$. If $v_n \sim v_0$, the cross section will be proportional to $\chi d\chi$. For large neutron velocities the cross section will behave like $\chi^2 d\chi$. For an estimate of the order of magnitude of the cross section, we set $R \sim 1$, and obtain for $v_n \gg v_0$ and $\chi \ll 1$

$$d\sigma^{(d)} \sim \frac{3}{8}(m/m')^2\sigma_0\,(p_n/p_0)\,\chi^2\,d\chi,$$
$$\sigma_0 = 4\pi\left(|a|^2 + \tfrac{3}{16}|b|^2\right). \qquad (34')$$

This expression depends on χ in the same way as $d\sigma^{(\nu i)}$ does [formula (18)]. The ratio of the cross sections is, in order of magnitude, equal to

$$d\sigma^{(\nu)}/d\sigma^{(d)} \sim (s/v_0)\,(1 - s^2/v_n^2)^{-3/2} \qquad (35)$$

and can be larger than unity if $v_n \sim s$; in general, however, $d\sigma^{(0)} \sim d\sigma^{(d)}$.

7. We saw earlier that the cross section for the scattering of neutrons with excitation of zero sound oscillations is determined by the poles of the function $\Phi(q, \omega)$ for $|\omega|\tau \gg 1$. If $|\omega|\tau \sim 1$, then Φ does not have poles for values of ω close to the real axis. For $|\omega|\tau \sim 1$ we cannot, therefore, separate out of the scattering cross section a term corresponding to the excitation of sharply defined collective oscillations of the Fermi liquid. On the other hand, if $|\omega|\tau \ll 1$, the function Φ again has poles for values of ω close to the real axis. These poles ($\omega = \eta_s v_0 q - i\gamma_s$) determine the dispersion law and the damping coefficient of the zero sound oscillations (expressions for the velocity $\eta_s v_0$ and the damping coefficient γ_s of the sound have been found in the work of Landau [1] and Khalatnikov and Abrikosov [6]).

Denoting the quantity Φ for $|\omega|\tau \ll 1$ by Φ_s, we have

$$\Phi_s(q, \omega) = \frac{\hbar\omega}{6\pi\eta_s^2}\left(\frac{d\tau_p}{d\varepsilon_p}\right)_\zeta (N_\omega + 1)\left\{\frac{\gamma_s}{(\omega - \eta_s v_0 q)^2 + \gamma_s^2} + \frac{\gamma_s}{(\omega + \eta_s v_0 q)^2 + \gamma_s^2}\right\}. \qquad (36)$$

Substituting (36) in (21), we obtain the cross section for the scattering of the neutron with excitation ($\omega > 0$) and absorption ($\omega < 0$) of zero-sound oscillations:

$$d\sigma^{(s)} = \frac{1}{2\pi}\left(\frac{m^*}{m'}\right)^2 |a|^2 \frac{v_0}{v_n}\,\omega\,(N_\omega + 1)\,\frac{1}{\eta_s^2} \times \left\{\frac{\gamma_s}{(\omega - \eta_s v_0 q)^2 + \gamma_s^2} + \frac{\gamma_s}{(\omega + \eta_s v_0 q)^2 + \gamma_s^2}\right\}\frac{dp_n'}{p_0^3}. \qquad (37)$$

We note that the cross section for the scattering of neutrons with small energy transfer ($|\omega| \ll \tau^{-1}$) is of the order $|\omega|\tau$; for $|\omega|\tau \ll 1$ we can therefore neglect the probability for direct scattering as compared to the probability for the scattering with excitation of ordinary sound.

If $\gamma_s = 0$, the cross section for excitation of ordinary sound* contains the function $\delta(\omega - \eta_s v_0 q)$ [see formula (37)]. Replacing $(2\pi\hbar)^{-3}dp_n'$ by $(2\pi)^{-3}dq$ and integrating over the angular part of the vector q, we find for the cross section for the excitation of ordinary sound with a wave vector in the interval $(q, q + dq)$

$$d\sigma^{(s)} = \pi\,(m^*/m')^2\,|a|^2\,(N_\omega + 1)\,(v_0/v_n)^2\,\hbar^3 q^2\,dq/\eta_s p_0^3. \qquad (38)$$

Excitation of ordinary sound is possible only if $v_n > \eta_s v_0$.

Comparing (37) and (32), we see that we can obtain the part of $d\sigma^{(s)}$ which depends on ω and q by making the replacements $\eta_0 \to \eta_s$, $\gamma_0 \to \gamma_s$ in the corresponding part of $d\sigma^{(0)}$. The relations for the scattering of neutrons with excitation of zero sound are therefore also valid for the scattering with excitation of ordinary sound. In particular, if $\gamma_s = 0$ and $\eta_s v_0 < v_n < 2\eta_s v_0$, the neutrons can not be scattered into an angle which is larger than some limiting angle χ_s. This angle is given by formula (16), if we replace ξ_0 by $\xi_s = v_n/\eta_s v_0$. As in the case of the zero sound, the damping of the ordinary sound leads to a "smearing out" of the limiting scattering angle. Here the scattering cross section for the neutron within the angular interval $d\chi$ (integrated over the absolute value of the vector p_n') near the angle χ_s is proportional to $\gamma_s^{1/2}$.

8. Unfortunately, the only known Fermi liquid — He^3—has the property that the absorption of slow neutrons is very strong. For energies of the order of 1° K the capture cross section for neutrons in He^3 is $\sigma_c \sim 10^5 \times 10^{-24}$ cm^2, whereas the scattering cross section is only $\sigma_0 \sim 10^{-24}$ cm^2. For every scattering event there will thus be a very large number of neutron capture events leading to a strong absorption of the neutron wave. Since the mean free path of the neutron with respect to capture is equal to $l_c \sim (\rho_0\sigma_c)^{-1} \sim 10^{-3}$ cm, the neutrons will be scattered primarily in the surface layer of the He^3, the effective thickness of which is $\sim 10^{-3}$ cm. Moreover, one must consider the fact that the liquid He^3 will be heated up as a consequence of the nuclear reactions caused by the capture of the neutrons (this energy amounts to 5×10^5 ev per captured neutron, which means that 10^{15} He^3 nuclei will be heated up by 1°K for every scattering event). All these complications make the investigation of the scattering of slow neutrons in liquid He^3 very difficult. One may hope, however, that it will be possible to carry out such experiments as time goes on.

The authors are grateful to L. D. Landau, S. V. Peletminskii, and L. P. Pitaevskii for useful comments.

*An expression for $d\sigma^{(s)}$ without account of the attenuation of sound has been found independently and by a different method by M. Kaganov.

[1] L. D. Landau, JETP **32**, 59 (1957), Soviet Phys. JETP **5**, 101 (1957).

[2] Yu. L. Klimontovich and V. P. Silin, JETP **23**, 151 (1952).

[3] L. D. Landau, JETP **30**, 1058 (1956), Soviet Phys. JETP **3**, 920 (1957).

[4] L. Van Hove, Phys. Rev. **95**, 249 (1954).

[5] A. A. Abrikosov and I. M. Khalatnikov, JETP **34**, 198 (1958), Soviet Phys. JETP **7**, 135 (1958).

[6] I. M. Khalatnikov and A. A. Abrikosov, JETP **33**, 1154 (1957), Soviet Phys. JETP **6**, 888 (1958).

Translated by R. Lipperheide
88

INFLUENCE OF THE NUCLEAR PHOTOEFFECT ON THE PRIMARY COSMIC RAY SPECTRUM

N. M. GERASIMOVA and I. L. ROZENTAL'

P. N. Lebedev Physics Institute, Academy of Sciences, U.S.S.R.

Submitted to JETP editor February 25, 1961

J. Exptl. Theoret. Phys. (U.S.S.R.) 41, 488-490 (August, 1961)

The effect of the nuclear photoeffect on the energy spectrum of high-energy primary cosmic rays is investigated. An estimate indicates that it is very improbable for very high-energy ($\sim 10^{18}$ ev) heavy nuclei of intergalactic origin to appear in the galaxy.

HIGH energy cosmic-ray nuclei disintegrate in the galaxy as a result of the nuclear photoeffect on stellar photons. The nuclear photoeffect on photons from the sun was considered earlier.[1,2] Assuming that the radiation spectrum of most stars is similar to the solar spectrum, let us estimate the effective energy of the nuclei subject to photodisintegration. The photoeffect occurs at a photon energy on the order of 10^7 ev in the system moving with the nucleus. The mean energy of the photons radiated by the stars in the galaxy is about 1 ev. Going over to the frame moving with the nucleus, we find that the nuclei of interest to us should have a Lorentz factor

$$\gamma \approx \varepsilon / 2\varepsilon_0 \cos^2(\alpha/2) \approx 10^7. \quad (1)$$

Here ε and ε_0 are the photon energies in the coordinate systems moving with the nucleus and with the galaxy, respectively; α is the angle between the directions of motion of the nucleus and the photon. Consequently the effective energy for the photodisintegration will be

$$E \approx \gamma Mc^2 A \approx 10^{16} A. \quad (2)$$

Thus, the photoeffect on heavy nuclei can change the spectrum of cosmic radiation only at very high energies.

We shall assume henceforth, in accordance with one of the prevalent notions,[3] that the highest energy in cosmic radiation is possessed by the heavy nuclei; to be specific, we shall assume these to be iron nuclei. The time variation of the number N(E) of iron nuclei of given energy is

$$\partial N(E)/\partial t = Q(E) - N(E)/T_{\text{nuc}} - N(E)/T_{\text{ph}}(E). \quad (3)$$

The first term in the right side is the energy spectrum of the cosmic rays at their source, while the second and third terms represent the decrease of the number of nuclei in a given energy interval, due to respective interactions with interstellar matter and with the photons, the mean interaction times being T_{nuc} and T_{ph}.

Since we assume the processes occuring in the galaxy to be stationary, i.e.,

$$\partial N/\partial t = 0, \quad (4)$$

we have

$$N(E) = T_{\text{nuc}} Q(E) [1 + T_{\text{nuc}}/T_{\text{ph}}(E)]^{-1}. \quad (5)$$

Let us assume that the differential energy spectrum of the cosmic rays, without account of the photoeffect (i.e., $T_{\text{ph}} \to \infty$), is given by the power function

$$T_{\text{nuc}} Q(E) \approx KE^{-\beta}. \quad (6)$$

The modified spectrum will have the following form:

$$N(E)\,dE = KE^{-\beta}\,dE\,[1 + T_{\text{nuc}}/T_{\text{ph}}(E)]^{-1}. \quad (7)$$

The ratio $T_{\text{nuc}}/T_{\text{ph}}$ (E) is equal to

$$T_{\text{nuc}}/T_{\text{ph}}(E) = cT_{\text{nuc}} \int_{\varepsilon_{0min}}^{\infty} \sigma_{\text{ph}}(\varepsilon)\, n(\varepsilon_0)\, d\varepsilon_0, \quad (8)$$

where $\sigma_{\text{ph}}(\varepsilon)$ is the photodisintegration cross section of the nucleus; $n(\varepsilon_0)\,d\varepsilon_0$ is the spectrum of the stellar photons, and ε and ε_0 are related by Eq. (1). The function $\sigma_{\text{ph}}(\varepsilon)$ has already been defined earlier.[2]

The photon spectrum was specified in terms of the Planck function for black-body radiation at T = 5800°K (kT = 0.5 ev). After suitable integration (with some simplification which does not appreciably alter the results) and averaging over the angles, assuming isotropic distribution of the photons in the galaxy, we obtain

$$\frac{T_{\text{nuc}}}{T_{\text{ph}}(E)} \approx \frac{cT_{\text{nuc}} c_g \bar{n}_G}{1.2} \left(\frac{\varepsilon_g}{2\gamma kT}\right)^2 \frac{\exp(-\varepsilon_g/2\gamma kT)}{(a_g + \varepsilon_g/2\gamma kT)^2} \left[1 + \frac{2}{a_g + \varepsilon_g/2\gamma kT}\right]. \quad (9)$$

Here c_g, a_g, and ε_g are parameters in the photoeffect cross section, which are given in the nota-

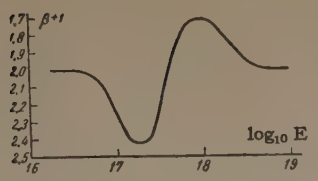

tion of[2] (for iron $c_g = 570$ mb, $a_g = 2.8$, and $\varepsilon_g = 13 \times 10^6$ ev), while $\bar{n}_G$ is the average photon density in the galaxy.

According to the available data,[4,5] the radiation energy density in the galaxy is approximately 0.3 ev/cm^3. If it is assumed that the average photon energy in the radiation from stars is about 1 ev, we get $\bar{n}_G \sim 0.3$ cm^{-3}. The maximum value of the ratio T_{nuc}/T_{ph} (E) for iron, attainable at $E \approx 6 \times 10^{17}$ ev, amounts then to 0.8.

The diagram shows the variation of the exponent of the integral spectrum of the nuclei of a given isotope of iron, due to photodisintegration. It must be emphasized that inasmuch the reactions (γ, n) and (γ, 2n) predominate in the region of giant resonance, there is no complete breakup of the heavy nuclei if T_{nuc}/T_{ph} (E) $\lesssim 1$. All that changes is the isotopic composition of the primary component, which is of galactic origin.

Let us consider now the influence of the photoeffect on cosmic rays that move in intergalactic space.* The lifetime of the iron nucleus in the galaxy is $T_{nuc} \approx 1.4 \times 10^8$ years. Since the density in intergalactic space is three orders of magnitude lower than in the galaxy, the average lifetime between collisions is about 10^{11} years there. However, this is longer than the age of the galaxy ($\sim 10^{10}$ years). We must therefore assume that the nuclei practically do not collide with nuclei of matter in the metagalaxy.

In order to estimate the density of the photons in the intergalactic region, we assume that all galaxies radiate in a fashion similar to ours, and the total radiation is proportional to the number of galaxies in the visible part of the world. Then the ratio of the density of the number of photons $\bar{n}_i$ in the intergalactic space to the density $\bar{n}_G$ will be

$$\bar{n}_i/\bar{n}_G \approx 4\pi R_i R_G^2 \eta. \qquad (10)$$

Here $R_G \approx 5 \times 10^{22}$ cm is the radius of the galaxy; we assume R_i to be equal to one-quarter of the radius of the entire visible part of the universe,† i.e., about ($^1/_4 \times 10^{28}$ cm; finally, a is the distribution density of the galaxies. According to astrophysical data,* a volume 5 million parsec in radius contains on the average some 300 galaxies with $\sim 10^{10}$ stars and about 30 galaxies with $\sim 10^{11}$ stars like our own galaxy. Since we start from the radiation density in our own galaxy, we assume that the equivalent radiation will be produced by 60 galaxies with 10^{11} stars. Then $\eta \approx 4 \times 10^{-75}$ galaxies per cubic centimeter, and

$$\bar{n}_i/\bar{n}_G \approx {}^1/_3.$$

According to Allen[5] $n_i/n_G \approx 1/4$.

Estimating on the basis of these figures the lifetime of the nuclei for the photoeffect, we obtain $T_{ph} \sim 10^9$ years. Therefore, if nuclei with energy $\sim 10^{18}$ ev were formed in the intergalactic space $\sim 10^{10}$ years ago, they could not be conserved, owing to the photoeffect, and there is no intergalactic component of the cosmic radiation spectrum with this value of energy.

On the other hand, if the nuclei are being produced at the present time, these estimates enable us to establish the dimensions of that region in space, from which they arrive into the galaxy. Ginzburg and Syrovat-skii[3] give a figure of 1.5×10^{26} cm for the dimensions of this region. The effect considered here reduces this radius by another factor of three, since the lifetime of the nuclei of higher energies is decreased by the photoeffect by one order of magnitude. Inasmuch as there are few new stars or other objects capable of serving as powerful sources of cosmic rays in that region, this fact makes also probable the conclusion that the intergalactic component of the cosmic rays makes no contribution to the corresponding part of the spectrum observed on earth.

The authors are grateful to V. L. Ginzburg and S. I. Syrovat-skii for discussions.

*Our attention was called to this question by E. L. Feĭnberg.

†We do not consider the red shift in this part of the universe, and we neglect the contribution to the radiation from the remaining part. A more accurate account of the red shift can result in only an insignificant correction.

*The authors take this opportunity to thank A. A. Korchak, S. B. Pikel'ner, and I. S. Shklovskii for information on the astrophysical data.

[1] G. T. Zatsepin, DAN SSSR 80, 577 (1951).

[2] N. M. Gerasimova and G. T. Zatsepin, JETP 38, 1245 (1960), Soviet Phys. JETP 11, 899 (1960).

[3] V. L. Ginzburg and S. I. Syrovat-skii, UFN 71, 411 (1960), Soviet Phys. Uspekhi 3, 504 (1961).

[4] H. Lambrecht and H. Zimmermann, Mat. Naturw. Reihe 5, 217 (1955—1956).

[5] C. W. Allen. Astrophysical Quantities, University of London, The Athlone Press, (1955).

Translated by J. G. Adashko
89

LOW-ENERGY LIMIT OF THE γN-SCATTERING AMPLITUDE AND CROSSING SYMMETRY

L. I. LAPIDUS and CHOU KUANG-CHAO

Joint Institute for Nuclear Research

Submitted to JETP editor February 27, 1961

J. Exptl. Theoret. Phys. (U.S.S.R.) 41, 491-494 (August, 1961)

The low energy limit for the γN scattering amplitude is derived with the aid of single-nucleon invariant amplitudes. Subsequent terms in ν for $Q^2 = 0$ and the expression for the limiting value of the first derivative in Q^2 as $Q^2 \to 0$ can be obtained by taking into account the conditions of crossing symmetry.

1. Low, Gell-Mann, and Goldberger showed [1] that the condition of relativistic and gauge invariance makes it possible to express the limiting value of the amplitudes for the scattering of low energy γ quanta on spin-$\frac{1}{2}$ particles and the limiting value of the derivative of the amplitude with respect to the frequency as $\nu \to 0$ in terms of the charge and magnetic moment of the particle. This result was later generalized [2] to the case of elastic scattering of γ quanta by particles with other spins and also to the case of bremsstrahlung. [3] The result for elastic scattering also holds when only CP invariance is assumed. Consideration of the single-nucleon terms in the dispersion relations for γN scattering [4-6] also leads to the limit theorem. (A similar result holds for bremsstrahlung. [7])

In the present note, we derive the limit theorem for γN scattering on the basis of the single-nucleon terms. The requirement of crossing symmetry for the invariant functions $T_i(\nu, Q^2)$ $(= 1, \ldots, 6)$ makes it possible to obtain additional terms for the limiting values of the functions $R_i(\nu, 0)$, which characterize the γN scattering matrix in the center-of-mass system, and also the limiting values of the derivatives of the amplitudes with respect to Q^2 as $\nu \to 0$. (For the definition of the quantities T_i and R_i see, e.g., [6].)

2. The invariant functions $T_i(\nu, Q^2)$ are related to the scalar functions $R_i(\nu, Q^2)$ $(i = 1, \ldots, 6)$ in the following way:

$$T_1 - T_3 = \frac{8MW^2}{(W^2-M^2)^2}\left[\nu - \frac{W-M}{W+M}\frac{Q^2}{M}\right](R_3 + R_4) - \frac{4W}{(M+W)}\left[1 - \frac{4Q^2W^2}{(W^2-M^2)^2}\right](R_1 + R_2),$$

$$T_2 - T_4 = \frac{8MW^2}{(W^2-M^2)^2}\left[1 + \frac{2W}{M}\frac{Q^2}{(W+M^2)}\right](R_3 + R_4) + \frac{4W}{(W+M)^2}\left[1 - \frac{4Q^2W^2}{(W^2-M^2)^2}\right](R_1 + R_2),$$

$$T_1 + T_3 = \frac{8MW^2}{(W^2-M^2)^2}\left[\nu - \frac{W-M}{W+M}\frac{Q^2}{M}\right](R_3 - R_4) + \frac{16W^3Q^2}{(W+M)(W^2-M^2)^2}(R_1 - R_2),$$

$$T_2 + T_4 = \frac{8MW^2}{(W^2-M^2)^2}\left[1 + \frac{2W}{M}\frac{Q^2}{(W+M)^2}\right](R_3 - R_4) - \frac{16W^3Q^2}{(W+M)^2(W^2-M^2)^2}(R_1 - R_2),$$

$$\frac{M\nu + Q^2}{W^2}T_5 = \frac{8W^2Q^2}{(W^2-M^2)^2}(R_5 - R_6) - (R_3 - R_4),$$

$$\frac{M\nu + Q^2}{W}T_6 = \left(2 - \frac{8W^2Q^2}{(W^2-M^2)^2}\right)(R_5 + R_6) + (R_3 + R_4), \quad (1)$$

where W is the total c.m.s. energy and ν and Q^2 are two invariants characterizing the kinematics of the process; $W^2 - M^2 = 2M\nu + 2Q^2$.

The pole terms for $T_i(\nu, Q^2)$ have the form [6]

$$T_1^0 = \frac{2e^2}{M}\frac{Q^2}{Q^4/M^2 - \nu^2}, \qquad T_2^0 = \frac{e^2}{M}\frac{\nu}{Q^4/M^2 - \nu^2}, \qquad T_3^0 = 0,$$

$$T_4^0 = -\frac{e^2(1+\lambda)^2}{M}\frac{\nu}{Q^4/M^2 - \nu^2},$$

$$T_5^0 = MT_6^0 = \frac{e^2(1+\lambda)}{M}\frac{Q^2}{Q^4/M^2 - \nu^2}, \quad (2)$$

where we have used the system of units in which $\hbar = c = 1$ and the magnetic moment is $\mu = e(1 + \lambda)/2M$.

For $Q^2 = 0$, it follows from (1) that

$$(T_1 - T_3)_0 = \frac{2W^2}{M\nu}(R_3 + R_4)_0 - \frac{4W}{W+M}(R_1 + R_2)_0,$$

$$(T_2 - T_4)_0 = \frac{2W^2}{M\nu^2}(R_3 + R_4)_0 + \frac{4W}{(W+M)^2}(R_1 + R_2)_0,$$

$$(T_1 + T_3)_0 = \frac{2W^2}{M\nu}(R_3 - R_4)_0, \quad (T_2 + T_4)_0 = \frac{2W^2}{M\nu^2}(R_3 - R_4)_0,$$

$$(T_5)_0 = -\frac{W^2}{M\nu}(R_3 - R_4)_0,$$

$$(T_6)_0 = \frac{W}{M\nu}[2(R_5 + R_6) + R_3 + R_4].$$

Differentiating the relations in (1) with respect to Q^2, we obtain, in the limit $Q^2 = 0$,

$$(T_1 - T_3)_0' = \frac{2W^2}{M\nu}(R_3 + R_4)_0' - \frac{4W}{W+M}(R_1 + R_2)_0'$$
$$- \frac{2(2W^3 + M^2W + M^3)}{M^2\nu^2(W+M)}(R_3 + R_4)_0$$
$$+ \frac{4}{W(W+M)}\left[\frac{W^4}{M^2\nu^2} - \frac{M}{W+M}\right](R_1 + R_2)_0,$$

$$(T_2 - T_4)_0' = \frac{2W^2}{M\nu^2}(R_3 + R_4)_0' + \frac{4W}{(W+M)^2}(R_1 + R_2)_0'$$
$$+ \frac{4}{M^2\nu^2}\left[\frac{W^3}{(W+M)^2} - M - \frac{M^2}{\nu}\right](R_3 + R_4)_0$$
$$- \frac{4}{(W+M)^2}\left[\frac{W^3}{M^2\nu^2} - \frac{1}{W} + \frac{2}{M+W}\right](R_1 + R_2)_0,$$

$$(T_1 + T_3)_0' = \frac{2W^2}{M\nu}(R_3 - R_4)_0'$$
$$- \frac{2(2W^3 + WM^2 + M^3)}{M^2\nu^2(W+M)}(R_3 - R_4)_0$$
$$+ \frac{4W^3}{(W+M)M^2\nu^2}(R_1 - R_2)_0,$$

$$(T_2 + T_4)_0' = \frac{2W^2}{M\nu^2}(R_3 - R_4)_0'$$
$$+ \frac{4(R_3 - R_4)_0}{M^2\nu^2}\left[\frac{W^3}{(W+M)^2} - M - \frac{M^2}{\nu}\right]$$
$$- \frac{4W^3}{(W+M)^2}\frac{(R_1 - R_2)_0}{M^2\nu^2},$$

$$(T_5)_0' = \frac{W^2}{M\nu}\left[\frac{2W^2}{M^2\nu^2}(R_5 - R_6)_0 - (R_3 - R_4)_0'\right.$$
$$\left. + \frac{M}{W^2\nu}(R_3 - R_4)_0\right],$$

$$(T_6)_0' = \frac{W}{M\nu}\left[-\frac{2W^2}{M^2\nu^2}(R_5 + R_6)_0\right.$$
$$+ (2R_5 + 2R_6 + R_3 + R_4)'$$
$$\left. - \frac{M+\nu}{W^2\nu}(2R_5 + 2R_6 + R_3 + R_4)\right]. \quad (4)$$

It is seen from (2) that the terms $T_1 - T_3$ and $T_2 + T_4$ do not contain poles for $Q^2 = 0$. It then follows from (1) that $(R_1 + R_2)_0$ and $(R_3 \pm R_4)_0/\nu$ are finite when $\nu \to 0$.

Since the functions $(T_2 \mp T_4)_0$ have a singularity of the form

$$\left[-\frac{e^2}{M} \mp \frac{e^2}{M}(1+\lambda)^2\right]\frac{1}{\nu},$$

it then follows from (1) that

$$\frac{(R_3 \pm R_4)_0}{\nu} = -\frac{e^2}{2M^2}[1 \pm (1+\lambda)^2] \quad (5)$$

as $\nu \to 0$, which is in accordance with the limit theorem.

Since T_5 and T_6 do not contain poles when $Q^2 = 0$, the quantity $(R_5 + R_6)/\nu$ should remain constant as $\nu \to 0$. Similarly, from the condition that $(T_1 \pm T_3)_0'$ contains a pole of the second order

$$(T_1 \pm T_3)_{0p}' = -2e^2/M\nu^2,$$

and that $\nu(T_2 - T_4)_0'$ does not contain a pole, it follows that

$$(R_1 \pm R_2)_0 = -e^2/M, \quad (6)$$

and $(R_3 \pm R_4)_0' \to$ const and $\nu(R_1 \pm R_2)_0' \to$ const as $\nu \to 0$.

Since

$$(T_5)_{0p}' = M(T_6)_{0p}' = -e^2(1+\lambda)/2M^2,$$

we conclude that

$$(R_5 \pm R_6)_0 = \pm e^2(1+\lambda)\nu/2M^2, \quad (7)$$

and $(2R_5 + 2R_6 + R_3 + R_4)_0' \to$ const as $\nu \to 0$.

We see that formulas (5)—(7) obtained from consideration of the pole terms (2) contain the results of the limit theorem for $Q^2 = 0$.

3. It is of interest to note that with the aid of the conditions of crossing symmetry one can obtain additional information on the low energy limit. It follows from crossing symmetry that, for example, the quantity $T_1 - T_3$ should be an even function of ν. If in the first relation of (3) we make the substitution

$$(R_1 + R_2)_0 = -\frac{e^2}{M} + \alpha_1\nu + \ldots,$$
$$(R_3 + R_4)_0 = -\frac{e^2}{2M^2}[1 + (1+\lambda)^2]\nu + \alpha_3\nu^2 + \ldots \quad (8)$$

and take into account the fact that $W = (M^2 + 2M\nu)^{1/2} \approx M(1 + \nu/M)$ for small ν, then from the condition that there is no linear dependence on ν we obtain the relation

$$\alpha_3 M - \alpha_1 = (e^2/M)\left[\tfrac{1}{2} + (1+\lambda)^2\right]. \quad (9)$$

It follows from the requirement of crossing symmetry that the quantity $\nu(T_2 - T_4)$ should be an even function of ν.

The absence of a linear dependence of the terms on ν leads to the relation

$$\alpha_3 M = (e^2/M)\left[\tfrac{3}{2} + (1+\lambda)^2\right]. \quad (10)$$

From (8)—(10) we have

$$(R_1 + R_2)_0 = -\frac{e^2}{M}\left(1 - \frac{\nu}{M}\right) + O(\nu^2),$$
$$(R_3 + R_4)_0 = -\frac{e^2}{2M^2}\left(1 - \frac{3\nu}{M}\right)\nu$$
$$- \frac{e^2}{2M^2}(1+\lambda)^2\left(1 - \frac{2\nu}{M}\right)\nu + O(\nu^3). \quad (11)$$

The functions $T_1 + T_3$, T_5, $(T_2 + T_4)$, and T_6 should be even functions of ν. Similar considerations lead to

$$(R_3 - R_4)_0 = -\frac{e^2}{2M^2}[1 - (1+\lambda)^2]\left(1 - \frac{2\nu}{M}\right)\nu + O(\nu^3), \quad (12)$$

and

$$[2(R_5 + R_6) + R_3 + R_4]_0$$

$$= -\frac{e^2}{2M^2}\lambda^2\left(1 - \frac{\nu}{M}\right)\nu + O(\nu^3), \qquad (13)$$

$$(R_5 + R_6)_0 = \frac{e^2(1+\lambda)}{2M^2}\nu$$

$$+ \frac{e^2}{4M^3}[\lambda^2 - 3 - 2(1+\lambda)^2]\nu^2 + O(\nu^3). \qquad (13')$$

The function $(T_1 - T_3)_0'$ is an even function of ν. Inserting in (4)

$$(R_3 + R_4)_0' = \alpha_3' + \ldots, \qquad (R_1 + R_2)_0' = \alpha_1'/\nu + \ldots,$$

we obtain from the condition that there is no term proportional to $1/\nu$

$$2M\alpha_3' - 2\alpha_1' = (e^2/M)[1 - 2(1+\lambda)^2].$$

A similar condition for the even function $\nu(T_2 - T_4)_0'$ leads to

$$2M\alpha_3' = -(e^2/M)[3 + 2(1+\lambda)^2].$$

Then $\alpha_1' = -2e^2/M^2$, and therefore

$$(R_1 + R_2)_0' = -2\frac{e^2}{M^2}\frac{1}{\nu} + O(1),$$

$$(R_3 + R_4)_0' = -\frac{e^2}{2M^2}[3 + 2(1+\lambda)^2] + O(\nu). \qquad (14)$$

The condition that the poles of the first order in the even functions $(T_1 + T_3)_0'$ and $\nu(T_2 + T_4)$ vanish leads to

$$(R_1 - R_2)_0 = -\frac{e^2}{M}\left(1 - \frac{3\nu}{M}\right) + O(\nu^2),$$

$$(R_3 - R_4)_0' = \frac{e^2}{2M^3}[-3 + 2(1+\lambda)^2] + O(\nu). \qquad (15)$$

Similar conditions for the functions $(T_5)_0'$ and $(T_6)_0'$ require that

$$(R_5 - R_6)_0 = -\frac{e^2(1+\lambda)}{2M^2}\nu + \frac{e^2}{4M^3}[-2 + 8(1+\lambda)$$

$$+ (1+\lambda)^2]\nu^2 + O(\nu^3),$$

$$(2R_5 + 2R_6 + R_3 + R_4)_0' = -\frac{e^2}{2M^3}(2\lambda^2 - 2\lambda - 1). \qquad (16)$$

It should be kept in mind that the expression for the limiting energy is valid for amplitudes in the center-of-mass system. The result obtained can be useful for analysis of the scattering of γ quanta by nucleons with the aid of the dispersion relation technique.

[1] F. Low, Phys. Rev. **96**, 1428 (1954); M. Gell-Mann and M. L. Goldberger, Phys. Rev. **96**, 1433 (1954).

[2] L. I. Lapidus and Chou Kuang-Chao, JETP **39**, 1286 (1960), Soviet Phys. JETP **12**, 898 (1961).

[3] F. E. Low, Phys. Rev. **110**, 974 (1958).

[4] N. N. Bogolyubov and D. V. Shirkov, Doklady Akad Nauk SSSR **113**, 529 (1957).

[5] T. Akiba and I. Sato, Progr. Theoret. Phys. (Kyoto) **19**, 93 (1958).

[6] L. I. Lapidus and Chou Kuang-Chao, JETP **41**, 294 (1961), Soviet Phys. JETP **14**, 210 (1962).

[7] S. M. Bilen'kii and R. M. Ryndin, JETP **40**, 819 (1961), Soviet Phys. **13**, 575 (1961).

Translated by E. Marquit
90

ELECTROMAGNETIC INTERACTION OF A NEUTRAL VECTOR MESON

I. Yu. KOBZAREV, L. B. OKUN', and I. Ya. POMERANCHUK

Institute for Theoretical and Experimental Physics, Academy of Sciences, U.S.S.R.

Submitted to JETP editor February 28, 1961

J. Exptl. Theoret. Phys. (U.S.S.R.) **41**, 495-498 (August, 1961)

The interaction between a neutral vector meson and a photon is considered. The two particles can transform into each other. In this connection the problem of diagonalization of the Green's function for the vector meson and photon is examined.

THE literature has been recently full of discussions on the existence of a hypothetical neutral vector meson ρ^0, endowed with strong interactions.[1-4] The interaction of the ρ^0 meson with the conserved current of strongly interacting particles j_s

$$\sqrt{4\pi}\, g B_\mu j_{s\mu}$$

(B_μ is the ρ^0 meson field, g is the coupling constant) resembles strongly the interaction of a photon with the current of charged particles j_e

$$\sqrt{4\pi}\, e A_\mu j_{e\mu}$$

(A_μ is the photon field, e is the electric charge). Since the spin and space and charge parities of the ρ^0 meson and photon are the same, the virtual transition $\rho^0 \to \gamma$ is possible since there exist strongly interacting charged particles, which contribute to both currents j_s and j_e.* From gauge invariance considerations it follows that the amplitude for such a transition will be of the form

$$P^{\rho\gamma}_{\mu\nu} = (\delta_{\mu\nu}k^2 - k_\mu k_\nu)\, P(k^2) \qquad (P(k^2) \sim ge),$$

where k is the momentum of the meson, μ, ν are polarization indices of the meson and photon. Since both j_s and j_e are conserved it follows that the second term in $P^{\rho\gamma}_{\mu\nu}$ never contributes and may be discarded. In what follows we shall take

$$P^{\rho\gamma}_{\mu\nu} = k^2 \delta_{\mu\nu} P(k^2).$$

The simplest diagram for $P(k^2)$ is shown in Fig. 1. Using the conventional way of calculating, one obtains from such a diagram a quadratically divergent expression, which violates gauge invariance. One must therefore discard the quadratically divergent part of the integral, just as is done in calculating vacuum polarization in electrodynamics. (Let us note that the loop under consideration is exactly the same as the loop involved in photon vacuum polarization.) The remaining part of the integral contains a logarithmic divergence. In electrodynamics this divergence is absorbed into charge renormalization. In the present case we must introduce for the ρ-γ transition a special constant.

FIG. 1

The existence of the ρ-γ transition leads[1] to the appearance of a pole at $k^2 = m^2$ (where m is the mass of the meson) in the amplitude for p-e (n-e) scattering, as a result of the diagrams shown in Fig. 2. The corresponding matrix element is of the form

$$M \sim eg \frac{1}{k^2 - m^2} k^2 P(k^2) \frac{1}{k^2} = \frac{egP(k^2)}{k^2 - m^2}.$$

Such a pole appears also in e-e scattering as a consequence of more complicated diagrams.

As a result of the ρ-γ transition it is possible to emit in electron collisions the ρ^0 meson with an amplitude, proportional to the corresponding vertex part (Fig. 3), which is given by

FIG. 2

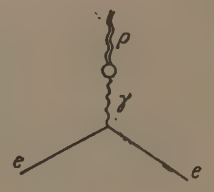

FIG. 3

*Within the framework of Sakata's model we may assume that

$$j_s = \bar{p}\gamma_\alpha p + \bar{n}\gamma_\alpha n + \bar{\Lambda}\gamma_\alpha \Lambda,$$

$$j_e = -\bar{p}\gamma_\alpha p + \bar{e}\gamma_\alpha e + \bar{\mu}\gamma_\alpha \mu$$

(in this connection see reference 2). The proton enters into both these currents.

$$ek^{-2}P(k^2)\,k^2|_{k^2=m^2} = eP(m^2).$$

We note that the amplitude for the ρ-γ transition chosen by us does not contribute to the photon vertex part at $k^2 = 0$, and therefore has no effect on the emission of real photons. If that were not the case Ward's identity in electrodynamics would be upset and the equality of the electromagnetic charges of the electron and the proton would no longer hold.[5]

We see that the presence of the ρ-γ transition leads in effect to the appearance of an interaction between the ρ^0 meson and the electric current, with a coupling constant equal to $eP(m^2) \sim e^2g$. We shall now carry out a more detailed discussion of this problem. We introduce the following D functions: for the ρ meson $D^{\rho\rho}$ (Fig. 4a), for the photon $D^{\gamma\gamma}$ (Fig. 4b), and also a new function $D^{\rho\gamma}$ for the diagram pictured in Fig. 4c. Let us note that the cross-hatched loops indicate the totality of diagrams (connected and disconnected).

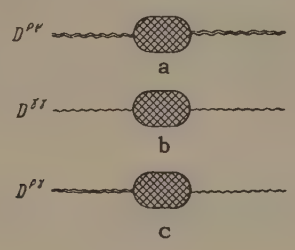

FIG. 4

Let us consider now electron-electron (e-e), electron-proton (e-p), electron-neutron (e-n), and proton-proton (p-p) scattering. The corresponding pole amplitudes are given by

$$M_{ne} = geD^{\rho\gamma}, \qquad M_{nn} = g^2D^{\rho\rho},$$

$$M_{pe} = geD^{\rho\gamma} + e^2D^{\gamma\gamma}, \qquad M_{pp} = g^2D^{\rho\rho} + 2geD^{\rho\gamma} + e^2D^{\gamma\gamma},$$

$$M_{ee} = e^2D^{\gamma\gamma} \qquad (1)$$

For simplicity we shall ignore the diagonal vacuum polarizations $P^{\rho\rho}$ and $P^{\gamma\gamma}$ and take into account only the amplitude $P^{\rho\gamma}$, which describes the totality of connected diagrams for the ρ-γ transition. By summing chains of diagrams we obtain

$$D^{\gamma\gamma} = 1/k^2 + P^2(k^2)/(k^2 - m^2 - k^2P^2(k^2)),$$

$$D^{\rho\rho} = 1/(k^2 - m^2 - k^2P^2(k^2)),$$

$$D^{\rho\gamma} = P(k^2)/(k^2 - m^2 - k^2P^2(k^2)). \qquad (2)$$

We now introduce diagonalized propagation functions for the photon and ρ meson:

$$D^{\gamma\gamma}_{diag} = 1/k^2, \qquad D^{\rho\rho}_{diag} = 1/(k^2 - m^2 - k^2P^2(k^2)).$$

It then follows from Eqs. (1) and (2) that

$$M_{ee} = e^2D^{\gamma\gamma}_{diag} + (eP)^2D^{\rho\rho}_{diag},$$

$$M_{nn} = g^2D^{\rho\rho}_{diag}, \qquad M_{ne} = gePD^{\rho\rho}_{diag},$$

$$M_{pe} = (g + eP)(eP)D^{\rho\rho}_{diag} + e^2D^{\gamma\gamma}_{diag}. \qquad (3)$$

The formulas (3) may be interpreted as follows: 1) the photon mass vanishes, as before; 2) the electric charge remains unchanged; 3) the pole of $D^{\rho\rho}_{diag}$ determines the renormalized mass M^2 of the ρ meson, where

$$M^2 - m^2 - M^2P^2(M^2) = 0 \text{ or } M^2 = m^2/(1 - P(M^2));$$

4) the renormalized charge for the interaction of the ρ meson with j_S is given by

$$g_{ren} = gZ^{1/2},$$

where

$$Z = [1 - P^2(M^2) - M^2\partial P^2/\partial k^2]^{-1}|_{k^2=M^2};$$

5) as a result of diagonalization an interaction of the ρ meson with the current j_e has been produced with the vertex part $P(k^2)$ and renormalized charge given by

$$h_{ren} = eP(M^2)\,Z^{1/2}.$$

Since $P(k^2)$ contains a logarithmic divergence h_{ren} cannot in fact be calculated but must be introduced as a new constant.

The diagonalization here performed can be illustrated by the following example. Consider the Lagrangian of the ρ and γ fields, containing the ρ-γ transition and the interaction with external currents J_S and J_e:

$$L = \tfrac{1}{2}B_\mu(k^2 - m^2)B_\mu + \tfrac{1}{2}A_\mu k^2A_\mu - A_\mu B_\mu\lambda k^2 - eJ_{e\mu}A_\mu - gJ_{s\mu}B_\mu$$

(A_μ and B_μ are respectively the photon and meson fields). Let us now introduce the renormalized (diagonal) fields*

$$A' = A - \lambda B, \quad B' = \sqrt{1-\lambda^2}B;$$
$$A = A' - \lambda B'/\sqrt{1-\lambda^2}, \quad B = B'/\sqrt{1-\lambda^2}.$$

Then the Lagrangian may be written in the form

$$A'_\mu k^2A'_\mu + B'_\mu(k^2 - M^2)B'_\mu - g_{ren}B'_\mu J_{s\mu} - eA'_\mu J_{e\mu} - hJ_{e\mu}B'_\mu,$$

where

$$M^2 = m^2/(1-\lambda^2), \quad g_{ren} = g/\sqrt{1-\lambda^2},$$

$$h = \lambda e/\sqrt{1-\lambda^2}.$$

It is seen that as a result of diagonalization the mass of the ρ meson and the strong interaction coupling constant g underwent renormalization,

*An analogous diagonalization procedure is contained in[6].

and the interaction of the ρ meson with the current J_e with the constant h appeared. The expressions obtained here for M^2, g_{ren} and h coincide with those obtained earlier in the case when $P(k^2) = \lambda = \text{const}$.

The authors express their gratitude to A. D. Galanin, B. L. Ioffe, and K. A. Ter-Martirosyan for useful discussions.

Note added in proof (July 14, 1961). The ρ-γ transition is discussed to some extent in the paper by Huff [R. W. Huff, Phys. Rev. 112, 1021 (1958)] with which we have become familiar after our work was sent to press.

[1] Y. Nambu, Phys. Rev. **106**, 1366 (1957).

[2] Y. Fuji, Progr. Theor. Phys. **21**, 232 (1959). I. Kobzarev and L. Okun', JETP **41**, 499 (1961), this issue p. 358.

[3] J. J. Sakurai, Phys. Rev. **119**, 1784 (1960).

[4] M. Gell-Mann and R. P. Feynman, Proc. of Tenth Rochester Conference, pp. 499, 508 (1960).

[5] M. Gell-Mann, Proc. of Tenth Rochester Conference, p. 792 (1960).

[6] S. Okubo, Nuovo cimento **16**, 963 (1960). Feinberg, Kabir, and Weinberg, Phys. Rev. Lett. **3**, 527 (1959). Cabibbo, Gatto, and Zemach, Nuovo cimento **16**, 168 (1960).

Translated by A. M. Bincer
91

ON THE THEORY OF THE VECTON

I. Yu. KOBZAREV and L. B. OKUN'

Institute for Theoretical and Experimental Physics, Academy of Sciences, U.S.S.R.

Submitted to JETP editor February 28, 1961

J. Exptl. Theoret. Phys. (U.S.S.R.) **41**, 499-506 (1959)

Consequences of the hypothesis that strong interactions arise as a result of the interaction of a neutral vector particle—the vecton—with the baryon current are considered. The problem of the origin in such a model of isotopic invariance, and, in particular, of the appearance of a π-meson triplet is discussed. Experimental possibilities of detecting the vecton are examined in detail.

INTRODUCTION

IN this paper we would like to make a number of remarks about a hypothetical neutral vector meson to which we shall from now on refer as the vecton and which we shall denote by ρ^0. The vecton is not a new entity in the physics of elementary particles. The idea that strong interactions, in analogy to electromagnetic interactions, are due to the exchange of neutral vector mesons has been widely discussed already in the 1930's and 1940's (cf. the well-known books of Wentzel[1] and Pauli[2]). However, at that time such a model was rejected because, firstly, charged mesons ($\pi^{\pm}$) were discovered, and secondly, within the framework of perturbation theory the vecton theory of strong interactions contradicted experiment: in particular, it was not possible to obtain the correct sign of the quadrupole moment of the deuteron.[2]

In the late 1950's theoreticians again turned to the vecton for an explanation of the electromagnetic properties of the nucleon (Nambu[3]) and of spin-orbit nuclear forces (Sakurai,[4] Breit[5]). These authors considered the vecton together with other mesons, both actual and hypothetical, basing their work explicitly or implicitly on the idea that all the known mesons and baryons are of an equally elementary nature. In addition to these papers there appeared the paper of Fujii,[6] in which the vecton was treated as the only elementary meson responsible for the interaction between the elementary baryons (proton, neutron and Λ hyperon). He treated the other mesons and baryons as compound particles (the Sakata model[7-9]).*

*The problem of the vecton in connection with the Sakata model was also considered by Feynman[10] and by Gell-Mann.[11]

STRANGENESS AND ISOTOPIC INVARIANCE

In common with Fujii[6] we assume that the Lagrangian for the strong interaction has the form

$$L_s = j_{s\alpha} B_\alpha, \tag{1}$$

where B_α is the vecton field, while the strong interaction current $j_{S\alpha}$ is given by

$$j_{s\alpha} = \sqrt{4\pi} g (\bar{\psi}_p \gamma_\alpha \psi_p + \bar{\psi}_n \gamma_\alpha \psi_n + \bar{\psi}_\Lambda \gamma_\alpha \psi_\Lambda). \tag{2}$$

In the approximation in which all the interactions with the exception of the strong interaction are switched off there is degeneracy between the three baryons. The consequences of this degeneracy have been examined in detail by Ohnuki et al.[12] We know from experiment that the strong interactions of the Λ particle are not identical with the strong interactions of the nucleons (the $\Lambda\Lambda\pi$ vertex is absent, the K-meson mass exceeds the π-meson mass by more than a factor of three, etc.). Consequently, there must exist a mechanism responsible for lifting the degeneracy between the Λ particle and the nucleons.

There exist several possible mechanisms for lifting the degeneracy. Some of these amount to the supposition that the Λ particle has some sort of an additional interaction compared to the nucleons; others amount to the supposition that it is the nucleon which has such an additional interaction. For example, Sakurai assumed that nucleons interact with a triplet of hypothetical nuclear mesons.

In our paper[13] we have assumed that there exists a neutral meson which interacts with the Λ hyperon and with the muon. This has enabled us to remove the degeneracy not only between Λ and n, but also between μ and e. Finally, it is possible to assume that the reason for the splitting lies in the bare mass of the Λ hyperon, which

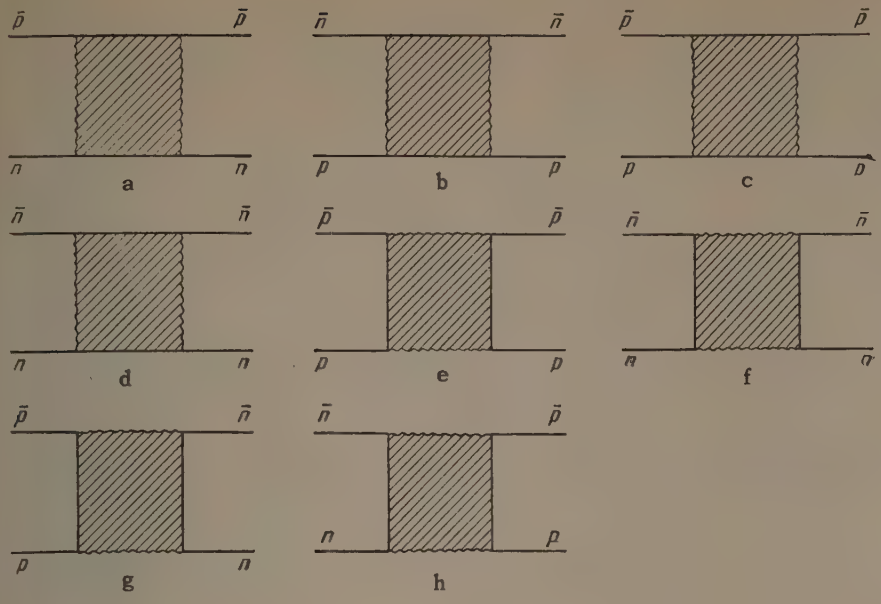

FIG. 1. a – $a(\bar{p}n)^2$, b – $a(\bar{n}p)^2$, c – $a(\bar{p}p)^2$, d – $a(\bar{n}n)^2$, e – $b(\bar{p}p)^2$, f – $b(\bar{n}n)^2$, g – $b(\bar{p}p)(\bar{n}n)$, h – $b(\bar{n}n)(\bar{p}p)$.

may be unequal to the bare masses of the proton and the neutron. The difference between the masses of the Λ hyperon and the nucleon will lead as a result of virtual processes to a difference in the strong interactions of these particles in spite of the fact that the "initial" strong interaction (2) is completely identical in the two cases. Thus, the bare mass of the Λ hyperon can be responsible for strangeness.

In order for strong interactions to be isotopically invariant within the framework of the scheme under consideration it is necessary and sufficient that the bare masses of the proton and the neutron should be equal, since it can be easily seen that the Lagrangian (1) is an isotopic scalar. Thus, the isotopic invariance of strong interactions with all its ramifications (the existence of isotopic multiplets, the relation between the interaction constants of the particles composing a given multiplet, the existence of selection rules with respect to isotopic spin, etc.) is a consequence of the symmetry of the current (2) with respect to the proton and the neutron and of the equality of the bare masses of these particles.

Apprehensions can arise that the Lagrangian (1) is too symmetric (since it contains only the neutral current) so that, for example, it will not yield a splitting between the π^0 meson and the π_0^0 meson (the hypothetical pseudoscalar meson of isotopic spin equal to zero). However, it can be easily seen that these apprehensions are unfounded. In order to do this we consider the diagrams representing the scattering of a nucleon by an antinucleon (Fig. 1) where the shaded regions denote virtual ρ mesons and closed nucleon loops. Since the ρ meson is an isotopic scalar, the contributions of diagrams a, b, c, d (Fig. 1) are all equal; we denote them by a. The contributions of diagrams e, f, g, h are also all equal; we denote them by b. The amplitudes for the different diagrams are shown in the caption for Fig. 1. We see that the $\bar{p}p$ and $\bar{n}n$ states are not diagonal; we introduce their linear combinations

$$\pi^0 = (\bar{p}p - \bar{n}n)/\sqrt{2}, \qquad \pi_0^0 = (\bar{p}p + \bar{n}n)/\sqrt{2}.$$

The sum of the amplitudes c—h can then be written in the form

$$a[(\bar{p}p)^2 + (\bar{n}n)^2] + b[\bar{p}p + nn]^2 = a[\pi^0]^2 + (a + 2b)[\pi_0^0]^2.$$

We see that 1) a splitting of the π^0 and π_0^0 states has occurred, 2) the π^0 state has the same amplitude as the $\pi^- = (\bar{p}n)$ and $\pi^+ = (\bar{n}p)$ states described by diagrams a and b. (We note that in the first approximation of perturbation theory b = 0 for the pseudoscalar state of the nucleon + antinucleon system.)

The Lagrangian (1) also does not lead to any undesirable isotopic degeneracies in a system of two or several nucleons. This can be easily understood if we note that the isotopic variables in the nucleon system are essentially superfluous: they contain no new information since in virtue of Pauli's principle the isotopic state of a system of nucleons is completely determined by its orbital and spin states. As a result of the above discussion we think that the introduction in addition to the ρ^0 meson of three other vector mesons "corresponding to the existence of the isotopic group" [4] is superfluous.

CONSERVATION OF CURRENT

It can be easily seen that the current $j_{s\alpha}$ is a conserved quantity. This leads to a number of

consequences. Firstly, the interaction (1) is renormalizable (cf., for example, [6]) in spite of the vector nature of the ρ^0 meson. Secondly, the $\Lambda\Lambda\rho$, nnρ and ppρ vertex parts renormalized taking virtual strong interactions into account are all equal to one another for $q^2 = 0$ where q is the vecton momentum. We shall from now on give the name vecton charges to such vertices for $q^2 = 0$.

This conclusion is completely obvious if we take into account the analogy between the vector current $j_{s\alpha}$ and the electromagnetic current.* The same analogy also enables us to conclude that the vecton charges of the compound baryons (Σ and Ξ) are also equal to the vecton charge of the nucleon and the Λ hyperon:

$$g_\Lambda = g_N = g_\Sigma = g_\Xi = g.$$

The vecton charges of all the antibaryons are equal to $-g$. The vecton charges of the K and π mesons must be equal to zero. The vecton charge of the nucleus must be equal to gA, where A is the number of nucleons in the nucleus.

POLE DIAGRAMS

Unfortunately, a rigorous physical interpretation can be given only to the vecton charge defined at the point $q^2 = \mu^2$ where μ is the vecton mass, and not at the point $q^2 = 0$ as has been done above. The magnitude of $g(q^2 = 0)$ could be obtained from experiment only provided the contribution of the pole diagram of the type of Fig. 2 would not be compensated by contributions of other diagrams. Strictly

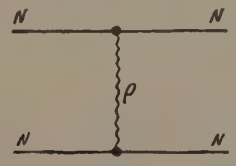

FIG. 2

speaking there are no reasons for the nonexistence of such compensation. On the other hand, we cannot prove that it must necessarily occur. Therefore, we shall draw attention to some properties of the pole diagram. It would be useful to determine whether these properties manifest themselves experimentally.

1) The cross section determined by the diagram of Fig. 2 does not decrease as the energy of the colliding nucleons increases (as was the case for the π-meson pole diagram), but tends to the constant limit

$$\sigma = 4\pi g^2/\mu^2.$$

2) The angular distribution of the nucleons has a maximum at 0°, with $d\sigma(0)\, d\Omega = 4g^2E^2/\mu^4$, where E is the energy of the nucleons in the center of mass system.

3) The scattering amplitude corresponding to the 0° angle determined by the diagram of Fig. 2 is purely real and increases linearly with E.

4) The diagram of Fig. 2 taken together with other diagrams (giving contributions to the imaginary part of the amplitude) leads to the existence of strong polarization in the scattering of high energy nucleons. Sakurai [4] has pointed out the possible role of this diagram in the explanation of the spin-orbit interaction.

We note that if the contribution of diagram 2 is not compensated then in the forward scattering of baryons the real part of the amplitude must be different from zero ($\mathrm{Re}\, f(0) \neq 0$), while there is no basis for this in the case of π and K mesons (their vecton charges are equal to zero). Moreover, in the case of baryons the real part must be negative: in the case of pp-scattering there must exist constructive interference with the Coulomb scattering. (At low energies, when the exchange of π mesons predominates, $\mathrm{Re}\, f > 0$, and the fact of the existence of nuclei is associated with this.) In the case of nuclei $\mathrm{Re}\, f(0°)$ must be proportional to A (in analogy to the fact that the amplitude of Coulomb scattering is proportional to Z). In order to observe this kind of coherent scattering of nucleons by nuclei we should separate out the small scattering angles when the momentum transferred to the nucleus is small compared to $m_\pi/A^{1/3}$ —the reciprocal nuclear dimensions. In the case of scattering by nuclei the possibility of compensation of the single meson diagram (Fig. 2) by other diagrams appears to be very probable due to the heavy absorption of the nucleon wave in the nucleus.*

We note that also in the case of scattering by a nucleon we can hope that there is no compensation only for low values of the transferred momentum. It is obvious that for large values of the transferred momentum the diagrams involving several virtual mesons will be significant. The experimentally observed angular distribution [15] falls off with angle much more rapidly than would follow from a single meson diagram.

*The problem of gauge invariance of the theory of heavy vector mesons interacting with a conserved current has been considered recently by V. Ogievetskii and I. Polubarinov (private communication).

*This remark is due to I. Ya. Pomeranchuk.

CONTRIBUTION TO THE ELECTROMAGNETIC FORM FACTOR OF THE NUCLEON

The vecton can make an essential contribution to the electromagnetic form factor of nucleons. The fact that the electric radius of the proton is $\sim \frac{1}{2}m_\pi$, while the electric radius of the neutron is nearly zero shows that the isovector and the isoscalar form factors of the nucleons are approximately equal (and compensate each other in the case of the neutron). This compensation seems strange since the isovector form factor might be expected to have a larger radius than the isoscalar form factor (the latter "begins" with three π mesons, while the former "begins" with two, cf. Fig. 3). Nambu[3] noted that the ρ meson, if it exists, should increase the radius of the isoscalar form factor and should make the compensation noted above more natural.

The contribution of the ρ meson to the electromagnetic form factor is described by a pole diagram (Fig. 4). This diagram corresponds to the amplitude

$$\alpha(q^2)\frac{q^2}{q^2-\mu^2},$$

where α is an unknown function of q^2; $\alpha(0) \neq 0$. (The factor q^2 in the numerator is determined by gauge invariance; for further details cf. [14].) Here, as before, we assume that the instability of the vecton does not appreciably affect the contribution of the pole diagram. If we assume that $\alpha(q^2)$ does not vary rapidly with increasing q^2, then for $q^2 \gg \mu^2$ the amplitude under consideration gives a contribution to the electric form factor of the nucleon which does not fall off with increasing q^2. Possibly this explains to some degree the appearance in the range $q \approx 0.7-0.9$ Bev of a plateau in the electric form factor of the proton recently discovered by Hofstadter's group.[16]

We note that from the fact that the isoscalar part of the anomalous magnetic moment of the nucleon is small it follows that the vecton pole diagram makes a small contribution to the anomalous magnetic moment of nucleons. Therefore,

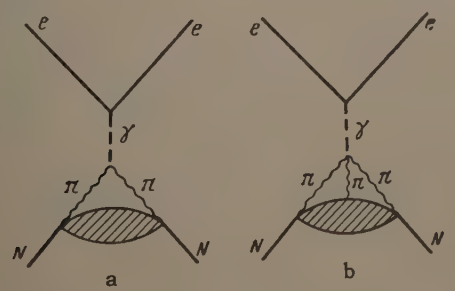

FIG. 3. a – isovector vertex, b – isoscalar vertex.

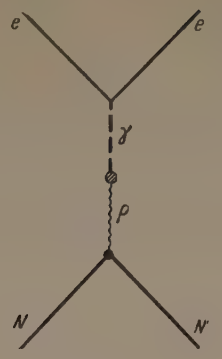

FIG. 4

generally speaking, the magnetic form factor should not have a plateau analogous to the electric form factor.

POSSIBILITIES OF EXPERIMENTAL DETECTION OF THE VECTON

The properties of the vecton should be significantly different, depending on whether its mass μ is greater than or less than $3m_\pi$. In the case when $\mu < 3m_\pi$ since the decay $\rho \to 2\pi$ is forbidden the ρ meson can decay only as a result of electromagnetic interactions with a lifetime of the order of

$$\sim 1/m_\pi e^2 \sim 10^{-20} - 10^{-21} \text{ sec.}$$

The principal decay is given by

$$\rho^0 \to \pi^0 + \gamma.$$

In this case the ρ^0 meson could be treated in the theory of strong interactions as an ordinary stable particle. But from the point of view of an experimenter, the ρ^0 meson would be as "good" a particle as the Σ^0 hyperon.

Unfortunately, this possibility is apparently contradicted by the presently available experimental data.

1. In the case when $\mu < m_K - m_\pi = 350$ Mev the decay

$$K^+ \to \rho^0 + \pi^+ \\ \downarrow \\ \pi^0 + \gamma$$

would be possible. The estimate made by Gomez et al[17] shows that data on the spectrum of the τ' decay exclude the possibility of the existence of the ρ^0 meson for $\mu < 320$ Mev.

2. The group at the California Institute of Technology[17] searched for the reaction

$$\gamma + p \to p + \rho^0.$$

The results of this experiment apparently exclude the possibility of the existence of a ρ^0 meson with a mass in the range 300 – 430 Mev. Somewhat earlier a less accurate search for the same photo-

production reaction $\gamma + p \rightarrow p + \rho^0$ carried out with the accelerator at Frascatti[18] led to the conclusion that the cross section for this reaction is $\sigma < 6 \times 10^{-31}$ cm^2 for a meson of mass $\mu \lesssim 500$ Mev. A search for singularities in the scattering of π^- mesons by protons on the threshold of production of a ρ^0 meson led to a negative result in the mass range $\mu \lesssim 370$ Mev (Pontecorvo, private communication).

3. In the annihilation of antiprotons $\bar{p} + p$ in addition to other strongly interacting particles ρ mesons should be emitted decaying into $\pi^0 + \gamma$:

$$\rho \rightarrow \pi^0 + \gamma$$

in the case when $\mu < 3m_\pi$. Annihilation with the participation of a ρ meson should be favored by the fact that the corresponding statistical weight contains the factor $2I + 1 = 3$. In such a case the fraction of the annihilation energy available to the charged particles should turn out to be[19] less than $2/3$, while experimentally[20] in the annihilation of $\bar{p}$ in a hydrogen bubble chamber the energy of the charged $\pi^\pm$ mesons amounts to $(64 + 4)$ % of the total energy.

4. A direct search for the ρ meson of $\mu < 3m_\pi$ in the annihilation $\bar{p} + p$ has apparently yielded a negative result.[21]

In view of the interest in this problem it appears desirable that these results be checked further. In this connection it is of interest to measure directly the number and the spectrum of the hard protons arising in the annihilation of antinucleons. In the case $m_K - m_\pi < \mu < 3m_\pi$ (350 Mev $\lesssim \mu \lesssim$ 420 Mev) the decay $K^+ \rightarrow \rho^0 + \pi^+$ is not possible. However, in this case the following decay can occur

$$\begin{array}{l} K^+ \rightarrow \rho^0 + e^+ + \nu \\ \qquad\quad \downarrow \\ \qquad\quad \pi^0 + \gamma, \end{array}$$

and this would lead to an apparent softening of the spectrum of the Ke_3 decay. Therefore, a measurement of the spectrum of the Ke_3 decay can give an answer to the problem of the existence of the ρ^0 meson in this mass range.

In the case when the mass of the ρ meson is greater than $3m_\pi$ the ρ meson will decay into three π mesons with a nuclear lifetime:

$$\rho \rightarrow \pi^+ + \pi^- + \pi^0, \quad \tau_{\rho^0} \sim 10^{-23} \text{ sec}.$$

For low values of $Q = \mu - 3m_\pi$ the probability of the $\rho \rightarrow 3\pi$ decay falls off as Q^4. In this case the instability of the ρ meson should be taken into account in an essential manner in constructing a theory of strong interactions in accordance with the proposed scheme. Experimentally a ρ meson with such a lifetime should appear as a 3π resonance.

It can be easily seen that in this case μ cannot be significantly smaller than m_K for otherwise the following decay would occur

$$\begin{array}{l} K^+ \rightarrow \rho^0 + e^+ + \nu \\ \qquad\quad \downarrow \\ \qquad\quad \pi^+ + \pi^- + \pi^0. \end{array}$$

The probability of the decay $K^+ \rightarrow e^+ + \nu + \rho$ is equal to

$$w = (G^2\beta^2/40\pi^3M^4)\,Q^5, \qquad (3)$$

where M is the nucleon mass, G is the coupling constant for the weak interaction, $Q = m_K - \mu$ and β is an unknown numerical coefficient. Since decay of strange particles is usually suppressed, it is sensible to take $\beta^2 \approx 0.1 - 0.01$.

The decay $K^+ \rightarrow \rho^0 + e^+ + \nu$, $\rho^0 \rightarrow \pi^+ + \pi^- + \pi^0$ would have the appearance of an anomalous τ decay. On taking into account the fact that among 2000 observed τ decays such decays were not observed we obtain for w the upper limit $w < 2.5 \times 10^3$ sec^{-1}. Comparing with (3) we obtain for $\beta^2 = 0.1$ the value $Q \leq 40$ Mev or $\mu \gtrsim 450$ Mev.

At the present time no experimental data are known which would contradict the possibility of the existence of a ρ meson with $\mu \gtrsim m_K$ with the fundamental decay

$$\rho \rightarrow 3\pi.$$

Such a meson should appear in the reactions of annihilation and of multiple production. The most direct answer to the problem of the existence of such a ρ meson would be given by a measurement of the recoil spectrum in the reactions*

$$p + d \rightarrow He^3 + \rho^0 \quad \text{(a)}, \qquad d + d \rightarrow He^4 + \rho^0 \quad \text{(b)},$$

$$\pi^+ + d \rightarrow p + p + \rho^0 \quad \text{(c)}, \qquad K^- + p \rightarrow \Lambda^0 + \rho^0 \quad \text{(d)}.$$

In the reactions (a), (b), (c) the recoil momentum of He^3, He^4, $p + p$ can be measured directly. In the reaction (d) the momentum of the Λ particle is equal to the total momentum of the decay products. If the ρ^0 meson exists, then in the recoil spectrum a peak should be observed corresponding to the production of the ρ^0 meson against the background of the spectrum of the various possible many-particle reactions. The cross section for the production of the ρ^0 meson in (a), (b), (c), (d) must be of nuclear order of magnitude. We note that the reaction (a) gives such a maximum corresponding to $\mu = 310 \pm 10$ Mev (experiments of the Berkeley group[22]). However, such a mass apparently contradicts the nonexistence of the de-

*The reaction (c) was proposed by N. G. Birger.

cay $K^+ \to \rho^0 + \pi^+$ (cf. above). A further investigation of the reaction (a) is necessary and, in particular, a check of whether an analogous maximum exists in the reaction

$$p + d \to H^3 + \rho^+.$$

If such a maximum exists, then the corresponding meson has an isotopic spin equal to unity, and has no relation whatsoever to the isosinglet particle considered by us. V. Baĭer (private communication) has drawn our attention to the fact that the existence of a ρ^0 meson would lead to a resonance in the scattering of electrons by positrons in the process $e^+ + e^- \to \mu^+ + \mu^-$ at an energy of $e^+ + e^-$ in their center-of-mass system equal to the mass of the ρ^0 meson. This resonance is determined by the diagram shown in Fig. 5.

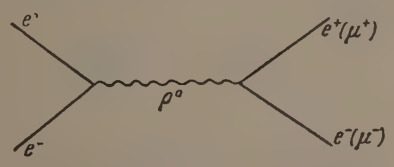

FIG. 5

The authors are grateful to V. Baĭer, N. G. Birger, V. I. Gol'danskii, Ya. B. Zel'dovich, V. Kolkunov, I. Ya. Pomeranchuk, B. M. Pontecorvo, and K. A. Ter-Martirosyan for a number of valuable comments.

[1] G. Wentzel, Einführung in die Quantentheorie der Wellenfelder, Edwards Bros., 1946.

[2] W. Pauli, Meson Theory of Nuclear Forces, Interscience, N.Y., 1946.

[3] Y. Nambu, Phys. Rev. **106**, 1366 (1957).

[4] J. J. Sakurai, Ann. Phys. **11**, 1 (1960); Phys. Rev. **119**, 1789 (1960); Nuovo cimento **16**, 388 (1960).

[5] G. Breit, Phys. Rev. **120**, 287 (1960).

[6] Y. Fujii, Progr. Theoret. Phys. (Kyoto) **21**, 232 (1959).

[7] S. Sakata, Progr. Theoret. Phys. (Kyoto) **16**, 686 (1956).

[8] L. B. Okun', JETP **34**, 469 (1958), Soviet Phys. JETP **7**, 322 (1958); Report at the Venice-Padua Conference, 1957.

[9] L. B. Okun', Proc. VIII Geneva Conv., 1958, p. 223.

[10] M. Gell-Mann, Proc. X Rochester Conf. 1960, p. 508.

[11] R. F. Feynman, Proc. X Rochester Conf. 1960, p. 501.

[12] Y. Ohnuki, Proc. X Rochester Conf. 1960, p. 843.

[13] I. Ya. Kobzarev and L. B. Okun', JETP (in press).

[14] Kobzarev, Okun', and Pomeranchuk, JETP **41**, 495 (1961), this issue p. 355.

[15] Cork, Wenzel, and Causey, Phys. Rev. **107**, 859 (1957).

[16] Bumiller, Croissiaux, and Hofstadter, Phys. Rev. Letters **5**, 263 (1960).

[17] Gomez, Burkhard, Daybell, Ruderman, Sands, and Talman, Phys. Rev. Letters **5**, 170 (1960).

[18] Bernardini, Querozoli, Salvini, Silverman, and Stoppini, Nuovo cimento **14**, 268 (1959).

[19] V. I. Gol'danskii and V. M. Maksimenko, JETP **39**, 841 (1960), Soviet Phys. JETP **12**, 584 (1961).

[20] Horwitz, Muller, Murray, and Tripp, Phys. Rev. **115**, 472 (1959).

[21] F. Solmitz, Proc. X Rochester Conf. 1960, p. 164.

[22] Abashian, Booth, and Crow, Phys. Rev. Letters **5**, 258 (1960).

Translated by G. Volkoff
92

A MECHANISM FOR ABSORPTION OF ENERGY BY ANISOTROPIC BODIES

M. Sh. GITERMAN

Institute for Physico-Technical and Radio Measurements

Submitted to JETP editor March 2, 1961

J. Exptl. Theoret. Phys. (U.S.S.R.) **41**, 507-511 (August, 1961)

A body located in a varying external field can execute periodic motion by absorbing the field energy and dissipating it in the viscous medium, if the magnetic susceptibility or electric polarizability of the body are anisotropic. The absorption coefficient has a resonant dependence on the frequency of the external field. In particular, only periodic oscillations of nuclei of a certain size are possible for the liquid—solid transition.

THE purpose of this research was to ascertain whether electromagnetic energy at audio frequencies (classical effect) can be absorbed, as a result of anisotropy of the magnetic susceptibility (or electric polarizability), by macroscopic bodies immersed in a liquid. Such bodies acquire in an external magnetic field a magnetic (or electric) moment of direction, in general, different than the field; under certain conditions this should lead to periodic motion of the body and to a corresponding absorption of energy. To be specific, we shall refer henceforth to the magnetic moment of an anisotropic nucleus of solid phase floating in a liquid. Let the nucleus be spherical with principal moments of inertia $I_x = I_y = I_z = I$, let the components of the magnetic susceptibility tensor be $\chi_x = \chi_y \neq \chi_z$, and let the external magnetic field be F.

We introduce two rectangular coordinate frames, one moving with axes xyz aligned with the principal inertia axes of the nucleus, and one stationary $\xi\eta\zeta$, with the ζ axis in the direction of the external field. The cosines of the angles between the direction of the external field and the axes of the moving frame will be designated γ_1, γ_2, and γ_3. They can be expressed in terms of the Euler angles θ, ψ, and φ:

$$\gamma_1 = \sin\varphi \sin\theta; \quad \gamma_2 = \cos\varphi \sin\theta; \gamma_3 = \cos\theta. \tag{1}$$

The equation describing the rotary motion of the nucleus has the form

$$d\mathbf{L}/dt = [\mathbf{MF}] - \beta\omega, \tag{2}*$$

where $\mathbf{L}$ is the angular momentum of the nucleus, ω is the angular velocity of rotation, $\mathbf{M}_i = \chi_i \mathbf{F}_i$ is the magnetic moment induced in the field $\mathbf{F}$, and β is the moment of the force of resistance to rotation in a viscous liquid.

*$[\mathbf{MF}] = \mathbf{M} \times \mathbf{F}$.

We project (2) on the axes of the moving coordinate system:

$$Id\omega_x/dt = -\Delta\chi F^2\gamma_2\gamma_3 - \beta\omega_x, \quad Id\omega_y/dt = \Delta\chi F^2\gamma_1\gamma_3 - \beta\omega_y,$$
$$Id\omega_z/dt = -\beta\omega_z. \tag{3}$$

It is quite obvious that undamped motion of the nucleus is possible in the presence of an anisotropy $\Delta\chi = \chi_z - \chi_x \neq 0$.

Euler's dynamic equations (3) must be solved simultaneously with Euler's kinematic equations

$$\omega_x = \dot{\psi}\gamma_1 + \dot{\theta}\cos\varphi, \quad \omega_y = \dot{\psi}\gamma_2 - \dot{\theta}\sin\varphi,$$
$$\omega_z = \dot{\psi}\gamma_3 + \dot{\varphi}. \tag{4}$$

It is also useful to employ the fact that the axes ξ, η, and ζ are stationary:

$$d\gamma_1/dt = \gamma_2\omega_z - \gamma_3\omega_y; \quad d\gamma_2/dt = \gamma_3\omega_x - \gamma_1\omega_z;$$
$$d\gamma_3/dt = \gamma_1\omega_y - \gamma_2\omega_x. \tag{5}$$

To ascertain the energy absorption, we are interested in the undamped solutions of the system (3)—(5). The last equation of (3) has only damped solutions $\omega_z = C\exp\{-\beta t/I\}$. Therefore, for sufficiently large t, we can assume

$$\omega_z = 0. \tag{6}$$

Multiplying the first two equations of (3) by γ_1 and γ_2 respectively, adding them, and using (5) we obtain $\gamma_1\omega_x + \gamma_2\omega_y = C_1\exp\{-\beta t/I\}$. For the reasons indicated above, we put

$$\gamma_1\omega_x + \gamma_2\omega_y = 0. \tag{7}$$

The physically obvious conditions (6) and (7) signify that the external field cannot cause the nucleus to rotate in either the plane perpendicular to the external field or in the plane xy where the susceptibility is symmetrical.

Substitution of (4) in (7) leads to the following

solution of the problem of periodic motion of the anisotropic nucleus:

$$\psi = \text{const}, \quad \varphi = \text{const}, \tag{8}$$

and the nutation angle θ is a solution of the differential equation

$$I\ddot{\theta} + \beta\dot{\theta} + \tfrac{1}{2}\Delta\chi F^2 \sin 2\theta = 0. \tag{9}$$

Assuming that the external field is a monochromatic wave $F = F_0 \cos pt$ and expanding $\sin 2\theta$ we obtain

$$\ddot{\theta} + 2\varkappa\dot{\theta} + \omega_0^2(1 + \cos 2pt)\left(1 - \tfrac{2}{3}\theta^2\right)\theta = 0,$$
$$\varkappa = \beta/2I, \ \omega_0^2 = F_0^2\Delta\chi/2I. \tag{10}$$

All the coefficients of (10) can be expressed in terms of the parameters of the substance and the radius R of the nucleus. The moment of the forces of resistance to the rotation of the sphere is [1] $\beta = 8\pi R^3\lambda$, where λ is the coefficient of viscosity of the liquid; the anisotropy of the susceptibility of the nucleus is $\Delta\chi = (\Delta\chi)_m 4\pi R^3\rho/3$, where $(\Delta\chi)_m$ is the anisotropy of the specific susceptibility (polarizability) of the solid phase, ρ is the density, and the principal moment of inertia of the sphere is $I = 8\pi\rho R^5/15$. Then

$$\varkappa = 7{,}5\lambda/\rho R^2, \ \omega_0^2 = 1{,}25\,(\Delta\chi)_m F_0^2 R^{-2}. \tag{11}$$

Equation (10) takes account also of the nonlinear terms. The solution of the linear differential equations contains constant factors determined by the boundary conditions. Account of the nonlinearity enables us to find the characteristics of the steady-state motion independently of the initial conditions, which is precisely the purpose of our investigation.

Assuming the nonlinearity small, we rewrite (10) in the form

$$\ddot{\theta} + 2\varkappa\dot{\theta} + \omega_0^2(1 + \alpha\cos 2pt)\theta + V(t, \theta) = 0,$$
$$V(t, \theta) = -\tfrac{2}{3}\omega_0^2(1 + \alpha\cos 2pt)\theta^3. \tag{12}$$

For convenience we have introduced in (12) the parameter $\alpha = 1$. In the linear approximation we have

$$\ddot{\theta} + 2\varkappa\dot{\theta} + \omega_0^2(1 + \alpha\cos 2pt)\theta = 0. \tag{13}$$

Equations similar to (12) and (13) are encountered in various problems where the parameters of the system have periodically variable parameters, as in the case of parametric resonance; these have been treated in an extensive literature. [2-6]

We consider the existence of periodic solutions of (13) first, after which we take account of the nonlinearity [Eq. (12)]. Periodic solutions of (13) are not obtained for all values of the coefficients

$\varkappa$ and ω_0, i.e., according to (11), not for all values of R. Let us investigate the dimensions R of nuclei capable of executing periodic motions in a field of a given frequency p. The figure, plotted in coordinates α and ω_0/p, shows the instability and stability regions of the solutions of the Mathieu equation, to which Eq. (13) reduces when $\varkappa = 0$. When friction is taken into account, the instability regions shrink and shift upward, the shift increasing with increasing ω_0 (for given p). The instability regions for $\varkappa \neq 0$ are shown shaded in the figure.

In our problem the periodic solutions of (13) are determined by the intersection of the line $\alpha = 1$ with the boundaries of the shaded regions. The number of intersections is finite, since the boundaries of the instability regions of the solutions shift upward with increasing ω_0/p. The fact that the abscissas of these points have a maximum abscissa denotes the existence of a minimum dimension R_{min} of the nucleus capable of executing periodic oscillations in the external field. It is likewise obvious that there exists a value R_{max}, determined by the abscissa of $(\omega_0/p)_{min}$ in the figure. Thus, periodic oscillations and absorption of energy from a specified external field $F = F_0 \cos pt$ by the nuclei are possible only if the nuclei have certain resonant dimensions R_i ($i = 1, 2, \ldots, n$), with $R_{max} \geq R_i \geq R_{min}$.

Mathieu equations [when $\alpha = 1$ in (13)], cannot be solved analytically, but the determination of the numerical values of the coefficients ω_0 and $\varkappa$, for which (13) has periodic solutions, is in principle a simple although cumbersome problem.* After compiling such a table, it is necessary to calculate the resonant nuclear radii R_i for the specific substance [$(\Delta\chi)_m$, λ in (11)] and for the specific experimental conditions (amplitude F_0 and frequencies $p_1, p_2, \ldots$, of the external field).

Turning now to Eq. (12), let us investigate the dependence of the amplitude of the nucleus oscillations at the frequency of the external field. Let the coefficients (11) of Eq. (12) be such that the periodic oscillations of the nucleus correspond to

*This effort is justified if suitable experiments are set up.

the first instability region in the figure. Since small nonlinearity is assumed, we seek an approximate solution of (12) in the form

$$\theta = A_1 \sin pt + B_1 \cos pt. \qquad (14)$$

Substituting (14) in (13) and equating the coefficients of sin pt and cos pt to zero we obtain

$$A_1(\omega_0^2 - p^2 - \omega_0^2/2) - \tfrac{1}{2}\omega_0^2 A_1 A^2 - 2\varkappa p B_1 + \tfrac{1}{3}\omega_0^2 A_1^3 = 0,$$

$$B_1(\omega_0^2 - p^2 + \omega_0^2/2) - \tfrac{1}{2}\omega_0^2 B_1 A^2 + 2\varkappa p A_1 - \tfrac{1}{3}\omega_0^2 B_1^3 = 0. \qquad (15)$$

In (15) we have introduced the oscillation amplitude $A = (A_1^2 + B_1^2)^{1/2}$.

To make the results clear, let us assume that the cubic terms in (15) are small and let us neglect the last terms in the left halves of (15).* Then the vanishing of the determinant of (15) leads to the following frequency dependence of the square of the oscillation amplitude:

$$A^2 = 2\omega_0^{-2}[\omega_0^2 - p^2 \pm (\omega_0^4/4 - 4\varkappa^2 p^2)^{1/2}]. \qquad (16)$$

The nucleus will execute periodic oscillations only if

$$\omega_0^2 > 4\varkappa p, \qquad (17)$$

i.e., the attenuation due to viscosity must not be too large.† Periodic oscillations are possible at external-field frequencies for which $A^2 > 0$. The condition $A^2 = 0$ determines the boundaries of the resonant frequency band.

Thus, the solution of (13) assumes the form

$$\theta = A \sin(pt - \delta), \quad \operatorname{tg}\delta = 2\varkappa p / [\omega_0^2/2 \pm (\omega_0^4/4 - 4\varkappa^2 p^2)^{1/2}],$$
$$A = \{2\omega_0^{-2}[\omega_0^2 - p^2 \pm (\omega_0^4/4 - 4\varkappa^2 p^2)^{1/2}]\}^{1/2}. \qquad (18)‡$$

The absorption coefficient γ is expressed in terms of the density of the dissipative function $F/V = \beta\theta^2/2V$ as

$$\gamma = 8\pi |F| / pF_0^2 V.$$

For a comparison with experimental data, it is necessary to average over the period of variation of the angle of revolution θ. As a result we obtain

$$\gamma = \frac{4\pi\beta p}{F_0^2\omega_0^2 V}\left[\omega_0^2 - p^2 \pm \left(\frac{\omega_0^4}{4} - 4\varkappa^2 p^2\right)^{1/2}\right]. \qquad (19)$$

As can be seen from (19), for nuclei of given dimension, the dependence of the coefficient of absorption on the frequency of the external field is of resonant character.

At each instant of time t of a real liquid-solid transition the nuclei have a certain distribution over the dimensions R. The distribution function N(R, t) can evidently be determined with the aid of the kinetic equation in the particle dimension space. We can then obtain (with account of the remarks made in the last two footnotes) the frequency dependence of the absorption coefficient and of the susceptibility (polarizability), suitable for direct comparison with experiments.

The energy-absorption mechanism considered above can be used to investigate the kinetics of the liquid-solid transition of magnetically-isotropic or electrically-isotropic bodies, the number of which is quite large. D. N. Astrov and A. V. Voronel' of the Laboratory of the Institute of Physico-Technical and Radio Measurements have observed electromagnetic absorption at acoustic frequencies in the melting and crystallization of benzene. This absorption was observed only during the phase transition process and not in the solid and liquid phases.

The author is grateful to I. E. Dzyaloshinskii for valuable advice and A. V. Voronel' for discussions.

*A more exact solution of (15) and an account of the higher harmonics of the nucleus [in addition to (14)] can be obtained by successive approximations.

†The criterion (17) agrees poorly with the condition that the Reynolds number be small, i.e., at such high frequencies the moment of the friction forces is proportional, generally speaking, to the angular velocity raised to a power higher than the first. The subsequent calculation is therefore only qualitative. The disparity indicated occurs only for resonances at the overtones of the external field (parametric resonance) and obviously not at undertones of the field (resonance of the n-th kind).

‡tg = tan.

[1] L. D. Landau and E. M. Lifshitz, Mekhanika sploshnykh sred (Mechanics of Continuous Media), 2d ed. Gostekhizdat, (1953).

[2] E. T. Whittaker and G. N. Watson, A Course in Modern Analysis, Cambridge University Press, (1940).

[3] A. A. Andronov and M. A. Leontovich, ZhRFKhO (Journal of the Russian Physical and Chemical Society) 59, 430 (1927).

[4] L. I. Mandel'shtam, Collected Works, vol. 2, AN SSSR (1947).

[5] L. D. Landau and E. M. Lifshitz, Mekhanika (Mechanics), Fizmatgiz (1958).

[6] N. N. Bogolyubov and Yu. A. Mitropol'skii Asimptoticheskie metody v teorii nelineĭnykh kolebanii (Asymptotic Methods in the Theory of Nonlinear Oscillations), Fizmatgiz, (1958).

Translated by J. G. Adashko
93

THEORY OF ELECTRIC CONDUCTIVITY OF SEMICONDUCTORS IN A MAGNETIC FIELD. II

Yu. A. FIRSOV and V. L. GUREVICH

Semiconductor Institute, Academy of Sciences, U.S.S.R.

Submitted to JETP editor March 6, 1961; resubmitted May 16, 1961

J. Exptl. Theoret. Phys. (U.S.S.R.) 41, 512-523 (August, 1961)

We obtain an expression for the diagonal element of the transverse conductivity tensor of a semiconductor in a strong magnetic field, taking the interaction between the conduction electrons with one another into account. We assume the conduction electron dispersion law to be isotropic and quadratic. The electron-phonon scattering is considered in the Born approximation. The general expression is studied for the case where the electrons satisfy Boltzmann statistics and where the electron-electron collisions are described also in the Born approximation. As an example of an application of this expression we evaluate the height of the resonance conductivity oscillations predicted in [1].

1. In a previous paper by the authors [1] (in the following referred to as I) we obtained an expression for the diagonal element of the transverse conductivity, σ_{xx}, of semiconductors in a strong magnetic field,* caused by the inelastic scattering of the conduction electrons by the lattice vibrations. We did not take then into account the electron-electron interaction. It is the aim of the present paper to take into account the influence of this interaction upon the conductivity for the case of an isotropic, quadratic electron spectrum.

One shows easily that because of the conservation of momentum during electron-electron collisions the quantity σ_{xx} is equal to zero for a system of mutually interacting electrons. It can be different from zero only owing to interaction with some other scatterers, for instance, phonons. In that case when there is a strong magnetic field present ($\sigma_{xx}/\sigma_{xy} \ll 1$), the role of the electron-electron interaction will only make itself felt in the renormalization of the electron-phonon scattering potential as far as the first non-vanishing approximation in the scattering—to which we restrict ourselves—is concerned.

To understand qualitatively the expected character of the effects we start with a phenomenological consideration, generalizing a method proposed by Doniach [2] to the case where there is a non-vanishing magnetic field H. Let a vibration with frequency ω and wave vector $\mathbf{q}$ propagate in an isotropic crystal. When we neglect the electron-electron interaction, the correction to the electron energy when this vibration is taken into account is of the form

$$U(\mathbf{r}, t) = u + u^* = c_q b_q e^{-i(\omega t - \mathbf{qr})} + c_q^* b_q^* e^{i(\omega t - \mathbf{qr})}. \quad (1)$$

The function $c_{\mathbf{q}}$ characterizes here the electron-phonon interaction (expressions for it for different cases are given, for instance, in I) and the dimensionless quantities $b_{\mathbf{q}}$ determine the vibrational amplitude. The extra term (1) in the energy causes the free charges in the crystal to be rearranged and this leads to a violation of local neutrality and hence to the appearance of an additional electrostatic potential which, taken together with (1), renormalizes the electron-phonon interaction. Since this effect is linear in the interaction we perform a renormalization of the first term in (1). The result for the second term is obtained by taking the complex conjugate of the first term.

Let the renormalized interaction be of the form

$$\tilde{u} = \tilde{u}_q(\omega)\, e^{i(\mathbf{qr} - \omega t)}.$$

The change in the electron density caused by it is determined by solving the equation for the density matrix ρ:

$$\partial\rho/\partial t + (i/\hbar)\,[\rho, \mathcal{H}] = 0, \quad (2)$$

where $\mathcal{H} = \mathcal{H}_0 + \tilde{u}$, $\mathcal{H}_0$ is the single-electron Hamiltonian operator while the square brackets indicate a commutator. Putting $\rho = \rho^0 + \rho'$ (ρ^0 is the equilibrium density matrix of a system of non-interacting electrons), we find

$$\rho'_{\Gamma\Delta} = -\frac{\rho^0_\Gamma - \rho^0_\Delta}{\varepsilon_\Delta - \varepsilon_\Gamma - \hbar\omega + i\nu}\, \tilde{u}_q(\omega) \langle \Gamma | e^{i\mathbf{qr}} | \Delta \rangle,$$

where Γ and Δ stand for the totality of quantum numbers characterizing the single-electron states when there is no perturbation, $\epsilon_\Gamma = \langle \Gamma | \mathcal{H}_0 | \Gamma \rangle$, ν is the adiabatic parameter corresponding to the

*The notation is the same as in I.

assumption of an infinitely slow switching on of the electron-phonon interaction ($\nu > 0$, $\nu \to 0$).

In the coordinate representation (σ is the spin variable) we have

$$\rho'_{\sigma\sigma'}(\mathbf{r}, \mathbf{r}') = \sum_{\Gamma\Delta} \rho'_{\Gamma\Delta} \psi^*_{\Delta}(\mathbf{r}, \sigma)\, \psi_{\Gamma}(\mathbf{r}', \sigma'),$$

from which we get for the Fourier component of the electron density

$$n_{\mathbf{q}} = \frac{1}{V_0} \sum_{\sigma} \int d^3 r e^{-i\mathbf{q}\mathbf{r}} \rho_{\sigma\sigma}(\mathbf{r}, \mathbf{r}) = -\frac{1}{\hbar V_0} K^0_{\mathbf{q}}(-\omega)\, \tilde{u}_{\mathbf{q}}, \qquad (3)$$

where V_0 is the normalizing volume and

$$K^0_{\mathbf{q}}(\omega) = \hbar \sum_{\Gamma\Delta} \frac{\rho^0_{\Delta} - \rho^0_{\Gamma}}{\varepsilon_{\Gamma} - \varepsilon_{\Delta} + \hbar\omega - i\nu} |\langle \Gamma | e^{i\mathbf{q}\mathbf{r}} | \Delta \rangle|^2. \qquad (4)$$

However, as we noticed earlier, the renormalized potential $\tilde{u}$ is the sum of the "bare" potential u and the electrostatic potential $e\varphi$, which is determined from the Poisson equation

$$\varepsilon_0 q^2 \varphi_{\mathbf{q}} = 4\pi e n_{\mathbf{q}}, \qquad (5)$$

whence

$$\tilde{u}_{\mathbf{q}} = \left[1 + \frac{4\pi e^2}{\varepsilon_0 \hbar q^2 V_0} K^0_{\mathbf{q}}(-\omega)\right]^{-1} u_{\mathbf{q}}. \qquad (6)$$

We now establish the connection between the renormalization coefficient in front of $u_{\mathbf{q}}$ in (6) and the permittivity of the crystal. To do this we note that Eq. (6) is independent of the actual form of the interaction, and depends only on the properties of its space and time periodicity. In particular, one may assume that $\mathbf{D} = -\epsilon_0 \nabla u$ is the "bare" electrical field, i.e., the electrical induction vector. In that case $\mathbf{E} = -\nabla \tilde{u}$ is the total electrical field and the coefficient connecting them,

$$\varepsilon_{\parallel}(\omega, \mathbf{q}) = \varepsilon_0 + \frac{4\pi e^2}{\hbar q^2 V_0} K^0_{\mathbf{q}}(-\omega) \qquad (7)$$

is the longitudinal component of the permittivity tensor, taking time and space dispersion into account.

If we do not take electron-electron interaction into account, the probability for an electron-phonon scattering is proportional to $|c_{\mathbf{q}}|^2$. The present calculation shows that taking this interaction into account is equivalent to replacing the transition probability $|c_{\mathbf{q}}|^2$ by

$$|c_{\mathbf{q}}|^2 \left\{\left[1 + \frac{4\pi e^2}{\varepsilon_0 \hbar q^2 V_0} \mathrm{Re}\, K^0_{\mathbf{q}}(\omega)\right]^2 + \left[\frac{4\pi e^2}{\varepsilon_0 \hbar q^2 V_0} \mathrm{Im}\, K^0_{\mathbf{q}}(\omega)\right]^2\right\}^{-1} \equiv \frac{|c_{\mathbf{q}}|^2}{A^2 + B^2}. \qquad (8)$$

In the Boltzmann statistics case and when the conduction electron spectrum is quadratic and isotropic one can easily evaluate the function (4) and according to Larkin[3]

$$\mathrm{Re}\, K^0_{\mathbf{q}}(\omega) = 2\frac{nV_0}{qv_T}\left[W\left(\frac{\omega}{qv_T} + \frac{q}{2q_T}\right) - W\left(\frac{\omega}{qv_T} - \frac{q}{2q_T}\right)\right], \qquad (9)$$

$$\mathrm{Im}\, K^0_{\mathbf{q}}(\omega) = V_0 \frac{n\sqrt{\pi}(1 - e^{-\hbar\omega\beta})}{qv_T} \exp\left[\frac{\hbar\omega\beta}{2} - \left(\frac{\omega}{qv_T}\right)^2 - \left(\frac{q}{2q_T}\right)^2\right],$$

$$W(x) = e^{-x^2} \int_0^x e^{u^2} du \qquad (10)$$

(n is the electron concentration and $\beta = 1/kT$) when there is no magnetic field. The form of these functions and therefore also of the expressions for A^2 and B^2 in (8) depends on the relation between v_T and ω/q. When $\omega/q \gg v_T$

$$A = 1 - 4\pi e^2 n / \varepsilon_0 m\omega^2 = 1 - \omega_p^2/\omega^2, \qquad (11)$$

B is exponentially small and expression (8) turns out to be larger than its renormalized value when ω is close to ω_p. This means physically that the electron-phonon interaction and thus also the scattering probability increases steeply when the phonon frequency approaches the frequency of the natural vibrations of the electron system, namely the plasma frequency ω_p.*

We note that the ratio ω/q is equal to the sound velocity w for acoustic phonons. But as a rule $v_T \gg w$ in the Boltzmann statistics region and it is thus practically impossible to excite plasma oscillations by sound if $H = 0$, since the inequality $\omega/q \gg v_T$ cannot be realized. When $\omega/q \ll v_T$

$$A = 1 + 4\pi n e^2 / \varepsilon_0 mkTq^2 = 1 + (\varkappa/q)^2$$

and the renormalized expression (6) turns out to be less than the unrenormalized expression by a factor $1 + (\varkappa/q)^2$ ($1/\varkappa$ is the Debye radius). This is due to the effect of the screening of the phonon potential, which decreases the electron-phonon interaction and thus also the scattering probability.

The magnetic field introduces additional complications in this picture. For instance, when $H = 0$ plasma effects are practically unobservable since the dispersion of the optical vibrations is small and one must select the impurity concentration specially in order that the frequency of the optical vibrations turn out to be near the plasma frequency. In a magnetic field, the plasma spectrum occupies a wide region of frequencies from

*This phenomenon is complicated by the fact that in the case of a sufficiently exact resonance the electron system may show a reciprocal influence on the phonons, changing the phonon frequency[2] (see also Appendix II).

ω_p to Ω ($\Omega = eH/mc$ is the Larmor frequency) and the equality between the plasma frequency and the frequency of the optical phonons is achieved much more simply.

Unfortunately an application of these simple methods to a rigorous analysis of the role played by the above-mentioned effects in transport phenomena is unjustified. The point is that phonons with wave vectors $q \gtrsim q_T$ are important for such phenomena, yet it does not follow directly at all that for such dimensions of the spatial inhomogeneity these effects can be described by the self-consistent field method with some kind of single-electron potential. This problem is essentially a many-particle one and one therefore needs solve it by means of many-particle quantum theory methods.

2. To construct a rigorous theory we start from Kubo's formula[4] for σ_{xx} in a form which is convenient for an expansion in powers of the electron-phonon interaction[5]

$$\sigma_{xx} = \frac{e^2\beta}{V_0} \operatorname{Re} \int_{-\infty}^{0} e^{\nu t} \left\langle e^{-\beta \mathcal{H}_1} T_C \left\{ \exp\left[\int U(z) \frac{dz}{i\hbar} \right] v^x(t)\, v^x(0) \right\} \right\rangle dt. \tag{12}$$

Here v^x is the operator of the x component of the total (summed over all electrons) velocity, T_C indicates ordering along the contour C, depicted in the figures by dot-dash lines,

$$U(z) = \exp(i\mathcal{H}_1 z/\hbar)\, U \exp(-i\mathcal{H}_1 z/\hbar), \tag{13}$$

$$\langle \ldots \rangle = \operatorname{Sp}(\ldots)/Z, \tag{14}$$

and Z is the partition function. Furthermore, $\mathcal{H} = \mathcal{H}_1 + U$, where $\mathcal{H}_1 = \mathcal{H}_e + \mathcal{H}_p$, $\mathcal{H}_e$ the Hamiltonian of a system of mutually interacting electrons in a magnetic field **H** which, when we choose the gauge **A** = (0, Hx, 0), is of the form

$$\mathcal{H}_e = \frac{\hbar^2}{2m} \sum_{i=1}^{N} \left[-\nabla_i^2 - 2ia^{-2} x_i \frac{\partial}{\partial y_i} + a^{-4} x^2 \right] + \frac{e^2}{2\varepsilon_0} \sum_{i \neq k} \frac{1}{|\mathbf{r}_i - \mathbf{r}_k|} \tag{15}$$

(N is the number of electrons, $\mathbf{r}_i$ the position coordinate of the i-th electron, $a^2 = c\hbar/eH$); $U = u + u^+$, where

$$u = \sum_{\mathbf{q}} \sum_{i} c_{\mathbf{q}} b_{\mathbf{q}} e^{i\mathbf{q}\mathbf{r}_i}, \tag{16}$$

$b_{\mathbf{q}}^+(b_{\mathbf{q}})$ the creation (annihilation) operator of a phonon in the state $\mathbf{q}$; and $\mathcal{H}_p$ the phonon Hamiltonian.

To study the properties of the operator $\mathcal{H}_e$ we introduce Jacobi variables

$$\rho_k = (\mathbf{r}_1 + \mathbf{r}_2 + \ldots + \mathbf{r}_k)/k - r_{k+1},$$
$$\rho_N \equiv \mathbf{r} = (\mathbf{r}_1 + \mathbf{r}_2 + \ldots + \mathbf{r}_N)/N. \tag{17}$$

Inversely

$$\mathbf{r}_k = \mathbf{r} - \frac{k-1}{k} \rho_{k-1} + \frac{1}{k+1} \rho_k + \ldots + \frac{1}{N} \rho_{N-1},$$
$$\mathbf{r}_N = \mathbf{r} - \frac{N-1}{N} \rho_{N-1}. \tag{18}$$

One verifies easily that in the new variables

$$\mathcal{H}_e = \mathcal{H}_0(\mathbf{r}) + \mathcal{H}_2(\rho), \tag{19}$$

where $\mathcal{H}_0(\mathbf{r})$ is the operator of the orbital motion of a free particle of charge Ne and mass Nm. The Hamiltonian $\mathcal{H}_2$ commutes with $\rho_N = \mathbf{r}$. In other words, one can split off the center-of-mass motion in the system of interacting electrons in a magnetic field, and the solution of the equation

$$\mathcal{H}_e \Psi_L = E_L \Psi_L \tag{20}$$

is of the form

$$\Psi_L = \psi_\lambda(\mathbf{r})\, F_l(\rho), \tag{21}$$

where $\psi_\lambda(\mathbf{r})$ are the orbital wave functions of a particle of charge Ne and mass Nm, characterizing "external" states, and $F_l(\rho)$ stands for all wave functions describing the "internal" states of the electron system. Similarly

$$E_L = E_l + \varepsilon_\lambda. \tag{22}$$

In the new variables

$$v_x = -(i\hbar/m)\, \partial/\partial x, \tag{23}$$

$$u = \sum_{\mathbf{q}} c_{\mathbf{q}} b_{\mathbf{q}} e^{i\mathbf{q}\mathbf{r}} \sum_{i} e^{i\mathbf{q}(\mathbf{r}_i - \mathbf{r})} \equiv \sum_{\mathbf{q}} c_{\mathbf{q}} b_{\mathbf{q}} e^{i\mathbf{q}\mathbf{r}} f_{\mathbf{q}}(\rho). \tag{24}$$

We assume the electron-phonon interaction to be weak and restrict ourselves, as in I, to the second-order term in the expansion of (12) in powers of U. To evaluate it we apply to (12) the standard method of disentangling exponential operator expressions under the T_C-product sign. In this way it turns out to be possible to write (12) as a sum of twelve terms, each of which corresponds to a diagram similar to the diagrams of Konstantinov and Perel',[5] but with the difference that all electron lines in it (except one) are proper ones, i.e., directed along the contour C. Each electron line going from the point z_2 to z_1 corresponds to a factor $\exp[E_L(z_1 - z_2)/i\hbar]$; the only improper electron line corresponds to an additional factor $\exp(-\beta E_L)$; each phonon line corresponds to a factor $(N_{\mathbf{q}} + 1)\exp[-i\omega_{\mathbf{q}}(z_1 - z_2)]$, if z_2 is earlier than z_1 (proper line) and to $N_{\mathbf{q}} \exp[-i\omega_{\mathbf{q}}(z_1 - z_2)]$ ($N_{\mathbf{q}}$ is the Planck function of the phonon frequency $\omega_{\mathbf{q}}$), if z_1 is earlier than z_2 (improper line); each vertex corresponds to a factor

$$c_{\mathbf{q}} \langle L | \Sigma e^{i\mathbf{q}\mathbf{r}_i} | L' \rangle = c_{\mathbf{q}} \langle \lambda | e^{i\mathbf{q}\mathbf{r}} | \lambda' \rangle \langle l | f_{\mathbf{q}} | l' \rangle; \tag{25}$$

the terminal t to a factor

$$\langle L|v^x|L'\rangle e^{i\omega_{LL'}t} = v^x_{\lambda\lambda'}e^{i\omega_{\lambda\lambda'}t}\delta_{ll'}, \tag{26}$$

and the terminal 0 to a factor

$$\langle M|v^x|M'\rangle = v^x_{\mu\mu'}\delta_{mm'}. \tag{27}$$

Here $\hbar\omega_{LL'} = E_L - E_{L'}$. In the final expression we integrate over z_1 and z_2 between limits that follow from the form of the diagram, and we sum over $\mathbf{q}$ and over all indices of the electron system.

By virtue of the properties of the functions (22), (25), (26), and (27) the matrix elements for transitions between internal states of the system enter as independent factors and therefore all diagrams have the common factors

$$\frac{1}{Z\hbar^2}e^{-\beta E_l}|\langle l|f_{\mathbf{q}}|m\rangle|^2|c_{\mathbf{q}}|^2\begin{Bmatrix}N_{\mathbf{q}}\\N_{\mathbf{q}}+1\end{Bmatrix}. \tag{28}$$

We want to sum the diagrams a to f (see figure) and the diagrams a′ to f′ which differ from the ones illustrated in the figure by the direction of the phonon line. Using the identity

$$v^x_{\lambda\lambda'}/(\nu + i\omega_{\lambda\lambda'}) = \langle\lambda|x - X_\lambda|\lambda'\rangle \tag{29}$$

(X_λ is the coordinate of the center of the Landau oscillator in the state λ) and using the matrix multiplication rules we find that diagram a is equal to

$$-\sum_{\lambda\lambda'}\sum_{\mu\mu'}\frac{e^{-\beta\varepsilon_{\lambda'}}}{\nu + i(\omega_{\mathbf{q}} + \omega_{\mu'\lambda'} + \omega_{ml})}\langle\mu'|e^{i\mathbf{qr}}|\lambda\rangle\langle\lambda|x - X_{\lambda'}|\lambda'\rangle$$
$$\times\langle\lambda'|e^{-i\mathbf{qr}}|\mu\rangle\langle\mu|x - X_\mu|\mu'\rangle$$
$$= -\sum_{\lambda'\mu'}\frac{e^{-\beta\varepsilon_{\lambda'}}}{\nu + i(\omega_{\mathbf{q}} + \omega_{\mu'\lambda'} + \omega_{ml})}$$
$$\times\langle\mu'|e^{i\mathbf{qr}}(x - X_{\lambda'})|\lambda'\rangle\langle\lambda'|e^{-i\mathbf{qr}}(x - X_{\mu'})|\mu'\rangle \tag{30}$$

(we have for the sake of simplicity not written down the factor (28) or the summation signs for summing over $\mathbf{q}$, l, and m). The expression for diagram b differs from (30) only by the general sign and by the fact that instead of the difference $x - X_{\mu'}$ the difference $x - X_{\lambda'}$ enters in it. The sum of diagrams a and b contains thus a factor

$$X_{\mu'} - X_{\lambda'} = (c\hbar/eH)\,q_y, \tag{31}$$

which is independent of the summation indices and is equal to

$$-\mathrm{Re}\sum_{\lambda\mu}(X_\mu - X_\lambda)X_\lambda\frac{e^{-\beta\varepsilon_\lambda}}{\nu + i(\omega_{\mathbf{q}} + \omega_{\mu\lambda} + \omega_{ml})}|\langle\mu|e^{i\mathbf{qr}}|\lambda\rangle|^2$$
$$+\mathrm{Re}\sum_{\lambda\mu}(X_\mu - X_\lambda)\frac{e^{-\beta\varepsilon_\lambda}}{\nu + i(\omega_{\mathbf{q}} + \omega_{\mu\lambda} + \omega_{ml})}$$
$$\times\langle\mu|xe^{i\mathbf{qr}}|\lambda\rangle\langle\lambda|e^{-i\mathbf{qr}}|\mu\rangle. \tag{32}$$

We show in the Appendix that the contribution to (12) from expressions of the form

$$\mathrm{Re}\sum_{\mathbf{q}}\sum_{LM}e^{-\beta E_L}|c_{\mathbf{q}}|^2|\langle l|f_{\mathbf{q}}|m\rangle|^2$$
$$\times\frac{\langle\lambda|e^{i\mathbf{qr}}|\mu\rangle\langle\mu|xe^{-i\mathbf{qr}}|\lambda\rangle}{\nu + i(\omega_{LM} \pm \omega)}\begin{Bmatrix}N_q\\N_q+1\end{Bmatrix} \tag{33}$$

is equal to zero. The second term in (32) which after summation over $\mathbf{q}$, l, and m reduces to the form (33), can thus at once be dropped.

When diagrams c, d, e, and f are summed the factor (31) can also be split off. In the sum of these four diagrams it is also possible to perform two summations, using the rules of matrix multiplication. If we drop terms which give a zero contribution by virtue of (33), we get for this sum

$$-\mathrm{Re}\sum_{\lambda\mu}(X_\mu - X_\lambda)X_\lambda\frac{e^{-\beta\varepsilon_\lambda}}{\nu + i(\omega_{\lambda\mu} - \omega_{\mathbf{q}} + \omega_{lm})}|\langle\lambda|e^{i\mathbf{qr}}|\mu\rangle|^2. \tag{34}$$

Finally, the sum of the diagrams a to f is

$$-\frac{2\pi}{\hbar^2}\sum_{\mathbf{q}}|c_{\mathbf{q}}|^2(N_{\mathbf{q}} + 1)\sum_{LM}(X_\mu - X_\lambda)$$
$$\times X_\lambda e^{-\beta E_L}|\langle L|\Sigma e^{i\mathbf{qr}_i}|M\rangle|^2\,\delta(\omega_{LM} - \omega_{\mathbf{q}}). \tag{35}$$

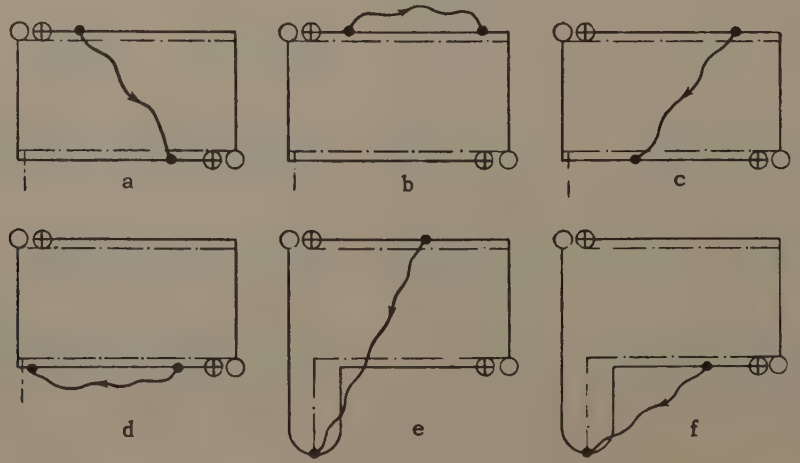

The sum of the diagrams a′ to f′ is the same expression, but with $-\omega_{\mathbf{q}}$ in the δ-function replaced by $\omega_{\mathbf{q}}$ and $N_{\mathbf{q}}+1$ by $N_{\mathbf{q}}$. Transposing in this expression the dummy summation indices L and M, adding this to (35) and taking into account the identity

$$e^{-\beta E_L}\delta(\omega_{LM}-\omega_{\mathbf{q}})(N_{\mathbf{q}}+1) = e^{-\beta E_M}\delta(\omega_{LM}-\omega_{\mathbf{q}})N_{\mathbf{q}} \tag{36}$$

and relation (35) we get finally

$$\sigma_{xx} = \frac{e^2\beta}{(2\pi)^3}\left(\frac{c}{eH}\right)^2\int d^3q\, q_y^2 |c_{\mathbf{q}}|^2 N_{\mathbf{q}}\Phi_{\mathbf{q}}(\omega_{\mathbf{q}}), \tag{37}$$

$$\Phi_{\mathbf{q}}(\omega) = Z^{-1}\sum_{LM}|\langle L|\sum e^{i\mathbf{q}\mathbf{r}_i}|M\rangle|^2 e^{-\beta E_L}\delta(\omega_{ML}-\omega). \tag{38}$$

(37) is exactly the same as Eq. (8) of I. The latter was derived from the formula of Kubo, Hasegawa, and Hashitsume [6] which expresses σ_{xx} in terms of the correlator of the operators of the velocity of the motion of the center of the Landau oscillator. But this formula itself was derived in [6] from an equation such as (12), using a number of additional assumptions. The present derivation starts directly from (12) and does therefore not depend on additional assumptions.

Moreover, it will be convenient for us to change in the expressions for $\Phi_{\mathbf{q}}(\omega)$ to a second quantization representation and to take a Gibbs average. To do this, we put

$$B_q = \sum_i e^{i\mathbf{q}\mathbf{r}_i} = \sum_\sigma\int d^3r\psi^+(\mathbf{r},\sigma)e^{i\mathbf{q}\mathbf{r}}\psi(r,\sigma)$$

$$= \sum_{\Gamma\Delta}\langle\Gamma|e^{i\mathbf{q}\mathbf{r}}|\Delta\rangle a_\Gamma^+ a_\Delta, \tag{39}$$

where $\psi(\mathbf{r},\sigma) = \Sigma_\Delta a_\Delta\psi_\Delta(\mathbf{r},\sigma)$ is the electron wave function in the second quantization representation, $a_\Delta(a_\Delta^+)$ is the annihilation (creation) operator for an electron in the state Δ. Then we have

$$\Phi_{\mathbf{q}}(\omega) = Z^{-1}\sum_{LM}\exp[-\beta(E_L-\mu N_L)]\,\delta$$

$$\times(\omega_{ML}-\omega)|\langle M|B_{\mathbf{q}}|L\rangle|^2, \tag{40}$$

where N is the particle number operator. According to I, $\Phi_{\mathbf{q}}(\omega)$ can be expressed in terms of $K_{\mathbf{q}}(\omega)$, the Fourier component of the two-particle retarded Green's function with pairwise equal arguments, through the formula

$$\Phi_{\mathbf{q}}(\omega) = \operatorname{Im}K_{\mathbf{q}}(\omega)/\pi(1-e^{-\hbar\omega\beta}). \tag{41}$$

In [3] a method was proposed to evaluate $K_{\mathbf{q}}(\omega)$ for the case $\mathbf{H}=0$; this method was generalized in a paper by the authors [7] for the case of a non-vanishing magnetic field. According to [7]

$$K_{\mathbf{q}}(\omega) = \Pi_{\mathbf{q}}(\omega)\Big/\left[1+\frac{4\pi e^2}{\varepsilon_0\hbar q^2 V_0}\Pi_{\mathbf{q}}(\omega)\right], \tag{42}$$

where $\Pi_{\mathbf{q}}(\omega)$ corresponds to the sum of all connected Matsubara diagrams (see [3] and [7]). Taking (37) and (41) into account we get then

$$\sigma_{xx} = \frac{e^2\beta}{(2\pi)^2}\left(\frac{c}{eH}\right)^2\int d^3q q_y^2\frac{\operatorname{Im}\Pi_q(\omega)}{\pi(1-e^{-\hbar\omega\beta})}|c_{\mathbf{q}}|^2 N_{\mathbf{q}}$$

$$\times\left\{\left[1+\frac{4\pi e^2}{\varepsilon_0\hbar q^2 V_0}\operatorname{Re}\Pi_{\mathbf{q}}(\omega)\right]^2+\left[\frac{4\pi e^2}{\varepsilon_0\hbar q^2 V_0}\operatorname{Im}\Pi_{\mathbf{q}}(\omega)\right]^2\right\}^{-1}. \tag{43}$$

We see that in the general case it is not at all possible to arrive at a simple renormalization of $|c_{\mathbf{q}}|^2$ of the form discussed in Sec. 1. However, in a number of cases, we have with fair accuracy

$$\Pi_{\mathbf{q}}(\omega) = K_{\mathbf{q}}^0(\omega), \tag{44}$$

where $K_{\mathbf{q}}^0(\omega)$ can be expressed by the sum (4) and corresponds to the simplest diagram which is of the form of a loop of two electron lines. [1,3,7]

When a strong magnetic field is present ($\alpha = \hbar\Omega/2kT \gg 1$) one can easily justify the approximation (44) for the case where the Born parameter is small $e^2/\epsilon_0\hbar v_T \ll 1$ (small effective masses and large values of ϵ_0 favor the satisfying of this inequality). However, there are grounds for hoping that in reality (44) is valid when the weaker condition $e^2n^{1/3}/\epsilon_0 kT \ll 1$ (average energy of the Coulomb interaction between the electrons small compared to the thermal energy) is satisfied.

If (44) is valid,

$$\sigma_{xx} = \frac{e^2\beta}{(2\pi)^2}\left(\frac{c}{eH}\right)^2\int d^3q q_y^2|c_{\mathbf{q}}|^2 N_{\mathbf{q}}\Phi_{\mathbf{q}}^0(\omega_{\mathbf{q}})$$

$$\times\left\{\left[1+\frac{4\pi e^2}{\varepsilon_0\hbar q^2 V_0}\operatorname{Re}K_{\mathbf{q}}^0(\omega)\right]^2+\left[\frac{4\pi e^2}{\varepsilon_0\hbar q^2 V_0}\operatorname{Im}K_{\mathbf{q}}^0(\omega)\right]^2\right\}^{-1},$$

$$\Phi_{\mathbf{q}}^0(\omega) = \operatorname{Im}K_{\mathbf{q}}^0(\omega)/\pi(1-e^{-\hbar\omega\beta}). \tag{45}$$

The renormalized interaction in (45) has, indeed, the form (8). Our rigorous theory justifies thus the application of the self-consistent field method in this case.

We obtained in I an expression for $\operatorname{Im}K_{\mathbf{q}}^0(\omega)$ for the case $H \neq 0$ in the form of a series which was particularly convenient to use in the quantum limiting case when it converges very rapidly*

$$\operatorname{Im}K_{\mathbf{q}}^0(\omega) = \pi(1-e^{-\hbar\omega\beta})\Phi_{\mathbf{q}}^0(\omega) = \frac{n\sqrt{\pi}V_0}{|q_z|v_T}(1-e^{-\hbar\omega\beta})$$

$$\times\exp\left(\frac{\hbar\omega\beta}{2}-\frac{q_\perp^2 a^2\operatorname{cth}\alpha}{2}\right)$$

$$\times\sum_{N=-\infty}^{\infty}I_N\left(\frac{q_\perp^2 a^2}{2\operatorname{sh}\alpha}\right)\exp\left[-\frac{(N\Omega-\omega)^2}{q_z^2 v_T^2}-\frac{q_z^2}{4q_T^2}\right]. \tag{46}$$

*cth = coth, sh = sinh.

Using similar methods we find

$$\operatorname{Re} K_q^0(\omega) = \frac{2nV_0}{|q_z| v_T} \exp\left(-\frac{q_\perp^2 a^2}{2} \operatorname{cth} \alpha\right) \sum_{N=-\infty}^{\infty} e^{\alpha N} I_N\left(\frac{q_\perp^2 a^2}{2 \operatorname{sh} \alpha}\right) \times \left[W\left(\frac{\hbar q_z^2/2m + \omega + N\Omega}{|q_z| v_T}\right) + W\left(\frac{\hbar q_z^2/2m - \omega + N\Omega}{|q_z| v_T}\right)\right]. \quad (47)$$

3. Using Eq. (45) we can in principle consider the effects caused by the Coulomb interaction between carriers which were mentioned in Sec. 1. Here we study one such effect. In I we predicted theoretically peculiar resonance oscillations of the transverse conductivity in a magnetic field which are caused by the scattering of the electrons by phonons with a non-vanishing limiting frequency ω_0 (optical phonons). The oscillation maxima are determined by the condition $\omega_0 = N_0\Omega$ (N_0 is an integer) and, for instance, when $\alpha \gg 1$ we have near $\omega_0 = \Omega$ ($N_0 = 1$)*

$$\sigma_{xx} = \sigma_{xx}^{cl} \frac{3\alpha}{2\sqrt{\pi\hbar\omega_0\beta}} \ln\frac{1}{\alpha|\delta|} = \sigma_{xx}^{cl} \frac{3(\hbar\omega_0\beta)^{1/2}}{4\sqrt{\pi}} \ln\frac{1}{\alpha|\delta|}, \quad (48)$$

where σ_{xx}^{cl} is the classical value of the low-temperature transverse conductivity evaluated in I and $\delta = (\omega_0 - \Omega)/\omega_0$. Expression (48), as also Eqs. (48) and (50) in I which are suitable for arbitrary N, give an infinite height of the oscillating peak for $\omega_0 = N_0\Omega$.

Mathematically, this infinity is caused by the fact that when ω_0 is exactly equal to $N_0\Omega$ the integral over q_z of the N_0-th term of the series (46) diverges at the lower limit. We did not consider in I the mechanisms limiting this infinity. If, however, we take these into account, the logarithm in (48) has a finite value at $\omega_0 = N_0\Omega$ and is equal to

$$\ln(1/\alpha\delta_c), \quad (49)$$

where $\delta_c \ll 1$. The second term in the denominator of (45) is proportional to the square of (46) and thus tends to infinity as $1/q_z^2$ when $q_z \to 0$. The Coulomb interaction between the scatterers is thus able to limit the height of the resonance peak. This mechanism is, of course, not the only one, but the cut-off determined by it can in a number of cases turn out to be the most effective one; in the present paper we shall evaluate it.

We restrict ourselves to one of the experimentally most interesting cases: $N_0 = 1$ (first oscillation), $\alpha = \hbar\Omega/2kT \gg 1$ (quantum limit). We shall here not be interested in the shape of the resonance line and simply evaluate σ_{xx} for $\Omega = \omega_0$. It is clear that small q_z ($q_z \ll q_T$) and $q_\perp \lesssim 1/a$ play a role in the resonance region. However, in the important region of q

$$\varkappa^2/q^2 \approx \varkappa^2 q_\perp^2 \sim \varkappa^2 a^2 \ll 1, \quad (50)$$

and when $q_\perp \sim 1/a$ the first term in the denominator in (45) can be assumed to be equal to unity. The interval $q_\perp \ll 1/a$ cannot play a role as long as the first term does not tend to zero in it. In actual fact, it takes on a zero value, generally speaking, but one can show that all contributions from the region of small $q_\perp$ are negligibly small, all the same.

Moreover, in the series (46) only the term with N = 1 will play a role and all other terms are exponentially small. Finally, for the interaction with the optical phonons

$$|c_q|^2 = A/q^2 \approx A/q_\perp^2,$$

where the expression for A was given in I. The problem is thus reduced to an evaluation of the following expression

$$\sigma_{xx} = \frac{ne^2\beta A}{2\pi^{3/2} v_T} N_q e^{\hbar\omega\beta/2} \int_0^\infty \frac{dq_z}{q_z} \int_0^\infty q_\perp dq_\perp I_1\left(\frac{q_\perp^2 a^2}{2 \operatorname{sh} \alpha}\right) \times \exp\left(-\frac{q_\perp^2 a^2}{2} - \frac{q_z^2}{4q_T^2}\right) \left\{1 + 4\pi\left(\frac{\varkappa}{q_\perp}\right)^4 \left(\frac{q_T}{q_z}\right)^2 \times \operatorname{sh}^2 \frac{\hbar\omega_0\beta}{2} I_1^2\left(\frac{q_\perp^2 a^2}{2 \operatorname{sh} \alpha}\right) \exp\left(-\frac{q_z^2}{2q_T^2} - q_\perp^2 a^2\right)\right\}^{-1}. \quad (51)$$

We take further into account that apart from exponentially small terms

$$I_1(q_\perp^2 a^2/2 \operatorname{sh} \alpha) = q_\perp^2 a^2/4 \operatorname{sh} \alpha,$$

and we change to new integration variables $x = q_\perp^2 a^2/2$, $y = q_z^2/4q_T^2$:

$$\sigma_{xx} = \frac{ne^2}{4\sqrt{\pi}\,\Omega^2 t_0} e^{-\hbar\omega_0\beta} \left(\frac{\hbar\omega_0}{kT}\right)^{3/2} \int_0^\infty x e^{-x} dx \times \int_0^\infty \frac{e^{-y} dy}{y + (\pi/16)(\varkappa a)^4 e^{-2(x+y)}}, \quad (52)$$

where $t_0 = (2\pi\hbar^2/A)(\hbar\omega_0/2m)^{1/2}$. When $(\varkappa a)^2 \ll 1$ the integral over y is equal to

$$\ln\frac{16}{\pi C_1 (\varkappa a)^4} + 2x, \quad (53)$$

where $C_1 = e^C$, $C = 0.577$ is Euler's constant. Performing the integration over x we get finally

$$\sigma_{xx} = \sigma_{xx}^{cl} \frac{3}{4\sqrt{\pi}} \sqrt{\hbar\omega_0\beta} \ln\frac{4e^2}{\sqrt{\pi C_1 (\varkappa a)^4}}, \quad (54)$$

where according to (49) of I

$$\sigma_{xx}^{cl} = (2ne^2/3m\Omega^2 t_0)\, \hbar\omega_0\beta e^{-\hbar\omega_0\beta}. \quad (55)$$

Comparing (48), (49), and (54) we find

*We note that in the corresponding Eq. (50) of I the coefficient $1/\pi^{1/2}$ was omitted by mistake.

$$\delta_c = \sqrt{\pi C_1}\,(\varkappa R)^2 / 4e^2, \tag{56}$$

where $R = mv_T c/eH$.

To elucidate when this mechanism of cut-off plays the main role we determine the cut-off, taking the dispersion of the optical phonons into account. Let the optical phonon frequency be

$$\omega_q = \omega_0 (1 - a_0^2 q^2), \tag{57}$$

where a_0 is of the order of the crystal lattice constant. Calculations completely similar to the ones we just performed give the following result

$$\delta_c = e\,(a_0 / a)^2. \tag{58}$$

This quantity is as a rule considerably less than (56).

We must finally give an estimate of the cut-off caused by the broadening of the energy levels due to collisions. Very rough estimates in a paper by Adams and Holstein[8] give

$$\delta_c = 1 / \Omega\tau, \tag{59}$$

where τ is a characteristic life time of the electron in the given state. Attempts to estimate this quantity more accurately run up against serious difficulties. From a comparison of (59) and (56) it is, however, clear that the electron-electron interaction may in a number of cases be the main mechanism restricting the height of the oscillations.

APPENDIX I

We show that an expression of the type

$$Z^{-1}\mathrm{Re}\sum_{\mathbf{q}} |c_{\mathbf{q}}|^2 N_{\mathbf{q}} \times \sum_{LM} (X_\lambda - X_\mu)\, e^{-\beta E_L} \frac{\langle L | x\Sigma e^{i\mathbf{q}\mathbf{r}_i} | M\rangle \langle M | \Sigma e^{-i\mathbf{q}\mathbf{r}_i} | L\rangle}{\nu + i\,(\omega_{LM} + \omega_{\mathbf{q}})} \tag{A.1}$$

when summed with the same expressions, where $N_{\mathbf{q}}$ and $\omega_{\mathbf{q}}$ are replaced by $N_{\mathbf{q}}+1$ and $-\omega_{\mathbf{q}}$ gives zero. We put

$$\mathrm{Re}\frac{\langle L | x\Sigma e^{i\mathbf{q}\mathbf{r}_i} | M\rangle \langle M | \Sigma e^{-i\mathbf{q}\mathbf{r}_i} | L\rangle}{\nu + i\,(\omega_{LM} + \omega_{\mathbf{q}})} = \pi\delta(\omega_{LM} + \omega_{\mathbf{q}}) \times \mathrm{Re}\{\langle L | x\Sigma e^{i\mathbf{q}\mathbf{r}_i} | M\rangle \langle M | e^{-i\mathbf{q}\mathbf{r}_i} | L\rangle\} + \mathrm{P}\frac{\mathrm{Im}\{\langle L | x\Sigma e^{i\mathbf{q}\mathbf{r}_i} | M\rangle \langle M | e^{-i\mathbf{q}\mathbf{r}_i} | L\rangle\}}{\omega_{LM} + \omega_{\mathbf{q}}} \tag{A.2}$$

(P indicates the principal value). The contribution in (A.1) from the first term in (A.2) to the sum with the same expression, but with $N_{\mathbf{q}}$ and $\omega_{\mathbf{q}}$ replaced by $N_{\mathbf{q}}+1$ and $-\omega_{\mathbf{q}}$ is zero. To verify that, it is sufficient to transpose in the expression with $N_{\mathbf{q}}+1$ the summation indices L and M, to replace $\mathbf{q}$ by $-\mathbf{q}$ and to take the identity (36) into account. We use further the relation

$$\mathrm{Im}\{\langle\lambda | xe^{i\mathbf{q}\mathbf{r}} | \mu\rangle \langle\mu | e^{-i\mathbf{q}\mathbf{r}} | \lambda\rangle\} = -\tfrac{1}{2}\frac{\partial}{\partial q_x} |\langle\lambda | e^{i\mathbf{q}\mathbf{r}} | \mu\rangle|^2. \tag{A.3}$$

However, by definition

$$\pi \sum_{\lambda\mu} \delta(\omega_{\lambda\mu} + \omega)\, |\langle\lambda | e^{i\mathbf{q}\mathbf{r}} | \mu\rangle|^2 e^{-\beta\varepsilon_\lambda} = Z^{-1}\Phi_{\mathbf{q}}^0(\omega), \tag{A.4}$$

where Z is the appropriate partition function. Using the representation (45) one obtains easily the rule for differentiating this function:

$$\frac{\partial}{\partial q_x}\Phi_{\mathbf{q}}^0(\omega) = -q_x a^2 \operatorname{cth}\alpha\, \Phi_{\mathbf{q}}^0(\omega) + \frac{q_x a^2}{2\operatorname{sh}\alpha}[\Phi_{\mathbf{q}}^0(\omega + \Omega) + \Phi_{\mathbf{q}}^0(\omega - \Omega)]. \tag{A.5}$$

Substituting (A.5) and (A.4) into (A.1) and taking into account that a non-vanishing contribution can only come from the second term in (A.2) we get finally the following expression for (A.1):

$$\frac{a^4}{2Z}\,\mathrm{P}\int\frac{d\omega}{\omega}\sum_{\mathbf{q}} q_x q_y |c_{\mathbf{q}}|^2 N_{\mathbf{q}}\,[\operatorname{cth}\alpha\,\Phi_{\mathbf{q}}(\omega - \omega_{\mathbf{q}}) - \Phi_{\mathbf{q}}(\omega - \omega_{\mathbf{q}} + \Omega)/2\operatorname{sh}\alpha - \Phi_{\mathbf{q}}(\omega - \omega_{\mathbf{q}} - \Omega)/2\operatorname{sh}\alpha]. \tag{A.6}$$

Since $\Phi_{\mathbf{q}}$, $|c_{\mathbf{q}}|^2$, and $\omega_{\mathbf{q}}$ are essentially even functions of q_x this expression vanishes which concludes our proof.

APPENDIX II

When analyzing the causes producing the cut-off of the oscillations we must bear in mind still the two following factors which occur because of the interaction between the phonons and the electrons: damping of the phonons and renormalization of their frequency, thanks to which there occurs for them an additional, rather strong dispersion. We show that both these factors are unimportant for the present problem.

We are interested in the case of a low electron concentration and a weak electron-phonon interaction. One can show that under those conditions when taking these effects into account it is sufficient to introduce renormalized phonon lines to each of which must be assigned a causal Green's function which is equal to[9,10]

$$iD(\mathbf{q}, z_1 - z_2) = \begin{cases} \int_{-\infty}^{\infty} \rho_{\mathbf{q}}(\omega) e^{-i\omega(z_1 - z_2)} d\omega, & \text{if the line is a proper one,} \\ \int_{-\infty}^{\infty} \rho_{\mathbf{q}}(\omega) e^{-\hbar\omega\beta - i\omega(z_1 - z_2)} d\omega, & \text{if the line is an improper one;} \end{cases} \quad (A.7)$$

$$\rho_{\mathbf{q}}(\omega) = \sum_{LM} e^{-\beta E_L} |\langle L | b_{\mathbf{q}} + b^{+}_{-\mathbf{q}} | M \rangle|^2 \delta(\omega - \omega_{ML}). \quad (A.8)$$

As a result we get instead of (37)

$$\sigma_{xx} = (e^2\beta / 8\pi^2)(c/eH)^2 \int_{-\infty}^{\infty} d\omega \int d^3q\, q_y^2 |c_{\mathbf{q}}|^2 \Phi_{\mathbf{q}}(\omega)\, \rho_{\mathbf{q}}(-\omega). \quad (A.9)$$

This expression corresponds to a sum of Matsubara diagrams with electron lines renormalized by taking phonons into account and with electron-phonon vertices.

In accordance with [9]

$$\rho_{\mathbf{q}}(\omega) = -\pi (1 - e^{-\hbar\omega\beta})^{-1} \operatorname{Im} \{D^T(\mathbf{q}, \omega_N)|_{\omega_N \to i\omega + \nu}\}, \quad (A.10)$$

where $D^T(\mathbf{q}, \omega_N)$ is the temperature dependent Green's function, and $\omega_N = 2\pi NkT/\hbar$. It satisfies the equation (cf. [10])

$$D^T(\mathbf{q}, \omega_N) = D_0^T(\mathbf{q}, \omega_N) + \hbar^{-2} D_0^T(\mathbf{q}, \omega_N) K_{\mathbf{q}}(-i\omega_N) D^T(\mathbf{q}, \omega_N).$$

According to Eq. (7b) of I, $|c_{\mathbf{q}}|^2 = 2\pi\hbar\omega_0 e^2/V_0 q^2 \epsilon_c$, $\epsilon_c^{-1} = \epsilon_0^{-1}(\infty) - \epsilon_0^{-1}(0)$. We have then

$$\rho_{\mathbf{q}}(\omega) = -\frac{2\omega_{\mathbf{q}}}{\pi(1 - e^{-\hbar\omega\beta})} \operatorname{Im} \left\{ \omega_{\mathbf{q}}^2 \left(1 - \frac{\varepsilon_0}{\varepsilon_c}\right) + \omega_{\mathbf{q}}^2 \frac{\varepsilon_0}{\varepsilon_c} \frac{1}{1 + \frac{4\pi e^2}{\varepsilon_0 \hbar V_0 q^2} \Pi_{\mathbf{q}}(\omega)} - \omega^2 \right\}^{-1}. \quad (A.11)$$

The poles of the function $D^T(\mathbf{q}, i\omega)$ give the renormalized phonon frequencies and the damping of the phonons due to their interaction with the electrons. In those $q_\perp$ and q_z regions where $\operatorname{Im} \Pi_{\mathbf{q}}(\omega)$ is large and leads to a limiting of the oscillations, the second term within the curly brackets in (A.11) is unimportant and in that region we obtain only an inappreciable shift of the resonance frequency* (when the coupling parameter is small, $\epsilon_0/\epsilon_c \ll 1$) Far from $\omega = N\Omega$ we obtain rather interesting singularities of the renormalized phonon spectrum, but they are unimportant for the present effect.

In conclusion we turn our attention to one interesting singularity of expression (A.9). For free phonons

$$\rho_{\mathbf{q}}(\omega) = N_{\mathbf{q}} \delta(\omega + \omega_{\mathbf{q}}) + (N_{\mathbf{q}} + 1) \delta(\omega - \omega_{\mathbf{q}}).$$

If we substitute this expression into (A.9) the integration over $d\omega$ disappears and we get Eq. (37). This is because when the electrons interact with free phonons there corresponds to a given value of the momentum transfer $\hbar\mathbf{q}$ a completely determined value of energy transfer $\hbar\omega_{\mathbf{q}}$. When the phonon damping is taken into account there occurs an uncertainty in the phonon energy and momentum. As a result the energy and momentum transfer are no longer connected with one another during electron-phonon collisions and σ_{xx} has the form of an integral over all possible values of the energy and momentum transfer (cf. [7]).

*We note that according to Born and Huang[11] the electron-electron interaction operator in an ionic crystal contains $\varepsilon_0(\infty)$, the permittivity on the plateau of the dispersion curve.

[1] V. L. Gurevich and Yu. A. Firsov, JETP **40**, 199 (1961), Soviet Phys. JETP **13**, 137 (1961).

[2] S. Doniach, Proc. Phys. Soc. (London) **73**, 849 (1959).

[3] A. I. Larkin, JETP **37**, 264 (1959), Soviet Phys. JETP **10**, 186 (1960).

[4] R. Kubo, J. Phys. Soc. Japan **12**, 570 (1957).

[5] O. V. Konstantinov and V. I. Perel', JETP **39**, 197 (1960), Soviet Phys. JETP **12**, 142 (1961).

[6] R. Kubo, H. Hasegawa, and N. Hashitsume, J. Phys. Soc. Japan **14**, 56 (1959).

[7] V. L. Gurevich and Yu. A. Firsov, JETP, in course of publication.

[8] E. N. Adams and T. D. Holstein, J. Phys. Chem. Solids **10**, 254 (1959).

[9] A. A. Abrikosov, L. P. Gor'kov, and I. E. Dzyaloshinskii, JETP **36**, 900 (1959), Soviet Phys. JETP **9**, 636 (1959).

[10] A. B. Migdal, JETP **34**, 1438 (1958), Soviet Phys. JETP **7**, 996 (1958).

[11] M. Born and Kun Huang, Dynamical Theory of Crystal Lattice (Russian translation), IIL, 1958, part II, Sec. 8. [Clarendon Press, Oxford, 1954].

Translated by D. ter Haar
94

NEGATIVE ABSORPTION COEFFICIENT PRODUCED BY DISCHARGES IN A GAS MIXTURE

V. A. FABRIKANT

Moscow Power Institute

Submitted to JETP editor March 7, 1961

J. Exptl. Theoret. Phys. (U.S.S.R.) **41**, 524-527 (August, 1961)

The probabilities for various processes are considered in an analysis of an electrical discharge in a mixture of two gases in which a negative absorption coefficient is obtained by selective excitation of atoms to a higher level and selective removal of atoms from a lower level.

1. Basov and Krokhin[1] have proposed a diagram that facilitates analysis of the necessary conditions for obtaining a negative absorption coefficient in an electrical discharge in a mixture of two gases.*

The assumptions used by these authors, however, correspond neither to actual conditions nor to the relations between atomic constants for vapors and gases used by Butaeva and Fabrikant[2] and by Ablekov, Pesin and Fabelinskii.[3] In [2] collisions between atoms and molecules of two components of a gas mixture were used to selectively remove atoms from a lower level; however, atoms were not selectively excited to an upper level.[1] This technique had been proposed in 1939 and is the original prototype of the method used in ammonia masers. This case is the opposite of that considered by Basov and Krokhin.

Entirely different results are obtained if calculations similar to those in [1] are used for the conditions pertaining to [2]. In particular, inequality (5) of [1] becomes completely different and the corresponding diagram contains only two regions, I and II; in contrast with [1], region IV, in which a negative absorption coefficient is impossible, no longer appears. It should also be noted that in [2] the discharge conditions were such that the Maxwellian electron energy did not appear explicitly, so that the relation between Θ_{i0} and Θ_{0i} given in [1] does not hold.

In [1] account is taken of collisions of the second kind with electrons in which atoms are transferred from level ϵ_i to level ϵ_0 while collisions of the second kind characterized by $\epsilon_i \to \epsilon_k$ are neglected. The principle of detailed balancing shows that the probability of collisions of the second kind increases as the distances between levels decrease.[5] Consequently the probability of $\epsilon_i \to \epsilon_k$ collisions of the second kind is greater than the probability of $\epsilon_i \to \epsilon_0$ transitions. Also, the quantity $1/\tau_{ik}$ cannot be neglected if $1/\tau_{i0}$ is retained. For example, in the case of mercury and zinc $1/\tau_{i0}$ is approximately 0 while $1/\tau_{ik} \approx 10^7$ sec^{-1}. The same situation holds for the inert gases.[6] It is well known that spontaneous transitions characterized by $\epsilon_i \to \epsilon_k$ in the optical frequency region generally have a strong inhibiting effect on the establishment of the required relation between the atomic populations in levels ϵ_i and ϵ_k.

2. We now derive the conditions that must be satisfied to obtain a negative absorption coefficient when the actual relations between the appropriate probabilities are taken into account. We first form the equations that describe selective removal of atoms from the lower level. Aside from a few changes our notation is essentially that used earlier in the theory of the gas discharge.[7] Thus, we have

$$dn_i^a/dt = -n_i^a(A_{ik} + \beta_{ik}) + n_0^a\alpha_{0i} + n_k^a\alpha_{ki}, \quad (1)$$

$$dn_k^a/dt = -n_k^a(A_{k0} + \beta_{k0} + B_{ab}) + n_0^a(\alpha_{0k} + B_{ba}) + n_i^a(A_{ik} + \beta_{ik}), \quad (2)$$

where n is the density of atoms or molecules; A_{ik} and A_{k0} are the probabilities for spontaneous transitions; $B_{ab} = n_0^b\sigma_{ab}v$, B_{ba} is the probability for collisions with impurity atoms or molecules (the impurity is the added component of the mixture); α_{0i}, α_{0k}, α_{ki} are the probabilities for electron collisions of the first kind; β_{i0}, β_{k0}, β_{ik} are the probabilities for electronic collisions of the second kind.

In writing Eqs. (1) and (2) we assume that

$$A_{i0} \ll A_{ik}, \ \alpha \ll \beta, \ \beta_{i0} \ll \beta_{ik}.$$

*The term "negative absorption coefficient" corresponds more closely to the terminology used by Einstein than the presently popular term "negative temperature."

The lifetimes are written in the form

$$\tau_i = 1/(A_{ik} + \beta_{ik}),\ \tau_k = 1/(A_{k0} + \beta_{k0} + B_{ab}). \quad (3)$$

Using Eqs. (1) and (2) we obtain the condition for producing a negative absorption coefficient in the steady state:

$$\frac{\alpha_{0i}(A_{k0} + \beta_{k0} + B_{ab}) + \alpha_{ki}(\alpha_{0k} + B_{ba})}{(\alpha_{0k} + \alpha_{0i} + B_{ab} n_k^b / n_0^b)(A_{ik} + \beta_{ik})} > 1. \quad (4)$$

Using Eq. (3) we can show that (4) is an extended version of inequality (10) of [2].

Using the approximations

$$\beta_{ik} \approx b_{ik}\beta_{i0},\quad \beta_{k0} \approx b_{k0}\beta_{i0}, \quad (5)$$

where b_{ik} and b_{k0} are essentially constants appreciably greater than unity, we obtain from Eq. (4)

$$\frac{B_{ab}}{\beta_{k0}} \gtrless \frac{b_{ik}[\exp\{(\varepsilon_i - \varepsilon_k)/kT_e\} + 1/b_{k0}]\,\eta_{ik} - \eta_{k0} - b_{ik}}{1 - b_{ik}(n_k^b/n_0^b)[\exp\{\varepsilon_i/kT_e\}\,\eta_{ik} - \exp\{\varepsilon_k/kT_e\}]} \quad (6)$$

(we have used the notation $\eta_{ik} \equiv 1 + A_{ik}/\beta_{ik}$). The > sign applies when the denominator is greater than zero while the < sign applies when the denominator is less than zero.

The equations for the lines on the A_{k0}/β_{k0}; A_{ik}/β_{ik} diagram are of the form

$$\frac{A_{ik}}{\beta_{ik}} = \frac{\exp\{-\varepsilon_i/kT_e\}}{b_{ik}}\,\frac{n_0^b}{n_k^b} - 1 - \exp\{-(\varepsilon_i - \varepsilon_k)/kT_e\}, \quad (7)$$

$$\frac{A_{ik}}{\beta_{ik}} = \frac{A_{k0}/\beta_{k0} + 1 - b_{ik}(1/b_{k0} - 1 + \exp\{(\varepsilon_i - \varepsilon_k)/kT_e\})}{b_{ik}(\exp\{(\varepsilon_i - \varepsilon_k)/kT_e\} + 1/b_{k0})}. \quad (8)$$

Equation (7) is physically meaningful only when

$$n_k^b/n_0^b < \exp\{-\varepsilon_i/kT_e\}/b_{ik}. \quad (9)$$

The inequality (9) is certainly not always satisfied in a gas discharge. In Eq. (8) the free term is always negative, in contrast with the case considered in [1]. If the condition in (9) is satisfied the diagram will contain four regions (cf. Fig. a) characterized by the following features: I) an impurity is not necessary, but is desirable; II) an impurity is necessary; III) an impurity is harmful; IV) it is impossible to obtain a negative absorption coefficient. Regions I and II vanish if the condition in (9) is not satisfied.

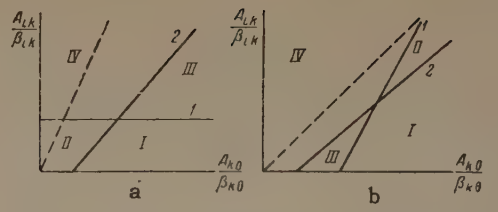

a – selective removal of atoms from the lower level; 1 – line (7), 2 – line (8); b – selective excitation of atoms to the upper level; 1 – line (14), 2 – line (15). Region I – impurity desirable, II – impurity necessary, III – impurity harmful, IV – effect impossible.

We now consider selective excitation of atoms to a level ϵ_i. In this case the starting equations are

$$dn_i^a/dt = -n_i^a(A_{ik} + \beta_{ik} + B_{ab}) + n_0^a(\alpha_{0i} + B_{ba}) + n_k^a\alpha_{ki}, \quad (10)$$

$$dn_k^a/dt = -n_k^a(A_{k0} + \beta_{k0}) + n_0^a\alpha_{0k} + n_i^a(A_{ik} + \beta_{ik}). \quad (11)$$

The condition for a negative absorption coefficient becomes

$$\frac{(\alpha_{0i} + B_{ba})(A_{k0} + \beta_{k0}) + \alpha_{0k}\alpha_{ki}}{(A_{ik} + \beta_{ik} + B_{ab})\alpha_{0k} + (A_{ik} + \beta_{ik})(\alpha_{0i} + B_{ba})} > 1. \quad (12)$$

The inequality (12) also represents an extended form of (10) of [2]. Consequently

$$\frac{B_{ba}}{\beta_{i0}} \gtrless \frac{(b_{ik}/b_{k0})[\eta_{ik}(1 + b_{k0}\exp\{(\varepsilon_i - \varepsilon_k)/kT_e\}) - (b_{k0}/b_{ik})\eta_{k0} - b_{ik}\exp\{(\varepsilon_i - \varepsilon_k)/kT_e\}]}{\exp\{\varepsilon_i/kT_e\}[\eta_{k0} - (b_{ik}/b_{k0})[\eta_{ik} - (n_0^b/n_i^b)\exp\{-\varepsilon_k/kT_e\}]}. \quad (13)$$

The equations for the lines on the A_{k0}/β_{k0}; A_{ik}/β_{ik} diagram are of the form

$$\frac{A_{ik}}{\beta_{ik}} = \frac{b_{k0}}{b_{ik}}\,\frac{A_{k0}}{\beta_{k0}} - \frac{b_{k0}}{b_{ik}}\left(\frac{n_0^b}{n_i^b}\exp\left\{-\frac{\varepsilon_k}{kT_e}\right\} - 1\right) - 1, \quad (14)$$

$$\frac{A_{ik}}{\beta_{ik}} = \frac{A_{k0}/\beta_{k0} - b_{ik}\exp\{(\varepsilon_i - \varepsilon_k)/kT_e\}(1 - 1/b_{k0}) - b_{ik}/b_{k0} + 1}{b_{ik}\exp\{(\varepsilon_i - \varepsilon_k)/kT_e\} + b_{ik}/b_{k0}}. \quad (15)$$

The free terms in Eqs. (14) and (15) are always negative.

The lines intersect when

$$n_i^b/n_0^b < \exp\{-\varepsilon_i/kT_e\}/b_{ik}. \quad (16)$$

In this case the diagram becomes that shown in Fig. b, where the shapes of the various regions are different from those in the diagram in [1]. If the excitation of impurity atoms becomes strong enough, the condition in (16) is violated and region III disappears.

Because of (5), for a given host material transfers are possible only in regions of the diagrams close to the dashed line. The slope of these lines is determined by the quantity $b_{k0}A_{ik}/b_{ik}A_{k0}$.

The value of diagrams of this kind is limited by the fact that the lines which divide the diagrams into various regions are displaced sharply for small changes in the electron temperature. In particular, shifts of this kind occur when the composition of the medium is changed in order to vary the quantity B_{ab}.

[1] N. G. Basov and O. I. Krokhin, JETP **39**, 1777 (1960), Soviet Phys. JETP **12**, 1240 (1961).

[2] F. Butaeva and V. Fabrikant, Issledovaniya po éksperimental'noĭ i teoreticheskoĭ fizike (Research in Experimental and Theoretical Physics), In memorian Acad. G. S. Landsberg, U.S.S.R. Acad. Sci. Press, 1959.

[3] Ablekov, Pesin, and Fabelinskii, JETP **39**, 892 (1960), Soviet Phys. JETP **12**, 618 (1961).

[4] V. Fabrikant, Elektronnye i ionnye pribory (Electron and Ion Devices) Proc. All-Union Electrotechnical Institute, 1940; Fabrikant, Vudynskii, and Butaeva, Bull. izobretenii (Invention Bulletin) **20**, 1959.

[5] V. Fabrikant, Dokl. Akad. Nauk SSSR **17**, 245 (1937).

[6] Javan, Bennett, and Herriot, Phys. Rev. Letters **6**, 106 (1961).

[7] V. Fabrikant, JETP **8**, 549 (1948); JETP **18**, 1127 (1948); Optika i spectroskopiya (Optics and Spectroscopy) **5**, 711 (1958).

Translated by H. Lashinsky
95

PLASMA IN A SELF-CONSISTENT MAGNETIC FIELD

N. N. KOMAROV and V. M. FADEEV

Submitted to JETP editor March 7, 1961

J. Exptl. Theoret. Phys. (U.S.S.R.) 41, 528-533 (August, 1961)

The stationary state of a multi-component plasma with axial symmetry in an external axial magnetic field is determined in the presence of an azimuthal plasma current by neglecting particle collisions and taking into account the proper magnetic field of the plasma. A Maxwellian velocity distribution is assumed with different longitudinal and transverse temperatures. Finally, the plasma is assumed to be neutral at each point.

IN 1950 Tamm [1] considered certain general relations for a plasma located in constant electric and magnetic fields by starting from a particular form of the particle distribution function. In a number of works, [2-5] more detailed plasma configurations were considered with neglect of collisions; in particular, [3-5] the case of cylindrical symmetry for the azimuthal magnetic field H_φ and longitudinal plasma current J_z were considered. It was shown that stationary plasma states can exist in the self-consistent self-magnetic field.

In the research that is described (also in the absence of collisions), a second case is considered in which the magnetic field H_z is longitudinal and the field J_φ is azimuthal, and all the quantities are independent of t, z, φ. The particle distribution densities, the proper magnetic fields and the currents of the multi-component plasma are found, and the external magnetic fields are determined for which stationary states exist.

The problem reduces to a solution of the set of n kinetic equations and two Maxwell equations:

$$v_r\frac{\partial f_i}{\partial r}+\left(\frac{q_i}{m_ic}\,v_\varphi\,\frac{1}{r}\,\frac{\partial}{\partial r}(rA)-\frac{q_i}{m_i}\,\frac{\partial\varphi}{\partial r}+\frac{v_\varphi^2}{r}\right)\frac{\partial f_i}{\partial v_r}$$
$$-\left(\frac{q_i}{m_ic}\,v_r\,\frac{1}{r}\,\frac{\partial}{\partial r}(rA)+\frac{v_\varphi v_r}{r}\right)\frac{\partial f_i}{\partial v_\varphi}=0; \qquad (1)$$

$$-\frac{\partial}{\partial r}\left[\frac{1}{r}\,\frac{\partial}{\partial r}(rA)\right]=\frac{4\pi}{c}\sum_i q_i\int v_\varphi f_i\,d\mathbf{v}, \qquad (2)$$

$$-\frac{1}{r}\,\frac{\partial}{\partial r}\left(r\,\frac{\partial\varphi}{\partial r}\right)=4\pi\sum_i q_i\int f_i\,d\mathbf{v}. \qquad (3)$$

Here q_i, m_i and f_i are respectively the charge, mass and distribution function of particles of the i-th type ($i = 1, 2, \ldots, n$); φ and A are the scalar and vector potentials, respectively.

The general solution of an equation of the form (1) is an arbitrary function of the first integrals of the equations of the characteristics:

$$C_{1i}=\tfrac{1}{2}m_i(v_r^2+v_\varphi^2)+q_i\varphi, \qquad C_{2i}=rv_\varphi+(q_i/m_ic)\,Ar.$$

As a boundary condition, we require that the distribution function $f_i(r, v)$ have the form

$$f_i(r_0,\mathbf{v})=\frac{n_{0i}}{\pi^{3/2}}\,\frac{m_i^{3/2}}{2T_\perp^i\sqrt{2T_\parallel^i}}$$
$$\times\exp\left\{-\frac{m_i}{2T_\perp^i}[v_r^2+(v_\varphi-v_{\varphi0}^i)^2]-\frac{m_i}{2T_\parallel^i}v_z^2\right\}$$

for any fixed value of $r = r_0$. Here n_{0i} and $v_{\varphi0}^i$ are respectively the density and velocity of the directed motion of particles of the i-th type at the point r_0; $T_\perp^i$ and $T_\parallel^i$ are the transverse and longitudinal temperatures of the particles, expressed in energy units. Solving the problem for the chosen boundary condition, we find the distribution function

$$f_i(r,\mathbf{v})=f_{0i}\exp\left(-\alpha_\perp^iC_{1i}-\beta_im_iC_{2i}-\tfrac{1}{2}\alpha_\parallel^im_iv_z^2\right);$$
$$f_{0i}=\frac{n_{0i}}{2^{3/2}\pi^{3/2}}\,m_i^{3/2}\alpha_\perp^i(\alpha_\parallel^i)^{1/2}$$
$$\times\exp\left[-\alpha_\perp^i\left(\frac{m_i}{2}\,v_{\varphi0}^{i2}-q_i\varphi(r_0)+\frac{q_i}{c}\,v_{\varphi0}^iA(r_0)\right)\right],$$
$$\beta_i=-v_{\varphi0}^i/T_\perp^ir_0, \qquad \alpha_\perp^i=1/T_\perp^i, \qquad \alpha_\parallel^i=1/T_\parallel^i.$$

The particle density n_i and the density of the azimuthal current of particles $P_{\varphi i}$ will be equal to

$$n_i=\int_{-\infty}^{\infty}f_i\,d\mathbf{v}=f_{0i}\left(\frac{2\pi}{m_i}\right)^{3/2}\frac{1}{\alpha_\perp^i\sqrt{\alpha_\parallel^i}}$$
$$\times\exp\left(\frac{m_i\beta_i^2r^2}{2\alpha_\perp^i}-\alpha_\perp^iq_i\varphi-\frac{\beta_iq_i}{c}\,Ar\right),$$

$$P_{\varphi i}=\int_{-\infty}^{\infty}v_\varphi f_i\,d\mathbf{v}=-\frac{\beta_ir}{\alpha_\perp^i}n_i=\bar v_{\varphi i}n_i,$$

where $\bar v_{\varphi i}=-\beta_ir/\alpha_\perp^i=\omega_ir$ is the mean azimuthal component of the velocity. Correspondingly we have for the mean squares of the velocity components;

$$\overline{v_{ri}^2}=1/m_i\alpha_\perp^i, \quad \overline{v_{\varphi i}^2}=1/m_i\alpha_\perp^i+\beta_i^2r^2/\alpha_\perp^{i2}, \quad \overline{v_{zi}^2}=1/m_i\alpha_\parallel^i.$$

We shall consider such states when there is only a magnetic field. In absence of external sources of the field E, it follows from the vanishing of the volume charge $\Sigma q_i n_i = 0$ that

$$-\beta_i q_i/c = a = \text{const}, \qquad m_i\beta_i^2/2\alpha_\perp^i = b = \text{const},$$
$$\sum_i q_i f_{0i} (2\pi/m_i)^{3/2} \left[\alpha_\perp^i \sqrt{\alpha_\parallel^i}\right]^{-1} = 0, \tag{4}$$

and there remains only the single Maxwell equation for the magnetic potential A:

$$-\frac{\partial}{\partial r}\left[\frac{1}{r}\frac{\partial}{\partial r}(rA)\right]$$
$$= \frac{4\pi}{c}\sum_i q_i f_{0i}\left(\frac{2\pi}{m_i}\right)^{3/2}\frac{1}{\alpha_\perp^i\sqrt{\alpha_\parallel^i}}\omega_i r \exp(br^2 + arA).$$

Transforming to the new function $\psi = br^2 + arA$ and introducing the variable $\rho = Lr^2$, where L is defined by the relation

$$L^2 = \frac{\pi}{c} a \sum_i q_i f_{0i} (2\pi/m_i)^{3/2} \omega_i / \alpha_\perp^i \sqrt{\alpha_\parallel^i},$$

we obtain the equation*

$$d^2\psi/d\rho^2 + e^\psi = 0,$$

the general solution of which has the form

$$e^\psi = 2C_1 \exp\{\sqrt{C_1}(\rho + C_2)\}[1 + \exp\{\sqrt{C_1}(\rho + C_2)\}]^{-2},$$

where C_1 and C_2 are arbitrary constants. Returning to the original variable, we find the following expression for the particle density n_i, the current J_i and the magnetic field H:

$$n_i = f_{0i}\left(\frac{2\pi}{m_i}\right)^{3/2}\frac{1}{\alpha_\perp^i\sqrt{\alpha_\parallel^i}} 2C_1 \frac{\gamma \exp\{\sqrt{C_1}Lr^2\}}{[1+\gamma\exp\{\sqrt{C_1}Lr^2\}]},$$
$$J_i = q_i\omega_i r n_i,$$
$$H = \frac{1}{r}\frac{\partial}{\partial r}(rA) = \frac{2L\sqrt{C_1}}{a}\frac{1-\gamma\exp\{\sqrt{C_1}Lr^2\}}{1+\gamma\exp\{\sqrt{C_1}Lr^2\}} - 2\frac{b}{a}, \tag{5}$$

where $\gamma = \exp(C_2\sqrt{C_1})$.

In these expressions the meaning of the coefficients γ and $L\sqrt{C_1}$ is not clear. To determine the coefficients we make use of the boundary conditions for the magnetic field. We denote the external magnetic field by H_∞; taking into account the relations

$$I = \sum_i I_i = \int_0^\infty \sum_i J_i\, dr = \frac{1}{2\pi}\sum_i q_i\omega_i N_i, \qquad N_i = \int_0^{2\pi}\int_0^\infty n_i r\, dr\, d\varphi,$$

where I_i and N_i are respectively the total azimuthal plasma current and the total number of particles of the i-th type per unit length of the plasma cylinder, we can write down the conditions for the magnetic field H at zero and at infinity in the form

$$H(0) = H_\infty + \frac{4\pi}{c} I, \qquad H(\infty) = H_\infty.$$

This yields

$$\gamma = -1 + \frac{4L\sqrt{C_1}}{a} \Big/ \frac{4\pi}{c} I.$$

For the density of particles at the center we have

$$n_{0i} = f_{0i}\left(\frac{2\pi}{m_i}\right)^{3/2}\frac{2C_1}{\alpha_\perp^i\sqrt{\alpha_\parallel^i}}\frac{4\pi}{c} I\left(-\frac{4\pi}{c} I + \frac{4L\sqrt{C_1}}{a}\right)\left(\frac{4L\sqrt{C_1}}{a}\right)^{-2}.$$

Then, by simple algebraic transformations, we get for γ and L:

$$\gamma = \frac{8\pi}{(4\pi I/c)^2}\sum_i n_{0i} m_i \overline{v_{ri}^2},$$
$$L\sqrt{C_1} = (1+\gamma)(4\pi I/c)^2/8\sum_i N_i m_i \overline{v_{ri}^2}.$$

Equations (5) now finally take the following form:

$$n_i = n_{0i}(1+\gamma)^2$$
$$\exp\{(1+\gamma)\lambda(r^2)\}[1+\gamma\exp\{(1+\gamma)\lambda(r^2)\}]^{-2},$$
$$J_i = q_i v_{\varphi i} n_i, \quad H = \frac{2\pi}{c} I(1+\gamma)\frac{1-\gamma\exp\{(1+\gamma)\lambda(r^2)\}}{1+\gamma\exp\{(1+\gamma)\lambda(r^2)\}} - H^*,$$
$$\lambda(r^2) = r^2(4\pi I/c)^2/8\sum_i N_i m_i \overline{v_{ri}^2},$$
$$H^* = 2b/a = m_i\omega_i c/q_i. \tag{6}$$

For analysis of the physical results, it is useful to obtain the set of equations:

$$H(0) = 2\pi I/c - 2\pi I\gamma/c - H^*,$$
$$H(\infty) = -2\pi I/c - 2\pi I\gamma/c - H^*.$$

From the equation

$$-\frac{\partial H_p}{\partial r} = \frac{4\pi}{c}\sum J_i$$

we have for the self field of the plasma

$$H_p = \frac{4\pi}{c} I \frac{1+\gamma}{1+\gamma\exp\{(1+\gamma)\lambda(r^2)\}}.$$

Equation (6) for the magnetic field can also be written in the form

$$H = \frac{4\pi}{c} I \frac{1+\gamma}{1+\gamma\exp\{(1+\gamma)\lambda(r^2)\}}$$
$$-\frac{2\pi}{c} I(1+\gamma) - H^* = H_p + H_\infty.$$

If Eq. (1) is multiplied by v_r and integrated over the velocity, we then get

$$m_i\overline{v_{ri}^2}\frac{\partial n_i}{\partial r} - \frac{q_i}{c} H\overline{v_{\varphi i}} n_i - \frac{1}{r}\overline{v_{\varphi i}}^2 m_i n_i = 0.$$

Summing this equation for all types of particles, making use of the expression for the current, and

*An equation of the same form has been obtained by F. M. Nekrasov in the plane case (private communication).

integrating over the coordinates, we obtain

$$\sum_i n_i m_i \overline{v_{ri}^2} + (H + H^*)^2 / 8\pi = (H_\infty + H^*)^2 / 8\pi. \qquad (7)$$

DISCUSSION OF RESULTS

We see that thus in the absence of collisions there exists a stationary state of a multi-component plasma with an external longitudinal magnetic field. The presence of an azimuthal plasma current I is characteristic of this state. The configurations of the plasma, current and magnetic field depend on the quantity γ. Actually, we see from (6) that the extrema for the density of particles will be at $r = 0$ for $\gamma \geq 1$, and at $r = 0$ and

$$r = \left[\frac{-8\pi \ln \gamma}{\pi(1+\gamma)(4\pi I/c)^2} \sum_i N_i m_i \overline{v_{ri}^2}\right]^{1/2}$$

for $\gamma < 1$.

The characteristic form of the curves for n_i and H are plotted in Figs. 1 and 2 for the two cases $\gamma < 1$ and $\gamma \geq 1$. In the case when the kinetic energy of the particles at the center is small in comparison with the energy of the plasma self field H_p on the axis of the cylinder, the density of the plasma has a "well" at the center and the magnetic field H in this region can even take a direction opposite to the direction of the external field H_∞. For $\gamma \geq 1$,

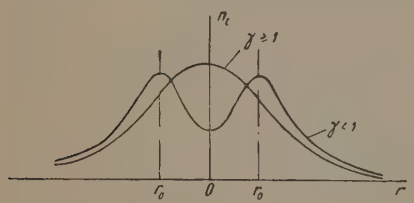

FIG. 1. Dependence of the concentration of particles of the i-th type on the radius for $\gamma \geq 1$ and $\gamma < 1$.

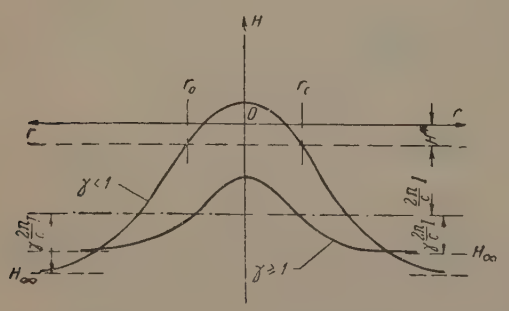

FIG. 2. Dependence of the magnetic field H on the radius for two cases $\gamma \geq 1$ and $\gamma < 1$. As $r \to \infty$, the field approaches the constant value H_∞.

the field H is always identical in direction with the external field, and the plasma has a maximum density at the center. The difference in the fields at the center and at infinity amounts to $4\pi I/c$. Thus the plasma possesses a diamagnetism, which is especially sharply pronounced for $\gamma < 1$.

It is seen from Eq. (6) that as the current I approaches zero the behavior of the field H depends on the quantity $\Sigma n_{0i} m_i \overline{v_{ri}^2}$. If the latter is constant or approaches zero more slowly than the current I ($\gamma \to \infty$), then $H \to H_\infty \to \infty$. In this case the self field of the plasma is almost nil. The particles are in a strong external magnetic field and interact weakly with one another; the decay curve (with distance) of the particle concentration is arbitrary; we have in the exponent

$$\pi r^2 \sum_i n_{0i} m_i \overline{v_{ri}^2} \Big/ \left(\sum_i N_i m_i \overline{v_{ri}^2}\right).$$

In the case $\gamma \to 1$ or $\gamma \to 0$, the field H approaches zero, but in this case the plasma configuration is spread out in space. In the last discussions, a constant number of particles N_i of each type has been assumed.

Equation (7) for the kinetic and magnetic pressures differs from the corresponding equation in the plane case only by the fact that the quantity $H + H^*$ appears in place of the field H. The quantity H^* has the physical meaning of the field which is necessary in order that the particle with mass m_i and charge q_i rotate with the cyclotron frequency ω_i about the axis of the cylinder, i.e., this is, as it were, that part of the field which is required to balance the centrifugal rotation forces of the plasma as a whole.

The first two equations of (4) are equivalent to the following conditions:

$$\overline{v_{\varphi i}}^2 q_i / m_i \overline{v_{ri}} = \text{const} \cdot r, \qquad \overline{v_{\varphi i}}^2 / \overline{v_{ri}^2} = \text{const} \cdot r^2$$

or

$$m_i \overline{v_{\varphi i}} / q_i = \text{const} \cdot r, \qquad m_i^2 \overline{v_{ri}^2} / q_i^2 = \text{const},$$

i.e., each type of particle rotates with a mean angular velocity that is independent of the radius; for particles with charges differing in sign, the directions of the angular velocities are different. The stationary states of the type under consideration exist only under the condition that the transverse temperatures of the particles of different types are inversely proportional to their masses. The azimuthal currents are principally connected with the light particles. Thus, in the case of an electron-ion plasma, the current will be created mainly by the electrons.

It can be shown that for the same absolute value of charge q_i, for instantaneous Larmor radii of particles of arbitrary type $r_{li} = m_i c v_\perp / eH$, the condition $\overline{r_{li}^2} = \text{const}$ is satisfied at each point.

Thus the results obtained make it possible to explain the behavior of the plasma upon application of a magnetic field, and to estimate the effect of diamagnetism. The application of an axial magnetic field to a plasma with an isotropic tempera-

ture distribution produces an ordered motion of the particles in the azimuthal direction, which leads to the appearance of a temperature anisotropy, since a part of the energy of random motion is transformed into ordered motion in the direction perpendicular to the field. The anisotropy produced can be estimated from a knowledge of the value of the total azimuthal current I_i and the total number of particles N_i of each type.

The states of the plasma considered admit of an arbitrary anisotropy in the temperature. However, it must be expected that its value will be limited by the criterion of stability.

In conclusion, the authors express their gratitude to R. A. Demirkhanov for constant interest in the work, and to I. I. Gutkin and A. I. Morozov for discussions.

[1] I. E. Tamm, Fizika plazmy i problema upravlyaemykh termoyadernykh reaktsiĭ (Plasma Physics and the Problem of Controlled Thermonuclear Reactions), vol. 1, Acad. Sci. Press, 1958, p. 3.

[2] A. I. Morozov and L. S. Solov'ev, JETP **40**, 1316 (1961), Soviet Phys. JETP **13**, 927 (1961).

[3] W. H. Bennett, Phys. Rev. **98**, 1584 (1955).

[4] S. Ciulli and M. Micu, Atomnaya energiya (Atomic Energy) **2**, 5 (1957).

[5] G. I. Budker, ibid. **1**, 9 (1956).

Translated by R. T. Beyer
96

THEORY OF SIMPLE FINITE-AMPLITUDE MAGNETOHYDRODYNAMIC WAVES IN A DISSIPATIVE MEDIUM

S. I. SOLUYAN and R. V. KHOKHLOV

Moscow State University

Submitted to JETP editor March 8, 1961

J. Exptl. Theoret. Phys. (U.S.S.R.) **41**, 534-543 (August, 1961)

The propagation of magnetic-sound waves of finite amplitude is analyzed by taking into account the dissipation of energy in the medium. The analysis method is based on a simplification of the initial magnetic hydrodynamic equations, which are valid for small initial perturbations and small energy dissipation. The concept of simple waves is extended to the case of dissipative media. The formation and "smearing out" of wave fronts are studied for different types of wave configurations. The spatial scales of the phenomena are determined.

1. INTRODUCTION

SIMPLE waves are known to play an important role in magnetohydrodynamics. Among the three types of simple waves existing in magnetohydrodynamics, greatest interest is attached to magnetic-sound waves. These are plane waves and if their velocity and magnetic-field vectors are specified in the xy plane at the initial instant, they remain in the same plane in the future. The theory of simple waves has been studied by several authors,[1-5] who integrated the system of hydrodynamic equations in the absence of energy dissipation and who investigated certain features in the propagation of fast and slow magnetic-sound waves. The dissipative terms of the equations of magnetohydrodynamics come into play only in connection with special problems in the structure of stationary shock waves. The most complete analysis of this type was made by Sirotina and Syrovat-skii.[6]

It is of interest, however, to analyze questions in the formation and "spreading" of discontinuities. This can be done only by examining "nonstationary" solutions, with account of energy-dissipation effects. Such an analysis has not yet been made for magnetohydrodynamics.

In the present paper we use an approximate method[7] to obtain solutions of the magnetohydrodynamic equations in the form of simple waves, with account of the dissipative terms of the equations. The method is based on the fact that the non-linearity of the medium and the energy dissipation in the medium are small. The solutions, which are carried to the second approximation, enable us to trace the spatial scales of the distortion of the simple waves for arbitrary orientation of the magnetic-field intensity vector **H**, and to study the mechanism of formation and "spreading" of the shock waves as well as to investigate their fronts. The relations obtained are applicable to the investigation of particular special limiting cases, the transition to which is very simple; the results agree with the data obtained previously by other methods.

2. FORMULATION OF THE PROBLEM AND DERIVATION OF THE APPROXIMATE EQUATIONS

Proceeding to an examination of the propagation of waves of finite amplitude in the half-plane xy, it is necessary in general to specify at the initial point ($x = 0$, $y = 0$) small perturbations of the velocities v_x and v_y, of the density ρ, of the pressure P, and of the magnetic field intensity h_y. Corresponding to these perturbations are accelerated and retarded magnetic-sound waves, which propagate without practically interacting with each other, owing to the difference in the phase velocities. In fact, in the first approximation (for infinitesimally small perturbations of v_x, v_y, ρ, P, and h_y) the following equation holds for the rate of propagation of the accelerated and retarded magnetic-sound waves $u_{1,2}$:[8]

$$u_{1,2}=\frac{1}{2}\left\{\left[u_0^2+\frac{H^2}{4\pi\rho_0}+\frac{H_x u_0}{\sqrt{\pi\rho_0}}\right]^{1/2}\pm\left[u_0^2+\frac{H^2}{4\pi\rho_0}-\frac{H_x u_0}{\sqrt{\pi\rho_0}}\right]^{1/2}\right\}. \quad (1)$$

Here $u_0=\sqrt{\gamma P_0/\rho_0}$ is the velocity of sound, P_0 is the pressure in the unperturbed medium, ρ_0 is the density of the unperturbed medium, and $\gamma = c_p/c_v$

is the ratio of the specific heats at constant volume.

Thus, the accelerated and retarded magnetic-sound waves can always be regarded separately, except in the particular case $H_y = 0$ and $H_x^2 \approx 4\pi\rho_0 u_0^2$, so nonlinear interactions between waves can manifest themselves only in the second order of smallness compared with nonlinear self-action of the waves.

The problem consists of finding the solutions of the system of magnetohydrodynamic equations in the form of simple waves propagating in a direction $x > 0$, when small perturbations of the velocity, density, pressure, and magnetic-field intensity are specified in some definite manner at the initial point, and the radiation conditions are satisfied at infinity. It is actually sufficient, for example, to specify at the point $x = 0$, $y = 0$ the x-component of the velocity, v_x, and assume v_y, ρ, h_y, and P to be specified in accordance with the formulas for infinitesimally small perturbations.

Thus, considering small velocities v_x and v_y, small deviations of the density ρ' and small deviations of the magnetic field intensity h_y from their equilibrium values ρ_0 and h_0, and specifying the equation of state in the form

$$P = P_0 + u_0^2\rho' + p, \tag{2}$$

we must assume that $v_x, v_y \ll u_{1,2}$, $\rho' \ll \rho_0$, $h_y \ll H_0$ and $p \ll P$, or, introducing the small parameter μ,

$$\frac{v_x}{u_{1,2}}, \frac{v_y}{u_{1,2}}, \frac{\rho'}{\rho_0}, \frac{h_y}{H_0} \sim \mu, \qquad p \sim \mu^2, \tag{3}$$

i.e., v_x, v_y, ρ' and h_y are of first order of smallness and p is of second order.

The bulk and shear viscosities η and ζ, the heat conduction κ, and the magnetic viscosity $\beta = c_0^2/4\pi\sigma$ (c_0 is the velocity of light and σ is the electric conductivity of the medium) are also assumed small quantities of the first order of smallness, i.e.,

$$\eta, \zeta, \varkappa, \beta \sim \mu. \tag{4}$$

In the case of infinitesimally small perturbations, i.e., in the first approximation, where the equations have no dissipative or nonlinear terms, the following solution holds true

$$v_x, v_y, \rho', h_y, P = F(t - x/u_{1,2}), \tag{5}$$

where F is an arbitrary function of its argument.

It is natural to assume that in the general case, under the assumptions (2) — (4) made above, the solution of the magnetohydrodynamic equations has essentially the form (5), but the form of the function F changes slowly with distance, i.e.,

$$v_x, v_y, \rho', h_y, P = F(\mu x, t - x/u_{1,2}). \tag{6}$$

By introducing the new variables $x' = \mu x$ and $\tau = t - x/u_{1,2}$ into the initial system of equations, we neglect everywhere the small terms of order μ^3 and higher. After simple but cumbersome transformations, the initial system reduces to the following four equations:

$$\frac{\partial\rho'}{\partial x} - \frac{1}{u_{1,2}}\left(1 - \frac{v_x}{u_{1,2}}\right)\frac{\partial\rho'}{\partial\tau} + \frac{\rho_0}{u_0^2}\left(1 - \gamma\frac{u_0^2\rho'}{u_{1,2}^2\rho_0} + \frac{u_0^2\rho'}{u_{1,2}^2\rho_0} - \frac{v_x}{u_{1,2}}\right)\frac{\partial v_x}{\partial\tau}$$
$$+ \frac{H_y\rho_0}{H_x u_0^2}\left(1 - \frac{v_x}{u_{1,2}}\right)\frac{\partial v_y}{\partial\tau}$$
$$- \frac{h_y}{4\pi u_0^2 u_{1,2}}\frac{\partial h_y}{\partial\tau} - \frac{1}{u_0^2 u_{1,2}^2}\left(\frac{4}{3}\eta + \zeta\right)\frac{\partial^2 v_x}{\partial\tau^2}$$
$$- \frac{1}{\rho_0 u_{1,2}^3}\frac{\gamma - 1}{\gamma}\frac{\varkappa}{c_v}\frac{\partial^2\rho'}{\partial\tau^2} - \frac{H_y}{u_0^2 u_{1,2}^2 H_x}\eta\frac{\partial^2 v_y}{\partial\tau^2} = 0, \tag{7}$$

$$\frac{\partial v_x}{\partial x} - \frac{1}{u_{1,2}}\left(1 + \frac{\rho'}{\rho_0}\right)\frac{\partial v_x}{\partial\tau} + \frac{1}{\rho_0}\left(1 - \frac{v_x}{u_{1,2}}\right)\frac{\partial\rho'}{\partial\tau} = 0, \tag{8}$$

$$\frac{\partial h_y}{\partial x} - \frac{1}{u_{1,2}}\left(1 - \frac{\rho'}{\rho_0}\right)\frac{\partial h_y}{\partial\tau}$$
$$- \frac{4\pi\rho_0}{H_x}\left(1 - \frac{v_x}{u_{1,2}}\right)\frac{\partial v_y}{\partial\tau} + \frac{4\pi}{u_{1,2}^2 H_x}\eta\frac{\partial^2 v_y}{\partial\tau^2} = 0, \tag{9}$$

$$\frac{\partial v_y}{\partial x} - \frac{1}{u_{1,2}}\frac{\partial v_y}{\partial\tau} - \frac{1}{H_x}\left(1 - \frac{v_x}{u_{1,2}}\right)\frac{\partial h_y}{\partial\tau} + \frac{H_y}{H_x\rho_0}\left(1 - \frac{v_x}{u_{1,2}}\right)\frac{\partial\rho'}{\partial\tau}$$
$$+ \frac{H_y}{H_x u_{1,2}}\left(\frac{h_y}{H_y} - \frac{\rho'}{\rho_0}\right)\frac{\partial v_x}{\partial\tau} + \frac{\beta}{u_{1,2}^2 H_x}\frac{\partial^2 h_y}{\partial\tau^2} = 0. \tag{10}$$

We have left the x unprimed throughout Eqs. (7) — (10).

It is well known that in the case of simple velocity waves the density, the pressure, and the magnetic-field intensity are functions of one and the same combination of the independent variables x and t. In the first approximation it follows from (7) — (10) that one can assume a combination of independent variables $(t - x/u_{1,2})$ and express v_x, v_y, ρ' and h_y (and consequently also P) simply in terms of each other:

$$\rho' = \frac{\rho_0}{u_{1,2}}v_x, \qquad h_y = -\frac{4\pi\rho_0 u_{1,2}}{H_x}v_y,$$
$$\rho' = -\frac{H_y\rho_0}{u_{1,2}H_x(1 - u_0^2/u_{1,2}^2)}v_y. \tag{11}$$

In the second approximation, however, if we keep v_x, v_y, ρ' and h_y dependent on the same combination $(t - x/u_{1,2})$, we can no longer express the velocity, density, magnetic field intensity, and pressure in terms of each other by the simple relations (11). It is natural to assume that these relations must be supplemented by small second-order terms. These are the second-order quadratic terms, and the terms due to energy dissipa-

tion, which are proportional to the derivatives with respect to τ with coefficients of order μ. Although v_x, v_y, ρ', and h_y may not have at the initial point a geometrically similar distribution with respect to τ, upon propagation of the initial perturbation into the region $x > 0$ the wave distributions of the velocity, of the density, of the pressure, and of the magnetic-field intensity should all vary in similar fashion.

The foregoing arguments are confirmed by an analysis of the structure of Eqs. (7) — (10), which were derived without any special assumptions regarding the connections between v_x, v_y, ρ' and h_y.

Finally, the simplest relationships (11) should in the second approximation be replaced by the following equations, which are compatible with each other (apart from arbitrary constant coefficients yet to be determined):

$$\rho' = \frac{\rho_0}{u_{1,2}} v_x + \frac{\rho_0}{u_{1,2}} \beta_1 v_x^2 + \gamma_1 \frac{\partial v_x}{\partial \tau}, \tag{12a}$$

$$v_x = \frac{u_{1,2}}{\rho_0} \rho' - \frac{u_{1,2}^2}{\rho_0^2} \beta_1 \rho'^2 - \frac{u_{1,2}^2}{\rho_0^2} \gamma_1 \frac{\partial \rho'}{\partial \tau}, \tag{12b}$$

$$h_y = -\frac{4\pi\rho_0 u_{1,2}}{H_x} v_y + \frac{4\pi\rho_0 u_{1,2} H_y}{H_x^2 (1 - u_0^2/u_{1,2}^2)} \beta_2 v_y^2 - \frac{4\pi u_{1,2}^2}{H_x} \gamma_2 \frac{\partial v_y}{\partial \tau}, \tag{12c}$$

$$v_y = -\frac{H_x}{4\pi\rho_0 u_{1,2}} h_y + \frac{H_x H_y}{(4\pi\rho_0 u_{1,2})^2 (1 - u_0^2/u_{1,2}^2)} \beta_2 h_y^2 + \frac{H_x}{4\pi\rho_0^2} \gamma_2 \frac{\partial h_y}{\partial \tau}, \tag{12d}$$

$$\rho' = -\frac{H_y \rho_0}{u_{1,2} H_x (1 - u_0^2/u_{1,2}^2)} v_y + \frac{H_y^2 \rho_0}{u_{1,2} H_x^2 (1 - u_0^2/u_{1,2}^2)^2} \beta_3 v_y^2 - \frac{H_y}{H_x (1 - u_0^2/u_{1,2}^2)} \gamma_3 \frac{\partial v_y}{\partial \tau}, \tag{12e}$$

$$v_y = -\frac{u_{1,2} H_x}{\rho_0 H_y} \left(1 - \frac{u_0^2}{u_{1,2}^2}\right) \rho' + \frac{u_{1,2}^2 H_x}{\rho_0^2 H_y} \left(1 - \frac{u_0^2}{u_{1,2}^2}\right) \beta_3 \rho'^2 + \frac{u_{1,2}^2 H_x}{\rho_0^2 H_y} \left(1 - \frac{u_0^2}{u_{1,2}^2}\right) \gamma_3 \frac{\partial \rho'}{\partial \tau}. \tag{12f}$$

Here β_i and γ_i are arbitrary constant coefficients, with γ_1, γ_2, and γ_3 all proportional to μ.

From the fact that v_x, v_y, ρ' and h_y are characteristics of a single wave process it follows that their x-variations should be described by identical equations. After substituting (12b) and (12f) into (7), (12a) into (8), (12d) into (9), as well as (12c) and (12e) in (10), and after replacing the second-order terms with the aid of relations (11), we can indeed reduce Eqs. (7) — (10) to an identical form. Simultaneously, by equating pairwise the coefficients of the nonlinear terms and the coefficients of the second derivatives we determine automatically and uniquely the values of β_i and γ_i.

It is now sufficient to solve one of the transformed equations, say the equation for the x component of the velocity, which has the form

$$\partial v_x/\partial x - \alpha v_x \partial v_x/\partial \tau = \delta \partial^2 v_x/\partial \tau^2, \tag{13}$$

$$\alpha = \frac{1}{2u_{1,2}^2} \left\{ (\gamma + 1) + \frac{(2-\gamma)(u_{1,2}^2 - u_0^2)^2}{(u_{1,2}^2 - u_0^2)^2 + H_y^2 u_0^2 / 4\pi\rho_0} \right\}, \tag{14}$$

$$\delta = \left\{ (u_{1,2}^2 - u_0^2)^2 (\eta + \beta\rho_0) - (u_{1,2}^2 - u_0^2) \frac{H_y^2}{4\pi\rho_0} \eta + \frac{H_y^2}{4\pi\rho_0} \left[u_0^2 \frac{\gamma - 1}{\gamma} \frac{\varkappa}{c_v} + u_{1,2}^2 \left(\frac{4}{3} \eta + \zeta \right) \right] \right\} \times \left\{ 2\rho_0 u_{1,2} \left[(u_{1,2}^2 - u_0^2)^2 + \frac{H_y^2}{4\pi\rho_0} u_0^2 \right] \right\}^{-1}. \tag{15}$$

Assuming v_x to be some definite function of t at the initial point, we can readily determine the corresponding solution of (13), since the substitution

$$v_x = \frac{2\delta}{\alpha W} \frac{\partial W}{\partial \tau} \tag{16}$$

reduces this equation to the usual form of heat-conduction equation. In the next section we shall consider the solutions of equation (13) at different boundary conditions.

However, before we proceed to the analysis of specific physical processes, it is appropriate to make the following remark concerning the preceding derivation. By supplementing relations (11) with derivatives with respect to τ we essentially deviate somewhat from the analysis of simple waves in the strict sense of this word, for we assume along with the dependence on the arbitrary combination ($\tau = t - x/u_{1,2}$) also a dependence on the derivative with respect to this combination of independent variables, albeit with a coefficient of order μ, made up of dissipated coefficients. This deviation must actually be regarded as a generalization of the concept of simple waves to include the case of dissipative media.

3. INVESTIGATION OF THE PROPAGATION OF MAGNETIC-SOUND WAVES AND OF THE STRUCTURE OF SHOCK WAVES

The case of sinusoidal boundary conditions ($v_x = v_{0x} \sin \omega t$) was considered by the authors in detail in a solution of the acoustic problem.[7] It is expedient here to consider only very briefly the final results of an analogous analysis for magnetic-sound waves for the purpose of comparing them with results obtained in ordinary hydrodynamics. We shall determine in passing the magnetohydrodynamic analogues of the Mach and

Reynolds numbers, which we need for the subsequent analysis.

The entire region of propagation of magnetic-sound waves ($x > 0$) can be subdivided into three sections. As the wave propagates towards the $x > 0$ direction the nonlinear effects bring about a distortion of the wave profile, so that at a point x_1, defined by the relation $kx_1 = 1/M$, a quasi-discontinuity is formed. Here $k = \omega/u_{1,2}$ is the wave number and $M = \frac{1}{2} f(u_{1,2}, u_0) v_{0x}/u_{1,2}$ is the magnetohydrodynamic analogue of the Mach number.* The function $f(u_{1,2}, u_0)$ is the expression in the curly brackets of (14), and is readily seen to be positive for all values of H and for any orientation of this field; its numerical value lies between $\gamma + 1$ and 3.

A comparison of x_1 with the analogous parameter of ordinary hydrodynamics, x_1^*, shows that

$$x_1 = x_1^* \frac{\gamma + 1}{f(u_{1,2}, u_0)} \left(\frac{u_{1,2}}{u_0}\right)^2 \qquad (17)$$

for equal initial perturbations v_{0x} and v_0. At the same time, by specifying a definite magnetic-field intensity vector, we can directly evaluate u_1 and u_2 graphically, as was done for example by Syrovat-skii,[9] and determine the characteristic points x_1 corresponding to these velocities simply in the form $x_1 \approx x_1^*(u_{1,2}/u_0)^2$.

The occurrence of the "discontinuity" is accompanied by a strong energy dissipation, which causes the quasi-discontinuous wave to be transformed in the second region ($x > x_1$) into an exponentially damped harmonic wave of frequency ω. This process can be regarded as completed at the point x_2, defined by the relation $kx_2 = 4\mathrm{Re}/M$, where $\mathrm{Re} = \alpha v_{0x}/2\omega\delta$ is the magnetohydrodynamic analogue of the Reynolds number, and takes into account the simultaneous influence of the bulk and shear viscosities, the heat conduction, and the magnetic viscosity of the medium. It is important to note that neither the characteristic points x_2 nor the amplitude of the signal at these points depend on the amplitude at the input of the system, v_{0x}. We can derive for the points x_1 a formula analogous to (17), but with cubic dependence on the velocity ratio.

In the third region ($x > x_2$) the propagation process can be described by the linear equations of magnetohydrodynamics, since the waves are already so weak that there are no nonlinear effects, and no reconversion of the sinusoidal wave into a shock wave takes place.

Without reporting the data obtained on the structure of the front of the shock wave, which are quite analogous to the earlier[7] solutions of the acoustic problem, we proceed directly to a determination of the solutions of greatest interest to magnetohydrodynamics.

Assume that at the initial point we are given the x component of velocity $v_x = v_{0x} \tanh(\tau/\tau_0)$, where $\tau_0 \gg (\alpha v_{0x}/2\delta)^{-1}$ and τ ranges from $-\infty$ to $+\infty$. Then the function W, which satisfies an equation similar to the heat-conduction equation, can be written in the form

$$W = \frac{1}{2\sqrt{\pi\delta x}} \int_{-\infty}^{\infty} \exp\left\{\frac{\tau_0}{\tau'} \int_0^{y/\tau_0} \mathrm{th}\, z\, dz - \frac{(\tau - y)^2}{4\delta x}\right\} dy, \quad \tau' \equiv \frac{2\delta}{\alpha v_{0x}}. \qquad (18)*$$

When $\tau_0/\tau' \gg 1$, i.e., at large magnetohydrodynamic Reynolds numbers, the integral (18) is calculated by the saddle-point method, so that from the relation defining the saddle point y_0 and from the value of v_x at this point [given by Eq. (16)] we can generally speaking find a solution in the form

$$\frac{\tau}{\tau_0} = \mathrm{Arth}\,\Phi - \frac{\alpha v_{0x} x}{\tau_0}\Phi, \quad \Phi = \mathrm{th}\frac{\tau}{\tau_0}. \qquad (19)‡$$

A graphic analysis of the solution obtained (Fig. 1) demonstrates quite clearly how the profile of the initial perturbation is distorted as the wave propagates. The degree of distortion of the initial perturbation is determined here by the value of the slope $X = \alpha v_{0x} x/\tau_0$, which increases in direct proportion to the distance covered by the wave from the entrance of the system. The "discontinuity" point corresponds to the distance $x_1 = \tau_0/\alpha v_{0x}$, and when $x > x_1$ the function Φ becomes multiple-valued, which is a physical absurdity. In this case, however, the solution (19) is itself not valid; the principal value of the in-

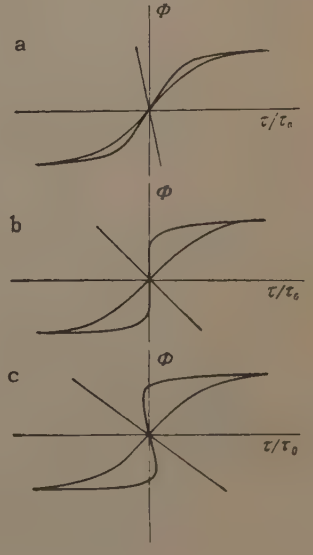

FIG. 1. Plot of the solutions of (19). $\tau/\tau_0 = f(\Phi)$ (heavy curve) is the sum of tanh Φ and a straight line with slope X: a – $|X| < 1$, b – $|X| = 1$, c – $|X| > 1$.

*In analogy with the acoustic analogue of the Mach number $M_{ac} = (\gamma + 1) v_0/2u_0$.

*th = tanh.

‡Arth = $\tanh^{-1}$.

tegral must now be calculated as the sum of its values over the small portions in the vicinity of the points y_1 and y_2, so that after calculating W_1 and W_2 and after substituting $W = W_1 + W_2$ in (16), the analysis of the form of v_x after formation of the "discontinuity" must be based on the expression

$$v_x = v_{0x}\frac{\operatorname{th}(y_1/\tau_0) + \operatorname{th}(y_2/\tau_0)\,e^{-Y}}{1+e^{-Y}}, \qquad (20)$$

where

$$|Y| = \left|\frac{\tau_0}{\tau'}\left[\int_0^{y_2/\tau_0}\operatorname{th} z\,dz - \int_0^{y_1/\tau_0}\operatorname{th} z\,dz\right] + \frac{(\tau-y_2)^2-(\tau-y_1)^2}{4\delta x}\right|.$$

The value of $|Y|$ is easy to calculate if it is recognized that $(\tau - y_{1,2}) = \pm\alpha v_{0x} x$ at the saddle point, and if the integrals of the hyperbolic tangents are expanded in powers of τ and only the first approximation is used. Then $v_x = v_{0x}\tanh(\tau/\tau')$, where τ' is the duration of the shock-wave front, has the value 1/Re when reduced to dimensionless form. Thus, the width $L_f = u_{1,2}\,\tau_f$ of the shock-wave front established near the point x_1 remains stationary (unlike a sinusoidal front) and is given by the formula

$$L_f = u_{1,2}\tau' = 2\frac{u_{1,2}}{v_{0x}}\left\{(u_{1,2}^2-u_0^2)^2[\eta+\beta\rho_0] - (u_{1,2}^2-u_0^2)\frac{H_y^2}{4\pi\rho_0}\eta\right.$$
$$\left.+\frac{H_y^2}{4\pi\rho_0}\left[u_0^2\frac{\gamma-1}{\gamma}\frac{\varkappa}{c_v}+u_{1,2}^2\left(\frac{4}{3}\eta+\zeta\right)\right]\right\}$$
$$\times\left\{\rho_0 u_{1,2}\left[(\gamma+1)\frac{H_y^2}{4\pi\rho_0}u_0^2+3(u_{1,2}^2-u_0^2)^2\right]\right\}^{-1}. \qquad (21)$$

Relation (21) goes in the limit into various particular magnetohydrodynamic discontinuities (parallel shock wave, perpendicular shock wave, singular oblique wave, etc.), which need not be analyzed here, since transitions of this type have been studied in detail by Sirotina and Syrovat-skii.[6] We need only point out here that the expressions determining the width of the front of the shock waves, obtained in [6] and in the present paper by different methods, coincide.

Particular interest is attached to an examination of the following boundary-value problems:

$$v_x = \begin{cases} -v_{0x}, & -\infty \leqslant \tau \leqslant 0, \\ +v_{0x}, & 0 \leqslant \tau \leqslant +\infty, \end{cases} \qquad (22)$$

i.e., when the x component of the velocity is specified at the initial point in the form of a discontinuous function with $L_f = u_{1,2}\tau_f = 0$. It is natural to expect the dissipative processes to predominate here from the very outset, so that the spatial scales of the established stationary width of the front will differ from those in the two preceding problems.

Thus, let the velocity v_x at the initial point be defined by (22). Then

$$W = \frac{1}{2\sqrt{\pi\delta x}}\left[\int_{-\infty}^{0}\exp\left\{-\frac{y}{\tau'}-\frac{(\tau-y)^2}{4\delta x}\right\}dy\right.$$
$$\left.+\int_0^{\infty}\exp\left\{\frac{y}{\tau'}-\frac{(\tau-y)^2}{4\delta x}\right\}dy\right] \qquad (23)$$

or, after reducing the exponential expressions to quadratic form, we obtain ($\tau' \equiv 2\delta/\alpha v_{0x}$)

$$W = \frac{1}{\sqrt{\pi}}\exp\left\{\frac{\alpha^2 v_{0x}^2 x}{4\delta}\right\}\left[e^{-\tau/\tau'}\int_{Z_-}^{\infty}e^{-z^2}dz - e^{\tau/\tau'}\int_{Z_+}^{-\infty}e^{-z^2}dz\right],$$

$$Z_{\mp} \equiv \frac{\tau \mp \alpha v_{0x} x}{2\sqrt{\delta x}}. \qquad (24)$$

The analysis of the spatial variation of v_x, carried out in accordance with (16), is now more difficult. First, for x sufficiently large to satisfy the condition $x \geq \tau/\alpha v_{0x}$ in the region $\tau \geq 2\sqrt{\delta x}$, the x component of the velocity is simply given by

$$v_x = v_{0x}\operatorname{th}(\tau/\tau'). \qquad (25)$$

The quantity τ', determines as before the duration of the front of the shock wave and its dimensionless value is 1/Re. Thus, at sufficiently large distances from the entrance to the system, the width of the shock-wave front displays no dependence on x and remains stationary.

Knowing the stationary duration of the front of the shock wave $\tau = \tau_{st}$, we can indicate a value x^1 beyond which $\tau = \tau_{st}$, namely:

$$x^1 = 2\delta/(\alpha v_{0x})^2. \qquad (26)$$

We determine by the same token the interval $[0, x^1]$ within which the stationary width of the front of the shock wave is established.

It remains only to determine the variation of τ_f in the indicated interval. This variation can readily be ascertained by starting from the following considerations. When $x < \tau/\alpha v_{0x}$ and $|\tau|$ is sufficiently large, one of the integrals in (24) can be neglected as having equal limits, so that we obtain $v_x = |v_{0x}|$. Assuming this approximation to be possible when the lower limits of the integrals in (24) are greater than unity in absolute value, we can express τ as a function of x:

$$\tau = 2\sqrt{\delta x} + \alpha v_{0x} x. \qquad (27)$$

However, even at the limiting point (26), the second term of formula (27) is $\sqrt{2}$ times less the first

one, so that the law of establishment of the stationary width of the shock-wave front can be simply determined to be

$$L_f = u_{1,2}\tau_f = 2u_{1,2}\sqrt{\delta x}, \qquad (28)$$

i.e., the growth in the width of the front of the shock wave is proportional to the square root of the distance from the entrance to the system covered by the wave before L_f reaches a stationary value.

Finally, it is interesting to consider the propagation of an arbitrary unit pulse, which for simplicity can be assumed to be triangular (Fig. 2a), in a certain interval $[0, \beta]$ such that the initial perturbation of the x component of the velocity remains of order μ while the area of the triangle P_{0x} remains constant, i.e.,

$$v_x = \begin{cases} 2P_{0x}\beta^{-1}(1-\tau/\beta), & 0 \leqslant \tau \leqslant \beta, \\ 0 & \tau < 0,\ \tau > \beta, \end{cases}$$

$$P_{0x} = \int_0^\beta v_{0x}\left(1 - \frac{\tau}{\beta}\right)d\tau. \qquad (29)$$

An exact analytic expression for v_x, obtained in accordance with (16) after calculating W and the logarithmic derivative is, however, rather cumbersome. It is therefore advantageous, without writing out the expression, to plot the variation of v_x with τ for different distances from the entrance to the system, obtained on the basis of the exact solution.

First, for sufficiently small distances $x \leq x^1 = \delta\beta^2/2\,(\alpha P_{0x})^2$, the distortion of the pulse is such that its profile can be broken up into four characteristic regions (Fig. 2b), so the maximum of the pulse amplitude shifts to the right of the point $\tau = 0$ and there are simultaneously formed on its edges gently sloping portions (regions I and IV), on which the profile of the pulse is described by the following equations:*

$$v_x = \frac{4}{\sqrt{2\pi}}\frac{P_{0x}}{\beta^2}\sqrt{\delta x}\exp\left\{-\frac{\tau^2}{4\delta x}\right\} \text{ for } \tau < -2\sqrt{\delta x}, \qquad (30)$$

$$v_x = \frac{4}{\sqrt{2\pi}}\frac{P_{0x}}{\beta^2}\sqrt{\delta x}\exp\left\{-\frac{(\beta-\tau)^2}{4\delta x}\right\} \text{ for } \tau > \beta. \qquad (31)$$

The boundaries of the first and fourth regions are defined as $\tau_I = -4\sqrt{\delta x}$ and $\tau_{IV} = \beta + 2\sqrt{\delta x}$, respectively. The second region, corresponding to the values of τ within the interval $\pm 2\sqrt{\delta x}$ from the point $\tau = 0$, is the region of the leading front of the pulse. When $x = x^1$ this region reaches a value 1/Re (in dimensionless units). In the third region the deviation of the pulse from its initial configuration is still insignificant when $x \leq x^1$.

*The magnetohydrodynamic Reynolds number is assumed to be much greater than unity, $Re \gg 1$.

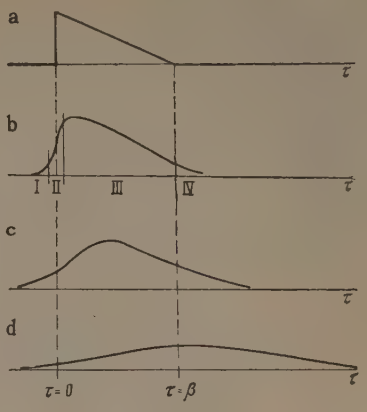

FIG. 2. Triangular unit pulse at different distances from the entrance to the system. a – $x = 0$, b – $x \leq x^1 = \delta\beta^2/2\,(\alpha P_{0x})^2$ c – $x^1 < x < x_2 = 4\,\mathrm{Re}/2\alpha P_{0x}\beta^{-2}$, d – $x \geq x_2$.

Further propagation of the pulse causes the maximum of v_x to shift in the direction $\tau \to \beta$ and broadens the regions I and IV and the region of the leading front at the expense of the third region (Fig. 2c), which is reduced. As the pulse attenuates, its form tends to be symmetrical, so that the duration of the front does not remain stationary, but increases as $\tau_f = 2\sqrt{\delta x}$, so long as the concept of τ_f retains in general a physical meaning.

At sufficiently large x, namely when $x \geq x_2 \approx \mathrm{Re}/2\alpha P_{0x}\beta^{-2}$ the following relation holds for all four regions (Fig. 2d):

$$v_x = \frac{2P_{0x}}{\beta}\exp\{-(\beta-\tau)^2/4\delta x\}/\sqrt{\mathrm{Re}}\sqrt{2\alpha P_{0x}x/\beta^2}. \qquad (32)$$

The parameter x_2 is quite analogous here to the corresponding parameter in the boundary problem $v_x = v_{0x}\sin\omega t$, while the parameter x^1 corresponds to the analogous parameter of the boundary-value problem (22).

The last thing to be emphasized here is that the pulse configuration of Fig. 2b corresponds to any single pulse at a definite distance from the entrance to the system.

4. CONCLUSION

The system of magnetohydrodynamic equations, in the case of small nonlinearity and low energy dissipation in the medium, reduces to a system of like equations similar to (13). In the case of dissipative media, the simple waves are regarded here as waves in which the density, velocity, pressure, and magnetic-field intensity depend not simply on a definite combination of independent variables ($\tau = t - x/u_{1,2}$), but also on the derivative with respect to this combination. An investigation of an equation such as (13) for one of the velocity components of the magnetic-sound waves v_x or v_y, for the magnetic field intensity h_y, or for the density ρ' enables us to study the laws of propagation of waves with different initial forms.

Such an analysis of waves of various configurations has shown, first, that in the absence of a discontinuity at the initial point ($x = 0$, $y = 0$), a discontinuity can be formed under certain conditions at a distance x_1, proportional to $1/M$, from the entrance of the system. Second, a discontinuity specified at the initial point becomes "spread out" as $\tau_f = 2\sqrt{\delta x}$, and attains at a distance $x^1 = 2\delta/(\alpha v_{0x})^2$ a dimensionless width $1/Re$. No further "smearing" of the front takes place only in the case of specially chosen functions (second and third boundary-value problems), for which $1/Re$ is thus found to be the stationary width of the front. Third, at a distance $x_2 \sim Re/M$, which is independent of the value of the initial perturbation, the amplitude of the wave is also independent of the amplitude at the entrance to the system, and wave propagation for $x > x_2$ can be described by the linear equations of magnetohydrodynamics.

[1] J. Bazer, Astrophys. J. **128**, 686 (1958).

[2] P. Lax, Comm. Pure Appl. Math. **10**, 537 (1957).

[3] A. G. Kulikovskii, DAN SSSR **121**, 987 (1958), Soviet Phys.-Doklady **3**, 743 (1959).

[4] R. V. Polovin, JETP **39**, 463 (1960), Soviet Phys. JETP **12**, 326 (1961).

[5] R. V. Polovin, UFN **72**, 33 (1960), Soviet Phys.-Uspekhi **3**, 677 (1961).

[6] E. P. Sirotina and S. I. Syrovat-skii, JETP **39**, 746 (1960), Soviet Phys. JETP **12**, 521 (1961).

[7] S. I. Soluyan and R. V. Khokhlov, Vestnik, Moscow State University, No. 3, 52 (1961).

[8] L. D. Landau and E. M. Lifshitz, Elektrodinamika sploshnykh sred (Electrodynamics of Continuous Media), Gostekhizdat, (1959).

[9] S. I. Syrovat-skii, Usp. Fiz. Nauk **62**, 247 (1957).

Translated by J. G. Adashko
97

SCATTERING OF GAMMA RAYS IN LIQUID He^3

A. A. ABRIKOSOV and I. M. KHALATNIKOV

Institute for Physics Problems, Academy of Sciences, U.S.S.R.

Submitted to JETP editor March 8, 1961

J. Exptl. Theor. Phys. (U.S.S.R.) 41, 544-548 (August, 1961)

Detailed formulas are derived for the frequency and angular distributions of the scattered radiation. Numerical estimates indicate a quite substantial magnitude for the effect, which makes possible its use in determining the velocity of "zero sound" in He^3.

SOME time ago, we investigated the problem of the scattering of light in liquid He^3.[1] One of the objects of this work was to examine the possibility of using Rayleigh scattering of light to determine the velocity of the so-called "zero," or high-frequency, sound ($\omega_s\tau \gg 1$, where τ is the time between collisions of the quasi-particles). The occurrence of this form of sound was predicted by Landau on the basis of his theory of a Fermi liquid.[2,3] Calculations[1] showed that the scattering of visible light is extremely small, and that detection of this effect would evidently lie beyond the bounds of experimental feasibility. However, since the scattering increases rapidly with frequency ($\sim \omega^4$ or ω^5), it was clear, even then, that an increase in the frequency of the electromagnetic radiation might significantly improve the conditions for observation.

Now, thanks to the discovery of the Mössbauer effect and the possibility it provides for the measurement of relatively insignificant variations in the energy of γ quanta, one may raise the question of the feasibility of determining the velocity of zero sound in He^3 using Rayleigh scattering of γ quanta. As we shall see below, this allows the effect to be enhanced by approximately five orders of magnitude, as compared with visible light.

Inasmuch as the change in the wave vector of the γ quantum equals the wave vector of the sound quantum, it is the angular range for which this latter quantity is sufficiently small which interests us:

$$q = 2\,(\omega/c)\sin(\theta/2) \ll p_0/\hbar, \qquad (1)$$

where p_0 is the Fermi boundary momentum. Only in this region does the concept of sound have meaning. The quantity $p_0/\hbar$ is of the same order as the reciprocals of the interatomic distances. To fulfill condition (1), therefore, we may employ the formulas already derived,[1] except that for the dielectric constant D we must use the expression $1 - 4\pi N_e e^2/m_e\omega^2$, where N_e and m_e are the number of electrons per unit volume and their mass, respectively, while ω is the frequency of the γ quanta. The derivative of D with respect to the density of atoms, $\partial D/\partial N$, clearly equals $-2\pi e^2/m_e\omega^2$, and in consequence, the coefficient of ω^4 becomes simplified while the extinction coefficient dh ceases to depend upon the frequency of the incident radiation (or, for a given q and $\Delta\omega$, upon the change in frequency of the γ quantum).

It is especially desirable to obtain the entire dispersion curve from ordinary ($\omega_s\tau \ll 1$) to zero sound ($\omega_s\tau \gg 1$). In this case the final equation (23) of[1] is sufficient, since it was derived under the assumption that $\tau\Delta\omega \gg 1$.

In view of this fact, we have made several changes in the derivations given previously.[1] In place of the form used in that paper for the collision integral, $I(n) = -\delta n/\tau$, where δn is the change in the distribution function, we have taken it in the form

$$I(n) = -\frac{1}{\tau}\left(\delta n - \int \delta n \frac{d\Omega_1}{4\pi} - 3\cos\theta \int \delta n \cos\theta_1 \frac{d\Omega_1}{4\pi}\right). \qquad (2)$$

This form for the collision integral insures that the conservation laws for momentum and particle number will be fulfilled, and makes it possible to go over to the hydrodynamic approximation (i.e., the case $\omega_s\tau \ll 1$).

We have already used this kinetic equation to investigate the dispersion of sound.[4] In addition it is assumed, as in[4], that the function $f(\chi)$ introduced in Landau's theory,[2] includes not only the zeroth, but also the first harmonic: $f = f_0 + f_1\cos\chi$. The rest of the calculations corresponded completely to those performed in[1].

As a result, the extinction coefficient turns out to be

$$dh = \left(\frac{e^2}{m_e c^2}\right)^2 \frac{p_0 m^*}{\pi^2\hbar^3}\hbar\Delta\omega n(\Delta\omega)\frac{(1+F_1/3)^2}{\tau(qv)^2}\xi^{-2}\frac{(\xi^*w^*-\xi w)/(\xi-\xi^*)-|w|^2(3|\xi|^2+1)}{\left|\left(1+\frac{1}{\xi\sigma}\right)\left(1+\frac{F_1}{3}\right)-w\left[\left(F_0-\frac{1}{\xi\sigma}\right)\left(1+\frac{F_1}{3}\right)+\xi^2\left(F_1-\frac{3}{\xi\sigma}\right)\left(1+\frac{1}{\xi\sigma}\right)\right]\right|^2}$$

$$\times\frac{1}{2}(1+\cos^2\theta)\frac{d\Omega}{4\pi}d\Delta\omega;$$

$$n(\Delta\omega)=\left[\exp\frac{\hbar\Delta\omega}{T}-1\right]^{-1},\quad \xi=\frac{i\Delta\omega\tau-1}{iqv\tau},\quad \sigma=iqv\tau,$$

$$v=p_0/m^*,\quad w=\frac{\xi}{2}\ln\frac{\xi+1}{\xi-1}-1,\quad F_0=f_0p_0m^*/\pi^2\hbar^3; \tag{3}$$

m^* is the effective mass of an excitation in He^3,

$$m^*=m_{He^3}(1+F_1/3).$$

In the limit $qv\tau\ll1$, $\Delta\omega\tau\ll1$, we obtain from Eq. (3)

$$dh=\frac{4}{45}\left(\frac{e^2}{m_ec^2}\right)^2\frac{p_0m^*}{\pi^2\hbar^3}\hbar\Delta\omega n(\Delta\omega)$$

$$\times\frac{(1+F_1/3)^2\tau(qv)^4}{[\Delta\omega^2-(u_1q)^2]^2+[^4/_{15}(1+F_1/3)\Delta\omega\tau q^2v^2]^2}$$

$$\times\frac{1}{2}(1+\cos^2\theta)\frac{d\Omega}{4\pi}d\Delta\omega;$$

$$u_1=v[^1/_3(1+F_0)(1+F_1/3)]^{1/2}, \tag{4}$$

u_1 is the velocity of sound in He^3 (see[2]). It can readily be seen from Eq. (4) that the frequency distribution corresponds to two narrow Rayleigh satellites whose frequencies are displaced relative to that of the fundamental line by $\Delta\omega=\pm u_1q$. The absence of a central line corresponding to the entropy fluctuations is due to our having neglected effects of order $1-c_p/c_V$ in choosing a collision integral of the form (2). Letting $\tau\to0$, we obtain from (4)

$$an=\frac{1}{8}\left(\frac{e^2}{m_ec^2}\right)^2\frac{p_0m^*}{\pi^2\hbar^3}\hbar\Delta\omega n(\Delta\omega)$$

$$\times[\delta(\Delta\omega-u_1q)+\delta(\Delta\omega+u_1q)]$$

$$\times(1+F_0)^{-1}\frac{1}{2}(1+\cos^2\theta)\,d\Omega d\Delta\omega. \tag{5}$$

In the opposite limit, $qv\tau\gg1$, we obtain two narrow satellites displaced from the fundamental line by $\Delta\omega=\pm u_2q$, where u_2 is the zero sound velocity, and a central plateau for $|\Delta\omega|<qv$. For the satellites we have

$$dh_1=\left(\frac{e^2}{m_ec^2}\right)^2\frac{p_0m^*}{\pi^2\hbar^3}\hbar\Delta\omega n(\Delta\omega)\frac{w^2(s)s^2}{\tau}\left(1+\frac{F_1}{3}\right)^2$$

$$\times\frac{A(s)}{B^2(s)}\left\{(|\Delta\omega|-u_2q)^2\right.$$

$$\left.+\frac{1}{\tau^2}\left[\frac{A(s)}{B(s)}s^2\left(1+\frac{F_1}{3}\right)\right]^2\right\}^{-1}\frac{1}{2}(1+\cos^2\theta)\frac{d\Omega}{4\pi}d\Delta\omega, \tag{6}$$

where

$$A(s)=\frac{1}{s^2-1}-\left(\frac{w(s)+1}{s}\right)^2-3w^2(s),$$

$$B(s)=\left(\frac{1}{s^2-1}-w(s)\right)\left(1+\frac{F_1}{3}\right)-2w^2(s)s^2F_1,$$

$$s=\frac{u_2}{v},\qquad w(s)=\frac{s}{2}\ln\frac{s+1}{s-1}-1,$$

while the quantity s satisfies the equation

$$w(s)=[F_0+F_1s^2/(1+F_1/3)]^{-1}. \tag{7}$$

In the limit as $\tau\to\infty$ we obtain from (6)

$$dh_1=\frac{1}{4}\left(\frac{e^2}{m_ec^2}\right)^2\frac{p_0m^*}{\pi^2\hbar^3}\hbar\Delta\omega n(\Delta\omega)\left(1+\frac{F_1}{3}\right)w^2(s)$$

$$\times\left[\frac{1}{s^2-1}-w(s)\left(1+\frac{F_1}{3}\right)-2w^2(s)s^2F_1\right]^{-1}$$

$$\times[\delta(\Delta\omega-u_2q)$$

$$+\delta(\Delta\omega+u_2q)]\frac{1}{2}(1+\cos^2\theta)\,d\Omega d\Delta\omega. \tag{8}$$

The central plateau depends little upon τ for $qv\tau\gg1$. We shall give, therefore, only the expression for the limit $\tau\to\infty$:

$$dh_2=\frac{1}{8}\left(\frac{e^2}{m_ec^2}\right)^2\frac{p_0m^*}{\pi^2\hbar^3}\hbar\Delta\omega n(\Delta\omega)\left(1+\frac{F_1}{3}\right)\frac{\Theta(qv-|\Delta\omega|)}{qv}$$

$$\times\left\{\left[1+\frac{F_1}{3}-\tilde{w}(\xi)\left(F_0\left(1+\frac{F_1}{3}\right)+\xi^2F_1\right)\right]^2\right.$$

$$\left.+\frac{\xi^2\pi^2}{4}\left[F_0\left(1+\frac{F_1}{3}\right)+\xi^2F_1\right]^2\right\}^{-1}\frac{1}{2}(1+\cos^2\theta)\,d\Omega d\Delta\omega, \tag{9}$$

where

$$\xi=\frac{\Delta\omega}{qv},\qquad \tilde{w}=\frac{\xi}{2}\ln\frac{1+\xi}{1-\xi}-1,\qquad \Theta(x)=\begin{cases}1 & x>0\\ 0 & x<0\end{cases}.$$

It should be pointed out that whether one or the other of the limiting cases occurs depends solely upon the relation between qv and $1/\tau$; i.e., upon the scattering angle of the light. This is clear in the case $qv\tau\ll1$, since $u_1\sim v$ and $\Delta\omega=qu_1\sim qv\ll1/\tau$. For $qv\tau\gg1$, however, both $\tau\Delta\omega\gg1$ (for the satellites, since $u_2\sim v$, and for the edge of the Doppler plateau) and $\tau\Delta\omega\ll1$ are possible. It can be shown with the aid of Eq. (3) that the case $qv\tau\gg1$, $\tau\Delta\omega\ll1$ is in actuality not a special one, but is described by Eq. (9), obtained under the assumption that $\Delta\omega\sim qv\gg1/\tau$.

Let us now make some numerical estimates. According to the most recent specific heat measurements on He^3 at low temperatures [5] the ratio of the effective mass to the mass of the He^3 atom $m^*/m = 2$. The remaining parameters (see [6]) are: $p_0/\hbar = 0.76 \times 10^8$ cm^{-1}, and $u_1 = 183$ m/sec, whence $F_0 = 6.95$, $F_1 = 3$, $v = 79.5$ m/sec, $s = u_2/v = 2.45$, $u_2 = 195$ m/sec, and $w(s) = 0.0625$.

For observation of the satellites it is essential that condition (1) be fulfilled. Inasmuch as we are dealing with small angles, this condition may be written in the form

$$\theta \ll \theta_1 = cp_0/\hbar\omega. \tag{10}$$

For $\hbar\omega \sim 10$ kev this yields $\theta_1 \sim 0.15 \approx 9°$.

Further, the degree of "quantization" of the process is of interest. This may be established by comparing $\hbar\Delta\omega$ with T. For the acoustical satellites quantum effects begin to play a part for angles exceeding

$$\theta_2 \sim cT/\hbar\omega u = 10^{-2}T \text{ (T in degrees)}. \tag{11}$$

It may therefore be presumed that a purely quantum situation prevails for the acoustical satellites at temperatures below 0.1° K and γ-quantum energies greater than 10 kev. It follows from this that only the Stokes satellite with $\hbar\Delta\omega \gg T$ will be observed.

To resolve the question of which form of sound will be observed it is necessary to compare qv with $1/\tau$. In accordance with [6] and Landau's paper [3] the quantity τ, which for $\hbar\Delta\omega \ll T$ has the form $\tau = 2.3 \times 10^{-12}T^{-2}$, (T in degrees), must in the case $\hbar\Delta\omega \gg T$ be replaced by

$$\tau = 1.6 \cdot 10^{12} (\Delta\omega)^{-2}, \text{ sec } (\Delta\omega \text{ in sec}^{-1}). \tag{12}$$

The limiting angles up to which the zero-sound satellite is observable are given by the relation $\Delta\omega = u_2 q \sim 1/\tau$, or

$$\theta_3 \sim 1.5 \cdot 10^{12}\ c/\omega u. \tag{13}$$

Angles smaller than θ_3 correspond to zero sound. Substitution of numerical data shows that θ_3 closely approximates θ_1, as determined by Eq. (10). (The order-of-magnitude agreement is quite obvious, but in this case there is also numerical agreement). As a consequence, only the zero-sound satellite will be observed over the whole angular range for which the study of acoustical satellites is feasible, for the energies and temperatures under consideration.

The amplitude of the scattering can be estimated with the aid of Eq. (18). As a result, one obtains

$$dI_1 = \int \frac{dh_1}{d\Delta\omega} d\Delta\omega \approx 5 \cdot 10^5 \hbar\omega\theta d\Omega, \text{ cm}^{-1}. \tag{14}$$

For an energy $\hbar\omega = 10$ kev and for angles $\sim 1°$, this yields $dI_1 \approx 10^{-4} d\Omega$ cm^{-1}. This is 10^5 times as great as the amplitude found for the optical region. This should clearly be regarded as a limiting figure. An increase in the γ-quantum energy does not lead to enhancement of the effect, since, in accordance with the condition (10), it is necessary in this case to take proportionately smaller scattering angles.

One of the characteristics of scattering in the zero-sound region is the central plateau. This corresponds to $\hbar\Delta\omega < vq$; i.e., its edge is approximately half-way between the undisplaced line and the satellite. The intensity of the plateau is given by Eq. (9), and is nearly independent of $\Delta\omega$. For $\Delta\omega/vq = \frac{1}{2}$, substitution of numerical values yields

$$dh_2 = 2 \cdot 10^9 d\ (\hbar\Delta\omega)\ d\Omega, \text{cm}^{-1}. \tag{15}$$

Over the whole plateau one finds, for $\hbar\omega = 10$ kev and $\theta = 1°$

$$dI_2 = \int \frac{dh_2}{d\Delta\omega} d\Delta\omega \approx 10^{-7}\ d\Omega, \text{cm}^{-1}.$$

Finally, let us consider the problem of γ-quantum scattering in liquid He^4. The appropriate formulas have been derived by Ginzburg.[7] Setting $\partial D/\partial N = -2\pi e^2/m_e\omega^2$ and taking the quantum factor into account, we obtain for the normal doublet

$$dh_1 = \tfrac{1}{8} (e^2/m_e c^2)^2\ (\rho/m^2 u_1^2)\ \hbar\Delta\omega n\ (\Delta\omega)\ [\delta\ (\Delta\omega - u_1 q) + \delta\ (\Delta\omega + u_1 q)]\ \tfrac{1}{2} (1 + \cos^2\theta)\ d\Omega d\Delta\omega, \tag{16}$$

where ρ is the density of the He^4, m is the atomic mass, and u_1 is the first-sound velocity. The intensity of the anomalous doublet associated with second sound is smaller by the factor

$$(c_p/c_v - 1)/(1 - u_2^2/u_1^2)^2$$

The restriction (10) on the angles and the estimate (11) of the quantum limit remain approximately correct for He^4 as well. At temperatures below 1° K, therefore, one can study a purely quantum situation. In this case we find, from Eq. (16), the intensity for the Stokes satellite

$$dI_1 = \int \frac{dh_1}{d\Delta\omega} d\Delta\omega = 4 \cdot 10^4 \hbar\omega\theta d\Omega, \text{cm}^{-1}.$$

The intensity of the anomalous doublet below 1°K is practically zero.

In conclusion, we express our thanks to Academician L. D. Landau for his consideration

of this work, and to V. P. Peshkov, at whose initiative this calculation was undertaken.

[1] A. A. Abrikosov and I. M. Khalatnikov, JETP **34**, 198 (1958), Sov. Phys. JETP **34**, 135 (1958).

[2] L. D. Landau, JETP **30**, 1058 (1956), Sov. Phys. JETP **3**, 920 (1957).

[3] L. D. Landau, JETP **32**, 59 (1957), Sov. Phys. JETP **5**, 101 (1957).

[4] I. M. Khalatnikov and A. A. Abrikosov, JETP **33**, 110 (1957), Sov. Phys. JETP **6**, 84 (1958).

[5] Brewer, Daunt and Sreedhar, Phys. Rev. **115**, 836 (1959).

[6] A. A. Abrikosov and I. M. Khalatnikov, Usp. Fiz. Nauk **46**, 177 (1958).

[7] V. L. Ginzburg, JETP **13**, 243 (1943).

Translated by S. D. Elliott
98

ABSORPTION OF HIGH-ENERGY PHOTONS IN THE UNIVERSE

A. I. NIKISHOV

P. N. Lebedev Physics Institute, Academy of Sciences, U.S.S.R.

Submitted to JETP editor March 8, 1961

J. Exptl. Theoret. Phys. (U.S.S.R.) 41, 549-550 (August, 1961)

The probability per unit length of path that a 10^{12}-ev γ quantum is converted into an electron pair as a result of a collision with a thermal photon is calculated. If the energy density of thermal photons in intergalactic space is taken as 0.1 ev cm^{-3}, the probability turns out to be 7×10^{-27}. Thus if the distance traversed is greater than 10^{26} cm, the attenuation of the γ-quantum flux may be appreciable.

THERE has recently been increasing interest in the possibility of observing point sources of high energy photons.[1] In this article, we shall consider the role of the reaction $\gamma + \gamma \to e^+ + e^-$ in the propagation of $10^{-12} - 10^{13}$-ev photons from sufficiently distant objects outside our galaxy.

The cross section for the conversion of two γ quanta into an electron pair is given by the expression* (see [2])

$$\sigma(s) = \tfrac{1}{2}\pi r_0^2 (1-v^2)\left\{(3-v^4)\ln\frac{1+v}{1-v} + 2v(v^2-2)\right\},$$

$$v = \sqrt{1-1/s},$$

$$r_0 = 2.8 \cdot 10^{-13} \text{ cm}, \quad s = (E\varepsilon/2m^2)(1-\cos\vartheta),$$

where s is the square of the c.m.s. γ-quantum energy, m is the mass of the electron, c = 1, E and ϵ are the energies of the colliding γ quanta in the laboratory system, θ is the angle between their momenta; $\sigma(s) \approx 10^{-25}$ cm^2 in the region of s of interest to us. At present, it is assumed that the density of photons with mean energy ~ 1 ev in intergalactic space is $\frac{1}{3}$ to $\frac{1}{10}$ the density in our galaxy. The density of light energy in the galaxy is $W_{gal} = 0.3 - 1$ ev.[3] It is thus readily seen that if the path traversed by high energy photons is $R \gtrsim 10^{26}$ cm, then the photon flux can be appreciably attenuated. Similar estimates indicate that the contribution to the attenuation of the photon beam as a result of interactions with nuclei or magnetic fields is much smaller.

We proceed to quantitative estimates. The probability per unit length of path that a quantum of energy E is converted into an electron pair in a collision with a thermal photon is

$$P = 2\int_0^\infty d\varepsilon n(\varepsilon)\int_0^1 z\sigma(s)\,dz, \quad z = \tfrac{1}{2}(1-\cos\vartheta),$$

$n(\epsilon)$ is the density of thermal photons in the energy interval $d\epsilon$. Replacing the integration over z by integration over $s = E\epsilon z/m^2$, we find that

$$P = 2\left(\frac{m^2}{E}\right)^2\int_0^\infty n(\varepsilon)\,\varepsilon^{-2}\varphi(s_0)\,d\varepsilon, \quad \varphi(s_0) = \int_1^{s_0} s\sigma(s)\,ds,$$

$$s_0 = \frac{E\varepsilon}{m^2}.$$

The values of $\varphi(s_0)$ in the interval $1 \le s_0 \le 10$ are shown in the figure. For larger s_0

$$\varphi(s_0) = 25\cdot 10^{-26}\{s_0(\ln 4s_0 - 2) + 3\}.$$

For the numerical estimate, we set

$$n(\varepsilon) = A\varepsilon^2/(e^{2\varepsilon} - 1).$$

This is a spectrum of the solar type, where kT = 0.5 and the photon energy is measured in electron-volts. To consider a specific case, we shall assume that the energy density of thermal photons in the universe is 0.1 ev cm^{-3}. Then the normalization factor is A = 0.22. Shown in the table are the numerical values of P for different γ-quantum energies and, as an example, the values of PR for an interesting star, Cygnus A (at a distance[4] $R_C = 6.6 \times 10^{26}$ cm). It is seen from the table that

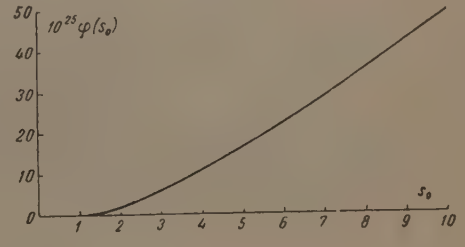

*It is readily seen that $\sigma(s)$ is obtained by multiplication of the inverse reaction by $2v^2$; the factor 2 results from the fact that the particles in the final state are not identical and v^2 results from the difference in the flux and statistical weight of these channels of the reaction.

10^{-12} E, ev	0.1	0.5	1	5	10	50
10^{27} P, cm^{-1}	0.05	5	7	4	2	0.7
PR_c	0.03	3	4.6	2.6	1.3	0.5

the maximum attenuation of the beam is e^{-PR} for $E = 10^{12}$ ev.

In principle, the effect can be used for an experimental estimate of the mean density of thermal photons in intergalactic space. The numerical value of this density is of interest for a number of astrophysical problems (see, e.g., [5], where the photodisintegration of high energy heavy nuclei in intergalactic space is discussed).

In conclusion, the author expresses his gratitude to V. L. Ginzburg for interesting discussions.

[1] G. Cocconi, Proceedings of the Moscow Cosmic Ray Conference, 1960, vol. 2, p. 309; Sekido, Yoshida, Komiya, Heno, and Murayama, ibid., vol. 3, pp. 137, 140; M. P. Savedoff, Nuovo cimento **13**, 12 (1959); P. Morrison, Nuovo cimento **7**, 858 (1958).

[2] A. I. Akiezer and V. B. Berestetskii, Kvantovaya élektrodinamika (Quantum Electrodynamics), 2nd ed., Fizmatgiz, 1959, p. 359.

[3] E. Feenberg and H. Primakoff, Phys. Rev. **73**, 449 (1948); C. W. Allen, Astrophysical Quantities, University of London, Athlone Press, 1955, pp. 228, 245.

[4] I. S. Shklovskii, Astronomicheskii zhurnal, **37**, 945 (1960), Soviet Astronomy **4**, 885 (1961).

[5] N. M. Gerasimova and I. L. Rozental', JETP **41**, 488 (1961), Soviet Phys. JETP **14**, 350 (1962).

Translated by E. Marquit
99

FIELD THEORY WITH NONLOCAL INTERACTION. I. CONSTRUCTION OF THE UNITARY S MATRIX

D. A. KIRZHNITS

P. N. Lebedev Physics Institute, Academy of Sciences, U.S.S.R.

Submitted to JETP editor March 8, 1961

J. Exptl. Theoret. Phys. (U.S.S.R.) **41**, 551-559 (August, 1961)

It is found that the impossibility of solving the nonlocal Tomonaga-Schwinger equations and the absence of analogous difficulties in the Lagrangian approach can be explained by the fact that these two approaches correspond to two essentially different nonlocal field theories, and not to two different representations of the same theory. By means of a simple representation found in this paper for the local S matrix in terms of retarded commutators, a unitary S matrix is constructed which corresponds to a nonlocal interaction. The matrix is completely relativistically invariant, and in the limit of local theory goes over into the usual S matrix.

1. INTRODUCTION

FOR a long time there has been interest in a field theory with a nonlocal interaction containing the product of field operators taken at noncoinciding points of space-time. Besides hopes for escape from the difficulties of existing field theory, and for the possibility of treating unrenormalizable interactions, there has recently been a basis for this interest in the expectation of experimental results on tests of quantum electrodynamics at small distances. It is not excluded that these experiments may give a negative result, i.e., that deviations from the predictions of existing theory may be detected. The introduction of a nonlocal interaction is evidently the simplest possibility for describing such deviations.

We shall here be discussing formal nonlocal theory, in which one uses a "rigid" form-factor, which is a prescribed function of the differences of the coordinates. The form of the function can be fixed as an additional condition (if the experiments mentioned earlier give a negative result, some characteristics of the form-factor can be found directly from experiment). Of course such a theory is of a preliminary, and at best phenomenological, nature. In spite of the existence of an extensive literature devoted to nonlocal theory, however, there is no definite answer to the question of the possibility of constructing even such a preliminary theory.

There are a number of problems that arise in the statement of the nonlocal problem with rigid form-factor; the most important of them will now be mentioned.

First is the problem of the freedom of the theory from mathematical contradictions.[1] By this we mean the possibility of satisfying Bloch's consistency condition. In this connection it must be noted that from the very beginning there is some inconsistency in the theory in question. This is that in a formally relativistically invariant theory there are inevitable motions at small distances with speeds larger than the speed of light. In itself this is not in contradiction with experiment, but the important question is whether or not this formal inconsistency will develop into a mathematical contradiction. The next problem, in order of importance, bears on the macroscopically causal character of the theory.[2] The existence of signals faster than light unavoidably brings with it violations of causality. The question is whether one can localize this violation in a small space-time region, and thus make it in a reasonable sense unobservable. A related question is that of the possibility of constructing a dispersion apparatus in nonlocal field theory.

Next, the requirement that the S matrix be unitary is extremely important. Examples have been given in the literature of nonlocal theories[3] in which this requirement was violated.

Finally, there are arguments[4] about the possible ineffectiveness of the form-factor in higher orders of perturbation theory. It is necessary that the form-factor lead to an effective removal of the divergences.

The remaining problems—renormalization, gauge invariance in electrodynamics, and so on—are not of such central significance.

In a series of papers, of which this is the first, an attempt will be made to show that the difficulties associated with the problems just listed can quite definitely be overcome and are not so deep as is generally supposed. In the present paper we consider the problems of consistency and unitarity, which can be studied without taking a concrete form for the form-factor.

3. THE MATHEMATICAL CONSISTENCY OF THE NONLOCAL THEORY

For definiteness we shall consider the pseudoscalar theory with pseudoscalar interaction; in the local case the interaction Hamiltonian is[1)]

$$H = g\int d\,1\ (\bar{\psi}(1)\gamma_5\psi(1))\varphi(1) = -L. \qquad (1)$$

The corresponding interaction Lagrangian differs from this expression only in sign.

Nonlocal generalizations of the theory can be made in two ways—by introducing the form-factor either in the Hamiltonian

$$H = g\int d(1)\,(\bar{\psi}(1')\,\gamma_5\psi(1''))\,\varphi(1'''), \qquad (2)$$

or in the interaction Lagrangian

$$\mathbf{L} = -\frac{g}{2}\int d(1)(\bar{\psi}(1')\gamma_5\psi(1'')\varphi(1''') + \text{Herm. adj.} \qquad (3)$$

Here $d(1) = d1'd1''d1'''F(1', 1'', 1''')$; F is the form-factor, which satisfies the condition

$$F(1', 1'', 1''') = F^*(1'', 1', 1'''),$$

so as to assure that the expression (2) is Hermitian, and which goes over into $\delta(1'-1'')\,\delta(1'-1''')$ in the limit of local theory. Here bold-face letters denote operators in the Heisenberg representation.

In the nonlocal theory based on the Hamiltonian (2) we immediately encounter a violation of the well known condition of consistency of the Tomonaga-Schwinger equation

$$[\mathcal{H}(1),\ \mathcal{H}(2)] = 0, \qquad (4)$$

where the points 1 and 2 are separated by a spacelike interval. We recall that Eq. (4) is the condition for the existence of the S matrix $S(\sigma)$ as a definite functional of the spacelike surface σ. Starting from the equation

$$i\delta S(\sigma)/\delta\sigma(1) = \mathcal{H}(1\,|\,\sigma)\,S(\sigma) \qquad (5)$$

and equating to each other the derivatives $\delta^2S/\delta\sigma(1)\,\delta\sigma(2)$ and $\delta^2S/\delta\sigma(2)\,\delta\sigma(1)$, we arrive at the consistency condition in general form[5]

$$[\mathcal{H}(1\,|\,\sigma),\ \mathcal{H}(2\,|\,\sigma)] = i\left\{\frac{\delta\mathcal{H}(2\,|\,\sigma)}{\delta\sigma(1)} - \frac{\delta\mathcal{H}(1\,|\,\sigma)}{\delta\sigma(2)}\right\}. \qquad (6)$$

Here and in the preceding equations $\mathcal{H}$ is the interaction Hamiltonian density. If this quantity does not depend on σ, we come back to the condition (4).[2)]

Furthermore one can also not avoid difficulties in the framework of the usual one-time formalism. Although the corresponding solution does exist, its relativistic invariance is violated in a fundamental way. The point is that the S matrix involves retarded commutators of the type

$$\theta(1-2)\,[\mathcal{H}(1),\ \mathcal{H}(2)],$$

which do not have invariant meaning because the commutator does not vanish outside the light cone (the function θ is zero when point 1 is earlier than point 2, and unity in the opposite case). Thus a nonlocal theory based on the use of the Hamiltonian (2) cannot be constructed at all.

On the other hand, a direct treatment of the Heisenberg equations that are based on the Lagrangian (3) does not encounter this sort of difficulties. Corresponding examples relating to the classical theory are well known.[3)] In quantum theory the solution by perturbation theory is always possible, and no violations of relativistic invariance occur in it.[4] In individual cases it may also be possible to find exact solutions of the field equations, which are also free from difficulties.[4)]

It is important to note that although the Heisenberg operators obtained with such a statement of the problem do not commute outside the light cone, this fact has no bearing on the difficulties under discussion, but indicates only a violation of microcausality.

The situation we have presented is often interpreted in the following rather unsatisfactory way. It is supposed that the two approaches that have been indicated correspond to the treatment of the same problem in two different representations—the interaction representation and the Heisenberg

[1)] In the equations that follow space-time arguments are denoted by numbers.

[2)] We emphasize that Eq. (6) is a direct consequence of Eq. (5). Therefore one can construct an infinite number of nonlocal Hamiltonians which satisfy the condition (6); it suffices to take a unitary operator $S(\sigma)$ and find $\mathcal{H}$ from Eq. (5). In this process, however, the causality condition is in general sharply violated. In the general case this condition is in no way connected with the condition of consistency. Only for the simplest Hamiltonian of the type (2) are the two conditions equivalent.

[3)] We note that difficulties also occur in the classical theory based on a Hamiltonian of the type (2) (cf. reference 6).

[4)] This situation occurs in the nonlocal analogue of the relativistic model which has been considered by Smolyanskii and the writer.[7]

representation. The presence of the difficulties in one representation and their absence in the other is explained either by a complete lack of equivalence of the representations, or by the concealed nature of difficulties in the second approach, based on the Lagrangian (3).

We must, however, pay attention to one essentially trivial fact, in the light of which the situation that has been described becomes completely clear. The point is that the nonlocal Hamiltonian (2) and Lagrangian (3) by no means correspond to the same problem. In fact, the Lagrangian (3) actually depends on higher derivatives of the fields, as one readily sees on expanding the integrand in Eq. (3) in series around one of the argument values. Along with this it is well known that even in a theory with the Lagrangian containing just the first derivative of the field φ the corresponding Hamiltonian necessarily includes a contact four-fermion term. In the present case there are derivatives of all orders, and therefore the Hamiltonian corresponding to Eq. (3) must have an extraordinarily complex structure with respect to both the field operators and the coupling constants (cf. papers by Katayama[8] and Hayashi[3]). In any case this Hamiltonian has nothing in common with Eq. (2).[5] The essential point is that the Hamiltonian obtained from Eq. (3) automatically satisfies the consistency condition (6) (it actually depends on the surface σ; for details see below).

Thus there are two essentially different nonlocal theories. The first, based on the use of the Hamiltonian (2), suffers from serious difficulties and is condemned to failure from the beginning.[6] The second, based on the Lagrangian (3), is free from such difficulties and calls for further study in the light of the other problems listed in the Introduction.

3. THE HEISENBERG FIELD EQUATIONS

When we consider the second type of theory the question of the unitarity of the S matrix becomes most acute.[3] We shall give some details of the corresponding calculations, in order on one hand to give an illustration of the assertions that have been made, and on the other, to introduce a number of concepts needed for what follows.

[5] The interaction Hamiltonian and Lagrangian differ in sign only in a local theory without higher derivatives. Already in local renormalized theory the Hamiltonian has a complex structure, owing to the presence of higher derivatives associated with the counter-terms.

[6] The relativistic Lee model relates to a theory of just this type (see reference 9).

Considering for simplicity only the equation for the field

$$(\Box - \mu^2)\,\varphi(1) = \mathrm{j}(1),$$

let us use the Yang-Feldman method of quantization. We have

$$\varphi(1) = \varphi(1) - \int d2\theta\,(1-2)\,D\,(1-2)\,\mathrm{j}(2), \qquad (7)$$

where $\varphi(1) \equiv \varphi_{\mathrm{in}}(1)$ is a solution of the free equation. We require that this operator shall also satisfy the free commutation rules $[\varphi(1), \varphi(2)] = iD(1-2)$; by this we uniquely determine also the commutation rules of the operator φ.

Let us then introduce the extremely convenient quantity[7]

$$\varphi(1,\sigma) = \varphi(1) - \int d2\theta\,(\sigma,\ 2)\ D\,(1-2)\,\mathrm{j}(2), \qquad (8)$$

which coincides with φ_{in} for $\sigma \to -\infty$, with φ_{out} for $\sigma \to +\infty$, and with the Heisenberg operator $\varphi(1)$ when the point 1 lies on σ (the symbol for this is $1|\sigma$). The operator $\varphi(1,\sigma)$ satisfies the free equation, but its commutation rules are by no means the free commutation rules [the actual commutation rules are automatically determined from Eq. (8)]. Therefore we separate out from $\varphi(1,\sigma)$ the part $\varphi_0(1,\sigma)$ that satisfies the free commutation rules:

$$\varphi(1,\sigma) = \varphi_0(1,\sigma) + \chi(1,\sigma),$$

where by definition $\chi(1,-\infty) = 0$. Then we can write

$$\varphi_0(1,\sigma) = U^{-1}(\sigma)\,\varphi(1)\,U(\sigma),$$

where U is a unitary operator.

It is clear from this that the connection between the operators in the Heisenberg and interaction representations is not unitary:

$$\varphi(1) = \varphi(1|\sigma) = U^{-1}(\sigma)\,\varphi(1)\,U(\sigma) + \chi(1|\sigma). \qquad (9)$$

It is precisely for this reason that the Heisenberg operators do not commute outside the light cone.

By means of $U(\sigma)$ we can construct the interaction Hamiltonian[8]

$$\mathcal{H}(1|\sigma) = i\,\frac{\delta U}{\delta\sigma(1)}\,U^{+},$$

[7] The quantity $\theta(\sigma; 1)$ is equal to unity if the point 1 is earlier than σ, and to zero in the opposite case. These cases differ in the sign of the normal dropped from 1 onto σ. Because of the timelike nature of this normal the definition has an invariant meaning.

[8] In a paper by Katayama[8] it is shown that the canonical formalism also leads to the same expression for the Hamiltonian, if this formalism is modified so as to apply to theories with higher derivatives.

which automatically satisfies the consistency condition (6) (cf. footnote [2)]). We can find the explicit forms of $\mathcal{H}$ and χ in the form of perturbation-theory series by expanding Eqs. (7) and (8) in power series in g. In particular, in the lowest order of perturbation theory we have

$$\mathcal{H}(1 \mid \sigma) = -\mathcal{L}(1),$$
$$\chi(1, \sigma) = \int d2d3\,(\theta(\sigma, 2) - \theta(\sigma, 3))\, D(1-3)\, \frac{\delta \mathcal{L}(2)}{\delta \varphi(3)}$$

Here and hereafter $\mathcal{L}(1)$ is the interaction Lagrangian density expressed in terms of the free operators

$$\mathcal{L}(1) = -g \int d[1]\, (\bar{\psi}(1')\, \gamma_5 \psi(1''))\, \varphi(1'''),$$
$$d[1] \equiv d(1)\, \tfrac{1}{3}\,(\delta(1-1') + \delta(1-1'') + \delta(1-1''')). \tag{10}$$

The second-order term in the expansion of $\mathcal{H}$, which is given at the end of the paper [Eq. (19)], depends explicitly on the surface σ; when it is substituted in the right member of Eq. (6) it exactly compensates the nonvanishing left member of that condition, and so on. As for the operator χ, it can be seen that it vanishes both in the limit of local theory and also in the limit $\sigma \to +\infty$.

This last fact is of importance in the solution of the problem of the unitarity of the S matrix. If the condition

$$\chi(1, +\infty) = 0, \tag{11}$$

is satisfied we can write

$$\varphi_{out}(1) = S^{-1} \varphi(1)\, S,$$

where $S = U(\infty)$ plays the role of the unitary S matrix of the theory. It is important to emphasize that the field equations in themselves by no means guarantee that the condition (11) is satisfied. In some types of field theory this condition is clearly violated in the fourth order of perturbation theory. Although, as Medvedev and Hayashi [3] have shown, this defect can be eliminated by introducing a charge-symmetrical Lagrangian, the situation in the higher orders of perturbation theory remains unclear.

Let us now return to the original equation (7) and formulate the principle for constructing its solution.[4] In local theory the solution can be represented in the form (cf. e.g., [10])

$$\varphi(1) = S^{+} T(\varphi(1)\, S) = \sum_{n=0}^{\infty} R_n(\varphi(1)), \tag{12}$$

where

$$R_n(\varphi(1)) = i^n \int d2 \ldots d(n+1)\, \theta(1-2)\, \theta(2-3) \ldots \theta$$
$$\times (n - (n+1))\, [\ldots [[\varphi(1)\, \mathcal{L}(2)]\, \mathcal{L}(3)] \ldots \mathcal{L}(n+1)] \tag{13}$$

is the retarded commutator integrated over the coordinates (cf. [11]).

An analysis of Eq. (7) shows that in nonlocal theory the retarded commutator R_n must be replaced by a quantity $\tilde{R}_n$ according to the following rules established by Bloch [4,9]:

a) One expands the complex commutator that appears in Eq. (13) according to the rules for commutators of products; one puts it in the form of a sum of terms, each of which is a product of "elementary" commutators (or anticommutators, if appropriate) of operators φ and ψ and of these operators themselves.

As an example we write out two characteristic terms which appear in R_3:

$$g^3 \int d[2]\, d[3]\, d[4]\, D(1-2'')\, \{D(3''-4''')(4', 4'')$$
$$\times (2', S(2''-3'), 3'') + \varphi(3''')\, \varphi(4''')$$
$$\times (3', S(3''-2'), S(2''-4'), 4'') + \ldots\}. \tag{14}$$

Here and in what follows

$$\{\psi(1)\, \bar{\psi}(2)\} = iS(1-2), \quad (n, m) \equiv (\bar{\psi}(n)\, \gamma_5 \psi(m)),$$
$$(n', S(n''-m) \ldots S(k-l'), l'') \equiv (\bar{\psi}(n')\, \gamma_5 S$$
$$\times (n''-m)\, \gamma_5 \ldots \gamma_5 S(k-l')\, \gamma_5 \psi(l'')).$$

b) One multiplies each elementary commutator by the function θ of the difference of the corresponding arguments, the argument subtracted being that with the larger index.

The respective factors for the terms written out in Eq. (14) are:

$$\theta(1-2''')\, \theta(2''-3')\, \theta(3'''-4'''),$$
$$\theta(1-2''')\, \theta(2'-3'')\, \theta(2''-4').$$

This rule assures the relativistic invariance of the result in the sense indicated above (see Sec. 2).

c) One divides each term that occurs in $\tilde{R}_n$ by a certain integer k which is defined below.

This rule is necessary to get the right local limit for $\tilde{R}_n$ when we let $\int d[l] \to 1$, $l', l'', l''' \to l$. In the local expression (13) all of the points $1, 2, \ldots n+1$ are ordered in time. But the local limit of $\tilde{R}_n$ also contains unordered points, for example, 3 and 4 in the second of the terms in Eq. (14). If we multiply this term by the sum $\theta(3-4) + \theta(4-3)$, which is equal to unity, we get two ordered terms, which, as is easily seen, make equal contributions to $\tilde{R}_n$. To get the right limit it is necessary to set $k = 2$. In the first of the terms in Eq. (14) there are no unordered terms and $k = 1$.

In the general case one must find all pairs of

[9)] The rule c) formulated here differs from the corresponding rule of Bloch in simplicity and convenience.

unordered points, insert for each such pair a sum of θ functions, and determine the number k as the number of terms so obtained which are different from zero. For example, in a term containing $\theta(1-2)\,\theta(2-3)\,\theta(2-4)\,\theta(3-5)$ the unordered pairs are (3, 4) and (4, 5). Multiplying this term by $[\theta(3-4)+\theta(4-3)][\theta(4-5)+(5-4)]$, we get k = 3, since on being multiplied by $\theta(3-5)$ the quantity $\theta(5-4)\,\theta(4-3)$ vanishes identically.

The main properties of a nonlocal retarded commutator constructed in this way—relativistic invariance and the correct local limit—are also preserved for commutators of more complex types, for example, $\tilde{\mathfrak{R}}_n(\mathcal{L}(1))$. In the next section we shall use the rules that have been formulated to construct the unitary S matrix.

4. CONSTRUCTION OF THE UNITARY S MATRIX

It has already been stated that although the solution of the nonlocal problem based on the Lagrangian (3) is always possible in principle, the question of the unitarity of the S matrix obtained in this way remains essentially open. The difficulties of investigating this incline one to renounce the dynamical principle altogether and go over to a direct construction of the S matrix in a form such that there is no doubt of its unitarity. We shall proceed along the line of a direct generalization of the S matrix of local theory, with the requirement that the equation to be found be relativistically invariant and provide the possibility of an inverse transition to the limit of the original local expression.

It has been shown above how one must carry out the corresponding generalization of the retarded commutator. Therefore the present problem can be regarded as solved if one can succeed in expressing the local S matrix in terms of retarded commutators. Such a representation of the S matrix is always possible. Nishijima[11] has found recurrence relations connecting T products with retarded commutators. There also exists a direct representation of the S matrix in terms of retarded commutators. To derive it we shall start from the usual expression for the local S matrix

$$S = T\exp\left\{i\int d1\,\mathcal{L}(1)\right\}$$

and regard $\mathcal{L}$ as proportional to the coupling constant g.[10]

[10] In the general case one can multiply $\mathcal{L}$ by a parameter which plays the role of g in the subsequent calculations, and which must be set equal to unity after the calculations are completed.

Differentiating this relation with respect to g, we find

$$g\frac{dS}{dg} = i\int d1T\,(\mathcal{L}(1)\,S) = iS\int d1\mathcal{L}_{\mathrm{H}}(1),$$

where, in complete analogy with Eq. (13), the Heisenberg-representation Lagrangian $\mathcal{L}_{\mathrm{H}}$ can be expressed in the form

$$\int d1\mathcal{L}_{\mathrm{H}}(1) = \int d1\sum_{n=0}^{\infty} R_n(\mathcal{L}(1)) \equiv \sum_{n=0}^{\infty}\mathfrak{R}_n.$$

Integrating the resulting equation, we find finally

$$S = \tilde{T}_g\exp\left\{i\int_0^g \frac{dg}{g}\sum_{n=0}^{\infty}\mathfrak{R}_n(g)\right\}, \tag{15}$$

where $\tilde{\mathrm{T}}_{\mathrm{g}}$ is the antichronological ordering with respect to charge (which must increase from left to right), and $\mathfrak{R}_{\mathrm{n}}$ is regarded as a function of the charge.

This expression has two important properties: it contains only retarded commutators, and instead of time ordering there is an ordering with respect to charge. This enables us to make a direct extension of Eq. (15) to the nonlocal theory,

$$S = \tilde{T}_g\exp\left\{i\int_0^g \frac{dg}{g}\sum_{n=0}^{\infty}\tilde{\mathfrak{R}}_n(g)\right\}, \tag{16}$$

where $\tilde{\mathfrak{R}}_{\mathrm{n}}$ is the retarded commutator of the nonlocal Lagrangians of Eq. (10), calculated according to the Bloch rules.

We have still to convince ourselves that the expression we have obtained is unitary. It is known that the condition for unitarity of any T exponential is that the exponent be antihermitian. In local theory the operator $\mathfrak{R}_{\mathrm{n}}$ is Hermitian by construction. It is easy to see that $\tilde{\mathfrak{R}}_{\mathrm{n}}$ also has this property. In fact, a complicated commutator occurring in $\mathfrak{R}_{\mathrm{n}}$ can always be broken up into pairs of terms whose components are each other's Hermitian adjoints. These components include elementary commutators with identical arguments, and therefore have a common set of θ functions and identical values of k. Therefore the transition from $\mathfrak{R}_{\mathrm{n}}$ to $\tilde{\mathfrak{R}}_{\mathrm{n}}$ does not involve a loss of the Hermitian property.[11]

We give the expansion of Eq. (16) to third order in g:

$$S = 1 + i\tilde{\mathfrak{R}}_0 - {}^1/_2((\tilde{\mathfrak{R}}_0)^2 - i\tilde{\mathfrak{R}}_1) - {}^1/_6\,i\,((\tilde{\mathfrak{R}}_0)^3 - 2i\tilde{\mathfrak{R}}_0\tilde{\mathfrak{R}}_1 - i\tilde{\mathfrak{R}}_1\tilde{\mathfrak{R}}_0 - 2\tilde{\mathfrak{R}}_2) + \ldots \tag{17}$$

The retarded commutators themselves have the forms (the notations are the same as in Eq. (14))

[11] We note that, independently of this fact, we could have taken the Hermitian part of $\tilde{\mathfrak{R}}_{\mathrm{n}}$ in the exponent of Eq. (16).

$$\tilde{\mathfrak{R}}_0 = -g\int d(1)\,(1',1'')\,\varphi(1''),$$

$$\tilde{\mathfrak{R}}_1 = -\frac{g^2}{2}\int d(1)\,d(2)\,\theta(1''-2'')\,D(1''-2'')\,(1',1'')\,(2',2'')$$
$$\times\theta(1''-2')\,(1',S(1''-2'),2'')\{\varphi(1''),\varphi(2'')\}$$
$$+\text{Herm. adj.}$$

$$\tilde{\mathfrak{R}}_2 = -\frac{g^3}{2}\int d(1)\,d(2)\,d(3)\,D(1''-2'')\,\varphi(3'')$$
$$\times(3\theta(1''-2'')\,\theta(2''-3')-\theta(1''-2'')$$
$$-2\theta(2''-3')+1)\{(1',1''),(2',S(2''$$
$$-3')\,3'')\}+\tfrac{1}{4}(3\theta(1''-2')-1)\,\theta$$
$$\times(2''-3')\{\{\varphi(1''),\varphi(2'')\}\varphi(3'')\}$$
$$\times(1',S(1''-2'),S(2''-3')\,3'')+\text{Herm. adj.}\quad(18)$$

As can be seen particularly clearly from the expression for $\tilde{\mathfrak{R}}_2$, the main difference between $\mathfrak{R}$ and $\tilde{\mathfrak{R}}$ is that the order of the processes of smearing out and of ordering is changed (the functions θ go under the signs of integration over the internal coordinates). This fact is in qualitative agreement with the well known theorem of Takahashi and Umezawa (cf. e.g., [5]) on the construction of the S matrix in a theory with higher derivatives. A detailed analysis of the expression we have obtained for the S matrix and, in particular, a formulation of the corresponding Feynman rules will be given later in this series.

We note that we would have arrived at this same expression for the S matrix, but by a more complicated way, if we had used the approach of Stueckelberg and Bogolyubov,[2,12] and determined the Hermitian part of the S matrix from the condition of unitarity and the antihermitian part from considerations like those used in the derivation of Eq. (16). The axiomatic approach with the use of the macrocausality condition to determine the antihermitian part of the S matrix has also been used earlier,[13] but the arguments in question were not fully developed. A paper by Stueckelberg and Wanders[2] relating to this same group of questions will be discussed in the next paper of this series, which is devoted to the problem of causality.

In conclusion we note that formally we can set up an effective Hamiltonian to correspond to the S matrix (16). For this purpose one must construct an S matrix with a variable upper limit, introducing into the integrand $\tilde{\mathfrak{R}}_n$ the factor $\theta(\sigma,1)\,\theta(\sigma,2)\ldots\theta(\sigma,n+1)$, and use the relation (5). As the result we get to the second order in g

$$\mathcal{H}(1\,|\,\sigma) = g\int d[1]\,(1',1'')\,\varphi(1'') - \frac{g^2}{2}\int d[1]\,d(2)\,\theta(\sigma,2)\,\theta$$
$$\times(2''-1'')\,D(1''-2'')\,(1',1'')\,(2',2'')+\theta(2'-1'')$$
$$\times(1',S(1''-2'),2'')\{\varphi(1''),\varphi(2'')\}+\text{Herm. adj.}\quad(19)$$

The method described in Sec. 3 leads to this same expression. We may suppose that this coincidence occurs in all orders of perturbation theory, and also the S matrix (16) itself must be equal to the operator $U(\infty)$. We emphasize, however, that the identification of the S matrix of the theory based on the nonlocal Lagrangian with this operator is possible only if the condition (11) is satisfied. Therefore the approach based not on the dynamical principle but on the direct introduction of the S matrix has definite advantages, primarily from the point of view of the condition for unitarity. It is this approach that is used in our further work.

I express my deep gratitude to I. E. Tamm and M. A. Markov for their interest in and attention to this work, to V. L. Ginzburg for a number of stimulating comments, and to A. A. Komar, V. Ya. Faĭnberg, and E. S. Fradkin for numerous discussions.

[1] M. A. Markov, JETP **26**, 527 (1953). Giperony i K-mezony (Hyperons and K Mesons), Fizmatgiz, 1958.

[2] M. Chrétien and R. Peierls, Nuovo cimento **10**, 668 (1953). E. C. G. Stueckelberg and G. Wanders, Helv. Phys. Acta **27**, 667 (1954).

[3] C. Hayashi, Progr. Theoret. Phys. **10**, 533 (1953); **11**, 226 (1954). B. V. Medvedev, Doklady Akad. Nauk SSSR **100**, 433 (1955).

[4] C. Bloch, Kgl. Danske Videnskab. Selskab, Mat-fys. Medd. **27**, No. 8 (1952).

[5] H. Umezawa, Quantum Field Theory, North Holland-Interscience, 1956.

[6] A. A. Komar and M. A. Markov, JETP **36**, 854 (1959), Soviet Phys. JETP **9**, 602 (1959).

[7] D. A. Kirzhnits and S. A. Smolyanskii, JETP **41**, 205 (1961), Soviet Phys. JETP **14**, 149 (1962).

[8] Y. Katayama, Progr. Theoret. Phys. **10**, 31 (1953).

[9] D. A. Kirzhnits, JETP **14**, 417 (1961), this issue p. 300.

[10] J. Schwinger, Phys. Rev. **17**, 765 (1957).

[11] K. Nishijima, Progr. Theoret. Phys. **17**, 765 (1957).

[12] N. N. Bogolyubov and D. V. Shirkov, Introduction to the Theory of Quantized Fields, Interscience, 1959.

[13] B. V. Medvedev, Doklady Akad. Nauk SSSR **103**, 37 (1955).

Translated by W. H. Furry
100

THE TRANSFORMATION MATRIX FOR THE PERMUTATION GROUP AND THE CONSTRUCTION OF COORDINATE WAVE FUNCTIONS FOR A MULTISHELL CONFIGURATION

I. G. KAPLAN

Institute of Chemical Physics, Academy of Sciences, U.S.S.R.

Submitted to JETP editor March 10, 1961

J. Exptl. Theoret. Phys. (U.S.S.R.) **41**, 560-568 (August, 1961)

We consider the orthogonal representation of the permutation group with an arbitrary type of reduction to subgroups. We introduce the matrix for transformation between representations with different types of reduction, which to a definite extent is the analog of the transformation matrix between different angular momentum coupling schemes, and we give a method for calculating this matrix in terms of the matrix elements of the standard Young-Yamanouchi representation. An expression is given for the coordinate wave function of a multishell configuration in terms of the vector-coupled coordinate wave functions of the individual shells.

1. INTRODUCTION

LET us consider a system of n identical particles placed in a central field. As examples of such a system, we have the nucleons in a nucleus (shell model) or the electrons in an atom. In those cases where the Hamiltonian of the system does not include spin interactions, all its properties are completely determined by assigning the coordinate wave function corresponding to a given value of the total orbital angular momentum and constructed including the spin and taking into account the Pauli principle (while for nucleons we must still also include the isotopic spin).* The splitting of the wave function into coordinate and spin parts is also often needed for a Hamiltonian of the most general type. Here the coordinate and spin functions must have permutation symmetry corresponding to dual Young patterns (associated representations).[1,2] However, until recently the problem of constructing a coordinate wave function for a configuration of several shells had not been solved in general form, except for those limiting cases which were treated by Jahn: 1) the particles have the same orbital angular momentum (a single shell);[3,4] 2) the particles have different orbital angular momenta, i.e., there is just one particle in each shell.[5] In [6] it is pointed out that Elliot in his dissertation treated the case where there is a single, unfilled, and several filled shells. However, unfortunately, these results were not published.

In the present paper we give a method for constructing the coordinate wave function of a multishell configuration in terms of the coordinate wave functions of the individual shells. In a succeeding paper we shall give the formulas for the fractional parentage coefficients of those configurations which make it possible to reduce the calculation of the matrix element of the energy operator and other physical quantities for a system of n particles to the already known matrix elements for two particles and one particle.

The problem of constructing functions with a definite permutation symmetry from the functions for subsystems, each of which has its own permutation symmetry, requires the study of the representations of the permutation group with arbitrary method of reduction to subgroups. In our work we introduce the transformation matrix which makes possible the transition between representations with different types of reduction to subgroups, and we give a method for calculating it. This matrix can be regarded as the analog of the matrix for transformation between different coupling schemes for angular momenta.[7]

Because the apparatus of the permutation group which is used in this paper is relatively little known to physicists, and also in order to systematize the basic definitions and notation, we felt it desirable to precede the presentation of our work

*We are talking about zeroth-order wave functions. By a coordinate function we mean a function which depends only on the spatial coordinates of the particles.

by giving the necessary information from the theory of the permutation group.

2. THE STANDARD REPRESENTATION OF THE PERMUTATION GROUP AND THE YOUNG OPERATORS

The irreducible representations of the permutation group on n symbols (S_n) are characterized by different symmetry schemes for the basis functions, the so-called Young patterns.[2,8] To described them we use the notation $[\lambda] \equiv [\lambda^{(1)}\lambda^{(2)} \ldots \lambda^{(m)}]$, where $\lambda^{(i)}$ is the number of boxes in the i-th row, $\lambda^{(1)} \geq \lambda^{(2)} \geq \ldots \geq \lambda^{(m)}$, and $\sum_{i=1}^{m} \lambda^{(i)} = n$. The number of linearly independent functions corresponding to a given Young pattern determines the dimensionality of the irreducible representation. The latter is equal to the number of ways of placing the integers from 1 to n into the boxes of the Young pattern in such a way that, reading from left to right in the rows and from top to bottom in the columns, the numbers will be arranged in increasing order. For example,

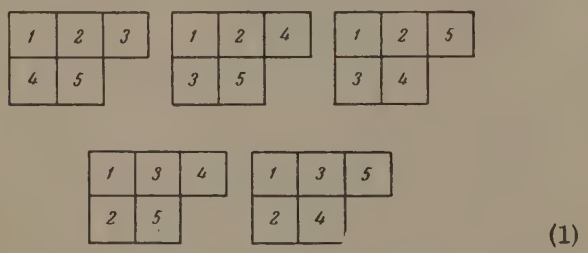

(1)

A Young pattern with a definite arrangement of numbers in it is called a Young tableau; in the following we shall use the abbreviation Y.T. The basis functions corresponding to each Y.T. can be chosen so that in making the transition from the group S_n to S_{n-1}, S_{n-2} etc., the irreducible representation $[\lambda]$ automatically splits into irreducible representations of the groups S_{n-1}, S_{n-2}, etc. The irreducible representation constructed in this fashion is said to be standard. Then each of the basis functions can be characterized by those irreducible representations to which it will belong in the reduction $S_n \to S_{n-1} \to S_{n-2} \to \ldots \to S_2$. This corresponds to the successive removal from the Y.T. of the boxes with the integers n, $n-1, \ldots$.

In place of the Y.T. it is convenient to characterize each of the basis functions by the Yamanouchi symbol (r) which is uniquely associated with the Y.T.[9] The symbol $(r) = (\sigma_1, \sigma_2, \ldots, \sigma_n)$, where σ_i is the number of the row in which the integer i appears. We shall say that $(r) = (\sigma_1 \ldots \sigma_n)$ lies higher than $(\bar{r}) = (\bar{\sigma}_1 \ldots \bar{\sigma}_n)$, if, for the first unequal pair of σ's we have the inequality $\sigma_i > \bar{\sigma}_i$.

The Young tableaux (1) correspond to the Yamanouchi symbols

$$(11122),\ (11212),\ (11221),\ (12112),\ (12121), \qquad (2)$$

which have been arranged in increasing order. The lowest Yamanouchi symbol corresponds to the Y.T. with the natural ordering of the integers. The Yamanouchi symbols corresponding to a given $[\lambda]$ can also be written without introducing the Y.T. if, in forming them, we remember that the arrangement of integers in the pattern must be subjected to the rule of lattice permutation which states: for any integer k appearing in the Yamanouchi symbol, we must satisfy the inequality $n(k) \geq n(k+1)$, where $n(k)$ gives the number of times that one meets the integer k among the first l numbers in the Yamanouchi symbol.

It is easily verified that the five symbols (2) satisfy the rule for lattice permutations and that no other symbol for [32] will satisfy this rule.

If we apply the permutations of the group S_n to the function of n numbers $\Phi_0 = \varphi_1(1)\,\varphi_2(2) \ldots \varphi_n(n)$, where the $\varphi_i(i)$ form an orthonormal system,* we obtain n! linearly independent functions $\Phi_p = P\Phi_0$. These functions transform among themselves under the action of permutations according to the so-called regular representation.[2] Linear combinations of the functions Φ_p, forming a basis for the irreducible representation, can be obtained by using the normalized Young operators:[5]

$$\omega_{rs}^{[\lambda]} = \left(\frac{f_\lambda}{n!}\right)^{1/2} \sum_P \langle [\lambda]\,(r) \mid P \mid [\lambda]\,(s) \rangle\, P, \qquad (3)$$

where f_λ is the dimensionality of the representation $[\lambda]$; (r) and (s) are Yamanouchi symbols, and P runs through the n! permutations. The matrices appearing in (3) form the orthogonal representation of the permutation group S_n. Young and Yamanouchi[8,9] have given formulas for the matrix elements of the matrix of a transposition of the type $P_{i,i-1}$ (cf. also [4]). All the other permutations can always be obtained as the product of appropriate transpositions.

We can form $(f_\lambda)^2$ different operators (3) for each $[\lambda]$. Correspondingly we can form the $(f_\lambda)^2$ functions:

$$|[\lambda]\,(r \mid s)\rangle = \omega_{rs}^{[\lambda]}\Phi_0. \qquad (4)$$

However, only those functions will transform into one another under the action of a permutation which have the same second index:[5]

*The number i can, for example, denote the set of coordinates of the i-th particle.

$$P|[\lambda](r|s)\rangle = \sum_{(t)} |[\lambda](t|s)\rangle \langle[\lambda](t)|P|[\lambda](r]\rangle. \quad (5)$$

For fixed (s) in Eq. (4), (r) runs through f_λ values which enumerate the basis functions of the $[\lambda]$ representation. Altogether, corresponding to the different values of (s), there are f_λ independent bases.* In those cases where there is no need to distinguish identical presentations, we shall agree to choose for the second index the lowest possible value and omit it in writing the symbol, for example, $|[\lambda](r)\rangle$.

The Yamanouchi symbols considered above number the basis functions which transform according to the standard orthogonal Young-Yamanouchi representation. However, in constructing the wave function of a system with definite permutation symmetry from the wave functions of subsystems, each having their own permutation symmetry, one needs to know the representations with arbitrary type of reduction into subgroups. The next section of the paper will be devoted to the study of such representations and also of the matrix for transforming between them.

3. NON-STANDARD REPRESENTATION OF THE PERMUTATION GROUP AND THE TRANSFORMATION MATRIX

If in treating some standard representation of the group S_n we go over to a subgroup S_{n_1}, it will split into irreducible representations of this subgroup. However, in considering the permutation of only the last $n - n_1 = n_2$ integers, a splitting into irreducible representations of the group S_{n_2} can in general not be achieved. This is related to the fact that the last integers as a rule do not form standard Young patterns. In the figure, the shaded boxes refer to the last n_2 integers. They do not correspond to any standard Young pattern. In this case we say that the Yamanouchi symbols of the last n_2 numbers are non-standard, and in the following we shall denote them by the letter ρ. Then the Yamanouchi symbol of the representation $[\lambda]$ can be written as $(r) = (r_1\rho_2)$, where r_1 is a

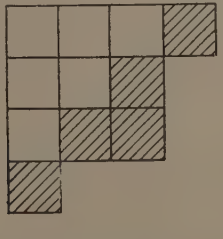

standard Yamanouchi symbol for the first n_1 numbers and ρ_2 is a non-standard Yamanouchi symbol for the last n_2 numbers. (In special cases, it may also be standard.)

Let us suppose that we are required to find that representation of the group S_n which, in the transition to the subgroup $S_{n_1} \times S_{n_2}$, would split into the irreducible representations $[\lambda_1] \times [\lambda_2]$. The possible patterns $[\lambda_1]$ and $[\lambda_2]$ are determined from the expansion

$$[\lambda] = \sum_{\lambda_1\lambda_2} c(\lambda\lambda_1\lambda_2)[\lambda_1]\times[\lambda_2], \quad (6)$$

which can easily be established from the character tables or by using Littlewood's theorem (cf. the Appendix). Thus

$$[32] = [2][3] + [2][21] + [11][21].$$

In place of the symbols (2), we shall now use the symbols (r_1r_2) to number the basis functions which are standard with respect to the first n_1 and the last n_2 numbers, namely,

$$((11)(111)),\ ((11)(112)),\ ((11)(121)),\ ((12)(112)),\ ((12)(121)). \quad (2a)$$

To find representations which are standard with respect to the last n_2 numbers, we apply the Young operator $\omega^{[\lambda_2]}_{r_2s_2}$ to the last n_2 numbers of the basis function of the standard representation $|[\lambda](r_1\bar{\rho}_2)\rangle$. For $\bar{\rho}_2$ we use the convention of choosing the symbol corresponding to the natural order of arrangement of the integers $n_1 + 1,\ n_1 + 2, \ldots, n_1 + n_2 = n$ in the Y.T., and for (s_2) the lowest symbol of the representation $[\lambda_2]$. Using formulas (3) and (5) we get

$$|[\lambda](r_1r_2)\rangle = \text{const}\cdot\omega^{[\lambda_2]}_{r_2s_2}|[\lambda](r_1\bar{\rho}_2)\rangle$$

$$= \sum_{\rho_2} |[\lambda](r_1\rho_2)\rangle\langle[\lambda](r_1\rho_2)|[\lambda](r_1r_2)\rangle. \quad (7)$$

The transformation matrix which accomplishes the transition from the basis functions of the standard representation to the basis functions of the representation with reduction type $S_{n_1} \times S_{n_2}$ is expressed in terms of the known matrix elements of the standard representation:

$$\langle[\lambda](r_1\rho_2)|[\lambda](r_1r_2)\rangle = N\sum_{P_2}\langle[\lambda_2](r_2)|P_2|[\lambda_2](s_2)\rangle$$

$$\times\langle[\lambda](r_1\rho_2)|P_2|[\lambda](r_1\bar{\rho}_2)\rangle. \quad (8)$$

The symbol $(r_1\rho_2)$ runs through all the Yamanouchi symbols of the pattern $[\lambda]$ which have for their first n_1 integers the symbol (r_1); P_2 are the permutations of the integers $n_1 + 1,\ n_1 + 2, \ldots, n$; N

*This is related to the fact that each irreducible representation appears in the resolution of the regular representation a number of times which is equal to its dimensionality. Consequently, in particular there follows the relation $\sum_\lambda (f_\lambda)^2 = n!$

is found from the condition of normalization of the function (7):

$$\sum_{\rho_2} (\langle [\lambda]\,(r_1\rho_2) \mid [\lambda]\,(r_1 r_2)\rangle)^2 = 1. \qquad (9)$$

We note that the matrices of the representation according to which the functions (7) transform do not depend on the choice of $\bar{\rho}_2$ and (s_2). The matrix elements (8) are different from zero only for those (r_1), (r_2), which belong to the representations $[\lambda_1]$, $[\lambda_2]$ which appear in the expansion (6). We express this condition symbolically in the form of a curly bracket:

$$\{\lambda\,(\lambda_1\lambda_2)\}. \qquad (10)$$

Obviously $\{\lambda_1(\lambda_1\lambda_2)\}$ is equivalent to $\{\lambda\,(\lambda_2\lambda_1)\}$. This symbol is in a certain sense analogous to the triangular condition for the addition of angular momenta. However, there is an essential difference from the addition of angular momenta. Whereas in the addition of angular momenta we are dealing with the direct product of representations of one and the same group (the rotation group), and in its expansion there appear the Clebsch-Gordan coefficients, in the expansion (6) a representation of the group S_n is expanded in representations of the subgroup $S_{n_1} \times S_{n_2}$. We cannot introduce Clebsch-Gordan coefficients in the usual sense.

In those cases where in the expansion of (6), $c(\lambda\lambda_1\lambda_2) > 1$, a further identification of the basis functions (7) is necessary. This is accomplished by the second index (s_2), which we choose starting from the lowest and so on. Then, the functions $|[\lambda](r_1(r_2|s_2))\rangle$ distinguished only by (s_2) will no longer be orthogonal to one another. However, the process of orthogonalization is easily carried out by considering the functions (7) as vectors in the orthogonal space of the standard basis (cf., for example, [10]). The scalar product of basis functions with different (s_2) is equal to

$$\sum_{\rho_2} \langle [\lambda]\,(r_1 r_2) \mid [\lambda]\,(r_1 (r_2 \mid s_2))\rangle \langle [\lambda[\,(r_1\rho_2) \mid [\lambda]\,(r_1 (r_2 \mid \bar{s}_2))\rangle. \qquad (9a)$$

For $n_2 = 2$, the matrix (8) has the simple form:

$$\langle [\lambda]\,(r_1\rho_2) \mid [\lambda]\,(r_1 r_2)\rangle = \begin{array}{c} \\ \rho_2' \\ \rho_2'' \end{array} \begin{array}{c} \begin{array}{cc} [2] & [11] \end{array} \\ \begin{vmatrix} \sqrt{\frac{d-1}{2d}} & -\sqrt{\frac{d+1}{2d}} \\ \sqrt{\frac{d+1}{2d}} & \sqrt{\frac{d-1}{2d}} \end{vmatrix} \end{array}, \qquad (11)$$

where $\rho_2 = (\sigma_{n-1}\sigma_n)$, and ρ_2' corresponds to $\sigma_{n-1} < \sigma_n$ and ρ_2'' to $\sigma_{n-1} \geq \sigma_n$; d is the axial distance between $n-1$ and n in the Y.T. corresponding to $(r_1\rho_2')$, and is defined as the number of single-box steps which are needed to move in the Y.T. from the integer $n-1$ to the integer n by moving from left to right and from top to bottom.[8]

For various questions associated with the treatment of configurations consisting of several shells, one needs to know the representations with arbitrary type of reduction to subgroups. We shall denote the type of reduction by Latin capitals; for example, $(r)^A$, $(r)^B$ denote Yamanouchi symbols with reduction types A and B. The absence of such a notation on the Yamanouchi symbol means that it refers to the standard type of reduction. Then, if the representation $[\lambda]$ is reduced to the subgroup $S_{n_1} \times S_{n_2} \times \ldots \times S_{n_k}$ where $(n_1 + n_2 + \ldots + n_k = n)$, then for its complete characterization we must give, in addition to the Young patterns $[\lambda_1], \ldots [\lambda_k]$, $k-2$ intermediate Young patterns and also the method for combining the $[\lambda_i]$ in the intermediate patterns (a situation which is analogous to the addition of k angular momenta, cf. [7,11]).

For example, for the case of the reduction type $(S_{n_1} \times S_{n_2}) \times S_{n_3}$, the basis functions of the transformed representation are obtained by applying two Young operators to the basis function of the standard representation, with an intermediate Young pattern of the first $n_1 + n_2$ numbers equal to $[\lambda_{12}]$. We write the Yamanouchi symbol of the standard representation in the form $(r_1\rho_2\rho_3)$, where $(r_1\rho_2) = (r_{12})$.* Then

$$|[\lambda]\,((r_1 r_2)\,\lambda_{12} r_3)\rangle = \text{const} \cdot \omega^{[\lambda_3]}_{r_3 s_3} \omega^{[\lambda_2]}_{r_2 s_2} |[\lambda]\,(r_1 \bar{\rho}_2 \bar{\rho}_3)\rangle$$
$$= \sum_{\rho_2\rho_3} |[\lambda]\,(r_1\rho_2\rho_3)\rangle \langle [\lambda]\,(r_1\rho_2\rho_3) \mid [\lambda]\,((r_1 r_2)\,\lambda_{12} r_3)\rangle. \qquad (12)$$

The transformation matrix is reduced to a product of two simpler matrices, which are obtained from formula (8):

$$\langle [\lambda]\,(r_1\rho_2\rho_3) \mid [\lambda]\,((r_1 r_2)\,\lambda_{12} r_3)\rangle$$
$$= \langle [\lambda_{12}]\,(r_1\rho_2) \mid [\lambda_{12}]\,(r_1 r_2)\rangle \langle [\lambda](r_{12}\rho_3) \mid [\lambda](r_{12} r_3)\rangle. \qquad (13)$$

The transformation matrices for the transition to the basis of a representation with a more complicated reduction type is found in similar fashion by applying appropriate sets of Young operators. The matrices of the transformed representation are calculated as usual from the formula

$$\langle [\lambda]\,(r)^A \mid P \mid [\lambda]\,(\bar{r})^A\rangle = \sum_{r,\,\bar{r}} \langle [\lambda]\,(r)^A \mid [\lambda]\,(r)\rangle$$
$$\times \langle [\lambda]\,(r) \mid P \mid [\lambda]\,(\bar{r})\rangle \langle [\lambda]\,(\bar{r}) \mid [\lambda]\,(\bar{r})^A\rangle. \qquad (14)$$

*Since the assignment of the Yamanouchi symbol automatically determines the Young pattern, to abbreviate the writing we shall omit the symbol for the Young pattern $[\lambda_i]$ in all those cases where no confusion can arise.

In applications it is frequently convenient to use the matrices for permutation operators constructed from "non-diagonal" matrix elements, in which the wave functions on the left and right sides have different types of reduction into subgroups:

$$\langle [\lambda]\,(r)^A \,|\, P \,|\, [\lambda]\,(r)^B \rangle. \tag{15}$$

These matrix elements appear as the coefficients in the expansion of the result of the operation of a permutation P on a function with reduction type B in terms of functions with reduction type A:

$$P\,|\,[\lambda]\,(r)^B\rangle = \sum_{(r)^A} |\,[\lambda]\,(r)^A\rangle \langle [\lambda]\,(r)^A \,|\, P \,|\, [\lambda]\,(r)^B\rangle. \tag{16}$$

The transformation matrices (8) and (13) may be regarded as special cases of the matrices (15) with $P \equiv 1$. The obvious generalization of formula (14) is

$$\langle [\lambda]\,(r)^A \,|\, P \,|\, [\lambda]\,(r)^B\rangle = \sum_{r,\,\bar{r}} \langle [\lambda]\,(r)^A \,|\, [\lambda]\,(r)\rangle \times \langle [\lambda]\,(r) \,|\, P \,|\, [\lambda]\,(\bar{r})\rangle \langle [\lambda]\,(\bar{r}) \,|\, [\lambda]\,(r)^B\rangle. \tag{14a}$$

Let us consider a special class of matrices (15), which we shall need in the following to find the coordinate fractional parentage coefficients of mixed configurations. Let us suppose that, under the action of the permutation P on $|\,[\lambda](r)^B\rangle$, we obtain a function in which the numbers are split up into the same groups as in $|\,[\lambda](r)^A\rangle$. Then we can apply the Wigner-Eckart[5] theorem* to each of these groups (its extension to finite groups has been given by Koster[12]). The matrix element (15) can be written as an integral of the product of two functions. If we choose P to be the identity operator, then from the point of view of the permutation group this is an irreducible tensor operator transforming according to the completely symmetric representation $[\lambda_g] \equiv [n]$; we denote such an operator by T^g. Since the direct product $[\lambda_g] \times [\lambda_i] = [\lambda_i]$ (there are no multiple representations in the expansion of the direct product), the Wigner-Eckart theorem takes the form

$$\langle [\lambda_i]\,(r_i) \,|\, T^g \,|\, [\bar{\lambda}_i]\,(\bar{r}_i)\rangle = \langle [\lambda_i] \,\|\, T^g \,\|\, [\lambda_i]\rangle\, \delta_{\lambda_i\bar{\lambda}_i}\delta_{r_i\bar{r}_i}, \tag{17}$$

i.e., the matrix element is diagonal with respect to $[\lambda_i](r_i)$ and does not depend on the Yamanouchi symbols. Therefore in this case equation (15) can be written in the form†

$$\langle [\lambda]^A \,\|\, P \,\|\, [\lambda]^B\rangle, \tag{18}$$

where the double bar means that the expression is independent of the Yamanouchi symbols, while A and B as before denote the types of reductions into subgroups, and the expressions are diagonal with respect to the $[\lambda_i]$ of the individual groups of numbers.

The simplest example of the matrix (18) is

$$\begin{aligned}\langle [\lambda]\,(r_1r_2) \,|\, P \,|\, [\lambda]\,(\bar{r}_2\bar{r}_1)\rangle &= \int \Phi^*\,([\lambda]\,(r_1r_2) \,|\, 12\,345)\, P_{13524}\, \Phi([\lambda]\,(\bar{r}_2\bar{r}_1) \,|\, 123\,45)\, d\tau \\ &= \int \Phi^*\,([\lambda]\,(r_1r_2) \,|\, 12\,345)\, \Phi\,([\lambda]\,(\bar{r}_2\bar{r}_1) \,|\, 345\,12)\, d\tau,\end{aligned} \tag{19}$$

Applying the Wigner-Eckart theorem individually to the groups of permutations of the numbers 12 and 345, we find that the expression is diagonal with respect to $[\lambda_1]$, $[\lambda_2]$ and independent of the Yamanouchi symbols.

4. CONSTRUCTION OF COORDINATE WAVE FUNCTIONS

Suppose we have a configuration consisting of two shells $l_1^{n_1} l_2^{n_2}$. In the absence of spin interactions, the energy levels are classified by assigning the permutation symmetry $[\lambda]$ of the whole configuration and the total orbital angular momentum L, and, in addition, a set of quantum numbers characterizing the energy levels of the individual shells $[\lambda_i]\,\alpha_i L_i$ (where the α_i distinguish terms with the same $[\lambda_i]\,L_i$). In the case of k shells it is necessary in addition to give $k-2$ intermediate symmetry patterns and intermediate orbital angular momenta.

In the work of Jahn,[5] for the case when all the orbital angular momenta of the particles are different, a formula was given which makes it possible to construct functions with symmetry $[\lambda]$ from functions with symmetries $[\lambda_1]$ and $[\lambda_2]$. In the final expression there enters the matrix whose calculation was not shown (except for the case of $n_2 = 2$). If in place of permutations of the orbital angular momenta we permute the coordinates of the particles and introduce a matrix of type (15), then by means of computations which are analogous to those carried out by Jahn we obtain the following expression for the orbital wave function of a two-shell configuration:

$$\begin{aligned}\Phi\,((l_1^{n_1}\,[\lambda_1]\,\alpha_1L_1,\ l_2^{n_2}\,[\lambda_2]\,\alpha_2L_2)\,[\lambda]\,(r)^ALM) &= \left\{\frac{f_\lambda}{f_{\lambda_1}f_{\lambda_2}}\frac{n_1!\,n_2!}{n!}\right\}^{1/2} \sum_{r_1r_2}\sum_{Q} \langle [\lambda]\,(r)^A \,|\, Q \,|\, [\lambda]\,(r_1r_2)\rangle\ Q \\ &\times \varphi\,(l_1^{n_1}\,[\lambda_1]\,(r_1)\,\alpha_1L_1,\ l_2^{n_2}[\lambda_2]\,(r_2)\,\alpha_2L_2;\ LM).\end{aligned} \tag{20}$$

The function φ describes the vector-coupled state

*This fact was brought to the author's attention by I. B. Levinson.

†The result (17) of the Wigner-Eckart theorem is trivial, since it follows from the orthonormality of the basis of the standard representation ($\langle [\lambda_i] \,\|\, T^g \,\|\, [\lambda_i]\rangle = 1$). However, the application of the theorem to the class of matrices (15) which we are considering gives the non-trivial result that (18) is independent of the Yamanouchi symbols and is diagonal with respect to $[\lambda_i]$.

with total angular momentum L and projection M. The symbols (r_1), (r_2) run through all the Yamanouchi symbols of the patterns $[\lambda_1]$ and $[\lambda_2]$, and Q are permutations of the coordinates of the particles between the shells. The choice of Q is not unique. We may choose for them any $n!/n_1!n_2!$ permutations from the set which are conjugate with respect to the subgroup $S_{n_1} \times S_{n_2}$.

As an example let us consider the case of $S_2 \times S_2$. We denote this subgroup of S_4 by H. It forms an invariant subgroup. The other elements can be obtained by multiplying the elements of H by the elements of the group S_4 which do not appear in it, until we exhaust the whole group:[10]

H:	1	P_{12}	P_{34}	$P_{12}P_{34}$
$P_{13}H$:	P_{13}	P_{123}	P_{134}	P_{1234}
$P_{23}H$:	P_{23}	P_{132}	P_{234}	P_{1342}
$P_{14}H$:	P_{14}	P_{124}	P_{143}	P_{1243}
$P_{24}H$:	P_{24}	P_{142}	P_{243}	P_{1432}
$P_{13}P_{24}H$:	$P_{13}P_{24}$	P_{1432}	P_{1324}	$P_{14}P_{23}$

Jahn uses the first column; we shall choose the permutations preserving the increasing order of enumeration of the particles within each shell:

Q	1	P_{123}	P_{23}	P_{1243}	P_{243}	$P_{13}P_{24}$
first shell	12	23	13	24	14	34
second shell	34	14	24	13	23	12

This choice of Q is made so that it is convenient for the later expansion of the wave function in terms of the fractional parentage coefficients, for which one has to split off the last particle from each of the shells.

For the case of k shells one can prove the following generalization of formula (20):

$$\Phi\left((l_1^{n_1}[\lambda_1]\,\alpha_1 L_1 \ldots l_k^{n_k}[\lambda_k]\,\alpha_k L_k)^B b_\lambda [\lambda]\,(r)^A b_L LM\right)$$
$$= c \sum_{r_1 \ldots r_k} \sum_{Q^B} \langle [\lambda]\,(r)^A \,|\, Q^B \,|\, [\lambda]\,(r_1 \ldots r_k)^B \rangle$$
$$\times\, Q^B \varphi\,(l_1^{n_1}[\lambda_1]\,(r_1) \ldots l_k^{n_k}[\lambda_k]\,(r_k)$$
$$\times\, (\alpha_1 L_1 \ldots \alpha_k L_k)^B b_L LM),$$
$$c = \left\{\frac{f_\lambda}{f_{\lambda_1} \cdots f_{\lambda_k}} \frac{n_1! \ldots n_k!}{n!}\right\}^{1/2}. \qquad (21)$$

Here A is the type of reduction of the representation $[\lambda]$ into subgroups, B is the method of coupling the $[\lambda_i]$ to form $[\lambda]$ and L_i to form L, which characterizes the structure of the function Φ; b_λ and b_L are sets of intermediate symmetry patterns and intermediate angular momenta necessary for complete characterization of a state, Q^B is the set of permutations which interchange the coordinates of particles between the shells and is determined by the method of coupling, B, of the shells. Thus, for successive symmetrization of the shells

$$Q^B = Q_{12\ldots k-1,\,k} Q_{12\ldots k-2,\,k-1} \ldots Q_{12},$$

where $Q_{12\ldots m-1,m}$ are the permutations of exchange between sets of particles of the first $m-1$ shells and the m-th shell.

APPENDIX

THE LITTLEWOOD THEOREM FOR THE PERMUTATION GROUP

To find all the possible $[\lambda]$ for the transition from the irreducible representation $[\lambda_1] \times [\lambda_2]$ of the subgroup $S_{n_1} \times S_{n_2}$ to the total group S_n, one can use Littlewood's theorem.[13] This theorem was proven by Littlewood for the group of linear transformations, and gives the expansion of the direct product of two irreducible representations of the linear group:

$$[\lambda_1] \times [\lambda_2] = \sum_\lambda c\,(\lambda_1 \lambda_2 \lambda)\,[\lambda]. \qquad (22)$$

Weyl showed that the bases of all irreducible representations of the linear group can be obtained by symmetrization of an arbitrary tensor of rank n according to the Young patterns with n boxes.[14] However, the n-th rank tensor symmetrized according to some Young pattern can simultaneously also serve as the basis for an irreducible representation of the group of permutations of n symbols, if we fix the components of the tensor and carry out the symmetrization over all Young tableaux. The fact that the expansion of the direct product of representations of the linear group contains the representation symmetrized according to some pattern $[\lambda]$ shows that for the permutation group also the representation $[\lambda]$ will appear in the symmetrization of the product $[\lambda_1] \times [\lambda_2]$. It can be shown that $c\,(\lambda\lambda_1\lambda_2)$ from Eq. (6) is equal to $c\,(\lambda_1\lambda_2\lambda)$ from (22), and therefore, to obtain the expansion (6), one can also use Littlewood's theorem, which is formulated as follows: to find the irreducible representations contained in the expansion of the direct product of the representations $[\lambda_1] \equiv [\lambda_1^{(1)}\lambda_1^{(2)} \ldots]$ and $[\lambda_2] \equiv [\lambda_2^{(1)}\lambda_2^{(2)} \ldots]$, we must successively add to the pattern $[\lambda_1]$, in all possible ways, $\lambda_2^{(1)}$ boxes with indices α, $\lambda_2^{(2)}$ boxes with indices β, etc., in such order that in the standard Young patterns which are formed the added indices satisfy the following two conditions: 1) there shall be no two identical indices in one column; 2) if we enumerate all the added indices from right to left successively through the rows, we obtain a lattice permutation of the expression $\alpha^{\lambda_2^{(1)}} \beta^{\lambda_2^{(2)}} \ldots$, i.e., among any m first terms the number of times we encounter α

is no less than the number of times that we encounter β, etc. As an example: $[21] \times [21]$:

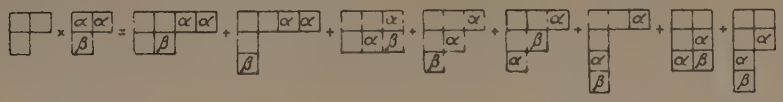

Collecting like terms, we finally get

$$[21] \times [21] = [42] + [411] + [33] + 2[321] + [3111] + [222] + [2211]. \quad (23)$$

In conclusion, I thank I. B. Levinson for useful advice and discussion and V. G. Neudachin for interest in the work and discussion of the results.

[1] B. L. Van Der Waerden, Die Gruppentheoretische Methode in der Quantenmechanik, Berlin, Springer, 1932.

[2] L. D. Landau and E. M. Lifshitz, Quantum Mechanics, Non-relativsitic Theory, Pergamon Press, 1958.

[3] H. A. Jahn, Proc. Roy. Soc. (London) **A205**, 192 (1951).

[4] H. A. Jahn and H. van Wieringen, Proc. Roy. Soc. (London) **A209**, 502 (1951).

[5] H. A. Jahn, Phys. Rev. **96**, 989 (1954).

[6] Elliott, Hope, and Jahn, Phil. Trans. Roy. Soc. **A246**, 241 (1953).

[7] Yutsis, Levinson, and Vanagas, Matematicheskii Apparat Teorii Momenta Kolichestva Dvizheniya (Mathematical Apparatus of the Theory of Angular Momentum), Press of the Academy of Sciences, Lithuanian S.S.R., (1960).

[8] D. E. Rutherford, Substitutional Analysis, Edinburgh, 1948.

[9] T. Yamanouchi, Proc. Phys.-Math. Soc. Japan **19**, 436 (1937).

[10] V. I. Smirnov, Kurs Vysshei Matematiki, (Course of Higher Mathematics), vol. 3, Chapter 1, Gostekhizdat, 1957.

[11] I. B. Levinson and V. V. Vanagas, Optika i Spektroskopiya (Optics and Spectroscopy) **2**, 10 (1957).

[12] G. F. Koster, Phys. Rev. **109**, 227 (1958).

[13] D. E. Littlewood, The Theory of Group Characters, Oxford, 1940, Chapter VI, page 94.

[14] H. Weyl, The Classical Groups, Princeton University Press, 1946.

Translated by M. Hamermesh
101

CONTRIBUTION TO THE THEORY OF HIGHLY COMPRESSED MATTER. II

A. A. ABRIKOSOV

Institute for Physics Problems, Academy of Sciences, U.S.S.R.

Submitted to JETP editor March 13, 1961

J. Exptl. Theoret. Phys. (U.S.S.R.) 41, 569-582 (August, 1961)

We investigate the interaction between electrons and ions in highly compressed matter. The possibility of superconductivity is discussed. We find the spectrum and the damping of the electron excitations of highly compressed hydrogen.

WE have studied earlier[1] a number of properties of highly compressed matter. In particular, we showed that the nuclei form a crystalline lattice at high density; we found the long-wavelength lattice vibrations spectrum. The present paper is mainly devoted to a study of the spectrum of electron excitations in highly compressed matter.

1. ELECTRON GREEN'S FUNCTION IN A CRYSTAL. ROLE OF THE STATIC LATTICE FIELD

It is well known (see [2]) that it is necessary to find the poles of the Fourier transform of the appropriate Green's function

$$G_{\alpha\beta}(\mathbf{x}-\mathbf{x}';\ t-t') = -i\langle T(\tilde{\psi}_\alpha(\mathbf{x},\ t)\,\tilde{\psi}^+_\beta(\mathbf{x}',\ t'))\rangle, \quad (1.1)$$

to obtain the excitation spectrum in an isotropic system; in (1.1) $\tilde{\psi}_\alpha$ is the Heisenberg operator and $\langle \ldots \rangle$ indicates averaging over the ground state. In the case under consideration the system is not isotropic, but possesses translational symmetry. Because of this we derive anew Lehmann's formula[3] applicable to such a system. We assume that the number of electrons is given, but at the same time we shall use a Hamiltonian $\hat{H}-\mu\hat{N}$ where μ is the value of the energy on the Fermi surface. The electron energy is then calculated from the level μ.

Introducing as usual[3,2] summation over intermediate states we find for $t > t'$*

$$G(\mathbf{x}, \mathbf{x}';\ t-t') = -i\sum_m \langle\Phi_0^*\tilde{\psi}(\mathbf{x},\ t)\,\Phi_m\rangle\langle\Phi_m^*\tilde{\psi}^+(\mathbf{x}',\ t')\,\Phi_0\rangle$$

$$= -i\sum_m \langle\Phi_0^*\psi(\mathbf{x})\,\Phi_m\rangle\langle\Phi_m^*\psi^+(\mathbf{x})\,\Phi_0\rangle$$

$$\times \exp\{-i(E_m-E_0)(t-t')\} \quad (1.2a)$$

and for $t < t'$

$$G(\mathbf{x}, \mathbf{x}';\ t-t') = i\sum_m \langle\Phi_0^*\psi^+(\mathbf{x}')\,\Phi_m\rangle\langle\Phi_m^*\psi(\mathbf{x})\,\Phi_0\rangle$$

$$\times \exp\{i(E_m-E_0)(t-t')\}, \quad (1.2b)$$

where the summation is over all possible states of the system, $E_m - E_0$ are the corresponding excitation energies (for a Hamiltonian $\hat{H}-\mu\hat{N}$), and $\psi(\mathbf{x})$ are the Schrödinger operators.

Because of the translational symmetry, the matrix elements of the kind $\langle\Phi_0^*\psi(\mathbf{x})\,\Phi_m\rangle$ must possess the properties of the Bloch wave functions of an electron in a periodic field, i.e., it must be possible to write them in the form

$$\langle\Phi_0^*\psi(\mathbf{x})\,\Phi_m\rangle = V^{-1/2}e^{i\mathbf{k}\mathbf{x}}u_{n\mathbf{k}}(\mathbf{x}),$$

$$\langle\Phi_0^*\psi^+(x)\,\Phi_m\rangle = V^{-1/2}e^{i\mathbf{k}\mathbf{x}}v_{n\mathbf{k}}(\mathbf{x}), \quad (1.3)$$

where $\mathbf{k}$ is the quasi-momentum and $u_{n\mathbf{k}}$ and $v_{n\mathbf{k}}$ are periodic functions of the coordinates. The index m, enumerating the excited states, corresponds to the collection of the numbers n and $\mathbf{k}$.

From (1.2) and (1.3) we get for the Fourier component of G with respect to $t-t'$

$$G(\varepsilon;\ \mathbf{x},\ \mathbf{x}') = \frac{1}{V}\sum_{\mathbf{k},\ n} e^{i\mathbf{k}(\mathbf{x}-\mathbf{x}')}\left\{\frac{u_{n\mathbf{k}}(\mathbf{x})\,u^*_{n\mathbf{k}}(\mathbf{x}')}{\varepsilon-\xi_n(\mathbf{k})+i\delta} + \frac{v_{n\mathbf{k}}(\mathbf{x})\,v^*_{n\mathbf{k}}(\mathbf{x}')}{\varepsilon+\xi_n(\mathbf{k})-i\delta}\right\}, \quad (1.4)$$

where $\xi_n(\mathbf{k}) = E_{n\mathbf{k}} - E_0$. The values of $\mathbf{k}$ in this sum are restricted to the basis cell in the reciprocal lattice. If we recollect the well-known commutation properties of the Schrödinger operators, we see easily that the functions $u_{n\mathbf{k}}$ and $v_{n\mathbf{k}}$ satisfy the following conditions

$$\frac{1}{V}\sum_{n,\ \mathbf{k}} e^{i\mathbf{k}(\mathbf{x}-\mathbf{x}')}\{u_{n\mathbf{k}}(\mathbf{x})\,u^*_{n\mathbf{k}}(\mathbf{x}') + v_{n\mathbf{k}}(\mathbf{x})\,v^*_{n\mathbf{k}}(\mathbf{x}')\} = \delta(\mathbf{x}-\mathbf{x}'),$$

$$\frac{1}{V}\sum_{n,\ \mathbf{k}} e^{-i\mathbf{k}(\mathbf{x}+\mathbf{x}')}\{v_{n\mathbf{k}}(\mathbf{x}')u^*_{n\mathbf{k}}(\mathbf{x}) + v_{n\mathbf{k}}(\mathbf{x})\,u^*_{n\mathbf{k}}(\mathbf{x}')\} = 0. \quad (1.5)$$

*We use units in which $\hbar = 1$. We have omitted for the sake of simplicity the spin indices.

We can expand the functions $u_{nk}(\mathbf{x})$ and $v_{nk}(\mathbf{x})$, which are periodic functions of the coordinates, in Fourier series

$$u_{nk}(\mathbf{x}) = \sum_{\mathbf{K}} u_{nk}(\mathbf{K})\, e^{i\mathbf{K}\mathbf{x}}, \quad v_{nk}(\mathbf{x}) = \sum_{\mathbf{K}} v_{nk}(\mathbf{K})\, e^{i\mathbf{K}\mathbf{x}}, \quad (1.6)$$

where the summation over $\mathbf{K}$ is over all periods of the reciprocal lattice. Substituting (1.6) into (1.4) and performing the Fourier transformation with respect to $\mathbf{x}$ and $\mathbf{x}'$ we get

$$G(\varepsilon; \mathbf{k}+\mathbf{K}, \mathbf{k}'+\mathbf{K}') = G(\varepsilon; \mathbf{K}, \mathbf{K}'; \mathbf{k})(2\pi)^3 \delta(\mathbf{k}-\mathbf{k}'),$$
$$G(\varepsilon; \mathbf{K}, \mathbf{K}'; \mathbf{k}) = \sum_n \left\{ \frac{u_{nk}(\mathbf{K})\, u^*_{nk}(\mathbf{K}')}{\varepsilon - \xi_n(\mathbf{k}) + i\delta} + \frac{v_{nk}(\mathbf{K})\, v^*_{nk}(\mathbf{K}')}{\varepsilon + \xi_n(\mathbf{k}) - i\delta} \right\}. \quad (1.7)$$

The spectrum of the electron excitation is according to (1.7), as also in the case of an isotropic Fermi system, determined by the poles of the Green's function, and these poles are independent of $\mathbf{K}$ and $\mathbf{K}'$. It will therefore be convenient for us to consider henceforth the diagonal element, i.e., $G(\epsilon; \mathbf{K}, \mathbf{K}; \mathbf{k})$ and introduce instead of the quasi-momentum $\mathbf{k}$ the momentum $\mathbf{p}: \mathbf{p} = \mathbf{k} + \mathbf{K}$. Such a function corresponds completely to the usual Green's function in an isotropic medium $G(\epsilon, \mathbf{p})$.

The function $G(\epsilon, \mathbf{p})$ has in the first approximation the form [2]

$$G^{(0)}(\varepsilon, \mathbf{p}) = \frac{1}{\varepsilon - \xi(\mathbf{p}) + i\delta\, \mathrm{sign}\, \xi(\mathbf{p})}, \quad (1.8)$$

where $\xi(\mathbf{p}) = \mathbf{p}^2/2m - p_0^2/2m$, $\delta \to +0$ (for p near to p_0 the function $\xi \approx u(p - p_0)$ where $u = p_0/m$). In the following we consider the change in this function under the influence of the interaction of the electrons with one another and with the ions in the lattice. We shall as usual write G in the form $(\epsilon - \xi + \Delta\mu - \Sigma)^{-1}$ and study the irreducible diagrams which give a contribution to the "self-energy part" Σ.

Before doing this, we consider the interaction of the electrons with the static lattice field. The diagrams for the G-function depicted in Fig. 1 are responsible for this interaction. We denote by a cross the vertex

$$Q(\varepsilon, \mathbf{p}; \varepsilon, \mathbf{p}+\mathbf{K}) = -4\pi Z e^2 (N/V)\, \mathbf{K}^{-2}, \quad (1.9)$$

where $\mathbf{K}$ is a reciprocal lattice vector. We first get rid of the vertices with $\mathbf{K} = 0$. We replace the Coulomb interaction law by $e^{-\alpha r}/r$. The contribution to $G(\epsilon, \mathbf{p})$ which is introduced by the lattice vertices with $\mathbf{K} = 0$ can be expressed by means of the self-energy part $\Sigma_{(1)} = -4\pi Z e^2 N/\alpha^2 V$. One sees easily that this part is exactly compensated by the diagram of Fig. 2, which arises from

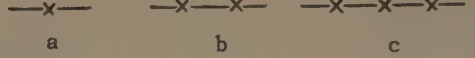

a b c

FIG. 1.

FIG. 2

the electron-electron interaction (the wavy line corresponds here to a Coulomb vertex $4\pi e^2/k^2$, where $\mathbf{k}$ is the momentum transfer). Indeed, the latter gives the self-energy part

$$\Sigma_{(2)} = -\frac{4\pi e^2}{\alpha^2} i \int G(\varepsilon, \mathbf{p})\, e^{i\varepsilon\tau} \frac{d^3p\, d\varepsilon}{(2\pi)^4} = \frac{4\pi e^2}{\alpha^2} \frac{N_e}{V} = \frac{4\pi e^2}{\alpha^2} Z \frac{N}{V}.$$

Both these and other diagrams can thus be dropped.

At first sight it seems that as soon as we get rid of the vertices with $\mathbf{K} = 0$, the corrections to $G(\mathbf{p}, \epsilon)$ from the interaction with the static lattice field will be at least of second order. However, in actual fact this is not always correct. We consider the simplest diagram of Fig. 1b assuming that the changes in momentum at the vertices compensate one another. We then get the following additional term in Σ

$$\Sigma = \left(4\pi Z e^2 \frac{N}{V}\right)^2 \sum_{0<|\mathbf{K}|} \frac{1}{\mathbf{K}^4} \frac{1}{\varepsilon - \xi(\mathbf{p}-\mathbf{K}) + i\delta\, \mathrm{sign}\, \xi(\mathbf{p}-\mathbf{K})}. \quad (1.10)$$

We are interested in the vicinity of the pole of G, in other words, in the point $\epsilon = \xi(\mathbf{p})$, and the region near the Fermi surface, i.e., $|\xi| \ll p_0^2/2m$, where p_0 is the limiting Fermi momentum, will be the most important one. One sees easily that for several values of the momentum $\mathbf{p}$ one (or several) of the differences $\xi(\mathbf{p}) - \xi(\mathbf{p}-\mathbf{K})$ becomes very small and the corresponding term in Σ very large.*

The equations $\xi(\mathbf{p}) = \xi(\mathbf{p}-\mathbf{K})$ determine surfaces in momentum space (the boundaries of the Brillouin zones). It is clear that near such boundaries Eq. (1.10) is no longer suitable. It is well known that intersections of the Fermi surface and the Brillouin zone boundaries make this surface more complicated, and in particular lead to the formation of open surfaces. If we assume that highly compressed matter has a body centered lattice (see [1]), the smallest distance to the boundary is equal to $\sqrt{2}\pi/a$, where a is the cube edge, or $\sqrt{2}\pi(2V/N)^{-1/3} = 3.52(N/V)^{1/3}$. If we

*This fact is well known from the theory of an electron in a weak periodic field (see [4]).

compare this with the Fermi momentum $p_0 = (3\pi^2 ZN/V)^{1/3} = 3.09\,(ZN/V)^{1/3}$, it is clear that for hydrogen the whole of the Fermi surface can be contained within the basis cell of the reciprocal lattice. The position is, however, already different for helium ($p_0 = 3.89\,(N/V)^{1/3}$). This conclusion remains valid also in the case where highly compressed matter has a face-centered cubic lattice.

One can show that in the case where the intersection takes place, in the regions near the intersections [at distances on the order of p_0e^2/u (where $u = p_0/m$)] the radius vector of the Fermi surface changes by an amount of the same order, and the velocity on the Fermi surface changes even by an amount of the order of p_0/m.

In the following we shall restrict ourselves for the sake of simplicity to a study of the electron spectrum of compressed hydrogen. Since there are no dangerous intersections the correction to Σ from the static lattice field will be a quantity of second order. We shall neglect such quantities in the following.

2. INTERACTION BETWEEN THE ELECTRONS

For what follows it is necessary to study the interaction between the electrons. The main characteristic of this interaction is the so-called vertex part Γ, in which all Feynman diagrams with four electron ends occur. Apart from the free Green's functions (1.8), the elements of such diagrams are the elementary vertices, due both to direct interaction of the electrons with one another and to their interaction with phonons.

The vertex corresponding to the electron Coulomb interaction is equal to $\Gamma_{01} = 4\pi e^2/\mathbf{k}^2$ and will be depicted by a wavy line in the diagrams (Fig. 3a).

FIG. 3

The electron-phonon vertex depends on the choice of the phonon field operators. If we take as the phonon operators $(NM/V)^{1/2}\mathbf{u}(\mathbf{x}, t)$, where $\mathbf{u}$ is the ion displacement and M the ion mass, we can easily obtain an expression for the elementary electron-phonon vertex by expanding the electron-ion interaction operator; it turns out to be equal to

$$\gamma_\alpha(\varepsilon, \mathbf{p}; \varepsilon+\omega, \mathbf{p}+\mathbf{k}+\mathbf{K}; \omega, \mathbf{k}) = 4\pi e^2 i\sqrt{N/VM}\,(\mathbf{k}+\mathbf{K})_\alpha/(\mathbf{k}+\mathbf{K})^2, \qquad (2.1)$$

where $\mathbf{k}$ lies within the confines of the basis cell of the reciprocal lattice.* In this expression the fact is manifest that the electrons possess not momentum, but quasi-momentum, which is conserved only accurate to an arbitrary reciprocal lattice period $\mathbf{K}$.

The simplest diagram for Γ due to the electron-phonon interaction is illustrated in Fig. 3b and is equal to

$$\Gamma_{02}(\varepsilon_p, \mathbf{p}; \varepsilon_q+\omega, \mathbf{q}+\mathbf{k}+\mathbf{K}; \varepsilon_p+\omega, \mathbf{p}+\mathbf{k}+\mathbf{K}'; \varepsilon_q, \mathbf{q}) = 4\pi e^2\omega_0^2 D_{\alpha\beta}(\omega, \mathbf{k})(\mathbf{k}+\mathbf{K})_\alpha(\mathbf{k}+\mathbf{K}')_\beta/(\mathbf{k}+\mathbf{K})^2(\mathbf{k}+\mathbf{K}')^2, \qquad (2.2)$$

where $\omega_0 = \sqrt{4\pi e^2 N/MV}$ and $D_{\alpha\beta}(\omega, \mathbf{k})$ is the Fourier component of the phonon Green's function (it corresponds to the dotted line) given by the equation

$$D_{\alpha\beta}(\mathbf{R}_l - \mathbf{R}_k, t-t') = -i\,(NM/V)\,\langle T\,(u_\alpha(\mathbf{R}_l, t)\,u_\beta(\mathbf{R}_k, t'))\rangle = \frac{1}{V}\sum_{\mathbf{k}}\int_{-\infty}^{\infty}\frac{d\omega}{2\pi}D_{\alpha\beta}(\mathbf{k}, \omega)\exp\{i\,[\mathbf{k}(\mathbf{R}_l - \mathbf{R}_k) - \omega(t-t')]\}. \qquad (2.3)$$

Here $\langle \ldots \rangle$ indicates an average over the ground state; $\mathbf{R}_i$ are the ion coordinates; the summation over $\mathbf{k}$ in the last formula is confined to the basis cell of the reciprocal lattice.

From the definition of the D-function we can easily obtain the relation

$$D_{\alpha\beta}(\mathbf{k}, \omega) = \sum_s \frac{v_\alpha(\mathbf{k}, s)\,v_\beta^*(\mathbf{k}, s)}{\omega^2 - \omega^2(\mathbf{k}, s) + i\delta}, \qquad (2.4)$$

where $\omega(\mathbf{k}, s)$ and $\mathbf{v}(\mathbf{k}, s)$ are the natural frequency and polarization vector of the s-th branch of the phonon spectrum, while

$$\sum_\alpha v_\alpha(\mathbf{k}, s)\,v_\alpha^*(\mathbf{k}, s) = 1.$$

In the case when the momentum transferred is not very small, we can restrict ourselves in first approximation to the simplest diagrams of Fig. 3a and b:

$$\Gamma_0(\varepsilon_p, \mathbf{p}; \varepsilon_q+\omega, \mathbf{q}+\mathbf{k}+\mathbf{K}; \varepsilon_p+\omega, \mathbf{p}+\mathbf{k}+\mathbf{K}'; \varepsilon_q, \mathbf{q}) = (4\pi e^2/(\mathbf{k}+\mathbf{K})^2)\,[\delta_{\mathbf{K}\mathbf{K}'} + \omega_0^2 D_{\alpha\beta}(\mathbf{k}) \times (\mathbf{K}+\mathbf{k})_\alpha(\mathbf{K}'+\mathbf{k})_\beta/(\mathbf{k}+\mathbf{K}')^2]. \qquad (2.5)$$

However, since the Coulomb forces have a long range, such a vertex part has a singularity for small momentum transfers. This singularity occurs according to Eq. (2.5) only in those Γ for which at least one of the $\mathbf{K}$ vanishes. The most

*We recall that the whole of this consideration is only applicable to hydrogen, so that we assume everywhere that $Z = 1$.

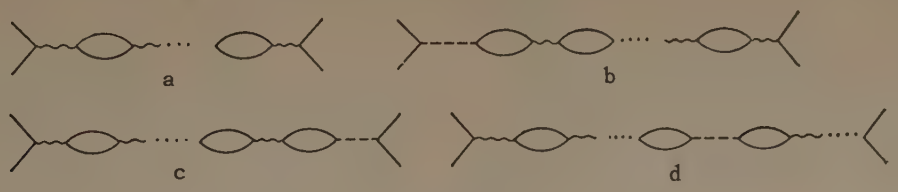

FIG. 4

important case is the one when $\mathbf{K} = \mathbf{K}' = 0$ for when $\mathbf{K} \neq 0$ and $\mathbf{K}' = 0$ the vertex is smaller by at least a factor $k/K_{min} \sim k/p_0$. We consider therefore only the case $\mathbf{K} = \mathbf{K}' = 0$, $k \ll p_0$. To describe this vertex correctly we must take terms of higher order into account.

One sees easily that the main role will be played by the corrections to Γ_0 corresponding to the diagrams of Fig. 4. In each such diagram the increase in the power of e^2 is compensated by a corresponding power of the large quantity $1/k^2$. The basic element of such diagrams is the loop formed by electron lines. Such a loop corresponds to the expression*

$$\Pi(\omega, \mathbf{k}) = 2i\int \frac{d\varepsilon}{2\pi}\frac{d^3\mathbf{p}}{(2\pi)^3} G_0(\mathbf{p}, \varepsilon)\, G_0(\mathbf{p}+\mathbf{k}, \varepsilon+\omega)$$
$$= \frac{p_0 m}{\pi^2}\left[1 - \frac{\omega}{2uk}\ln\left(\frac{\omega+uk+i\delta\,\mathrm{sign}\,\omega}{\omega-uk+i\delta\,\mathrm{sign}\,\omega}\right)\right], \qquad (2.6)$$

where $\delta \to +0$.

Summing all diagrams which do not contain phonon lines (Fig. 4a) we get

$$4\pi e^2/(k^2 + 4\pi e^2\Pi). \qquad (2.7)$$

In the case $\omega \ll uk$ this formula gives $4\pi e^2/(k^2+\kappa^2)$, where κ is the reciprocal of the Debye radius and is equal to

$$\varkappa = \sqrt{4p_0 m e^2/\pi}. \qquad (2.8)$$

The summation of the loops is simply equivalent to taking the Debye screening into account.

We now turn to the diagrams containing a phonon line. It was shown in [1] that the lattice vibration spectrum in the region of the small momenta consists of three acoustical branches, one of which corresponds to longitudinal vibrations while the other two correspond to the transverse vibrations (apart from small terms of the order of e^2/u). Since the electrons interact only with the longitudinal phonons [one sees this easily from Eqs. (2.2) and (2.4); see also the last footnote] the expression $k_\alpha k_\beta k^{-2} D_{\alpha\beta}(\omega, \mathbf{k})$ will in the case $\omega \ll uk$ simply correspond to

$$1/(\omega^2 - \omega_l^2(k) + i\delta), \qquad (2.9)$$

where ω_l is the frequency of the longitudinal phonons, which was found in [1]

$$\omega_l = \omega_0 [k^2/(k^2+\varkappa^2)]^{1/2}. \qquad (2.10)$$

We obtained Eq. (2.10) with account of the Debye screening. All electron loops strung along the D-line are thus already taken into account in Eqs. (2.9) and (2.10) when $\omega \ll uk$. If $\omega \gtrsim uk$, Eq. (2.9) is no longer valid. However, as in (2.7), the whole of the difference consists in that one must substitute the more general expression $4\pi e^2\Pi$ for κ^2. If we perform this substitution formally in Eq. (2.10) for ω_l and substitute this into (2.9) we obtain the complete D-function also for the case $\omega \gtrsim uk$.

There remains now for us to sum all diagrams of Figs. 4b, c, d. One sees easily that these diagrams differ from the diagram of Fig. 3b by the replacement of both electron-phonon vertices by more general expressions which take screening into account. The summation of the necessary diagrams causes each electron-phonon vertex to be simply multiplied by $k^2/(k^2 + 4\pi e^2\Pi)$. The total expression for Γ has thus for small transfers $\mathbf{k}$ and ω the form

$$\Gamma(\mathbf{k}, \omega) = \frac{4\pi e^2}{k^2 + 4\pi e^2\Pi}\left[1 + \frac{\omega_l^2}{\omega^2 - \omega_l^2 + i\delta}\right].$$

Substituting Eq. (2.10) for ω_l and taking the substitution $\kappa^2 \to 4\pi e^2\Pi$ into account we find finally

$$\Gamma(\mathbf{k}, \omega) = \frac{4\pi e^2\omega^2}{(\omega^2 - \omega_0^2)k^2 + 4\pi e^2\Pi\omega^2 + i\delta}. \qquad (2.11)$$

Let us consider the limiting cases. When $\omega \ll uk$ this expression becomes

$$\Gamma(\omega \ll uk) = \frac{4\pi e^2\omega^2}{\omega^2(k^2+\varkappa^2) - \omega_0^2 k^2 + i\delta}. \qquad (2.12)$$

When $k \to 0$ (in the following $c_l = \omega_0/\kappa$)

$$\Gamma \to 4\pi e^2/\varkappa^2 \quad \text{when } uk \gg \omega \gg c_l k,$$
$$\Gamma \to 4\pi e^2\omega^2/\omega_0^2 k^2 \quad \text{when } \omega \ll c_l k. \qquad (2.13)$$

The last formula is not completely exact. If we take into account corrections from "transverse" terms in the D-function it is clear that it is valid only if $\omega \gg c_t k$ (c_t is the velocity of the trans-

*If the loop π arises after a phonon line, it may depend on $k + K$. However, in that case, according to Eq. (2.1), there occurs in the corresponding electron-phonon vertex a factor K_α/K^2 instead of k_α/k^2, and this leads to a decrease of the diagram by the factor $k/K \sim k/p_0$.

verse phonons which is of the order of $\sqrt{e^2/u}\,c_l$). When $\omega \ll c_t k$ we have $\Gamma \sim 4\pi e^2 \kappa^{-2} (c_t/c_l)^2$. Equation (2.12) at $\omega = \omega_l(k)$ has a pole corresponding to longitudinal phonons (in actual fact there are also poles from the transverse phonons, but they occur with small coefficients of the order of e^2/u).

When $\omega \gg uk$ we have $\Pi \to -Nk^2/Vm\omega^2$ and neglecting the term $\omega_0^2 k^2$ as compared to $4\pi e^2 \Pi \omega^2$ ($\sim \omega_0^2 k^2 M/m$) in the denominator of (2.11) we get

$$\Gamma_\omega \equiv \Gamma(\omega \gg uk) = \frac{4\pi e^2 \omega^2}{k^2(\omega^2 - 4\pi e^2 N/mV + i\delta)}. \qquad (2.14)$$

The pole in Γ_ω at $\omega_p = \sqrt{4\pi e^2 N/mV}$ corresponds to plasma oscillations. The dispersion of these oscillations arises from the next term in the expansion in Eq. (2.6)

$$\Pi \approx -Nk^2/Vm\omega^2 - p_0^5 k^4/5\pi^2 m^3 \omega^4.$$

Taking this last term into account we get for the pole

$$\omega_p^2 = \omega_p^2(0) + \tfrac{3}{5} u^2 k^2. \qquad (2.15)$$

From (2.14) we find the following limiting formula

$$\Gamma \to -mV\omega^2/Nk^2, \qquad \omega_p \gg \omega \gg uk. \qquad (2.16)$$

3. SUPERCONDUCTIVITY

We consider now whether superconductivity is possible in highly compressed matter. To solve this problem we apply the simple and clear method of Cooper,[5] by means of which the possibility of the formation of bound electron pairs was first demonstrated. According to Cooper the equation for the wave function of a bound electron pair can be written in the momentum representation in the form

$$(2\xi(\mathbf{p}) - E)\, a_{\mathbf{p}} + \frac{1}{V} \sum_{|\mathbf{p}'| > p_0} U_{\mathbf{p}\mathbf{p}'} a_{\mathbf{p}'} = 0. \qquad (3.1)$$

We substitute for the effective interaction $U_{\mathbf{p}\mathbf{p}'}$ the electron-electron vertex part $\Gamma(p_1 p_2; p_3 p_4)$ in which $\mathbf{p}_1 = -\mathbf{p}_2 = \mathbf{p}$, $\mathbf{p}_3 = -\mathbf{p}_4 = \mathbf{p}'$, $\epsilon_1 = \epsilon_2 = \xi(\mathbf{p})$, $\epsilon_3 = \epsilon_4 = \xi(\mathbf{p}')$, i.e., $\mathbf{k} = \mathbf{p} - \mathbf{p}'$, $\omega = \xi(\mathbf{p}) - \xi(\mathbf{p}')$.

In the integral term in Eq. (3.1) the domain of integration over $d^3\mathbf{p}$ is divided into two. In the first region $|\mathbf{p} - \mathbf{p}'| \ll p_0$ and in the second region $|\mathbf{p} - \mathbf{p}'| \sim p_0$. Since the region $|\mathbf{p} - \mathbf{p}'| \lesssim \kappa$ makes a relatively small contribution, we can assume in the first region that $|\mathbf{p} - \mathbf{p}'| \gg \kappa$ and use Eq. (2.5) with $\mathbf{K} = \mathbf{K}' = 0$, which in the present case gives

$$U_{\mathbf{p}\mathbf{p}'} = \frac{4\pi e^2}{(\mathbf{p} - \mathbf{p}')^2} \frac{[\xi(\mathbf{p}) - \xi(\mathbf{p}')]^2}{[\xi(\mathbf{p}) - \xi(\mathbf{p}')]^2 - \omega_0^2}, \qquad |\mathbf{p} - \mathbf{p}'| \ll p_0. \qquad (3.2)$$

This potential can approximately be written in the form ($\kappa \ll |\mathbf{p} - \mathbf{p}'| \ll p_0$)

$$U_{\mathbf{p}\mathbf{p}'} = \begin{cases} 4\pi e^2/(\mathbf{p} - \mathbf{p}')^2 & \text{for } |\xi(\mathbf{p}) - \xi(\mathbf{p}')| > \omega_0 \\ 0 & \text{for } |\xi(\mathbf{p}) - \xi(\mathbf{p}')| < \omega_0 \end{cases}. \qquad (3.3)$$

When we substitute this potential into the second term of Eq. (3.1) we must bear in mind that the coefficients $a_{\mathbf{p}'}$ need not depend on the direction of $\mathbf{p}'$. We can thus integrate over the angle between $\mathbf{p}$ and $\mathbf{p}'$. Taking it into account that we shall in the following be interested in the values $|\mathbf{p}| \approx |\mathbf{p}'| \approx p_0$ we obtain in that case

$$\frac{4\pi e^2}{p_0^2}\left(\ln\frac{p_0}{\varkappa} + c_1\right)\frac{1}{V}\sum_{p'} a_{\mathbf{p}'},$$
$$|\xi(\mathbf{p}) - \xi(\mathbf{p}')| > \omega_0, \quad \xi(\mathbf{p}) > 0, \qquad (3.4)$$

where c_1 is a constant of the order of unity.

We now consider the integral over the second region $|\mathbf{p} - \mathbf{p}'| \sim p_0$.

It is now necessary to take into account the contribution of all phonon branches to the D-function (and also the vertices with $\mathbf{K}, \mathbf{K}' \neq 0$). According to Eqs. (2.5), the phonon term in Γ has then in the region $|\xi(\mathbf{p}) - \xi(\mathbf{p}')| \lesssim \omega_0$ the same order of magnitude as the electron term, while in the region $|\xi(\mathbf{p}) - \xi(\mathbf{p}')| \gg \omega_0$ it is appreciably less than the electron term (see [1]). Bearing in mind that the interaction potential depends in the region $|\mathbf{p} - \mathbf{p}'| \sim p_0$ weakly on the angle between $\mathbf{p}$ and $\mathbf{p}'$ we can approximately write it in the form

$$U_{\mathbf{p}\mathbf{p}'} = \begin{cases} 4\pi e^2 c_2/p_0^2, & |\xi(\mathbf{p}) - \xi(\mathbf{p}')| \lesssim \omega_0 \\ 4\pi e^2 c_3/p_0^2, & |\xi(\mathbf{p}) - \xi(\mathbf{p}')| \gg \omega_0 \end{cases}. \qquad (3.5)$$

Here, c_2 and c_3 are constants of the order of unity, and $c_3 > 0$. As to the constant c_2, its sign depends on the relation between the two terms in (2.5) in the region $k \sim p_0$, which can be found only by evaluating the phonon spectrum in the short-wavelength region.

When we substitute the potential (3.5) into the integral term of Eq. (3.1) we get two terms. The term which contains a summation over the region $|\xi(\mathbf{p}) - \xi(\mathbf{p}')| > \omega_0$ is similar to expression (3.4) and contributes to the constant c_1 which combines with $\ln(p_0/\kappa)$.

After all transformations Eq. (3.1) becomes of the form

$$(2\xi(\mathbf{p}) - E)\, a_{\mathbf{p}} + A\frac{1}{V} \sum_{\substack{|\xi(\mathbf{p}) - \xi(\mathbf{p}')| < \omega_0 \\ \xi(\mathbf{p}') > 0}} \times a_{\mathbf{p}'} + B\frac{1}{V} \sum_{\substack{|\xi(\mathbf{p}) - \xi(\mathbf{p}')| > \omega_0 \\ \xi(\mathbf{p}') > 0}} a_{\mathbf{p}'} = 0, \qquad (3.6)$$

where

$$A = 4\pi e^2 c_2/p_0^2, \qquad B = (4\pi e^2/p_0^2)(\ln(p_0/\varkappa) + c_1).$$

In the various regions of $\xi(\mathbf{p})$ we have

$$(2\xi(\mathbf{p}) - E)\, a_p = -A\alpha - B\beta, \quad \xi(\mathbf{p}) < \omega_0,$$
$$(2\xi(\mathbf{p}) - E)\, a_p = -B(\alpha + \beta), \quad \xi(\mathbf{p}) > \omega_0, \qquad (3.7)$$

where

$$\alpha = \frac{1}{V} \sum_{0<\xi(\mathbf{p}')<\omega_0} a_{p'}, \qquad \beta = \frac{1}{V} \sum_{\xi(\mathbf{p}')>\omega_0} a_{p'}.$$

We find from these equations a_p and after that α and β. As a result we get the following equations for α and β

$$\alpha\left(1 + \frac{1}{2}\frac{p_0^2}{\pi^2 u} A \ln\frac{\omega_0}{\Delta}\right) + \beta \cdot \frac{1}{2}\frac{p_0^2}{\pi^2 u} B \ln\frac{\omega_0}{\Delta} = 0,$$
$$\alpha \cdot \frac{1}{2}\frac{p_0^2}{\pi^2 u} B \ln\frac{p_0 u}{\omega_0} + \beta\left[1 + \frac{1}{2}\frac{p_0^2}{\pi^2 u} B \ln\frac{p_0 u}{\omega_0}\right] = 0,$$

where $2\Delta = -E$ is the pair binding energy.

Assuming that $(p_0^2/\pi^2 u)\, B \ln(p_0 u/\omega_0) \ll 1$ we find the following equation to determine Δ

$$1 + \frac{1}{2}\frac{p_0^2}{\pi^2 u} A \ln\frac{\omega_0}{\Delta} = 0. \qquad (3.8)$$

As we have already noted earlier the sign of the constant A can be either positive or negative. The question, whether or not this equation has a solution, i.e., whether or not there are bound pairs, thus remains an open one. We are thus led to the conclusion that the possibility of the appearance of superconductivity is determined by the properties of the short-wavelength phonons, and the problem posed here can therefore not be solved without completely determining the phonon spectrum. We can only state on the basis of Eq. (3.8) that if superconductivity occurs the order of magnitude of the quantity Δ is given by the relation

$$\Delta \sim \omega_0 \exp(-\pi u / e^2).$$

This means that superconductivity is an exponentially small effect and that the magnitude of the gap decreases under compression ($u = p_0/m = m^{-1}(3\pi^2 N/V)^{1/3}$).

4. ELECTRON SPECTRUM

We now consider how the interaction of the electrons with one another and with the phonons influences the electron excitation spectrum. We shall evaluate all quantities in the first non-vanishing order in e^2. We shall then neglect superconducting effects, i.e., we shall assume the distance from the Fermi boundary to be large compared to Δ. We have illustrated in Fig. 5 the first-order diagrams for the self-energy part, where the electron line corresponds to the complete G-function (it was shown in Sec. 1 that one need not take into account the diagram of Fig. 2).

FIG. 5

The expression for Σ can thus be written in the form*

$$\Sigma(\mathbf{p}, \varepsilon) = i\int \frac{d^3\mathbf{p}_1}{(2\pi)^3}\frac{d\varepsilon_1}{2\pi} \times \Gamma(\mathbf{p}_1 - \mathbf{p}, \varepsilon_1 - \varepsilon)\frac{1}{\varepsilon_1 - \xi(\mathbf{p}_1) + \Delta\mu - \Sigma(\mathbf{p}_1, \varepsilon_1)}, \qquad (4.1)$$

where Γ corresponds to expression (2.5). When small values of the momentum $\mathbf{p}_1 - \mathbf{p}$ are important in the integral one must take into account diagrams of the next order. One sees easily that it is sufficient in that case to take into account the diagrams of Fig. 6, i.e., take for Γ in Eq. (4.1) expression (1.9). Since we are interested in the excitation spectrum we shall in the following only be interested in the vicinity of the pole of G, i.e., we shall put $\epsilon \approx \xi(\mathbf{p})$.

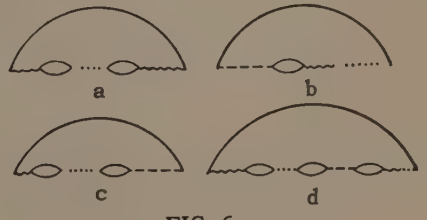

FIG. 6

We first split off from Γ the simple Coulomb term $\Gamma_1 = 4\pi e^2/(\mathbf{p}_1 - \mathbf{p})^2$. We denote the corresponding part of Σ by Σ_1. One sees easily that the values $\epsilon_1 = \xi(\mathbf{p}_1) \sim p_0 u$ are important in the integral in (4.1). We can thus neglect the term $\Sigma(\mathbf{p}_1, \epsilon_1)$ in the denominator of the integrand. Integrating,† we get

$$\Sigma_1(\mathbf{p}, \varepsilon) = -\int_{|\mathbf{p}_1|<p_0} \frac{d^3\mathbf{p}_1}{(2\pi)^3}\frac{4\pi e^2}{(\mathbf{p} - \mathbf{p}_1)^2}$$
$$= \frac{e^2}{\pi}\left(-p_0 + \frac{p^2 - p_0^2}{2p}\ln\frac{p + p_0}{|p - p_0|}\right). \qquad (4.2)$$

The first term within the bracket corresponds to the value Σ_1 at $p = p_0$ and must be included in μ. The second term in (4.2) has for $|p - p_0| \ll p_0$ the form

*Non-diagonal components $G(\varepsilon; \mathbf{k}; K, K')$ may occur under the integral sign in (4.1) together with the corresponding term in Γ, but we can neglect them since these components themselves are at least of first order in e^2/u.

†The first-order diagram given in Fig. 5a with $G = G^0$ is important here. The integral (4.1) contains for such a diagram a factor $e^{i\epsilon_1\tau}$ where $\tau \to +0$. Thanks to this, the contour of the integral over ε_1 is closed in the upper half-plane.

$$\Sigma_1' = (e^2\xi/\pi u)\ \ln\left(2p_0 u/\xi\right). \tag{4.3}$$

We shall see below that $\Sigma(\mathbf{p}, \epsilon) - \Delta\mu \ll \xi$. We can therefore in the integrand in (4.1) replace the Green's function by the free one. We get thus

$$\Sigma(\mathbf{p}, \varepsilon) - \Sigma_1(\mathbf{p}, \varepsilon) = i\int \frac{d^3p_1}{(2\pi)^3}\frac{d\varepsilon_1}{2\pi}\left[\Gamma(\mathbf{p}_1 - \mathbf{p}, \varepsilon_1 - \varepsilon) - \Gamma_1(\mathbf{p}_1 - \mathbf{p}, \varepsilon_1 - \varepsilon)\right]\frac{1}{\varepsilon_1 - \xi(p_1) + i\delta\ \mathrm{sign}\ \xi(p_1)}. \tag{4.4}$$

We perform several transformations in this integral (see the paper by Migdal[6]). Instead of ϵ_1 and $\cos(\widehat{\mathbf{pp}_1})$ we introduce new integration variables $\epsilon_1 - \epsilon = \omega$ and $|\mathbf{p}_1 - \mathbf{p}| = k$. The integral is then transformed to

$$\Sigma - \Sigma_1 = \frac{i}{(2\pi)^3 p}\int_0^\infty kdk \int_{|p-k|}^{p+k} p_1 dp_1 \times \int_{-\infty}^{\infty} d\omega\left[\Gamma(k, \omega) - \Gamma_1(k)\right]\frac{1}{\varepsilon + \omega - \xi(p_1) + i\delta\ \mathrm{sign}\ \xi(p_1)}. \tag{4.5}$$

We now write $\Gamma - \Gamma_1$ as the sum of three terms

$$\Gamma - \Gamma_1 = \Gamma_2 + \Gamma_3 + \Gamma_4, \tag{4.6}$$

where

$$\Gamma_2 = -\frac{4\pi e^2}{k^2}\frac{4\pi e^2\,\Pi}{k^2 + 4\pi e^2\,\Pi},$$

$$\Gamma_3 = \frac{4\pi e^2\omega_0^2 k^2}{\left[(\omega^2 - \omega_0^2)k^2 + 4\pi e^2\,\Pi\omega^2 + i\delta\right]\left[k^2 + 4\pi e^2\,\Pi\right]},$$

$$\Gamma_4 = \Gamma - \frac{4\pi e^2\omega^2}{(\omega^2 - \omega_0^2)k^2 + 4\pi e^2\,\Pi\omega^2 + i\delta}. \tag{4.7}$$

Correspondingly, we also break up $\Sigma - \Sigma_1$ into three parts: $\Sigma - \Sigma_1 = \Sigma_2 + \Sigma_3 + \Sigma_4$.

We shall see that values of $k \ll p_0$ are important in the integrals for Σ_2 and Σ_3. We can thus simplify the integral in (4.5). We shall assume that $|p - p_0| \ll p_0$ and introduce a new variable $\xi = u(p_1 - p_0)$. The integrals for Σ_2 and Σ_3 then become of the form

$$\Sigma_n = \frac{i}{(2\pi)^3 u}\int_0^\infty kdk \int_{\xi - uk}^{\xi + uk} d\xi_1 \int_{-\infty}^{\infty} d\omega\,\Gamma_n(\omega, k)\frac{1}{\varepsilon + \omega - \xi_1 + i\delta\ \mathrm{sign}\ \xi_1}.$$

It is important here that Γ_2 and Γ_3 decrease at large ω as $1/\omega^2$. We can thus integrate over ξ_1 before integrating over ω. Integrating we get

$$\Sigma_n = \frac{i}{(2\pi)^3 u}\int_0^\infty kdk \int_{-\infty}^{\infty} d\omega\Gamma_n(\omega, k)\ln\left|\frac{\xi - \varepsilon - \omega - uk}{\xi - \varepsilon - \omega + uk}\right| + \frac{\pi}{(2\pi)^3 u}\int_0^\infty kdk \int_{\xi - \varepsilon - uk}^{\xi - \varepsilon + uk} d\omega\Gamma_n(\omega, k)\ \mathrm{sign}\ (\varepsilon + \omega).$$

We are interested in the pole of the G-function, i.e., the case $\epsilon \approx \xi$. The first term of the foregoing equation then tends to zero. This follows from the fact that Γ_2 and Γ_3 are even functions ω [see (4.7) and Eq. (2.6) for Π], while $\ln|(\omega + uk)/(\omega - uk)|$ is an odd function. There remains thus from the integration over ξ_1 only the residue around the pole. Taking into account the fact that Γ_2 and Γ_3 are even, we find

$$\Sigma_n = \frac{\mathrm{sign}\varepsilon}{(2\pi)^3 u}\left[\int_0^{|\varepsilon|/u} kdk \int_0^{uk} d\omega + \int_{|\varepsilon|/u}^{\infty} kdk \int_0^{|\varepsilon|} d\omega\right]\Gamma_n = \frac{\mathrm{sign}\,\varepsilon}{(2\pi)^2 u}\int_0^{|\varepsilon|} d\omega \int_{\omega/u}^{\infty} kdk\,\Gamma_n(\omega, k). \tag{4.8}$$

We consider Σ_2 first. Since the general case is difficult we study two limiting cases: $|\epsilon| \ll u\kappa$ and $|\epsilon| \gg u\kappa$, where κ is the reciprocal of the Debye radius. In the case $\epsilon \ll u\kappa$ we can in Eq. (4.8) for Σ_2 substitute Π for $\omega \ll k$. This follows from the fact that when $k \gtrsim \kappa$ the frequency $\omega \ll uk$, while for $k \ll \kappa$ the quantity Γ_2 does no longer depend on Π ($4\pi e^2\Pi \sim \kappa^2$). When $\omega \ll uk$ we have, up to terms of the order ω/uk, $4\pi e^2\Pi \approx \kappa^2$. If we substitute this value into the integral we find

$$\Sigma_2 \approx \mathrm{Re}\,\Sigma_2 = -\frac{\mathrm{sign}\,\varepsilon}{(2\pi)^2 u}\int_0^{|\varepsilon|} d\omega \int_{\omega/u}^{\infty} \frac{kdk\,4\pi e^2\kappa^2}{k^2(k^2 + \kappa^2)} = -\frac{e^2}{\pi u}\varepsilon\left(\ln\frac{\kappa u}{|\varepsilon|} + 1\right). \tag{4.9}$$

To find the imaginary part of Σ_2 we must take into account the next term of the expansion of Π in terms of ω/uk. According to (2.6) $4\pi e^2\Pi \approx \kappa^2(1 + i\pi|\omega|/2uk)$. Substituting this into the equation for Γ_2 we obtain

$$\mathrm{Im}\,\Sigma_2 = -\frac{\mathrm{sign}\,\varepsilon}{(2\pi)^2 u}\int_0^{|\varepsilon|} d\omega \int_{\omega/u}^{\infty} dk\,\frac{4\pi e^2\kappa^2\pi\omega}{2u(k^2 + \kappa^2)} = -\frac{\pi e^2\,\varepsilon\,|\varepsilon|}{16u^2\kappa}. \tag{4.10}$$

We see easily that in the opposite limiting case $|\epsilon| \gg \kappa u$ the region $k \sim \kappa$, $\omega \sim u\kappa$ is important in the integral (4.8) for Σ_2. Because of this we must consider the upper limit of the integral over ω to be infinite. After that we change the order of integration over ω and k. If we introduce new variables $z = \omega/uk$ and $y = k/\kappa$ one can easily integrate over y and we get

$$\Sigma_2 = -\frac{1}{2}e^2\kappa(\beta_1 + i\beta_2)\ \mathrm{sign}\ \varepsilon, \tag{4.11}$$

where β_1 and β_2 are dimensionless constants which are respectively equal to the real and the imaginary part of the integral

$$\beta_1 + i\beta_2 = \int_0^1 dz\left(1 - z\,\mathrm{th}\,z + \frac{i\pi}{2}z\right)^{-1/2} \tag{4.12}*$$

*th = tanh.

(we take here the value of the radical with the positive imaginary part).

We now turn to Σ_3. We can also here distinguish two limiting cases: $|\epsilon| \ll \omega_0$ and $|\epsilon| \gg \omega_0$. According to (4.8) we can in the first case substitute

$$\Gamma_3 \approx \frac{4\pi e^2 \omega_0^2 k^2}{[-\omega_0^2 k^2 + 4\pi e^2 \Pi\omega^2 + i\delta][k^2 + 4\pi e^2 \Pi]}.$$

The real part of Σ_3 is obtained if we take the principal value of the integral over k, which corresponds to the region $p_0 \gtrsim k \gtrsim \kappa$. Bearing in mind that $\omega < |\epsilon| \ll \omega_0 \ll u\kappa$ we can replace $4\pi e^2\Pi$ by κ^2. Apart from logarithmic terms, we then find*

$$\mathrm{Re}\,\Sigma_3 = -(e^2/\pi u)\,\varepsilon \ln (p_0/\kappa). \qquad (4.13)$$

The imaginary part of Σ_3 occurs because of the residue of the pole arising from the first bracket in the denominator of Γ_3 and also because of the imaginary correction to Π in the second bracket in the denominator of Γ_3. The pole corresponds to the point $k^2 = \kappa^2\omega^2/\omega_0^2$ (we note that in that point $k \sim \omega/c_1 \gg \omega/u$). The residue from this pole gives

$$(\mathrm{Im}\,\Sigma_3)_1 = -e^2\varepsilon^3/6u\omega_0^2. \qquad (4.14)$$

One sees easily that the second term of $\mathrm{Im}\,\Sigma_3$ exactly compensates the contribution from $\mathrm{Im}\,\Sigma_2$ in this region:

$$(\mathrm{Im}\,\Sigma_3)_2 = \pi e^2 \varepsilon\,|\varepsilon|/16u^2\kappa. \qquad (4.15)$$

In the second limiting case $|\epsilon| \gg \omega_0$ we must use the complete expression (4.7) for Γ_3. Since the integration over ω and k is mainly over the region $\omega \sim \omega_0$, $k \sim \kappa$ we may perform the substitution $4\pi e^2\Pi \approx \kappa^2$ when evaluating the real part of Σ_3. Moreover, we can in first approximation put the limit of the integration over ω equal to infinity. If after this we interchange the order of integration over ω and k, we get

$$\int_0^\infty kdk \int_0^{uk} d\omega \approx \int_0^\infty kdk \int_0^\infty d\omega,$$

since $k \sim \kappa$. One sees easily that the principal value of $\int_0^\infty d\omega$ vanishes. This leads to the following interesting result. If we combine the real parts of the different terms of Σ of the form (4.4), (4.9), and (4.13) with $\epsilon \approx \xi$, it turns out that in the case $\epsilon \ll \omega_0$ all logarithmic terms cancel one another.† On the other hand, when $\epsilon \gg \omega_0$ we have $\mathrm{Re}\,\Sigma_3 \approx 0$ and there thus remains in $\mathrm{Re}\,\Sigma$ the term $(e^2/\pi u)\,\epsilon \ln (p_0/\kappa)$. One can observe the appearance of a logarithmic term if one calculates $\mathrm{Re}\,\Sigma_3$, including logarithmic terms, for the case $|\epsilon| \sim \omega_0$. We get then

$$\mathrm{Re}\,\Sigma_3 = \frac{\mathrm{sign}\,\varepsilon}{(2\pi)^2 u} \int_0^{|\varepsilon|} d\omega \int_{\omega/u}^\infty kdk\, \frac{4\pi e^2\omega_0^2 k^2}{[(\omega^2-\omega_0^2)k^2 + \kappa^2\omega^2][k^2+\kappa^2]}$$

$$\approx \frac{\mathrm{sign}\,\varepsilon e^2}{\pi u} \int_0^{|\varepsilon|} d\omega\, \frac{\omega_0^2}{\omega^2-\omega_0^2} \ln \frac{p_0}{\kappa}$$

$$= -\frac{e^2}{2u\pi}\,\omega_0 \ln \left|\frac{\varepsilon+\omega_0}{\varepsilon-\omega_0}\right| \ln \frac{p_0}{\kappa}.$$

Combining all logarithmic terms in Σ we find

$$\frac{e^2}{\pi u}\left(\varepsilon - \frac{\omega_0}{2} \ln \left|\frac{\varepsilon+\omega_0}{\varepsilon-\omega_0}\right|\right) \ln \frac{p_0}{\kappa}. \qquad (4.16)$$

We now turn to the imaginary part of Σ_3 for $|\epsilon| \gg \omega_0$. It arises from the residue in Γ_3 which only occurs when the condition $\omega < \omega_0$ is satisfied. We find thus

$$\mathrm{Im}\,\Sigma_3 = -\frac{2\pi^2 e^2}{(2\pi)^2 u}\,\mathrm{sign}\,\varepsilon \int_0^{\omega_0} \frac{\omega^2}{\omega_0^2-\omega^2}\,d\omega.$$

This integral does in actual fact not diverge, since the pole in k can not lie above p_0, i.e., $\kappa^2\omega^2/(\omega_0^2-\omega^2) \ll p_0^2$. Restricting ourselves to the order of the logarithmic terms we get

$$\mathrm{Im}\,\Sigma_3 = -(e^2\omega_0/2u)\,\mathrm{sign}\,\varepsilon \ln (p_0/\kappa). \qquad (4.17)$$

As far as additional terms in $\mathrm{Im}\,\Sigma_3$ due to the imaginary part of Π are concerned, one sees easily that they are of relative order $\omega_0/u\kappa \ll 1$ in comparison with (4.17).

There now only remains the last term, Σ_4. We have chosen the function Σ_4 especially in such a way that it vanishes when $k \ll p_0$. Only values $k \sim p_0$ will therefore be important in the integral. We can write in this region Γ_4 in the form [see (2.5)]

$$\Gamma_4(\mathbf{k},\omega) = \frac{4\pi e^2}{k^2}\,\omega_0^2 \left(\frac{1}{k^2}\sum_s \frac{|\mathbf{v}(s,\mathbf{k})\,\mathbf{k}|^2}{\omega^2-\omega^2(s,\mathbf{k})+i\delta} - \frac{1}{\omega^2-\omega_0^2+i\delta}\right). \qquad (4.18)$$

The momentum $\mathbf{k}$ can then take on any value, and we must substitute in $\mathbf{v}(\mathbf{k})$ and $\omega(\mathbf{k})$ the value of this vector, which is reduced to the basis cell of the reciprocal lattice by the subtraction of the appropriate vector $\mathbf{K}$. The integral for Σ_4 can be written in a form similar to (4.6), but we must take into account that expression (4.18) is anisotropic and that we must therefore still integrate over $d\varphi$ in (4.5). Since for an exact calculation

*Knowledge of the short-wavelength part of the phonon spectrum is required to attain high accuracy. This applies to Eqs. (4.16) and (4.17).

†We shall show later that Σ_4 does not contain such terms.

we need to know $\omega(s, \mathbf{k})$ and $v(s, \mathbf{k})$ in the short-wavelength region $k \sim p_0$, we can only estimate its order of magnitude.

In the region $k \sim p_0$ the integral over p_1 in (4.5) is taken between the limits 0 and $\sim 2p_0$. The situation here corresponds exactly to the case considered by Migdal.[6] One sees easily that the principal value of the integral over ξ_1 gives a correction to μ ($\sim \omega_0 e^2/u$), and the part obtained from the residue of the pole can be written in the form

$$\frac{\pi}{(2\pi)^4 u}\int d\varphi \int_0^{\sim 2p_0} k dk \int_{-\varepsilon}^{\varepsilon} d\omega \Gamma_4(\omega, \mathbf{k}).$$

In the case $|\epsilon| \ll \omega_0$ the imaginary part of that integral vanishes and the real part is of the order $e^2\epsilon/u$. When $\epsilon \gg \omega_0$ there are both a real and an imaginary part. Both are of the order $e^2\omega_0/u$.

We have thus determined all terms which make up the self-energy part Σ. The pole of the G-function is obtained from the solution of the equation $\epsilon - \xi + \Delta\mu - \Sigma = 0$, i.e., $\epsilon = \xi + \Sigma(\epsilon = \xi) - \Delta\mu$. It is well known[2] that the real and the imaginary parts of the pole of the G-function determine the energy of the excitations and their damping:

$$\varepsilon(p) = \xi(p) + \mathrm{Re}\,\Sigma - \Delta\mu, \qquad \gamma = -\mathrm{Im}\,\Sigma.$$

Combining all results obtained in the foregoing we get

$$\varepsilon(p) = \begin{cases} \xi(p)(1 + e^2\alpha_1/\pi u), & \xi \ll \omega_0 \\ \xi(p)[1 + (e^2/\pi u)(\ln(2p_0/\varkappa) - 1)], & \omega_0 \ll \xi \ll \varkappa u \\ \xi(p)[1 + (e^2/\pi u)\ln(2p_0 u/\xi(p))], & \varkappa u \ll \xi \ll u p_0 \\ \xi(p)[1 + (e^2 m/\pi p)\ln((p + p_0)/|p - p_0|)], & \xi \sim u p_0 \end{cases} \tag{4.19}$$

$$\gamma = \frac{e^2}{u} \cdot \begin{cases} \xi^3/6\omega_0^2, & \xi \ll \omega_0 \\ {}^1/_{16}\pi\xi|\xi + u\varkappa + \omega_0 \operatorname{sign}\xi\,[{}^1/_2 \ln(p_0/\varkappa) + \alpha_2], & \omega_0 \ll \xi \ll u\varkappa. \\ {}^1/_2 \beta_2 u\varkappa \operatorname{sign}\xi, & \xi \gg \varkappa u \end{cases} \tag{4.20}$$

The constants α_1 and α_2 depend here on the parameters of the short-wavelength part of the phonon spectrum, while the constant β is expressed in terms of the integral (4.12). The change in the "velocity on the Fermi surface" which is given by Eq. (4.19) corresponds in the region $\omega_0 \ll \xi \ll u\varkappa$ to the equation of Gell-Mann[7] for the electronic specific heat.

In conclusion the author uses this opportunity to express his gratitude to Academician L. D. Landau for numerous discussions of this paper.

[1] A. A. Abrikosov, JETP **39**, 1797 (1960), Soviet Phys. JETP **12**, 1254 (1961).

[2] V. M. Galitskii and A. B. Migdal, JETP **34**, 139 (1958), Soviet Phys. JETP **7**, 96 (1958).

[3] H. Lehmann, Nuovo cimento **11**, 342 (1954).

[4] R. E. Peierls, Quantum Theory of Solids, Clarendon Press, Oxford, 1955.

[5] L. N. Cooper, Phys. Rev. **104**, 1189 (1956).

[6] A. B. Migdal, JETP **34**, 1438 (1958), Soviet Phys. JETP **7**, 996 (1958).

[7] M. Gell-Mann, Phys. Rev. **106**, 369 (1957).

Translated by D. ter Haar
102

INVESTIGATION OF THRESHOLD ANOMALIES IN THE CROSS SECTIONS FOR COMPTON SCATTERING AND PHOTOPRODUCTION OF π^0 MESONS

G. K. USTINOVA

P. N. Lebedev Physics Institute, Academy of Sciences, U.S.S.R.

Submitted to JETP editor March 14, 1961

J. Exptl. Theoret. Phys. (U.S.S.R.) **41**, 583-587 (August, 1961)

Compton scattering on protons near the threshold for the production of π^0 and π^+ mesons, and photoproduction of π^0 mesons near the π^+-meson threshold, are examined phenomenologically. It is shown that if one takes into account the fact that near threshold the mesons are produced predominatly in the s-state one will obtain a peculiar energy dependence for the cross sections for elastic γp scattering and for photoproduction of neutral mesons. Analytic expressions are obtained for the total and differential cross sections for the Compton process and for π^0 photoproduction near the thresholds. Some numerical estimates of the effects to be expected are also given.

1. As is known, the unitarity of the full scattering matrix leads to a characteristic influence of one process on another in the threshold region.[1-3] In this connection Compton scattering is of particular interest; since the cross section for this process is comparatively small the effects due to the production of new particles with a large rest mass are particularly noticeable. Capps and Holladay[2] were the first to discover an anomaly in the total Compton effect cross section at the first threshold, by expanding the cross section near threshold in powers of the final state momentum. By utilizing dispersion relations, Lapidus and Chou Kuang-chao[4] obtained the characteristic threshold energy dependence for the cross section for Compton scattering and for photoproduction of neutral mesons. In the present work we investigate local threshold effects for these processes by the method of Baz',[3] generalized to include photons.

2. Let us investigate the energy dependence of the Compton effect on protons near the threshold for photoproduction of π^+ mesons ($E_t^+ = 150$ Mev). Let the z axis be taken along the direction of the momentum of the incident photon. In that case the z component of the angular momentum operator of the photon has the values ± 1, corresponding to right and left circular polarization, and the basic states of the photon + nucleon system are those in which the nucleon and photon spins are parallel or antiparallel.

For the two polarization cases the electric vector $\mathbf{E}$ is of the form[5]

$$\mathbf{E}_{n,a} = -e^{ik_0 z}\mathbf{e}_+ \chi_\pm + \mathbf{F}_{n,a} r^{-1} e^{ik_0 r};$$

$$\mathbf{F}_{n,a} = \sum_{l=1}^{\infty} \sqrt{2\pi(2l+1)} \sum_{j=l-1/2}^{l+1/2} C_{l\,1/2}(j,\ 1\pm 1/2;\ 1,\ \pm 1/2)$$

$$\times (2ik_0)^{-1} \Big\{ (S_{lj}^{M} - 1) \sum_{m=-1/2}^{m=1/2} C_{l\,1/2}(j,\ 1\pm 1/2;\ 1\pm 1/2 - m,\ m)$$

$$\times \mathbf{X}_{l,\,1\pm 1/2-m}\chi_m + i(S_{lj}^{E} - 1) \sum_{m=-1/2}^{m=1/2} C_{l\,1/2}(j,\ 1\pm 1/2;\ 1$$

$$\pm 1/2 - m,\ m)\Big[\frac{r}{r}\mathbf{X}_{l,\,1\pm 1/2-m}\Big]\chi_m\Big\}, \qquad (1)$$

where $\mathbf{e}_+$, $\chi_\pm$ are the spin functions of the photon and nucleon respectively, $\mathbf{k}_0$ is the wave vector of the relative photon—nucleon motion, $\mathbf{X}_{lm}$ is the vector spherical harmonic for $I = l$; $C_{l\frac{1}{2}}(j, M;\ M-m,\ m)$ is the Clebsch-Gordan coefficient, and $S_{lj}^{M} = \exp\{2i\delta_{lj}^{M}\}$ and $S_{lj}^{E} = \exp\{2i\delta_{lj}^{E}\}$ are the elements of the scattering matrix for magnetic and electric multipoles.

Near threshold the mesons are produced in the s state. The total angular momentum in the final state is $I = \frac{1}{2}$ since the spin of the meson is zero. The parity of the final state is $(-)$. The total angular momentum of the initial state is composed of the angular momentum of the photon l and the spin of the nucleon $\frac{1}{2}$, so that we must have the equality $l \pm \frac{1}{2} = I = \frac{1}{2}(-)$. It therefore follows that the photoproduction is due to electric dipole radiation in the state in which the photon and nucleon spin are antiparallel. Then, following Baz',[3,6] one may assume that

$$S^{E}_{1\,1/2} = |S^{0\,E}_{1\,1/2}| \exp\{2i\delta^{E}_{1/2}\}\,(1 - a_1 kR),$$

$$S^{E}_{lj} = |S^{0\,E}_{lj}| \exp\{2i\delta^{E}_{lj}\},\quad (l \neq 1,\ j \neq \tfrac{1}{2}),$$

$$S^{M}_{lj} = |S^{0M}_{lj}| \exp\{2i\delta^{M}_{lj}\}. \qquad (2)$$

Analogously, if D_l stands for the matrix element for the photoproduction of π^0 mesons, then near the threshold for the production of π^+ mesons the conservation of angular momentum and parity leads to the conclusion that

$$D_0 = |D_0^{(0)}| \exp\{i\delta_0\}\,(1 - a_2 kR),$$
$$D_l = |D_l^{(0)}| \exp\{i\delta_l\} \quad (l \neq 0). \qquad (3)$$

In Eqs. (2) and (3) $S^0_{lj} = |S^0_{lj}| \exp\{2i\delta_{lj}\}$ and $D_l^{(0)} = |D_l^{(0)}| \exp\{i\delta_l\}$ are the values of S_{lj} and D_l at the threshold E_t^+ ($k = 0$, where k is the momentum vector of the relative π^+-meson-nucleon motion); δ_{lj} and δ_l are real phase shifts respectively for the scattering of photons of various multipolarities and scattering of π^0 mesons in l state (at $k = 0$). The coefficients a_1 and a_2 are determined, in accordance with Baz' and Okun',[6] by

$$|S^{0\,E}_{1\,1/2}|\, a_1 = m_0'^2/2, \quad |D_0^{(0)}|\, a_2 = m_0' m_0''/2, \qquad (4)$$

where m_0' appears in the matrix element for direct photoelectric production of π^+ mesons in s states: $M_0 = (kR)^{1/2} m_0'$, and m_0'' is analogous to m_0' but in the matrix element for "internucleon charge exchange" of π^0 mesons in s states.

From a knowledge of the energy dependence of S_{lj} one can calculate the energy dependence of the cross section for Compton scattering near the threshold for π^+ production:

$$\sigma_c(\theta, E) = \sigma_c(\theta,\ E_t^+) - \mathrm{Re}\, a_1 kR F_a^* G^E_{a1}, \qquad (5)$$

$$G^E_{a1} = \frac{\sqrt{6\pi}}{2k_0} S^{0\,E}_{1\,1/2} \left\{ \frac{2}{3}\left[\frac{r}{r} X_{1,1}\right]\chi_{-1/2} - \frac{\sqrt{2}}{3}\left[\frac{r}{r} X_{1,0}\right]\chi_{1/2} \right\}. \qquad (6)$$

If one chooses the unit vector $\mathbf{n}$ in the direction of $\mathbf{F}_\alpha$ and the unit vector $\mathbf{m}$ in the direction of $G^E_{\alpha 1}$ then

$$\mathbf{F}_a = e^{i\alpha(\theta)} |F_a| \mathbf{n} = e^{i\alpha(\theta)} \sqrt{\sigma_c^a(\theta, E_t^+)}\, \mathbf{n},$$

$$G^E_{a1} = \exp(2i\delta^E_{1/2}) |G^E_{a1}| \mathbf{m} = (1/2k_0) |S^{0\,E}_{1/2}| \exp(2i\delta^E_{1/2})\, \mathbf{m}, \qquad (7)$$

and if we denote the angle between $\mathbf{n}$ and $\mathbf{m}$ by $\beta(\theta)$, we will get

$$\sigma_c(\theta, E) = \sigma_c(\theta, E_t^+) - (k_0/4\pi) \sqrt{\sigma_c^a(\theta, E_t^+)} \times \sigma^{+\prime}_{ph}(|k|) \cos\beta(\theta) \begin{cases} \sin(2\delta^E_{1/2} - \alpha(\theta)), & E > E_t^+ \\ \cos(2\delta^E_{1/2} - \alpha(\theta)), & E < E_t^+ \end{cases}, \qquad (8)$$

where $\sigma^{+\prime}_{ph}(|k|) = 2\pi |S^{0E}_{1/2}|\, a_1 |k| R/k_0^2$ coincides with the cross section for direct photoelectric production of positive mesons above threshold E_t^+, $\sigma_C(\theta, E_t^+)$ is the Compton cross section at the threshold E_t^+, $\alpha(\theta)$ is the phase of the amplitude at $E = E_t^+$, and $\sigma_C^a(\theta, E_t^+)$ is the cross section for Compton scattering of photons fully polarized antiparallel to the proton spin.

For $\theta = 0°$ it turns out that

$$\sigma_c(0, E) = \sigma_c(0, E_t^+) - (k_0/4\pi) \sqrt{\sigma_c^a(0, E_t^+)} \times \sigma^{+\prime}_{ph}(|k|) \begin{cases} \sin(2\delta^E_{1/2} - \alpha(0)), & E > E_t^+ \\ \cos(2\delta^E_{1/2} - \alpha(0)), & E < E_t^+, \end{cases} \qquad (9)$$

i.e., $\beta(0) = 0$. For other angles it is not possible to obtain a similar exact formula because of the infinite number of interference terms. If, on the other hand, we limit ourselves to the dipole approximation and take into account that the phase shifts are small ($\delta_{lj} \sim e^2 k_0/M \sim 0.001$) so that $\sin\delta_{lj} = \delta_{lj}$ and $\cos\delta_{lj} = 1$, then we find for the elastic scattering cross section through an arbitrary angle

$$\sigma_c(\theta, E) = \sigma_c(\theta, E_t^+) - \sigma^{+\prime}_{ph}(|k|)/4\pi \times \begin{cases} \frac{1}{2}[|S^{0\,E}_{1/2}| + \frac{1}{4}(3\cos^2\theta - 1)|S^{0\,E}_{3/2}| + \frac{1}{2}\cos\theta\,[2|S^{0M}_{1/2}| + |S^{0M}_{3/2}|] \\ \qquad - \frac{3}{4}(1 + \cos\theta)^2], \quad E > E_t^+; \\ [-\frac{1}{4}(3\cos^2\theta - 1)|S^{0\,E}_{3/2}|(\delta^E_{1/2} - \delta^E_{3/2}) + \frac{1}{2}\cos\theta\,[2|S^{0M}_{1/2}|(\delta^E_{1/2} - \delta^M_{1/2}) \\ \qquad + |S^{0M}_{3/2}|(\delta^E_{1/2} - \delta^M_{3/2})] - \frac{3}{4}(1 + \cos\theta)^2 \delta^E_{1/2}], \quad E < E_t^+. \end{cases} \qquad (10)$$

The energy dependence of the total cross section for the Compton process is given by

$$\sigma_c(E) = \sigma_c(E_t^+) - \sigma^{+\prime}_{ph}(|k|) \begin{cases} \frac{1}{2}[|S^{0\,E}_{1/2}| - 1], & E > E_t^+ \\ \delta^E_{1/2}, & E < E_t^+ \end{cases}. \qquad (11)$$

All the analysis above refers to the case of unpolarized particles. It is relevant, however, that only the photon-nucleon combination with antiparallel spins contributes to the singularity. It is therefore possible to generalize the formulas to the case of arbitrary polarization. Thus in the case of Eq. (8) we get

$$\sigma_c(\theta, E, \xi^0, \zeta^0) = \sigma_c(\theta, E_t^+, \xi^0, \zeta^0) - (k_0/4\pi)(1 - \xi^0_3 \zeta^0_z) \times \sqrt{\sigma_c^a(\theta, E_t^+)}\, \sigma^{+\prime}_{ph}(|k|) \cos\beta(\theta) \begin{cases} \sin(2\delta^E_{1/2} - \alpha(\theta)), & E > E_t^+ \\ \cos(2\delta^E_{1/2} - \alpha(\theta)), & E < E_t^+, \end{cases} \qquad (12)$$

where $\boldsymbol{\zeta}^0$ (ζ^0_x, ζ^0_y, ζ^0_z) is the polarization vector of the incident proton, $\boldsymbol{\xi}^0$ (ξ^0_1, ξ^0_2, ξ^0_3) is the Stokes parameter of the incident electromagnetic radiation; ξ^0_3 is the degree of circular polarization of the incident photon. The same factor has to be introduced in all other formulas as well. For totally polarized particles with antiparallel spins ($\xi^0_3 \zeta^0_z = -1$) the singularity in the cross section is twice as large as in the unpolarized case, and for parallel spins ($\xi^0_3 \zeta^0_z = 1$) the singularity disappears.

3. The energy dependence of the Compton scattering cross section near the threshold for photo-

production of neutral mesons ($E_t^0 = 145$ Mev) can be formally obtained from the previous equations if it is remembered that S_{lj} satisfies at the threshold E_t^0 the condition $|S_{lj}^0| = 1$.[3] Therefore everywhere in Eqs. (8) — (12) all threshold quantities should be evaluated at 145 Mev (i.e., E_t^+ should be replaced by E_t^0) and $|S_{lj}^0|$ should be set equal to unity. For example, instead of Eq. (10) we get for the γp-scattering cross section near the threshold for π^0 production the following expression

$$\sigma_c(\theta, E) = \sigma_c(\theta, E_t^0) - (1/4\pi)\,\sigma_{ph}^0(|k'|) \times \begin{cases} 0, & E > E_t^0 \\ -[\frac{1}{4}(3\cos^2\theta - 1)(\delta_{1/2}^E - \delta_{3/2}^E) + \frac{1}{2}\cos\theta\,[2(\delta_{1/2}^E - \delta_{3/2}^M) \\ \quad + (\delta_{1/2}^E - \delta_{3/2}^M)] - \frac{3}{4}(1+\cos\theta)^2\,\delta_{1/2}^E], & E < E_t^0 \end{cases} \quad (13)$$

where all δ_{lj} stand for the real phase shifts of Compton scattering at the threshold E_t^0 ($k' = 0$), and $\sigma_{ph}^0(|k'|) = 2\pi a\,|k'|\,R/k_0^2$ coincides with the cross section for the photoproduction of π^0 mesons above the threshold E_t^0: k' is the π^0-meson-nucleon relative-motion vector.

4. The differential cross section for photoproduction of π^0 mesons near the threshold E_t^+ may be written with the help of Eq. (3) as follows

$$\sigma_{ph}^0(\theta, E) = \frac{k'}{k_0}\left|\sum_{l=0}^{\infty}\frac{2l+1}{2\sqrt{k_0 k'}}D_l P_l(\cos\theta)\right|^2 = \sigma_{ph}^0(\theta, E_t^+) - \frac{k_0}{2\pi}\sqrt{\sigma_{ph}^0(\theta, E_t^+)}\,\sigma_{ph}^{+\pi}(|k|)\begin{cases}\sin(\delta_0 - \gamma(\theta)), & E > E_t^+ \\ \cos(\delta_0 - \gamma(\theta)), & E < E_t^+\end{cases} \quad (14)$$

or, if we introduce the known phase shifts δ_1 and δ_3 for s-wave scattering in states with isotopic spin $\frac{1}{2}$ and $\frac{3}{2}$ respectively,

$$\sigma_{ph}^0(\theta, E) = \sigma_{ph}^0(\theta, E_t^+) - (2k_0/6\pi)\sqrt{\sigma_{ph}^0(\theta, E_t^+)}\,\sigma_{ph}^{+\pi}(|k|) \times \begin{cases}[-(M/m-1)\sin(\delta_1 - \gamma(\theta)) + (M/m+1)\sin(\delta_3 - \gamma(\theta))], & E > E_t^+ \\ [-(M/m-1)\cos(\delta_1 - \gamma(\theta)) + (M/m+1)\cos(\delta_3 - \gamma(\theta))], & E < E_t^+.\end{cases} \quad (15)$$

Here M is the nucleon and m the meson mass; $\gamma(\theta)$ is the phase of the amplitude

$$f_{ph}^0(\theta, E_t^+) = e^{i\gamma(\theta)}\sqrt{\sigma_{ph}^0(\theta, E_t^+)}$$

at the threshold E_t^+, and we have used the abbreviation

$$\sigma_{ph}^{+\pi}(|k|) = 2\pi\,|D_0^{(0)}|\,a_2\,|k|\,R/k_0^2. \quad (16)$$

For the total cross section for the production of neutral mesons near the threshold for positive mesons we get

$$\sigma_{ph}^0(E) = \sigma_{ph}^0(E_t^+) - \begin{cases}|D_0^{(0)}|\,\sigma_{ph}^{+\pi}(|k|), & E > E_t^+ \\ 0, & E < E_t^+.\end{cases} \quad (17)$$

5. The formulas (8) — (13) and (15) are valid as long as $kR \ll 1$, $k'R \ll 1$, i.e., $k, k' \ll 1/R$, where $R = \hbar/mc = 1.4 \times 10^{-13}$ cm is the range of the meson-nucleon interaction. The width of the threshold singularities is of the same order. It is reasonable to make the estimates at k and k' $= 0.124 \times 10^{13}$ cm^{-1}, which corresponds to a distance away from the threshold of $E - E_t = k^2/2\mu = 2.5$ Mev (this should make it possible to resolve the singularities in the Compton effect cross section near the thresholds for the production of π^0 and π^+ mesons [$\mu = mM/(m+M)$].

Let us investigate the behavior of the Compton scattering cross section near the threshold E_t^+, as given by Eq. (10). If we take the phase shifts δ_{lj} from Gell-Mann, Goldberger, and Thirring[5] we get

$$\sigma_c(\theta, E) = \sigma_c(\theta, E_t^+) + (1/4\pi)\,\sigma_{ph}^+(|k|) \times \begin{cases}0.00021 + 0.00001\cos\theta, & E > E_t^+ \\ 0,00017 - 0,00041\cos\theta + 0.00057\cos^2\theta, & E < E_t^+,\end{cases} \quad (18)$$

i.e., at all angles the cross section increases on both sides of the threshold (the singularity is in the form of a cusp, cf. [4]).

This is also the form of the singularity in the total Compton effect cross section according to Eq. (11). The size of the anomaly is determined by the cross section for meson photoproduction. It can be obtained, according to the calculations by Feld, by making use of perturbation theory (which is quite reliable near threshold) with a small correction for the finiteness of the nucleon mass and the possibility of meson charge exchange scattering in the field of the nucleon:[7]

$$\sigma_{ph}(|k|) = 4\pi\,|\zeta|^2\,\sigma_0 = 4\pi\,|\zeta|^2\,25k/k_0 \ \mu b; \quad \zeta = \zeta_r + i\zeta_i,$$
$$\zeta_r = 0.105, \quad \zeta_i = -0.127k'R \text{ — for } \pi^0 \text{ mesons}$$
$$\zeta_r = 1, \quad \zeta_i = 0.057\,kR \text{ — for } \pi^+ \text{ mesons.} \quad (19)$$

Taking the threshold values of the Compton cross section from Capps,[8] we find that 2.5 Mev away from the threshold the relative increase in the cross section at individual angles amounts to 10 — 30% above threshold and 30 — 50% below threshold.

Since the cross section for s-wave production of neutral mesons is approximately 100 times smaller than the corresponding cross section for charged mesons [see Eq. (19)], it follows that the singularity in the Compton process cross section at the threshold E_t^0 will amount to a fraction of a percent. The total cross section for π^0 photoproduction decreases by 1 — 2% at 25 Mev above the threshold E_t^+.

In conclusion I would like to express my deep gratitude to Professors V. I. Gol'danskii and Ya. A. Smorodinskii for directing this research and to A. I. Baz' for valuable remarks.

[1] E. P. Wigner, Phys. Rev. **73**, 1002 (1948).
[2] R. H. Capps and W. G. Holladay, Phys. Rev. **99**, 931 (1955).
[3] A. I. Baz', JETP **33**, 923 (1957), Soviet Phys. JETP **6**, 709 (1958); JETP **32**, 478 (1957), Soviet Phys. JETP **5**, 403 (1957).
[4] L. I. Lapidus and Chou Kuang-chao, JETP **38**, 201 (1960), Soviet Phys. JETP **11**, 147 (1960); JETP **39**, 112 (1960), Soviet Phys. JETP **12**, 82 (1960).
[5] Gell-Mann, Goldberger, and Thirring, Phys. Rev. **95**, 1612 (1954).
[6] A. I. Baz' and L. B. Okun', JETP **35**, 757 (1958), Soviet Phys. JETP **8**, 526 (1959).
[7] B. T. Feld, Ann. of Phys. **4**, 189 (1958).
[8] R. H. Capps, Phys. Rev. **106**, 1031 (1957); **108**, 1032 (1957).

Translated by A. M. Bincer
103

MAGNETOACOUSTIC RESONANCE IN STRONG MAGNETIC FIELDS

A. V. BARTOV, E. K. ZAVOĬSKII, and D. A. FRANK-KAMENETSKII

Submitted to JETP editor March 18, 1961

J. Exptl. Theoret. Phys. (U.S.S.R.) **41**, 588-591 (August, 1961)

In a plasma in which the magnetic energy is comparable with the electron rest energy (i.e., the electron cyclotron frequency is of the same order as the plasma frequency), the resonance frequency of magnetic sound (as a function of the concentration) passes through a maximum in a constant magnetic field. Near the peak, the magnetoacoustic resonance can be produced and observed under nonlinear conditions (for a changing concentration) and can be used for ionization of the plasma.

In previous researches on magnetoacoustic resonance in a plasma,[1-3] it was assumed that the plasma frequency ω_0 was large in comparison with the cyclotron frequencies ω_e and ω_i. Under such conditions, the resonant frequency of magnetic sound is seen to be essentially dependent on the concentration. Under the same conditions, the observation and use of magnetoacoustic resonance becomes more difficult. The opinion[4] has already been voiced that the detailed character of the resonance can be shown to be practically unattainable because of the action of the same phenomenon on the plasma concentration. It is impossible to agree with this, in principle, since there can be no doubt of the complete possibility of observing magnetoacoustic resonance under strictly controlled linear conditions, in which the resonance fields have low amplitude and the concentration of the plasma is formed and maintained by other independent means of action. However, magnetoacoustic resonance has been observed experimentally under nonlinear conditions,[2] when the creation of the plasma and the resonance action on it were carried out by the same variable field. Moreover, it seemed that the ionization process also continues very effectively under conditions of magnetoacoustic resonance[5]; this ionization is associated by its very nature with a continuous change of the concentration.

In order to account for the possibility of resonance phenomena of the magnetoacoustic type in a plasma with a time-dependent concentration, we assume the limitation made earlier:

$$\omega_0^2 \gg \omega_e^2$$

and consider the case in which the plasma frequency is of the order of or less than the electron cyclotron frequency. This case exists either in a rarefied plasma (where the plasma frequency is low) or in very strong magnetic fields (where the cyclotron frequency is high).

A plasma in which the cyclotron frequency is high in comparison with the collision frequency is known as magnetized (in relation to the collisions). If the cyclotron frequency is higher than the plasma frequency, then the electrostatic oscillations are magnetized; it is customary to call such a plasma oscillation magnetized. We note that the ratio

$$\omega_0^2 / \omega_e^2 = 4\pi nmc^2 / H^2$$

is of the order of the ratio of the electron rest energy to its magnetic energy. Thus, a plasma is magnetized in oscillation if its magnetic energy is larger than the rest energy of the electrons.

We consider first a rarefied plasma in which the number of electrons per unit length is small. Then, in accord with [3], the resonance frequency of the magnetic sound in the case of purely radial propagation is close to the lower hybrid frequency.[6] The formula developed in[3] for the lower hybrid frequency is valid only in the case when the plasma frequency is high in comparison with the cyclotron frequencies. By equating the coefficient a_{20} to zero in the general dispersion equation [Eq. (52) of [3]], we easily obtain a general expression for the lower hybrid frequency in the form

$$\omega_h^2 = \omega_i\omega_e \frac{\omega_0^2 + \omega_i\omega_e}{\omega_0^2 + \omega_e^2}. \qquad (1)$$

If we assume $\omega_0^2 \gg \omega_i\omega_e$, we then get the approximate formula given in [3].

The general behavior of the lower hybrid frequency as a function of the density was also pointed out by Körper.[7] For $\omega_0^2 \ll \omega_i\omega_e$, the lower hybrid frequency approaches the ion cyclotron frequency, and for $\omega_0^2 \gg \omega_i\omega_e$, the geometric mean of the electron and ion cyclotron frequencies. However, it is

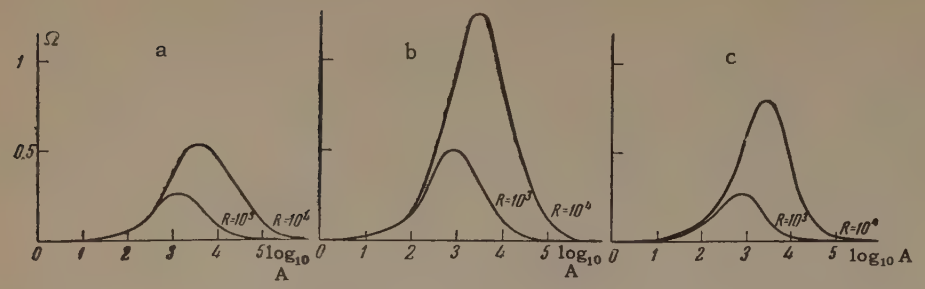

Dependence of Ω on A for B = 1840 (hydrogen), R = 10^3 and 10^4 for different values of cot θ: a – $\cot^2\theta = 0$, b – $\cot^2\theta = 10^{-3}$, c – $\cot^2\theta = 10^{-2}$ (the curves in drawing c are plotted in an ordinate scale reduced by a factor of 10).

important to note that there exists a wide intermediate region $\omega_e^2 \gg \omega_0^2 \gg \omega_i\omega_e$ in which the approximate expression for the lower hybrid frequency has the form

$$\omega_h^2 \approx \omega_0^2\omega_i/\omega_e. \qquad (2)$$

Here the lower hybrid frequency is proportional to the plasma frequency, i.e., to the square root of the concentration. For a small number of electrons per unit length, the resonant frequency of magnetic sound must behave in the same way. The heavier the ions, the greater the width of this region.

For a given magnetic field (ω_e = const) in a dense plasma, the resonant frequency of magnetic sound decreases, and, in a rarefied plasma, increases with the concentration. It must pass through a maximum in the intermediate region. Near the maximum, the concentration dependence of the resonant frequency should be weak and, with account of the finite width of the resonance, the resonance can be observed in a wide range of concentrations in the case of a sufficiently broad maximum.

In order to represent the concentration dependence of the resonant frequency in general form for a constant magnetic field, it is convenient to introduce dimensionless variables in a somewhat different way from what was done in [3]. Preserving the definition of the dimensionless frequency

$$\Omega = \omega^2/\omega_i\omega_e, \qquad (3)$$

the square of the Alfvén index of refraction

$$A = \omega_0^2/\omega_i\omega_e \qquad (4)$$

and the ratio of the cyclotron frequencies

$$B = \omega_e/\omega_i, \qquad (5)$$

we introduce new dimensionless parameters:

$$R = k_1^2c^2 / \omega_i\omega_e = k_1^2\tilde{r}_i\tilde{r}_e, \quad \operatorname{tg}\theta = k_1/k_3. \qquad (6)^*$$

Here ω is the resonant, ω_0 the plasma, ω_e and ω_i the electron and ion cyclotron angular frequencies, k_1 and k_3 are the radial and longitudinal wave numbers; $\tilde{r}_e$ and $\tilde{r}_i$ are the cyclotron radii for the velocity of light, $\tilde{r} = c/\omega$. The angle θ lies between 0 and $\pi/2$.

*tg = tan.

Expanding the dispersion equation in powers of Ω, we reduce it to the form

$$\Omega^5 - b_4\Omega^4 + b_3\Omega^3 - b_2\Omega^2 + b_1\Omega - b_0 = 0;$$
$$b_4 = 3A + B + 2R(1 + \operatorname{ctg}^2\theta),$$
$$b_3 = A^2 + 3AB + B^2 - [2A + B + R(1 + \operatorname{ctg}^2\theta)]^2,$$
$$b_2 = (A + B)[A + R(1 + \operatorname{ctg}^2\theta)]^2 - AB(A + R),$$
$$b_1 = AR[A + R + BR\operatorname{ctg}^2\theta(1 + \operatorname{ctg}\theta)],$$
$$b_0 = AR^2\operatorname{ctg}^2\theta(1 + \operatorname{ctg}^2\theta). \qquad (7)^*$$

If we neglect all the coefficients except b_2 and b_1, then we obtain the approximate formula (for $\cot^2\theta \ll 1$)

$$\Omega = \left(1 + \frac{BR}{A+R}\operatorname{ctg}^2\theta\right)\Big/\left(\frac{A}{R} + 1 + \frac{B}{A}\right), \qquad (8)$$

which is identical with the "long cylinder approximation."[3] This approximation gives the root for Ω closest to unity if the parameters A and R are large and AR(A + R)/B ≫ 1.

In dimensionless form, the concentration dependence of the resonant frequency for a constant magnetic field is represented as the dependence of Ω on A for constant R. Under ordinary experimental conditions, the long-cylinder approximation is shown to be sufficiently accurate. In this approximation, for $\theta = \pi/2$ ($k_3 = 0$, i.e., purely radial oscillations), the maximum lies at $A = \sqrt{BR}$ and the maximum value of the dimensionless frequency is

$$\Omega_m = \sqrt{BR}/(2B + \sqrt{BR}). \qquad (9)$$

For $k_3 \neq 0$ the expressions for the location and height of the maximum are obtained very crudely and we shall not write them down. As is seen from the graphs, the position of the maximum is shifted slightly, but the height of it increases sharply: resonance becomes possible at frequencies above the hybrid.[3]

The phenomenon under consideration of the maximum of the resonance frequency of the magnetic sound as a function of concentration for a constant magnetic field is of great value for interpretation of experiments on the magnetoacoustic resonance under nonlinear conditions.[2] Far from the maximum, resonance is possible

*ctg = cot.

only for strictly fixed concentration of the plasma. In the region close to the maximum, the magnetoacoustic resonance can occur and be observed even for variable concentration. In particular, the ionization with the help of magnetic sound[5] should effectively take place precisely in the region of concentration close to the condition of maximum. Experiments whose detailed description will be published later confirm the existence of a maximum and the remaining qualitative conclusions of the theory.

[1] D. A. Frank-Kamenetskii, J. Tech. Phys. **30**, 899 (1960), Soviet Phys.-Technical Physics **5**, 842 (1961).

[2] A. P. Akhmatov and P. I. Blinov et al., JETP **39**, 536 (1960), Soviet Phys. JETP **12**, 376 (1961).

[3] D. A. Frank-Kamenetskii, JETP **39**, 669 (1960), Soviet Phys. JETP **12**, 469 (1961).

[4] K. Körper, Z. Naturforsch. **15a**, 220 (1960).

[5] Zavoĭskii, Kovan, Patrushev, Rusanov, and Frank-Kamenetskii, J. Tech. Phys. (U.S.S.R.) (in press).

[6] Auer, Hurwitz, and Miller, Phys. Fluids **1**, 501 (1958).

[7] K. Körper, Z. Naturforsch. **12a**, 815 (1957).

Translated by R. T. Beyer
104

SOME PROCESSES INVOLVING HIGH-ENERGY NEUTRINOS

Ya. I. AZIMOV and V. M. SHEKHTER

Leningrad Physico-Technical Institute, Academy of Sciences, U.S.S.R.

Submitted to JETP editor March 21, 1961

J. Exptl. Theoret. Phys. (U.S.S.R.) 41, 592-599 (August, 1961)

Cross sections for processes of the type $\bar{\nu} + e^- \to \pi^- + \pi^0$, $\bar{\nu} + p \to \Lambda + \mu^+$, and $\mu^- + p \to \Lambda + \nu$ are calculated by taking into account the form factors for weak V-A coupling.

1. INTRODUCTION

A rather large number of recent papers [1-6] is devoted to processes that can occur when high energy neutrinos are absorbed. The most complete listing of such processes appears in Pontecorvo's article.[1] Lee and Yang[3] have analyzed experiments which could yield various information of interest for the theory of weak interactions. A number of authors[2,6] have studied the possibility of a practical experimental arrangement.

Since such an experiment will be possible in the comparatively near future, it is expedient to calculate the cross sections for various processes which occur when a neutrino is absorbed. Such a computation has been performed for a number of reactions, namely for elastic neutrino-electron scattering ($\bar{\nu} + e^- \to \bar{\nu} + e^-$ and $\nu + e^- \to \nu + e^-$)[7,8] and for the reactions $\bar{\nu} + p \to n + e^+$ and $\nu + n \to p + e^-$.[3-5]

In the present article cross sections are calculated for processes leading to the formation of two particles which occur when a neutrino is absorbed by an electron, a proton, or a neutron. Besides those indicated above, the following reactions are possible (their thresholds, in the laboratory system, are given in parentheses)

$$\nu + e^- \to \nu + \mu^-,\ \bar{\nu} + e^- \to \bar{\nu} + \mu^-\ (10{,}9\ \text{Bev}); \quad (1)$$

$$\bar{\nu} + e^- \to \pi^- + \pi^0\ (74\ \text{Bev}),\ \bar{\nu} + e^- \to K^- + \pi^0\ (387\ \text{Bev}),$$
$$\bar{\nu} + e^- \to K^- + K^0\ (963\ \text{Bev}),\ \bar{\nu} + e^- \to \bar{K}^0 + \pi^-\ (398\ \text{Bev}); \quad (2)$$

$$\bar{\nu} + p \to n + \mu^+\ (113\ \text{Mev}),\ \nu + n \to p + \mu^-\ (110\ \text{Mev}),$$
$$\bar{\nu} + p \to \Lambda + e^+\ (195\ \text{Mev}),\ \bar{\nu} + p \to \Lambda + \mu^+\ (319\ \text{Mev}), \quad (3)$$

$$\bar{\nu} + p \to \Sigma^0 + e^+\ (289\ \text{Mev}),\ \bar{\nu} + p \to \Sigma^0 + \mu^+\ (420\ \text{Mev}),$$
$$\bar{\nu} + n \to \Sigma^- + e^+\ (295\ \text{Mev}),\ \bar{\nu} + n \to \Sigma^- + \mu^+\ (426\ \text{Mev}).$$

In each of the reactions of (2) or (3), only two particles take part in the strong interactions. Their presence leads to the appearance of weak-interaction form factors, which essentially enter in all the formulas. Since strong interactions are absent in case (1), form factors of this kind do not arise.

Processes (1) and (2) will be examined further in Sec. 2, and processes (3) and further in Sec. 3. The reaction $\nu + n \to \Sigma^+ + e^-(\mu^-)$ is not included among the latter since it is forbidden in the Feynman—Gell-Mann scheme.[7] Section 4 deals with processes which are the inverse of (3) in the sense that the μ meson is absorbed by the nucleon and the neutrino arises in the final state. Processes of this kind involving the absorption of an electron have been discussed earlier.[9,10]

It will be assumed everywhere that the weak interaction includes only the V and A variants. It should not be forgotten that all processes in (2) and (3) occurring with the participation of electrons, as well as the second reaction in (1), can take place only if the electron and μ-meson neutrinos are identical (keeping in mind that the incident neutrinos are generated in $\pi_{\mu 2}$ and $K_{\mu 2}$ decay).

2. PROCESSES OCCURRING WHEN NEUTRINOS ARE ABSORBED BY ELECTRONS

Among the inelastic processes that occur when neutrinos interact with electrons, the reactions (1) have the lowest threshold. These reactions have been discussed earlier by, for example, Blokhintsev.[11] Their cross sections are given by the expressions (the index I refers to the reaction involving ν, II to that with $\bar{\nu}$)

$$\sigma_I = (G^2/\pi)\mathscr{E}^2 (1 - m_\mu^2/\mathscr{E}^2)^2,$$
$$\sigma_{II} = (G^2/3\pi)\mathscr{E}^2 (1 - m_\mu^2/\mathscr{E}^2)^2 (1 + m_\mu^2/2\mathscr{E}^2), \quad (4)$$

where $\mathscr{E}^2 \equiv (p_\nu + p_e)^2 = 2m_e W_\nu$ is the square of the total energy in the center-of-mass system and $G = 1.41 \times 10^{-49}$ erg-cm^3 is the Feynman-Gell-Mann constant. At a neutrino energy $W_\nu = 20$ Bev we have $\sigma_I = 7 \times 10^{-41}$ cm^2 and $\sigma_{II} = 3 \times 10^{-41}$ cm^2. At large energies (W_ν is expressed in Bev), σ_I

$= 1.6 \times 10^{-41} W_\nu \text{ cm}^2$ and $\sigma_{II} = \sigma_I/3$, just as for the elastic scattering of a neutrino by an electron.

Especially interesting is the reaction

$$\bar{\nu} + e^- \to \pi^- + \pi^0. \tag{5}$$

In the Feynman–Gell-Mann scheme[7] the weak interaction responsible for this process has the same structure as the interaction between charged π mesons and the electromagnetic field. For this reason the total cross section for reaction (5)

$$\sigma = \frac{2G^2}{3\pi} \frac{k^3}{\mathscr{E}} F^2(\mathscr{E}^2) \tag{6}$$

[$k = (\mathscr{E}^2/4 - m_\pi^2)^{1/2}$ is the π-meson momentum in the center-of-mass system] contains $F(\mathscr{E}^2)$, which is the continuation of the electromagnetic form factor of the π meson into the region of timelike values of the argument. The determination of $F(\mathscr{E}^2)$ is a very interesting physical problem. Unfortunately the threshold of reaction (5) is very high.

When $W_\nu = 100$ Bev we have $\sigma = 3.3 \times 10^{-41} \times F^2(\mathscr{E}^2)$ cm^2. It must be remembered that since $\mathscr{E}^2 > 0$, $F(\mathscr{E}^2)$ can be several times greater than unity. According to Frazer and Fulco,[12] for example, $F(\mathscr{E}^2) \sim 2$ when $W_\nu = 100$ Bev. In the laboratory system both mesons travel forwards with practically equal energy. In the center-of-mass system the angular distribution assumes the form $\sin^2 \vartheta \, d\Omega$, where ϑ is the angle between the directions of incident and emerging particles; this is the result of neglecting the mass of the electron.

The same interaction as in process (5) can give rise to a completely analogous reaction, $\bar{\nu} + e^- \to K^- + K^0$. Its cross section is determined from formula (6) with the additional isotopic factor $\frac{1}{2}$; here $F(\mathscr{E}^2)$ is the continuation of the electric form factor of the K meson. The processes $\bar{\nu} + e^- \to K^- + \pi^0$ and $\bar{\nu} + e^- \to \bar{K}^0 + \pi^-$ are due to another interaction, responsible for one that causes lepton decays of hyperons and K mesons and has no electromagnetic analog. Here again formula (6) is correct with the added factor $\frac{1}{2}$, but

$$k = \{\mathscr{E}^4 - 2\mathscr{E}^2(m_K^2 + m_\pi^2) + (m_K^2 - m_\pi^2)^2\}^{1/2}/2\mathscr{E},$$

and $F(\mathscr{E}^2)$ coincides with the form factor that determines the K_{e3} decay. Whereas $F^2(0) = 1$ for $\bar{\nu} + e^- \to \pi^- + \pi^0$ and $K^- + K^0$, $F^2(0) \sim \frac{1}{30}$ in the case of $\bar{\nu} + e^- \to K^- + \pi^0$ (see, for example,[13] and[14]).

All these processes are no less interesting than reaction (5), but their thresholds lie fantastically high. Still higher are the thresholds for the formation of baryon pairs in the collision between $\bar{\nu}$ and e^-. The reaction $\bar{\nu} + e^- \to n + \bar{p}$, for example, begins at $W_\nu = 3450$ Bev.

3. ABSORPTION OF NEUTRINOS BY PROTONS

Processes involving the absorption of neutrinos or antineutrinos by nucleons [enumerated in (3)] are more accessible for experimental investigation. A typical process of this kind is the reaction

$$\bar{\nu} + p \to \Lambda + \mu^+, \tag{7}$$

whose matrix element, as is known, has the form

$$\begin{aligned}(G/\sqrt{2})\,(\bar{v}_\nu \gamma_\alpha (1+\gamma_5) v_\mu)\,(\bar{u}_\Lambda \{\gamma_\alpha (f_1 - g_1\gamma_5) \\ + \sigma_{\alpha\beta}(p_p - p_\Lambda)_\beta (f_2 + g_2\gamma_5) \\ + (p_p - p_\Lambda)_\alpha (f_3 + g_3\gamma_5)\}\, u_p)\end{aligned} \tag{8}$$

[the metric $(1, -1, -1, -1)$ is used, $\gamma_5 = i\gamma_0\gamma_1\gamma_2\gamma_3$, and $\sigma_{\alpha\beta} = (\gamma_\alpha\gamma_\beta - \gamma_\beta\gamma_\alpha)/2$]. The form factors f_i and g_i $(i = 1, 2, 3)$ are functions of the invariant

$$Q^2 \equiv (p_p - p_\Lambda)^2 = (m_\Lambda - m_p)^2 - 2m_p W_\Lambda, \tag{9}$$

where W_Λ is the kinetic energy of the Λ hyperon in the laboratory system. The quantity Q^2 is uniquely associated with the emission angle of the Λ and can vary within the limits

$$\begin{aligned}(2\mathscr{E}^2)^{-1}\{-(\mathscr{E}^2 - m_p^2)(\mathscr{E}^2 - m_\Lambda^2 - m_\mu^2) + 2m_p^2 m_\mu^2 \\ - (\mathscr{E}^2 - m_p^2)[(\mathscr{E}^2 - m_\Lambda^2 - m_\mu^2)^2 \\ - 4m_\Lambda^2 m_\mu^2]^{1/2}\} \leqslant Q^2 \leqslant (2\mathscr{E}^2)^{-1}\{-(\mathscr{E}^2 - m_p^2)(\mathscr{E}^2 - m_\Lambda^2 - m_\mu^2) \\ + 2m_p^2 m_\mu^2 + (\mathscr{E}^2 - m_p^2)[(\mathscr{E}^2 - m_\Lambda^2 - m_\mu^2)^2 - 4m_\Lambda^2 m_\mu^2]^{1/2}\},\end{aligned} \tag{10}$$

where again $\mathscr{E}^2 \equiv (p_\nu + p_p)^2 = m_p^2 + 2m_p W_\nu$ is the square of the total energy in the center-of-mass system. At higher energies, when $(\mathscr{E}^2 - m_\Lambda^2)/m_\mu^2 \gg 1$, (10) is simplified and assumes the form

$$-\mathscr{E}^2(1 - m_p^2/\mathscr{E}^2)(1 - m_\Lambda^2/\mathscr{E}^2) \leqslant Q^2 \leqslant 0. \tag{11}$$

The expression for the antineutrino capture cross section at a given Q^2 is rather cumbersome and is given in the Appendix [formulas (A.1) to (A.3)]. Since the form factors are, apparently, small for large $|Q^2|$, in the limit $W_\nu \gg m_p$ the expression simplifies to

$$\begin{aligned}d\sigma = (2\pi)^{-1} G^2 d(-Q^2)\,[|f_1|^2 + |g_1|^2 \\ + (-Q^2)(|f_2|^2 + |g_2|^2)].\end{aligned} \tag{12}$$

In the case of the processes $\bar{\nu} + p \to n + \mu^+(e^+)$ and $\nu + n \to p + \mu^-(e^-)$ the form factors f_3 and g_2 go to zero as a result of isotopic invariance. The dependence of f_1 and f_2 on Q^2 in the Feynman–Gell-Mann scheme is moreover well known from experiments on the scattering of fast electrons,[15] and equals (μ_n and μ_p are the anomalous magnetic moments of the neutron and proton)

$$\begin{aligned}f_1 \approx \Phi(Q^2), \quad f_2 \approx \frac{\mu_p - \mu_n}{2m_p}\Phi(Q^2) = +\frac{3.71}{2m_p^2}\Phi(Q^2); \\ \Phi(Q^2) = (1 - Q^2a^2/12)^{-2}, \quad a = 0.8 \cdot 10^{-13} \text{ cm}.\end{aligned} \tag{13}$$

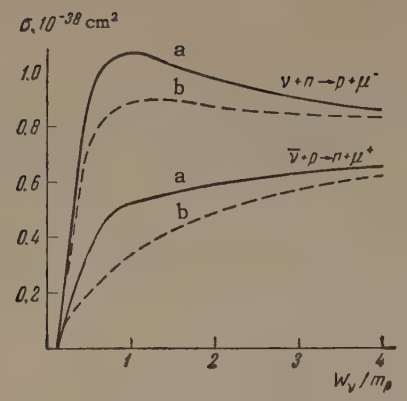

Dependence of cross sections for the reactions $\bar{\nu} + p \to n + \mu^+$ and $\nu + n \to p + \mu^-$ on the incident neutrino energy. The solid curves correspond to the possibility of case a) from formula (14), the dotted to case b).

At the present time it is impossible to say anything definite about the dependence of the form factors g_1 and g_3 on Q^2. It is only known that $g_1(0) = -1.2$. In [3-5] it was assumed that, like f_1 and f_2, $g_1 = -1.2\,\Phi(Q^2)$, and cross sections for the processes $\bar{\nu} + p \to n + e^+$ and $\nu + n \to p + e^-$ at various (anti) neutrino energies were calculated in this approximation. In both processes the "pseudoscalar" form factor g_3 yields a negligibly small contribution. In the reactions $\bar{\nu} + p \to n + \mu^+$ and $\nu + n \to p + \mu^-$, however, the contribution from g_3 is substantial. Goldberger and Treiman,[16] using dispersion techniques, found that $m_\mu g_3(-m_\mu^2) \approx 8\, g_1(0)$ when $Q^2 = -m_\mu^2$ and that $g_3(Q^2) \sim 1/(-Q^2 + m_\pi^2)$ at small Q^2. Such a dependence of g_3 on Q^2 cannot, strictly speaking, be extended to $-Q^2 \gg m_\pi^2$, but it can be adopted as an estimate. An alternate possibility is the weaker dependence $g_3 \sim \Phi(Q^2)$ for small Q^2.

The figure shows the total cross sections for the reactions $\bar{\nu} + p \to n + \mu^+$ and $\nu + n \to p + \mu^-$ as a function of incident (anti) neutrino energy W_ν. Relations (13) are adopted for the vector form factors. [Although f_1 falls off, apparently, more slowly than $\Phi(Q^2)$ when $-Q^2$ is of the order of $8 \times 10^{26} - 2 \times 10^{27}$ cm^{-2}, the correction necessitated by this fact would not be very great at these energies.] Two possibilities are considered for g_1 and g_3:

$$\text{a)}\ m_\mu g_3(Q^2) \approx 8 g_1(Q^2),\ g_1(Q^2) \approx -1.2\Phi(Q^2);$$

$$\text{b)}\ m_\mu g_3(Q^2) \approx 8 g_1(0)\,(m_\mu^2 + m_\pi^2)/(-Q^2 + m_\pi^2),\quad g_1(Q^2) \approx -1.2\Phi(Q^2). \qquad (14)$$

Cases a) and b) are shown in the figure by the solid and dotted lines respectively. When W_ν exceeds 500 Mev, the curve for case b) practically coincides with the cross section for the reaction that leads to the formation of e instead of μ. A similar agreement occurs for the curve of case a) only beyond 4 Bev. The difference is principally due to the component proportional to $g_3^2 m_\mu^2$, which in case a) is large for all Q^2, and in case b) is large only for small Q^2. The interference terms are insignificant since $g_3 m_\mu$ is multiplied by m_μ, which is small in comparison with the other energy quantities in (A.3). Analogously, the differential cross sections of electron and μ-meson reactions in case a) differ essentially in the term $g_3^2 m_\mu^2 (-Q^2) \times (-Q^2 + m_\mu^2)/2$ in (A.3). Therefore, if indeed $m_\mu g_3 \gg g_1$, then by investigating experimentally the quantity

$$\frac{8\pi}{G^2 m_\mu^2} \frac{(\mathscr{E}^2 - m_p^2)^2}{(-Q^2)(-Q^2 + m_\mu^2)} \left[\frac{d\sigma_\mu}{d(-Q^2)} - \frac{d\sigma_e}{d(-Q^2)} \right], \qquad (15)$$

we can determine with good accuracy the dependence of g_3 on Q^2. Here, of course, expression (15) must not depend on $\mathscr{E}^2$.

It is, no doubt, impossible to regard the hypotheses (14) as proved. There is no basis for assuming, for example, that f_1 and g_1 have the same order of magnitude for all Q^2. It can be noted that the cross sections for the processes $\bar{\nu} + p \to n + e^+$ and $\nu + n \to p + e^-$ differ only in the sign of the term containing $f_1 g_1$. If for some Q^2 one of these form factors is much smaller than the other, the cross sections in this region must coincide. Otherwise they will differ considerably.

Reactions (3), which involve the formation of strange particles, are also very interesting to study. When evaluating the order of magnitude of the cross sections it is possible to neglect in (A.3) or (12) the form factors f_2, g_2, f_3, and g_3 and consider that $f_1 = -g_1 = \text{const}$ when $-Q^2 \lesssim m_K^2$ and that $f_1 = g_1 = 0$ when $-Q^2 > m_K^2$.[10,14] In this approximation the cross sections for the processes

$$\bar{\nu} + p \to \Lambda + \mu^+ (e^+),\ \bar{\nu} + p \to \Sigma^0 + \mu^+ (e^+),\quad \bar{\nu} + n \to \Sigma^- + \mu^+ (e^+)$$

tend in the limit of $W_\nu \to \infty$ to the value $4 \times 10^{-39}\, |f_1|^2 \text{cm}^2$. If we assume that $|f_1|^2 \sim 1/20$, which is similar to what apparently occurs in the decay $\Lambda \to p + e^- + \bar{\nu}$, $\sigma \sim 2 \times 10^{-40} \text{cm}^2$. When $W_\nu = 1$ Bev the cross sections for the production of Λ and Σ hyperons reach 0.7 and 0.6 of the limiting value.

4. THE PROCESS $\mu^- + p \to \Lambda + \nu$

Considerable information about the weak interactions of strange particles can be obtained by studying the process

$$\mu^- + p \to \Lambda + \nu, \qquad (16)$$

as well as the completely analogous reactions $\mu^- + p \to \Sigma^0 + \nu$ and $\mu^- + n \to \Sigma^- + \nu$. A similar process involving the participation of an electron has been previously examined by one of the authors.[10] Great experimental difficulties are associated with the observation of this process, principally because of the fact that Λ hyperons are hard to detect against the large background.* As was observed several years ago by L. B. Okun', however, process (16) is more favorable in this respect. The fact is that the threshold for the photoproduction of π^- in the collision between a μ^- meson and nucleon, 166 Mev, exceeds the 82 Mev threshold for reaction (16). The thresholds for all other processes capable of leading to the formation of π^- mesons in a μ^--p interaction lie still higher. Thus in the energy region between the thresholds the Λ hyperon can be observed through the decay into a π^- meson ($\Lambda \to p + \pi^-$). This is impossible in the case of electrons, since the thresholds lie in the reverse order due to the smallness of m_e.

The expression for the matrix element of reaction (16) is analogous to that for (8), and the limits for variations of Q^2 [determined from Eq. (9)] are given by formula (10) if we make the exchanges $m_p \leftrightarrow m_\Lambda$ and $\mathscr{E} \to \mathscr{E}_1$, where $\mathscr{E}_1^2 \equiv (p_\mu + p_p)^2 = (m_p + m_\mu)^2 + 2m_p W_\mu$ and W_μ is the kinetic energy of the μ meson in the laboratory system.

The expression for the cross section of process (16) (if the beam of μ mesons is unpolarized) is given by formulas (A.4) — (A.3) of the Appendix. In the case of pure V-A coupling it will assume the form

$$d\sigma_0 = \frac{G^2}{2\pi} \frac{\mathscr{E}_1^2 - m_\Lambda^2}{[(\mathscr{E}_1^2 - m_p^2 - m_\mu^2)^2 - 4m_p^2 m_\mu^2]^{1/2}} \frac{f_1^2 d(-Q^2)}{|v_\mu|}, \qquad (17)$$

where v_μ is the velocity of the μ meson in the laboratory system. If f_1 is considered to be a constant, the total cross section is

$$\sigma_0 = \frac{G^2}{2\pi} \frac{f_1^2}{|v_\mu|} \mathscr{E}_1^2 (1 - m_\Lambda^2 / \mathscr{E}_1^2)^2. \qquad (18)$$

Again assuming $f_1^2 \sim 1/20$, we find that for the cross section at the photoproduction threshold ($W_\mu = 166$ Mev) $\sigma_0 = 0.7 \times 10^{-41}$ cm^2.

*B. Pontecorvo has indicated the interesting possibility of discovering Λ particles produced in the reaction $e^- + p \to \Lambda + \nu$. All π^0 mesons formed in the interaction of the beam of electrons with the target decay in the target. The π^0 mesons can appear in the space behind the target only as a result of the decay of a strange particle. Registering a π^0 meson is thus equivalent to observing a Λ.

Real μ mesons generated in $\pi_{\mu 2}$ or $K_{\mu 2}$ decay are always polarized. In this case the cross section for process (16) is given by the more complicated expression of (A.3) — (A.8), which for pure V-A coupling has the form

$$d\sigma = d\sigma_0 (1 - \zeta v_\mu),$$

where ζ is the polarization vector of the μ meson, definable as the average value of the spin in its rest system. According to (19), in pure V-A coupling azimuthal asymmetry of Λ hyperon emission does not arise, and the polarization of the μ meson leads only to the suppression or strengthening of the process according to whether the meson spin is directed forwards or backwards. We also point out that in the case of V-A coupling the Λ hyperon is completely polarized in a direction opposite to its own momentum in the center-of-mass system, independently of the polarization of the μ meson. If the meson spin is not parallel to its momentum and $f_1 \neq -g_1$, or if the contribution of other form factors is substantial, then, as follows from (A.4) and (A.7), azimuthal asymmetry of the type $p_\Delta \zeta_\perp$ arises in Λ-particle emission. When time parity is not conserved, an asymmetry of the type $p_\Delta [p_\mu \zeta]$ would also be added.

If ζ is expressed in terms of the μ and π meson momenta in the laboratory system, $d\sigma/d\sigma_0$ is according to (A.5) equal to

$$\varkappa = 2m_\mu^2 (E_\pi - E_\mu) / (m_\pi^2 - m_\mu^2) E_\mu, \qquad (20)$$

where E_π and E_μ are the total energies of the mesons in the laboratory system. Since

$$[E_\pi (m_\pi^2 + m_\mu^2) - p_\pi (m_\pi^2 - m_\mu^2)] / 2m_\pi^2 \leqslant E_\mu \leqslant [E_\pi (m_\pi^2 + m_\mu^2) + p_\pi (m_\pi^2 - m_\mu^2)] / 2m_\pi^2 \qquad (21)$$

($p_\pi = \sqrt{E_\pi^2 - m_\pi^2}$), in (20) χ varies within the limits

$$2m_\mu^2 / [(E_\pi - p_\pi)^2 + m_\pi^2] \geqslant \varkappa \geqslant 2m_\mu^2 / [(E_\pi + p_\pi)^2 + m_\pi^2]. \qquad (22)$$

When $E_\pi = 300$ Mev, for example, and when 74 Mev $\leq W_\mu = E_\mu - m_\mu \leq 187$ Mev, these limits are equal to 1.63 and 0.07, and when $E_\pi \gg m_\pi$, $2 \geq \chi \geq 0$. When studying reaction (16) the upper limit of χ decreases, since the left inequality in (21) must be replaced by $E_\mu \geq (m_\Lambda^2 - m_p^2 - m_\mu^2)/2m_p = 188$ Mev.

The authors thank L. B. Okun' and B. Pontecorvo for discussing the possibility of observing the reactions considered in Sec. 4.

APPENDIX

A. The differential cross section for the reaction $\bar{\nu} + p \to \Lambda + \mu^+$ can be written as

$$d\sigma = \frac{G^2}{4\pi} \frac{d(-Q^2)}{(\mathscr{E}^2 - m_p^2)^2} A, \qquad (A.1)$$

where A is a function of the invariants $\mathscr{E}^2 = (p_p + p_\nu)^2$, $Q^2 = (p_p - p_\Lambda)^2$, and $\Delta^2 = (p_p - p_\mu)^2$, of which only two are independent, since

$$\mathscr{E}^2 + Q^2 + \Delta^2 = m_p^2 + m_\Lambda^2 + m_\mu^2. \qquad (A.2)$$

The quantity $A(\mathscr{E}^2, Q^2, \Delta^2)$ is expressed in terms of the form factors $f_i(Q^2)$ and $g_i(Q^2)$ introduced into (8):

$$\begin{aligned}
A = {} & |f_1 - g_1|^2 (-\Delta^2 + m_\Lambda^2)(-\Delta^2 + m_p^2 + m_\mu^2) \\
& + |f_1 + g_1|^2 (\mathscr{E}^2 - m_p^2)(\mathscr{E}^2 - m_\Lambda^2 - m_\mu^2) \\
& + [|f_2|^2 + |g_2|^2]\{Q^2[(\mathscr{E}^2 - m_p^2)(\Delta^2 - m_\Lambda^2) \\
& + (\mathscr{E}^2 - m_\Lambda^2)(\Delta^2 - m_p^2)] - m_\mu^2[(m_\Lambda^2 - m_p^2)(\mathscr{E}^2 - \Delta^2) \\
& + \tfrac{1}{2}(-Q^2 + m_\mu^2)(m_p^2 + m_\Lambda^2 + Q^2)]\} \\
& + 2\,\mathrm{Re}\, f_2 g_2^* (m_\Lambda^2 - m_p^2)[Q^2(\mathscr{E}^2 - \Delta^2) + m_\mu^2(m_\Lambda^2 - m_p^2)] \\
& + \tfrac{1}{2}[|f_3|^2 + |g_3|^2] m_\mu^2 (-Q^2 + m_\mu^2)(-Q^2 + m_\Lambda^2 + m_p^2) \\
& + m_p m_\Lambda (-Q^2 + m_\mu^2)\{2[|g_1|^2 - |f_1|^2] \\
& + (2Q^2 + m_\mu^2)[|g_2|^2 - |f_2|^2] - m_\mu^2[|g_3|^2 - |f_3|^2]\} \\
& + [Q^2(\mathscr{E}^2 - \Delta^2) + m_\mu^2(m_\Lambda^2 - m_p^2)] \\
& \times 2\,\mathrm{Re}\,[f_1 g_2^* (m_\Lambda - m_p) - g_1 f_2^* (m_\Lambda + m_p) \\
& + (f_2 f_3^* + g_2 g_3^*)\tfrac{1}{2} m_\mu^2] \\
& + 2\,\mathrm{Re}\,(f_1 f_2^* + g_1 g_2^*) m_p [Q^2(Q^2 - m_p^2 + m_\Lambda^2) \\
& + m_\mu^2(\mathscr{E}^2 - m_\Lambda^2 - m_\mu^2)] \\
& + 2\,\mathrm{Re}\,(f_1 f_2^* - g_1 g_2^*) m_\Lambda [Q^2(Q^2 - m_\Lambda^2 + m_p^2) \\
& + m_\mu^2(\Delta^2 - m_p^2 - m_\mu^2)] + 2\,\mathrm{Re}\,(f_1 f_3^* + g_1 g_3^*) m_\mu^2 m_p \\
& \times (-\Delta^2 + m_\Lambda^2) + 2\,\mathrm{Re}\,(f_1 f_3^* - g_1 g_3^*) m_\mu^2 m_\Lambda (\mathscr{E}^2 - m_p^2).
\end{aligned} \qquad (A.3)$$

After renaming the indices, formulas (A.1) — (A.3) are of course correct for all the processes of antineutrino absorption in (3), and it is possible to neglect the contribution from f_3 and g_3 in reactions involving formation of e because of the smallness of m_e. In the case of the process $\bar{\nu} + p \to n + \mu^+(e^+)$ the form factors f_3 and g_2 reduce to zero. The cross section for the analogous process involving the absorption of a neutrino $[\nu + n \to p + \mu^-(e^-)]$ is also described by formulas (A.1) — (A.3) if we reverse the sign of g_1 and g_3.

B. For the reaction $\mu^- + p \to \Lambda + \nu$ with a polarized beam of μ^- mesons, the cross section in the laboratory system equals

$$\begin{aligned}
d\sigma = {} & \frac{G^2}{8\pi |v_\mu|} \frac{d(-Q^2)\,(d\varphi/2\pi)}{(\mathscr{E}_1^2 - m_p^2 - m_\mu^2)[(\mathscr{E}_1^2 - m_p^2 - m_\mu^2)^2 - 4m_p^2 m_\mu^2]^{1/2}} \\
& \times \{A_1 - 2m_p B\, p_\mu \zeta - 2m_\mu C\, p_\Lambda \zeta_\perp + 4m_p m_\mu D\, p_\Lambda [p_\mu \zeta]\},
\end{aligned} \qquad (A.4)$$

where φ is the azimuthal angle of the vector p_Λ, ζ is the depolarization vector of the μ meson, and $\zeta_\perp$ is its component orthogonal to the momentum ($\zeta_\perp = \zeta - p_\mu(\zeta p_\mu)/p_\mu^2$).

If μ mesons are produced in the decay of π^- mesons, they will be completely polarized along their own momentum in the π rest system. In the laboratory system

$$\zeta = -\frac{2m_\mu p_\pi}{m_\pi^2 - m_\mu^2} + \frac{W_\mu p_\mu}{(m_\pi^2 - m_\mu^2) p_\mu^2}[(m_\pi + m_\mu)^2 + 2m_\mu W_\pi], \qquad (A.5)$$

where W_π and W_μ are the kinetic energies of the mesons.

The expression for A_1 coincides with (A.3) if we substitute

$$\Delta^2 \to \mathscr{E}_1^2 \equiv (p_p + p_\mu)^2 = (m_p + m_\mu)^2 + 2m_p W_\mu,$$
$$\mathscr{E}^2 \to \Delta_1^2 = m_p^2 + m_\Lambda^2 + m_\mu^2 - \mathscr{E}_1^2 - Q^2.$$

The quantities B, C, and D are given by the formulas

$$B = B_1 - \frac{(\mathscr{E}_1^2 - m_p^2 - m_\mu^2)(\mathscr{E}_1^2 + Q^2 - m_p^2) - 2m_\mu^2 (m_\Lambda^2 + m_p^2 - Q^2)}{(\mathscr{E}_1^2 - m_p^2 - m_\mu^2)^2 - 4m_p^2 m_\mu^2} C, \qquad (A.6)$$

$$\begin{aligned}
B_1 = {} & |f_1 - g_1|^2 (\mathscr{E}_1^2 - m_\Lambda^2) + 2\,\mathrm{Re}\, f_2 g_2^* (m_\Lambda^2 - m_p^2)(\mathscr{E}_1^2 - m_\Lambda^2) \\
& + [|f_2|^2 + |g_2|^2][(-\Delta_1 + m_p^2)(-Q^2 - m_\Lambda^2 + m_p^2) \\
& + \tfrac{1}{2} m_\mu^2 (m_\Lambda^2 + m_p^2 - Q^2)] - \tfrac{1}{2}[|f_3|^2 + |g_3|^2] m_\mu^2 (m_\Lambda^2 \\
& + m_p^2 - Q^2) + m_p m_\Lambda \{2[|g_1|^2 - |f_1|^2] \\
& + (2Q^2 - m_\mu^2)[|g_2|^2 - |f_2|^2] + m_\mu^2[|g_3|^2 - |f_3|^2]\} \\
& + 2\,\mathrm{Re}\,[f_1 g_2^* (m_\Lambda - m_p) - g_1 f_2^* (m_\Lambda + m_p)](\mathscr{E}_1^2 - m_\Lambda^2) \\
& - \mathrm{Re}\,(f_2 f_3^* + g_2 g_3^*)[Q^2(\Delta_1 - m_\Lambda^2) + m_\mu^2(m_\Lambda^2 - m_p^2)] \\
& + \mathrm{Re}\,(f_1 f_2^* + g_1 g_2^*) m_p (\mathscr{E}_1^2 - Q^2 - 2m_\Lambda^2 + m_p^2) \\
& + \mathrm{Re}\,(f_1 f_2^* - g_1 g_2^*) m_\Lambda (\Delta_1^2 - 2Q^2 - 2m_p^2 + m_\Lambda^2 + m_\mu^2) \\
& + \mathrm{Re}\,(f_1 f_3^* + g_1 g_3^*) m_p (-\Delta_1^2 + m_\Lambda^2 + m_\mu^2) \\
& + \mathrm{Re}\,(f_1 f_3^* - g_1 g_3^*) m_\Lambda (-\Delta_1^2 + m_\Lambda^2 - m_\mu^2),
\end{aligned} \qquad (A.7)$$

C is obtained from (A.7) by reversing the sign of g_1, f_3, and g_3 and by the substitution $m_\Lambda \leftrightarrow m_p$ and $\mathscr{E}_1^2 \leftrightarrow \Delta_1^2$;

$$\begin{aligned}
D = {} & \mathrm{Im}\,[(f_1 f_2^* - g_1 g_3^*)(m_\Lambda - m_p) + (f_1 f_3^* - g_1 g_2^*)(m_\Lambda + m_p) \\
& - (f_2 f_3^* + g_2 g_3^*) Q^2].
\end{aligned} \qquad (A.8)$$

D is different from zero only when time parity is not conserved, since otherwise all the form factors are real.

In conclusion let us observe that if it is possible to neglect m_μ^2 in (A.3), (A.7), and (A.6),

$$(\mathscr{E}_1^2 - m_p^2) B_1 + (\Delta_1^2 - m_\Lambda^2) C = A_1, \qquad (A.9)$$

so that in (A.4)

$$A_1 - 2m_p B p_\mu \zeta = A_1 (1 - v_\mu \zeta). \qquad (A.10)$$

Note added in proof (July 13, 1961). Analogously to the situation occurring in the annihilation of an electron-positron pair (recently noted by Baĭer and Sokolov[17]), there is a resonance in the reaction $\bar{\nu} + e^- \to \bar{\nu} + \mu^-$, connected with the pos-

sibility of a process going via an intermediate π^- meson. Near resonance the cross section is described by the formula

$$\sigma = 16\pi\lambda^2 \left(\frac{m_e}{m_\mu}\right)^2 \frac{m_\pi^4}{(m_\pi^2 - m_\mu^2)^2} \frac{(\Gamma m_\pi)^2}{(\mathscr{E}^2 - m_\pi^2)^2 + (\Gamma m_\pi)^2},$$

where λ is the Compton length of the π meson and Γ is the probability of its decay. The height of the peak is 1.3×10^{-4} mb, but unfortunately its width is insignificantly small: $\Gamma \approx 3 \times 10^{-8}$ ev.

The same formula is correct for the cross section of the process $\bar{\nu} + e^- \to \bar{\nu} + e^-$ with the additional small factor

$$(m_e/m_\mu)^2 [1 - (m_\mu/m_\pi)^2]^{-2} = 1{,}3 \cdot 10^{-4}.$$

[1] B. M. Pontecorvo, JETP **37**, 1751 (1959), Soviet Phys. JETP **10**, 1236 (1960).

[2] M. Schwartz, Phys. Rev. Lett. **4**, 306 (1960).

[3] T. D. Lee and C. N. Yang, Phys. Rev. Lett. **4**, 307 (1960).

[4] N. Cabibbo and R. Gatto, Nuovo cimento **15**, 304 (1960).

[5] Y. Yamaguchi, Progr. Theoret. Phys. **23**, 1117 (1960).

[6] Collection, K fizike neĭtrino vysokikh énergii (On the Physics of High Energy Neutrinos), Dubna, 1960.

[7] R. P. Feynman and M. Gell-Mann, Phys. Rev. **109**, 193 (1958).

[8] V. M. Shekhter, JETP **34**, 257 (1958), Soviet Phys. JETP **7**, 179 (1958).

[9] V. B. Berestetskii and I. Ya. Pomeranchuk, JETP **36**, 1321 (1959), Soviet Phys. JETP **9**, 936L (1959).

[10] V. M. Shekhter, JETP **38**, 1343 (1960), Soviet Phys. JETP **11**, 967L (1960).

[11] D. I. Blokhintsev, Usp. Fiz. Nauk **62**, 381 (1957).

[12] W. R. Frazer and J. R. Fulco, Phys. Rev. Lett. **2**, 365 (1959).

[13] L. B. Okun', Usp. Fiz. Nauk **68**, 449 (1959), Ann. Rev. Nuc. Sci. **9**, 61 (1959).

[14] V. M. Shekhter, JETP **36**, 1299 (1959), Soviet Phys. JETP **9**, 920L (1959).

[15] Hofstadter, Bumiller, and Yearian, Revs. Modern Phys. **30**, 482 (1958).

[16] M. L. Goldberger and S. B. Treiman, Phys. Rev. **111**, 354 (1958).

[17] V. N. Baĭer and V. V. Sokolov, JETP **40**, 1233 (1961), Soviet Phys. JETP **13**, 866 (1961).

Translated by Mrs. J. D. Ullman
105

ELECTROMAGNETIC FORM FACTOR OF THE NEUTRAL PION

HSIEN TING-CH'ANG and HU SHIH-K'E

Joint Institute for Nuclear Research

Submitted to JETP editor March 22, 1961

J. Exptl. Theoret. Phys. (U.S.S.R.) 41, 600-602 (August, 1961)

The possibility of determining the electromagnetic form factor of the π^0 meson in the process $e^+ + e^- \to \pi^0 + \gamma$ is discussed.

ONE may hope that it will soon be possible to perform experiments using head-on electron and positron beams from the accelerator. In this connection it is interesting to note that the electromagnetic form factor of the π^0 meson can be measured with the help of the reaction

$$e^+ + e^- \to \pi^0 + \gamma. \qquad (1)$$

Below we shall consider the dependence of this process on the form factor of the π^0 meson. Recognizing the fact that the effective Hamiltonian for the interaction of the pseudoscalar π^0 meson with electromagnetic fields must be invariant under spatial translations and rotations, we write it in the form

$$H_i = \iiint d^4x\, d^4y\, d^4z \widetilde{F}\,((x-z)^2,\ (y-z)^2,$$
$$\times (x-y)^2)\, \varepsilon_{\alpha\beta\rho\sigma} \frac{\partial A_\alpha(x)}{\partial x_\beta} \frac{\partial A_\rho(y)}{\partial y_\sigma} \Phi_0(z), \qquad (2)$$

where Φ_0 and A_α are the field of the pseudoscalar π^0 meson and the electromagnetic field, and $\epsilon_{\alpha\beta\rho\sigma}$ is the completely antisymmetric unit tensor of fourth rank.

Restricting ourselves to lowest order perturbation theory for the electromagnetic interaction between the electron and the positron, we can draw the Feynman graph for process (1) as shown in Fig. 1. The matrix element corresponding to this graph has the form

$$\langle q, k | S | p_e, p_p \rangle$$
$$= -\frac{e}{(2\pi)^2} \frac{1}{\sqrt{q_0 k_0}} \varepsilon_{\mu\beta\rho\sigma} (v^-(-\mathbf{p}_p)\, \gamma_\mu u(\mathbf{p}_e))\, e_\rho$$
$$\times (p_p + p_e)_\beta\, k_\sigma\, (p_e + p_p)^{-2}$$
$$\times F((p_e + p_p)^2,\ 0,\ m_{\pi^0}^2)\, \delta(p_p + p_e - q - k), \qquad (3)$$

where p_p, p_e, k and q are the four-momenta of the positron, electron, photon, and π^0 meson, e_ρ is the polarization vector of the photon,

FIG. 1

$F(k_1^2, k_2^2, k_3^2)$ is the Fourier transform of the function $\widetilde{F}$ in (2) in momentum space and is, by definition, the electromagnetic form factor of the π^0 meson.

The total cross section for process (1) is

$$\sigma(E) = \frac{e^2}{4\pi} \frac{1}{6} \frac{(1-x)^3 (1+2y)}{(1-4y)^{1/2}} F^2(-E^2,\ 0,\ m_{\pi^0}^2), \qquad (4)$$

where E is the total energy in the center of mass system, $x = m_{\pi^0}^2/E^2$, $y = m_e^2/E^2$, and m_{π^0} and m_e are the masses of the π^0 meson and the electron. We see from (4) that the measurement of $\sigma(E)$ yields information on the electromagnetic form factor of the π^0 meson.

In order to estimate the magnitude of $\sigma(E)$, we replace $F^2(-E^2, 0, m_{\pi^0}^2)$ in (4) by $F^2(0, 0, m_{\pi^0}^2)$, which is connected with the lifetime of the π^0 meson, τ, through the relation

$$F^2(0, 0, m_{\pi^0}^2) = 8\pi / m_{\pi^0}^3 \tau. \qquad (5)$$

Taking $\tau = (2.3 \pm 0.8) \times 10^{-16}$ sec,[1] we find from (4)

$$\sigma(E) = f(E)\, \sigma, \qquad \sigma = (1.4^{+0.7}_{-0.4}) \cdot 10^{-35}\ \text{cm}^2, \qquad (6)$$

the function f(E) is shown in Fig. 2.

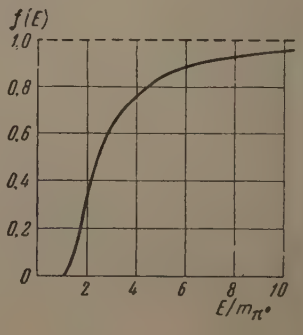

FIG. 2. Dependence of the function f(E) on the energy of the electron-positron pair.

It is also interesting to note that the above-mentioned experiment yields some information on the contribution of the intermediate 3π state to the form factor of the π^0 meson.

Using the standard technique of dispersion relations, we can easily show (see, for example,[2]) that

$$\frac{1}{2\pi\sqrt{\pi q_0}}\varepsilon_{\mu\beta\rho\sigma}\bar{v}\gamma_\mu u\cdot e_\rho K_\beta k_\sigma F(K^2, 0, m_{\pi^0}^2)$$
$$= e_\rho\bar{v}\gamma_\mu u\int d^4z e^{-i(k+K)z/2}\left\langle \mathbf{q}\left|T\left(I_\mu\left(\frac{z}{2}\right)I_\rho\left(-\frac{z}{2}\right)\right)\right|0\right\rangle, \quad (7)$$

where $I_\rho(z/2)$ is the current of strongly interacting particles. To simplify the formulas, we write further

$$F(K^2, 0, m_{\pi^0}^2) \equiv F(\nu), \quad (8)$$

where $\nu = -K^2$. Using (7), it is easily shown that $F(\nu)$ is an analytic function in the ν plane with a cut from $4m_{\pi^0}^2$ to ∞. The dispersion relation for $F(\nu)$ is then written in the form

$$F(\nu) = F(0) + \frac{\nu}{\pi}\int_{4m_{\pi^0}^2}^{\infty}\frac{\operatorname{Im}F(\nu')}{\nu'(\nu'-\nu)}d\nu', \quad (9)$$

where $\operatorname{Im}F(\nu')$ is given by

$$\frac{1}{2\pi\sqrt{\pi q_0}}\varepsilon_{\mu\beta\rho\sigma}\bar{v}\gamma_\mu u\cdot e_\rho K_\beta k_\sigma \operatorname{Im}F(K^2, 0, m_{\pi^0}^2)$$
$$= (2\pi)^4\bar{v}\gamma_\mu u\sum_n\langle \mathbf{q}|I_\rho(0)|n\rangle\langle n|I_\mu(0)|0\rangle\,\delta^4(K-P_n), \quad (10)$$

where $n = 2\pi, 3\pi, \ldots$ We shall restrict our discussion to the two intermediate states $n = 2\pi$ and 3π.

The contribution from the intermediate 2π state can be determined from the knowledge of: 1) the structure of the nucleon (the vertex function $\langle 2\pi|I_\mu(0)|0\rangle$) and 2) the photoproduction of the pion on a nucleon (the vertex function $\langle \mathbf{q}|I_\rho(0)|2\pi\rangle$). It can then be expected that we obtain an estimate of the contribution of the intermediate 3π state by subtracting the contribution of the intermediate 2π state from $F(\nu)$. Since the problems 1) and 2) have not yet been solved with sufficient accuracy, we are unable to make this estimate. We shall only discuss what conclusions can be drawn from a measurement of $F(\nu)$ in this situation.

It is seen at once from (9) that for small $\nu(\nu \ll 4m_{\pi^0}^2)$

$$F(\nu) \sim F(0) + a\nu, \quad (11)$$

where a is some contsant. For larger $\nu(\nu < 4m_{\pi^0}^2)$, when the contributions from the intermediate 2π and 3π states are both in resonance and have about the same resonance energy, we have

$$F(\nu) \sim F(0) + b\nu/(\nu_0 - \nu), \quad (12)$$

where b is a constant and ν_0 is the square of the resonance energy of the intermediate 2π state. If the experiment indicates that the form factor of the π^0 meson has the form (12), we conclude that either the intermediate 3π state gives a negligible contribution to the form factor or its contribution is appreciable but its resonance energy is about equal to the resonance energy of the 2π state. If, on the other hand, the experiment shows that $F(\nu)$ has a form which is very different from (12), this will mean that the intermediate 3π state gives a large contribution and either has no resonance character or, if it does have one, then the resonance energy is far away from ν_0.

The authors thank Prof. M. A. Markov, who directed their attention to this problem, and also Chou Kuang-chao and the participants of Prof. Markov's seminar for discussions.

[1] Glasser, Seeman, and Stiller, Proc. of the 1960 Ann. Int. Conf. on High Energy Phys. at the University of Rochester, p. 30 (1960).

[2] S. M. Berman and D. A. Geffen, Nuovo cimento 18, 1192 (1960).

Translated by R. Lipperheide
106

A NEUTRAL MODEL FOR INVESTIGATION OF $\pi\pi$ SCATTERING

A. V. EFREMOV, CHOU HUNG-YUAN, and D. V. SHIRKOV

Joint Institute for Nuclear Research; Institute of Mathematics, Siberian Division, Academy of Sciences, U.S.S.R.

Submitted to JETP editor March 20, 1961

J. Exptl. Theoret. Phys. (U.S.S.R.) **41**, 603-611 (August, 1961)

An equation describing the scattering of low energy neutral pseudoscalar mesons is investigated. A general solution of the equation is derived, similar to that obtained by Castillejo, Dalitz, and Dyson[12] for the Low equation. Two different types of asymptotic behavior of the solutions at high energies are possible. If the amplitude decreases as $(\ln E)^{-1}$ at high energies, the solution corresponds to the renormalizable perturbation theory. In the second case, when the amplitude decreases as E^{-4}, the solution does not correspond to perturbation theory. In a certain sense it can be connected with the nonrenormalizable Lagrangian $[(\partial\varphi/\partial x_n)(\partial\varphi/\partial x_n)]^2$. This second solution possesses some interesting properties. In particular, it becomes degenerate when the interaction is switched off.

1. INTRODUCTION

ATTEMPTS have been made in recent years to construct a theory of strong interactions in the low-energy region by starting from the analytic properties of the scattering amplitudes in the form proposed by Mandelstam[1] and from the unitarity conditions.

The arguments were based on the premise that the phenomena in the low-energy region admit of description in closed form. Mathematically this hypothesis reduces to the assumption that the behavior of an analytic function is determined in a small region by the near-lying singularities.[2]

The restriction to the low-energy region enables us to write down an approximate unitarity condition in which only two-particle intermediate states are taken into account. This approximate unitarity condition, together with the spectral representation, makes it possible to write down[1,3] a closed system of nonlinear integral equations for the scattering amplitude as a function of two variables.

In view of the complexity of such equations, still another approximation is made by representing the scattering amplitude in the form of a small number of first terms of its expansion and Legendre polynomials. Chew and Mandelstam[4] have obtained in this manner a closed system of nonlinear integral equations for the lower partial waves of the pion-pion scattering. Subsequently analogous equations were obtained for several other processes (see[5,6] and others). In the analysis of the anti-Hermitian part of the amplitude in the cross integral, these authors use analytic continuations in the Legendre polynomials into the region $|\cos\theta| > 1$. But the use of only the first terms of the Legendre series leads to large errors,[7-9] which are particularly large at high-energy crossing processes. The integrals of the higher partial waves are found to be divergent, and the solutions of the equations are unstable against small perturbations in the region of high energies. Analytic continuation in Legendre polynomials, in particular, led to contradictions[10] when attempts were made to determine the parameters of the resonance of the p-phase of $\pi\pi$ scattering from the πN scattering and from the nucleon structure, and also to the impossibility of obtaining a stable solution of $\pi\pi$ scattering equations with large p-wave.[11]

Thus, the use of analytic continuation in Legendre polynomials leads in final analysis to a contradiction of the original assumption that the low-energy region is closed. The foregoing difficulties can raise doubts concerning the possibility of constructing a closed theory of strong interactions at lower energies. In our opinion, however, there are still not enough grounds for such pessimism. It is quite possible that the foregoing difficulties can be overcome by a somewhat different approach, proposed in[8,9], to the derivation of equations for the partial waves. In this deduction no use is made of analytic continuations in Legendre polynomials, and the equations for the partial waves differ from the Chew-Mandelstam

equations in the structure of the crossing integrals. These integrals have, in particular, better convergence at high energies.

The aforementioned program may make it possible to describe the phenomena at low energies without internal contradictions. For this purpose, naturally, it is necessary to solve numerically the equations for partial waves of different processes, and above all for the pion-pion scattering. The latter were obtained by Hsien Ting-ch'an, Ho Tso-hsin, and Zoellner, and in simpler form under the assumption that the d and f waves are negligibly small compared with the s and p waves, as was done in [8]. In the derivation of these equations, only rigorously proved dispersion relations for forward scattering were used.

To solve these equations numerically it is necessary to have an idea of at least some general properties of the solutions of equations of this type. However, an analytic investigation of the equations derived in [8] is a complicated matter. We therefore consider first the neutral analogue of the system of equations obtained in [8]. This analysis will lead to several important consequences, which must be taken into consideration in the analytic investigation and numerical solution of such equations.

2. EQUATION AND BEHAVIOR OF SOLUTION AT HIGH ENERGIES

In the case considered here, the scattering amplitude A is a scalar function of three ordinary invariant arguments

$$s = 4(\nu + 1), \qquad u = -2\nu(1 + c), \qquad t = -2\nu(1 - c), \tag{2.1}$$

where $\nu = q^2/\mu^2$ and $c = \cos\theta$; q and θ are the momentum and scattering angle in the center-of-mass system. By virtue of the crossing symmetry, A is symmetrical under commutation of any pair of arguments (2.1). Consequently its Legendre series contains only even l. In accordance with our program,[8,9] we identify the forward scattering amplitude with the s-wave

$$A(\nu, c) = A_0(\nu) \equiv A(\nu). \tag{2.2}$$

Using the symmetry of the amplitude with respect to commutation of s and u, and taking into account the fact that

$$A(\nu) = \lim_{\varepsilon \to +0} A(\nu + i\varepsilon),$$

we obtain

$$A(-\nu - 1) = A^*(\nu). \tag{2.3}$$

The unitarity condition for the s-wave can be written in the form

$$\mathrm{Im}A(\nu) = K(\nu)|A(\nu)|^2, \qquad \nu > 0;$$

$$K(\nu) = \sqrt{\nu/(\nu + 1)}. \tag{2.4}$$

This formula is accurate only up to the threshold of the first inelastic process at $\nu = 3$. We shall assume, however, that (2.4) is valid for all positive ν, presupposing that this assumption hardly influences the solution at small ν. Formula (2.4) limits the function $A(\nu)$, and consequently in writing the dispersion relation it is sufficient to employ one subtraction, which we perform at the symmetrical point $\nu = -1/2$. We obtain

$$A(\nu) = \lambda + \frac{\nu + 1/2}{\pi} \int_0^\infty \frac{\mathrm{Im}\, A(\nu')}{\nu' + 1/2} \left\{ \frac{1}{\nu' - \nu} + \frac{1}{\nu' + \nu + 1} \right\} d\nu'. \tag{2.5}$$

From (2.5) it is seen that the assumption

$$\lim_{\nu \to \infty} \mathrm{Im}\, A(\nu) = C > 0$$

leads to a logarithmic growth of the real part, and consequently, to a contradiction. Consequently $A(\infty) = 0$, and we can therefore write the equation for $A(\nu)$ without subtraction:

$$A(\nu) = \frac{1}{\pi} \int_0^\infty \mathrm{Im}\, A(\nu') \left\{ \frac{1}{\nu' - \nu} + \frac{1}{\nu' + \nu + 1} \right\} d\nu'. \tag{2.6}$$

From (2.6) it also follows that

$$\lambda = \frac{2}{\pi} \int_0^\infty \frac{\mathrm{Im}\, A(\nu')}{\nu' + 1/2}\, d\nu' > 0. \tag{2.7}$$

Thus, Eq. (2.6) without subtraction is mathematically equivalent to Eq. (2.5) with subtraction. It follows therefore that the arbitrariness in the solution, connected with the parameter λ, is not a consequence of the subtraction.

3. SOLUTION OF THE EQUATION

We first introduce a new variable

$$\omega = (2\nu + 1)^2, \quad A(\nu) = B(\omega). \tag{3.1}$$

Equations (2.4) and (2.6) assume the form

$$\mathrm{Im}\, B(\omega) = k(\omega)|B(\omega)|^2, \qquad \omega > 1;$$

$$k(\omega) = [(\sqrt{\omega} - 1)/(\sqrt{\omega} + 1)]^{1/2} = K(\nu) \tag{3.2}$$

and

$$B(\omega) = \frac{1}{\pi} \int_1^\infty \frac{\mathrm{Im}\, B(\omega')}{\omega' - \omega}\, d\omega'. \tag{3.3}$$

Equation (3.3) is solved by the method of Castillejo, Dalitz, and Dyson.[12] We consider for this purpose the function $B(z)$ in the complex plane $z = \omega + iy$. The function $B(z)$ has the fol-

lowing properties: 1) it is analytic in the plane z with cut [1, ∞), and

$$B^*(z) = B(z^*), \qquad \operatorname{Im} B(\omega + i0) = k(\omega)\,|B(\omega + i0)|^2;$$

2) it is a generalized R-function, i.e.,

$$\operatorname{Im} B(z) = \lambda(z) \operatorname{Im} z,$$

$$\lambda(z) = \frac{1}{\pi}\int_1^\infty k(\omega')\,\frac{|B(\omega')|^2}{|\omega' - z|^2}\,d\omega' > 0,$$

consequently B(ω) has zeros nowhere except on the real axis and at an infinitely remote point; 3) when $\omega \le 1$ we have B(ω) > 0; 4) it can have any number of isolated zeros on the segment of (1, ∞).

Let us consider the function

$$H(z) = 1/B(z). \tag{3.4}$$

H(z) has the following properties: 1) it is analytic and in complex plane with cut [1, ∞), whereupon H*(z) = H(z*) and Im H(ω + i0) = −K(ω) on the cut; 2) it is a generalized R-function and consequently has no zeros if Im z ≠ 0; 3) it has no poles anywhere except at (1, ∞), where any number of isolated poles of first order is possible (this follows from 2), since higher-order poles do not have the properties of the R-function); 4) it has no zeros on the real axis.

We can therefore write the following general expression for H(z):

$$H(z) = \frac{1}{\lambda} - \frac{z}{\pi}\int_1^\infty \frac{k(\omega')\,d\omega'}{\omega'(\omega' - z)} - cz - zR(z), \tag{3.5}$$

where

$$R(z) = \sum_n \frac{R_n}{\omega_n(\omega_n - z)}, \qquad 1 < \omega_n < \infty. \tag{3.6}$$

Let us verify the property 2). From (3.5) we have

$$\operatorname{Im} H(z) = -\operatorname{Im} z\,(\lambda'(z) + c + \sum_n R_n/|\omega_n - z|^2),$$

with

$$\lambda'(z) = \frac{1}{\pi}\int_1^\infty \frac{k(\omega')\,d\omega'}{|\omega' - z|^2} > 0.$$

It follows therefore that

$$R_n \geqslant 0, \qquad c \geqslant 0. \tag{3.7}$$

Let us verify now property 4). When ω < 1 H(ω) is a monotonically decreasing function and in order for it not to have any zeros on this interval it is therefore sufficient to have

$$1/\lambda \geqslant I(1)/\pi + c + R(1), \tag{3.8}$$

where

$$I(\omega) = \omega\int_1^\infty \frac{k(\omega')\,d\omega'}{\omega'(\omega' - \omega)} = \pi - 2\sqrt{x}\,Q_0(\sqrt{x}) - \frac{2}{\sqrt{x}}\,Q_0\left(\frac{1}{\sqrt{x}}\right),$$

$$x = \frac{\nu}{\nu + 1}, \tag{3.9}$$

and $Q_0(x) = \frac{1}{2}\ln[(x+1)/(x-1)]$ is the Legendre function of the second kind.

As a result we obtain a solution of (3.3) in the form

$$B(\omega) = \lambda/[1 - \lambda I(\omega)/\pi - \lambda c\omega - \lambda\omega R(\omega)]. \tag{3.10}$$

Here R(ω) is determined from (3.6) while the constants γ, c, and R_n satisfy the conditions (3.7) and (3.8). The limitation (2.7) is a consequence of these conditions.

4. COMPARISON WITH PERTURBATION THEORY

Let us establish the correspondence between (3.10) and the results of perturbation theory. Assuming λ to be small and expanding the denominator of (3.10), we obtain

$$A(\nu) = \lambda + \frac{\lambda^2}{\pi} I[(2\nu + 1)^2] + \lambda^2 c\omega + \lambda^2\omega R(\omega) + O(\lambda^3). \tag{4.1}$$

The first two terms of (4.1) correspond to the diagram of first and second orders of perturbation theory, based on the Lagrangian

$$L_{int}^{(0)} = (4\pi/3)\,\lambda\varphi^4. \tag{4.2}$$

The fourth term corresponds to the pole contributions of the diagrams corresponding to the second order of perturbation theory for a Lagrangian of the following form (see in this connection Dyson's paper[13])

$$L_{int}^{(1)} = \sum_n g_n \Phi_n(x)\,\varphi^2(x), \tag{4.3}$$

where the fields Φ_n describe unstable particles with masses $m_n > 2$. The correspondence between g_n, λ, m_n, ω_n, and R_n can be readily established in perturbation theory.

The third term can be set in correspondence with the non-renormalized Lagrangian

$$L_{int}^{(2)} = f\left\{\left(\frac{\partial\varphi}{\partial x_n}\frac{\partial\varphi}{\partial x_n}\right)^2 - \frac{\varphi^4}{3}\right\}, \tag{4.4}$$

where $f = 2\pi\lambda^2 c$. Naturally, the correspondence with the Lagrangian (4.4) is arbitrary to a higher degree, since we cannot construct a consistent perturbation theory for such a Lagrangian. However, as shown by one of us (A.E.), such a correspondence can be established in the nonrelativistic theory.

We defer the discussion of this interesting fact and confine ourselves at the present time to an

analysis of the terms of (4.1) corresponding to the Lagrangian (4.2).

Calculating the s-wave, we obtain from (4.2)

$$A_{\text{p.t.}}(\nu) = \lambda_0 + \frac{\lambda_0^2}{\pi} A^{(2)}_{\text{p.t.}}(\nu) + \ldots, \tag{4.5}$$

where the amplitude is renormalized at the point x $\nu = 0$, i.e., $\lambda_0 = A_{\text{p.t.}}(0)$ and

$$A^{(2)}_{\text{p.t.}} = 6 - 2\sqrt{x}\,Q_0(\sqrt{x}) - \frac{4}{\sqrt{x}}\,Q_0\left(\frac{1}{\sqrt{x}}\right) - 2\frac{1-x}{x}\,Q_0^2\left(\frac{1}{\sqrt{x}}\right). \tag{4.6}$$

Expressions (4.5) and (4.6) must be compared with the first terms of (4.1), which can be written in the new normalization in the form (4.5), with

$$A^{(2)}_{\text{i.e.}} = 2 - 2\sqrt{x}\,Q_0(\sqrt{x}) - \frac{2}{\sqrt{x}}\,Q_0\left(\frac{1}{\sqrt{x}}\right). \tag{4.7}$$

Let us compare the second-order terms in (4.6) and (4.7). Near the threshold we obtain: a) from perturbation theory

$$A^{(2)}_{\text{p.t.}} \approx -\tfrac{8}{3}x - \tfrac{52}{45}x^2 - \tfrac{248}{315}x^3 + \ldots;$$

b) from the solution of the integral equation

$$A^{(2)}_{\text{i.e.}} \approx -\tfrac{8}{3}x - \tfrac{16}{15}x^2 - \tfrac{24}{35}x^3 + \ldots.$$

At the threshold of the first inelastic process we get for $\nu = 3$

$$A^{(2)}_{\text{p.t.}}(3) = -3.521, \qquad A^{(2)}_{\text{i.e.}}(3) = -3.323.$$

We see therefore that in the region of low energies the solution of the integral equation corresponds with good accuracy to the perturbation-theory results. The error in the second-order term amounts at $\nu = 3$ only to 6 percent. This agreement confirms the hypothesis that the low-energy region can be described in closed form.

5. RESONANT BRANCH OF SOLUTION

It follows from (3.10) that as $\nu \to \infty$ the solution admits of two different asymptotic approximations:

$$A(\nu) \approx \pi / 2 \ln \nu, \tag{5.1}$$

corresponding to the absence of non-renormalizable interactions, and

$$A(\nu) \approx -1/c\nu^2, \tag{5.2}$$

which corresponds to the non-renormalizable Lagrangian (4.4). These asymptotic expansions do not depend on the part of the R-function corresponding to the unstable particles. We shall henceforth confine ourselves for simplicity to the case when there are no unstable particles or, what is equivalent, to the case when the phase does not vanish when $0 < \nu < \infty$. Then the solution does not admit of resonance in the case (5.1), and is resonant in the case of (5.2) and for small λ at the point

$$\nu_r = \tfrac{1}{2}\{(\lambda c)^{-1/2} - 1\} = \tfrac{1}{2}\{\sqrt{\pi\lambda/2f} - 1\}. \tag{5.3}$$

If λ and f are of the same order of magnitude, the resonance is in the low-energy region.

The resonant solution for small λ can be written in the form

$$A(\nu) = \frac{\lambda}{2} \Big/ \left[1 - \frac{2\nu+1}{2\nu_r+1} - i\frac{\lambda}{2}K(\nu)\,\theta(\nu)\right] + \frac{\lambda}{2} \Big/ \left[1 + \frac{2\nu+1}{2\nu_r+1} + i\frac{\lambda}{2}K(-1-\nu)\,\theta(-1-\nu)\right]. \tag{5.4}$$

In the limit, as $\lambda \to 0$, the imaginary part of $A(\nu)$ is approximated by the δ-functions:

$$\operatorname{Im} A(\nu) \approx \tfrac{1}{2}\pi\lambda\left(\nu_r + \tfrac{1}{2}\right)\{\delta(\nu - \nu_r) - \delta(\nu + \nu_r + 1)\}, \tag{5.5}$$

and the real part is approximated by the pole terms

$$\operatorname{Re} A(\nu) \approx \frac{\lambda}{2}\left(\nu_r + \frac{1}{2}\right)\left\{\frac{1}{\nu_r - \nu} + \frac{1}{\nu_r + \nu + 1}\right\}. \tag{5.6}$$

Thus, for fixed ν_r, the width of the resonance tends to zero in proportion to λ, and at $\lambda = 0$ we obtain a non-zero solution. The scattering phase changes abruptly from 0 to π at the resonance point ν_r, the position of which is arbitrary. Thus, the solution is degenerate when $\lambda = 0$.

We note that in this case the d-wave A_2 will be proportional to the first degree of λ. It is expressed, however, in terms of a crossing integral with large denominator and is consequently small. Thus, for example, when $\nu_r = 3$ and $0 < \nu < 6$, the numerical estimates yield

$$5A_2(\nu)/A_0(\nu) \lesssim 6\%.$$

It is quite probable that the solutions for the charged case also have an arbitrariness of the type (3.10). It can be shown that the solutions of the charged system should decrease at infinity. In addition to the logarithmic branch, corresponding to renormalized perturbation theory, branches can exist in which the decrease at infinity is faster. When the interactions are turned off, these branches should lead to discontinuous phases, similar to what was described above.

Let us make a few remarks on the possibility of obtaining the solutions (3.10) by the "N/D method" of Chew and Mandelstam (see [4]).

The form of the integral representation for the function D depends essentially on the asymptotic form of the phase as $\nu \to \infty$. This representation

is determined with accuracy to a polynomial of degree n,[14,15] where

$$n = [\delta(0) - \delta(\infty)]/\pi.$$

The choice of representation in the form (V.12) of [4] corresponds to n = 0. By the same token, Chew and Mandelstam have earlier excluded the possibility of an odd number of resonances in the partial waves. Therefore the equations such as (V.11) and (V.12) of [4] cannot describe solutions of the form (5.4). Resonant solutions such as (5.4) call for the use of a second subtraction in (V.12).

We note that a similar conclusion was reached by Taylor in his latest paper.[16]

We note also that in our opinion the equations of the "N/D method," such as (V.11) and (V.12), cannot ensure crossing symmetry of the real part of the amplitude.

6. DISCUSSION OF RESULTS

Let us make first one formal remark. Solutions (5.1) and (5.2) recall in many respects the model expressions for the Green's functions in the renormalizable and non-renormalizable theories proposed in[17,18].

Solution (5.1) is analogous to the expression for the photon Green's function. This solution satisfies the spectral representation without subtraction, [i.e., Eq. (2.6)]. However, if we attempt the expansion in powers of λ under the sign of the spectral integral, we obtain after integration logarithmically divergent integrals in each order in λ. On the other hand, if we carry out one subtraction in the spectral representation, i.e., if we go over to (2.5), these divergences do not arise.

The solution (5.2) corresponds in this sense to the non-renormalizable theory. If we expand the integrand in (2.6) in powers of λ and f, we obtain integrals whose degree of divergence increases with the power of f. These divergences cannot be removed by any finite number of subtractions. The solution (5.2) has thus no correspondence with perturbation theory. There are no grounds, however, for discarding this solution and for confining ourselves to solutions of type (5.1), which actually are analytic continuations of perturbation theory to the region of not small values of λ. Solutions such as (5.2) are degenerate when the interaction is turned off. As was noted by Bogolyubov,[19] solutions of this type are of great interest in many problems of statistical physics. We see now that such solutions can also turn out to be important in the theory of elementary particles. It is known that the 33-resonance in πN-scattering is sufficiently narrow. A similar conclusion is reached also from preliminary estimates of p-resonance in $\pi\pi$ scattering. However, it is very difficult to obtain a narrow 33-resonance.[20,21] Even greater difficulties arise when attempts are made to obtain a narrow p-resonance in $\pi\pi$ scattering.[22,23] Solutions such as (5.2) lead to narrow resonances in a natural manner.

On the basis of the explicit form of the solution (3.10), we can draw the following important conclusion.

The integral equations obtained from the dispersion relations, from unitarity conditions, and from crossing symmetry do not lead to an ambiguous description of the scattering processes. In order to determine the solution completely, it is necessary to specify an (infinite!) set of parameters.

This fact is not surprising. The dispersion relations reflect only the very general properties of the theory, such as causality and relativistic invariance, and do not give any details on the specific interaction mechanism. In this sense, the situation in relativistic dispersion theory corresponds fully to the situation in the nonrelativistic models (see, for example, [13]).

Thus, in order to obtain a theory from the integral dispersion equations, it is necessary to specify many other properties of the solutions of these equations. For example, in the neutral case under consideration, it is sufficient to specify the value of the amplitude at the threshold of the process, to state the asymptotic behavior at infinity, and to stipulate that the scattering phase not vanish. Similar limitations can be imposed by introducing fixed subtraction constants. The threshold value is specified by the first subtraction. Specification of the second subtraction constant (i.e., the derivative of the amplitude at the threshold) is equivalent, in the absence of phase zeros, to fixing the asymptotic behavior. This method of fixing the solution is the most convenient in numerical solution of the integral equations.

We can now speculate somewhat on the physical meaning of the parameters defining the solutions.

We can, first, establish a correspondence between these parameters and Lagrangians of the type (4.2), (4.3), and (4.4). It may turn out here that an important role is played in pion physics by interactions which are not renormalizable in perturbation theory (see [24] in this connection). In other words, the dispersion approach may de-

cide, through comparison with experiment, the existence of non-renormalizable strong interactions.

Second, it can be assumed that the parameters under consideration take into account the influence of inelastic processes on the elastic processes in the low-energy region. We arrive thereby at the possibility of a phenomenological account of inelastic processes in the two-particle approximation scheme.

In conclusion we note that analysis shows the essential properties of the neutral model, to which this section was devoted, to be possessed also by the scattering of charged pions. The results of an investigation of a real charged case will be reported in future articles.

The authors consider it their pleasant duty to thank N. N. Bogolyubov, D. I. Blokhintsev, and A. A. Logunov for useful discussions.

[1] S. Mandelstam, Phys. Rev. **112**, 1344 (1959).

[2] G. Chew, Ann. Rev. Nucl. Sci. **9**, 29 (1959).

[3] K. A. Ter-Martirosyan, JETP **39**, 827 (1960), Soviet Phys. JETP **12**, 575 (1961).

[4] G. Chew and S. Mandelstam, Phys. Rev. **119**, 467 (1960).

[5] W. Fraser and J. Fulco, Phys. Rev. **117**, 1609 (1960).

[6] W. Fraser and J. Fulco, Phys. Rev. **117**, 1603 (1960).

[7] Hsien Ting-ch'an, Ho Tso-hsin, and W. Zoellner, JETP **39**, 1668 (1960), Soviet Phys. JETP **12**, 1165 (1961).

[8] Efremov, Meshcheryakov, Shirkov, and Chou, Proc. 1960 Ann. Intern. Conf. on High-Energy Physics at Rochester, Interscience, 1961, p. 279.

[9] Efremov, Meshcheryakov, Shirkov, and Chou, Nucl. Phys. **22**, 202 (1961).

[10] Bowcock, Cottingham, and Lurie, Phys. Rev. Lett. **5**, 386 (1960).

[11] G. Chew and S. Mandelstam, Preprint UCRL-9126.

[12] Castillejo, Dalitz, and Dyson, Phys. Rev. **101**, 543 (1956).

[13] F. J. Dyson, Phys. Rev. **106**, 157 (1957).

[14] F. D. Gakhov, Kraevye zadachi (Boundary-Value Problems), Gostekhizdat 1958, Chapter 2.

[15] N. I. Muskhelishvili, Singular Integral Equations, Nordhoff, Groningen, 1953, Chapter 5.

[16] J. G. Taylor, The Low Energy Pion-Pion Interaction—I, preprint, 1961.

[17] P. I. Redmond and J. L. Uretsky, Rev. Lett. **1**, 147 (1958).

[18] Bogolyubov, Logunov, and Shirkov, JETP **37**, 805 (1959), Soviet Phys. JETP **10**, 574 (1959).

[19] N. N. Bogolyubov, Physica **26**, Suppl. S1 (1960).

[20] Dyson, Ross, Salpeter, Schweber, Sundaresan, Visscher, and Bethe, Phys. Rev. **95**, 1644, (1954); see also H. Bethe and F. de Hoffmann, Mesons and Fields, II, Secs. 41 and 42, N.Y., Row, Peterson and Co., 1955.

[21] G. Salzman and F. Salzman, Phys. Rev. **108**, 1619 (1957).

[22] G. Chew, Proc. 1960 Ann. Intern. Conf. on High-Energy Physics of Rochester, Interscience 1961, p. 273.

[23] B. Bransden and J. Moffat, A Numerical Determination of Coupled s and p Amplitudes for Pion-Pion Scattering, CERN-preprint, 1961.

[24] B. Lee and M. Vaughn, Phys. Rev. Lett **4**, 578 (1960).

Translated by J. G. Adashko
107

RADIATIVE CORRECTIONS IN PION DECAYS

Ya. A. SMORODINSKII and HU SHIH-K'E

Joint Institute for Nuclear Research

Submitted to JETP editor March 23, 1961

J. Exptl. Theoret. Phys. (U.S.S.R.) **41**, 612-615 (August, 1961)

Radiative corrections to pion decays are calculated. The spectra of real photons emitted together with μ mesons and electrons are different in shape. The ratio of the decay probabilities, therefore, depends on the common cut-off parameter for the photon spectrum in both channels. The contribution of radiation effects to the total decay probability (decay with emission of any photon) is 3.93%. This correction is primarily determined by the ratio of the photon emission probabilities from the electron and the μ meson. Expressions for the lepton and photon spectra in π decays are given.

RADIATIVE corrections in weak interactions have been the subject of many papers.[1-9] It was shown in this work that the form of these corrections is different in different processes. In β decay, where there are two charged particles of the same helicity in the final state, one finds integrals which diverge at the upper limit owing to the interaction between these particles (together with the effect of their proper masses). In μ decay, on the other hand, in which the charged particles also have the same helicity but one is absorbed in the beginning and the other created in the end of the process, the corresponding integrals compensate each other* and the corrections can be calculated.

The divergence in the first case is apparently connected with general difficulties of the four-fermion interaction. However, in the second case we should expect that the major part of the effect is due to the emission of real photons with comparatively low energies, so that the magnitude of the correction is, for the most part, simply determined by the probability for such a decay. It is natural that the emission of quanta will have a comparatively large effect on the angular and energy distribution of the reaction products, but will affect the magnitude of the total probability only weakly. Thus, in the μ — e decay, the Michel parameter, which determines the spectrum of the electrons, is changed by 5% owing to the radiative corrections, whereas the lifetime of the μ meson changes only by 0.5%. The radiative corrections should play a similar role in the case of the two possible types of pion decay.

Recent investigations of the pion decay[10,11] have shown that the experimental value of the ratio of the electron and the muon decay probabilities of the π meson is close to the value predicted by the Feynman-Gell-Mann theory. The theoretical value is, without radiative corrections,[12]

$$R_0 = \frac{(W_{e\nu})_0}{(W_{\mu\nu})_0} = \frac{(m_\pi^2 - m_e^2)^2}{(m_\pi^2 - m_\mu^2)^2}\,\frac{m_e^2}{m_\mu^2} = 1.282\cdot 10^{-4}, \qquad (1)$$

where $(W_{e\nu})_0$ and $(W_{\mu\nu})_0$ are the uncorrected probabilities for the electron and muon decay of the π meson, respectively. Radiative corrections to both decay types have been calculated by Berman[6] (also by Kinoshita[8]), who showed that the correction to the ratio (1) is surprisingly large and reaches the value of 14%.

Berman calculated, in the usual manner, the sum of the "radiative corrections" and the "probability for the emission of real soft photons." This quantity depends on the cut-off energy of the quanta or, what is the same thing, on the observed energy loss of the electrons ΔE (the result computed below corresponds to $\Delta E = 0.25$ Mev). It is clear that the correction can be large in this case if the shape of the photon spectrum is very different in the two decays. In this case the cut-off will separate out different parts of the lepton spectrum. The calculations show that this is indeed the reason for the large size of the correction. This circumstance has also been noted by Kinoshita;[8] but he did not give all the formulas.

In the present paper we shall repeat all these calculations; our formula for the correction to the

*If the graphs are drawn such that the decay is described as the transformation of one charged particle into another (μ into e, p into e), the divergent integral occurs when the helicity of the charged particle changes.

decay probability differs somewhat from that of Kinoshita (but the numerical value of our correction is almost the same as Kinoshita's). We shall also give formulas for the photon spectra. The lepton spectrum obtained by us agrees with that calculated by Ioffe and Rudik,[14] Vaks and Ioffe,[15] and Bludman and Ruderman.[16].

The calculations are carried out in the standard manner. The emission of virtual nucleons is neglected, since the corresponding terms contain the nucleon mass in the denominator (see, for example, [17]). Choosing a coordinate system in which the π meson is initially at rest, we have for the radiative decay probability[8]

$$\frac{W_{ev\gamma}}{(W_{ev})_0}=\frac{\alpha}{\pi}\left\{b(\mu)\left[\ln\frac{\lambda}{m_\pi}-\ln(1-\mu^2)-\frac{1}{2}\ln\mu+\frac{3}{4}\right]\right.$$
$$\left.-\frac{\mu^2(10-7\mu^2)}{2(1-\mu^2)^2}\ln\mu+\frac{2(1+\mu^2)}{(1-\mu^2)}L(1-\mu^2)+\frac{(15-21\mu^2)}{8(1-\mu^2)}\right\}, \quad (2)$$

$$L(x)=\int_0^x\frac{\ln(1-t)}{t}\,dt=-\sum_{k=1}^{\infty}\frac{x^k}{k^2}\ (|x|\leqslant 1),$$

$$b(\mu)=2\left(\frac{1+\mu^2}{1-\mu^2}\ln\mu+1\right). \quad (3)$$

In these formulas λ is the infrared cut-off parameter and μ is the ratio of the lepton and pion masses.

The spectra of the photons and leptons are given by the formulas

$$dW_{ev\gamma}(\varepsilon_\gamma)=(W_{ev})_0\frac{\alpha}{\pi}\left\{-\frac{2}{\varepsilon_\gamma}+\frac{(4-5\mu^2-2\varepsilon_\gamma)}{(1-\mu^2)^2}\right.$$
$$+\frac{\mu^2}{(1-2\varepsilon_\gamma)(1-\mu^2)^2}+\left[\frac{(1+\mu^2)}{(1-\mu^2)}\frac{1}{\varepsilon_\gamma}\right.$$
$$\left.\left.-\frac{2(1-\mu^2-2\varepsilon_\gamma)}{(1-\mu^2)^2}\right]\ln\frac{1-2\varepsilon_\gamma}{\mu^2}\right\}d\varepsilon_\gamma, \quad (4)$$

$$dW_{ev\gamma}(\varepsilon_e)=(W_{ev})_0\frac{\alpha}{\pi}\left\{\frac{4}{(1-\mu^2)(1+\mu^2-2\varepsilon_e)}\left[\varepsilon_e\ln\frac{\varepsilon_e+\sqrt{\varepsilon_e^2-\mu^2}}{\varepsilon_e-\sqrt{\varepsilon_e^2-\mu^2}}\right.\right.$$
$$\left.-2\sqrt{\varepsilon_e^2-\mu^2}\right]+\frac{(1+\mu^2-2\varepsilon_e)}{(1-\mu^2)^2}$$
$$\left.\times\ln\frac{\varepsilon_e+\sqrt{\varepsilon_e^2-\mu^2}-\mu^2}{\varepsilon_e-\sqrt{\varepsilon_e^2-\mu^2}-\mu^2}\right\}d\varepsilon_e, \quad (5)$$

where

$$\varepsilon_\gamma=E_\gamma/m_\pi,\quad \varepsilon_e=E_e/m_\pi.$$

Formula (5) agrees with the formula of Bludman and Ruderman.[16]

$\Delta E_e/m_e$		0.5	10	20	30	Total energy region
$\left(\frac{R_0-R}{R_0}\right)\cdot 10^2$	Berman	13.9	7.6	6.1	5.3	3.9[8]
	This work	14.0	7,8	6,5	5.8	3,93

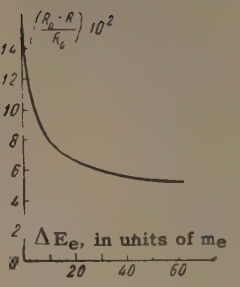

Dependence of the ratio $(R_0-R)/R_0$ on the cut-off parameter.

If we take account of all Feynman graphs with emission of a virtual photon up to order e^2, we obtain for the probability of non-radiative electron (or muon) decay of the π meson

$$W_{ev}=(W_{ev})_0\left\{1+\frac{\alpha}{\pi}\left[-\frac{3}{2}\ln\frac{L}{m_\pi}-b(\mu)\left(\ln\frac{\lambda}{m_\pi}-\frac{1}{2}\ln\mu\right.\right.\right.$$
$$\left.\left.\left.+\frac{3}{4}\right)+\frac{(3-2\mu^2)}{(1-\mu^2)}\ln\mu-\frac{3}{8}\right]\right\}, \quad (6)$$

where L and λ are the upper and lower limits of the energy of the virtual photons, respectively. The difference between Kinoshita's formula[8] and ours consists in the fact that in the former the term $-3/8$ is replaced by $-1/4$ (after the mass correction).

Summing (2) and (6), we find for the total (radiative + non-radiative) decay probability for the pion

$$\frac{W_{ev}+W_{ev\gamma}}{(W_{ev})_0}=1+\frac{\alpha}{\pi}\left\{-\frac{3}{2}\ln\frac{L}{m_\pi}-b(\mu)\ln(1-\mu^2)\right.$$
$$+\frac{(6-20\mu^2+11\mu^4)}{2(1-\mu^2)^2}\ln\mu$$
$$\left.+\frac{2(1+\mu^2)}{(1-\mu^2)}L(1-\mu^2)+\frac{(6-9\mu^2)}{4(1-\mu^2)}\right\}. \quad (7)$$

In Kinoshita's work[8] the last term (after the mass correction) is replaced by $(13-19\mu^2)/8(1-\mu^2)$. With the help of formula (7) we can compute the radiative correction to (1).

For the probability of emission of a lepton with energy less than $E_{max}-\Delta E$ we find

$$\frac{W_{ev\gamma}(E<E_{max}-\Delta E)}{(W_{ev})_0}=\frac{\alpha}{\pi}\left\{-b(\mu)\left(\ln\frac{m_\pi}{2\Delta E}+2\ln(1-\mu^2)\right.\right.$$
$$\left.-\frac{3}{4}\right)+\frac{2(1+\mu^2)}{(1-\mu^2)}\left[L(1-\mu^2)-L\left(\frac{2}{1-\mu^2}\frac{\Delta E}{m_\pi}\right)\right]$$
$$-\left[\frac{\mu^2(10-7\mu^2)}{2(1-\mu^2)^2}+\frac{4(1-3\mu^2)}{(1-\mu^2)^3}\frac{\Delta E}{m_\pi}\right]\ln\mu$$
$$\left.+\left[\frac{(15-21\mu^2)}{8(1-\mu^2)}-\frac{4(1+2\mu^2)}{(1-\mu^2)^2}\frac{\Delta E}{m_\pi}\right]\right\}. \quad (8)$$

Formula (8) goes over into Kinoshita's formula[8] if we neglect the terms linear in ΔE.

We can now write down the formula for the correction to the ratio of the probabilities of the electron and muon decays in which the leptons have an energy which differs from the maximal value by no more than the amount ΔE. Substituting

the numerical values of the constants, we obtain

$$R(\Delta E) = R_0\left\{1 - (4.647\cdot 10^{-3})\left[30.12 - 4.611\left(\ln\frac{2\Delta E_e}{m_e} - \frac{2\Delta E_e}{m_\pi}\right) - L\left(\frac{2\Delta E_e}{m_\pi}\right)\right]\right\}. \quad (9)$$

A comparison between our numerical results and those of Berman[6] and Kinoshita[8] is given in the table.

For an illustration, we show the dependence of the ratio on the cut-off parameter ΔE_e in the figure. We note that for $\Delta E_e = 10$ Mev, which is the value assumed in the experiments of reference 11, we have $R = 1.198 \times 10^{-4}$ [the experimental value is $R = (1.18 \pm 0.08) \times 10^{-4}$].

We express our gratitude to L. Okun', Chu Hung-yuan, Chu Kuang-chao, Ho Tso-hsiu, Hsien Ting-ch'ang, and Wang-j'ung for a useful discussion of this work.

[1] Behrends, Finkelstein, and Sirlin, Phys. Rev. 101, 866 (1956).

[2] T. Kinoshita and A. Sirlin, Phys. Rev. 107, 593 and 638 (1957).

[3] T. Kinoshita and A. Sirlin, Phys. Rev. 113, 1652 (1959).

[4] T. Kinoshita and A. Sirlin, Phys. Rev. Lett. 2, 177 (1959).

[5] S. M. Berman, Phys. Rev. 112, 267 (1958).

[6] S. M. Berman, Phys. Rev. Lett. 1, 468 (1958).

[7] Ya. A. Smorodinskii and Ho Tso-hsiu, JETP 38, 1007 (1960), Soviet Phys. JETP 11, 724 (1960).

[8] T. Kinoshita, Phys. Rev. Lett. 2, 477 (1959).

[9] Durand III, Landovitz, and Marr, Phys. Rev. Lett. 4, 620 (1959).

[10] A. O. Vaisenberg, Usp. Fiz. Nauk 70, 429 (1960), Soviet Phys.-Uspekhi 3, 195 (1960).

[11] T. Fujii et al., Bull. Amer. Phys. Soc. 5, 71 (1960).

[12] L. B. Okun', Usp. Fiz. Nauk 68, 449 (1959), Ann. Rev. Nuc. Sci. 9, 61 (1959).

[13] R. P. Feynman and M. Gell-Mann, Phys. Rev. 109, 193 (1958).

[14] B. L. Ioffe and A. I. Rudik, Doklady Akad. Nauk SSSR 82, 359 (1952).

[15] V. G. Vaks and B. L. Ioffe, JETP 35, 221 (1958), Soviet Phys. JETP 8, 151 (1959).

[16] S. A. Bludman and M. A. Ruderman, Phys. Rev. 101, 910 (1956).

[17] Kwo She-hung, Acta Phys. Sinica 16, 299 (1960).

Translated by R. Lipperheide
108

EXCESS NEGATIVE CHARGE OF AN ELECTRON-PHOTON SHOWER AND ITS COHERENT RADIO EMISSION

G. A. ASKAR'YAN

P. N. Lebedev Physics Institute, Academy of Sciences, U.S.S.R.

Submitted to JETP editor March 24, 1961

J. Exptl. Theoret. Phys. (U.S.S.R.) 41, 616-618 (August, 1961)

We investigate the excess of electrons in an electron-photon shower. This excess is caused by annihilation of the positrons in flight and by the Compton and δ-electrons in the cascade. It is shown that at the maximum of the shower the excess may comprise ten percent of the total number of shower particles. The Cerenkov radiation from this excess charge in a dense medium is estimated. It is indicated that this radio emission from showers produced by high-energy accelerator particles or cosmic rays in blocks of dense matter can be recorded and used. The possibility of recording radio waves from penetrating particle showers in the moon's ground, by apparatus dropped on the lunar surface, and in underground layers on the Earth in which radio waves can propagate, is also noted.

1. EXCESS NEGATIVE CHARGE OF ELECTRON-PHOTON SHOWER

THREE processes contribute to the formation of an excess of electrons in a cascade, namely annihilation of the positrons in flight and dragging of the Compton and δ-electrons into the shower cascade. Let us estimate this excess charge.

We write the equation for the average number of electrons n_- and of positrons n_+ with energies of interest to us in the form

$$\dot{n}_- = \Phi(t) - n_-/\tau_- + \dot{n}_{\delta, C}, \quad \dot{n}_+ = \Phi(t) - n_+/\tau_+,$$

where $\Phi(t, n_\pm, n_\gamma)$ is a function of the electron and positron pair production by γ rays and shower particles, $\dot{n}_{\delta, C}$ is the number of Compton and δ-electrons with energies of interest to us produced per unit time by the quanta and shower particles, $\tau_\pm$ is the lifetime of the charged particles prior to energy loss to production of the γ quanta. We put $1/\tau_+ = 1/\tau_- + 1/\tau_a$, where τ_a is the lifetime of the positron prior to annihilation.

Subtracting the equation for n_+ from the equation for n_- we obtain for the excess particles $\nu = n_- - n_+$ the equation

$$\dot{\nu} + \nu/\tau_- = n_+/\tau_a + \dot{n}_{\delta, C} \approx n_+/\tau_a.$$

The value of ν can be estimated by putting $n_+/\tau_a \approx Ae^{t/T_+}$, where T_+ is the characteristic build-up time of the number of annihilating positrons. For this case we obtain

$$\nu \approx Ce^{-t/\tau_-} + \frac{Ae^{t/T_+}}{1/T_+ + 1/\tau_-} \approx \frac{n_+}{\tau_a(1/T_+ + 1/\tau_-)} \qquad t \gg \tau_-.$$

It is easy to see that $T_+ \sim \tau_-$, and therefore $\nu \sim n_+\tau/\tau_a$. Inasmuch as $\tau \approx l_{rad}/c$ and $\tau_a \approx 1/N_e\sigma_a c$, where the annihilation cross section is

$$\sigma_a \approx \pi r_0^2 (mc^2/E_+) \ln(2E_+/mc^2),$$

and the radiational length

$$l_{rad} = 137/4ZN_e r_0^2 \ln(183/Z^{1/3}),$$

we obtain

$$\frac{\tau}{\tau_a} \approx \frac{137}{4Z}\left(\frac{mc^2}{E_+}\right)\frac{\ln(2E/mc)}{\ln(183/Z^{1/3})} \approx \frac{B}{ZE_+}.$$

This ratio is independent of the density of the medium, and depends only on its atomic number Z and on the particle energy. For example, when $Z \approx 10$, with a mean particle energy at the maximum of shower development $E \approx 10^8$ ev, we obtain $\tau/\tau_a \sim 0.1$, i.e., the number of moving electrons in the shower can exceed the number of positrons by some ten percent.

2. COHERENT RADIO EMISSION FROM THE SHOWER

The presence of a moving uncompensated charge in a shower may increase by many orders of magnitude a flash of Cerenkov, bremsstrahlung, or transition radiation in the radio range. Various possibilities of recording cosmic showers by radio emission bursts have been discussed numerous times (see, for example,[1]). Coherent amplification of the radio emission from the excess charge increases the chances of registering

the showers by radio. Indeed, in the range of wavelengths greater than the dimensions of the cluster, the intensity of radiation is proportional to ν^2. This value is the greater the more particles in the shower, so that radio registration of powerful electron-photon showers becomes preferable.

The density of the medium determines the dimensions of the localized region of shower particles and the range of wavelengths in which the radiation is coherent. A flash of coherent radiation is produced when there are created in the shower a large number of particles of such energy that the positron annihilation becomes noticeable, but the range of the positrons is still not too small. In air, the shower dimensions and the wavelengths radiated are of the order of hundreds of meters. In dense media, the coherent radio emission is in the $\sim 1-100$ cm wavelength range. Interest attaches to registering the flash of radio emission from a shower created in a block of dense matter by a high-energy particle (from outer space or from an accelerator), since it is possible to estimate from the intensity of the flash the number of particles in the shower and the energy of the primary particle. The radiation power is greatly dependent on the energy E_0 of the primary particle:

$$\Delta J_\omega \approx (e^2\nu^2/c)\,\omega\Delta\omega \approx 3\,(10^{-16}E_0)^2 \cdot \text{mw for}$$

$$\Delta\omega \sim 0.1\omega \sim 2\cdot 10^9\ (\lambda \sim 10\ \text{cm});$$

For example, when $E_0 \approx 10^{18}$ ev, the radiation power is $\Delta J_\omega \approx 30$ w. It is obviously expedient to use media in which the shower has minimum dimensions, since this permits the use of higher frequencies, where the Cerenkov radiation is more intense.

We note that other mechanisms for the separation of charges in the shower are possible. For example, V. I. Gol'danskii indicated (private communication) that the polarization of a shower by the earth's magnetic field can give rise to coherent radio emission. To him is also due the idea of using the transition radiation to register such a shower as it arrives to the earth's surface.

Increased efficiency of registration of cosmic particles and showers of superhigh energies may yield valuable information on rare processes involving gigantic energies and occurring in outer space. We consider below a possible method of remote registration of penetrating particles by using flashes of radio emission produced underground, either on earth or on the moon.

3. REGISTRATION OF PENETRATING PARTICLES AND SHOWERS UNDERGROUND ON EARTH AND ON THE MOON

The presence of extensive underground zones in which radio waves can propagate was noted recently.[2] It was established that the surface layer of the earth screens the internal zone completely against external electromagnetic interference. The small attenuation of the radio waves (particularly in substances such as rock salt, marble, granite, etc.), the dielectric constant of the rocks, and the absence of radio interference at great depths offer hope of effective registration of cosmic particles of high penetrating ability, for example muons, by means of the Cerenkov radiation of the radio waves emitted when the particles penetrate deeply underground or when a shower is produced there by these particles.

Let us estimate the effective signal produced by the shower: the radiated power due to the motion of the excess shower charge is $\Delta J_\omega \sim (e^2\nu^2/c)\,\omega\Delta\omega \sim 30\,\mu$w when $\nu \sim 10^7$ and $\Delta\omega \sim 0.1\omega \sim 2\times 10^8$ $(\lambda - 1)$ meters. Estimates of the absorption path l, for not too short wavelengths, $l \approx \sqrt{\epsilon}c/2\pi\sigma$ (see[3]), based on values of the conductivity σ of pure rocks such as salt, marble, or granite (see, for example,[4]), show that the absorption paths are greater than the distance R of interest to us, which is on the order of a kilometer to the point of reception. The field intensity of a signal equivalent to the radiated power is $\mathcal{E} \approx (e\nu/cR)\sqrt{\omega\Delta\omega} \sim 30\,\mu$v/m, which is many times greater than the level of internal noise of an ordinary receiver ($\mathcal{E}_{\text{noise}} \approx 0.1\,\mu$v/m — see, for example,[3] p. 88).

It must be noted that the dimensions of rocks in which interactions can be registered are commensurate with the radiation length for a muon in a dense medium (on the order of several kilometers), thus permitting more efficient registration of the muons by means of the electron-photon showers that they produce. The absence of external radio interference allows amplifiers with low internal noise to be used and to register flashes of radio emission from groups of mesons of a shower produced in the atmosphere, or from individual mesons.

We note that the generation of radio waves by cosmic particles and by showers should be more intense in the ground of the moon, which has no magnetic field or atmosphere, and which permits all cosmic rays of any energy to reach its surface; the absorption of radio waves in the ground of the

moon should in this case be small even near the surface. This facilitates the registration of flashes of radio emission of showers in the ground by means of suitable apparatus dropped on the moon.

In general, the importance of ground-wave radio communication on the moon will apparently be great, owing to the lack of a Heavyside layer and to the large curvature of the moon's surface, which makes it impossible otherwise to communicate by radio between two remote objects on the moon's surface.

[1] J. Jelley, Cerenkov Radiation and Its Applications, Pergamon, 1958, Chapter II, Section 5.

[2] Radio-Electronics, **31**, No. 10, 6 (1960).

[3] Al'pert, Ginzburg, and Feĭnberg, Rasprostranenie radiovoln (Propagation of Radio Waves), Gostekhizdat, (1953).

[4] Sb. fizicheskikh konstant (Collection of Physical Constants), ONTI, 1937, p. 202.

Translated by J. G. Adashko
109

ON THE MAXIMUM VALUE OF THE COUPLING CONSTANT IN FIELD THEORY

A. A. ANSEL'M, V. N. GRIBOV, G. S. DANILOV, I. T. DYATLOV, and V. M. SHEKHTER

Leningrad Physico-Technical Institute, Academy of Sciences, U.S.S.R.

Submitted to JETP editor March 24, 1961

J. Exptl. Theoret. Phys. (U.S.S.R.) **41**, 619-628 (August, 1961)

It is assumed that the interactions between elementary particles are characterized by an effective range that depends only on the mass of the particles transmitting the interaction. It is shown that if all masses (and consequently interaction ranges) are fixed, then unitarity and analyticity limit the possible values of the πN interaction coupling constant, as well as the absolute value of the $\pi\pi$ scattering amplitude at zero energy (in the case when the latter is negative). The proof is carried out by means of dispersion relations for the inverse of the forward scattering amplitude.

1. INTRODUCTION

IN modern field theory particle masses and coupling constants between fields describing these particles appear as independent quantities, whose values must be given by experiment. This is true both of the Hamiltonian form of the theory, where renormalization is performed in such a way as to make the renormalized charge and mass the same as the observed ones, and of the dispersion relations approach, in which the location of the singularities of the scattering amplitude and the residues of the pole terms are identified with the experimental values of the particles' masses and coupling constants. One might, however, ask the following question: could not the values of the particle masses impose some restrictions on the coupling constants? The example of nonrelativistic theory with point interaction shows that such a situation is possible; in that example the magnitude of the renormalized coupling constant cannot be in excess of a certain critical value, determined by the masses of the particles.[1,2]

In the relativistic theory no such precise limitation can be proved. This is related to the circumstance that the interaction between particles is effectively smeared out by the existence of virtual processes. On the other hand, it has been assumed in field theory, beginning with Yukawa, that if an interaction is due to the exchange of a particle of mass μ then the effective range of the interaction is of the order of $\hbar/\mu c$, regardless of the interaction strength. If one accepts this point of view, i.e., if it is assumed that the range of the interaction is determined by the masses only, then it becomes possible to deduce limitations on the coupling constants.

In this paper we consider scattering of π mesons by nucleons. Analogous considerations are, apparently, valid for other processes (for example scattering of K mesons by nucleons), however the existence of unphysical regions in the dispersion relations for these processes complicates their analysis.

We find it convenient to make use of dispersion relations for the inverse of the forward scattering amplitude. These dispersion relations possess a number of peculiar properties, although mathematically they are a consequence of the direct dispersion relations. In the first place, they are sensitive to the zeros of the scattering amplitude. The number of these zeros is limited; it is shown below that if the high energy behavior of the cross section does not differ much from a constant, then the forward scattering amplitude of charged pions on nucleons can have in the complex plane one, two or three zeros; the $\pi\pi$-scattering amplitude either has no zeros, or has one or two zeros; the Compton effect amplitude has no zeros. In the second place, although the "inverse" dispersion relations are an identity with respect to the coupling constant, in distinction to the usual dispersion relations they do not represent a term by term identity after the integrands have been expanded in a power series in the charge.

In addition to restrictions on the coupling constants, i.e., on the residues of the pole terms in the scattering amplitudes, it also turns out to be possible to obtain restrictions on the scattering amplitude at zero energy (scattering length) when the latter is negative. In conclusion we discuss the following question: might not the observed pion-nucleon interaction coupling constant have the maximum value allowable by the prescribed masses?

It is possible to give certain indirect arguments in favor of such a hypothesis.

2. SCATTERING OF π^0 MESONS ON PROTONS

Let us consider first scattering of π^0 mesons on protons. This case is simpler than the scattering of charged mesons because the imaginary part of the forward scattering amplitude differs in this case on the left and right cuts by its sign only. The dispersion relations for $A^0(\omega)$, including the form of the pole term, are easily written down following, for example, the work of Goldberger et al,[3] taking into account the fact that $A^0(\omega) = [A^+(\omega) + A^-(\omega)]/2$, where $A^\pm$ are the forward scattering amplitudes for $\pi^\pm$ mesons on protons:

$$A^0(\omega) = A^0(\mu) + 2f^2\omega_0\left[\frac{1}{\omega_0^2-\omega^2} - \frac{1}{\omega_0^2-\mu^2}\right] + \frac{1}{\pi}\int_{\mu^2}^{\infty} \operatorname{Im} A^0(\omega')\left[\frac{1}{\omega'^2-\omega^2} - \frac{1}{\omega'^2-\mu^2}\right] d\omega'^2. \quad (1)$$

Here ω is the energy of the π meson in the laboratory system, μ is the mass of the π meson, $f^2 = 0.08$ is the meson-nucleon coupling constant, $\omega_0 = \mu^2/2m$, and m is the nucleon mass. According to the optical theorem we have

$$\operatorname{Im} A^0(\omega) = (k/4\pi)\,\sigma^0(\omega), \quad (2)$$

where $\sigma^0(\omega)$ is the total π^0-meson-proton interaction cross section.

It is clear from Eq. (1) that, as a function of the complex variable ω^2, $A^0(\omega)$ is an R-function, i.e., the sign of its imaginary part is the same as the sign of the imaginary part of ω^2, and consequently it can have zeros only on the real axis.[1] The inverse function $h^0(\omega) = -1/A^0(\omega)$ is also an R-function and has poles only at the zeros of the function $A^0(\omega)$, i.e., on the real axis. The most general dispersion relation that it satisfies is of the form

$$h^0(\omega) = \frac{1}{\pi}\int_{\mu^2}^{\infty} \operatorname{Im} h^0(\omega')\frac{d\omega'^2}{\omega'^2-\omega^2} + \sum_n \frac{R_n}{\omega_n^2-\omega^2} + b + b_1\omega^2. \quad (3)$$

The constants ω_n^2, R_n, b and b_1 are real; furthermore $b_1 \geq 0$ and $R_n \geq 0$. The latter is necessary in order that $h^0(\omega)$ be an R-function in the ω^2-plane. The dispersion relation (3) has been written without subtractions since $\operatorname{Im} h^0(\omega) = \operatorname{Im} A^0(\omega)/|A^0(\omega)|^2$ goes at large ω like $1/\omega$, if the cross section $\sigma^0(\omega)$ is approximately constant. Besides, two more subtractions in the variable ω^2 would not change the discussion that follows. Actually, some of the terms written on the right side of Eq. (3) drop out. Thus, the quantities b and b_1 are equal to zero if the cross section does not decrease at large energies at least as fast as $1/\omega$. And as regards the sum of the pole terms, it will be shown in the following section that it contains only one term with $\omega_1^2 < \omega_0^2$, if $A^0(\mu) < 0$, and one more term with $\omega_0^2 < \omega_2^2 < \mu^2$, if $A^0(\mu) > 0$. All this, however, is irrelevant for what follows.

The residue of the function $A^0(\omega)$ at the pole, proportional to the coupling constant f^2, equals $-(dh/d\omega^2)^{-1}\big|_{\omega^2=\omega_0^2}$. It is therefore easy to obtain the following expression for the coupling constant:

$$\frac{1}{f^2} = 2\omega_0\left[\frac{1}{\pi}\int_{\mu^2}^{\infty}\frac{\operatorname{Im} A^0(\omega')}{|A^0(\omega')|^2}\frac{d\omega'^2}{(\omega'^2-\omega_0^2)^2} + \sum_n \frac{R_n}{(\omega_n^2-\omega_0^2)^2} + b_1\right]. \quad (4)$$

As a result of the positive nature of R_n and b_1 it follows from here that

$$\frac{1}{f^2} > \frac{2\omega_0}{\pi}\int_{\mu^2}^{\infty}\frac{\operatorname{Im} A^0(\omega')}{|A^0(\omega')|^2}\frac{d\omega'^2}{(\omega'^2-\omega_0^2)^2}. \quad (5)$$

The idea of the subsequent discussion consists of the following. At low energies, when it is possible to limit oneself in the scattering amplitude to s-waves only, one has*

$$\operatorname{Im} A^0(\omega')/|A^0(\omega')|^2 = k' \equiv \sqrt{\omega'^2-\mu^2},$$

and the range of the variable k', within which this assertion is valid, is determined by the inequality $k'\rho \ll 1$ (ρ is the range of the π-meson—nucleon interaction). If one accepts the hypothesis mentioned in the introduction, that the quantity ρ is determined by the masses of the particles only and does not depend on the renormalized coupling constant, then the integral on the right side of Eq. (5) will certainly contain a small region ($k'\rho \ll 1$), whose size is independent of f^2, where the integrand is equal to $k'(\omega'^2-\omega_0^2)^{-2}$. Since the entire integral can only be larger than the result of the integration over this small region, it follows that the quantity f^{-2} is bounded from below by a certain expression which depends only on the masses of the particles.

Below we shall obtain a more precise inequality based on replacing the integrand by a quantity independent of f^2 at all energies. We have for $\operatorname{Im} A^0/|A^0|^2$

$$\frac{\operatorname{Im} A^0(\omega)}{|A^0(\omega)|^2} = \frac{k\sigma^0(\omega)}{4\pi\sigma_e^0(\omega, 0)} \geqslant k\frac{\int \sigma_e^0(\omega, \theta)\, d\Omega/4\pi}{\sigma_e^0(\omega, 0)}. \quad (6)$$

Here $\sigma^0(\omega)$ is as before the total π^0-meson-proton interaction cross section, and $\sigma_e^0(\omega, \theta)$ is the dif-

*Strictly speaking, this equality applies only to pure isotopic states, however the refinements connected with this remark are trivial and do not lead to any new results.

ferential elastic scattering cross section through the angle θ. We next carry out a phase shifts expansion of the right side of Eq. (6):*

$$\frac{\operatorname{Im} A^0(\omega)}{|A^0(\omega)|^2} \geqslant k \frac{\sum |a_l|^2 (2l+1)}{|\sum a_l (2l+1)|^2} \geqslant k \frac{\sum |a_l|^2 (2l+1)}{[\sum |a_l| (2l+1)]^2}. \quad (7)$$

We shall, further, assume that the partial wave amplitudes a_l decrease rapidly for $l > l_0(k) = k\rho(k)$, where $\rho(k)$ is the interaction range characteristic of the given energy. If the effective dimensions of the system do not increase indefinitely with increasing k, then there exists a certain maximum ρ, such that at all energies the a_l are vanishingly small if $l > l_0 = k\rho$. It should be emphasized that the quantity ρ need not coincide with the quantity $\rho(k)$ as $k \to \infty$. It is easy now to observe that the right side of the inequality (7) reaches a minimum, when all the a_l are equal to each other. Thus

$$\frac{\operatorname{Im} A^0(\omega)}{|A^0(\omega)|^2} \geqslant k \Big/ \sum_{l=0}^{l_0} (2l+1) = \frac{k}{(l_0+1)^2} = \frac{k}{(k\rho+1)^2}. \quad (8)$$

For $k\rho \ll 1$ one obtains the correct value $\operatorname{Im} A/|A|^2 = k$. Substituting Eq. (8) into Eq. (5) and performing the integration we find

$$\frac{1}{f^2} > \frac{4\omega_0}{\pi}\left[\frac{2\rho}{(1+\rho^2)^2} + \frac{2\rho(1-\rho^2)}{(1+\rho^2)^3}\ln\rho + \frac{\pi}{4}\frac{1-6\rho^2+\rho^4}{(1+\rho^2)^3}\right]. \quad (9)$$

In Eq. (9) we have set $\mu = 1$ and have neglected the small quantity ω_0 in comparison with unity. The choice of the quantity ρ is fairly arbitrary. Since the π-meson-nucleon interaction proceeds via the exchange of at least two π mesons one might expect that $\rho \sim 1/2$. Then $f^2 < 60$ ($\omega_0 = 0.07$). When $\rho = 1$, $f^2 < 100$; when $\rho = 0$, $f^2 < 15$. Let us also note that even if ρ were to increase with energy an estimate of f^2 would still be possible. One would only need to take into account this k-dependence of ρ when carrying out the integration in Eq. (8). Such a dependence, however, is of little importance since the main contribution to the integral in Eq. (5) comes from $\omega' \sim \mu$.

The limitation here obtained on the magnitude of the residue has the following meaning: as f^2 goes through a certain critical value the scattering amplitude ceases to satisfy the unitarity and analyticity requirements. That this is so can be clearly seen in the example of nonrelativistic theory.[2]

The magnitude of the residue of the pole term in the amplitude for the scattering of π^0 mesons on protons, in contrast to the residue in the amplitudes for the scattering of charged mesons, is proportional to the small quantity ω_0. This numerically worsens the estimate of f^2 and results in a complete disappearance of the inequality in the limit when the nucleon mass becomes infinite. It is therefore of interest to study the amplitude for the scattering of charged mesons on protons. We shall show in what follows that in this case one obtains a much stronger restriction on f^2.

*The inclusion of nucleon spin leads to no new results, naturally.

3. ZEROS OF THE FORWARD SCATTERING AMPLITUDE

In order to obtain restrictions on the residue of the amplitude for the scattering of charged π mesons on nucleons, it is necessary to know the number and the location in the complex ω-plane of the zeros of the amplitude. In this section we shall derive a formula for the number of zeros and will discuss their location.

Let us consider the amplitude $A^+(\omega)$ for the scattering of π^+ mesons on protons and the amplitude $A^-(\omega)$ for the scattering of π^- mesons on protons, which is connected to A^+ by the crossing symmetry condition. $A^+(\omega)$ is a function analytic in the complex ω-plane except for the two cuts from $\omega = \mu$ to $\omega = +\infty$ and from $\omega = -\mu$ to $\omega = -\infty$, and the pole at $\omega = \omega_0 = \mu^2/2m$. On the right cut the imaginary part of $A^+(\omega)$ is positive above the cut [$\operatorname{Im} A^+(\omega) = k\sigma^+(\omega)/4\pi$] and differs by a sign below the cut. On the left cut the situation is reversed: the imaginary part is positive below the cut and equal to $k\sigma^-(\omega)/4\pi$ and negative above the cut. [$\sigma^{\pm}(\omega)$ are the total interaction cross sections for π^+ and π^- mesons with protons.]

Consider the integral

$$\frac{1}{2\pi i}\oint \frac{A^{+\prime}(\omega)}{A^+(\omega)}\,d\omega \quad (10)$$

where the contour consists of lines enclosing both cuts on both sides joined at infinity by two large semicircles. According to Cauchy's theorem, the integral is equal to the number of zeros (k) minus the number of poles (p) of the function $A^+(\omega)$ contained inside the contour (in our case p = 1). On the other hand the integral is equal to the increment in the phase of the function on traversing the contour, divided by 2π:

$$k - p = \Delta\varphi / 2\pi. \quad (11)$$

As will be seen from what follows the increment $\Delta\varphi$ depends on the signs of the real quantities $A^+(\mu)$ and $A^+(-\mu) = A^-(\mu)$, i.e., on the signs of the scattering lengths. Let us assume for defi-

niteness sake that $A^+(\mu) < 0$ and $A^-(\mu) > 0$ and start calculating $\Delta\varphi$ by beginning to traverse the contour at $\omega = \mu$. Then the initial value of the phase, $\varphi(\mu)$, may be taken equal to π $[A^+(\mu) < 0]$. The value of the phase at the point $\omega = +\infty + i\epsilon$ will lie between zero and π if the total interaction cross section (and, consequently, the imaginary part of the amplitude) does not vanish anywhere. The total cross section is determined by many partial waves and we shall assume that not all scattering phase shifts can be simultaneously equal to multiples of π. This assumption can be proved theoretically, since the phase shifts corresponding to large orbital angular momenta can be calculated from diagrams with lowest in mass intermediate states.[4]

Let us now assume that the asymptotic behavior of the amplitude $A^+(\omega)$ at large ω has the character ω^n, where n is an odd integer. n must be odd in order that the imaginary part of $A^+(\omega)$ be negative above the left cut. On traversing the large semicircle, joining the points $+\infty + i\epsilon$ and $-\infty + i\epsilon$, the phase increment amounts to $n\pi$. As one proceeds along the upper edge of the left cut, the phase varies between $n\pi$ and $(n+1)\pi$ and consequently is equal to $(n+1)\pi$ [an even multiple of π since $A^-(\mu) > 0$] at the point $\omega = -\mu$. Continuing these considerations it is easy to show that the total phase increment upon traversing the contour equals $\Delta\varphi = 2\pi n$. From here, according to Eq. (11), we get

$$k = n + p \qquad (A^+(\mu) < 0, \quad A^-(\mu) > 0). \tag{12a}$$

It is easy to see that Eq. (12a) remains valid if $A^+(\mu) > 0$, $A^-(\mu) < 0$, but

$$k = n + p - 1 \qquad (A^+(\mu) < 0, \quad A^-(\mu) < 0), \tag{12b}$$

$$k = n + p + 1 \qquad (A^+(\mu) > 0, \quad A^-(\mu) > 0). \tag{12c}$$

If the asymptotic form of the amplitude does not have a pure power law character, but rather is multiplied by a slowly varying function (for example, by $\sim \ln^{-2}\omega$, which would insure the decreasing of the total cross section[5]), then Eqs. (12) remain valid. If instead the behavior of the amplitude at infinity is governed not by an integral power of ω, then it is easy to show that the n in Eqs. (12) is equal to the odd integer nearest to the exponent of ω in the asymptotic form of the amplitude. It should be added that in view of the positive nature of the imaginary parts on the cuts the scattering amplitude cannot, apparently, have an asymptotic behavior that depends on the direction in the complex plane along which the point at infinity is approached.

If it is accepted that at large energies the total cross section is approximately constant $(n = 1)$, then it follows from Eq. (12) that the forward scattering amplitude of π^+ mesons on protons has one $[A^\pm(\mu) < 0]$, two $[A^\pm(\mu)$ of opposite signs], or three $[A^\pm(\mu) > 0]$ zeros. Qualitatively the location of these zeros can be easily determined by investigating the amplitude $A^+(\omega)$ for real values of ω in the interval $(-\mu, \mu)$. For ω close to ω_0 $A^+(\omega)$ tends to $+\infty$ if ω lies to the left of ω_0, and to $-\infty$ if $\omega > \omega_0$. It therefore follows that in the case when $A^+(\mu) < 0$ and $A^-(\mu) < 0$ the single zero of the amplitude lies on the real axis to the left of the point ω_0. When $A^+(\mu) > 0$, $A^-(\mu) < 0$, the amplitude has two zeros: one to the left and one to the right of the point ω_0. When $A^+(\mu) < 0$, $A^-(\mu) > 0$ (the experimentally observed situation) one has various possibilities. The two zeros of the amplitude could both lie to the left of ω_0, or both to the right of ω_0, or lie in the complex plane (in which case they must be, of course, complex conjugate). All the cases with three zeros can be obtained from these last ones by the addition of a zero on the real axis to the right of ω_0.

The amplitude for π^0 mesons scattering on protons $\{A^0(\omega) = [A^+(\omega) + A^-(\omega)]/2$, $A^0(\omega) = A^0(-\omega)\}$ has two poles at the points ω_0 and $-\omega_0$, and has consequently either two zeros if $A^0(\mu) < 0$ (which corresponds to the experimental data), or four zeros if $A^0(\mu) > 0$. In the first case these zeros are either on the real axis between $-\omega_0$ and ω_0, placed symmetrically with respect to the origin, or on the imaginary axis. In the second case one must add to them a zero to the right of ω_0 and a zero to the left of $-\omega_0$. In the ω^2-plane this corresponds to what has been said in the previous section.

In an analogous manner it is easy to show that in electrodynamics the amplitude for forward scattering of photons on electrons has no zeros $[A(0) = -e^2/m < 0]$, and the amplitude for scattering of π mesons on π mesons has either no zeros, or one, or two zeros.

4. SCATTERING OF CHARGED π MESONS ON PROTONS AND $\pi\pi$ SCATTERING

Let us return to the estimate of the residue of the pole term in the amplitude for the scattering of π^+ mesons on protons, $A^+(\omega)$. As was shown in the preceding section this function may have one, two or three zeros distributed in various ways. The most interesting, from the point of view of obtaining restrictions on the coupling constant, is the case of two complex zeros and, pos-

sibly, one more zero to the right of ω_0. All the other variants can be discussed in a manner analogous to the one described below, and lead to stronger inequalities on the coupling constant — hence may be considered as being included in the estimate obtained below.

Let ω_1 and $\omega_2 = \omega_1^*$ be the complex zeros of $A^+(\omega)$, and ω_3 the additional zero ($\omega_3 > \omega_0$). Consider the functions

$$F^+(\omega) = A^+(\omega)\,(\omega+\mu)/(\omega-\omega_1)(\omega-\omega_2),$$
$$H^+(\omega) = -1/F^+(\omega), \qquad (13)$$

which are R-functions (the imaginary parts of these functions due to the pole terms and on the right cut have the same sign as Im $A^+(\omega)$, and the opposite sign on the left cut). $F^+(\omega)$ has two zeros at $\omega = -\mu$ and $\omega = \omega_3$ and a pole at $\omega = \omega_0'$, $H^+(\omega)$ has poles at $\omega = -\mu$, ω_3 and a zero at $\omega = \omega_0$; both functions behave for large ω approximately like constants [$A^+(\omega) \sim \omega$]. The dispersion relation for $H^+(\omega)$ has the form

$$H^+(\omega) = \frac{1}{\pi}\int_\mu^\infty d\omega' \frac{\operatorname{Im} A^+(\omega')}{|A^+(\omega')|^2}\frac{|\omega'-\omega_1|^2}{\omega'+\mu}\left[\frac{1}{\omega'-\omega}-\frac{1}{\omega'-\omega_0}\right]$$
$$-\frac{1}{\pi}\int_\mu^\infty d\omega' \frac{\operatorname{Im} A^-(\omega')}{|A^-(\omega')|^2}\frac{|\omega'+\omega_1|^2}{\omega'-\mu}\left[\frac{1}{\omega'+\omega}-\frac{1}{\omega'+\omega_0}\right]$$
$$-\frac{|\omega_1+\mu|^2}{A^-(\mu)}\left[\frac{1}{\mu+\omega}-\frac{1}{\mu+\omega_0}\right]+R_3\left[\frac{1}{\omega_3-\omega}-\frac{1}{\omega_3-\omega_0}\right]. \qquad (14)$$

A subtraction has been performed at the point $\omega = \omega_0$ in Eq. (14) and the fact that $H(\omega_0) = 0$ has been taken into account, so that for ω close to ω_0 $H(\omega)$ is of the form $H(\omega) \approx H'(\omega_0)(\omega-\omega_0)$. As can be seen from the relation between $H^+(\omega)$ and $A^+(\omega)$, the magnitude $-2f^2$ of the residue of the function $A^+(\omega)$ is proportional to $-1/H'(\omega_0)$. Consequently

$$\frac{1}{2f^2} = \frac{\omega_0+\mu}{|\omega_0-\omega_1|^2}\left\{\frac{1}{\pi}\int_\mu^\infty \frac{\operatorname{Im} A^+}{|A^+|^2}\frac{|\omega'-\omega_1|^2\,d\omega'}{(\omega'-\omega_0)^2(\omega'+\mu)}\right.$$
$$+\frac{1}{\pi}\int_\mu^\infty \frac{\operatorname{Im} A^-}{|A^-|^2}\frac{|\omega'+\omega_1|^2\,d\omega'}{(\omega'+\omega_0)^2(\omega'-\mu)}$$
$$\left.+\frac{|\omega_1+\mu|^2}{A^-(\mu)}\frac{1}{(\mu+\omega_0)^2}+\frac{R_3}{(\omega_3-\omega_0)^2}\right\}. \qquad (15)$$

We can now proceed in the same manner as in estimating the residue of the function $A^0(\omega)$, i.e., estimate Im $A^\pm/|A^\pm|^2$ by Eq. (8) and then strengthen the inequality by throwing away the last terms in Eq. (15). If the small quantity ω_0 is neglected everywhere, we arrive at the following inequality:

$$\frac{1}{f^2} > \frac{4I_1}{\pi}\left[1+\frac{1}{\omega_1}+\frac{1}{\omega_1^*}+\frac{I_2}{I_1|\omega_1|^2}\right];$$
$$I_1 = \int_1^\infty \frac{d\omega'}{k'\omega'(k'\rho+1)^2}, \qquad I_2 = \int_1^\infty \frac{\omega'\,d\omega'}{k'(k'\rho+1)^2}, \qquad \mu = 1. \qquad (16)$$

Let us set $1/\omega_1 = x + iy$; then the polynomial in the square brackets $[(I_2/I_1)(x^2+y^2)+2x+1]$ has a minimum at $y = 0$ and $x = -I_1/I_2$. For the quantity f^2 we obtain the estimate

$$\frac{1}{f^2} > \frac{4I_1}{\pi I_2}(I_2-I_1) = \frac{4}{\pi\rho}\varphi(\rho)[1-\varphi(\rho)];$$
$$\varphi(\rho) = \frac{\rho^2}{(1+\rho^2)}+\frac{\pi}{2}\frac{\rho(1-\rho^2)}{(1+\rho^2)^2}+\frac{2\rho^2\ln\rho}{(1+\rho^2)^2}. \qquad (17)$$

For $\rho = \frac{1}{2}$ $f^2 < 1.7$; for $\rho = 1$ $f^2 < \pi$, for $\rho = 0$ $f^2 < 0.5$. These estimates are somewhat better than those obtained in Sec. 2. It is interesting that corresponding to the maximum value of f^2 the position of the zero turns out to be on the left cut, i.e., at a place where the true scattering amplitude cannot vanish. Indeed,

$$\omega_1 = -I_2/I_1 = -\varphi(\rho) < -1. \qquad (18)$$

This circumstance is related to the fact that we have not formulated quantitatively the condition that the total cross section must not vanish anywhere. It is obvious that the restriction obtained on f^2 has been greatly overestimated as compared with the true one. From Eq. (18) follow numerical values for ω_1 for various choices of ρ. For $\rho = \frac{1}{2}$ $\omega_1 = -2.8$; for $\rho = 1$ $\omega_1 = -2$; for $\rho = 0$ $\omega_1 \to -\infty$.

In what follows we consider the question whether the pion-nucleon interaction is the maximal possible given the masses of the particles. Had we been able to give a good estimate for the critical constant, beyond which unitarity and analyticity of the theory are violated, then this question could be answered by comparing this quantity with the observed value $f^2 = 0.08$. The value of the critical coupling, obtained from Eq. (17) with $\rho = \frac{1}{2}$, $f^2_{cr} = 1.7$ is 20 times larger than the observed value. This, of course, means nothing since our restriction has been so greatly overestimated.

One can compare the location of the zeros of the amplitude, as obtained from Eq. (18), with the location of the true zeros which can be determined from experimental data, and see to what extent they agree. At that one should remark that since experimentally $A^+(\mu) < 0$, $A^-(\mu) > 0$, it follows that $A^+(\omega)$ has two zeros. It is shown in the Appendix that it follows from experiment that $\omega_{1,2} = -0.9 \pm 0.5\,i$. These numbers are in qualitative agreement with the zeros obtained from Eq. (18) by requiring that f^2 be maximal, if it is taken into account that this requirement must be supplemented

by the condition that $\sigma^{\pm}(\omega)$ must be larger than a certain minimum value, beyond which $\omega_{1,2}$ develops an imaginary part. It may be that this comparison may serve as an indirect indication that the meson-nucleon interaction is maximal.

Restrictions on the residues of the pole terms can be easily obtained also in the presence of bound states in the theory. In contrast to the nonrelativistic theory[2] the upper bound on the coupling constant may depend here on the energy differences of the bound states and increase as this difference decreases.

Let us show now that also the scattering amplitudes at zero energy, i.e., the scattering lengths, are restricted in absolute magnitude, provided that they are negative. Qualitatively this can be understood as follows. At low energies ($k\rho \ll 1$, where k is the momentum and ρ is the interaction range) the scattering amplitude is of the form $a/(1-ika)$, where a is the scattering length. For $\omega < \mu$, $k = +i\sqrt{\mu^2-\omega^2}$, so that the amplitude is written here in the form $a/(1+a\sqrt{\mu^2-\omega^2})$. This expression has a pole at $|k| = \sqrt{\mu^2-\omega^2} = 1/a$. If $a < 0$ and $|a|$ is very large then this pole falls into the region of applicability of our formula ($k\rho \ll 1$). Therefore, if it is known that in the given theory there are no bound states with small binding energies, the quantity $|a|$ cannot be too large. For $a > 0$ the pole passes into the second sheet of the complex plane and the restriction disappears. In that case we are dealing with a situation analogous to singlet np scattering.

Let us consider π-meson–π-meson scattering, restricting ourselves for the sake of simplicity to the case when the crossed reaction is the same as the direct reaction. If the scattering length is negative then, according to the results obtained above, the scattering amplitude has no zeros and the dispersion relation for the inverse function may be written in a form analogous to Eq. (3)*

$$h(\omega) = \frac{1}{\pi}\int_{\mu^2}^{\infty} \frac{d\omega'^2}{\omega'^2-\omega^2}\frac{\operatorname{Im} A(\omega')}{|A(\omega')|^2}. \qquad (19)$$

The scattering length is $a = -1/h(\mu)$. Hence

$$-\frac{1}{a} = \frac{1}{\pi}\int_{\mu^2}^{\infty} \frac{d\omega'^2}{\omega'^2-\mu^2}\frac{\operatorname{Im} A(\omega')}{|A(\omega')|^2}$$

$$> \frac{1}{\pi}\int_{\mu^2}^{\infty} \frac{d\omega'}{\omega'^2-\mu^2}\frac{k'}{(k'\rho+1)^2} = \frac{2}{\pi\rho}, \qquad (20)$$

$$|a| < \pi\rho/2. \qquad (21)$$

If the $\pi\pi$ interaction is characterized by a range $\rho \sim 1/2$ then $|a| < \pi/4$. Since this result most certainly represents a great overestimate it is, apparently, to be expected that if the $\pi\pi$ scattering lengths are found experimentally to be negative, they will turn out to be of the order of $0.1\,\hbar/\mu c$, and not $\hbar/\mu c$ as is frequently asserted.

Analogous inequalities may be also obtained for the πp scattering lengths. For example, for the π^0-meson–proton scattering amplitude one obtains

$$|a| < \pi\rho/\varphi(\rho), \qquad (22)$$

where $\varphi(\rho)$ is given by Eq. (17). For $\rho = 1/2$, $|a| < 4.3$. Experimentally the value of this length is ~ -0.02.

5. CONCLUSIONS

Despite the hypothetical nature of the assumption that a range independent of the interaction strength exists, we are convinced that unitarity and analyticity do in fact impose restrictions on the possible values of the coupling constant. This raises the question whether the π-meson–nucleon interaction, as well as other strong interactions of various particles, is the maximal possible given the values of the masses of the particles. Formulating the question in this fashion presupposes that the magnitude of the renormalized coupling constant may vary to some extent independently of the masses. Such an assumption seems reasonable at the present time since in field theory masses and coupling constants appear as independent quantities as a result of the infinite renormalizations. As regards a "future" theory, in which definite values of coupling constants will be correlated with strictly determined particle masses, we remark that in the first place in such a theory the coupling constants themselves will have definite numerical values, and in the second place no such theory exists as yet.

An example of maximal coupling in the nonrelativistic case is provided by the deuteron formula for nucleon-nucleon scattering. In this case the connection between the location of the pole and the size of the residue of the scattering amplitude corresponds to the strongest interaction possible.[2]

The idea that the strong interactions that are present in nature are in a certain sense as strong as possible seems rather attractive, although at this time it cannot be formulated theoretically in a precise manner or verified experimentally.

In conclusion the authors would like to express their gratitude to Ya. B. Zel'dovich, who stimulated

*For positive a, the right side of Eq. (19) would also contain the pole term corresponding to the zero of $A(\omega)$. The presence of this negative term would make it impossible to obtain an estimate.

their interest in this question. We are also grateful to I. Ya. Pomeranchuk and V. A. Anisovich for constructive remarks.

APPENDIX

DETERMINATION OF THE ZEROS OF THE AMPLITUDE FOR THE FORWARD SCATTERING OF π MESONS ON PROTONS

The dispersion relation with one subtraction at $\omega = \omega_0$ for the function $-(\omega-\omega_1)(\omega-\omega_2)/(\omega-\omega_0)A^+(\omega)$ can be written as follows ($\mu = 1$)

$$a(\omega) - 2b(\omega)\xi + c(\omega)\eta = 0, \qquad (A.1)$$

where

$$\xi = (\omega_1 + \omega_2)/2, \quad \eta = \omega_1\omega_2, \qquad (A.2)$$

$$a(\omega) = \frac{\omega_0^2}{2f^2} + \frac{\omega^2}{(\omega-\omega_0)A^+(\omega)} + \frac{\omega-\omega_0}{\pi}\int_1^\infty d\omega'\omega'^2\left[\frac{\operatorname{Im}A^+(\omega')}{|A^+(\omega')|^2}\frac{1}{(\omega'-\omega_0)^2(\omega'-\omega)} + \frac{\operatorname{Im}A^-(\omega')}{|A^-(\omega')|^2}\frac{1}{(\omega'+\omega_0)^2(\omega'+\omega)}\right],$$

$$b(\omega) = \frac{\omega_0}{2f^2} + \frac{\omega}{(\omega-\omega_0)A^+(\omega)} + \frac{\omega-\omega_0}{\pi}\int_1^\infty d\omega'\omega'\left[\frac{\operatorname{Im}A^+(\omega')}{|A^+(\omega')|^2}\frac{1}{(\omega'-\omega_0)^2(\omega'-\omega)} - \frac{\operatorname{Im}A^-(\omega')}{|A^-(\omega')|^2}\frac{1}{(\omega'+\omega_0)^2(\omega'+\omega)}\right],$$

$$c(\omega) = \frac{1}{2f^2} + \frac{1}{(\omega-\omega_0)A^+(\omega)} + \frac{\omega-\omega_0}{\pi}\int_1^\infty d\omega'\left[\frac{\operatorname{Im}A^+(\omega')}{|A^+(\omega')|^2}\frac{1}{(\omega'-\omega_0)^2(\omega'-\omega)} + \frac{\operatorname{Im}A^-(\omega')}{|A^-(\omega')|^2}\frac{1}{(\omega'+\omega_0)^2(\omega'+\omega)}\right]. \qquad (A.3)$$

It follows from Eq. (A.1) that no matter what two values are chosen for ω after evaluating the expressions (A.3) the combinations

$$\xi = (a_1c_2 - a_2c_1)/2\,(b_1c_2 - b_2c_1),$$

$$\eta = (a_1b_2 - a_2b_1)/(b_1c_2 - b_2c_1) \qquad (A.4)$$

(a_1 and a_2 ... are the values of the functions a ... for those choices of ω) should lead to the same values of ξ and η. The verification of this assertion is by itself equivalent to an additional verification of the dispersion relations. It turns out to be simplest to evaluate (A.3) at the points $\omega = \pm 1$ since, on the one hand, it is then not necessary to evaluate the integral in the principal value sense and, on the other hand, the following quantities are known

$$A^+(1) = a_3\left(1 + \frac{\mu}{m}\right),$$

$$A^+(-1) = \left(\frac{2}{3}a_1 + \frac{1}{3}a_3\right)\left(1 + \frac{\mu}{m}\right),$$

where a_1 and a_3 are the scattering lengths of Orear.[6] In the numerical integration in Eq. (A.3) we have set $\omega = \pm 1$. The values of the real and imaginary parts of $A^\pm(\omega)$ were taken from[7].

As a result of integration and evaluation of Eq. (A.4) we find $\xi = -0.88$, $\eta = 0.96$. Consequently $\omega_{1,2} = -0.88 \pm 0.44i$. Since the size of the imaginary part of $\omega_{1,2}$ depends on the difference of two rather similar numbers (it is equal to $\sqrt{\eta - \xi^2}$) it is unlikely that our determination is very accurate. For this reason we give in the text the value $\omega_{1,2} = -0.9 \pm 0.5\,i$.

Note added in proof (July 14, 1961). From a different point of view the question of the strength of the coupling has also been discussed by Chew and Frautschi.[8]

[1] M. A. Ruderman and S. Gasiorowicz, Nuovo cimento **8**, 861 (1958). Castillejo, Dalitz, and Dyson, Phys. Rev. **101**, 453 (1956).

[2] Gribov, Zel'dovich, and Perelomov, JETP **40**, 1190 (1961), Soviet Phys. JETP **13**, 836 (1961).

[3] Goldberger, Miyazawa, and Oehme, Phys. Rev. **99**, 986 (1955).

[4] L. B. Okun' and I. Ya. Pomeranchuk, JETP **36**, 300 (1959), Soviet Phys. JETP **9**, 207 (1959).

[5] V. N. Gribov, Nucl. Phys. **22**, 249 (1961). V. B. Berestetskii and I. Ya. Pomeranchuk, JETP **39**, 1078 (1960), Soviet Phys. JETP **12**, 752 (1960).

[6] J. Orear, Phys. Rev. **96**, 176 (1954).

[7] Klepikov, Meshcheryakov, and Sokolov, preprint, Joint Inst. Nuc. Res., 1960; J. W. Cronin, Phys. Rev. **118**, 824 (1960).

[8] G. F. Chew and S. C. Frautschi, Phys. Rev. Lett. **5**, 580 (1960).

Translated by A. M. Bincer
110

APPLICATION OF THE POLE METHOD TO THE ANALYSIS OF EXPERIMENTAL DATA ON πp INTERACTIONS

V. I. RUS'KIN and D. S. CHERNAVSKII

P. N. Lebedev Physics Institute, Academy of Sciences, U.S.S.R.

Submitted to JETP editor March 27, 1961

J. Exptl. Theoret. Phys. (U.S.S.R.) **41**, 629-632 (August, 1961)

Various kinematic characteristics of the process $\pi + N \to \pi + \pi + N$ are examined. On this basis, a method is proposed for separating other events from events due to the pole diagram considered by Chew and Low.[1] The problem of improving the extrapolation procedure proposed by Chew and Low is discussed.

THE pole method proposed by Chew and Low[1] for studying the πp interactions has lately achieved great popularity. The inelastic interaction of a π meson with a nucleon, for example the reaction $\pi^- + p \to \pi^- + \pi^0 + p$ ($\pi^- + \pi^+ + n$), is described in this method by the diagram of Fig. 1.

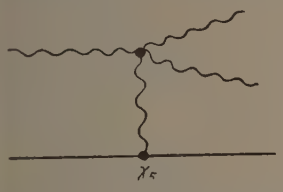

FIG. 1. The pole diagram for the process $\pi + N \to \pi + \pi + N$. The straight lines correspond to nucleons; the wavy lines correspond to π mesons.

The cross section $\sigma_{\pi p}$ for the πp interaction is in this case related to other quantities in the following manner[1]:

$$F(\omega^2, \Delta^2) = \frac{\partial^2 \sigma_{\pi p}}{\partial \Delta^2 \partial \omega^2} (\Delta^2 + \mu^2)^2$$

$$= \frac{f^2}{4\pi} \frac{\Delta^2}{q_0^2 \mu^2} \sqrt{\omega^2 (\omega^2 - 4\mu^2)}\, \sigma_{\pi\pi}(\omega), \qquad (1)$$

where f^2 is the coupling constant, equal to 0.08; μ is the π-meson mass; m is the nucleon mass; q_0 is the momentum of the primary π meson in the laboratory coordinate system (l.s.); ω is the energy of the two secondary π mesons in their center of mass system (c.m.s.); $\sigma_{\pi\pi}$ is the cross section for the mutual scattering of two π mesons; Δ^2 is the square of the four-momentum of the intermediate π meson related to the recoil energy of the nucleon: $\Delta^2 = 2mT$ (T is the kinetic energy of the recoil nucleon in the l.s.).

Thus, by measuring the quantities $\sigma_{\pi p}$, Δ^2, and ω one can obtain information about $\sigma_{\pi\pi}(\omega)$. For this it is sufficient, as has been shown in [1], to extrapolate the quantity $F(\omega^2, \Delta^2)$ from the region $\Delta^2 > 0$ to the point $\Delta^2 = -\mu^2$. At this point

$$\sigma_{\pi\pi} = -4\pi f^{-2} F(\omega^2, -\mu^2)\, q_0^2 [\omega^2 (\omega^2 - 4\mu^2)]^{-1/2}.$$

If all the experimentally recorded cases are indeed due to the diagram of Fig. 1 then, in accordance with (1), $F(\omega^2, \Delta^2)$ must depend linearly on Δ^2, and the extrapolation procedure in this case is simple and does not introduce a large error.

However, in addition to the possibility represented by the diagram of Fig. 1 the process may occur in other ways as well. For example, the following competing processes have been discussed in the literature: a) the so-called head-on collisions described by the statistical theory[2] and characterized by an isotropic distribution of the secondary particles in the c.m.s.; b) processes in which there is a πN interaction in the final state, the diagram for which is given in Fig. 2.

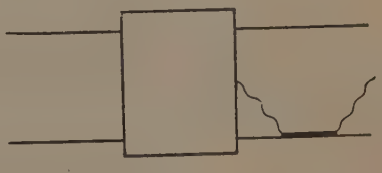

FIG. 2. Diagram of the process taking into account the πN interaction in the final state (the thick line represents the isobar 3/2, 3/2).

Moreover, terms can appear in the cross section which represent interference between matrix elements of different diagrams.* If the aforementioned processes make the same contribution to the cross section (or, more accurately, to the quantity $F(\omega^2, \Delta^2)$) as does the diagram of Fig. 1, then F will no longer depend linearly on Δ^2, but will be given in the general case by the polynomial

$$F(\omega^2, \Delta^2) = a_0 + a_1 (\Delta^2/\mu^2) + a_2 (\Delta^2/\mu^2)^2 + \ldots$$

*It is impossible to assume that the contribution due to the diagram of Fig. 1 will be predominant for small Δ^2, since in accordance with (1) the quantity $F(\omega^2, \Delta^2)$ also tends to zero as $\Delta^2 \to 0$.

It should be emphasized that in this case all the terms of the polynomial (up to the fourth-degree term) must be of the same order (in absolute value) within the region $|\Delta^2/\mu^2| \lesssim 1$.

In this connection it appears to us to be reasonable to pick out in advance from the experimental material those cases which are indeed due to the process shown in Fig. 1.* We consider below one of the possible methods of making such a selection. The method is based on the qualitative difference in the kinematic characteristics of the various processes. At the present time it is impossible to consider all the processes. Therefore, in addition to the pole process we shall discuss only the most "competitive" processes a) and b).

We investigate the kinematic characteristics of the process shown in Fig. 1 for a π-meson energy $E_{lab} = 1$ Bev in the l.s., since the experimental data[3,4] refer to this energy. We first assume that $\sigma_{\pi\pi}(\omega)$ is constant in the range $0.3 \leq \omega \leq 0.7$ Bev. Then on integrating (1) with respect to Δ^2 over the range consistent with the conservation laws we can easily obtain the quantity $d\sigma_{\pi p}/d\omega$, i.e., the distribution of events with respect to the magnitude of ω. This distribution is shown in Fig. 3. It is bell-shaped with a maximum at $\omega = 0.55$ Bev and has a half width $\Delta\omega \sim 0.3$ Bev.

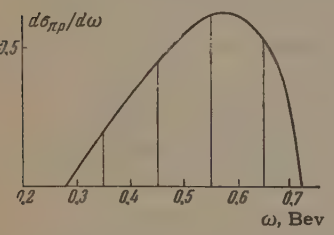

FIG. 3. The distribution $d\sigma_{\pi p}/d\omega$ calculated for the diagram of Fig. 1; ω is the energy of the two π mesons in their c.m.s.

The angular distribution of the nucleons in the c.m.s. of the nucleon and the primary π meson can be easily obtained by assuming $\omega = \overline{\omega} = 0.55$ Bev. It has the form

$$d\sigma \sim \frac{1.13 - \cos\theta}{(1.2 - \cos\theta)^2} d\cos\theta.$$

From this it can be seen that the angular distribution is fairly broad. Therefore, this characteristic cannot be utilized for discriminating between the pole process and, for example, a "head-on" collision.

The distribution of the π mesons with respect to the angle φ between them (in the c.m.s.) is shown in Fig. 4. Curve 1 corresponds to the process of Fig. 1;* curve 2 corresponds to the process for which a "πN isobar" of mass $\mathfrak{M} = 1.3$ m, isospin $T = 3/2$ and spin $J = 3/2$ is formed in the final stage. This process corresponds to the diagram of Fig. 2.† The dotted curve was obtained on the assumption of isotropic distribution of all the particles (π mesons and nucleon) in the c.m.s. taking the conservation of momentum into account.[6] It can be seen from the diagram that curves 2 and 3 are close to one another, but curve 1 is appreciably different.

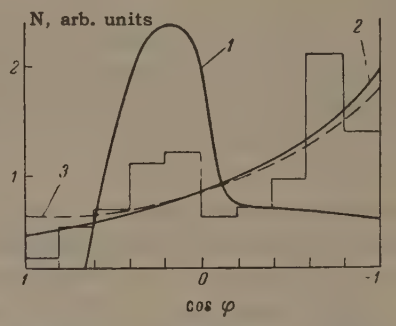

FIG. 4. Distribution with respect to the angle φ between two π mesons in the c.m.s. The curves correspond to: 1 – the pole diagram of Fig. 1, 2 – the process in which the isobar participates, 3 – isotropic angular distribution. The histogram represents the experimental data of[4]. All the curves are normalized in the same way (N is the number of events).

We note that an estimate of the interference between the matrix elements of the processes considered here can also be made using the curves of Fig. 3. Indeed, we can always choose the angle φ as one of the independent angular variables. Then the regions of overlap of the curves of Fig. 3 give some information about the order of magnitude of the interference terms. It can be seen from the graph that even if all the processes make equal contributions the interference between them is still not very great. It is impossible to estimate in advance the total contribution of the diagram of Fig. 1 to the process of πN interaction since it

*Of course, in this case, the statistical accuracy in the determination of $\sigma_{\pi p}$ [or more precisely, of the quantity $F(\omega^2, \Delta^2)$] will be reduced, but the accuracy of the extrapolation will be significantly increased.

*In obtaining this it was assumed that the angular distribution of the π mesons in their c.m.s. (denoted in the following by $\pi\pi$ system) is isotropic. In actual fact (for example, if there exists a resonance $\pi\pi$ interaction in the $T = 1$ and $J = 1$ state) this distribution can depend on the angle ϑ measured from the direction of motion $\mathbf{n}$ of the primary π meson in the $\pi\pi$ system. However, in our case this fact is immaterial, for owing to the broad angular distribution in the c.m.s. the distribution of the directions $\mathbf{n}$ in the $\pi\pi$ system is nearly isotropic.

†Analogous calculations of angular correlations have already been carried out earlier by Rus'kin and Usik.[5] They were utilized in one of the variants of the statistical theory of multiple production.

depends on the magnitude of $\sigma_{\pi\pi}$, which must itself be determined from experiment.

Experimentally the angular correlation of the π mesons has been measured only by Walker, Hushfur and Shepard[4] at an energy of $E_{lab} = 1$ Bev. Their data are represented by the histogram in Fig. 4. It can be seen that there exist two well resolved maxima: near $\cos\varphi = 0.2$ and $\cos\varphi = -0.8$. Comparison with the curves shows that the region near the first maximum is due to processes taking place in accordance with the diagram of Fig. 1, while the neighborhood of the second maximum is due to other processes. The area under the first maximum amounts to approximately one-third of the total area. Thus, the pole part does not give rise to a dominant contribution to the cross section, but amounts to approximately one-third of the cross section.

The whole discussion has been carried out on the assumption that $\sigma_{\pi\pi}(\omega)$ is a smooth function of the energy ω in the range $\omega \sim 0.3 - 0.7$ Bev. However, at the present time there are some indications of the resonance character of this function. If the resonance occurs in the neighborhood of $\omega_r \sim 0.55$ Bev,[3] then this merely improves the conditions for resolving the maxima in the angular distribution with respect to φ (Fig. 4). If the resonance occurs at $\omega_r \sim 0.7$ Bev, then at an energy of $E_{lab} = 1$ Bev the criteria for performing the separation become worse, but they will again be good at a higher energy. For this it is sufficient to have $\omega_r < \omega_{max}$, where ω_{max} is the maximum value of ω consistent with the conservation laws: $\omega_{max} = (2E_{lab}m + m^2 + \mu^2)^{1/2} - m$. We note that the separation of the maxima in the distribution over the angle φ is significantly improved if we do not utilize all the experimental material, but pick out from it the cases corresponding to small values of Δ^2.

From the above discussion it follows that the angular correlation of the mesons in the c.m.s. can serve as a good criterion for ensuring that the selected cases actually correspond to the diagram of Fig. 1.

In conclusion the authors express their gratitude to E. L. Feĭnberg and I. M. Dremin for a number of valuable comments.

[1] G. F. Chew and F. E. Low, Phys. Rev. **113**, 1640 (1959).

[2] Belen'kii, Maksimenko, Nikishov, and Rozental', Usp. Fiz. Nauk **62**, 1 (1957).

[3] D. D. Andersen and N. N. Schmitz, Proc. 1960 Annual International Conference on High Energy Physics at Rochester, Univ. of Rochester, 1961.

[4] Walker, Hushfur, and Shepard, Phys. Rev. **104**, 527 (1956).

[5] V. I. Rus'kin and L. N. Usik, JETP **38**, 929 (1960), Soviet Phys. JETP **11**, 669 (1960).

[6] V. A. Astaf'ev, JETP **36**, 98 (1959), Soviet Phys. JETP **9**, 70 (1959).

Translated by G. Volkoff
111

PION-NUCLEON AMPLITUDE WITH ACCOUNT OF ππ INTERACTION

A. D. GALANIN and A. F. GRASHIN

Institute for Theoretical and Experimental Physics, Academy of Sciences, U.S.S.R.

Submitted to JETP editor March 30, 1961

J. Exptl. Theoret. Phys. (U.S.S.R.) **41**, 633-643 (August, 1961)

Dispersion relations for the invariant πN amplitudes similar to those used by Bowcock et al[7] are considered. The relations contain additional subtractions in the energy s (one subtraction) and momentum transfer t (two subtractions). They are regarded as integral equations with kernels dependent on the S, P, and D wave ππ scattering amplitudes. All quadratures obtained in the solution of the integral equations are evaluated for a simple phase shift model which is a generalization of the effective interaction range approximation. Simple analytic expressions for the contribution of ππ interaction to the πN amplitude are obtained. It is shown that in previous calculations[3-9] the convergence of the integrals along the cut $t \geq 4\mu^2$, where μ is the pion mass, is not sufficiently rapid; conclusions based on these calculations are therefore not reliable.

1. INTRODUCTION

SEVERAL attempts have recently been made to calculate the πN amplitudes for small values of the invariants s and t on the basis of the Mandelstam representation.[1,2] The solution of this problem would relate the ππ-scattering, πN-scattering, NN-scattering, and nucleon electromagnetic form factors. The simplest way of solving this problem is to use dispersion relations to extrapolate the πN amplitudes from the $\pi + N \to \pi + N$ scattering channel where the imaginary parts of the amplitudes are known from experiment.[3-8] Then the use of unitarity in the two-meson approximation for the $N + \bar{N} \to \pi + \pi$ annihilation channel turns these relations into simple linear integral equations; the solution of these equations is in the form of quadratures dependent on the ππ scattering amplitudes.

The main defect of the previous calculations is the insufficiently rapid decrease of the integrands in the integrations along the annihilation cut $t \geq 4\mu^2$, where t is the square of the total energy in the annihilation channel and μ is the pion mass. As a result, the calculations are inconsistent since, on the one hand, the use of unitarity in the two-meson approximation assumes that we are concerned with only small values of t, while, on the other hand, the integrals obtained in the solution of the equations depend strongly on the behavior of the amplitudes for large t. Moreover, in several papers[3-6] numerical integration was used to carry out the calculations; this makes the consideration of the various problems requiring a knowledge of the πN amplitudes very complicated. We note also that Efremov, Meshcheryakov, and Shirkov[6] made use of a patently incorrect simplification in their equations (see below); as a result, their results must be revised.

Bowcock, Cottingham, and Lurie[7] (see also [8] and [9]) obtained simple analytic expressions for the πN amplitudes in a model with a sharp ππ resonance; however, this was achieved at the price of not using the correct solution of the integral equations. For this reason it is not clear whether the contributions they obtain from the cut $t \geq 4\mu^2$ are consistent with the two-meson approximation or not, i.e., whether they are a consequence of ππ interaction or of heavier intermediate states in the unitarity condition.

In this work we attempt to improve the method used in [7] by introducing additional subtractions and correctly solving the integral equations thus obtained. In a simple ππ phase model which is a generalization of the effective interaction range approximation, all the integrals are evaluated and simple analytic expressions are obtained for the contributions from the cut $t \geq 4\mu^2$. In this model the ππ interaction is specified by a number of parameters which are unknown at present. The scattering length[3,4,6] and Breit-Wigner resonance[7-9] approximations used previously are special cases of our model. The πN amplitudes we obtain can easily be used in various problems involving nucleons and pions; this will be done in separate papers.

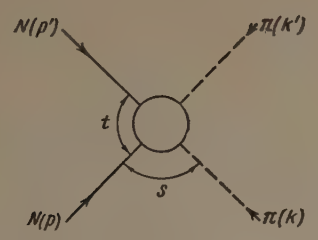

2. EQUATIONS FOR THE INVARIANT πN AMPLITUDES

We use the system of units in which $\hbar = c = \mu = 1$ and the following notations for the invariants (see Fig. 1):

$$t = (p + p')^2,\ \nu = (p - p')(k - k')/4m,$$
$$s = (p + k)^2 = m^2 + 1 - t/2 + 2m\nu,$$
$$u = (p + k')^2 = m^2 + 1 - t/2 - 2m\nu,$$
$$p^2 = p'^2 = m^2 = 1/\varepsilon^2, \qquad \varepsilon = 0.15, \qquad k^2 = k'^2 = 1. \tag{1}$$

In the $\pi + N \to \pi + N$ channel the invariant s is related to the total energy ω of the incident pion in the laboratory system of coordinates by

$$\omega = (s - m^2 - 1)/2m.$$

In considering the πN amplitudes in the annihilation channel, it is convenient to use the variables x and $\bar{\theta}$ (the square of the pion 3-momentum and the angle between the vectors p and -k, respectively, in the center-of-mass system in this channel), which are related to t and ν by

$$t = 4(1 + x), \tag{1'}$$
$$\nu = \sqrt{t/4m^2 - 1}\,\sqrt{t/4 - 1}\cos\bar{\theta}.$$

The pion-nucleon amplitude is specified by the invariant functions $A^{(\pm)}$ and $B^{(\pm)}$ (in the usual notation[10,11]), which satisfy dispersion relations in ν (or, equally, in s) for fixed momentum transfer t. We use these relations as a starting point. Instead of $A^{(\pm)}$ we consider the functions with definite helicity[12,13]

$$F^{(\pm)} = (1 - t/4m^2)A^{(\pm)} + \nu B^{(\pm)}, \tag{2}$$

which, as will be apparent in the following, have some advantages over the $A^{(\pm)}$.

The dispersion relation for $F^{(+)}$ is

$$F^{(+)}(\nu, t) = F_p^{(+)}(\nu, t) + F^{(+)}(0, t) + \frac{1}{\pi}\int_{(m+1)^2}^{\infty} \mathrm{Im}\,F^{(+)}(s', t)\left[\frac{1}{s' - s(\nu,t)} + \frac{1}{s' - u(\nu,t)} - \frac{2}{s' - s(0,t)}\right]ds', \tag{3}$$

where the notation for the pole terms is

$$F_p^{(\pm)} = \nu B_p^{(\pm)}; \qquad B_p^{(\pm)} = g_r^2\left(\frac{1}{m^2 - s} \mp \frac{1}{m^2 - u}\right). \tag{4}$$

with $g_r^2 = 4\pi g^2$, $g^2 = 14.5$.

We consider the analytic properties in t of $\mathrm{Im}\,F^{(+)}(s', t)$ and of the subtraction term $F^{(+)}(0, t)$. The subtraction term has the cuts $t \geq 4$ and $t \leq -4m$, and $\mathrm{Im}\,F^{(+)}(s', t)$ has cuts for $t \geq t(c_{13}) \geq 4$ and $t \leq t(c_{12}) < -4m$, where c_{12} and c_{13} are the boundary curves in Mandelstam's[1] notation. The contributions from the left-hand cuts can be expanded in powers of t; this gives a series in powers of $|t/t_{\mathrm{eff}}| < |t|/4m = \epsilon|1 + x|$. Keeping just two terms of this expansion and combining them with similar terms from the right-hand cuts (which is equivalent to using a dispersion relation in t with two subtractions), we obtain

$$F^{(+)}(\nu, t) = F_p^{(+)}(\nu, t) + \mathcal{F}^{(+)}(0, t) + \frac{1}{\pi}\int_{(m+1)^2}^{\infty} \mathrm{Im}\,\mathcal{F}^{(+)}(s', t)\left[\frac{1}{s' - s(\nu,t)} + \frac{1}{s' - u(\nu,t)} - \frac{2}{s' - s(0,t)}\right]ds' + \frac{t^2}{\pi}\int_4^{\infty} F_{ann}^{(+)}(\nu, t')\frac{dt'}{(t' - t)\,t'^2}, \tag{5}$$

$$\mathcal{F}^{(+)}(0, t) = F^{(+)}(0,0) + t\left[\frac{\partial}{\partial t}F^{(+)}(0, t)\right]_{t=0},$$
$$\mathrm{Im}\,\mathcal{F}^{(+)}(s', t) = \mathrm{Im}\,F^{(+)}(s', 0) + t\left[\frac{\partial}{\partial t}\mathrm{Im}\,F^{(+)}(s', t)\right]_{t=0} \tag{6}$$

which is accurate to order $\epsilon^2(1 + x)^2$.

The last term in Eq. (5) gives the exact contribution (with two subtractions) of the cut $t \geq 4$; $F_{ann}^{(+)}$ signifies the annihilation part of the absorptive part of the amplitude $F^{(+)}$. For $t \leq 16$ only two-meson states contribute to $F_{ann}^{(+)}$; their contribution can be obtained by extrapolating $\mathrm{Im}\,F^{(+)}$ from the physical region of the $N + \bar{N} \to \pi + \pi$ channel.[1,14] The extrapolation can be carried out by means of an expansion in Legendre polynomials $P_l(\cos\bar{\theta})$.[13] This expansion in annihilation harmonics is equivalent to a series in powers of $[\nu/\nu(c_{13})]^2$ and converges in the region between the boundary curves* c_{13}:

$$-\nu(c_{13}) \leqslant \nu \leqslant \nu(c_{13}), \qquad \nu(c_{13}) \geqslant 2.75.$$

For accuracy of order $\leq(\nu/2.75)^2$ we can keep just the lowest harmonic; by using unitarity† this

*The minimum value (equal to 2.75) of ν on the curve c_{13} occurs for $t = 4.5m$.

†We note that the unitarity condition for the functions (2) has the same form as in the scalar theory and leads to the simple expressions (7) and (10).

can be expressed in terms of the S wave phase shift $\delta_0(x)$ for $\pi\pi$ scattering:

$$F^{(+)}_{ann}(\nu, x) = e^{-i\delta_0(x)} \sin\delta_0(x)\ F^{(+)}_0(x). \tag{7}$$

In Eq. (7) and in the following we use the notation

$$(F^{(\pm)}_l(x);\ B^{(\pm)}_l(x)) = \frac{1}{2}\int_{-1}^{1} P_l(\cos\bar\theta)\,(F^{(\pm)}(\cos\bar\theta, x);\ B^{(\pm)}(\cos\bar\theta, x))\,d\cos\bar\theta \tag{8}$$

for the annihilation harmonics.

For the other invariant amplitudes we obtain

$$B^{(+)}(\nu, t) = B^{(+)}_p(\nu, t) + \frac{1}{\pi}\int_{(m+1)^2}^{\infty} \operatorname{Im}\mathcal{B}^{(+)}(s', t)\left[\frac{1}{s'-s(\nu,t)} - \frac{1}{s'-u(\nu,t)}\right]ds' + \frac{t^2}{\pi}\int_4^\infty B^{(+)}_{ann}(\nu, t')\,\frac{dt'}{(t'-t)\,t'^2},$$

$$F^{(-)}(\nu, t) = F^{(-)}_p(\nu, t) + \nu[\mathcal{F}^{(-)}(\nu_0, t) - \mathcal{F}^{(-)}_p(\nu_0, t)]/\nu_0|_{\nu_0=0} + \frac{1}{\pi}\int_{(m+1)^2}^{\infty} \operatorname{Im}\mathcal{F}^{(-)}(s', t)\left[\frac{1}{s'-s(\nu,t)} - \frac{1}{s'-u(\nu,t)} - \frac{4\nu}{(s'-s(0,t))^2}\right]ds' + \frac{t^2}{\pi}\int_4^\infty F^{(-)}_{ann}(\nu, t')\,\frac{dt'}{(t'-t)t'^2},$$

$$B^{(-)}(\nu, t) = B^{(-)}_p(\nu, t) + \mathcal{B}^{(-)}(0, t) - \mathcal{B}^{(-)}_p(0, t) + \frac{1}{\pi}\int_{(m+1)^2}^{\infty} \operatorname{Im}\mathcal{B}^{(-)}(s', t)\left[\frac{1}{s'-s(\nu,t)} + \frac{1}{s'-u(\nu,t)} - \frac{2}{s'-s(0,t)}\right]ds' + \frac{t^2}{\pi}\int_4^\infty B^{(-)}_{ann}(\nu, t')\,\frac{dt'}{(t'-t)\,t'^2}, \tag{9}$$

where $\mathcal{F}^{(-)}$ and $\mathcal{B}^{(\pm)}$, as in Eq. (6), denote two terms in the expansions of $F^{(-)}$ and $B^{(\pm)}$ in powers of t. We note that for the amplitudes $F^{(-)}$ and $B^{(-)}$ it would be possible to make no subtractions in the energy variable, but in this case the original dispersion relations would contain arbitrary terms $\nu a(t)$ and $b(t)$ of the same form as the subtraction terms.[11] Thus, the introduction of subtractions to improve the convergence of the integrals over the energy does not increase the number of unknown parameters.

The lowest harmonics of the functions $F^{(-)}_{ann}$ and $B^{(\pm)}_{ann}$ are expressed in terms of the P and D wave $\pi\pi$ scattering phase shifts $\delta_1(x)$ and $\delta_2(x)$ by

$$B^{(+)}_{ann}(\nu, x) = 3\nu e^{-i\delta_2(x)} \sin\delta_2(x)\,[B^{(+)}_1(x) - B^{(+)}_3(x)]\,/\,W\sqrt{-x},$$
$$F^{(-)}_{ann}(\nu, x) = 3\nu e^{-i\delta_1(x)} \sin\delta_1(x)\ F^{(-)}_1(x)/W\sqrt{-x},$$
$$B^{(-)}_{ann}(\nu, x) = e^{-i\delta_1(x)} \sin\delta_1(x)\ [B^{(-)}_0(x) - B^{(-)}_2(x)],$$
$$W = \sqrt{1 - \varepsilon^2(1 + x)}. \tag{10}$$

The extrapolation of the functions (10) from the physical region of the $N + \bar N \to \pi + \pi$ reaction to the region $x \sim 1$ is made on the upper side of the cut $x \geq 0$ ($t \geq 4$), where we take $W(-x)^{1/2} = -i\,|W(-x)^{1/2}|$.

Equations (5) and (9) are similar to those used in [7]; they differ only in the presence of additional subtractions. The subtraction terms in (5) and (9) can be expressed in terms of the S, P, and D pion-nucleon scattering lengths (see the Appendix); in $F^{(\pm)}$ they can be expressed in terms of only the S and P scattering lengths. The s' integration is over the physical region for πN scattering along the line $t = 0$, $s' \geq (m + 1)^2$; the main contribution comes from energies of several hundred Mev, where the πN amplitudes are rather accurately known.

For numerical calculations it is essential to express the first term in the expansion of $\operatorname{Im} F^{(\pm)}(s', t)$ in powers of t in terms of the total cross sections $\sigma_t(\pi^{(\pm)}p)$ for $\pi^{(\pm)}p$ interactions:

$$\operatorname{Im} F^{(\pm)}(s, 0) = \operatorname{Im}\mathcal{F}^{(\pm)}(s, 0) = E_{c.m.}p_{c.m.}\,[\sigma_t(\pi^- p) \pm \sigma_t(\pi^+ p)]/2m. \tag{11}$$

Here $E_{c.m.}$ and $p_{c.m.}$ are the total energy and momentum in the center-of-mass system. This procedure gives significantly higher accuracy than calculating with the πN phase shifts.

The relations (5) and (9) are thus equations of the form

$$(F^{(\pm)}(\nu, t);\ B^{(\pm)}(\nu, t)) = (\tilde F^{(\pm)}(\nu, t);\ \tilde B^{(\pm)}(\nu, t)) + \frac{t^2}{\pi}\int_4^\infty \frac{(F^{(\pm)}_{ann}(\nu, t');\ B^{(\pm)}_{ann}(\nu, t'))\,dt'}{(t'-t)\,t'^2} \tag{12}$$

where $\tilde F^{(\pm)}$ and $\tilde B^{(\pm)}$ are known functions without singularities on the line $t = 4$ and $F^{(\pm)}_{ann}$ and $B^{(\pm)}_{ann}$ are certain integrals of $F^{(\pm)}$ and $B^{(\pm)}$. By solving these equations we obtain the amplitudes for small values of the invariants with an accuracy of order

$$|t|^2/16m^2, \qquad |\nu|^2/8, \tag{13}$$

due to the expansions used above.*

Similar equations were obtained by Ishida et al.[4] They differ from (5) and (9), however, in that they contain integrals of $\operatorname{Im} A^{(\pm)}$ and $\operatorname{Im} B^{(\pm)}$ in an unphysical region along the line $u = \text{const}$, $s \geq (m + 1)^2$; it is therefore difficult to estimate with sufficient reliability the contribution from

*We emphasize that the parameters in (13) define the accuracy of the solution of the problem within the two-meson approximation; the study of the conditions under which the latter is applicable is the self-consistency question. From general considerations one can expect that higher-mass intermediate states in the unitarity condition will give additional contributions of order $(t/16)^2$ and $(t/4m)^2$.

that part of the region of integration where they used an incorrect expansion in Legendre polynomials.

3. SOLUTION OF THE EQUATIONS

When Eq. (12) is written in terms of the annihilation harmonics (8) with the substitutions (7) and (10), it has the form of a well known integral equation[15,16] whose solution can be written in terms of the auxiliary function (meson form factor)

$$\varphi_l(x) = \exp\left[\frac{x-\xi}{\pi}\int_0^\infty \frac{\delta_l(x')\,dx'}{(x'-x)(x'-\xi)}\right]. \qquad (14)$$

A subtraction at some point ξ is used to improve the convergence for $x' \to \infty$. In order to calculate (14) we approximate the ππ phase shifts by

$$x^l \sqrt{x}\,\mathrm{ctg}\,\delta_l(x) = X(x), \qquad (15)^*$$

where X(x) is a polynomial of arbitrary degree. The phase shift (15) corresponds to the ππ amplitude

$$\lambda_l(x) = ix^l\sqrt{-x}/(X(x) + x^l\sqrt{-x}),$$

$$\lambda_l(x+i0) = e^{i\delta_l(x)}\sin\delta_l(x), \qquad (16)$$

defined on the whole plane with a cut for $x \geq 0$ and poles at the points $x = x_k$ ($k = 1, 2, \ldots n$) which are the roots of the equations $X(x) + x^l(-x)^{1/2} = 0$, $\mathrm{Re}(-x)^{1/2} \geq 0$. Generally speaking, these poles have no physical significance, but just represent the effects of the left-hand cut $x \leq -1$, which the "true" ππ amplitude with the correct analytic properties must have.

Substituting (15) into (14) and transforming the integral into a contour integral around the cut $x \geq 0$, we obtain

$$\varphi_l(x) = \frac{\Pi_{k=1}^n (x-x_k)}{X(x) + x^l\sqrt{-x}}. \qquad (17)$$

We consider now the solution for $F^{(+)}$, which can be written in the form†

$$F_0^{(+)}(x) = \tilde{F}_0^{(+)}(x) + \frac{(1+x)^2}{2\pi i}\varphi_S(x) \times \int_0^\infty \frac{\tilde{F}_0^{(+)}(x')\,[\varphi_S^{-1}(x'-i0) - \varphi_S^{-1}(x'+i0)]\,dx'}{(x'-x)(1+x')^2}, \qquad (18)$$

$$\tilde{F}_0^{(+)}(x) = \mathcal{F}^{(+)}(0,x) + \varepsilon g_r^2\left[-1 + \frac{\varepsilon(1+2x)}{4W\sqrt{-x}}\ln\frac{\varepsilon(1+2x)+2W\sqrt{-x}}{\varepsilon(1+2x)-2W\sqrt{-x}}\right] + \frac{2}{\pi}\int_1^\infty \frac{\mathrm{Im}\,\mathcal{F}^{(+)}(\omega,x)}{\omega+\varepsilon(1+x)}\left[\frac{\omega+\varepsilon(1+x)}{2W\sqrt{-x}} \times \ln\frac{\omega+\varepsilon(1+x)+W\sqrt{-x}}{\omega+\varepsilon(1+x)-W\sqrt{-x}} - 1\right]d\omega. \qquad (19)$$

For the higher harmonics $F_l^{(+)}(x) = \tilde{F}_l^{(+)}(x)$. The subtraction term in (19) can be expressed in terms of the experimental πN amplitude with an accuracy of $\epsilon^2(1+x)$ (see the Appendix); it is

$$\mathcal{F}^{(+)}(0,x) = \varepsilon g_r^2\tilde{\alpha}(x), \quad \tilde{\alpha}(x) = 0.95 + 0.2(1+x). \qquad (20)$$

The last term in (19) can be neglected, since it is a correction of order $\leq \epsilon^2 x$ to the subtraction term, as can be seen by expanding the integrand in powers of

$$\left|\frac{W\sqrt{-x}}{\omega+\varepsilon(1+x)}\right|^2 \sim \left|\frac{W\sqrt{-x}}{\omega_{\mathrm{eff}}+\varepsilon(1+x)}\right|^2 \sim \varepsilon x \qquad (21)$$

and calculating the lowest order term (the value $\omega_{\mathrm{eff}} \approx 2.4$ corresponds to the 33 resonance).

The integration over x which remains in (18) can be put into a form analogous to the integration in (14) by noting that

$$\frac{-2x^l\sqrt{-x}}{\Pi_{k=1}^n (x-x_k)} \qquad (22)$$

is the analytic continuation of the function $\varphi_l^{-1}(x-i0) - \varphi_l^{-1}(x+i0)$ to the whole plane with the cut $x \geq 0$ and coincides with it on the upper side of the cut. Summing all the harmonics in reverse, we obtain finally

$$F^{(+)}(\nu,x) = \tilde{F}^{(+)}(\nu,x) + i\varepsilon g_r^2\lambda_S(x)\left\{\tilde{\alpha}(x) - 1 + \frac{\varepsilon(1+2x)}{2\sqrt{-x}} \times \ln\left(1+2x+\frac{2\sqrt{-x}}{\varepsilon}\right) + L_{n+1}^{(S)}(x)/\sqrt{-x}\right\}, \qquad (23)$$

where the polynomial $L_{n+1}^{(S)}(x)$ of degree $n+1$ is found from the conditions that the expression in the curly brackets vanish at the points $x = -1$ and $x = x_k$ ($k = 1, 2, \ldots, n$) along with its first derivative at the point $x = -1$.* The conditions at $x = -1$ are equivalent to the presence of two subtractions in (18). In the integration of the logarithmic term in (19), W has been replaced by unity

*ctg = cot.

†The solution (18) is unique if we require that $F_0^{(+)}(x)/x^2\varphi_S(x)$ go to zero as $|x|$ becomes infinite; this is fulfilled if we require that the function $F_0^{(+)}(x)/\varphi_S(x)$, which has no cut for $x \geq 0$, satisfy a dispersion relation with two subtractions (cf.[13]).

*For actually calculating the polynomial $L_{n+1}^{(S)}$, it is convenient to write it in the form $L_1(x) + (1+x)^2 L_{n-1}(x)$, where the first degree polynomial $L_1(x)$ is first determined from the conditions at $x = -1$, i.e., it is independent of the x_k.

and the contribution from the cut $x \lesssim -m^2$ ($t \lesssim -4m^2$) which remains after the integral in (18) is transformed into a contour integral has been dropped; this gives an accuracy of $\epsilon^2(1+x)$.

We call attention to the compensation of the subtraction and pole (of order ϵg_r^2) terms in (19) and (23); these appear in the combination* $\tilde{\alpha}(x) - 1 \approx \epsilon(1+x)$. A similar compensation also occurs in the subsequent terms of the expansion (7) which depend on D-wave and higher $\pi\pi$ phase shifts. This makes the contribution of $\pi\pi$ interaction to $F^{(+)}$ smaller by an additional factor ϵ and increases the relative error due to the corrections that have been neglected in calculating this contribution. This compensation shows that in no case may one neglect the contribution of $B^{(+)}$ to the absorptive part in the equation for $A^{(+)}$, as was done by Efremov, Meshcheryakov, and Shirkov[6] [see Eq. (5.3) in their first paper]. Notwithstanding this fundamental distortion of the equation, they obtained the same S-wave $\pi\pi$ scattering length as was obtained in papers by Sato et al[3] and Ishida et al,[4] where this contribution was included. This is apparently a consequence of the fact that in both cases the main contribution comes from the region of impermissibly large values $x \gtrsim m$, where this compensation does not occur.

The solutions for the other invariant amplitudes can be obtained in a similar way. Thus, for $B^{(+)}$ we expand the additional absorptive part in powers of $\epsilon(1+2x)/2x^{1/2}$ and keep just the lowest order term to obtain

$$B^{(+)}(\nu, x) = \tilde{B}^{(+)}(\nu, x) + 5i\nu\varepsilon g_r^2 \lambda_D(x)\{x^{-1} + L_{n+1}^{D}(x)/x^2\sqrt{-x}\}, \quad (24)$$

where the polynomial $L_{n+1}^{D}(x)$ is determined in a manner analogous to that in which $L_{n+1}^{(S)}(x)$ is determined. For simplicity we denote the number of poles in the D-wave $\pi\pi$ scattering amplitude by the same letter n that we use for the S wave amplitude. Since the absorptive part vanishes like $x^{5/2}$ near $x = 0$, the expansion in powers of $\epsilon(1+2x)/2x^{1/2}$ does not, in practice, introduce errors near $x = 0$; it provides an accuracy of $\epsilon x^{1/2}$ for the integration region $x \gtrsim 1$. Corrections of order ϵ to the contribution of the D-wave scattering to $B^{(+)}$ need not be taken into account, since they are of the same order of magnitude as the D-wave contributions to $F^{(+)}$, which we neglected.

*This result was obtained previously for the amplitudes at the point $\nu = 0$, $t = 4\mu^2$ where they determine the peripheral interaction.[17,18]

The solutions for $F^{(-)}$ and $B^{(-)}$, which depend on the P-wave $\pi\pi$ scattering, are expressed in terms of the annihilation harmonics

$$\frac{1}{W\sqrt{-x}}\tilde{F}_1^{(-)}(x) = \frac{1}{3\nu_0}[\mathcal{F}^{(-)}(\nu_0, x) - \mathcal{F}_p^{(-)}(\nu_0, x)]\Big|_{\nu_0=0} + \frac{\varepsilon^2 g_r^2(1+2x)}{2W^2 x}\left[1 - \frac{\varepsilon(1+2x)}{4W\sqrt{-x}}\ln\frac{\varepsilon(1+2x)+2W\sqrt{-x}}{\varepsilon(1+2x)-2W\sqrt{-x}}\right], \quad (25)$$

$$\tilde{B}_0^{(-)}(x) - \tilde{B}_2^{(-)}(x) = \mathcal{B}^{(-)}(0, x) - \mathcal{B}_p^{(-)}(0, x) + \frac{3\varepsilon g_r^2}{4W^2}\left\{\frac{1+\varepsilon^2/4x}{W\sqrt{-x}}\ln\frac{\varepsilon(1+2x)+2W\sqrt{-x}}{\varepsilon(1+2x)-2W\sqrt{-x}} - \frac{\varepsilon(1+2x)}{x}\right\}, \quad (26)$$

where we have dropped the terms similar to the last term in (19), since they are corrections of order $\epsilon^2 x$ to (25) and (26). We obtain finally

$$F^{(-)}(\nu, x) = \tilde{F}^{(-)}(\nu, x) + 3i\nu\lambda_P(x)\{\tilde{f}(x) + L_{n+1}^{(P)}(x)/x\sqrt{-x}\}, \quad (27)$$

$$B^{(-)}(\nu, x) = \tilde{B}^{(-)}(\nu, x) + i\lambda_P(x)\{\tilde{b}(x) + M_{n+1}^{(P)}(x)/x\sqrt{-x}\}, \quad (28)$$

where $\tilde{f}(x)$ and $\tilde{b}(x)$ denote the functions (25) and (26) with the additional replacements

$$W \to 1,$$

$$\ln\frac{\varepsilon(1+2x)+2W\sqrt{-x}}{\varepsilon(1+2x)-2W\sqrt{-x}} \to 2\ln\left(1 + 2x + \frac{2\sqrt{-x}}{\varepsilon}\right). \quad (29)$$

The polynomials in (27) and (28) are determined analogously to those in (23) and (24).

We call attention to the fact that (25), like (19), is decreased by a factor of order ϵ. However, this is due to the smallness of both the subtraction and pole terms and not to their compensation; therefore this factor should apparently also occur in the corrections we have neglected in obtaining the original equations [see the derivation of Eqs. (5) and (9)]. In this case, the main error in (25) is due to the error in the subtraction term which amounts to a correction of order $\epsilon(1+x)/3$ to the pole term and must be set equal to zero for the accuracy stated above (see the Appendix).

Comparison of the amplitudes in Eqs. (23), (24), (27), and (28) with Eq. (12) shows that the solution of the integral equations actually amounts to a calculation of the contribution to the πN amplitudes from the annihilation cut $t \geq 4$ due to $\pi\pi$ interaction.

We now discuss the convergence of the integrals over the annihilation cut which we obtained in the solution; this convergence, along with the errors in the integrands, determines the accuracy of the calculations of the $\pi\pi$-interaction terms. The solution of Eq. (12) in the two-meson approxima-

tion, i.e., with the absorptive parts (7) and (10), is logically justifiable only if the result is independent of the behavior of the amplitudes in the region where they are not known, which is the region $x \gtrsim m$ ($t \gtrsim 4m$). Clearly this requires sufficiently rapid convergence of integrals of the type (18) in the region $x' < m$, and thus a corresponding behavior of the harmonics like (19) and the auxiliary functions like (22). In this latter region we have effectively

$$\tilde{F}_0^{(+)} \sim x, \qquad [\tilde{B}_1^{(+)} - \tilde{B}_3^{(+)}]/W\sqrt{-x} \sim 1/x, \tag{30}$$

$$\tilde{F}_1^{(-)}/W\sqrt{-x} \sim \text{const}, \qquad \tilde{B}_0^{(-)} - \tilde{B}_2^{(-)} \sim 1/\sqrt{x},$$

and therefore convergence of the type $dx'/x'^{5/2}$, for example, which would give a contribution of order $\epsilon^{3/2}$ from the region $x' \gtrsim m$, requires the presence of at least one pole in the $\pi\pi$ amplitude (16). Only poles which lie sufficiently near improve the function (22) in the region $x' < m$. This shows the importance for the "true" $\pi\pi$ amplitude of the left-hand cut $x \leq -1$, which is represented in the model (15), (16) by unphysical poles.

It is also not hard to see that the previously-considered simpler scattering length[3,4,6] and sharp $\pi\pi$ resonance[7-9] models lead, in a scheme with one subtraction in t, to integrals of the form $dx'/x'^{1/2}$ for $x' < m$; a large contribution must therefore come from the impermissible region of integration $m \lesssim x' \lesssim m^2$, where the quantities in (30) are replaced by factors that converge somewhat more rapidly. For these models, the introduction of a second subtraction, like that used in the present work, leads to convergence of the form $dx'/x'^{3/2}$ in the region $x' < m$ and makes possible the calculation of the $\pi\pi$ terms with an accuracy of $\epsilon^{1/2}$. Then corrections of order $\epsilon(1+2x)/2x^{1/2}$ must be neglected in (25) along with corrections of order $\epsilon^2(1+2x)^2/4x$ in (26); this is equivalent to substituting in Eqs. (27) and (28)

$$\tilde{f}(x) = \varepsilon^2 g_r^2 (1+2x)/2x,$$

$$\tilde{b}(x) = \mathcal{B}^{(-)}(0,0) - \mathcal{B}_p^{(-)}(0,0) + \frac{3\varepsilon g_r^2}{4}\left\{\frac{2}{\sqrt{-x}}\ln\left(1+2x+\frac{2\sqrt{-x}}{\varepsilon}\right) - \frac{\varepsilon(1+2x)}{x}\right\}. \tag{31}$$

the contributions from the $\pi\pi$ interaction we have neglected corrections of order $\epsilon^2(1+x)^2$ and ϵ^2. However, the amplitude $F^{(+)}$ [Eq. (23)] is decreased by an extra factor ϵ due to compensation of the $\pi\pi$ terms, and its relative accuracy is therefore determined by the parameters ϵ and ϵx. The $\pi\pi$ term in the amplitude $B^{(+)}$ [Eq. (24)] is small because of the small D-wave $\pi\pi$-scattering amplitude and therefore corrections of order ϵ and ϵx have been dropped in calculating it. The relative accuracy of the $\pi\pi$ terms in (27) and (28) is determined by the parameters ϵ^2 and $\epsilon^2 x^2$.

2. The accuracy described in item 1 is attained only for "good" meson form factors which provide sufficiently rapid convergence of the integrals along the annihilation cut $t \geq 4$ and thus lead to relatively insignificant contributions ($\lesssim \epsilon$ for $F^{(+)}$ and $B^{(+)}$ and $\lesssim \epsilon^2$ for $F^{(-)}$ and $B^{(-)}$) from the region of integration $t \gtrsim 4m$. The behavior of the form factors is improved by singularities of the $\pi\pi$ amplitude in the unphysical region within a radius $|x| < m$. In the worst case the $\pi\pi$ terms have an approximate accuracy of $\epsilon^{1/2}$ or $(\epsilon x)^{1/2}$.

3. Peripheral πN interaction is due to the contribution from the S-wave $\pi\pi$-scattering amplitude. The reduction of this contribution to $F^{(+)}$ because of the compensation described above must make it more difficult to fulfill the conditions under which the asymptotic formulas[17] can be applied for the partial amplitudes with large angular momentum l. The disagreement[17] of the theoretical and experimental $l = 2$ phases is apparently a consequence of the fact that the role of terms neglected in the calculation, namely $B^{(-)}$, which is due to P-wave $\pi\pi$ scattering, and further peripheral terms such as four-meson terms and pole-terms, is sharply increased by the compensation.

4. In previous calculations[3-9] the integrals do not converge rapidly enough, and the $\pi\pi$ terms must depend in an essential way on the amplitudes in the region $|t| \gtrsim 4m$ in which the behavior of the amplitudes is not known at present. Therefore, conclusions concerning the $\pi\pi$ interaction drawn on the basis of these calculations must be considered unreliable.*

The authors are grateful to B. L. Joffe, I. Ya. Pomeranchuk, and K. A. Ter-Martirosyan for discussions and useful comments.

4. CONCLUSIONS

1. The method used in the present work allows us to obtain the invariant πN amplitudes in the two-meson approximation with an accuracy of about $(t/4m)^2$; consequently, in the calculation of

*Ball and Wong[19] have also shown that the results of Frazer and Fulco[5] are unreliable and that subtractions must be introduced.

APPENDIX

CALCULATION OF SUBTRACTION TERMS

The subtractions at $\nu = 0$ which enter the original dispersion relations can be expressed in terms of subtractions at $s = s_0 = (m+1)^2$ by

$$F^{(+)}(0,t) - F_p^{(+)}(0,t) = F^{(+)}(s_0,t) - F_p^{(+)}(s_0,t) - \frac{2}{\pi}\left(1+\frac{t}{4m}\right)^2 \int_1^\infty \frac{\operatorname{Im} F^{(+)}(\omega,t)\,d\omega}{(\omega-1)(\omega+t/4m)(\omega+1+t/2m)}, \tag{A.1}$$

$$\frac{1}{\nu_0}[F^{(-)}(\nu_0,t) - F_p^{(-)}(\nu_0,t)]|_{\nu_0=0} = \frac{F^{(-)}(s_0,t) - F_p^{(-)}(s_0,t)}{1+t/4m} - \frac{2}{\pi}\left(1+\frac{t}{4m}\right)^2 \int_1^\infty \frac{\operatorname{Im} F^{(-)}(\omega,t)\,d\omega}{(\omega-1)(\omega+t/4m)^2(\omega+1+t/2m)}. \tag{A.2}$$

The analogous relations for $B^{(-)}$ are obtained by replacing $F^{(+)}$ in (A.1) by $B^{(-)}$. By keeping just two terms in the expansion of (A.1) and (A.2) in powers of t, we obtain the relations we need for the functions $\mathcal{F}^{(\pm)}$ and $\mathcal{B}^{(-)}$. Thus, for example, for $\mathcal{F}^{(+)}$ we have

$$\mathcal{F}^{(+)}(0,t) = \mathcal{F}^{(+)}(s_0,t) - \mathcal{F}_p^{(+)}(s_0,t) - \frac{2}{\pi}\int_1^\infty \frac{\operatorname{Im}\mathcal{F}^{(+)}(\omega,t)\,d\omega}{\omega(\omega^2-1)} - \frac{t}{2\pi m}\int_1^\infty \frac{\operatorname{Im}\mathcal{F}^{(+)}(\omega,0)(2\omega+1)\,d\omega}{\omega^2(\omega+1)^2}. \tag{A.3}$$

The main contribution of the integral terms in (A.3) can be expressed in terms of the πN cross section[20] by using (11); this gives a value $-0.10 - 0.02(1+x)$. In calculating the remaining part of the integral terms we consider just the resonant 33 phase shift[21]; this gives $-0.08(1+x)$. The first term in (A.3) is expressed in terms of the S and P scattering lengths by

$$\mathcal{F}^{(+)}(s_0,t)/4\pi = \tfrac{1}{3}(1+\varepsilon)(2a_3+a_1) + \tfrac{4}{3}(1+x)(1+\varepsilon)\left[2a_{33}+a_{31}+\tfrac{1}{2}(2a_{13}+a_{11})\right]. \tag{A.4}$$

The lengths a_3, a_1, a_{33}, and a_{31} are quite accurately known,[21,22] but reliable values of a_{13} and a_{11} are not available and we neglect them. This gives an error which we estimated by using the 200- to 300-Mev data[22] and assuming the P phases to vary with energy as $p^3_{c.m.}$; this gave a contribution to (A.4) of order $\epsilon^2(1+x)$. Substituting also the pole term, which gives the main contribution to (A.3), we obtain finally

$$\mathcal{F}^{(+)}(0,x) = \varepsilon g_r^2 \tilde{\alpha}(x), \quad \alpha(x) = 0.95 + 0.2(1+x) \tag{A.5}$$

with a relative error of order $\epsilon^2(1+x)$.

In a completely analogous way we obtain

$$\frac{1}{\nu_0}[\mathcal{F}^{(-)}(\nu_0,x) - \mathcal{F}_p^{(-)}(\nu_0,x)]|_{\nu_0=0} = \varepsilon g_r^2[a+b(1+x)], \quad |a|,\ |b| \sim \varepsilon^2. \tag{A.6}$$

In the subtraction term $\mathcal{B}^{(-)}(0,x) - \mathcal{B}_p^{(-)}(0,x)$ the main contribution comes from the term

$$\mathcal{B}^{(-)}(s_0,x)/4\pi = \tfrac{1}{6}\varepsilon(a_1-a_3) + \tfrac{2}{3}m(a_{33}-a_{31}+a_{11}-a_{13}) - (1+x)[\varepsilon(a_{33}-a_{13}) - 4m(d_{35}-d_{33}+d_{13}-d_{15})]. \tag{A.7}$$

We neglect the dependence of (A.7) on the D lengths d. To estimate the error thus introduced we use the analysis of the data at energies above 300 Mev[23] and assume that the D phases vary with energy as $p^5_{c.m.}$. This gives a D-length contribution of order $\epsilon^2(1+x)$ to (A.7). Therefore the main error comes from the contribution of $a_{11} - a_{13}$ which we do not take into account and which apparently amounts to not more than 20%. We obtain finally

$$[\mathcal{B}^{(-)}(0,x) - \mathcal{B}_p^{(-)}(0,x)]/4\pi = 0.9 + 0.3(1+x) \tag{A.8}$$

with an error of $A + b(1+x)$, $|A| \lesssim 0.2$, $|b| \sim \epsilon^2$.

[1] S. Mandelstam, Phys. Rev. **112**, 1344 (1958); **115**, 1741, 1752 (1959).

[2] M. Cini and S. Fubini, Ann. of Phys. **10**, 352 (1960).

[3] Sato, Takahashi, and Ueda, Progr. Theor. Phys. **22**, 617 (1959).

[4] Ishida, Takahashi, and Ueda, Progr. Theor. Phys. **23**, 731 (1960).

[5] W. R. Frazer and J. R. Fulco, Phys. Rev. Lett. **2**, 365 (1959); Phys. Rev. **117**, 1609 (1960).

[6] Efremov, Meshcheryakov, and Shirkov, JETP **39**, 438, 1099 (1960), Soviet Phys. JETP **12**, 308 (1961).

[7] Bowcock, Cottingham, and Lurie, Nuovo cimento **16**, 918 (1960); **19**, 142 (1961).

[8] S. C. Frautschi, Phys. Rev. Lett. **5**, 159 (1960).

[9] S. C. Frautschi and J. D. Walecka, Phys. Rev. **120**, 1486 (1960).

[10] Chew, Goldberger, Low, and Nambu, Phys. Rev. **106**, 1337 (1957).

[11] A. C. Finn, Phys. Rev. **119**, 1786 (1960).

[12] M. Jacob and G. C. Wick, Ann. of Phys. **7**, 404 (1959).

[13] W. R. Frazer and J. R. Fulco, Phys. Rev. **117**, 1603 (1960).

[14] S. Mandelstam, Phys. Rev. Lett. **4**, 84 (1960).

[15] R. Omnes, Nuovo cimento **8**, 316 (1958).

[16] N. I. Muskhelishvili, Singular Integral Equations, P. Noordhoff N. V., Groningen 1953.

[17] A. D. Galanin, JETP **38**, 243 (1960), Soviet Phys. JETP **11**, 177 (1960).

[18] Galanin, Grashin, Joffe, and Pomeranchuk, JETP **37**, 1663 (1959), Soviet Phys. JETP **10**, 1179 (1960); Nuclear Phys. **17**, 181 (1960).

[19] J. S. Ball and D. Y. Wong, Phys. Rev. Lett. **6**, 29 (1961).

[20] Klepikov, Meshcheryakov, and Sokolov, preprint.

[21] Barnes, Rose, Giacomelli, Ring, Miyake, and Kinsey, Phys. Rev. **117**, 226 (1960).

[22] B. Pontecorvo, Report to the Ninth High-energy Physics Conference, Kiev 1959.

[23] Walker, Davis, and Shephard, Phys. Rev. **118**, 1612 (1960).

Translated by M. Bolsterli
112

CONTRIBUTION TO THE THEORY OF PLASMA FLUCTUATIONS

A. I. AKHIEZER, I. A. AKHIEZER, and A. G. SITENKO

Physico-Technical Institute, Academy of Sciences, Ukrainian S.S.R.; Khar'kov State University

Submitted to JETP editor March 30, 1961

J. Exptl. Theoret. Phys. (U.S.S.R.) 41, 644-654 (August, 1961)

Spectral distributions and correlation functions are derived for various fluctuating quantities (electron and ion densities, electron and ion current densities, electric and magnetic fields, particle distribution functions). The possible difference between the electron and ion temperatures is taken into account. The cross sections for the scattering of electromagnetic waves on plasma fluctuations are determined. It is shown that the possibility of propagation of Langmuir oscillations as well as of high-frequency sound waves (in a nonisothermal plasma) leads to the appearance of satellites in the spectrum of the scattered radiation. When a constant magnetic field is applied, the scattered-radiation spectrum contains satellites due to the possibility of propagation of Langmuir, Alfven, and magnetic-sound waves in the plasma.

1. A study of plasma fluctuations can be of interest to plasma physics. Since it yields directly the spectrum of the plasma oscillations, such a study can serve to determine many plasma parameters (density, temperature) and can probably help explain the role of oscillations in transport processes and in the establishment of equilibrium in the plasma. This paper deals with a theoretical determination of the spectral distributions and correlation functions of various fluctuating quantities (including the particle distribution function) and a determination of the cross section for the scattering of electromagnetic waves on fluctuations in a plasma without collisions. We consider here free plasma as well as plasma in a uniform magnetic field, and take into account the possible difference between the electron and ion temperatures.*

2. Fluctuations in a plasma which is in complete statistical equilibrium can be investigated in the general theory (Callen and Welton,[4] Leontovich and Rytov,[5,6] Landau and Lifshitz[7]) by using the known dielectric-constant tensor of the plasma.† In particular, the space-time Fourier components of the correlation functions of the current density $\mathbf{j}(\mathbf{r}, t)$ can be determined from

$$\langle j_i j_j \rangle_{\mathbf{k}\omega} \equiv \int \langle j_i(\mathbf{r}, t)\, j_j(\mathbf{r}', t') \rangle\, e^{-i\mathbf{k}(\mathbf{r}-\mathbf{r}')+i\omega(t-t')}\, d\mathbf{r}\, dt = \frac{\hbar}{1-e^{-\hbar\omega/T}} \frac{1}{2i} (\alpha_{ij} - \alpha_{ji}^*), \quad (1)$$

where $\alpha_{ij}(\mathbf{k}, \omega)$ is the tensor relating the Fourier components of the current $j_i(\mathbf{k}, \omega)$ and the potential $\tilde{A}_i(\mathbf{k}, \omega)$ of the external field:

$$j_i(\mathbf{k}, \omega) = c^{-1} \alpha_{ij}(\mathbf{k}, \omega)\, \tilde{A}_j(\mathbf{k}, \omega)$$

(the symbol $\langle \ldots \rangle$ denotes averaging over the fluctuations). The tensor α_{ij}, as follows from Maxwell's material equations, is connected with the dielectric-constant tensor $\epsilon_{ij}(\mathbf{k}, \omega)$ by the relation

$$\alpha_{ij} = \tfrac{1}{2} \omega^2 \{\Lambda^0_{ij} - \Lambda^{-1} \Lambda^0_{ik} \lambda_{kl} \Lambda^0_{lj}\}, \quad (2)$$

where

$$\Lambda^0_{ij} = \eta^2 (k_i k_j k^{-2} - \delta_{ij}) + \delta_{ij}, \quad \Lambda_{ij} = \Lambda^0_{ij} - \delta_{ij} + \varepsilon_{ij}; \quad \Lambda^{-1}\lambda_{ij} = (\Lambda^{-1})_{ij}, \quad \Lambda = \det \Lambda_{ij}, \quad \eta = kc/\omega. \quad (2')$$

We note that the equation $\Lambda(\mathbf{k}, \omega) = 0$ is the dispersion equation of the system. Consequently the spectral distribution of the fluctuations has sharp maxima near the natural frequencies of the system.*

*The particle-density fluctuations in a free plasma were determined in a paper by Salpeter,[1] with which we became acquainted after completing the present work (the results of[1] coincide with the ones we obtained by a different method). The scattering of electromagnetic waves by Langmuir plasma oscillations was considered earlier.[2] Scattering with small frequency variation in the presence of a magnetic field is treated by Dougherty and Farley.[3]

†Equations for the spatial correlation functions of particle systems with electromagnetic interaction are derived in the papers by Tolmachev, Tyablikov, and Klimontovich.[8-10] The correlation functions of microcurrents were calculated by Shafranov[11] from the laws of motion. The spatial dispersion as it affects the fluctuations was treated by Bass and Kaganov[12] and by Silin.[13]

*Relation (1) can be derived, according to Landau and Lifshitz,[7] from the expression of the rate of change of the plasma energy under the influence of the external field

$$\dot{U} = (2c)^{-1} \operatorname{Re} \sum_{\mathbf{k},\omega} i\omega j^*(\mathbf{k}, \omega)\, \tilde{A}(\mathbf{k}, \omega).$$

The dielectric tensor constant of a free plasma has the form

$$\varepsilon_{ij}(\mathrm{k}, \omega) = k_i k_j k^{-2} \varepsilon_l(k, \omega) + (\delta_{ij} - k^{-2} k_i k_j)\, \varepsilon_t(k, \omega),$$

where ϵ_l and ϵ_t are the longitudinal and transverse dielectric constants of the plasma

$$\varepsilon_l = 1 + (ak)^{-2}\,[1 - \varphi(z) - \varphi(\mu z) + \tfrac{1}{2} i \sqrt{\pi} z\,(e^{-z^2} + \mu e^{-\mu^2 z^2})],$$

$$\varepsilon_t = 1 - 2\frac{\Omega^2}{\omega^2}\left[\varphi(z) - \frac{i}{2}\sqrt{\pi} z e^{-z^2}\right]; \quad \varphi(z) = z e^{-z^2}\int_0^z e^{t^2} dt \qquad (3)$$

($z = \omega/ks$, $\mu^2 = M/m$, $a^2 = (8\pi e^2 n_0)^{-1} T$, $\Omega^2 = 4\pi e^2 n_0/m$, and $s^2 = 2T/m$; n_0 is the equilibrium density of the electrons, while m and M are the electron and ion masses (the plasma is assumed nondegenerate).

Substitution of (3) into (1) and (2) leads to the following expressions for the Fourier components of the correlators of the charge densities and of the transverse current in the plasma

$$\langle \rho^2 \rangle_{k\omega} = \frac{T}{2\pi}\frac{k^2}{\omega}\frac{\operatorname{Im}\varepsilon_l}{|\varepsilon_l|^2} = \frac{T(ak)^3}{4\sqrt{\pi} as} \times \frac{e^{-z^2} + \mu e^{-\mu^2 z^2}}{[1 + (ak)^2 - \varphi(z) - \varphi(\mu z)]^2 + (\pi/4) z^2 (e^{-z^2} + \mu e^{-\mu^2 z^2})^2},$$

$$\langle j_t^2 \rangle_{k\omega} = \frac{T}{2\pi}\omega(\eta^2 - 1)^2 \frac{\operatorname{Im}\varepsilon_t}{|\eta^2 - \varepsilon_t|^2} = \frac{T\omega}{\sqrt{\pi}}\left(\frac{\omega}{\Omega}\right)^2 \frac{(1-\eta^2)^2 z e^{-z^2}}{[\omega^2(1-\eta^2)/\Omega^2 - 2\varphi(z)]^2 + \pi z^2 e^{-2z^2}}. \qquad (4)$$

It follows from these expressions that when $ka \gtrsim 1$ the principal role in the fluctuations of ρ and j is played by the low-frequency oscillations. The frequency of the fluctuations increases with decreasing ka and at $ka \ll 1$ the only frequencies remaining in the spectrum are those close to the natural frequencies of the longitudinal (in the spectrum of ρ) and transverse (in the spectrum of j_t) oscillations of the plasma ($\omega \gg ks$):

$$\langle \rho^2 \rangle_{k\omega} = \tfrac{1}{4} T k^2 \delta(\omega - \omega_p), \qquad \omega_p = \Omega\left(1 + \tfrac{3}{4} k^2 s^2\right),$$

$$\langle j_t^2 \rangle_{k\omega} = \tfrac{1}{2} T \Omega^4 \omega^{-2} \delta(\omega - \omega_t), \quad \omega_t = \sqrt{k^2 c^2 + \Omega^2}. \qquad (5)$$

Integrating $\langle \rho^2 \rangle_{k\omega}$ with respect to the frequencies (which is most readily done with the aid of the Kramers-Kronig relations, see[7]), we derive the well known formula for the spatial Fourier component of the charge-density fluctuation

$$\langle \rho^2 \rangle_k \equiv \frac{1}{2\pi}\int_{-\infty}^{\infty} \langle \rho^2 \rangle_{k\omega}\, d\omega = \frac{T}{4\pi a^2}\frac{(ak)^2}{1 + (ak)^2}. \qquad (6)$$

From this we can then obtain the mean frequency of the plasma space-charge fluctuations

$$\overline{\omega^2} \equiv \left\{\int_{-\infty}^{\infty} \langle \rho^2 \rangle_{k\omega}\, d\omega\right\}^{-1} \int_{-\infty}^{\infty} \omega^2 \langle \rho^2 \rangle_{k\omega}\, d\omega = \Omega^2 + \tfrac{1}{2}(ks)^2.$$

Finally, (6) leads to the following expression for the correlation function of the charge density

$$\langle \rho(\mathbf{r}', t)\, \rho(\mathbf{r}'', t) \rangle = 2e^2 n_0 \left[\delta(\mathbf{r}) - \frac{1}{4\pi a^2}\frac{e^{-r/a}}{r}\right], \quad \mathbf{r} = \mathbf{r}' - \mathbf{r}''. \qquad (7)$$

Analogously we can determine the correlation function for the density of the total current

$$\langle \mathbf{j}(\mathbf{r}', t)\, \mathbf{j}(\mathbf{r}'', t) \rangle = 3e^2 n_0 (T/m)\, \delta(\mathbf{r}). \qquad (8)$$

The spectral distributions of the fluctuations of the electric and magnetic fields **E** and **H** are also expressed in terms of ϵ_l and ϵ_t:

$$\langle \mathbf{E}^2 \rangle_{k\omega} = \frac{8\pi T}{\omega}\left(\frac{\operatorname{Im}\varepsilon_l}{|\varepsilon_l|^2} + 2\frac{\operatorname{Im}\varepsilon_t}{|\eta^2 - \varepsilon_t|^2}\right),$$

$$\langle \mathbf{H}^2 \rangle_{k\omega} = \frac{16\pi T}{\omega}\eta^2 \frac{\operatorname{Im}\varepsilon_t}{|\eta^2 - \varepsilon_t|^2}. \qquad (9)$$

Inserting (3) and integrating with respect to ω, we obtain

$$\langle \mathbf{E}^2 \rangle_k = 8\pi T\left(1 + \tfrac{1}{2}\frac{1}{1 + a^2 k^2}\right), \qquad \langle \mathbf{H}^2 \rangle_k = 8\pi T.$$

From this we readily determine the correlation functions for the fields

$$\langle \mathbf{E}(\mathbf{r}', t)\, \mathbf{E}(\mathbf{r}'', t) \rangle = 8\pi T\left[\delta(\mathbf{r}) + \frac{1}{8\pi a^2}\frac{e^{-r/a}}{r}\right],$$

$$\langle \mathbf{H}(\mathbf{r}', t)\, \mathbf{H}(\mathbf{r}'', t) \rangle = 8\pi T \delta(\mathbf{r}). \qquad (10)$$

3. Using the well-known expression for the dielectric constant of a degenerate electron gas[14] we can use (1) to determine the spectral distribution of the fluctuations in an electron gas with $T \ll mv_0^2/2$ (v_0 — boundary velocity). In particular, we have for $\langle \rho^2 \rangle_{k\omega}$

$$\langle \rho^2 \rangle_{k\omega} = \tfrac{3}{4}\frac{\hbar\zeta k^2}{1 - e^{-\hbar\omega/T}}\left\{\tfrac{1}{2} z\theta(1 - |z|) \times \left[\left(\zeta + 1 - \frac{z}{2}\ln\frac{1+z}{1-z}\right)^2 + \left(\frac{\pi z}{2}\right)^2\right]^{-1} + \delta\left(\zeta + 1 - \frac{z}{2}\ln\left|\frac{z+1}{z-1}\right|\right)\operatorname{sign} z\right\},$$

$$\theta(z) = \begin{cases} 0, & z < 0 \\ 1, & z > 0 \end{cases}, \qquad (11)$$

where $z = \omega/kv_0$ and $\zeta = (kv_0/\Omega)^2/2$.

4. The fluctuations in a plasma situated in a constant homogeneous magnetic field $\mathbf{H}_0$ are also determined by the general formula (1). (The components of the tensor ϵ_{ij} of a plasma in a magnetic field are known[15,16].)

If we disregard the thermal motion of the plasma particles ($\omega \gg ks$), then ϵ_{ij} has the form[17]

$$\varepsilon_{ij} = \begin{pmatrix} \varepsilon_1 & -i\varepsilon_2 & 0 \\ i\varepsilon_2 & \varepsilon_1 & 0 \\ 0 & 0 & \varepsilon_3 \end{pmatrix},$$

$$\varepsilon_1 = 1 - \frac{\Omega^2}{\omega^2 - \omega_H^2}, \quad \varepsilon_2 = \frac{\omega_H}{\omega}\frac{\Omega^2}{\omega^2 - \omega_H^2},$$

$$\varepsilon_3 = 1 - \frac{\Omega^2}{\omega^2}, \quad \omega_H = \frac{eH_0}{mc}. \tag{12}$$

In this case relation (1) becomes ($T \gg \hbar\omega$)

$$\langle j_i j_l \rangle_{k\omega} = \tfrac{1}{4} T\omega \Lambda^0_{ik}\lambda_{kl}\Lambda^0_{lj}\delta\,(A\,(\eta^2 - \eta_1^2)\,(\eta^2 - \eta_2^2)),$$

$$A = \varepsilon_1 \sin^2\vartheta + \varepsilon_3 \cos^2\vartheta, \tag{13}$$

where $\eta_{1,2}$ are the refractive indices of the ordinary and extraordinary waves, and λ_{ij} is determined by formula (2′) (ϑ is the angle between $\mathbf{H}_0$ and $\mathbf{k}$).

Equating the argument of the δ -function to zero, we obtain the dispersion equation for the high-frequency plasma oscillations. The equation $A = 0$ determines here the frequencies of the Langmuir oscillations of the plasma in a magnetic field

$$\omega_\pm^2 = \tfrac{1}{2}(\Omega^2 + \omega_H^2) \pm \tfrac{1}{2}[(\Omega^2 + \omega_H^2)^2 - 4\Omega^2\omega_H^2\cos^2\vartheta]^{1/2}.$$

With the aid of (13) we can find the spectral distribution of the charge-density fluctuations in a plasma at high frequencies ($\omega \gg ks$):

$$\langle \rho^2 \rangle_{k\omega} = \frac{T}{4}\left(\frac{k\omega}{\Omega}\right)^2 \frac{(\omega^2 - \omega_H^2)^2}{\omega^4\cos^2\vartheta + (\omega^2 - \omega_H^2)^2\sin^2\vartheta}\,\{\delta(\omega - \omega_+)$$

$$+ \delta(\omega + \omega_+) + \delta(\omega - \omega_-) + \delta(\omega + \omega_-)\}. \tag{14}$$

5. We now proceed to determine separately the electron and ion density fluctuations, and also the fluctuations of the plasma-particle distribution functions, without assuming the electron and ion temperatures T^e and T^i to be equal. Since the energy exchange between the electrons and ions is much slower than exchange between like particles, we can regard a nonisothermal plasma as a quasi-equilibrium system and apply the general methods of fluctuation theory to the fluctuations produced in this plasma.

To determine the fluctuations of the particle distribution functions we must introduce into the kinetic equations that define these functions the random forces $y^{e,\,i}(\mathbf{v}, \mathbf{r}, t)$ (the indices e and i will henceforth denote electrons and ions):*

$$\left\{\frac{\partial}{\partial t} + \mathbf{v}\frac{\partial}{\partial \mathbf{r}} + \frac{e}{m}\mathbf{E}\frac{\partial}{\partial \mathbf{v}}\right\} F^e(\mathbf{v}, \mathbf{r}, t)$$

$$= -\frac{1}{\tau^e} f^e(\mathbf{v}, \mathbf{r}, t) + y^e(\mathbf{v}, \mathbf{r}, t),$$

$$\left\{\frac{\partial}{\partial t} + \mathbf{v}\frac{\partial}{\partial \mathbf{r}} - \frac{e}{M}\mathbf{E}\frac{\partial}{\partial \mathbf{v}}\right\} F^i(\mathbf{v}, \mathbf{r}, t)$$

$$= -\frac{1}{\tau^i} f^i(\mathbf{v}, \mathbf{r}, t) + y^i(\mathbf{v}, \mathbf{r}, t), \tag{15}$$

where $F_0^{e,\,i}$ are the Maxwellian distribution functions for the electrons and ions, $f^{e,\,i} = F^{e,\,i} - F_0^{e,\,i}$ are the deviations of the distribution functions from Maxwellian, and $\tau^{e,\,i}$ are the relaxation times, which will tend to infinity in the final results. For simplicity we consider first only longitudinal plasma oscillations; in this case

$$\operatorname{div}\mathbf{E} = 4\pi e\{\delta n^e - \delta n^i\} = 4\pi e\int (F^e - F^i)\,d\mathbf{v}, \quad \operatorname{rot}\mathbf{E} = 0. \tag{16}*$$

Taking the time derivative of the entropy of the electron and ion system (separately for specified values of the electron and ion energies and numbers), we obtain

$$\dot{S} = -\int d\mathbf{r}\,d\mathbf{v}\,(\dot{x}^e X^e + \dot{x}^i X^i),$$

$$\dot{x}^{e,\,i} = -\frac{1}{\tau^{e,\,i}} f^{e,\,i} + y^{e,\,i}, \qquad X^{e,\,i} = \frac{f^{e,\,i}}{F_0^{e,\,i}}.$$

Using further the method developed by Landau and Lifshitz[19] and by Abrikosov and Khalatnikov[18] we obtain the following expression for the mean values of the products of the random forces

$$\langle y^a(\mathbf{v}, \mathbf{r}, t)\, y^b(\mathbf{v}', \mathbf{r}', t')\rangle$$

$$= \delta_{ab}\,2(\tau^a)^{-1} F_0^a(\mathbf{v})\,\delta(\mathbf{v} - \mathbf{v}')\,\delta(\mathbf{r} - \mathbf{r}')\,\delta(t - t'), \tag{17}$$

where the indices a and b label the type of particle (a, b ≡ e, i). We now must use (15) and (16) to express the distribution functions and the various physical quantities defined by them in terms of the random forces, and average these forces with the aid of (17). For the Fourier components of the fluctuations of the electron and ion densities we obtain

$$\delta n^e(\mathbf{k}, \omega) = i\frac{k}{\omega}\frac{1}{\varepsilon(k, \omega)}\{Y^e_{k\omega}(1 + 4\pi\varkappa^i) + Y^i_{k\omega}4\pi\varkappa^e\},$$

$$\delta n^i(\mathbf{k}, \omega) = i\frac{k}{\omega}\frac{1}{\varepsilon(k, \omega)}\{Y^e_{k\omega}4\pi\varkappa^i + Y^i_{k\omega}(1 + 4\pi\varkappa^e)\};$$

$$Y^a_{k\omega} = \int \frac{\mathbf{kv}}{k}\left(\omega - \mathbf{kv} + \frac{i}{\tau^a}\right)^{-1} y^a(\mathbf{v}, \mathbf{k}, \omega)\,d\mathbf{v}, \tag{18}$$

where $\epsilon = 1 + 4\pi(\varkappa^e + \varkappa^i)$, where $\varkappa^{e,\,i}$ are the electric susceptibilities of the electrons and ions:

$$\varkappa^a(k, \omega) = -\frac{e^2}{k^2}\frac{1}{T^a}\int F_0^a(v)\frac{\mathbf{kv}}{\omega - \mathbf{kv} + i0}\,d\mathbf{v}. \tag{19}$$

*This method is a generalization of the one employed by Abrikosov and Khalatnikov [18] to find the distribution-function fluctuations in an equilibrium Fermi system.

*rot $\mathbf{E}$ = curl $\mathbf{E}$.

Averaging of Y leads, according to (17) and (19), to the expressions $e^2\langle Y^a Y^b\rangle_{k\omega} = 2\delta_{ab}\omega T^a \operatorname{Im}\kappa^a(k,\omega)$. Using next Eq. (18) we obtain ultimately*

$$e^2\langle|\delta n^e|^2\rangle_{k\omega} = \frac{2k^2}{\omega|\varepsilon|^2}\{T^e|1+4\pi\varkappa^i|^2\operatorname{Im}\varkappa^e + T^i|4\pi\varkappa^e|^2\operatorname{Im}\varkappa^i\},$$

$$e^2\langle|\delta n^i|^2\rangle_{k\omega} = \frac{2k^2}{\omega|\varepsilon|^2}\{T^e|4\pi\varkappa^i|^2\operatorname{Im}\varkappa^e + T^i|1+4\pi\varkappa^e|^2\operatorname{Im}\varkappa^i\},$$

$$e^2\langle\delta n^e\delta n^i\rangle_{k\omega} = e^2\langle\delta n^i\delta n^e\rangle^*_{k\omega} = \frac{2k^2}{\omega|\varepsilon|^2}\{T^e(1+4\pi\varkappa^i)(4\pi\varkappa^i)^*\operatorname{Im}\varkappa^e + T^i(1+4\pi\varkappa^e)^*(4\pi\varkappa^e)\operatorname{Im}\varkappa^i\}. \quad (20)$$

From these formulas we can readily obtain the spectral distribution of the charge-density fluctuations:

$$\langle\rho^2\rangle_{k\omega} \equiv e^2\langle|\delta n^e - \delta n^i|^2\rangle_{k\omega} = \frac{2k^2}{\omega|\varepsilon|^2}\operatorname{Im}\{T^e\varkappa^e + T^i\varkappa^i\}. \quad (21)$$

When $T^e = T^i$, this expression goes into the first expression in (4).

We note that in the region of the small phase velocities ($\omega/k \ll s^e$ and s^i) we have

$$\langle\rho^2\rangle_{k\omega} = \frac{2\sqrt{\pi}}{k}e^2 n_0\left(\frac{1}{s^e}+\frac{1}{s^i}\right)\left(1+\frac{1}{a^2k^2}\right)^{-1},$$

($a^{-1} = \sqrt{k_e^2 + k_i^2}$, $k_{e,i}^2 = 4\pi e^2 n_0/T^{e,i}$). If $s^e \gg \omega/k \gg s^i$ and $T^e \gg T^i$, then

$$\langle\rho^2\rangle_{k\omega} = \frac{1}{4}BT^e\frac{k^4}{k_e^2+k^2}\{\delta(\omega-\omega_s(k)) + \delta(\omega+\omega_s(k))\};\ \omega_s(k) = \frac{\Omega_i}{\sqrt{k_e^2+k^2}}k,$$

where $\Omega_i^2 = 4\pi e^2 n_0/M$;

$$B = \left[1+\frac{s_e}{s_i}\frac{T^i}{T^e}\exp\left\{-\left(\frac{\Omega_i}{s_i}\right)^2\frac{1}{k_e^2+k^2}\right\}\right]\Big/\left[1+\frac{s_e}{s_i}\times\exp\left\{-\left(\frac{\Omega_i}{s_i}\right)^2\frac{1}{k_e^2+k^2}\right\}\right].$$

(In particular, if $\ln(T^e/T^i) \ll (\Omega_i/s_i)^2(k^2+k^2)^{-1}$, then $B = 1$.) We see that in a highly non-isothermal plasma with $T^e \gg T^i$ the correlation function of the charge density has a sharp maximum at $\omega = \pm\omega_s(k)$, corresponding to the possibility that specific sound oscillations propagate in the plasma.† At large phase velocities ($\omega/k \gg s^e, s^i$) the principal role in the charge-density fluctuations is played by electrons, and $\langle\rho^2\rangle_{k\omega}$ is determined by the formula (5) with $T = T^e$.

Let us express now the Fourier component of the distribution-function fluctuation in terms of the random forces

$$f^e(\mathbf{v}) = \frac{4\pi e^2}{k^2}\frac{1}{T^e}\frac{\mathbf{kv}F_0^e(v)}{\omega-\mathbf{kv}+i/\tau^e}(\delta n^e - \delta n^i) + \frac{i}{\omega-\mathbf{kv}+i/\tau^e}y^e(\mathbf{v}),$$

$$f^i(\mathbf{v}) = -\frac{4\pi e^2}{k^2}\frac{1}{T^i}\frac{\mathbf{kv}F_0^i(v)}{\omega-\mathbf{kv}+i/\tau^i}(\delta n^e - \delta n^i) + \frac{i}{\omega-\mathbf{kv}+i/\tau^i}y^i(\mathbf{v}).$$

Using (17), we obtain the distribution-function correlators*

$$\langle f^a(\mathbf{v})f^b(\mathbf{v}')\rangle_{k\omega} = 2\pi\delta_{ab}F_0^a(v)\delta(\mathbf{v}-\mathbf{v}')\delta(\omega-\mathbf{kv}) \pm 2\pi\cdot 4\pi e^2k^{-2}F_0^a(v)F_0^b(v')S^{ab}(\mathbf{v},\mathbf{v}'), \quad (22)$$

where the upper (or lower) sign is taken in the case of like (unlike) particles and

$$S^{ab} = \frac{1}{T^a}\frac{\mathbf{kv}}{\omega-\mathbf{kv}+i0}\frac{1}{\varepsilon}\delta(\omega-\mathbf{kv}') + \frac{1}{T^b}\frac{\mathbf{kv}'}{\omega-\mathbf{kv}'-i0}\frac{1}{\varepsilon^*}\delta(\omega-\mathbf{kv}) + \frac{4}{\omega}\frac{1}{T^aT^b}\frac{\mathbf{kv}}{\omega-\mathbf{kv}+i0}\frac{\mathbf{kv}'}{\omega-\mathbf{kv}'-i0}\frac{\operatorname{Im}(T^e\varkappa^e+T^i\varkappa^i)}{|\varepsilon|^2}.$$

6. We now generalize the obtained results to include a plasma in a constant homogeneous magnetic field $\mathbf{H}_0$. In this case the kinetic equations can be written (in Fourier components) as

$$-iG^a(\mathbf{v},\mathbf{k},\omega)f^a(\mathbf{v},\mathbf{k},\omega) \mp e\mathbf{E}\frac{\mathbf{v}}{T^a}F_0^a(v) = y^a(\mathbf{v},\mathbf{k},\omega),$$

$$G^e = \omega - \mathbf{kv} + i\frac{e[\mathbf{vH}_0]}{mc}\frac{\partial}{\partial\mathbf{v}}, \qquad G^i = \omega - \mathbf{kv} - i\frac{e[\mathbf{vH}_0]}{Mc}\frac{\partial}{\partial\mathbf{v}}. \quad (23)\dagger$$

We can use (23) to relate the fluctuations of the electron and ion currents with the random forces

$$j_i^a = \pm ieY_i^a - i\omega\varkappa_{ij}E_j, \qquad Y_i^a = \int v_i(G^a)^{-1}y^a\,d\mathbf{v}$$

[the upper sign pertains to the electrons ($a = e$) and the lower to the ions ($a = i$)]. Here $(G^a)^{-1}$ is the operator inverse to G^a, $\mathbf{E}$ is the fluctuation of the electric field, and κ_{ij}^a are the tensors of the electric susceptibility of the electrons and ions of the plasma in a magnetic field. Expressing $\mathbf{E}$ in terms of $\mathbf{j} = \mathbf{j}^e + \mathbf{j}^i$ with the aid of Maxwell's equations we obtain

$$j_i^a = \pm ieY_i^a - 4\pi\varkappa_{ij}^a Q_{jl}j_l,$$

$$Q_{ij} = k_ik_jk^{-2} - (\eta^2-1)^{-1}(\delta_{ij} - k^{-2}k_ik_j). \quad (24)$$

*Salpeter[1] derived the expression for $\langle|\delta n^e|^2\rangle_{k\omega}$ by a different method.

†These oscillations were investigated by Tonks and Langmuir[20] and by Gordeev.[21]

*The fluctuations of the distribution function of a gas (without account of the self-consistent fields) was investigated by Kadomtsev.[25]

†$[\mathbf{vH}_0] = \mathbf{v}\times\mathbf{H}_0$.

(The field $\mathbf{E}$ is not assumed potential, for in general the longitudinal and transverse oscillations cannot be separated in the presence of a magnetic field.)

Introducing for simplicity of notation a (2×3)-dimensional current-density vector j_α, which combines the two currents j^e $(\alpha = 1, 2, 3)$ and j^i $(\alpha = -1, -2, -3)$ we rewrite (24) in the form

$$\mathfrak{M}_{\alpha\beta} j_\beta = ieY_\alpha, \quad j_\alpha = \begin{pmatrix} j^e \\ j^i \end{pmatrix}, \quad Y_\alpha = \begin{pmatrix} Y^e \\ -Y^i \end{pmatrix},$$

$$\mathfrak{M}_{\alpha\beta} = \begin{pmatrix} I + 4\pi\varkappa^e Q & 4\pi\varkappa^e Q \\ 4\pi\varkappa^i Q & I + 4\pi\varkappa^i Q \end{pmatrix}. \tag{24'}$$

Recognizing that $\det \mathfrak{M}$ differs from the determinant of the matrix Λ [see (2')] only by a factor $(\eta^2 - 1)^{-2}$, we write the solution of (24') in the form

$$j_\alpha = ie\Lambda^{-1}\mu_{\alpha\beta}Y_\beta,$$

where $\mu_{\alpha\beta}\mathfrak{M}_{\beta\gamma} = \delta_{\alpha\gamma}\Lambda$.

We must now average the products of the currents over the random forces with the aid of (17). (The fact that (23) contains additional terms due to the field $\mathbf{H}_0$, not contained in (15), does not change the expression for S, and consequently does not change the expression for $\langle y^a y^b \rangle_{k\omega}$.) Noting that

$$e^2 \langle Y_i^a Y_j^b \rangle_{k\omega} = -i\delta_{ab}\omega T^a (\varkappa_{ij}^a - \varkappa_{ji}^{a*}),$$

we obtain finally an expression for the correlators of the electron and ion currents

$$\langle j_i^a j_j^b \rangle_{k\omega} = -i\omega |\Lambda|^{-2} \{\mu_{il}^{ae}\mu_{jm}^{be*} T^e (\varkappa_{lm}^e - \varkappa_{ml}^{e*}) + \mu_{il}^{ai}\mu_{jm}^{bi*} T^i (\varkappa_{lm}^i - \varkappa_{ml}^{i*})\}, \tag{25}$$

where μ_{ij}^{ab} are the elements of the matrix μ:

$$\mu = \begin{pmatrix} \mu^{ee} & \mu^{ei} \\ \mu^{ie} & \mu^{ii} \end{pmatrix}.$$

From (25) we readily obtain the spectral distribution of the fluctuations of the total current density

$$\langle j_i j_j \rangle_{k\omega} = -i\omega |\Lambda|^{-2} \mu_{il}^t \mu_{jm}^{t*} \{T^e (\varkappa_{lm}^e - \varkappa_{ml}^{e*}) + T^i (\varkappa_{lm}^i - \varkappa_{ml}^{i*})\}, \tag{26}$$

where the tensor μ^t is related with the tensor

$$\mathfrak{M}_{ij}^t = (\eta^2 - 1)^{-1} (\eta^2 k^{-2} \varepsilon_{il} k_l k_j - \Lambda_{ij})$$

by the equation $\mu_{il}^t \mathfrak{M}_{lj}^t = \delta_{ij}\Lambda$ [we note that $\det \mathfrak{M}^t = (\eta^2 - 1)^{-2}\Lambda$].

Using Maxwell's equations we obtain with the aid of (25) and (26) the correlators of all the quantities of interest to us.

In particular, the correlators of the electron-density fluctuations and of the magnetic-field fluctuations have the form

$$e^2 \langle |\delta n^e|^2 \rangle_{k\omega} = \frac{k_i k_j}{\omega^2} \langle j_i^e j_j^e \rangle_{k\omega},$$

$$\langle \delta H_i \delta H_j \rangle_{k\omega} = \left(\frac{4\pi}{\omega}\right)^2 \frac{\eta^2}{(\eta^2 - 1)^2} e_{ilm} e_{jl'm'} k^{-2} k_l k_{l'} \langle j_m j_{m'} \rangle_{k\omega},$$

$$e \langle \delta n^e \delta H_j \rangle_{k\omega} = -\frac{4\pi i}{c\omega} \frac{\eta^2}{\eta^2 - 1} e_{jm'l} \frac{k_m k_{m'}}{k^2} \{\langle j_m^e j_l^e \rangle_{k\omega} + \langle j_m^e j_l^i \rangle_{k\omega}\}, \tag{27}$$

where $e\ldots$ is a completely antisymmetrical third-rank tensor.

As already noted, the correlation functions have sharp maxima near values of ω and $\mathbf{k}$ satisfying the dispersion equation $\Lambda(\mathbf{k}, \omega_n(\mathbf{k})) = 0$ (the index n labels the type of oscillations). It is easy to establish the form of the correlation functions near such maxima. For example, for the quantity $\langle j_i j_j \rangle_{k\omega}$ we have

$$\langle j_i j_j \rangle_{k\omega} = B_{ij}(\mathbf{k}, \omega)\, \delta(\omega \pm \omega_n(\mathbf{k})),$$

$$B_{ij} = -i\pi\omega \left|\frac{\partial\Lambda}{\partial\omega}\right|^{-1} \mu_{il}^t \mu_{jm}^{t*} \frac{T^e (\varkappa_{lm}^e - \varkappa_{ml}^{e*}) + T^i (\varkappa_{lm}^i - \varkappa_{ml}^{i*})}{\operatorname{Im}\Lambda}.$$

If $\omega/k \gg s_e, s_i$, then this formula goes into Eq. (13) with $T = T^e$.

We note also that if $\eta \gg 1$ the correlators of the particle densities and the charge density in the presence of a magnetic field are determined by the same formulas (20) and (21) as in the case of a free plasma. Here we must take κ and ϵ to mean the longitudinal components of the corresponding tensors, for example $k^{-2}k_i k_j \epsilon_{ij}$ (this conclusion does not hold true only near the poles of the correlation functions, corresponding to the propagation of fast and slow magnetic-sound waves).*

To find the correlators of the distribution functions it is necessary to express, with the aid of Maxwell's equations, the fluctuation of the electric field in terms of the fluctuation of the distribution functions and, after substituting the resultant expression (23), to average in accordance with (17). We do not give the corresponding expressions here.

7. We consider now the scattering of electromagnetic waves by fluctuations in a plasma. In a free plasma this scattering is determined only by the fluctuations of the electron density; for a plasma in a magnetic field $\mathbf{H}_0$ it is necessary to take additional account, generally speaking, of the magnetic-field fluctuations $\delta\mathbf{H}$ (the fluctuations of the ion density are insignificant because of the large ion mass). The electric field of the scattered waves obviously satisfies the equation

$$\left(\operatorname{rot}\operatorname{rot} + \frac{1}{c^2}\frac{\partial^2}{\partial t^2}\right)\mathbf{E}' = -\frac{4\pi e}{c^2}\frac{\partial}{\partial t}(n_0\mathbf{v}' + \delta n^e \mathbf{v}),$$

*These waves were investigated by Stepanov[22,24] and Bernstein.[23]

where $\mathbf{v}$ is the average electron velocity due to the field of the incident wave $\mathbf{E} = \mathbf{E}^0 \exp(i\mathbf{k}_0 \cdot \mathbf{r} - i\omega_0 t)$:

$$\mathbf{v} = i\frac{e}{m}\frac{\omega_0^2\mathbf{E} - \omega_H^2(\mathbf{hE})\mathbf{h} - i\omega_0\omega_H[\mathbf{hE}]}{\omega_0(\omega_0^2 - \omega_H^2)}, \quad \mathbf{h} = \frac{\mathbf{H}_0}{H_0}$$

and $\mathbf{v}'$ is the electron velocity associated with the scattered wave:

$$\frac{d\mathbf{v}'}{dt} = \frac{e}{m}\mathbf{E}' + \frac{e}{mc}[\mathbf{v}'\mathbf{H}_0] + \frac{e}{mc}[\mathbf{v}\delta\mathbf{H}]$$

(We assume that $v, v' \ll c$). From these relations follows an equation for the field of the scattered wave with frequency $\omega = \omega_0 + \Delta\omega$ and a wave vector $\mathbf{k} = \mathbf{k}_0 + \mathbf{q}$:

$$\Lambda_{ij}(\mathbf{k},\omega)E_j'(\mathbf{k},\omega) = E_j^0\left\{\frac{\omega_0}{\omega}(\delta_{ij} - \varepsilon_{ij}^0)\frac{\delta n^e(\mathbf{q},\Delta\omega)}{n_0} + i\frac{e}{mc}\frac{\omega_0}{\Omega^2}(\delta_{il} - \varepsilon_{il})e_{lkm}(\delta_{kj} - \varepsilon_{kj}^0)\delta H_m(\mathbf{q},\Delta\omega)\right\},$$

where $\epsilon_{ij} = \epsilon_{ij}(\omega)$ and $\epsilon_{ij}^0 = \epsilon_{ij}(\omega_0)$ [the tensor ϵ_{ij} is determined from (12)].

To find the scattering coefficient we must divide the intensity of the scattered wave by the $\mathbf{k}_0$-component of the Poynting vector of the incident wave

$$S_0 = \frac{c}{8\pi}\eta_0|E^0|^2\left(1 - \frac{|\mathbf{e}_0\mathbf{k}_0|^2}{|\mathbf{e}_0|^2k_0^2}\right);$$

$$\mathbf{e}_0 = \left(i; \quad -\frac{\varepsilon_2^0}{\eta_0^2 - \varepsilon_1^0}; \quad \frac{i}{2}\frac{\eta_0^2\sin 2\vartheta_0}{\eta_0^2\sin^2\vartheta_0 - \varepsilon_3^0}\right), \quad \eta_0 = \frac{ck_0}{\omega_0}$$

(ϑ_0 is the angle between $\mathbf{H}_0$ and $\mathbf{k}_0$). We give only the final results.

In the absence of a magnetic field, the differential scattering coefficient for an unpolarized wave is

$$d\Sigma = \frac{1}{4\pi}\left(\frac{e^2}{mc^2}\right)^2\left(\frac{\omega}{\omega_0}\right)^2\sqrt{\frac{\varepsilon}{\varepsilon_0}}(1 + \cos^2\theta)\langle|\delta n^e|^2\rangle_{q\Delta\omega}\, do\, d\omega, \tag{28}$$

where θ is the scattering angle, do the element of solid angle $\mathbf{k}$, $\epsilon \equiv \epsilon(\omega) = 1 - \Omega^2/\omega^2$, and $\epsilon_0 = \epsilon(\omega_0)$. We note that this formula admits of arbitrary frequency variations. When $\Delta\omega \ll \omega_0$ the factor $(\omega/\omega_0)^2\sqrt{\epsilon/\epsilon_0}$ becomes equal to unity, and (28) goes into the well-known formula for the scattering on fluctuations with small frequency variation (see, for example,[7]).

In the presence of a magnetic field, $d\Sigma$ has the form

$$d\Sigma = \frac{1}{2\pi}\left(\frac{e^2}{mc^2}\right)^2\left(\frac{\omega_0\omega}{\Omega^2}\right)^2 R\left\{|\xi|^2\langle|\delta n^e|^2\rangle_{q\Delta\omega} - \frac{en_0}{mc}\frac{\omega}{\Omega^2}\mathrm{Im}(\xi A_i\langle\delta n^e\delta H_i\rangle_{q\Delta\omega}) + \frac{n_0}{4\pi mc^2}\frac{\omega^2}{\Omega^2}A_i^*A_j\langle\delta H_i\delta H_j\rangle_{q\Delta\omega}\right\} do\, d\omega,$$

$$R = \eta^3\left\{\eta_0\left(|\mathbf{e}_0|^2 - \frac{|\mathbf{e}_0\mathbf{k}_0|^2}{k_0^2}\right)\varepsilon_{ij}e_i^*e_j^0\right\}^{-1}, \quad \xi = (\varepsilon_{ij}^0 - \delta_{ij})e_i^*e_j^0,$$

$$A_i = (\varepsilon_{kl} - \delta_{kl})e_k^*e_{lmi}(\varepsilon_{mj}^0 - \delta_{mj})e_j^0, \tag{29}$$

where $\mathbf{e}$ is the polarization vector of the scattered wave

$$\mathbf{e} = \left(\frac{\varepsilon_2}{\eta^2 - \varepsilon_1}\sin\varphi + i\cos\varphi; \quad -\frac{\varepsilon_2}{\eta^2 - \varepsilon_1}\cos\varphi + i\sin\varphi; \quad \frac{i}{2}\frac{\eta^2\sin 2\vartheta}{\eta^2\sin^2\vartheta - \varepsilon_3}\right)$$

[ϑ is the angle between $\mathbf{H}_0$ and $\mathbf{k}$, while φ is the angle between the planes $(\mathbf{k}_0, \mathbf{H}_0)$ and $(\mathbf{k}, \mathbf{H}_0)$]. The quantities $\langle|\delta n^e|^2\rangle$, $\langle\delta n^e\delta H_i\rangle$ and $\langle\delta H_i\delta H_j\rangle$ are determined from (27).

8. If the electron and ion temperatures are equal and there is no magnetic field* the spectrum of the scattered radiation consists of the Doppler-broadened principal line ($\Delta\omega \lesssim qs_i$) and of sharp maxima at $\Delta\omega = \pm\Omega$ if $aq \ll 1$. If in addition $\omega_0 \gg \Omega$, then the integral scattering coefficient (in a given angle interval) has the form

$$d\Sigma = \frac{n_0}{4}\left(\frac{e^2}{mc^2}\right)^2\frac{1 + 2(aq)^2}{1 + (aq)^2}(1 + \cos^2\theta)\, do; \quad q = \frac{2\omega_0}{c}\sin\frac{\theta}{2}. \tag{30}$$

Whether the electron and ion temperatures are equal or not, the coefficient of scattering is determined for small changes in temperature ($\Delta\omega \ll qs_i$) by the formula

$$d\Sigma = \frac{n_0}{2\sqrt{\pi}}\left(\frac{e^2}{mc^2}\right)^2\frac{a}{s_i}\frac{(aq)^3}{[1 + (aq)^2]^2}(1 + \cos^2\theta)\, do\, d\omega. \tag{31}$$

If $\Delta\omega \gg qs_e$ the scattering is only on the Langmuir oscillations. In this region, for arbitrary relation between T^e and T^i, the form of $d\Sigma$ is

$$d\Sigma = \frac{e^2T^eq^2}{16\pi(mc^2)^2}\frac{\omega^2}{\omega_0^2}\sqrt{\frac{\varepsilon}{\varepsilon_0}}(1 + \cos^2\theta)\{\delta(\Delta\omega - \Omega) + \delta(\Delta\omega + \Omega)\}\, do\, d\omega. \tag{32}$$

In a strongly nonisothermal plasma ($T^e \gg T^i$) an additional sharp maximum appears in the frequency interval between the central (Doppler) maximum and the Langmuir satellites when $\Delta\omega = \omega_s(q)$. This maximum is connected with the possibility of propagation of specific sound oscillations in the plasma. In the case of greatest interest, when $\Delta\omega/qs_i \gg \ln(T^e/T^i)$, the scattering coefficient for $\Delta\omega \sim \omega_s(q)$ is equal to

$$d\Sigma = \frac{e^2k_e^4T^e(1 + \cos^2\theta)}{16\pi(mc^2)^2(k_e^2 + q^2)}\{\delta(\Delta\omega - \omega_s(q)) + \delta(\Delta\omega + \omega_s(q))\}. \tag{33}$$

9. In the presence of a magnetic field, as follows from the results of Sec. 6, the scattered-radiation spectrum contains, along with the Doppler-broadened principal lines, sharp maxima connected with the possibility of propagation of

*Various particular cases occurring under these conditions have been studied in detail for small changes of frequency ($\Delta\omega \ll \omega_0$) by Dougherty and Farley.[3]

various natural modes in the plasma (two types of Langmuir oscillations, Alfven waves, and also fast and slow magnetic-sound waves in the case when $T^e \gg T^i$). We give here the final expression only for the scattering coefficient on the Langmuir oscillations ($\Delta\omega \sim \omega_\pm$), which is simplest in form

$$d\Sigma = \frac{e^2q^2T^e}{8\pi(mc^2)^2}\frac{\omega^2\omega_0^2}{\Omega^6}R|\xi|^2\frac{(\Delta\omega)^2[(\Delta\omega)^2-\omega_H^2]^2}{(\Delta\omega)^4\cos^2\tilde{\vartheta}+[(\Delta\omega)^2-\omega_H^2]^2\sin^2\tilde{\vartheta}}$$
$$\times\{\delta(\Delta\omega-\omega_+)+\delta(\Delta\omega+\omega_+)+\delta(\Delta\omega-\omega_-)$$
$$+\delta(\Delta\omega+\omega_-)\}\,do\,d\omega, \qquad (34)$$

where $\tilde{\vartheta}$ is the angle between $\mathbf{q}$ and $\mathbf{H}_0$.

When $\omega_0 \gg \omega_+$ and $T^e = T^i$, we can determine the integral scattering coefficient (in a given angle interval). It is then sufficient to retain in (29) only the first term proportional to $\langle|\delta n^e|^2\rangle$; the relative contributions of the second and third terms to the integral coefficient amounts to s/c and $(s/c)^2$. If $(\Delta\omega)_{eff}$ denotes the effective frequency interval in which $\langle|\delta n^e|^2\rangle$ is different from zero [we note that $(\Delta\omega)_{eff} \lesssim \omega_+$], then the integral scattering coefficient, for $(\Delta\omega)_{eff} \ll \omega_0 \sin\theta$, will be

$$d\Sigma = \frac{n_0}{4}\left(\frac{e^2}{mc^2}\right)^2\left(\frac{\omega_0}{\Omega}\right)^4(R|\xi|^2)_{\omega=\omega_0}\frac{1+2(aq)^2}{1+(aq)^2}\,do. \qquad (35)$$

[We note that in general the second and third terms in the differential scattering coefficient (29) cannot be neglected.]

[1] E. E. Salpeter, Phys. Rev. **120**, 1528 (1960).

[2] Akhiezer, Prokhoda, and Sitenko, JETP **33**, 750 (1957), Soviet Phys. JETP **6**, 576 (1958).

[3] J. P. Dougherty and D. T. Farley, Proc. Roy. Soc. **A259**, 79 (1960).

[4] H. B. Callen and T. A. Welton, Phys. Rev. **83**, 34 (1951).

[5] M. A. Leontovich and S. M. Rytov, JETP **23**, 246 (1952).

[6] S. M. Rytov, Teoriya élektricheskikh fluktuatsii i teplovogo izlucheniya (Theory of Electric Fluctuations and Thermal Radiation), AN SSSR, 1953.

[7] L. D. Landau and E. M. Lifshitz, Élektrodinamika sploshnykh sred (Electrodynamics of Continuous Media), Gostekhizdat, 1957.

[8] V. V. Tolmachev, DAN SSSR **112**, 842 (1957) and **113**, 301 (1957), Soviet Phys.-Doklady **2**, 85 (1957) and **2**, 124 (1958).

[9] S. V. Tyablikov, ibid. **114**, 1210 (1957), translation **2**, 299 (1958).

[10] Yu. L. Klimontovich, JETP **34**, 173 (1958), Soviet Phys. JETP **7**, 119 (1958).

[11] V. D. Shafranov, Collection: Fizika plazmy i problema upravlyaemykh termoyadernykh reaktsii (Plasma Physics and the Problem of Controllable Thermonuclear Reactions), vol. 4, AN SSSR, 1958, p. 416.

[12] F. G. Bass and M. I. Kaganov, JETP **34**, 1154 (1958), Soviet Phys. JETP **7**, 799 (1958).

[13] V. P. Silin, Radiofizika (Radiophysics) **2**, 198 (1958).

[14] J. Lindhard, Mat.-Fys. Medd. Dan. Vid. Selsk. **28**, No. 8 (1954).

[15] M. E. Gertsenshteĭn, JETP **27**, 180 (1954).

[16] A. G. Sitenko and K. N. Stepanov, JETP **31**, 642 (1956), Soviet Phys. JETP **4**, 512 (1957).

[17] Al'pert, Ginzburg, and Feĭnberg, Rasprostranenie radiovoln (Propagation of Radio Waves), Gostekhizdat 1953.

[18] A. A. Abrikosov and I. M. Khalatnikov, JETP **34**, 198 (1958), Soviet Phys. JETP **7**, 135 (1958).

[19] L. D. Landau and E. M. Lifshitz, JETP **32**, 618 (1957), Soviet Phys. JETP **5**, 512 (1957).

[20] L. Tonks and I. Langmuir, Phys. Rev. **33**, 195 (1929).

[21] G. V. Gordeev, JETP **27**, 19 (1954).

[22] K. N. Stepanov, JETP **35**, 1155 (1958), Soviet Phys. JETP **8**, 808 (1959).

[23] I. B. Bernstein, Phys. Rev. **109**, 10 (1958).

[24] K. N. Stepanov, Ukr. Phys. J. **4**, 678 (1959).

[25] B. B. Kadomtsev, JETP **32**, 943 (1957), Soviet Phys. JETP **5**, 771 (1957).

Translated by J. G. Adashko
113

Letters to the Editor

METHOD OF FINDING LOCAL SOURCES OF HIGH-ENERGY PHOTONS

G. T. ZATSEPIN and A. E. CHUDAKOV

P. N. Lebedev Physics Institute, Academy of Sciences, U.S.S.R.

Submitted to JETP editor June 6, 1960

J. Exptl. Theoret. Phys. (U.S.S.R.) **41**, 655-656 (August, 1961)

DATA on processes connected with cosmic rays in many astronomical objects are of great importance to the solution of many astrophysical problems. Such data can be obtained from the high-energy photons arriving at the earth without being deflected.

Cocconi[1] proposed to locate on the celestial sphere sources of photons with $E \sim 10^{12}$ ev by measuring the relative delay in the passage of a front of a developing air shower through scintillators.[2]

It seems to us that showers from primary photons with energy $E \sim 10^{12}$ ev, in a solid angle $\Omega \sim 10^{-3}$ sr, can be registered more reliably and with much simpler means by using the Cerenkov radiation produced by the shower in the atmosphere. For this purpose, the light flash should be registered with a photomultiplier placed at the focus of a large parabolic mirror. The angular resolution of such a system can be reduced to $\pm 1°$.

It is advisable to use several paraboloids with parallel orientation to distinguish between separate showers by the time coincidences of the pulses. It is possible in this case to register showers for which the number of light quanta gathered on the photocathode is greater than 200.[3] Calculations of the intensity of Cerenkov glow of a sea-level shower produced by a primary 10^{12}-ev photon yields a flux of ~ 50 quanta/m^2. To register such showers the area of the parabolic mirror should be 4 m^2. In spite of many shortcomings (the observations can be made only in moonless and cloudless nights) the proposed procedure seems more promising than that of Cocconi,[1] at any rate when searching for photons from known radioastronomical objects.

If the apparatus is located on a mountain and if large-area mirrors are used, primary photons of lower energy can be registered. At high energies, the ratio of the photon effect to the cosmic-ray background can be improved by using penetrating-particle detectors connected for anticoincidence.

An advantage of the proposed method, in addition to the possibility of placing the apparatus at sea level, is the relatively large effective area of shower registration (on the order of 10^5 m^2), so that high statistical accuracy can be attained; the latter is very important, since the optimistic estimates given in [1] for the intensity of the high-energy photons from radioastronomical objects are highly overestimated. A likely estimate can be made by counting the number of neutral pions generated when cosmic-ray particles collide inside an object with atomic nuclei of disperse matter (gas or dust).

Using the experimental data on cosmic rays in the atmosphere and assuming that the cosmic rays in radio nebulae have an energy spectrum similar to that of the particles incident on earth [i.e., $F_c(E)\,dE = AE^{-(\gamma+1)}\,dE$ with $\gamma \cong 1.7$ when $E > E_{min}$ and $F_c(E) = 0$ when $E < E_{min}$], we can write for the number of photons produced by passage of the cosmic rays through a layer of matter of thickness dx

$$dF_{ph}(E) = K_{ph}F_c(E)\,dx/\lambda_0, \quad K_{ph} \approx 2 \cdot 10^{-2},$$

$$\lambda_0 = 1{,}5 \cdot 10^2 \text{ g/cm}^2$$

Therefore, integrating over the volume of the entire object and expressing the constant A in terms of the cosmic-ray energy density ϵ_c,

$$\varepsilon_c = 4\pi c \int_{E_{min}}^{\infty} EF_c(E)\,dE,$$

we can obtain in simple fashion the following estimate for the intensity of the flux of photons with energy greater than E at a distance R from the object:

$$I_{ph}(>E) \sim 10^{-5} E_{min}^{\gamma-1} E^{-\gamma} c R^{-2} \bar{\varepsilon}_c M,$$

where E_{min} ($\sim 10^{-3}$ erg) is the minimum energy of the cosmic-ray particles in the object, c is the velocity of light, while $\bar{\epsilon}_c$ and M are the energy density of the cosmic rays and the mass of the gas in the object, determined from the relation

$$\bar{\varepsilon}_c M = \int \varepsilon_c(\mathbf{r})\,\rho(\mathbf{r})\,dV,$$

where ρ is the density of the gas and integration is over the entire volume of the object.

The flux of cosmic-ray particles at the earth is $I_c\ (>E) = 5 \times 10^{-5} E^{-\gamma}$ erg-cm^{-2} sec^{-1} sr^{-1}. The expected fraction of showers from the photons inside a solid angle $\Omega = 10^{-3}$ is

$$\Delta = (I_{ph}/I_c)\cdot 10^3 = 5\cdot 10^{10}\bar{\epsilon}_c MR^{-2} \approx 2\cdot 10^9 \overline{H^2} MR^{-2}$$

(if it is assumed that $\bar{\epsilon}_c = \overline{H^2}/8\pi$, where H is the intensity of the magnetic field). If, for example, we assume for the Crab nebula $H = 3 \times 10^{-3}$ oe, $M = 10^{33}$ g, and $R = 10^{22}$ cm, then $\Delta = 2 \times 10^{-7}$. If (as in the center of the galaxy) $H = 10^{-3}$, $M = 10^{38}$, and $R = 2 \times 10^{22}$, then $\Delta = 5 \times 10^{-4}$.

Thus, even the most favorable estimates yield rather low values for the photon intensity. Recognizing, however, that the cosmic-ray spectrum in many objects can be richer in high-energy particles than is the spectrum on earth, and also that only the order of magnitude of most astrophysical quantities is known, it seems advantageous to investigate by the above-described method the most promising objects (such as the center of the galaxy or the radio nebulae).

[1] J. Cocconi, Trans. Intl. Conf. on Cosmic Rays, vol. 2, AN USSSR, 1960, p. 327.

[2] B. Rossi, ibid. p. 16.

[3] Chudakov, Nesterova, Zatsepin, and Tukish, ibid. p. 36.

Translated by J. G. Adashko
114

TUNNEL EFFECT BETWEEN THIN LAYERS OF SUPERCONDUCTORS

N. V. ZAVARITSKII

Institute for Physics Problems, Academy of Sciences, U.S.S.R.

Submitted to JETP editor June 7, 1961

J. Exptl. Theoret. Phys. (U.S.S.R.) **41**, 657-659 (August, 1961)

As is well known, the chemical potentials of the electrons of metals in electrical contact are equalized. Contact can also be accomplished by tunneling transfer of electrons through a layer of insulator separating the metals. If a potential difference is applied to the layer of insulator, the current produced depends not only on the dimensions of the insulator, but also on the distribution of electron states near the energy corresponding to the chemical potential. According to the present theory of superconductivity,[1,2] the transition of a metal from the normal into the superconducting state is accompanied by a change in the distribution density of electrons ρ; if $\rho = N(0)$ in the normal state, then in the superconducting state the density of "unpaired" electrons (for $E > 0$) or holes (for $E < 0$)*

$$\rho_s(E) = N(0)\,|E|\,[E^2 - \Delta^2]^{-1/2}, \quad E \geqslant \Delta,$$
$$\rho_s(E) = 0, \quad E < \Delta, \qquad (1)$$

where E is the energy, measured from the chemical potential, and $\Delta(T)$ is the width of the gap in the energy spectrum of the electrons of the superconductor. A change in the electron density distribution will, evidently, produce a change in the current when the applied voltage is less than Δ/e. This effect has recently been found[3] and also confirmed.[4] In these experiments, however, the measurements were carried out in a temperature region where the smearing out of the electron distribution, due to the influence of temperature on the Fermi distribution, affects the results appreciably.

In the present paper we report on a study of the tunnel effect at temperatures down to $\sim 0.1°$ K. The specimens were metal films of thickness $\sim 10^{-5}$ cm, condensed at 300° K onto a glass surface in the form of a ~ 1 mm wide strip. The measurements were made on the overlap regions of strips of successively condensed metals. An oxidized aluminum layer, or in some experiments a BaF_2 film, was used as insulator. The resistance of the specimens was $10^4 - 10^6$ ohm. The tunneling transfer between Al and Al, In, Sn, and Pb was mainly studied. The temperature of the specimens was reduced by adiabatic demagnetization of a paramagnetic salt.[5] It was possible with the apparatus to achieve brief heating of the specimen to $\sim 4°$ K before the measurements.† In an experiment, current-voltage characteristics were measured between metals in the normal ($J_n - V$) and superconducting ($J_S - V$) states. The dependence of the current on temperature and on a magnetic field parallel to the plane of the specimen was measured.

The $J_n - V$ characteristic is linear up to $\sim 10^{-3}$ v for the tunneling transfer of electrons between metals in the normal state (at a temperature above the transition temperature or in a field greater than the critical magnetic field).

*The paired electrons are only important in the equalization of chemical potentials. Their contribution in the tunneling current is negligibly small.

†The heating served to remove the frozen-in fields from the specimens. These fields, frozen-in during the adiabatic demagnetization, led to a spreading of the $\sigma(V)$ dependence.

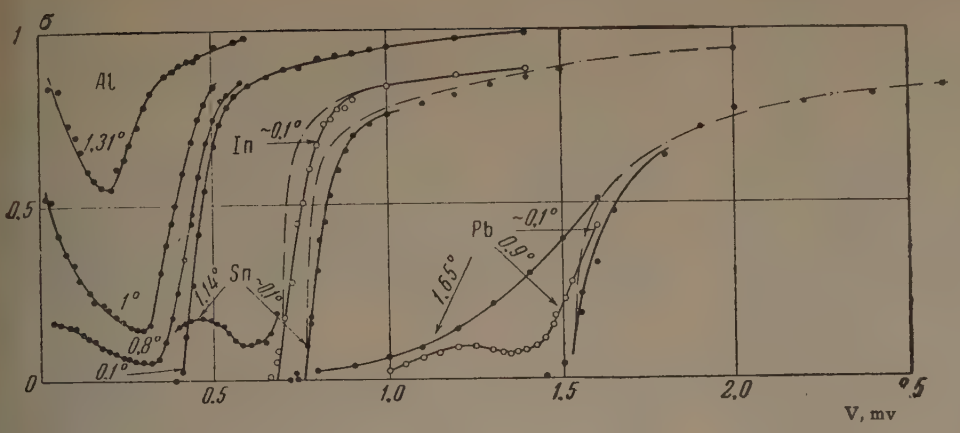

FIG. 1. The reduced conductivity $\sigma = J_S/J_n$ for tunneling transitions between Al and Al, In, Sn, and Pb films. The dashed lines indicate results calculated from relation (2).

A departure from linearity is observed for large potential differences, related to the penetration of electrons through the potential barrier. Figure 1 shows the change in the J – V characteristic when the metals go over into the superconducting state.

Let us consider the results obtained at ~ 0.1° K. It is evident that if the spread of the Fermi distribution f(E/T) is negligibly small, the current due to the tunnel effect between superconductors will only appear if the applied voltage $V \geq (\Delta_1+\Delta_2)/e$, where Δ_1 and Δ_2 are the gap widths in the superconductors being studied. With this condition we can deduce $\Delta_1 + \Delta_2$ from the data of Fig. 1 and then Δ for Al, In, Sn and Pb. It was found that for the Al specimens only the ratio $2\Delta/kT_C = 3.37 \pm 0.10$ remains constant, while the value of Δ changed correspondingly with the critical temperature of the specimen (T_C varied from 1.35 to 1.45° K). For the remaining metals the following values were found: (Δ is given in millielectron volts):

$$\Delta_{In} = 0.505 \pm 0.01, \quad \Delta_{Sn} = 0.56 \pm 0.01,$$

$$\Delta_{Pb} = 1.33 \pm 0.02\,\text{Mev}, \quad 2\Delta_{In}/kT_c = 3.45 \pm 0.07,$$

$$2\Delta_{Sn}/kT_c = 3.47 \pm 0.07, \quad 2\Delta_{Pb}/kT_c = 4.26 \pm 0.08.$$

The electron distribution density in the superconductor $\rho_S(E)$ can be determined from the voltage dependence of the conductivity ratio $\sigma = J_S/J_n$. It is easy to show[4] that if the probability of tunneling penetration of the barrier is the same for the normal and superconducting states, then

$$\sigma = \frac{1}{V}\int \rho_{s1}(E)\,\rho_{s2}(E-V)\left\{f\left(\frac{E-V}{kT}\right) - f\left(\frac{E}{kT}\right)\right\} dE. \quad (2)$$

Using the values of Δ obtained above, the σ(V) dependence for the pairs of superconductors studied can be calculated from (2). The results of this calculation are shown in Fig. 1, from which it is seen that the values of σ calculated theoretically and obtained in the experiments are close to one another. Some difference is only observed in the immediate neighborhood of $\Delta_1 + \Delta_2$.

We now discuss the change in σ(V) on increasing the temperature. It can be seen from Fig. 1 that for Al in the temperature region $T \lesssim T_C$, an increase in σ is observed not only for $eV \sim \Delta_1 + \Delta_2$, but also for $eV \sim \Delta_1 - \Delta_2$. The effect of the appearance of a current for $\Delta_1 - \Delta_2$, as a result of the spread of the f(E/T) distribution, was discussed in detail.[3,4] Our data for the pair Al-Pb agree with those given in these papers. Similar results were obtained for the Al-Sn pair. The existence of the additional maximum in σ at $eV = \Delta_1 - \Delta_2$ is most clearly seen in the Al-Al pair. The ratio σ decreases several fold in the range from V = 0 to $eV = 2\Delta$.

As can be seen from Fig. 1, the potential difference at which the sharp increase in σ for Al-Al occurs changes with temperature. This variation is evidently produced by the variation of the width of the gap Δ with temperature, which can therefore be determined from the data of Fig. 1. The Δ(T) dependence is shown in Fig. 2. The form of the variation with temperature is close to that which follows from the present theory.

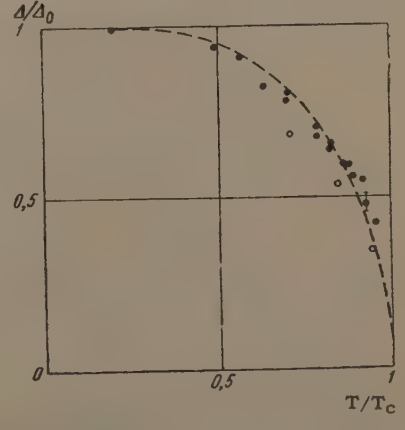

FIG. 2. The dependence of the gap width Δ in Al on temperature: ● – from measurements on the Al–Al pair ($\Delta_0 = 0.41$ Mev, $T_c = 1.4 \pm 0.02$°K); ○ – for the Al–Sn pair ($T_{cAl} = 1.34$°K); the dashed curve shows the theoretical Δ(T) dependence.

The results obtained thus show that the tunneling effect between $\sim 10^{-5}$ cm thick superconducting films can be explained satisfactorily by the present theory of superconductivity, and the ratio $2\Delta/kT_c$ is not a universal constant. The ratio $2\Delta/kT_c$ obtained on thin films is close to the value determined by other methods on bulk specimens. However, while results of investigations on bulk specimens indicate the existence of strong anisotropy of Δ in a number of metals, no noticeable anisotropy was found in the investigation of the tunnel effect in thin films of superconductors. For example, although the anisotropy of Δ in tin is as much as $\sim 30\%$, according to measurements on the heat capacity[5] and on the absorption of ultrasonics,[6] the $\sigma(V)$ dependence is close to that which follows from an isotropic model. It is possible that this arises because the thickness of the films studied was much smaller than the coherence distance of the electrons of the superconductor.

In conclusion, I express my thanks to P. L. Kapitza and A. I. Shal'nikov for their interest in this work.

[1] Bardeen, Cooper, and Schrieffer, Phys. Rev. 108, 1175 (1957).

[2] Bogolyubov, Tolmachev, and Shirkov, Novyĭ metod v teorii sverkhprovodimosti (A New Method in the Theory of Superconductivity) AN SSSR, 1958.

[3] J. Giaever, Phys. Rev. Letters 5, 147, 464 (1960).

[4] Nicol, Shapiro, and Smith, Phys. Rev. Letters 5, 461 (1960).

[5] N. V. Zavaritskii, JETP 33, 1085 (1957), Soviet Phys. JETP 6, 837 (1958).

[6] Bezuglyĭ, Galkin, and Korolyuk, JETP 36, 1951 (1959), Soviet Phys. JETP 9, 1388 (1959). Morse, Olsen, and Gavenda, Phys. Rev. Letters 3, 15 (1959).

Translated by R. Berman
115

THE SPECIAL ROLE OF OPTICAL BRANCHES IN THE MÖSSBAUER EFFECT

Yu. KAGAN

Submitted to JETP editor June 15, 1961

J. Exptl. Theoret. Phys. (U.S.S.R.) 41, 659-661 (August, 1961)

1. Recently two experimental groups have detected an anomalous temperature behavior of the Mössbauer effect in SnO_2[1] (radiator Sn^{119}) and Dy_2O_3[2] (radiation Dy^{161}). It appeared that in these materials the effect exists at high temperatures, and its fall-off with increasing T occurs much more slowly than would be expected starting from the actual values of the Debye temperature and a simple theoretical description of the effect.[3]

In the present note we give the results of an analysis of the effect of optical branches of the crystal on the magnitude of the Mössbauer effect, which makes it possible in particular to explain the observed regularities.

2. The probability of the Mössbauer effect in a crystal of arbitrary symmetry, when the radiator is one of the atoms in the elementary cell (j), is given by the expression[4]

$$W_j = \exp\{-Z_j\}, \qquad (1)$$

$$Z_j = R\frac{v_0}{(2\pi)^3}\sum_\alpha \int_\xi \frac{|\mathbf{q}\mathbf{V}_j(\mathbf{f}, \alpha)|^2}{\hbar\omega(\mathbf{f}, \alpha)}[2\bar{n}(\mathbf{f}, \alpha)+1]\,d^3f \qquad (2)$$

(where the notation is all the same as in [4]).

If we use the orthonormality of the complex amplitudes $\mathbf{V}_j^\xi(\mathbf{f}, \alpha)$, one can show that for any atom in the cell and for arbitrary direction of the γ quantum we have the relation

$$(2\pi)^{-3} v_0 \sum_\alpha \int_\xi |\mathbf{q}\mathbf{V}_j(\mathbf{f}, \alpha)|^2\,d^3f = 1. \qquad (3)$$

It then follows from (2) and (3) that at T = 0 the effect is determined by the average over branches and phase space of the value of $1/\omega(\mathbf{f}, \alpha)$, where the probability density distribution is given by the quantity $|\mathbf{q}\cdot\mathbf{V}_j(\mathbf{f}, \alpha)|^2$.

This result enables us to draw the important conclusion that the probability of the Mössbauer effect will be the larger the greater the relative magnitude of the amplitude of oscillation of the atom in the highest-lying optical branches in the fundamental region of the phase space of the reciprocal lattice.

Let us compare crystals with one and with several atoms in the unit cell, which have similar characteristic acoustic frequencies (that is, similar Debye temperatures). If we have the same radiator in both cases, it follows from (2) and (3) that the Mössbauer effect in the polyatomic lattice will, in general, occur with higher probability.

The presence of optical branches in the crystal can markedly change the temperature dependence of the effect. In fact, the temperature excitation of optical phonons begins at much higher temperatures compared with acoustic phonons. Therefore, if the role of optical branches in vibrations of the atoms of the j-th type is significant, W_j drops with temperature more slowly compared with the monatomic lattice with the same Debye temperature.

In the limiting case where the optical branches play a predominant role, W_j changes slowly with temperature, so long as kT does not become of the order of the characteristic energy of the optical phonons.

3. To find the frequency spectrum and relative values of the amplitudes of oscillation for different branches, one must solve the eigenvalue problem for the dynamical matrix $C_{jj'}^{\alpha\beta}(\mathbf{f})$.[5] Let us consider a lattice with two atoms in the elementary cell. If for simplicity we assume that the dynamical matrix can be reduced to diagonal form simultaneously for all values of $\mathbf{f}$ and j, j', then the qualitative analysis of the vibration problem can be carried through completely.

As $\mathbf{f} \to 0$ for the acoustic branch which corresponds to polarization along the ξ axis, we have

$$V_1^\xi / V_2^\xi = \sqrt{m_1 / m_2}, \tag{4}$$

while for an optical phonon with the same direction of polarization:

$$V_1^\xi / V_2^\xi = -\sqrt{m_2 / m_1}. \tag{4'}$$

If $m_1 \gg m_2$, we see that for a heavy atom the contribution to Z_j in (2) for small $\mathbf{f}$ is due mainly to the acoustical branch, while for the light atom it is mainly from the optical branch. Which situation will hold for arbitrary $\mathbf{f}$ depends essentially on the nature of the interaction between the atoms. If the interaction between the heavy atoms is greater than all other interactions, so that the inequality

$$|C_{11}^{\xi\xi}(\mathbf{f})| \gg |C_{12}^{\xi\xi}(\mathbf{f})|, \quad |C_{22}^{\xi\xi}(\mathbf{f})| \tag{5}$$

holds in the fundamental part of phase space, then with increasing $\mathbf{f}$ the heavy atom "slips over" into the optical branches. Since the phase volume corresponding to small wave vectors is small, Z_j for the heavy atom will be determined for the most part by the optical branches. As a consequence, we get a large Mössbauer effect for a heavy radiator at T = 0, and a weak dependence of the effect on temperature.

The results found give a good qualitative explanation of the observed temperature dependence of the effect.[1,2] Though the elementary cell in SnO_2 and Dy_2O_3 contains more than two atoms, it is obvious that all the arguments remain unchanged.

If the predominant interaction is that between different atoms or the interaction between light atoms, then as $\mathbf{f} \to 0$, just as for arbitrary $\mathbf{f}$, in the optical branches the predominant vibration will be that of the light atom. As a result, in such a lattice one will observe a weaker temperature dependence even for the light radiator. The case of a cubic lattice, which is considered in detail in [6], taking account of the interaction with nearest neighbors, corresponds to just this variant.

[1] V. A. Bryukhanov et al., JETP (in press).
[2] Sklyarevskii, Samoĭlov, and Stepanov, JETP (in press).
[3] W. M. Visscher, Annals of Physics **9**, 194 (1960).
[4] Yu. Kagan, JETP **40**, 312 (1961), Soviet Phys. JETP **13**, 211 (1961).
[5] M. Born and K. Huang, Dynamical Theory of Crystal Lattices, 1954.
[6] Yu. Kagan and V. A. Maslow, JETP **41**, 1296 (1961), Soviet Phys. JETP **14**, (1962).

Translated by M. Hamermesh
116

POLARIZATION OF LAMBDA HYPERONS GENERATED ON LIGHT NUCLEI BY NEGATIVE 2.8-Bev/c PIONS

Yu. S. KRESTNIKOV and V. A. SHEBANOV

Institute of Theoretical and Experimental Physics, Academy of Sciences, U.S.S.R.

Submitted to JETP editor June 15, 1961

J. Exptl. Theoret. Phys. (U.S.S.R.) **41**, 661-663 (August, 1961)

MANY experimental investigations[1,3] were devoted to the polarization of Λ hyperons generated in π^-p and π^--nucleus collisions at pion energies greater than 2 Bev. In a preliminary communication[1] we reported a freon bubble chamber[4] investigation of the transverse polarizations of the Λ particles produced in the reactions

$$\pi^- + A \to \Lambda + K + A' + n\pi, \tag{1}$$

$$\pi^- + A \to \Sigma^0 + K + A' + n\pi. \qquad \Sigma^0 \to \Lambda + \gamma \tag{1'}$$

Number of Λ decays $\Lambda \to p + \pi^-$	Number of negative pions from Λ decays, emitted			$\alpha\bar{p}$	Number of negative pions from Λ decays, emitted in the S plane			$(\alpha\bar{p})'$
	Upward	Downward	In the plane of creation and indeterminate cases		To the right	To the left	Indeterminate cases	
564	242	272	50	-0.11 ± 0.08	277	265	22	0.04 ± 0.08
Including 106 paired cases	41	58	7	-0.32 ± 0.19	54	46	6	0.15 ± 0.19

at 2.8 Bev/c on light nuclei (C, F, Cl). The asymmetry coefficient obtained in this investigation (in 183 Λ-decay events)

$$\alpha\bar{p} = 2(N_\uparrow - N_\downarrow)/(N_\uparrow + N_\downarrow) = -0{,}30 \pm 0{,}15$$

resulted in noticeable probability for a negative value of $\alpha\bar{p}$.

To improve the statistics, we analyzed more than 350 additional Λ particles (on top of the 183 decays) registered in a chamber and corresponding to reactions (1) and (1′) at 2.8 Bev/c. The average Λ-particle momentum in the spectrum was 650 Mev/c. The K^0-decay admixture was less than 7 percent of the number of Λ decays. The total number of particles was 564, and 106 events corresponded to bound creation of $\Lambda + K^0$ and $\Sigma^0 + K^0$ in the reactions

$$\pi^- + A \to \Lambda + K^0 + A' + m\pi, \qquad (2)$$

$$\pi^- + A \to \Sigma^0 + K^0 + A' + m\pi, \quad \Sigma^0 \to \Lambda + \gamma, \qquad (2')$$

where $\bar{m} = 1.2 \pm 0.15$.[5]

The measured values of $\alpha\bar{p}$ are listed in the table. It is seen from this data that slightly more negative pions are emitted downward from the Λ-particle creation plane, but the value of $\alpha\bar{p}$, obtained from 564 Λ decays, is close to zero; on the other hand the value -0.32 ± 0.19, obtained from the paired cases of bound creation $\Lambda(\Sigma^0) + K^0$ is subject to large statistical error. Therefore, as before,[1] we cannot conclude with certainty that $\alpha\bar{p}$ is negative.

We also investigated the right-left asymmetry for the obtained Λ decays. The asymmetry coefficient is in this case

$$(\alpha\bar{p})' = 2(N_\rightarrow - N_\leftarrow)/(N_\rightarrow + N_\leftarrow),$$

where $N_\rightarrow$ and $N_\leftarrow$ is the number of negative pions from Λ-hyperon decay, emitted to the right and to the left of the plane S defined by the vectors $\mathbf{p}_\Lambda$ and $\mathbf{p}_{\pi\,\mathrm{prim}} \times \mathbf{p}_\Lambda$. Such an asymmetry arises if parity is not conserved in the creation of strange particles in strong interactions.[6]

In the latter case the resultant longitudinal polarization of Λ hyperons leads to a front-back and left-right asymmetry. As noted in [7] measurement of $(\alpha\bar{p})'$ excludes the systematic error due to the method used to select the Λ decays. It is seen from the table that no right-left asymmetry is observed, within the limits of statistical errors.

The measurement of the front-back asymmetry is made difficult by the uncertain efficiency of observing the Λ decays, due either to the smallness of decay-particle ranges or to the small angles between them. In order to reduce these uncertainties to a minimum, we used only cases of pair creation (106 cases), which were selected most carefully.[5] Upon correcting for the foregoing uncertainties we found the fraction of the protons emitted backward in the Λ-particle c.m.s. to be 0.53 ± 0.08. This is in good agreement with the value 0.5, expected if parity is conserved during the process of creation of the Λ particle.

In conclusion, I am deeply grateful to A. I. Alikhanov and A. G. Meshkovskii for discussions, and to Ya. Ya. Shalamov, V. P. Rumyantseva and N. S. Khropov for help with the work.

[1] Barmin, Krestnikov, Pershin, Rumyantseva, Shalamov, and Shebanov, JETP **39**, 1229 (1960), Soviet Phys. JETP **12**, 857 (1961).

[2] Ivanovskaya, Kuznetsov, Prokesh, and Chuvilo, JETP **40**, 708 (1961), Soviet Phys. JETP **13**, 495 (1961).

[3] Wang, Wang, Veksler, Vrana, Ting, Ivanov, Kim, Kladnitskaya, Kuznetsov, Nguyen, Nikitin, Solov'ev, Khofmokl', and Cheng, JETP **39**, 1854 (1960), Soviet Phys. JETP **12**, 1292 (1961).

[4] Blinov, Lomanov, Meshkovskii, Shalamov, and Shebanov, PTÉ (Instruments and Exptl. Techniques), No. 1, 35 (1958).

[5] Shalamov, Shebanov, and Grashin, JETP **40**, 1302 (1961), Soviet Phys. JETP **13**, 917 (1961).

[6] V. G. Solov'ev, DAN SSSR **129**, 68 (1959), Soviet Phys.-Doklady **4**, 1255 (1960).

[7] Kuznetsov, Ivanovskaya, Prokesh, and Chuvilo, Proc. 1960 Conf. on High-Energy Physics, Rochester, 1960, p. 384.

Translated by J. G. Adashko
117

PARITY NONCONSERVATION IN STRONG INTERACTIONS AND NUCLEAR FISSION

V. V. VLADIMIRSKII and V. N. ANDREEV

Institute for Theoretical and Experimental Physics, Academy of Sciences, U.S.S.R.

Submitted to JETP editor June 23, 1961

J. Exptl. Theoret. Phys. (U.S.S.R.) 41, 663-665 (August, 1961)

RECENTLY, in connection with the discovery of nonconservation of parity in weak interactions, attempts have been made to determine the degree of nonconservation in strong interactions. We can expect the admixture of parity-nonconserving interaction in the nuclear forces to be of order $f^2/\hbar c \approx 10^{-14}$ if we include, in addition to the exchange of π mesons, the virtual exchange of leptons. Gell-Mann and Rosenfeld[1] found that under certain assumptions it is possible to have emission of a nucleon-antinucleon pair with the strong coupling constant $g/\sqrt{\hbar c}$, and the absorption of the pair by weak interaction with the weak coupling constant $f/\sqrt{\hbar c}$. The admixture of such a parity-nonconserving interaction into the strong interaction amounts to $\sim fg/\hbar c \approx 10^{-7}$. Within the framework of the universal Fermi interaction, a similar result is obtained for a four-fermion interaction and an interaction in which two fermions and two bosons participate.[2]

The possibility of observing experimentally the admixture of parity-nonconserving interaction results from the fact that selection rules hinder the parity-conserving transitions. Blin-Stoyle[3] investigated the possibility of observing a pseudoscalar admixture in nuclear γ transitions. A comparison of the computations with the experimental data shows that the admixture of nuclear states which do not conserve parity is $F \leq 10^{-4} - 10^{-5}$. An increase in accuracy of the measurements by 2 — 3 orders of magnitude is required in order to reach the theoretical value $F \sim 10^{-7}$.

Further possibilities for detecting nonconservation of parity in strong interactions may be given by investigations of nuclear fission. The most important fact in this case is that the value of the fission threshold, according to the hypothesis of A. Bohr[4] and the data of Stokes et al,[5] depends on the spin and parity of the fissioning nucleus. If it turns out that the barrier for fission of a nucleus with nonconservation of parity is lower than the barrier for fission with conservation of parity, then the admixture of parity-nonconserving states, after passing through the barrier will be greater than the value F in the ratio of the barrier factors P_1 and P_2. The maximum enhancement can be obtained in the case of spontaneous fission, in which the ratio of the barrier penetrabilities is $\sim 10^{6 \cdot \Delta E}$, where ΔE is the difference in heights of the barriers in Mev. Thus in the case of spontaneous fission it would be sufficient to have a difference in barrier heights $\Delta E \geq 1$ Mev in order that $FP_1/P_2 \sim 1$.

A difference in barrier heights of this order was found by Stokes et al[5] in investigating the fission of even-even nuclei, and by Simmons and Henkel[6] in investigating nuclei with odd A. For odd nuclei the probability of spontaneous fission is, on the average, 10^{-4} of the probability for spontaneous fission of the neighboring even-even nuclei. This fact was explained by Newton[7] and Wheeler[8] as an effect of raising of the barrier with the spin and parity of the ground state above the ground state at the saddle point. To explain the smaller probability of spontaneous fission of nuclei with odd A, it was necessary to assume that this rise, the so-called "restricting energy," amounts to ~ 1 Mev.

Several effects may occur in experiments from nonconservation of parity in strong interactions:

1) Increase in fission probability because of the contribution of fission with nonconservation of parity. This effect can be observed only when one makes a comparison with theoretical calculations of fission probability. However, because there is no quantitative theory of fission, this effect cannot be detected.

2) Observation of the asymmetry in emergence of the light (or heavy) fragment along the direction of and opposite to the direction of the nuclear spin, i.e., an asymmetry of the form $1 + a\sigma \cdot \mathbf{p}$, which is possible only when we have nonconservation of spatial parity. Such an asymmetry occurs as a result of the interference of states of one parity with states of the opposite parity and is maximal for $FP_1/P_2 \sim 1$.

One can suggest a mechanism for the appearance of spatial asymmetry. According to [9], in a sufficiently elongated nucleus the external nucleons with large angular momentum are located in the neighborhood of one of the ends, producing a pear-shaped deformation. We denote the wave functions of the states in which σ is directed along the two opposite directions relative to the "pear" by ψ_1 and ψ_2. If parity is conserved, two combinations of these states are possible: the even state $\psi_+ = \psi_1 + \psi_2$, and the odd state $\psi_- = \psi_1 - \psi_2$. If there is a weak parity violation, combinations of these functions must appear. In a nucleus with

positive parity, we get $\psi = \psi_+ + F\psi_-$. After passing through the barrier, whose penetrabilities for the states ψ_+ and ψ_- are equal respectively to P_2 and P_1, we form a state

$$\psi = P_2\psi_+ + P_1F\psi_- = P_2\left[\left(1+\frac{P_1}{P_2}F\right)\psi_1 + \left(1-\frac{P_1}{P_2}F\right)\psi_2\right],$$

i.e., a state with a pear-shaped deformation which is correlated with the spin. An analogous result is obtained for a nucleus with negative parity.

The estimates given above for the values of P_1/P_2 and F show that the spatial asymmetry can be quite large in certain nuclei. An experiment for observing spatial asymmetry can be carried out with polarized nuclei which have a spin in the ground state and a relatively high probability for spontaneous fission:[10] Bk^{249} ($T_{sp.f.} = 6 \times 10^8$ yr), Cf^{249} ($T_{sp.f.} = 1.5 \times 10^9$ yr), Es^{253} ($T_{sp.f.} = 7 \times 10^5$ yr) and possibly Am^{241} ($T_{sp.f.} \geq 2 \times 10^{14}$ yr).[11]

3) The appearance of longitudinal polarization of secondary neutrons, associated with the fact that the direction of the spin of the fragments formed in fission may be correlated with the direction of motion of the fragments. The observation of longitudinal polarization of neutrons can be carried out with unpolarized nuclei.

4) The occurrence of circular polarization of γ quanta, associated with a possible transition of the mixture of even and odd wave functions in the fission fragment.

The authors express their gratitude to I. S. Shapiro for many useful comments.

[1] M. Gell-Mann and A. H. Rosenfeld, Ann. Revs. of Nucl. Sci. 7, 409 (1957).

[2] R. J. Blin-Stoyle, Phys. Rev. 118, 1605 (1960).

[3] R. J. Blin-Stoyle, Phys. Rev. 120, 181 (1960).

[4] A. Bohr, Paper No. 911, Vol. 2, p. 151, First International Conference on Peaceful Uses of Atomic Energy, Geneva, 1955.

[5] Stokes, Northop, and Boyer, Paper No. 659, Vol. 15, page 179, Second International Conference on Peaceful Uses of Atomic Energy, Geneva, 1958.

[6] J. E. Simmons and R. L. Henkel, Phys. Rev. 120, 198 (1960).

[7] J. O. Newton, Progr. in Nucl. Phys. 4, 234 (1955).

[8] J. A. Wheeler, p. 1103, Proc. Intern. Conf. on Nuclear Reactions, Amsterdam, 1956.

[9] V. V. Vladimirskii, JETP 32, 822 (1957), Soviet Phys. JETP 5, 673 (1957).

[10] E. Hyde and G. Seaborg, Handbuch der Physik, Vol. 42, 1957.

[11] V. L. Mikheev et al, JETP 37, 859 (1959), Soviet Phys. JETP 10, 612 (1960).

Translated by M. Hamermesh
118

TRANSVERSE POTENTIAL DIFFERENCE THAT IS EVEN WITH RESPECT TO THE MAGNETIC FIELD, OBSERVED IN TIN

V. N. KACHINSKII

Institute of Crystallography, Academy of Sciences, U.S.S.R.

Submitted to JETP editor, July 4, 1961

J. Exptl. Theoret. Phys. (U.S.S.R.) 41, 665-667 (August, 1961)

AT the present time there are only three papers dealing with the experimental study, in large magnetic fields, of the even e.m.f. (even relative to the magnetic field direction), which —like the Hall effect—appears in the plane perpendicular to the current; the experiments have been conducted on single crystals of gallium,[1] tin,[2] and copper.[3] In the last case this phenomenon is attributed to the motion of carriers in open trajectories.

We have carried out an investigation, which was described in [2], on cylindrical specimens of pure tin ($\rho_{290°K}/\rho_{4.2°K} = 60\,000$) of various orientations in fields up to 7 koe. The voltage proportional to the resistance due to inaccurate disposition of the contacts amounted to several percent of the measured effect.

The rotation diagram of the even voltage is given in the figure for one of the specimens— Sn-11; for comparison, the rotation diagram of the resistance in the magnetic field is given. (The quantity E_{qy} plotted in the diagram in the projection of the vector of the even electric field $\mathbf{E}_q$ on the y axis; the x and z axes are directed along the current $\mathbf{j}$ and field $\mathbf{H}$, respectively. Since $\mathbf{E}_q \perp \mathbf{H}$, it follows that E_{qy} coincides with $|\mathbf{E}_q|$ except in sign.) For directions leading to open trajectories, the even voltage attains a maximum (as in the case of copper[3]); it does not, however, disappear for intermediate directions of the magnetic field when there are no open trajectories (with the exception of the direction $\mathbf{H} \parallel$ proj.[001]).* A rotation dia-

*The symbol proj. [001] means the direction of the projection of the [001] axis in the plane of rotation of the magnetic field.

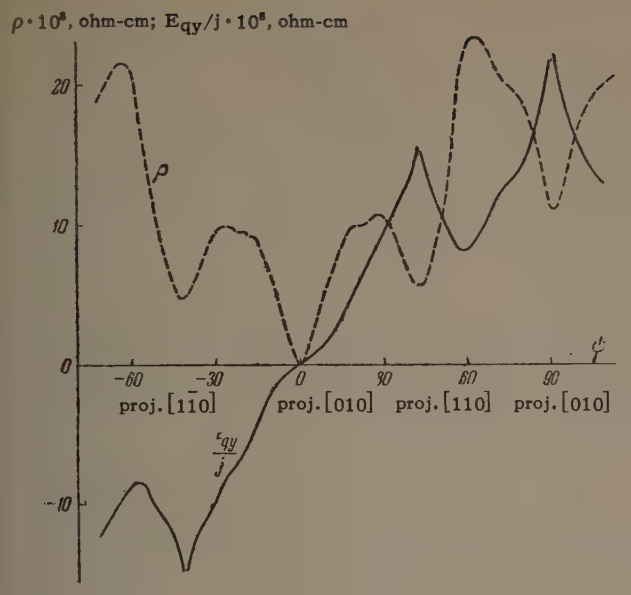

Rotation diagram E_{qy}/j (j is the current density) for specimen Sn-11; the specimen axis lies in the (010) plane and makes an angle of 27° with the [001] direction. Magnetic field is 6.9 koe.

gram of this type is characteristic of all the tin specimens, with the exception of those oriented parallel and perpendicular to the [001] axis. In the latter case the even effect is absent.

It seems possible to us that the occurrence of the even voltage can be explained as due to the appearance of closed carrier orbits elongated in one direction, oriented so that the direction of elongation makes with the current direction an angle not equal to 0° or 90°. (Open trajectories can be considered as particular cases with limiting elongation.) From this viewpoint singularities in the behavior of the even voltage can be explained on the basis of a knowledge of the form of the Fermi surface. In the case of tin the Fermi surface is such (see [5]) that elongated orbits passing through several elementary cells in reciprocal space exist for all directions of the magnetic field which are not parallel to the [001] axis and the (001) plane. For all these directions of the magnetic field an even voltage arises (with the exception of the case when **H** ∥ proj.[001] i.e., when the direction of elongation is perpendicular to the current) which attains a maximum when open trajectories appear. In copper the Fermi surface has a more symmetrical form [7] and elongated orbits only occur in directions close to open trajectory directions. Therefore, the even voltage in copper has the form of separate "peaks"; unlike in tin, there is no even voltage between them.[3] To some extent our viewpoint confirms the mention of the presence of an even voltage in bismuth,[6] which has closed Fermi surfaces in the form of strongly elongated ellipsoids.

As Klauder and Kunzler [3] showed, a knowledge of the vector of the even field E_q and the resistance field allows, when open trajectories appear, the direction of these trajectories in space to be determined. However, concerning the sharpness of the peaks, it is possible that their smearing is caused by the imperfect structure of the crystal (of a growth-structure type), which it is impossible to avoid in practice. This fact reduces the reliability of such a determination. The assertion by these authors that the rotation diagrams of the even voltage and the resistance of one specimen are adequate for the complete disclosure of the Fermi surface topology is true only in the simplest case; this apparently led to the authors making the error of incorrectly describing the particular directions of the magnetic field in copper (cf. [7]). At the same time a study of the even voltage together with the resistance in a series of specimens of various orientations can give more complete information about the Fermi surface than the study of the resistance alone. In particular, whatever the particular directions of the open trajectories the singularities appearing are always maxima in the case of the even transverse voltage, whereas singularities of the resistance can be minima (tin) or maxima (metals of the first group, tin for some orientations).

The author is grateful to A. I. Shal'nikov and N. A. Brilliantov for their interest, to Yu. P. Gaĭdukov for discussions, and to S. Volkov for help in the work.

[1] J. Yahia and J. A. Marcus, Phys. Rev. **113**, 137 (1959).

[2] V. N. Kachinskii, DAN SSSR **135**, 818 (1960), Soviet Phys.-Doklady **5**, 1260 (1960).

[3] J. R. Klauder and J. E. Kunzler, Phys. Rev. Letters **6**, 179 (1961).

[4] Lifshitz, Azbel', and Kaganov, JETP **31**, 63 (1956), Soviet Phys. JETP **4**, 41 (1957).

[5] Alekseevskii, Gaĭdukov, Lifshitz, and Peschanskii, JETP **39**, 1201 (1960), Soviet Phys. JETP **12**, 837 (1961).

[6] R. A. Connell and J. A. Marcus, Phys. Rev. **107**, 940 (1957).

[7] N. E. Alekseevskii and Yu. P. Gaĭdukov, JETP **37**, 672 (1959), Soviet Phys. JETP **10**, 481 (1960). Yu. P. Gaĭdukov, JETP **37**, 1281 (1959), Soviet Phys. JETP **10**, 913 (1960).

Translated by K. F. Hulme
119

POSSIBLE ASYMPTOTIC BEHAVIOR OF ELASTIC SCATTERING

V. N. GRIBOV

Leningrad Physico-Technical Institute, Academy of Sciences, U.S.S.R.

Submitted to JETP editor July 6, 1961

J. Exptl. Theoret. Phys. (U.S.S.R.) **41**, 667-669 (August, 1961)

UNTIL recently, elastic scattering at high energies s and at small transferred momenta t (region of the diffraction peak) was described exclusively on the basis of the classical picture of diffraction from a black body, in which the invariant scattering amplitude A(s, t) has the form

$$A(s, t) = s f(t). \tag{1}$$

Recently, owing to the progress in the study of the analytic properties of the scattering amplitudes,[1] it became possible to approach the asymptotic behavior of the scattering amplitude in a somewhat less phenomenological fashion. It turned out here[2] that an asymptotic behavior such as (1) cannot be reconciled in simple fashion with the unitarity and analycity conditions. It was simple to reconcile diffraction with a slowly decreasing cross section, such as from a grey sphere. At the present time it is not clear whether a classical diffraction pattern is produced at all in the scattering of high-energy particles.

In this connection, we wish to discuss in the present note a different type of asymptotic behavior, which in spite of having a few unusual features is theoretically feasible and does not contradict the experimental values. Before we formulate this asymptotic behavior [see (4a) and (4b) below], let us see how it is deduced from the analytic properties of A(s, t). We consider the scattering of identical spinless particles with mass μ, which are the lightest in theory.

The physical region corresponds to $t < 0$. If we continue A(s, t) into the region $t > 4\mu^2$, then A(s, t) can be regarded as the scattering amplitude of particles having a squared energy t in the c.m.s. and having a nonphysical squared momentum transfer s. The asymptotic behavior at large values of s and at the values of t referred to here was investigated in [2], where it was shown that it cannot have the form $sf(t)$. Regge[3] has shown that in nonrelativistic theory, at large momentum transfers, A(s, t) behaves as $s^{l(t)}$, where $l(t)$ is the position of the pole of the partial wave f_l as a function of the momentum l in the complex plane. He also showed that the poles are determined by the possible bound and resonant states. When $t < 4\mu^2$, these poles go to the real axis of the complex l plane and $l(t)$ decreases with t. In a future more detailed paper we shall show that in field theory the amplitudes of the partial waves are also analytic functions of l, and that the asymptotic behavior of A(s, t) as $s \to \infty$ is determined by the nearest singularities of f_l on the side of the larger l. If we now assume that the nearest singularity in the l plane is a simple pole, we arrive at the same asymptotic behavior of $s^{l(t)}$ with real l for $t < 4\mu^2$ as in the nonrelativistic theory. In the nonrelativistic theory, however, there is only one channel (t, the energy). In the relativistic energy, on the other hand, the region $t < 0$ is a new physical region (where s is the energy) which is of principal interest to us. In this region, A(s, t) should satisfy the unitarity conditions. As shown by Frautschi,[4] it follows from the unitarity condition and from the Mandelstam representation that

$$|A(s, 0)| < Cs \ln^2 s. \tag{2}$$

This means that $l(0) \leq 1$. If we assume that the strongest possible interaction is realized, then $l(0) = 1$. If we write for small t

$$l(t) = 1 + \gamma t, \tag{3}$$

then we obtain

$$A(s, t) \sim s e^{\gamma t \xi}, \qquad \xi = \ln s \tag{4}$$

and consequently, A(s, t) decreases rapidly with increasing t at high energies, so that the significant interval of t is of the order of $-1/\xi$ (it is readily shown that $\gamma > 0$). If we take crossing symmetry into account we obtain the following expressions for the imaginary (A_1) and real (D) parts of A(s, t) when $t \sim -1/\xi$:

$$A_1(s, t) = Cs e^{\gamma t \xi}, \tag{4a}$$

$$D(s, t) = Cs(-\gamma t) e^{\gamma t \xi}. \tag{4b}$$

Let us list the main properties of such an asymptotic scattering behavior: 1) the total interaction cross section is constant at high energies, so that $A_1(s, 0) = Cs$; 2) the elastic-scattering cross section tends to zero as $1/\xi$; 3) the scattering amplitude in the significant region becomes pure imaginary because of the factor $-\gamma t$ in (4b); 4) the region of momentum transfer significant for the elastic scattering decreases with increasing energy: $\sqrt{-t} \sim \xi^{-1/2}$; 5) the amplitudes of the partial waves

$$a_l(s) = \tfrac{1}{2}\int_{-1}^{1} P_l(z)\, A(s,\ t)\, dz$$

as functions of l (or, what is more convenient, as functions of the impact parameter $\rho = 1/p$) behave in the following fashion:

$$a_l(s) \equiv a(\rho,\ s) = \begin{cases} \frac{C}{\gamma\xi} e^{-\rho^2/\gamma\xi}\left[i + \frac{1}{\xi}\right], & \rho \ll \gamma\xi \\ \sim s^{l(4\mu^2)} e^{-2\mu\rho}, & \rho \gg \gamma\xi \end{cases},$$

i.e., an important role is played in the scattering by impact parameters $\rho \sim (\gamma\xi)^{1/2}$ for which $a(\rho, s) \sim 1/\xi$. This behavior means that the particles become grey with respect to high-energy interaction, but increase in size, so that the total cross section remains constant.

If we assume, as was done above, that the asymptotic behavior is determined by the position of the pole of the partial wave as a function of l, for example for $\pi\pi$-scattering, then, inasmuch as the partial waves of different processes are related by the unitarity condition, it can be shown that in general the processes with partial waves that have poles for the same value of l will be $N + \bar{N} \to 2\pi$, $N + \bar{N} \to N + \bar{N}$, etc, and consequently the behavior of the amplitudes of the reactions $\pi + N \to \pi + N$, $N + N \to N + N$ etc. will be similar to (4a) and (4b), with the same value of γ as for $\pi\pi$ scattering.

Chu and Frautschi [5] expressed in several articles the conviction that the asymptotic behavior of large momentum transfers in the nonphysical region should have common features in relativistic and nonrelativistic theory. It was emphasized, in particular, that the condition that the total cross section be constant, which calls for a pole at $l = 1$, is indeed the condition for the interaction force to have a maximum. These authors have disregarded, however, the fact that $l(t)$ is an analytic function of t, a consequence of which is the extraordinary nature of the described scattering picture.

Ordinary diffraction arises only if the partial waves have a pole at $l = 1$ when $t < 4\mu^2$, or have no pole when $t > 4\mu^2$. As will be shown in a more detailed article, the partial wave must have for this purpose complicated analytic properties, which have no nonrelativistic analogue.

In conclusion I wish to express my deep gratitude to I. Ya. Pomeranchuk, L. D. Landau, and I. T. Dyatlov for useful discussion and for valuable remarks.

[1] S. Mandelstam, Phys. Rev. **112**, 1344 (1958).
[2] V. N. Gribov, Nucl. Phys. **22**, 246 (1961).
[3] T. Regge, Nuovo cimento **14**, 952 (1959); **18**, 957 (1960).
[4] Froissart. Preprint.
[5] G. Chew and S. Frautschi, Phys. Rev. Lett. **5**, 12 (1960).

Translated by J. G. Adashko
120

Contents of Coming Issues

SOVIET PHYSICS JETP VOLUME 14, NUMBER 3 MARCH, 1962

CONTENTS

	Russian Reference	
Exchange Interaction and Magneto-Optical Effects in Ferrite Garnets . . . . . G. S. Krinchik and M. V. Chetkin	41,	673
Measurement of the Longitudinal Polarization of Electrons Emitted in Beta Decay of Au^{198} . . . . . R. O. Avakyan, G. L. Bayatyan, I. E. Vishnevskii, and E. V. Pushkin	41,	681
Spin Dependence of Weak Interaction in the Process $\mu^- + p \to n + \nu$. . . . L. B. Egorov, C. V. Zhuravlev, A. E. Ignatenko, A. V. Kuptsov, ... Li Hsuan-ming, and M. G. Petrashku	41,	684
The Nature of Low Temperatures Magnetic Transformations in Ferrites Possessing Compensation Points . . . . . K. P. Belov	41,	692
Low Temperature-Magnetic Transformation in Lithium Ferrite-Chromites . . . . . A. N. Goryaga and Lin Chang-ta	41,	696
Anomalies in the Physical Properties of Gadolinium Ferrite Garnet in the Low Temperature Region . . . . . A. V. Ped'ko	41,	700

Alpha-Particle Spectra and the Differential Cross Sections of the Reaction $H^3(t, 2n)He^4$ at 90° . . . . . A. M. Govorov, Li Ha Youn, G. M. Osetinskii, V. I. Salatskii, and I. V. Sizov 41, 703

Experimental Verification of the Charge Invariance Principle in the $d + d \rightarrow He^4 + \pi^0$ Reaction for 400-Mev Deuterons . . . . . Yu. K. Akimov, O. V. Savchenko, and L. M. Soroko 41, 708

Neutron Polarization in the $T(d, n)He^4$ Reaction . . . . . I. S. Trostin, V. A. Smotryaev, and I. I. Levintov 41, 725

Superconducting Properties of Freshly Deposited Mercury Films . . . . . I. S. Khukhareva 41, 728

Energy Spectrum and Time Dependence of the Intensity of Solar Cosmic-Ray Protons . . . . . A. N. Charakhch'yan, V. F. Tulinov, and T. N. Charakhch'yan 41, 735

Interaction Between 9-Bev Protons and Protons . . . . . V. A. Kobzev, Yu. T. Lukin, Zh. S. Takibaev, G. R. Tsadikova, and E. V. Shalagina 41, 747

Anomalous Doppler Effect in a Plasma . . . . . M. A. Gintsburg 41, 752

On the Theory of Spin-Lattice Relaxation in Liquid Solutions of Electrolytes . . . . . K. A. Valiev and M. M. Zaripov 41, 756

Scattering Equations for Low Energies . . . . . V. V. Malakhov 41, 762

Width and Shape of Mössbauer Lines in Solid Solutions . . . . . M. A. Krivoglaz 41, 765

Determination of the $K^+ \rightarrow 2\pi + \gamma$ Decay Amplitude from the Dispersion Equations and the Unitarity Conditions . . . . . I. G. Ivanter 41, 773

Minimal Number of Partial Waves in Reactions Involving the Formation of Several Particles . . . . . Hsien Ting-ch'ang and Ch'en Ts'ung-mo 41, 784

Coordinate Fractional Parentage Coefficients for a Configuration Consisting of Several Shells . . . . . I. G. Kaplan 41, 790

Interaction between the Surface and Nuclei Containing a Nucleon in Excess of a Closed Shell . . . . . V. N. Guman 41, 800

Effect of Zero Vibrations of the Shape of Heavy Nuclei on the Probability of Alpha Decay . . . . . V. G. Nosov 41, 806

Symmetry Properties of Strong Interactions . . . . . V. M. Shekhter 41, 810

Analytic Properties of the Total πN-Interaction Cross Section as a Function of Virtuality . . . . . I. M. Dremin 41, 821

Second Sound, the Convective Mechanism of Thermal Conductivity, and Exciton Excitation in Superconductors . . . . . V. L. Ginzburg 41, 828

τ-Decay and $\tau\pi$ Interaction . . . . . J. Wolf and W. Zöllner 41, 835

Transport Phenomena in a Paramagnetic Gas . . . . . Yu. Kagan and L. Maksimov 41, 842

Determination of the Hyperfine Splitting Energy of the 1s Muonium State . . . . . A. O. Vaĭsenberg 41, 853

π^-p Interaction at 7 Bev . . . . . I. M. Gramenitskii, I. M. Dremin, and D. S. Chernavskii 41, 856

The High-Frequency Dielectric Permittivity of a Plasma . . . . . V. P. Silin 41, 861

Fissionability of Nuclei by High-Energy Protons . . . . . N. A. Perfilov 41, 871

Single-Particle Excited States and the Model Description of Light Nuclei . . . . . V. G. Neudachin and V. N. Orlin 41, 874

The Upper Critical Field of Superconducting Alloys . . . E. A. Shapoval 41, 877

Absorption of Electromagnetic Waves in a Plasma . . . . . V. I. Perel' and G. M. Éliashberg 41, 886

Effect of Superfluidity of Atomic Nuclei on the Stripping and Pick-Up Reactions . . . . . B. L. Birbrair 41, 894

The Nature of Collective Levels in Nonspherical Nuclei . . . . . D. F. Zaretskii and M. G. Urin 41, 898
Upper Limit of Neutrino, Graviton, and Baryon Density in the Universe . . . . . Ya. B. Zel'dovich and Ya. A. Smorodinskii 41, 907
Electron and Positron Polarization Correlation in Relativistic Pairs . . . . . Ya. B. Zel'dovich 41, 912
The $\Sigma^+ \to p + e^+ + e^-$ and $\Sigma^+ \to p + \mu^+ + \mu^-$ Decays . . . . . I. V. Lyagin and E. Kh. Ginzburg 41, 914
Analysis of the Distributions of Transverse Momenta of Pions and Strange Particles . . . . . N. N. Roĭnishvili 41, 919
Analytical Properties of a Square Diagram with Nondecaying Masses . . . . . V. N. Gribov, G. S. Danilov, and I. T. Dyatlov 41, 924
Threshold Singularities in the Total Pion Scattering Cross Section . . . . N. P. Klepikov, V. R. Rokityanskii, Yu. G. Rudoĭ, F. V. Sayevskii, ... V. V. Fedorov, and V. A. Yudin 41, 937
Peculiarities of Motion of Charged Quasi-Particles in a Variable and Inhomogeneous Electromagnetic Field . . . . . I. M. Lifshitz, A. A. Slutskin, and V. M. Nabutovskii 41, 939
Production of Lepton Particle Pairs on a Coulomb Center . . . . . M. A. Kozhushner and E. P. Shabalin 41, 949
Collective Gyromagnetic Ratio of Odd Atomic Nuclei . . . . . Yu. T. Grin' and I. M. Pavlichenkov 41, 954
Neutron Force Function in the Optical Model . . . . . Yu. P. Elagin, V. A. Lynl'ka, and P. I. Nemirovskii 41, 959
The Formation of High-Energy Pion Beams . . . . . Yu. P. Nikitin, I. Ya. Pomeranchuk, and I. M. Shmushkevich 41, 963
Contribution to the Theory of Electromagnetic Fluctuations in a Plasma . . . . . V. P. Silin 41, 969
Theory of Relativistic Coulomb Scattering. I. . . . . V. G. Gorshkov 41, 977

LETTERS TO THE EDITOR

The Cosmic-Ray Equator as Determined by the Second Soviet Spaceship . . I. A. Savenko, P. I. Shavrin, V. E. Nesterov, and N. V. Pisarenko 41, 985
Nonlinear Properties of Three-Level Systems . . . . . V. M. Faĭn, Ya. I. Khanin, and É. G. Yashchin 41, 986
Negative Conductivity in Induced Transitions . . . . . N. G. Basov, O. N. Krokhin, L. M. Lisitsyn, E. P. Markhin, ... and B. D. Osipov 41, 988
Which is Heavier, Muoinium-1 or Muonium-2? . . . . . L. B. Okun' and B. M. Pontecorvo 41, 989

SOVIET PHYSICS JETP VOLUME 14, NUMBER 4 APRIL, 1962

Study of Three-Prong Stars Produced in Nuclear Emulsion by Inelastic pn Interactions at 9 Bev . . . . . V. A. Botvin, Zh. S. Takibaev, I. Ya. Chasnikov, N. P. Pavlova, and É. G. Boos 41, 993
Anisotropic Fission of U^{238} Induced by 3-Mev Neutrons . . . . . I. A. Baranov, A. A. Protopopov, and V. P. Éĭsmont 41, 1003
Investigation of Hypernuclei Produced by 8.8 Bev Protons . . . . . V. A. Tumanyan, M. G. Sarinyan, D. A. Galstyan, A. R. Kanetsyan, ... M. E. Arustamova, and G. S. Sarkisyan 41, 1007

(γ, n) -Reaction Thresholds for Silicon Isotopes . . . . . A. K. Berzin and R. P. Meshcheryakov 41, 1013
Electrostatic Instability of an Intense Electron Beam in a Plasma . . . . . M. V. Nezlin 41, 1015
The Ne^{21}(n, α) O^{18} Reaction on Slow Neutrons . . . . . A. I. Abramov and M. G. Yutkin 41, 1023
Elastic Scattering of 2.8 Bev/c π^- Mesons on Neutrons . . . . . Yu. D. Bayukov, G. A. Leksin, and Ya. Ya. Shalamov 41, 1025
Spectrum of Electrons Emitted in the Decay of Negative Muons in Nuclear Emulsion . . . . . A. O. Vaĭsenberg, E. A. Pesotskaya, and V. A. Smirnitskii 41, 1031
Nonstationary Elastic Slowing Down of Neutrons in Graphite and Iron . . . . . A. I. Isakov 41, 1037
Inelastic Scattering of Protons on F^{19} Nuclei . . . . . S. S. Vasil'ev, E. A. Romanovskii, and G. F. Timushev 41, 1040
Absorption of Nuclear-Active Cosmic-Ray Particles in Air . . . . . G. Bozoki, E. Fenyves, T. Sandor, O. Balea, M. Batagui, E. Friedlander, B. Betev, ... Sh. Kavalakov, and L. Mitrani 41, 1043
A Method for Studying Elastic Scattering at High Energies . . . . . V. N. Kuz'min 41, 1046
Ionization of Argon by Atoms and Singly or Doubly Charged Ions of Neon and Argon . . . . . V. V. Afrosimov, R. N. Il'in, V. A. Oparin, E. S. Solov'ev, and N. V. Fedorenko 41, 1048
Some Observations on the Solidification of Helium . . . . . A. I. Shalnikov 41, 1056
Motion of Charges in Liquid and Solid Helium . . . . . A. I. Shal'nikov 41, 1054
Asymmetry of Double Mott Scattering of 45 — 245 kev Electrons . . . . . P. E. Spivak, L. A. Mikaélyan, I. E. Kutikov, V. F. Apalin, I. I. Lukashevich, ... and G. V. Smirnov 41, 1064
Inelastic Interaction of Protons and Nucleons at 9 Bev . . . . . T. Visky, I. M. Gramenitskii, Z. Korbel, A. A. Nomofilov, M. J. Podgoretsky, ... L. Rob, V. N. Strel'tsov, D. Tuvdéndorzh, and M. S. Kvastunov 41, 1069
Electron Paramagnetic Resonance in Concentrated Aqueous Solutions of VO^{2+} . . . . . N. S. Garif'yanov, B. M. Kozyrev, R. Kh. Timerov, and N. F. Usacheva 41, 1076
Concerning the Fermi Surface of Tin . . . . . N. E. Alekseevskii and Yu. P. Gaĭdukov 41, 1079
Nuclear Magnetic Resonance in Metallic Thallium . . . . . Yu. S. Karimov and I. F. Shchegolev 41, 1082
Photodeuterons from Al^{27} . . . . . E. D. Makhnovskii 41, 1091
Slow Ions Produced in Gases Upon Passage of Fast Atom and Ion Beams . . . . . I. P. Flaks, G. N. Ogurtsov, and N. V. Fedorenko 41, 1094
Two-Electron Charge Exchange of Protons in Helium During Fast Collisions . . . . . V. I. Gerasimenko 41, 1104
Particle Acceleration by Passage of a Hydromagnetic Wave Front . . . . . V. P. Shabanskii 41, 1107
Energy Level Shift in Plasma Atoms . . . . . L. E. Pargamanik 41, 1112
Quantum Theory of the Dielectric Tensor of an Electron Plasma in a Magnetic Field . . . . . P. S. Zyryanov and V. P. Kalshnikov 41, 1119
Calculation of the Fraction of High-Energy Electrons and Photons Near the Axis of Extensive Air Showers . . . . . I. V. Rakobol'skaya 41, 1125
Degree of Growth of Matrix Elements in the Axiomatic Approach . . . . . B. V. Medvedev and M. K. Polivanov 41, 1130
Thermal Conductivity of Pure Superconductors and Absorption of Sound in Superconductors . . . . . B. T. Geĭlikman and V. É. Kresin 41, 1142
Theory of Plasma Diffusion in a Magnetic Field . . . . . V. L. Gurevich and Yu. A. Firsov 41, 1151
Coherent Phenomena in the Radiation of Identical Oscillators Constituting a Crystal . . . . . C. Muzicar 41, 1168

"Metallic" Reflection of Neutrons . . . . . I. I. Gurevich and P. É. Nemirovskii 41, 1175
Interference Between Direct and Resonance Capture of Slow Neutrons . . . . . I. Lovas 41, 1178
Linear Polarization of Gamma Rays Produced in the (d, pγ) Stripping Reaction . . . . . N. Menyhard and J. Zimanyi 41, 1185
Elimination of Ambiguities in Phase Shift Analysis . . . . . N. P. Klepikov 41, 1187
Transformation of Sound and Electromagnetic Waves at the Boundary of a Conductor in a Magnetic Field . . . . . V. M. Kontorovich and A. M. Glutsyuk 41, 1195
A Model for Anomalous Muon Interaction . . . . . I. Yu. Kobzarev and L. B. Okun' 41, 1205
Analytic Properties of the Square Diagram with Decay Masses . . . . . V. N. Gribov, G. S. Danilov, and I. T. Dyatlov 41, 1215
Theory of Reactions Involving the Formation of Three Particles Near Threshold τ Decay . . . . . V. N. Gribov 41, 1221
Effect of External Fields on the Motion and Growth of Bubbles in Boiling Liquids . . . . . G. A. Askar'yan 41, 1231
Proposed Relation Between the Position of a Pole of the Scattering Amplitude and the Value of the Residue of the Pole . . . . . L. A. Khalfin 41, 1233
Transport Equation for a Degenerate System of Fermi Particles . . . . . G. M. Éliashberg 41, 1241
Concerning the Electromagnetic Structure of the K Meson . . . . . A. A. Startsev 41, 1252
On the Theory of the Spin Echo . . . . . A. R. Kessel' 41, 1254
A New Method of Calculating the Energy Spectrum of Carriers in Semiconductors . . . . . G. E. Pikus 41, 1258
Correlation of Motion of Four Nucleons in the Po^{212} Nucleus . . . . . I. M. Band, L. A. Sliv, and Yu. I. Kharitonov 41, 1274
Photoproduction of Neutrinos on Electrons and Neutrino Radiation from Stars . . . . . V. I. Ritus 41, 1285
Possibility of Polarization of an Electron Beam due to Relativistic Radiation in a Magnetic Field . . . . . I. M. Ternov, Yu. M. Loskutov, and L. I. Korovina 41, 1294
The Mössbauer Effect in Mono- and Diatomic Cubic Lattices . . . . . Yu. Kagan and V. A. Maslov 41, 1296
Correlation Between the Mean Number and Mean Energy of Fission Neutrons and the Properties of the Fissioning Nucleus . . . . . V. P. Kovalev and V. S. Stavinskii 41, 1304
A New Treatment of the Gravitational Field . . . . . A. M. Brodskii, D. Ivanenko, and G. A. Sokolik 41, 1307
The $K + N \rightarrow \Lambda(\Sigma) + \gamma$ Processes . . . . . L. I. Lapidus and Chou Kuang-chao 41, 1310
Nuclear Recoil in the Equivalent Photon Method . . . . . A. M. Badalyan 41, 1315
Adiabatic Perturbation of Discrete Spectrum States . . . . . A. M. Dykhne 41, 1324
A More Precise Determination of the Kinetic Coefficients of a Plasma . . . . . O. V. Konstantinov and V. I. Perel' 41, 1328

LETTERS TO THE EDITOR

Scattering of 7 — 8 Bev Negative Pions on Nucleons with Large Momentum Transfer . . . . . R. A. Aripov, V. G. Grishin, L. V. Silvestrov, and V. N. Strel'tsov 41, 1330
Anisotropy of the Odd Photomagnetic Effect . . . . . I. K. Kikoin and S. D. Lazarev 41, 1332
Resistance of Thin Single-Crystal Wires . . . . . B. N. Aleksandrov and M. I. Kaganov 41, 1333

SOVIET PHYSICS JOURNALS

Translations of the 1961 Originals—*Published in English by the American Institute of Physics with the cooperation of the National Science Foundation.*

Publication year July, 1961—June, 1962.

Soviet Physics—JETP

A translation, beginning with 1955 issues of *Zhurnal Eksperimental'noi i Teoreticheskoi Fiziki* of the USSR Academy of Sciences. Leading physics journal of Soviet Union. Similar to "The Physical Review" in quality and range of topics. Outstanding new work is most likely to appear in this journal.

Vols. 13 and 14 comprising twelve issues, approx. 4000 pp.
$75 domestic, $79 foreign
Libraries $50 domestic, $54 foreign. Single copies, $8*

Soviet Physics—SOLID STATE

A translation, beginning with 1959 issues of *Fizika Tverdogo Tela* of the USSR Academy of Sciences. Offers results of theoretical and experimental investigations in the physics of semiconductors, dielectrics, and on applied physics associated with these problems. Also publishes papers on electronic processes taking place in the interior and on the surface of solids.

Vol. 3 comprising twelve issues, approx. 3800 pp.
$70 domestic, $74 foreign
Libraries $45 domestic, $49 foreign. Single copies, $8*

Soviet Physics—TECHNICAL PHYSICS

A translation, beginning with 1956 issues of *Zhurnal Tekhnicheskoi Fiziki* of the USSR Academy of Sciences. Contains work on plasma physics and magnetohydrodynamics, aerodynamics, ion and electron optics, and radio physics. Also publishes articles in mathematical physics, the physics of accelerators, and molecular physics.

Vol. 6 comprising twelve issues, approx. 2000 pp.
$55 domestic, $59 foreign
Libraries $35 domestic, $39 foreign. Single copies, $5*

Soviet Physics—ACOUSTICS

A translation, beginning with 1955 issues of *Akusticheskii Zhurnal* of the USSR Academy of Sciences. Devoted principally to physical acoustics but includes electro-, bio-, and psychoacoustics. Mathematical and experimental work with emphasis on pure research.

Vol. 7 comprising four issues, approx. 500 pp.
$12 domestic, $14 foreign
(No library discounts.) Single copies, $4

Soviet Physics—DOKLADY

A translation, beginning with 1956 issues of the physics sections of *Doklady Akademii Nauk SSSR*, the proceedings of the USSR Academy of Sciences. All-science journal offering four-page reports of recent research in physics and borderline subjects.

Vol. 6 comprising twelve issues, approx. 1500 pp.
$35 domestic, $38 foreign
Libraries $25 domestic, $28 foreign*
Single copies Vols. 1 and 2, $4;
Vols. 3 through 5, $8.00
Vol. 6 and subsequent issues, $4.00

Soviet Physics—CRYSTALLOGRAPHY

A translation, beginning with 1957 issues of the journal *Kristallografiya* of the USSR Academy of Sciences. Experimental and theoretical papers on crystal structure, lattice theory, diffraction studies, and other topics of interest to crystallographers, mineralogists, and metallurgists.

Vol. 6 comprising six issues, approx. 1000 pp.
$25 domestic, $27 foreign
Libraries $15 domestic, $17 foreign. Single copies, $5*

SOVIET ASTRONOMY—AJ

A translation, beginning with 1957 issues of *Astronomicheskii Zhurnal* of the USSR Academy of Sciences. Covers various problems of interest to astronomers and astrophysicists including solar activity, stellar studies, spectroscopic investigations of radio astronomy.

Vol. 5 comprising six issues, approx. 1100 pp.
$25 domestic, $27 foreign
Libraries $15 domestic, $17 foreign. Single copies, $5*

Soviet Physics—USPEKHI

A translation, beginning with September, 1958, issue of *Uspekhi Fizicheskikh Nauk* of the USSR Academy of Sciences. Offers reviews of recent developments comparable in scope and treatment to those carried in *Reviews of Modern Physics*. Also contains reports on scientific meetings within the Soviet Union, book reviews, and personalia.

Vol. 4 comprising six issues, approx. 1700 pp.
(Contents limited to material from Soviet sources)
$45 domestic, $48 foreign
Libraries $30 domestic, $33 foreign. Single copies, $8*

**For libraries of nonprofit academic institutions.*